# Investigating the Ikaros Family of Transcription Factors Within Macrophages in Inflammatory Bowel Disease


**By**

**JAGJEET KAUR SONDH**


**A thesis submitted to the University of Birmingham for the degree of DOCTOR OF PHILOSOPHY**




UNIVERSITY OF BIRMINGHAM


**Institute of Immunology and Immunotherapy**

**College of Medical and Dental Sciences**

**University of Birmingham**


**May 2022**

UNIVERSITY OF
BIRMINGHAM

## University of Birmingham Research Archive

### e-theses repository

This unpublished thesis/dissertation is copyright of the author and/or third parties. The intellectual property rights of the author or third parties in respect of this work are as defined by The Copyright Designs and Patents Act 1988 or as modified by any successor legislation.

Any use made of information contained in this thesis/dissertation must be in accordance with that legislation and must be properly acknowledged. Further distribution or reproduction in any format is prohibited without the permission of the copyright holder.

# Abstract

The Ikaros Family of transcription factors ***Aiolos***, ***Eos***, ***Helios***, ***Ikaros*** and ***Pegasus*** are a family of zinc finger proteins involved in the regulation of genes within a plethora of immune cells. Studies have suggested the family play a role in mediating Regulatory T cell (Treg) and T helper 17 (Th17) responses within Inflammatory Bowel Disease (IBD) but much of the detail of their function and expression is undocumented. This thesis examines the expression and roles of the family in IBD and the associated autoimmune liver disease Primary Sclerosing Cholangitis (PSC). Using qPCR and immunohistochemistry, we investigated the expression of the Ikaros family in blood derived CD4+ T Cells, myeloid cells, and whole bowel and liver tissue from diseased and healthy individuals. I also used an siRNA knockdown of Eos (siEos) within THP-1 derived macrophages to investigate changes in phenotype and function. We report altered expression of family members within diseased bowel and liver in CD4+ T cells, but also myeloid cells. This includes previously unreported expression of the family within macrophage populations, with changes observed in macrophage subtypes. Ikaros family members were present in both the bowel and liver with greater numbers of Eos and Helios-expressing macrophages found in diseased bowel. Importantly, Eos expression was elevated in monocytes from both Biologic Naïve and anti-TNFalpha treated patient samples in comparison to Control, with novel correlations between Ikaros family members and liver clinical markers also identified. Using siRNA, we found siEos macrophages have reduced phagocytic capacity and upregulated proinflammatory mediator production suggesting Eos promotes a regulatory macrophage phenotype. Together, our results suggest a novel role for the Ikaros family within macrophage phenotype in bowel and liver disease.

# Acknowledgements

Firstly, thank you to the University of Birmingham for my PhD scholarship and Professor Subrata Ghosh for awarding me this PhD position. This thesis would not have been possible without the support of some truly amazing people who I'll forever be grateful for:

Firstly, to Dr Trish Lalor. I don't think I can ever thank you enough for everything - from believing in me and supporting me through all the (many) trials and tribulations in this project, I'm honestly eternally grateful!

To all the members of the Lalor group, both past and present, thank you guys so much! Laura, Pantelitsa and Ellie thank you for just being amazing and I'm so glad we got to share this whole experience together (and the craziness of working in a pandemic too!). To Dr Emma Shepherd, thank you for your support and motivation, to Dr Stuart Hunter, thanks for being a great desk buddy and getting all my pop culture references, and Dr Lozan Sheriff, thank you for all your advice and support!

Thank you to members of the CLGR past and present - to Manjit Braitch for help with ELISAs and always maintaining a positive attitude, Samita Patel for your help with IHC training, to Dr Evaggelia Liaskou, thanks for your help with monocyte/macrophage cultures and Subin Modit for cutting all the tissue sections. To my friends, thank you guys for helping me stay sane/realise there is a life outside the lab!

To both the liver and IBD clinical teams and patients who helped with sample collection in this project, thank you all so much! Special thanks to Dr Marietta Iacucci and Dr

Uday Shivaji for help with collecting IBD samples. Thank you to Dr Dave Withers for your support and organising mouse material – thank you Veronika Matei for helping with this! Thank you to Dr Graham Wallace for your support and guidance- I had such an amazing time working with you during my master's and it really encouraged me to pursue a PhD.

Finally, to my mum Sukhvinder and my sister Jasminder – thank you both so much! I wouldn't have been able to do this PhD or literally anything else had it not been for both of you and your constant support and belief in me. I dedicate this thesis to both of you.

# Contents

*Abstract* ..... *II*

*Acknowledgements* ..... *III*

*List of Figures* ..... *XI*

*List of Tables* ..... *XVII*

*List of Abbreviations* ..... *XIX*

*Chapter 1: Introduction* ..... *1*

**1.1 Inflammatory Bowel Disease** ..... **2**

1.1.1 Ulcerative Colitis and Crohn's Disease ..... 2

1.1.2 Crohn's Disease ..... 3

1.1.3 Ulcerative Colitis ..... 3

1.1.4 Symptoms of Inflammatory Bowel Disease ..... 4

1.1.5 Epidemiology of Inflammatory Bowel Disease ..... 7

1.1.6 Causes of IBD ..... 9

1.1.6.1 Environmental Factors ..... 10

1.1.6.2 Immune Response in the Bowel ..... 10

1.1.6.3 Epithelial Barrier Dysfunction & Microbial Factors ..... 10

1.1.6.4 Genetic Factors Which Alter IBD Susceptibility ..... 11

1.1.7 IBD Pathogenesis ..... 12

1.1.7.1 Mucosal Structure of the Colon ..... 12

1.1.7.2 The Colon Under Homeostatic Conditions ..... 14

1.1.7.3 The Colon in Inflammatory Bowel Disease ..... 15

1.1.8 Diagnosis and Management of Inflammatory Bowel Disease ..... 17

1.1.9 Outlook for IBD Management ..... 20

**1.2 The Liver** ..... **22**

1.2.1 The Gut-Liver Axis ..... 22

1.2.2 Structure and Function of the Liver ..... 24

1.2.3 Cell Types Within the Liver ..... 26

1.2.3.1 Kupffer Cells and Liver Disease ..... 26

1.2.4 Liver Disease ..... 28

1.2.4.1 Primary Sclerosing Cholangitis ..... 29

1.2.4.2 PSC-IBD ..... 30

**1.3 Monocytes and Macrophages** ..... **33**

1.3.1 Monocytes ..... 33

1.3.2 THP-1 ..... 35

1.3.3 Macrophages ..... 36

1.3.3.1 Differentiation of Monocytes to Macrophages ..... 38

1.3.3.2 Macrophage Polarisation and Subsets ..... 39

1.3.3.2.1 Proinflammatory M1 Macrophages ..... 39

1.3.3.2.2 Regulatory M2 Macrophages ..... 40

1.3.3.3 Macrophage Plasticity ..... 43

1.3.3.4 Macrophages in IBD and Disease ..... 44

**1.4 CD4+ T Lymphocytes** ..... **47**

1.4.1 Tregs and Th17 Cells ..... 48

1.4.1.1 Tregs ..... 48

1.4.1.2 Th17 ..... 49

1.4.1.3 Th17/Treg Balance in IBD ..... 50

**1.5 The Ikaros Family of Transcription Factors ..... 53**
1.5.1 Ikaros Family: Structure ..... 54
1.5.2 Expression of the Ikaros Family ..... 56
1.5.3 Regulation of Gene Transcription ..... 56
1.5.4 The Ikaros Family in Disease ..... 57
1.5.5 Ikaros ..... 59
1.5.5.1 The Role of Ikaros ..... 59
1.5.5.2 Ikaros Isoforms and Splice Variants ..... 60
1.5.5.3 Ikaros, CK2 and Cell Cycle Control ..... 62
1.5.5.4 Ikaros Expression in Cells and Tissue ..... 64
1.5.5.5 Ikaros in Disease ..... 65
1.5.6 Aiolos ..... 66
1.5.6.1 Aiolos and its Role in B Cells ..... 67
1.5.6.2 Role of Aiolos in Disease ..... 67
1.5.7 Eos ..... 68
1.5.7.1 Eos Expression and Function in Immune Cells ..... 70
1.5.7.2 Eos in Disease ..... 71
1.5.8 Helios ..... 72
1.5.8.1 Helios Expression in Tissue ..... 73
1.5.8.2 Cellular Expression of Helios ..... 73
1.5.8.3 Role of Helios in Disease ..... 74
1.5.9 Pegasus ..... 75
1.5.9.1 The Role of Pegasus in Development ..... 76
1.5.9.2 Pegasus and Its Role in Platelet Development and Disease ..... 77

**1.6 Summary, Hypothesis and Aims ..... 78**

***Chapter 2: Methods ..... 80***

**2.1 Ethics and Use of Human Biomaterials ..... 81**

**2.2 Cell Culture ..... 82**
2.2.1. Peripheral Blood Mononuclear Cells (PBMCs) ..... 82
2.2.1.1 Isolation and Culture of Peripheral Blood Mononuclear Cells (PBMCs) ..... 82
2.2.1.2 Selection of CD4 Positive (CD4+) PBMCs ..... 83
2.2.1.3 Enrichment of Monocytes From PBMCs ..... 83
2.2.1.4 Polarisation of PBMC-Derived Monocytes into Macrophages ..... 85
2.2.2 THP-1 ..... 87
2.2.2.1 Culture of THP-1 Cells ..... 87
2.2.2.2 THP-1 Differentiation to Macrophages in Vitro ..... 87

**2.3 Flow Cytometric Analysis of Protein Expression ..... 88**
2.3.1 Extracellular and Intracellular Staining of Proteins ..... 88
2.3.2 Flow Cytometry: Compensation Beads ..... 91
2.3.3 Eos Antibody Titration ..... 92
2.3.4 Flow Cytometry: Sorting Cells ..... 93

**2.4 Cell Harvesting and RNA Extraction ..... 94**

**2.5 Real-Time Quantitative Polymerase Chain Reaction (RT- qPCR) ..... 95**
2.5.1 cDNA Preparation ..... 95
2.5.2 qPCR: Methodology ..... 96
2.5.3 Analysis of PCR Data ..... 98

**2.6 Immunohistochemistry ..... 98**
2.6.1 Haematoxylin and Eosin Staining ..... 98
2.6.2 3,3'-Diaminobenzidine (DAB) Immunohistochemistry ..... 99
2.6.3 Opal Dye™ for Multiplex Staining ..... 102

**2.7 RNASeq Methodology ..... 105**
2.7.1 Resection Sample Processing for Bulk RNASeq Analysis ..... 105

**2.8 Western Blotting for Protein Quantification ..... 107**
2.8.1 BCA Assay ..... 107
2.8.2 Western Blot Protocol ..... 108

**2.9 Enzyme-Linked ImmunoSorbent Assay (ELISA) ..... 111**
2.9.1 IL-10 ELISA ..... 111
2.9.2 IL-12 ELISA ..... 111

**2.10 Testing Effects of Pomalidomide on Macrophage Ikaros Family Expression . 112**

**2.11 Short interference RNA (siRNA) ..... 113**
2.11.1 Silencer Select & Lipofectamine RNAiMAX Reagent ..... 113
2.11.2 siRNA Experimental Design ..... 113
2.11.3 Vybrant™ Phagocytosis Assay ..... 116
2.11.4 Proteome Profiler - Human Cytokine Array ..... 117

**2.12 Graphing and Statistical Analysis ..... 118**

***Chapter 3: The Role of The Ikaros Family in Treg and Th17 Polarisation and Plasticity ..... 120***

**3.1 Introduction ..... 121**
3.1.1 Aiolos Influences Th17 and Treg Polarisation ..... 121
3.1.2 Eos Promotes Treg Polarisation and Prevents Th17 Development ..... 122
3.1.3 Helios is a Marker of Tregs ..... 124
3.1.4 Ikaros is Key to Treg and Th17 Polarisation ..... 125

**3.2 Results ..... 128**
3.2.1 Sorting of Tregs Vs Non-Tregs from PBMCs ..... 128
3.2.2. Expression of Ikaros Family Members in Treg Populations ..... 131
3.2.3 Protein Expression of The Ikaros Family in Tregs and Non-Tregs ..... 133
3.2.4 Mild UC Inflammation is Associated with Lower Expression of the Ikaros Family ..... 136

**3.3 Discussion ..... 138**
3.3.1 Summary ..... 139

***Chapter 4: Ikaros Family Expression Within The Bowel And Liver ..... 140***

**4.1 Introduction ..... 141**

**4.2 Results ..... 142**
4.2.1 Inflammatory Bowel Disease Upsets the Normal Structure of the Bowel ..... 144
4.2.2 Crohn's Disease and Ulcerative Colitis Disrupts Bowel Structure ..... 146
4.2.3 The Ikaros Family is Expressed Within the Bowel Tissue ..... 149
4.2.4 Higher Expression of Aiolos and Ikaros mRNA is Found in Diseased Tissue Samples ... 156
4.2.5 Liver Inflammation Perturbs Liver Structure ..... 158
4.2.5.1 Donor Liver has a Regular Liver Structure, Interspersed With Fatty Droplets ..... 158
4.2.5.2 Immune Infiltration and Fibrosis is Common in PSC ..... 160
4.2.6 Ikaros Family Expression in Liver ..... 162
4.2.6.1 Aiolos Expression is Elevated in Diseased Tissue ..... 162

4.2.6.2 PSC Tissue Has Significantly Higher Expression Levels of Eos in Comparison to Donor ..... 163
4.2.6.3 Helios Expression is Significantly Higher in PSC Liver in Comparison to NASH and PSC-IBD ..... 163
4.2.6.4 Ikaros is Expressed in Diseased and Donor Liver Tissue ..... 163
4.2.6.5 PSC and PSC-IBD Liver Express Greater Protein Levels of Pegasus ..... 164
4.2.7 Primary Sclerosing Cholangitis Liver has Higher Expression of the Ikaros Family at a RNA level in Comparison to Donor Liver ..... 170
4.2.8 Expression of Ikaros Family RNA Correlates with Markers of Disease Severity ..... 172
**4.3 Discussion ..... 184**
4.3.1 What Happens to Tissue Structure in IBD? ..... 184
4.3.2 Phenotypic Changes in PSC Tissue ..... 186
4.3.3 Ikaros Family Expression in the Liver and Bowel ..... 186
4.3.3.1 Ikaros Family Expression Within the Bowel ..... 187
4.3.3.2 Ikaros Family Expression Within the Liver ..... 190
4.3.4 Ikaros Family Correlations with Liver Clinical Data ..... 193
4.3.5 Summary ..... 196
***Chapter 5: Ikaros Family Expression Within Monocytes and Macrophages ... 198***
**5.1 Introduction ..... 199**
**5.2 Results ..... 201**
5.2.1 Quantitation of Macrophages in the Healthy, Crohn's Disease and Ulcerative Colitis Bowel Biopsies ..... 201
5.2.2 Quantitation of Macrophages in the Liver ..... 204
5.2.3 Basal Expression of the Ikaros Family in Monocytes and the THP-1 Cell Line ..... 206
5.2.4 Polarising the THP-1 Cell Line into Macrophages ..... 210
5.2.5 Polarised THP-1 Derived Macrophages Express Macrophage Subtype-Specific Surface Markers ..... 213
5.2.6 RNA Expression of the Ikaros family in THP-1 derived Macrophage Populations ..... 216
5.2.7 Protein Expression of Ikaros Family Members in THP-1-Derived Macrophages ..... 218
5.2.8 Blood Derived M2 Macrophage Subtypes Secrete the Highest Levels of IL-10, Whilst M1 Macrophages Produce Most IL-12 ..... 223
5.2.9 Primary Monocyte-Derived Macrophages Express Defined Surface Markers Specific to Macrophage Subtypes ..... 226
5.2.10 Polarisation of PBMC-Derived Monocytes into Various Macrophage Populations Alters the Expression of the Ikaros Family ..... 229
5.2.11 Ikaros Family Transcription Factors are Co-expressed with CD68 in Kupffer Cells ..... 231
5.2.12 CD68-Expressing Macrophages in the Bowel Co-express the Ikaros Family of Transcription Factors ..... 234
5.2.13 RNASeq Data Analysis From CD Resections ..... 240
5.2.13.1 Hierarchical Clustering for Macrophage Genes in Resection Samples ..... 240
5.2.13.2 Pegasus Expression is Highest in Stricture Regions, With Ikaros Expression Higher in Distal Regions ..... 245
5.2.13.3 Ikaros Has the Highest VIP Score of All Ikaros Family Members, With Greatest Expression in Distal Regions ..... 247
**5.3 Discussion ..... 249**
5.3.1 Elevated Expression of Macrophages in Diseased Bowel ..... 249
5.3.2 Macrophages Play a Key Role in Liver Disease ..... 249
5.3.3 Monocytes and THP-1 cells Express the Ikaros Family ..... 251
5.3.4 Establishing our Monocyte to Macrophage Culture Method ..... 252
5.3.5 Ikaros Family in Macrophage Populations ..... 253

5.3.6 All Ikaros Family Members Co-Express With CD68 ....255
5.3.7 Limitations of Our IHC Study ....257
5.3.8 RNASeq Data Analysis ....259
5.3.9 Summary ....264

***Chapter 6: Impact of IBD and Therapeutic Intervention on Ikaros Family Expression ....267***

**6.1 Introduction ....268**
6.1.1 Thalidomide, Lenalidomide and Pomalidomide: Immunomodulatory Drugs and The Ikaros Family ....268
6.1.2 The Ikaros Family and Thalidomide ....272

**6.2 Results ....274**
6.2.1 Short-term Pomalidomide Culture Alters Ikaros Family Expression ....274
6.2.2 Pomalidomide Addition Alters Expression of the Ikaros Family in Macrophages ....277
6.2.3 Freezing and Thawing Cells Alters Expression of Ikaros Family Members Compared to Freshly Isolated Cells ....279
6.2.4 Diseased Patient Macrophages have Differential Expression of Ikaros Family Transcription Factors in Comparison to Control ....281
6.2.5 Elevated Levels of IL-12 Secretion Are Found in M1 Populations Isolated From Untreated IBD Blood ....283
6.2.6 Impact of Anti-TNFα treatment on Ikaros Family Expression in Macrophages ....285
6.2.6.1 Anti-TNFα Treatment Increases Expression of Eos in Monocytes ....285
6.2.6.2 Anti-TNFα Treatment Lowers Ikaros Expression in Macrophage Populations ....286
6.2.6.3 Helios Expression is Elevated in M2c Macrophage Populations Following Anti-TNFα Treatment ....286

**6.3 Discussion ....290**
6.3.1 Pomalidomide Targets Expression of all Ikaros Family Members ....290
6.3.2 Expression of the Ikaros Family in Frozen PBMC Samples ....293
6.3.3 Expression of the Ikaros Family in Biologic Naïve IBD Samples ....294
6.3.4 Impact of Infliximab Therapy on Ikaros Family Expression ....298
6.3.5 Summary ....302

***Chapter 7: Selective Eos Knockdown In Macrophages ....304***

**7.1 Introduction ....305**

**7.2 Results ....306**
7.2.1 Lipofectamine RNAiMAX and Silencer Select Significantly Reduce Eos Expression in THP-1-derived MΦ Macrophages ....306
7.2.2 Eos Knockdown Macrophages Retain Cell Viability During Culture ....308
7.2.3 The Lipofectamine RNAiMAX Method is Sufficient to Knockdown Eos in a 96 Well Plate Culture ....310
7.2.4 Eos Knockdown Within Macrophages Impacts Their Phagocytic Capacity ....312
7.2.5 Eos Knockdown is Sustained Post siRNA Treatment Following Addition of Complete Medium ....314
7.2.6 Eos knockdown in Macrophages Reduces IL-2 Secretion but Increases IL-17E and IL-8 secretion ....316

**7.3 Discussion ....320**
7.3.1 Eos Knockdown Effects the Phagocytic Capacity of Macrophages ....320
7.3.2 Summary and Limitations of this Chapter ....325

***Chapter 8: Concluding Discussion ....327***

**8.1 Key Conclusions of my Thesis ..... 328**
**8.2 Significance of Key Findings ..... 333**
**8.3 Future Directions of Work ..... 334**
**8.4 Conclusion ..... 335**
***References ..... 336***
***Appendix A: Chapter 2 Methods Supplementary Material ..... 351***
**A.1 Immunohistochemistry Supplementary Material ..... 351**
A.1.1 3,3'-diaminobenzidine (DAB) Staining Controls ..... 351
A.1.1.1 Live Tissue DAB Controls: Mouse IgG ..... 351
A.1.1.2 Live Tissue DAB Controls: Rabbit IgG ..... 352
A.1.1.3 Bowel Tissue Controls: Mouse and Rabbit IgG ..... 353
A.1.2 Opal Dye™ Staining Controls ..... 354
A.1.2.1 Bowel Mouse and Rabbit IgG ..... 354
A.1.2.2 Liver Mouse and Rabbit IgG ..... 355
A.1.3 Immunohistochemistry (IHC) Semi-Quantitative Analysis ..... 356
A.1.3.1 DAB: Percentage Area DAB+ ..... 356
A.1.3.2 IHC DAB Semi-Quantitative Analysis: CD68 Counting ..... 356
A.1.3.3 IHC Opal™ Semi-Quantitative Analysis ..... 356
**A.2 ELISA Reagent Preparation ..... 357**
A.2.1 IL-10 ELISA Reagent and Standard Curve Preparation ..... 357
A.2.2 IL-12 ELISA Reagent and Standard Curve Preparation ..... 357
**A.3 Patient Blood Samples ..... 358**
***Appendix B: The Ikaros Family and Mouse Models ..... 359***
**B.1 Introduction ..... 359**
B.1.1 IBD Mouse Models ..... 359
B.1.2 Ikaros Family Mouse Models ..... 360
**B.1.3 Results ..... 362**
B.1.3.1 Eos and Helios Are Greatly Upregulated in CD11b+F4/80+ Mice Colon Macrophages 363
**B.1.4 Discussion ..... 365**

# List of Figures

***Chapter 1 - Introduction***


| Figure | Figure Title | Page |
|---|---|---|
| 1.1 | Historical Timeline of Inflammatory Bowel Disease | 5 |
| 1.2 | Comparison Between Crohn's Disease and Ulcerative Colitis | 6 |
| 1.3 | Global Prevalence of Inflammatory Bowel Disease in 2015 | 8 |
| 1.4 | Causes of IBD | 9 |
| 1.5 | Transverse and Longitudinal Cross Section Views of the Structure of the Colon | 13 |
| 1.6 | Structure of the Gut and its Role in Inflammatory Bowel Disease | 18 |
| 1.7 | Summary of Causes, Diagnostic Methods and Treatment Methods for Inflammatory Bowel Disease | 21 |
| 1.8 | The Gut-Liver Axis | 23 |
| 1.9 | Schematic Diagram of Liver Structure | 25 |
| 1.1 | Polarisation of Monocytes Into M1, M2a And M2c Macrophage Populations | 42 |
| 1.11 | Factors Influencing the Plasticity of Regulatory T Cells and T helper 17 (Th17) Cells | 52 |
| 1.12 | Structure and Function of Ikaros Family Members | 55 |
| 1.13 | Ikaros and the Nucleosome-Remodelling and Histone Deacetylate (NuRD) Complex Can Regulate Gene Transcription | 58 |
| 1.14 | Schematic of Ikaros Isoforms | 61 |
| 1.15 | Ikaros and CK2 Mediated Gene Transcription | 63 |
| 1.16 | Ikaros Phosphorylation Enables Cell Cycle Progression | 64 |
| 1.17 | Proposed Regulation Pathways of Aiolos | 68 |
| 1.18 | Proposed Regulation Pathways of Eos | 72 |
| 1.19 | Proposed Regulation Pathways of Helios | 75 |


***Chapter 2 - Methods***


| Figure | Figure Title | Page |
|---|---|---|
| 2.1 | The MACS® Miltenyi Biotec Pan Monocyte Isolation Kit | 85 |
| 2.2 | Lipofectamine RNAiMAX and Silencer Select Protocol Walkthrough | 114 |


***Chapter 3 - The Role of The Ikaros Family in Treg and Th17 Polarisation and Plasticity***


| Figure | Figure Title | Page |
|---|---|---|
| 3.1 | Influence of Ikaros Family Members on Regulatory T Cell (Treg) and T helper 17 (Th17) Gene Expression | 126 |

| | | |
|---|---|---|
| 3.2 | Gating Strategy For Sorting of Tregs and Non-Tregs From Peripheral Blood Mononuclear Cells (PBMCs) | 129 |
| 3.3 | Confirming Treg Vs Non-Treg Sorting Through Expression of FoxP3 | 130 |
| 3.4 | Expression of the Ikaros Family in Sorted Tregs and Non-Tregs | 132 |
| 3.5 | Gating Strategy For Identifying Treg And Non-Treg Populations | 134 |
| 3.6 | Expression of the Ikaros Family in Tregs and Non-Tregs | 135 |
| 3.7 | Relative Expression Levels of Helios, Ikaros and Pegasus are Lower in Ulcerative Colitis in Comparison to Hemochromatosis | 137 |


***Chapter 4 - Ikaros Family Expression Within the Bowel and Liver***


| Figure | Figure Title | Page |
|---|---|---|
| 4.1 | Structure of the Normal Colon | 145 |
| 4.2 | Haematoxylin and Eosin Staining of Crohn's Diseased Tissue | 147 |
| 4.3 | Haematoxylin and Eosin Staining of Ulcerative Colitis Bowel Tissue | 148 |
| 4.4 | Expression of Aiolos in Uninflamed and Inflamed Bowel | 151 |
| 4.5 | Eos Expression in Inflamed Bowel in Comparison to Uninflamed | 152 |
| 4.6 | Expression of Helios in Uninflamed and Inflamed Bowel | 153 |
| 4.7 | Ikaros Expression in Inflamed Bowel in Comparison to Uninflamed | 154 |
| 4.8 | Expression of Pegasus in Uninflamed and Inflamed Bowel | 155 |
| 4.9 | Relative Expression Levels of Aiolos and Ikaros is Higher in Biopsies From Patients With UC in Comparison to Healthy Donors | 157 |
| 4.10 | Haematoxylin and Eosin Staining of Donor Liver Tissue | 159 |
| 4.11 | Haematoxylin and Eosin Staining of Primary Sclerosing Cholangitis Liver Tissue | 161 |
| 4.12 | Expression of Aiolos in Donor, Non-alcoholic Steatohepatitis (NASH), Primary Sclerosing Cholangitis (PSC) and PSC-Inflammatory Bowel Disease (PSC-IBD) Liver Tissue | 165 |
| 4.13 | Expression of Eos in Donor, Non-alcoholic Steatohepatitis (NASH), Primary Sclerosing Cholangitis (PSC) and PSC-Inflammatory Bowel Disease (PSC-IBD) Liver Tissue | 166 |
| 4.14 | Expression of Helios in Donor, Non-alcoholic Steatohepatitis (NASH), Primary Sclerosing Cholangitis (PSC) and PSC-Inflammatory Bowel Disease (PSC-IBD) Liver Tissue | 167 |
| 4.15 | Expression of Ikaros in Donor, Non-alcoholic Steatohepatitis (NASH), Primary Sclerosing Cholangitis (PSC) and PSC-Inflammatory Bowel Disease (PSC-IBD) Liver Tissue | 168 |
| 4.16 | Expression of Pegasus in Donor, Non-alcoholic Steatohepatitis (NASH), Primary Sclerosing Cholangitis (PSC) and PSC-Inflammatory Bowel Disease (PSC-IBD) Liver Tissue | 169 |

| | | |
|---|---|---|
| 4.17 | Diseased Liver has Higher Relative Expression Levels of the Ikaros Family in Comparison with Donor Liver | 171 |
| 4.18 | Correlations Between Aiolos and Patient Liver Function Markers in Non-alcoholic Steatohepatitis Liver | 173 |
| 4.19 | No Clear Correlation Exists Between Eos and Patient Liver Function Markers in Non-alcoholic Steatohepatitis Liver | 174 |
| 4.20 | A Trend For Correlation Exists Between Helios and Body Mass Index in Non-alcoholic Steatohepatitis Liver | 175 |
| 4.21 | Correlations Between Ikaros and Patient Liver Function Markers in Non-alcoholic Steatohepatitis Liver | 176 |
| 4.22 | A Negative Correlation Exists Between Pegasus and Body Mass Index in Non-alcoholic Steatohepatitis Liver | 177 |
| 4.23 | Correlations Between Aiolos and Patient Liver Function Markers in Primary Sclerosing Cholangitis Liver | 179 |
| 4.24 | A Positive Trend Exists Between Eos and Body Mass Index in Primary Sclerosing Cholangitis Liver | 180 |
| 4.25 | A Strong Positive Correlation Exists Between Helios and Body Mass Index in Primary Sclerosing Cholangitis Liver | 181 |
| 4.26 | Correlations Between Ikaros and Patient Liver Function Markers in Primary Sclerosing Cholangitis Liver | 182 |
| 4.27 | Correlations Between Pegasus and Patient Liver Function Markers in Primary Sclerosing Cholangitis Liver | 183 |
| 4.28 | Summary Diagram For Chapter 4 | 197 |


***Chapter 5 - Ikaros Family Expression Within Monocytes and Macrophages***


| Figure | Figure Title | Page |
|---|---|---|
| 5.1 | Expression of CD68 in the Bowel | 202 |
| 5.2 | CD68-Expressing Macrophage Expression in Uninflamed and Inflamed Bowel | 203 |
| 5.3 | CD68+ Macrophage Staining in Liver | 205 |
| 5.4 | Monocytes From Peripheral Blood Mononuclear Cells Have Similar Expression Levels of the Ikaros Family of Transcription Factors as the THP-1 Cell Line | 207 |
| 5.5 | THP-1 Derived Macrophage Flow Cytometry Gating Strategy | 208 |
| 5.6 | THP-1 Cells Express Protein Levels of Aiolos, Eos, Helios And Ikaros | 209 |
| 5.7 | Differentiated THP-1 M2c Macrophages Secrete the Most IL-10 | 211 |
| 5.8 | Differentiated THP-1 M1 Macrophages Secrete the Most IL-12 | 212 |
| 5.9 | THP-1 Derived Macrophage Flow Cytometry Gating Strategy | 214 |
| 5.10 | Markers of Macrophage Differentiation | 215 |

| | | |
|---|---|---|
| 5.11 | Polarisation of THP-1s into Different Macrophage Populations Alters the RNA Expression of the Ikaros Family | 217 |
| 5.12 | Polarisation of THP-1s Into Different Macrophage Populations Alters the Protein Expression of the Ikaros Family | 220 |
| 5.13 | THP-1 –Derived Macrophages Express Protein Levels of Aiolos, Eos, Helios and Ikaros | 222 |
| 5.14 | Blood-derived M2 Macrophages Secrete IL-10 | 224 |
| 5.15 | Blood-derived M1 Macrophages Secrete IL-12 | 225 |
| 5.16 | Gating Strategy For Flow Cytometry Analysis of Surface Markers Present on Primary Monocyte-derived Macrophages | 227 |
| 5.17 | Flow Cytometry Analysis of Surface Markers Present on Primary Monocyte-Derived Macrophages | 228 |
| 5.18 | Polarisation of PBMC-Derived Monocytes Into Different Macrophage Populations Alters The Expression of the Ikaros Family | 230 |
| 5.19 | Ikaros Family Members Co-localise with CD68-Expressing Macrophage Expression in Primary Sclerosing Cholangitis (PSC) Tissue | 232-233 |
| 5.20 | Aiolos Co-localises with CD68-Expressing Macrophages in Uninflamed and Inflamed Bowel Tissue | 235 |
| 5.21 | Eos Co-localises with CD68-Expressing Macrophages in Uninflamed and Inflamed Bowel Tissue | 236 |
| 5.22 | Helios Co-localises with CD68-Expressing Macrophages in Uninflamed and Inflamed Bowel Tissue | 237 |
| 5.23 | Ikaros Co-localises with CD68-Expressing Macrophages in Uninflamed and Inflamed Bowel Tissue | 238 |
| 5.24 | Pegasus Co-localises with CD68-Expressing Macrophages in Uninflamed and Inflamed Bowel Tissue | 239 |
| 5.25 | Dendrogram Showing Outcome of Hierarchical Clustering for Macrophage Genes in Resection Samples | 242 |
| 5.26 | VIP Scores Separate Key Macrophage Genes in Key Anatomical Compartments in the Injured Colon | 244 |
| 5.27 | Distribution of Ikaros Family Gene Expression in Key Anatomical Compartments in the Injured Colon | 246 |
| 5.28 | VIP Scores Separate Ikaros Family Genes in Key Anatomical Compartments in the Injured Colon | 248 |
| 5.29 | Summary of Findings From Chapter 5 | 266 |

***Chapter 6 - Impact of IBD and Therapeutic Intervention on Ikaros Family Expression***


| Figure | Figure Title | Page |
|---|---|---|
| 6.1 | Chemical Structure of Thalidomide and Its Derivatives | 270 |
| 6.2 | Pomalidomide-Mediated Degradation of Ikaros | 271 |
| 6.3 | Pomalidomide Addition Alters Expression of the Ikaros Family in Macrophages | 275 |
| 6.4 | Prolonged Pomalidomide Culture Alters Expression of the Ikaros Family in Macrophages | 278 |
| 6.5 | Comparison of Fresh and Frozen Peripheral Blood Mononuclear Cells-derived Monocyte to Macrophage Culture | 280 |
| 6.6 | Comparison of Ikaros Family Levels in Control and Biologic Naïve Diseased Patient Samples | 282 |
| 6.7 | Biologic Naïve Inflammatory Bowel Disease (IBD) M1 Macrophages Secrete Greater IL-12 in Comparison to Control | 284 |
| 6.8 | Expression of Eos in Control and Anti-TNFα Treated IBD Patient Samples | 287 |
| 6.9 | Expression of Ikaros in Control and Anti-TNFα treated IBD patient samples | 288 |
| 6.10 | Expression of Helios in Control and Anti-TNFα treated IBD patient samples | 289 |
| 6.11 | Summary Diagram Of Chapter 6 | 303 |


***Chapter 7 - Selective Eos Knockdown In MΦ Macrophages***


| Figure | Figure Title | Page |
|---|---|---|
| 7.1 | Lipofectamine RNAiMAX and Silencer Select Reduces Eos Expression | 307 |
| 7.2 | Lipofectamine RNAiMAX and Silencer Select Have Minimal Impact On Cell Viability | 309 |
| 7.3 | Lipofectamine RNAiMAX and Silencer Select Reduces Eos Expression | 311 |
| 7.4 | Eos Knockdown Suggests A Reduction in Phagocytic Capacity of PMA-Polarised THP-1 Macrophages | 313 |
| 7.5 | Eos Knockdown is Sustained Post siRNA Treatment And Following Addition of Complete Medium | 315 |
| 7.6 | Eos Knockdown in THP-1 Macrophages Alters Cytokine Secretion | 317 |
| 7.7 | Eos Knockdown in THP-1 Macrophages Alters Chemokine Secretion | 319 |
| 7.8 | Summary Diagram for Chapter 7 | 326 |

***Chapter 8 – Concluding Discussion***


| Figure | Figure Title | Page |
|---|---|---|
| 8.1 | Key Conclusions of This Thesis | 332 |


***Appendices A&B***


| Figure | Figure Title | Page |
|---|---|---|
| A.1 | Representative Images of Isotype Matched Control Mouse IgG Liver Sections | 351 |
| A.2 | Representative Images of Isotype Matched Control Rabbit IgG Liver Sections | 352 |
| A.3 | Representative Images of Isotype Matched Control Rabbit and Mouse IgG Bowel Sections | 353 |
| A.4 | Representative Images of Isotype Matched Control Rabbit and Mouse IgG For Opal Dye Staining On Bowel Tissue | 354 |
| A.5 | Representative Images of Isotype Matched Control Rabbit and Mouse IgG For Opal Dye™ Staining on Primary Sclerosing Cholangitis Liver Tissue | 355 |
| B.1 | Gating Strategy for Flow Cytometry Analysis of Mice Colons | 363 |
| B.2 | Helios and Eos are Upregulated Within *Citrobacter rodentium* Mice Colon Macrophages | 364 |

# List of Tables


***Chapter 1 – Introduction***

| Table | Table Title | Page |
|---|---|---|
| 1.1 | Montreal Classification System | 19 |
| 1.2 | Phenotypic Differences Between Crohn's Disease (CD) and Primary Sclerosing Cholangitis- CD (PSC-CD) | 31 |
| 1.3 | Phenotypic Differences Between Ulcerative Colitis (UC) and Primary Sclerosing Cholangitis- UC (PSC-UC) | 31 |
| 1.4 | Monocyte Subsets | 35 |
| 1.5 | Differences Between M1 and M2 Macrophage Populations | 43 |
| 1.6 | T Helper Cell Subsets | 47 |
| 1.7 | Genes Encoding the Five Members of the Ikaros Family | 53 |
| 1.8 | Aims and Objectives of Each Thesis Chapter | 78-79 |

***Chapter 2 – Methods***

| Table | Table Title | Page |
|---|---|---|
| 2.1 | Primary Monocyte to Macrophage Polarising Conditions | 86 |
| 2.2 | THP-1 to Macrophage Polarising Conditions | 88 |
| 2.3 | List of Flow Cytometry Antibodies | 89-90 |
| 2.4 | List of Antibodies Used for Flow Cytometry Compensation | 91 |
| 2.5 | Conditions Assayed For Optimisation of Unconjugated Anti-Eos Antibody And Appropriate Secondary Antibody For Flow Cytometry | 93 |
| 2.6 | List of Antibodies Used For Sorting Tregs and Non-Tregs | 94 |
| 2.7 | Qiagen RNA Extraction Kits Used For Appropriate Starting Materials | 95 |
| 2.8 | One Reaction Mix of iSCRIPT ™ cDNA Synthesis Kit | 95 |
| 2.9 | Steps for cDNA Synthesis | 96 |
| 2.1 | Components of One Taq Man ® Universal Master Mix Reaction | 96 |
| 2.11 | Assay ID For Target Genes Used in This Thesis | 97 |
| 2.12 | PCR Cycles and Steps | 97 |
| 2.13 | Analysing PCR Data | 98 |
| 2.14 | Haematoxylin and Eosin Staining of Paraffin Embedded Tissue | 99 |
| 2.15 | 3,3'-Diaminobenzidine (DAB) Protocol of Paraffin Embedded Tissue | 101-101 |
| 2.16 | Antibodies and Their Dilutions Used in 3,3'-Diaminobenzidine (DAB) | 102 |
| 2.17 | Opal Dye™ Multiplex Protocol of Paraffin Embedded Tissue | 103-104 |
| 2.18 | Antibodies and Their Dilutions Used in Opal Dye™ Staining of Tissue | 105 |

| | | |
|---|---|---|
| 2.19 | Genes For Identifying Macrophage Populations From RNASeq Data | 107 |
| 2.20 | Antibody Dilutions Used in Western Blotting | 110 |
| 2.21 | Lipofectamine RNAiMAX Cell Seeding Conditions | 114 |
| 2.22 | Lipofectamine RNAiMAX Opti-Mem Media to Lipofectamine RNAi Max Ratio | 114 |
| 2.23 | Lipofectamine RNAiMAX Opti-Mem Media to siRNA Ratio | 115 |
| 2.24 | Diluted Lipofectamine RNAiMAX Reagent to Diluted siRNA Ratio | 115 |
| 2.25 | Lipofectamine RNAiMAX siRNA-Lipid Complex and Final siRNA Concentration Per Well | 115 |
| 2.26 | Vybrant Phagocytosis Assay Conditions | 116 |

***Chapter 4 - Ikaros Family Expression Within the Bowel and Liver Chapter***

| Table | Table Title | Page |
|---|---|---|
| 4.1 | Demographic Results For Liver Transplant Patients With Non-alcoholic Steatosis (NASH) and Primary Sclerosing Cholangitis (PSC) Used in this Investigation | 143 |
| 4.2 | Changes in Tissue Architecture in CD and UC Distinguishable by Biopsies and Resections | 185 |
| 4.3 | Summary of Clinical Data Correlations | 193 |

***Chapter 5 - Ikaros Family Expression Within Monocytes and Macrophages***

| Table | Table Title | Page |
|---|---|---|
| 5.1 | RNASeq Resection Patient Samples and Clinical Data | 241 |

***Chapter 6 - Impact of IBD and Therapeutic Intervention on Ikaros Family Expression***

| Table | Table Title | Page |
|---|---|---|
| 6.1 | Statistical Analysis of 24-hour Pomalidomide Addition to MΦ and M1 Macrophages | 276 |

***Appendices A & B***

| Table | Table Title | Page |
|---|---|---|
| A.1 | Patient Blood Samples Used in Chapter 6 | 358 |
| B.1 | Antibody Panel For Mice Colon Staining | 362 |

# List of Abbreviations

| | |
|---|---|
| ALL | Acute Lymphoblastic Leukaemia |
| AML | Acute Myeloid Leukaemia |
| B-ALL | B- Cell Acute Lymphoblastic Leukaemia |
| CD | Crohn's Disease |
| CD68+ | CD68 Positive |
| CNS | Central Nervous System |
| DAB | 3,3'-Diaminobenzidine |
| DAMPs | Danger Associated Molecular Patterns |
| DC | Dendritic Cells |
| DSS | Dextran Sodium Sulphate |
| EAE | Experimental Autoimmune Encephalomyelitis |
| GF | Growth Factors |
| GI | Gastrointestinal |
| GM-CSF | Granulocyte Macrophage Colony Stimulating Factor |
| GWAS | Genome Wide Association Study |
| HFE | Hemochromatosis |
| HSC | Hepatic Stellate Cells |
| HSCs | Hematopoietic Stem Cells |
| IBD | Inflammatory Bowel Disease |
| IF | Ikaros Family |
| IFNγ | Interferon Gamma |
| IHC | Immunohistochemistry |
| IL | Interleukin |
| ILCs | Innate Lymphoid Cells |
| iNOS | Inducible Nitric Oxide Species |
| LP | Lamina Propria |
| LPS | Lipopolysaccharide |
| LSEC | Liver Sinusoidal Endothelial Cells |
| M-CSF | Macrophage Colony Stimulating Factor |
| M1 | Proinflammatory macrophages |
| M2 | Regulatory macrophages |
| MDMs | Monocyte Derived Macrophages |
| MHC | Major Histocompatibility Complex |
| MMPs | Matrix metalloproteinases |
| MΦ | Macrophage |
| NAFLD | Non-alcohol associated fatty liver disease |
| NASH | Non-alcoholic Steatohepatitis |
| NO | Nitric Oxide |
| NOD2 | Nucleotide Binding Oligomerization Domain Containing 2 |

| | |
|---|---|
| PAMPs | Pathogen Associated Molecular Patterns |
| PBC | Primary Biliary Cirrhosis |
| PCR | Polymerase Chain Reaction |
| PMA | Phorbol 12-myristate 13-acetate |
| Pom. | Pomalidomide |
| PRRs | Pattern Recognition Receptors |
| PSC | Primary Sclerosing Cholangitis |
| RA | Rheumatoid Arthritis |
| ROS | Reactive Oxidative Species |
| scRNASeq | Single Cell RNA Sequencing |
| SEM | Standard Error Mean |
| siEos | Silencer Select Eos Targeting siRNA |
| siGAPDH | Silencer Select GAPDH Positive siRNA |
| siRNA | Small Interfering RNA |
| SLE | Systemic Lupus Erythematosus |
| SNPs | Single Nucleotide Polymorphisms |
| T-ALL | T cell Acute Lymphoblastic Leukaemia |
| T1D | Type 1 Diabetes |
| T2D | Type 2 Diabetes |
| TF | Transcription Factor |
| Tfh | T Follicular Helper Cells |
| Th1 | T Helper 1 |
| Th17 | T Helper 17 Cell |
| Th2 | T Helper 2 |
| TLR | Toll Like Receptor |
| TNBS | Trinitrobenzene Sulphonic Acid |
| TNF$\alpha$ | Tumour Necrosis Factor Alpha |
| Treg | Regulatory T Cell |
| UC | Ulcerative Colitis |
| WT | Wild Type |

# Chapter 1: Introduction

## 1.1 Inflammatory Bowel Disease

Inflammatory Bowel Disease (IBD) is a chronic inappropriate immune response to the normal microbiota within the intestine, associated with rising morbidity (1-5). A relapsing condition, IBD presents as two main manifestations, Crohn's Disease (CD) and Ulcerative Colitis (UC) and impacts both adults and children (4, 6-10). The aetiology of IBD is unknown and no cure has been identified (6, 11, 12). IBD was first identified during the industrial revolution and some studies suggest around 0.5% of populations in the westernised world are now impacted by IBD. It is hypothesised that the incidence of IBD will continue to rise in the future (5, 6, 11, 12). In IBD, it's believed that an inappropriate immune response to pathogens within the gastrointestinal area coupled with particular genetic susceptibilities, results in a continued inflammatory immune response within the gut, leading to loss of function, deterioration and scarring of the tissue (3, 5, 13).

IBD manifests as a chronic condition with phases of recurrence, relapse, and remission (1, 2, 11). Although IBD displays low mortality, it has a greater association with disability impacting the quality of life through its association with various secondary diseases such as Primary Sclerosing Cholangitis (PSC) and Cardiovascular Disease (CVD) (2, 6, 7, 10, 11). This thus contributes to the need to find better management and treatment of the disease (14).

### 1.1.1 Ulcerative Colitis and Crohn's Disease

Our knowledge of IBD dates back to 1875 when UC was first described by Wilks and Moxon (Figure 1.1) (6, 15). CD was later identified as a disease impacting the terminal ileum (6, 15-17). In previous studies, it was believed that CD was associated with a T helper 1 (Th1) phenotype whereas in UC, T helper 2 (Th2) cells played a greater role,

however we now know it is the concerted action of a number of immune cell types which contribute to IBD pathogenesis (See 1.1.7) (4).

### 1.1.2 Crohn's Disease

CD is associated with a Th1 immune profile and comprises of discontinuous transmural inflammation in the terminal ileum and colon (9, 18). CD can lead to the development of fistulas and in severe cases, stricturing which requires surgical resections to remove the diseased tissue (3, 19). CD can impact growth as approximately 50% of CD patients are 10% shorter than the average general population (1). Relapse is common with 20-30% of patients with CD relapsing after surgery (1). CD mortality is itself highly linked to GI and respiratory diseases (5). Some studies also suggest CD has a higher mortality rate than UC (5).

### 1.1.3 Ulcerative Colitis

UC is restricted to the colon and is associated with Th2 cells (20). UC manifests as continuous superficial submucosal and mucosal colon inflammation (3, 18, 20). Patients go on to develop ulcers, crypt abscesses, increased neutrophil infiltration in the lamina propria (LP) and a decrease in mucin production from goblet cells (20). UC is more common in men than women (20). In comparison to CD, fistulas and strictures are less common in UC, although increased cancer risk is more prevalent in these patients (21). UC mortality is also linked to infection and GI diseases (5). The most common disease association of UC is with PSC, with UC present in approximately 75% of PSC cases (22).

### 1.1.4 Symptoms of Inflammatory Bowel Disease

Symptoms of IBD vary from patient to patient, with many studies suggesting underlying genetic differences cause the variation in severity of symptoms (Figure 1.2) (9). The main IBD manifestations include fever, abdominal pain, weight loss, bloody stool, rectal bleeding, and diarrhoea (2, 4, 8, 16). In IBD patients, if symptoms are mis-managed, the colon and or rectum become ulcerated which results in fistulas and stenosis in CD and megacolon in UC (4). Depression, anaemia, and malnutrition are also common in IBD patients (14, 23).

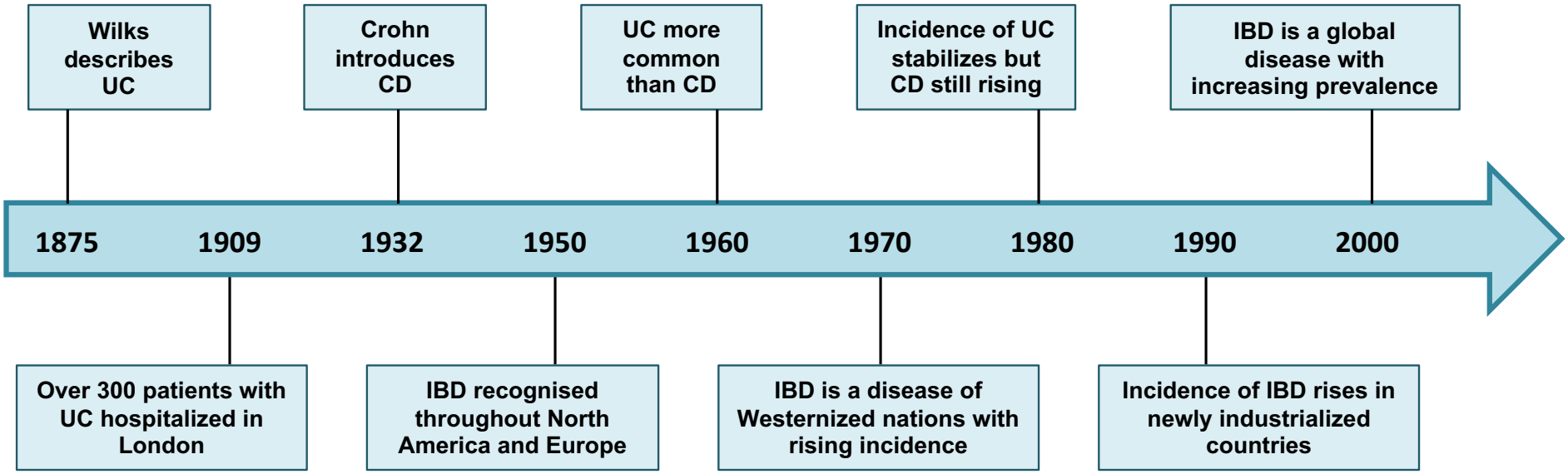



**Figure 1.1: Historical Timeline of Inflammatory Bowel Disease**
Diagram depicting key events in the history of Inflammatory Bowel Disease (IBD) from the first description of Ulcerative Colitis (UC) in 1875 to the growing presence of IBD in the 2000s. Adapted from Kaplan (2015). *CD;* Crohn's Disease, *UC;* Ulcerative Colitis.

| Crohn's Disease | Ulcerative Colitis |
| --- | --- |
|  |  |
| Discontinuous inflammation<br><br>Impacts the whole of the gastrointestinal tract<br><br>**Th1** associated cytokines such as IL-1 and IL-6<br><br>Risk of cancer less common<br><br>Risk of fistulas and strictures common | Restricted to a specific region of the colon<br><br>Extensive continuous mucosal inflammation<br><br>**Th2** associated cytokines such as IL-4 and IL-5<br><br>Risk of cancer more common<br><br>Risks of fistulas and strictures less common |

**Figure 1.2: Comparison Between Crohn's Disease and Ulcerative Colitis**
Differences between Crohn's Disease and Ulcerative Colitis exist in their impact on regions of the gastrointestinal tract and their risk of cancer and strictures. Th1; T helper 1 cells, Th2; T helper 2 cells. Figures adapted from *Crohnscolitisfoundation.org* (2018). Table adapted from Ouyang *et al.,* (2006).

### 1.1.5 Epidemiology of Inflammatory Bowel Disease

Patients are typically diagnosed with IBD around the ages of 18 - 35, with a quarter diagnosed before the age of 20 (5, 6). The most recent epidemiological study by the *Global Burden of Disease Study (GBD) 2017 IBD Collaborators* found that globally, an estimated 3.9 million women and 3 million men suffer from some form of IBD (14). IBD was historically associated with Caucasians and industrialized areas, converging in Europe and North America (6). The highest incidence rates of IBD are still seen in Europe and North America (Figure 1.3) (1, 24). Approximately 2.5 – 3 million people are affected by some form of IBD in Europe, while an estimated 2 million people suffer from IBD in America (6, 11, 25). The UK has one of the highest prevalence's in Europe, with a rate of 464.5/100,000 reported in the most recent data set (14, 25). The USA overall has the highest rates of IBD, and this contributes immensely to global incidence reporting of IBD (14).

The frequency of cases of IBD however appears to be stabilising in westernised countries with a rise in low–incidence and emerging westernized regions such as South Asia and the Middle East (6). Levels are beginning to increase, with a rise seen in Africa and East Asia too, with historically higher levels being observed in China in recent years (5). Early onset and prevalence of IBD is still high and the hypothesis is that IBD prevalence will rise in the coming years (6, 11, 24). Thus with 0.5% of the global population suffering from IBD, coupled with rising cases and an ageing IBD population with co-morbidities, investigating IBD and identifying its causes and potential cure is of great interest globally (11).

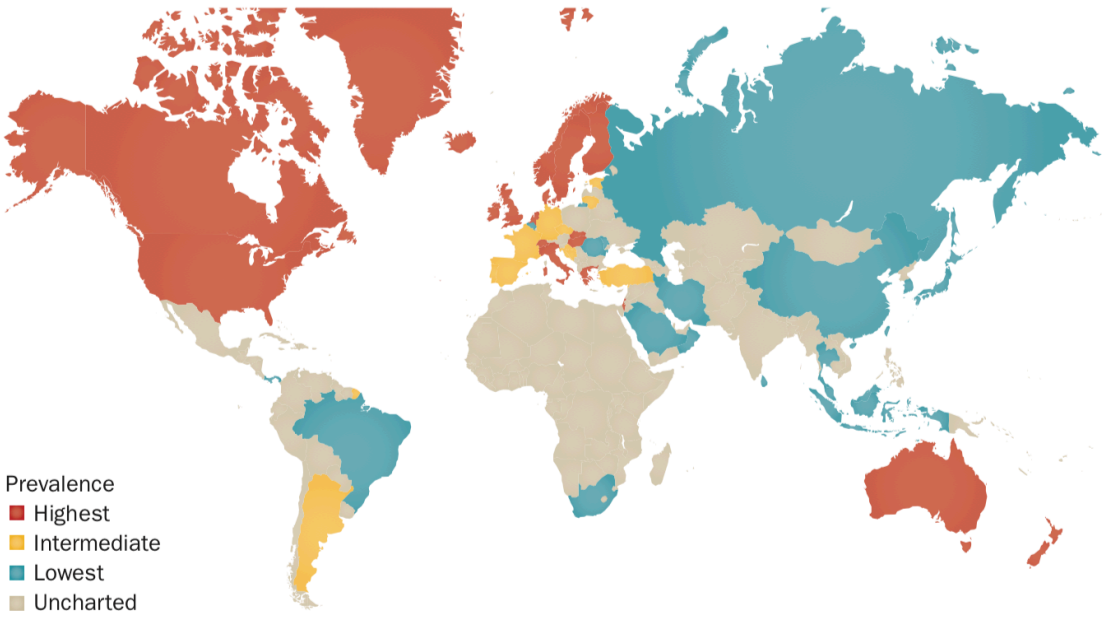



**Figure 1.3: Global Prevalence of Inflammatory Bowel Disease in 2015**
Coloured ranges from red (as highest) to grey (as unchartered) are used to highlight the prevalence of Inflammatory Bowel Disease (IBD) globally. Figure adapted from Kaplan (2015).

### 1.1.6 Causes of IBD

There are numerous contributing factors associated with IBD, with many working in combination to contribute to the pathogenesis (1, 2, 5, 13). The four major causes of IBD include **immune dysregulation**, **genetic predisposition**, epithelial barrier dysfunction and **microbial flora composition**, and susceptibility to **environmental factors** (Figure 1.4) (9, 18).

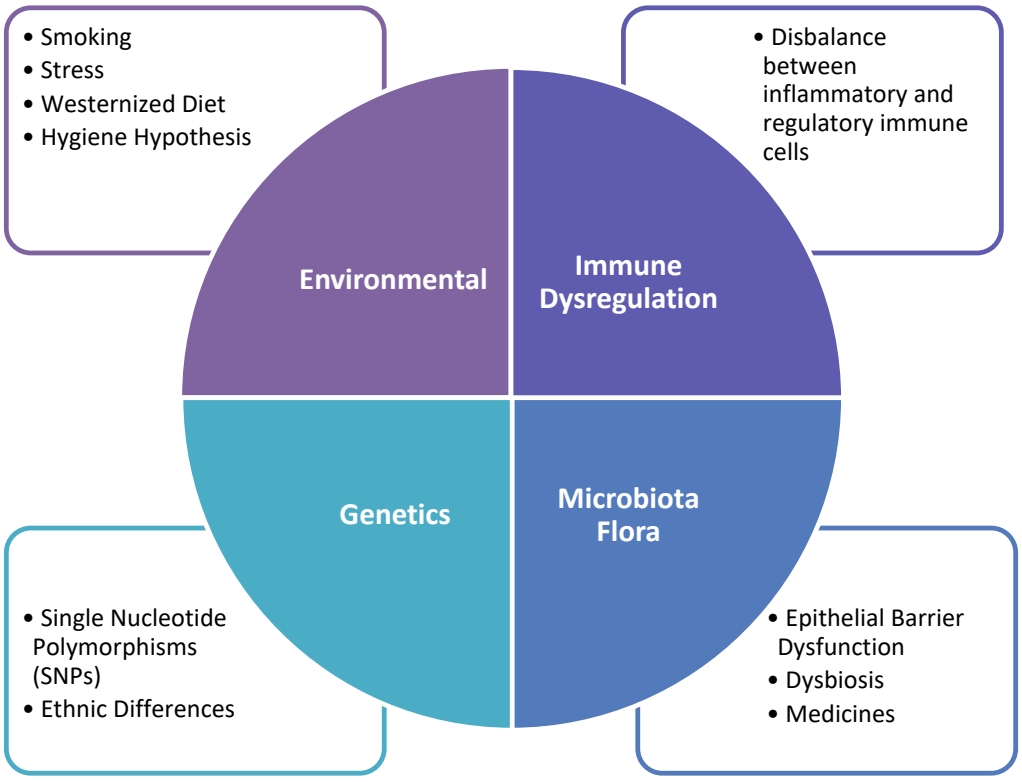



**Figure 1.4: Causes of IBD**
Risk factors of IBD can be grouped into four broad categories: Environmental, Immune Dysregulation, Genetics and Microbiota Flora. Key risk factors associated with each category are highlighted in the figure.

#### 1.1.6.1 Environmental Factors

Exposure to factors within an individual's environment (their diet, living conditions and geographical location) are believed to drive IBD development. Studies have shown immigrants have dissimilar incidence and severity of IBD in comparison to those who remain in their home country (5). Environmental risk factors for IBD include cigarette smoking and urbanisation including consumption of westernised diet, hygiene status and pollution (1, 3, 5).

#### 1.1.6.2 Immune Response in the Bowel

Mucosal homeostasis between effector and regulatory cells is needed to maintain tissue integrity in the bowel, with immune dysregulation a major cause of IBD (2, 8, 9). Imbalance between regulatory and proinflammatory immune cells is believed to be a major contributor to the dysregulated immune response seen in many IBD patients (Section 1.1.7). Defects in macrophages are also a major contributor to IBD pathogenesis and are discussed in greater detail in this thesis (Section 1.3.3.5).

#### 1.1.6.3 Epithelial Barrier Dysfunction & Microbial Factors

The intestinal flora mainly comprises bacterial species with archaea, fungi and protozoa also found (26, 27). In the gastrointestinal tract, the colon has the highest amount of bacteria within the body which help to metabolise dietary components (26). ***Dysbiosis*** is an imbalance of the gut microbiota composition caused by changes in the commensal nature of the gut microflora and is associated with IBD (1, 4, 28). Changes in the microbiota composition in IBD have been identified in the clinic, and risk factors include medicines and antibiotics, whereas probiotics and supplements

which contain live 'healthy' microorganisms, could help attenuate dysbiosis seen in IBD (1, 3, 5, 9). Dysbiosis can increase gastrointestinal permeability which can then lead the epithelial barrier to become 'leaky' (termed *'leaky gut'*), which enables passage of harmful pathogens into the LP (Section 1.1.7) (13, 29). Microorganisms such as *Escherichia coli* (*E. coli*), salmonella and viruses are thought to be risk factors for developing IBD (5, 30). Specific bacterial strains have been associated with the development of UC and CD such as *Actinobacteria* and *Proteobacteria* (4, 28). *E. coli* infection has been linked to CD with studies showing *E. coli* can be found in the macrophages of CD patients, but not UC (9, 30, 31).

#### 1.1.6.4 Genetic Factors Which Alter IBD Susceptibility

Patients who develop IBD are thought to be genetically predisposed, with some studies suggesting that genetics account for 20% of an individual's risk (3, 9, 32, 33). Many genes have been identified in Genome Wide Association Studies (GWAS), with several of those involved in the response to pathogenic insult (5, 9). GWAS can be used to associate allele frequency of certain variants in cases and controls and is an efficient unbiased method to analyse data (13). Such studies have highlighted single nucleotide polymorphisms (SNPs) associated with IBD including CARD9, CARD15, NOD2, IBD5-associated organic transporter gene (OCTN), IL-10, IL-12, IL23R and STAT3 (3, 9, 11, 34). Over 200 SNPs are now thought to correlate with an increase in IBD genetic susceptibility (11, 13). In CD, 140 susceptible loci found have been found and of these 30% are also found in UC and 50% are found in other genetic diseases (32). CD-associated SNPs include innate immune genes such as TLR4, STAT3, CARD9, and adaptive immunity SNPs in IL-12B and IRF5 (which has a role in autophagy) (13). SNPs for UC have been identified in genes including HNF4A and

LAMB1 which has a role in epithelial barrier and is linked to Human Leukocyte Antigen (HLA) defects (30). Genetically, there is a higher risk of CD in the Jewish diaspora, specifically in the Ashkenazi Jews community (13). A link is also seen in twins and first-degree relatives with a risk higher in Jewish relatives in comparison to non-Jewish (13). A greater risk of IBD is also seen in familial generations which suggests environmental impact of IBD may trigger genetic predispositions in people and their offspring (5).

### 1.1.7 IBD Pathogenesis

#### 1.1.7.1 Mucosal Structure of the Colon

IBD is a disease of the gastrointestinal tract, impacting the bowel and most often, the colon. The colon is an average of 1.5m in length with a proximal and distal end and is the major site for inflammation and damage in IBD (35). The main functions of the colon are to retain water, electrolytes and nutrients, whilst moving waste to the rectum for excretion (35, 36). Water is absorbed via osmosis and an osmotic gradient is established by absorption of electrolytes including sodium *via* sodium channels, creating an electrochemical gradient (36). The gut microbiota, which houses the largest collection of microorganisms within the human body contains bacteria, archaea, hormones, neurotransmitters, and metabolites which aid digestion and influence the gut but also the brain, liver, and kidneys (29, 37, 38).

The colon consists of four layers: the mucosa, submucosa, muscularis propria and serosa (Figure 1.5) (35, 36, 39).

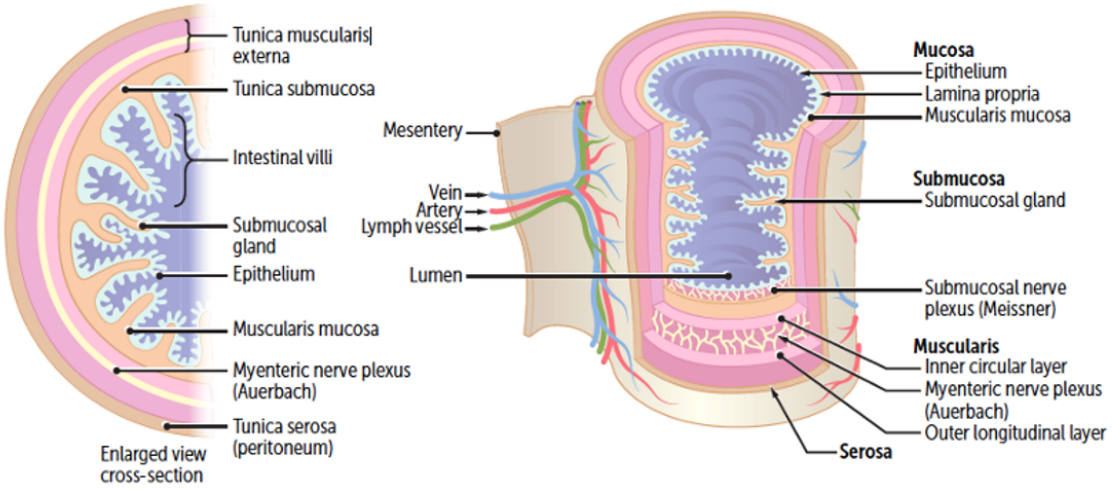



**Figure 1.5: Transverse and Longitudinal Cross Section Views of the Structure Of the Colon**
Cross sectional views of the different layers of the colon highlighting the four main components of the tissue structure: the mucosa, submucosa, muscularis and serosa. Components of each section are also highlighted in the diagram. Figure adapted from *Quizlet*, 2016.

The mucosa is the innermost layer of the colon and is comprised of three layers designed to increase the surface area: the epithelium, the LP, and muscular mucosa (35, 39). Epithelial cells face the intestinal lumen and thus are the first cells to encounter pathogens (35). The epithelial barrier has a high renewal capacity and contains goblet cells, enteroendocrine cells and enterocytes (35, 40). Crypts are immersed between the epithelium and the LP and are full of numerous folds which again provide increased surface area to sample contents in the colon (35, 39). The crypt undergoes continued cell renewal with stem cell precursors present forming different cell types of the bowel including goblet cells and enterocytes (35, 39). Enterocytes can differentiate into cells including goblet cells which secrete mucus (26). Mucus produced by goblet cells forms a protective layer which can trap pathogenic bacteria preventing it from entering the LP (26). In IBD, it is common for mucin production to be perturbed. Enterocytes can also mediate endocytosis of pathogenic

antigens, and then present these to Antigen Presenting Cells (APC) such as macrophages (26). The second layer of the mucosa the LP, contains lymph nodes, connective tissue and is infiltrated with immune cells to mount an immune response to infiltrating pathogens (35). These include macrophages, Dendritic Cells (DC), and T and B Cells, which will be discussed in this thesis in further detail (26). The final layer of the mucosa is the muscular mucosa which is a smooth muscle layer which aids the movement of items within the bowel (35). Below the mucosa is the sub mucosa (35, 39). This is a connective tissue containing protective immune cells, lymphatics, nervous connections and arteries (35, 39). It is through these connections that the gut is able to influence the brain through the brain-gut axis and the liver through the gut-liver axis (41). The penultimate layer of the colon is termed the muscularis propria composed of two smooth muscle layers. One is responsible for elongation of the colon whilst the other functions to constrict the gut to move food from the proximal to distal end of the colon (39). The final layer of the colon is the serosa, a protective layer containing squamous epithelial cells known as the epithelium or mesothelium and acts as a barrier to foreign insults (35, 39).

#### 1.1.7.2 The Colon Under Homeostatic Conditions

Under homeostatic conditions, the epithelial barrier and mucus layer both work to prevent pathogenic material entering the LP, whilst allowing access to commensals and dietary antigens to develop tolerance (Figure 1.6) (40). Tight junctions found at the base and apex of the epithelial barrier restrict access to the LP and can regulate permeability of the epithelial barrier to generate oral tolerance or a defence response to pathogens (2, 9). In the LP, a homeostatic balance between regulatory and inflammatory innate and adaptive immune cells exists so that insults can be

competently dealt with (34). Tissue resident macrophages recognise Pathogen Associated Molecular Patterns (PAMPs) using Pattern Recognition Receptors (PRRs) on their surface to respond to pathogens (30). Macrophages and DC present major histocompatibility complex (MHC) which displays PAMPs to activate CD4+ and CD8+ T Cells *via* co-stimulatory molecules resulting in the production of T effector cells to remove the pathogenic insult (Section 1.4) (2, 42). Following the successful removal of pathogens, Tregs and macrophages then work together through mediators such as IL-10 and TGF-β to restore tissue (4, 43). In IBD however, this level of regulation and homeostatic balance is lost, leading to inflammation and tissue destruction within the bowel.

#### 1.1.7.3 The Colon in Inflammatory Bowel Disease

Disruption of the intestinal epithelial cell barrier is believed to be a key triggering event for IBD enabling uncontrolled access to the LP (8). Proinflammatory cytokines such as TNFα and IFNγ can increase the permeability of the barrier (9). Apoptosis of cells further increases the permeability of the epithelial barrier driving loss of ions and water, enabling passage of antigens through to the LP (9). IFNγ also causes endocytosis and destruction of tight junction transmembrane proteins by micropinocytosis (9). The intestinal epithelial barrier is also involved in electrolyte transfer and if disturbed, can lead to diarrhoea, a major symptom of IBD seen in almost all UC cases (9). A decrease in tight junction proteins enables pathogens to enter the LP and activate immune cells causing the release of pro-inflammatory cytokines which in turn influence tight junctions contributing to the '*leakiness'* of the barrier (2).

APC recognition of PAMPs by PRRs leads to activation of the adaptive immune response resulting in an influx of innate cells, lymphocytes, proinflammatory cytokines,

and enhanced production of eicosanoids, chemokines and ROS (2, 4). An influx of lymphocytes, neutrophils and monocytes is observed during initial inflammation in the mucosa caused by the release of chemoattracts such as CCL2 and CCL5 from surrounding cells (9, 26). Common PAMPs seen in the colon include Lipopolysaccharide (LPS), a component of the cell wall of gram-negative bacteria, Lipoteichoic acid (LTA), a component of the cell wall of gram-positive bacteria, beta glucans found on fungi and double stranded-RNA (4, 26). PRRs found on macrophages include TLRs '*Type I transmembrane glycoproteins*' or TLRs, with TLR2, TLR4 and TLR5 also expressed in normal intestinal epithelial cells, with an increase in TLR2/4 seen in IBD (2, 26).

Macrophages play a key role in IBD and are some of the first immune cells to respond to pathogens (2, 26, 44). Colon macrophages and those present in the LP are distinct to macrophages elsewhere as they have a more regulated response to microbes to prevent an inappropriate inflammatory response in the gut (26). As we will discuss in detail in Section 1.3.3, studies have shown that during gut inflammation, monocytes are recruited to the bowel through the CCL2/CCR2 axis, where they then differentiate into a proinflammatory monocyte-derived macrophage (MDM) phenotype (26, 45). These macrophages contribute to production of proinflammatory mediators such as IFNγ, creating the perfect stimulatory environment for polarisation of more proinflammatory Th cell subsets such as Th1 and Th17 cells (18, 37, 44). Together, these perpetuate an inflammatory microenvironment preventing the recruitment and or polarisation of regulatory cell subsets such as regulatory Th cells (Tregs) in IBD. Numerous studies have demonstrated a reduced presence of Tregs in the intestinal mucosa and patient blood in IBD in comparison to healthy (2, 46). Contrastingly, elevated Th17 levels producing proinflammatory mediators such as IL-17A and IL-17F

perpetuate inflammation and disturb the Treg/Th17 regulatory balance (See Section 1.4) (47, 48). Thus collectively, the concerted action of innate cells such as macrophages can influence effector T Cell responses which when inappropriate, contributes to IBD pathogenesis by disturbing the regulatory response.

### 1.1.8 Diagnosis and Management of Inflammatory Bowel Disease

Diagnosis of IBD heavily relies on lab confirmation and endoscopy (1). In the clinic, colonoscopies are used to aid diagnosis with the Montreal Classification System used to classify the severity and forms of IBD (Table 1.1) (11, 25). The colon however is quite difficult to sample, and biopsies may be superficial, sampling only the mucosa (49). Hence stool samples can also provide another diagnostic method (49). Bowel ultrasonography alongside a faecal calprotectin value of over 50-100ug/g can also be indicative of IBD (50). However, its key to note that due to the broad spectrum of IBD manifestations some patients display no symptoms, presenting difficulties in diagnosis (22).

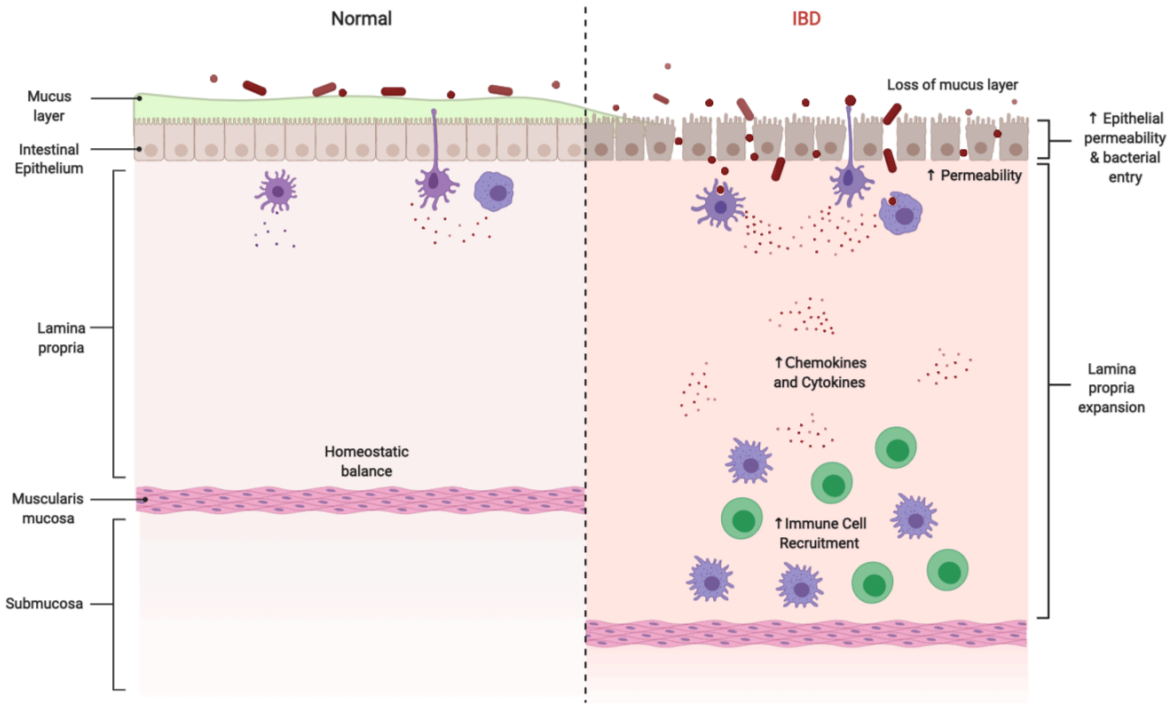



**Figure 1.6: Structure of the Gut and its Role in Inflammatory Bowel Disease**
The gut consists of four layers: The intestinal epithelium, mucus layer, epithelial layer, and the lamina propria. Under homeostatic conditions, bacteria remain in the intestinal lumen with passage through the tight junctions of the intestinal epithelium carefully controlled. The epithelial layer and mucus layer enable a level of control and prevent bacterial pathogens entering the lamina propria. In the lamina propria, a homeostatic balance between regulatory and inflammatory innate and adaptive immune cells are at a balance producing cytokines to supress a prolonged immune response. In IBD (right hand side of figure), a host of genetic and environmental factors lead to the breakdown of the mucosal and epithelial layer through the apoptosis of mucus producing goblet cells and epithelial cells which creates leaky tight junctions. This increases epithelial permeability, enabling the passage of pathogenic bacteria into the lamina propria. This then activates an immune response in the lamina propria, causing a rise in immune cell recruitment and increase in cytokines and chemokines contributing to the chronic inflammation observed in IBD. Purple cells, Macrophages; Green Cells, CD4+ T Cells. Figure adapted from Zhang *et al.,* 2017 and made using *BioRender.com*.

**Table 1.1: Montreal Classification System**

| Clinical Factors | |
|---|---|
| **Age** | **A1:** < 16 years<br>**A2:** 17 - 40 years<br>**A3:** > 40 years |
| **Disease Location** | **L1:** Ileal<br>**L2:** Colonic<br>**L3:** Ileocolonic<br>**L4:** Isolated upper disease |
| **Disease Behaviour** | **B1:** Nonstricturing, nonpenetrating<br>**B2:** Stricturing<br>**B3:** Penetrating |

**L4:** Can be added to L1-L3 when upper gastrointestinal disease is present
**p:** Perianal disease modifier that can be added to B1-B3 if relevant
*Adapted from Nakase et al., (2021)*

Treatments for IBD are currently focussed on repressing inflammation and promoting remission and for this, early diagnosis is key (1, 7). Current treatment methods include biologics and corticosteroids, alongside promoting a healthy lifestyle including a well-balanced diet and weight management (9, 11, 12). Biologics are popular as they provide a favourable outcome for patients by preventing exacerbation of disease (11, 12). They include anti-TNFalpha (anti-TNF$\alpha$) targeting Infliximab and IL-12 targeting Ustekinamab (6, 11, 12, 52, 53). The more gut specific Vedolizumab which targets the integrin subunit alpha4beta7 ($\alpha4\beta7$), is also available for IBD management (9, 53). Anti-TNF$\alpha$ therapies such as Infliximab have shown the greatest promise in promoting remission in UC and CD (8, 9). TNF$\alpha$ is an attractive target as it contributes significantly to inflammation in IBD with high levels found in the mucosa, serum and stool of CD patients (9). Anti-TNF$\alpha$ antibody can also induce apoptosis in T cells and monocytes (9). The difficulty with many biologics however is that they are systemically

delivered and not localised with systemic consequences (9). Some individuals may not respond to drugs or show reduced responses over time. Here individuals can develop antibodies against therapies and become '*non-responders'* (9, 53). According to Roda *et al.,* (2016), 10-30% of patients are non-responders to drugs and then of those who are responsive, approximately 23-46% of them later develop non-responsiveness (53). Aside from biologics, more traditional anti-inflammatory therapies such as steroids and aminosalicylates are often used as first line therapies in IBD (54). Other drugs with anti-inflammatory benefit have also been trialled. Thalidomide an immunomodulatory drug (IMiD) has been shown in some studies to promote remission in IBD (7, 12). This category of drugs is of particular interest and thus will be covered in detail in Section 6.1.

### 1.1.9 Outlook for IBD Management

IBD is a chronic condition and thus treatment can become expensive due to the costs of medication and the chronic nature of the disease (1, 2). A US study suggests that IBD patients have 3-fold higher healthcare costs in comparison to healthy controls (IBD: Control, $22,987: $6,956) (23). Alongside costs and inaccessibility to medication, treatment-resistant IBD can lead to the development of strictures in CD and a higher risk of cancer in UC and thus it is imperative to maintain remission in patients (21, 23). Importantly, dysregulation within the bowel can lead to issues with related organs through its bidirectional relationships. One such relationship is the *Gut-Liver* axis.

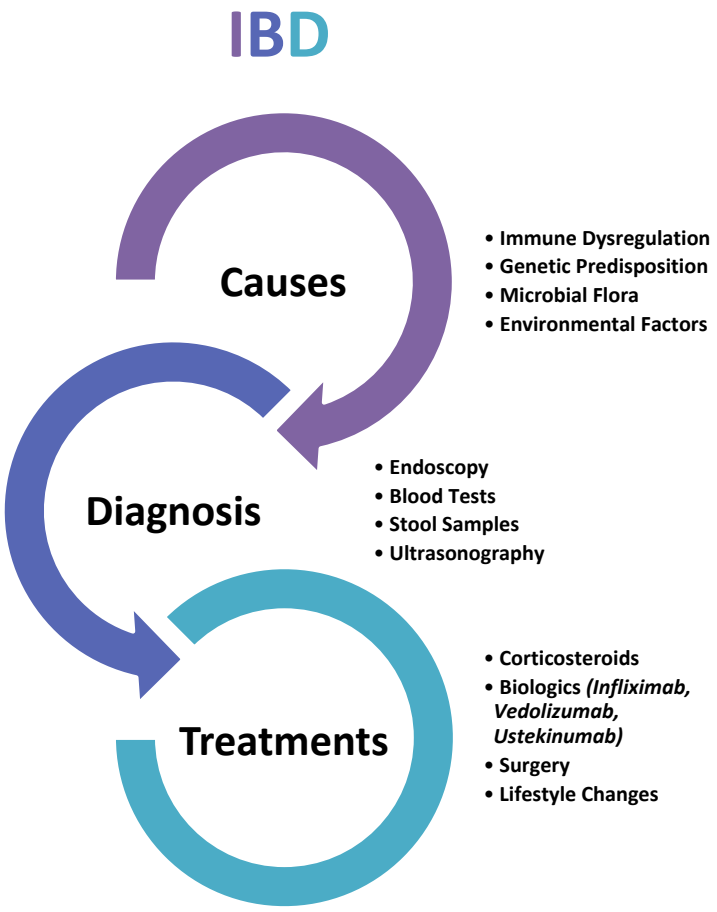



**Figure 1.7: Summary of Causes, Diagnostic Methods and Treatment Methods for Inflammatory Bowel Disease**
Summarised are the causes, diagnostic methods used in the clinic and treatment options available to patients suffering from Inflammatory Bowel Disease (IBD).

## 1.2 The Liver

### 1.2.1 The Gut-Liver Axis

The liver is linked closely to the gastrointestinal tract with the relationship between the two termed the *Gut-Liver axis* (55). The liver is well positioned below the gut, therefore is poised to recognise, and remove pathogens entering the body through the oral cavity efficiently (56). For this reason, both the liver and bowel need to show a great deal of immunotolerance as they are constantly exposed to exogenous entities (56). The liver also contains the biliary tree with ducts that enable modification and transport of bile to the duodenum (57). Through this bidirectional relationship, in disease a '*leaky gut'* filled with toxic compounds coupled with *dysbiosis* can make the liver susceptible to damage through translocation of PAMPs or Danger Associated Molecular Patterns (DAMPs) (29). Bacteria can move from the gut into the liver through the portal circulation where an immune response can be activated which could ultimately damage the liver (29). Dysbiosis in turn could contribute to the development of various liver diseases (Figure 1.8) (29, 58).

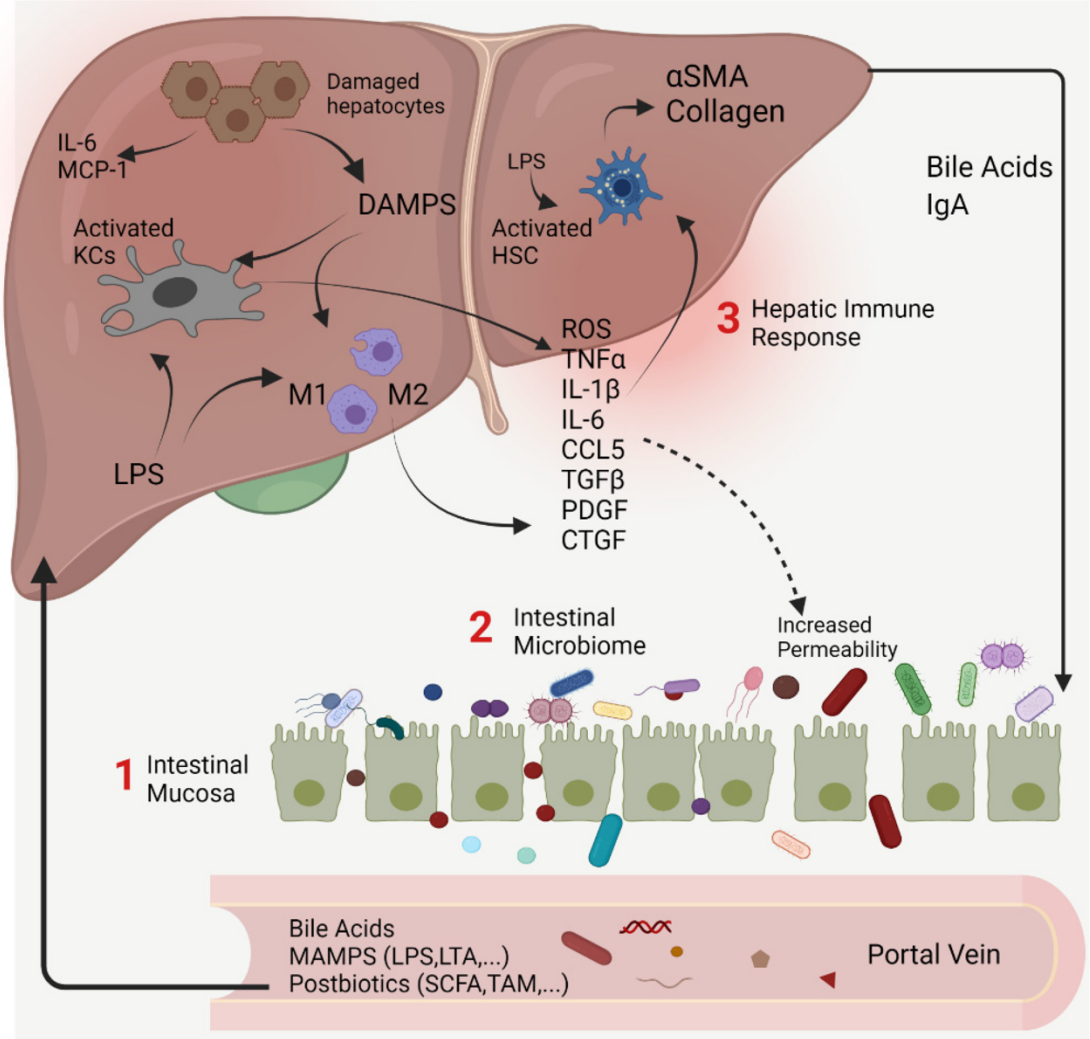



**Figure 1.8: The Gut-Liver Axis in Disease**
A bidirectional relationship exists between the liver and the bowel, linked through the portal vein which communicate through the (1) intestinal mucosa, (2) the intestinal microbiome and (3) immune cells (hepatic immune response shown in figure). The liver also provides bile and IgA antibodies to the bowel, with the bowel through the microbiome transporting antigens into the liver, highlighting the multitude of ways in which the gut and liver communicate with one another. α-SMA, alpha smooth muscle actin; DAMPs, damage associated molecular patterns; HSCs, hepatic stellate cells; IL, interleukin; CCL5, chemokine (C-C motif) ligand 5; KCs, Kupffer cells; LPS, lipopolysaccharides; LTA, lipoteichoic acid; M1, macrophage type1; M2, macrophage type 2; MAMPs, microbe-associated molecular patterns; CCL2/MCP-1, chemokine (C-C motif) ligand 2/monocyte chemoattractant protein-1; PDGF, platelet-derived growth factor; ROS, reactive oxygen species; SCFA, short-chain fatty acids; TMA, trimethylamine; TGFβ, transforming growth factor beta; TNF-α, tumour necrotizing factor alpha. Figure adapted from Kalo *et al.,* 2021.

### 1.2.2 Structure and Function of the Liver

The liver is a large organ, encompassing approximately 2-3% of an individual's total body weight, and plays a key role in many processes necessary for the human body to function such as detoxification, metabolism, and the immune system (55-57, 59). The liver contains two lobes: the left and right (Figure 1.9) (57). The right lobe is larger and contains segments *V,VI,VII* and *VIII* whereas the left lobe is smaller and contains segments *I,II,III* and *IV* (57). Both arterial (via the hepatic artery) and venous blood (via the portal vein) is supplied to the liver, which then perfuses throughout the liver through the sinusoidal bed (55-57, 59). The liver receives 75% of its blood supply from the portal vein and the remaining volume from the hepatic artery (55).

The liver is organised into hexagonal functional units called *lobules* containing hepatocytes, bile ducts and access to the portal vein and hepatic artery, altogether known as the *portal triad* (Figure 1.9B) (55, 57, 59). The lobules are the *'smallest functional units'* of the liver (Figure 1.9C) (14, 60). The abundant blood supply through the liver transports oxygen, nutrients and gut-derived or systemic pathogenic material which can activate the immune response as it flows through the sinusoids (liver capillaries) (56). Blood flows in the direction from the portal area to hepatic vein causing a gradient to form throughout the liver creating different functional zones in the acinus (59, 60). The distance from arterial blood forms these three zones for hepatocytes: Zones *I*, *II* and *III*. Zone I is called the *periportal* region and is closest to the portal vein, oxygenated blood, and nutrients, and has a higher rate of perfusion and therefore hepatocytes in this area have greater functional roles including cholesterol and bile formation (55, 60). Zone II is called the *transition* zone and Zone III, which is closest to the hepatic artery, is called the *pericentral* zone (55, 60). Zone III is furthest from the portal triad and cells here are involved in glycolysis and glycogen

synthesis (55, 60). The liver also contains the *Disse* space which is the space around the sinusoids, between endothelial cells and the basolateral membrane of hepatocytes (55, 60). The Disse space contains fenestrations and microvilli which enable access to the blood supply for hepatocytes (55).

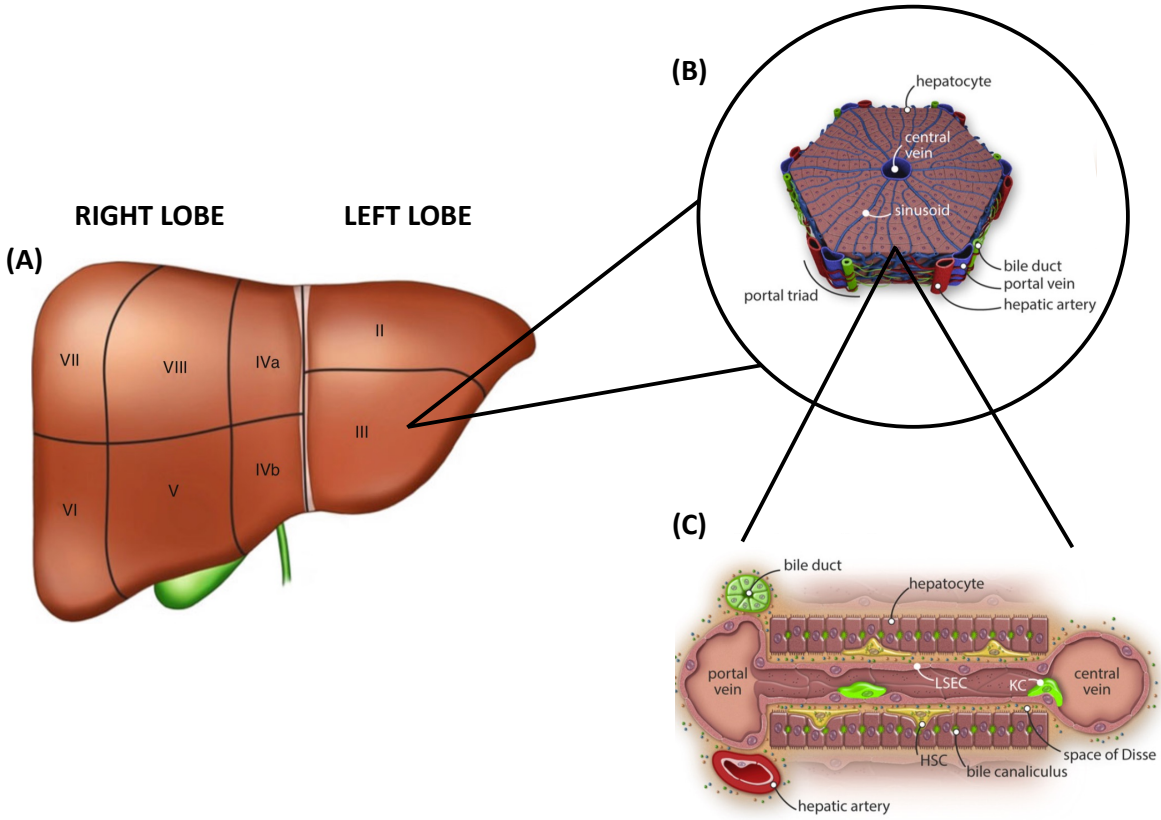



**Figure 1.9: Schematic Diagram of Liver Structure**
**(A**) Schematic of the structure of the liver showing the right and left lobes, with locations of the different segments in each lobe. **(B)** Describes the hexagonal structure of a liver lobule, highlighting the key components of each lobule including sinusoids, and the portal triad. **(C)** The livers' functional unit known as the *acinus* depicts the key cellular and structural components needed for liver function. LSEC, Liver Sinusoidal Endothelial Cells; KC, Kupfer Cells; HSC, Hepatic Stellate Cell. Figures adapted from Youssef *et al.,* 2015 (A) and van Grunsven, 2017 (B&C).

### 1.2.3 Cell Types Within the Liver

The liver contains a combination of epithelial, stromal, and immune cells with functions necessary to promote homeostasis (56). The major cell type in the liver is hepatocytes, followed by the second most prevalent, cholangiocytes (also known as Biliary Epithelial Cells, (BECs)) (57). Other common cell types include stellate cells, Kupffer cells and Liver sinusoidal endothelial cells (LSECs) (55, 59). Hepatocytes, the main cell type found in the liver, are 25-40μm in size and are involved in metabolism, production of proteins, removal of toxins and can also detect pathogens, behaving as APC through their expression of MHCI (55, 56, 59). Bile is a key compound produced by hepatocytes and is transported from hepatocytes into bile canaliculi where it then enters the duodenum or is stored in the gallbladder (55). This bile is needed to emulsify and metabolise lipids and fats for digestion and thus links the liver with the gut (38, 39, 55). Cholangiocytes also aid bile production and secretion (60). The liver is also enriched with many immune cell types due to its encounters with pathogenic entities in systemic and portal blood. Resident DC behave as APC to activate T Cells and the adaptive immune response (56). The liver also contains abundant NK cells, helping to maintain innate immunity, whilst priming cells for the adaptive immune response (56). Another key immune cell type in the liver are resident macrophages.

#### 1.2.3.1 Kupffer Cells and Liver Disease

*Kupffer cells* are resident liver macrophages which are yolk sac derived and play an important role in liver biology (Discussed further in Section 1.3.3) (61-63). Macrophages within the liver account for 90% of total body macrophages (59). Kupffer cells are found in the perisinusoidal space and their main role is to maintain homeostasis within the liver through defence and tissue repair (64). These cells are

self-sustaining, and functions include endocytosis, phagocytosis, and secretion of cytokines, chemokines, and GFs (61, 62, 64). Mass deletion of Kupffer cells leaves the liver susceptible to foreign insult, thus macrophages play a key role in liver immunity (56). Kupffer cells can remove apoptotic hepatocytes to prevent release of DAMPs via efferocytosis (65). Kupffer cells produce factors such as TGF-β and PDGF which are needed for stellate cell survival and maintenance of liver architecture (63). Cytokines and chemokines produced by Kupffer cells can also help mediate inflammation, fibrosis, and wound repair during the resolution phase (63, 65).

Deviations in Kupffer cell function can greatly contribute to liver disease, where macrophages are highly activated (66). In disease, Kupffer cells contribute to fibrogenesis, fibrolysis, alongside inflammation (61). In liver injury, monocytes are recruited through CCL2 and MCP-1 which is produced by various cells in the liver including Kupffer cells (See Section 1.3) (63). These recruited monocytes differentiate into proinflammatory macrophages and exacerbate inflammation, however Kupffer cells themselves can also initiate inflammation (61). In PSC, a disease with a strong association with IBD, macrophages are linked to the pathogenesis suggesting insights from targeting macrophages in PSC may impact IBD research (67). Similar to the bowel, two populations of macrophages are found in liver disease i.e., resident and newly recruited MDMs (61). As in the bowel, MDM monocytes are recruited to the liver through the CCL2/CCR2 (Section 1.1.7)(61). Greater CCL2 expression is seen on Kupffer cells, with more CCR2 on recruited monocytes, again similar to what is seen in IBD (18, 61). Lipotoxic hepatocytes release DAMPs, that can aggravate Kupffer cells to release proinflammatory cytokines (65). Kupffer cells also recruit other immune cells through the release of cytokines leading to the polarisation of Th1 and Th17 cells (61). Contrastingly, Kupffer cells are also involved in tissue restoration in the resolution

phase (63). Thus, similar to the injured bowel, broadly targeting macrophages for therapy is not ideal as cells are needed for both host defence, tissue repair and fibrosis regulation (63). Thus, a nuanced response to targeting specific proinflammatory cells or promoting the function of restorative cells is required.

### 1.2.4 Liver Disease

The liver can fail due to issues including immune dysregulation, viral infection (Hepatitis B and C), excessive alcohol or drug intake and obesity (55, 59). *Cirrhosis* is inflammation and irreversible fibrosis of the liver, which coincides with end-stage liver disease (29, 56). In Cirrhosis, the liver is unable to function efficiently which can then have secondary consequences in other organs or lead to hepatocellular carcinoma (*HCC*) (55). *HCC* is the most common liver cancer and in many cases is secondary to Cirrhosis arising due to Non-alcoholic fatty liver disease (NAFLD), Non-alcoholic steatohepatitis (NASH), Hepatitis B/C infection or in some cases autoimmune diseases such as primary biliary cirrhosis (PBC) or PSC (55).

NASH is a global health crisis caused by excessive fat deposition within the liver in the context of insulin resistance and often obesity (29, 68). It is the end stage of NAFLD and in both, an accumulation of fat leads to inflammation within the liver which stimulates fibrosis (68). Dysbiosis within the gut is also believed to affect NAFLD by causing a ‘leaky gut’ which alters bile production, increases inflammation and insulin resistance (29). In my thesis, NASH liver samples were used in certain experiments as a chronic disease control.

#### 1.2.4.1 Primary Sclerosing Cholangitis

Primary Sclerosing Cholangitis (PSC) is a chronic autoimmune cholestatic disease which impacts the biliary tree and results in inflammation and fibrosis within the liver and is associated with IBD (22, 29). Its estimated that globally the prevalence of PSC is 0.024% (69). PSC begins with portal inflammation and progresses to biliary fibrosis due to the accumulation of bile within the liver (22, 29). No effective treatment for PSC is available with many patients developing cholangiocarcinoma thus needing a liver transplant to survive (20, 22). PSC is more common in men than women and is rare in children, with an incidence of approximately 0.2/100,000 a year (22).

There is still a lack of understanding of the aetiology of PSC, but some hypothesises have been proposed. Specific HLA-susceptible loci have been associated with PSC in GWAS studies, suggesting errors in immune sensing are key to pathophysiology (70). Studies also highlight a role for macrophages and myeloid cells in the development of PSC (30). A key hypothesis suggests PSC may arise due to the bidirectional relationship between the bowel and the liver. Here an antigen in both the liver and gut activates the PSC pathway or T cells activated in the bowel migrate into the liver causing autoimmunity (22, 71). There is also growing evidence supporting association between IBD and PSC, with UC present in approximately 75% of PSC cases (22). However little genetic overlap exists between both diseases, and studies have shown only 5% of IBD risk loci identified via GWAS studies are associated with PSC (22). The rising occurrence of IBD alongside PSC however has led to the identification of a unique disease entity, named PSC-IBD.

#### 1.2.4.2 PSC-IBD

PSC-IBD was first described in 1965 but is still not well defined, and many PSC patients may develop IBD, but are asymptomatic and thus may go undiagnosed (22, 69, 70). PSC-IBD impacts around 50-80% of PSC patients who go onto to develop pancolitis, with a higher risk of colorectal cancer (22, 69). Of all cases, around 0.8-5.6% cases of UC develop into PSC-IBD, with 0.4-6.4% of CD developing into PSC-IBD (22, 69). In Europe and North America, its estimated 60-80% of PSC cases develop into PSC-IBD (69). PSC-IBD involves extensive colitis, development of colorectal cancer, liver failure and cholangiocarcinoma (70). Although UC is the most common form of IBD in these patients, PSC-CD can also exist, although it is less severe than PSC-UC (22). Stricturing is rare in PSC-IBD but colorectal cancer is much more prevalent with a threefold higher risk contributing to the higher risk of mortality in PSC-IBD (22). PSC-IBD patients have a higher mortality rate due to a *'high prevalence of pancolitis, rectal sparing and backwash ileitis'* in comparison to PSC or IBD alone (5, 22, 70) (69). Differences between the phenotypes of PSC-IBD and UC or CD alone are described below (Table 1.2 & 1.3). Studies have shown CD (or no IBD) has better outcome for PSC survival in comparison to UC alone (20). It is believed PSC-IBD has less dramatic symptoms and is '*quiescent'* in comparison to IBD or PSC alone due to less intense colitis and in some cases, asymptomatic cholangitis (69).

**Table 1.2: Phenotypic Differences Between Crohn's Disease (CD) and Primary Sclerosing Cholangitis- CD (PSC-CD)**

| | CD | PSC-CD |
|---|---|---|
| **Location of Inflammation** | Restricted to one region | Colitis and Ileocolitis |
| **Intensity of Inflammation** | Greater inflammation | Reduced inflammation |
| **Penetration of Disease** | Greater penetrating disease | Less intense penetrating disease |
| **Risk of Colorectal Cancer** | Present | Greater |

**Table 1.3: Phenotypic Differences Between Ulcerative Colitis (UC) and Primary Sclerosing Cholangitis- UC (PSC-UC)**

| | UC | PSC-UC |
|---|---|---|
| **Pancolitis** | Absent | Present |
| **Intensity of Inflammation** | Greater Inflammation | Less inflammation |
| **Steroid Use** | Greater steroid use | Reduced steroid use |
| **Risk of Flares** | Greater | Reduced |
| **Risk of Colorectal Cancer** | Present | Greater |

Both the *leaky gut* theory and dysbiosis are hypothesised to contribute to PSC-IBD pathogenesis, alongside theories on autoantibodies and 'lymphocyte-homing' (69). The *leaky gut* theory suggests that the leaky permeable mucosal barrier in the gut as a result of IBD, enables pathogens to translocate into the liver which leads to the

development of PSC (22, 69). The '*lymphocyte-homing'* theory similarly suggests that cells activated within the bowel, migrate into the liver where they then cause disease (69). Dysbiosis is also linked to PSC-IBD with the disrupted gut microbiota and barrier believed to enable translocation of toxic compounds into the liver (9, 13, 22, 29). Differences in the composition of the microbiota have been reported with an increase in *Escherichia* and *Ruminococcus* bacterial species seen in PSC-IBD (69). Alongside this, the gut microbiome can influence bile acid composition and cholesterol handling, supporting the influence of the gut-liver axis in PSC-IBD (22, 29). It is important to identify the common mediators which play a role in PSC, IBD and PSC-IBD, and monocytes, macrophages and CD4+ T Cells are such.

## 1.3 Monocytes and Macrophages

### 1.3.1 Monocytes

Monocytes are dynamic bone marrow-derived innate immune cells involved in inflammation, immune surveillance, and homeostasis (72, 73). Monocytes are found in the blood, spleen and bone marrow and make up approximately 4-10% of the circulating leukocyte population (73, 74). These cells are multi-functional removing pathogens by release of Reactive Oxygen Species (ROS) and Nitric Oxide (NO) but can also guide T Cell responses to influence inflammation (73). In disease, however monocytes can contribute to processes such as angiogenesis and liver fibrosis (75). Development of monocytes is controlled by the cytokine, macrophage colony stimulating factor (M-CSF) which is produced by stromal cells (42, 73). M-CSF is constitutively expressed under resting conditions enabling constant monocyte production and replenishment (42). Monocytes can differentiate into DC in lymph nodes becoming APC to influence adaptive immune responses (74). Most importantly for this body of work, monocytes can differentiate into macrophages and thus are implicated in both phagocytosis and repair (74). Monocyte differentiation into macrophage subsets depends on the tissue environment and can contribute to disease by prolonging the inflammatory response (73).

There are three broad subsets of monocytes defined by their differential expression of CD14 and CD16: *classical*, *intermediate*, and *non-classical* (Table 1.4) (76). CD14 is the cell surface LPS co-receptor on monocytes (74, 77). This receptor can form a complex with MD2 and TLR4 to enable LPS signalling and can activate an immune response to pathogenic entities (78). CD16, another cell surface marker, is the FcγRIII

receptor involved in cell signalling and together both CD14 and CD16 are key markers of monocyte phenotype (77).

*Classical* monocytes are the most prevalent representing roughly 85-90% of circulating monocytes, followed by *intermediate* at approximately 5-10% and then *non-classical* representing around 10% of the total monocyte population (73, 76, 77). *Classical* monocytes have a high expression of CD14, but lack expression of CD16 ($CD14^{high++}CD16^{-}$/$CD14^{+}CD16^{-}$) (73). *Intermediate* cells contrastingly express high CD14 but have low expression of CD16 ($CD14^{++}CD16^{+}$/$CD14^{+}CD16^{+}$)(73, 77). *Non-classical* monocytes again differ as they possess low CD14 expression but have higher CD16 expression ($CD14^{low}CD16^{high}$/$CD14^{+}CD16^{++}$/$CD14^{dim}CD16^{+}$) (73, 77). The proportions of these subsets have been found to be altered in different diseases, although there is still uncertainty about their roles (73, 76). For example, CD16-expressing monocytes are upregulated during infection although their purpose is unknown (77). In IBD, $CD14^{high}$ monocytes which are proinflammatory in nature, express TNF$\alpha$, IL-6 and IL-1$\beta$ and accumulate in mucosa (45). In CD, these monocytes can then go on to produce IL-23 which promotes a Th1 and Th17 phenotype (45). Thus, it has been suggested that monocytes may be able to exacerbate inflammation by interacting with T cells (45). Contrastingly, they may also promote repair and homeostasis by enabling recruitment of other innate cells such as neutrophils (45).

**Table 1.4: Monocyte Subsets**

| | Classical | Intermediate | Non-Classical |
|---|---|---|---|
| |  |  |  |
| **Frequency in Circulating Blood** | 85-90% | 5-10% | 10% |
| **CD16 Expression** | - | +<br>low | +/++<br>high |
| **CD14 Expression** | ++<br>high | ++<br>high | +<br>low |

### 1.3.2 THP-1

Using primary cells for experimental science has many benefits as they reflect the human phenotype however there are some limitations to their use such as need to sample patients, challenges in collecting a sufficient volume of blood, heterogeneity in patient samples, and limited proliferation *in vitro* (78, 79). During the COVID pandemic, cell lines have proved beneficial in allowing research to continue in situations (such as this project) where patients sample access was halted due to clinical burden. Cell lines can be advantageous because they are readily available and can be stored for a long period, whilst remaining homogenous (43). For my project, I used the THP-1 cell line. This cell line is an immortalised monocyte-like cell line derived from acute monocytic leukaemia, which can be differentiated into macrophage-like cells (43, 74, 80). THP-1 cells in comparison to blood-derived monocytes are readily available, and easy to use as they are robust and expand greatly (78, 81).

Phorbol 12-myristate 12-acetate (PMA) is used to differentiate THP-1s into a macrophage-like phenotype and was a method used in my thesis for macrophage culture (Section 2.2.2.2) (78, 81). THP-1 derived macrophages are resistant to apoptosis, phagocytose opsonised particles and develop a macrophage phenotype

similar to MDMs (79). However, as THP-1s are derived from a malignant cell origin, there are obvious differences in phenotypes between these cells and primary monocytes (78). Nevertheless, THP-1 cells can provide a means to assay monocytes and macrophages in a controlled manner and thus were sufficient for us to test our hypothesis during the lack of primary cells.

### 1.3.3 Macrophages

Macrophage, translating to '*big'* and '*eat'* in Greek are integral to innate immunity and are needed to maintain tissue homeostasis, playing a part in both innate and adaptive immune responses through their role as APC (30, 75, 79). Macrophages are long lived, highly specialised and key to intestinal homeostasis (79, 82). Alongside maintaining immune homeostasis, macrophages are needed for tissue development, surveillance, phagocytosis, host defence, tissue repair and remodelling (73, 81). Macrophages are a heterogenous population of cells with individual phenotypes localised to specific regions such as microglial cells in the central nervous system, histocytes in the spleen, Kupffer cells in the liver (Section 1.2.3.1), alveolar macrophages in the lungs and osteoclasts in the bone (34, 73, 75).

Macrophages arise from two origins; monocytes or from embryonic progenitors (73). Tissue derived macrophages arise from bone-marrow derived monocytes (with a life span of 3-4 days) found in the periphery (30). Tissue resident macrophages deriving from the yolk sac behave as the first line of defence and respond to and phagocytose pathogens without mounting an inappropriate immune response (30, 45). Resting or non-activated macrophages (M0, henceforth MΦ) along with memory macrophages can also be found residing in tissue (73). Resident macrophages undergo apoptosis when removed and are then replenished by MDMs (79).

Macrophages can produce ROS and prostaglandins which have antimicrobial properties to control invading pathogens (42, 77). Macrophages are also a source of NO (83). Nitric Oxide Species (NOS) are present in three forms: neuronal, inducible, and constitutive NOS (83). Inducible NOS (iNOS) is present on macrophages and is released upon activation via cytokines, transcription factors such as NF-κB and LPS enabling efficient removal of pathogens (83). Enabling efficient removal of pathogens is a key role of macrophages, which occurs through the process of *phagocytosis*. Phagocytosis is key to pathogen removal and is the process wherein opsonised pathogens are ingested into the phagosome which fuses with the endosome and lysosome (79). The lysosome is highly acidic and produces proteases to destroy pathogens (79). Defects in the cells ability to phagocytose can have detrimental consequences in the immune response which will be discussed in greater detail later in this chapter.

CD206, a mannose receptor, is a well described surface marker on phagocytic macrophages used as a marker of alternatively activated macrophages in phenotypic studies (78, 79). Activated macrophages also express CD80 and CD86 which are co-stimulatory molecules and aid antigen presentation (75). Cluster of Differentiation 68 (CD68) is a common, highly expressed glycoprotein marker of macrophages found in the lysosome (45). CD68 is mainly used as a diagnostic marker as it is highly expressed and thus was used in our work as a marker of macrophages (45). In the gut, markers of intestinal macrophages include CD68, CD64, CD14, CD11b and CD163 although not all will be co-expressed (44).

There are two main definitions of macrophages arising from MΦ: *inflammatory* macrophages, termed *M1*, which are classically activated and produce high levels of IL-12 and low levels of IL-10 (34). The second population is termed *anti-inflammatory*,

*wound healing,* and *repair* macrophages, denoted as *M2* (81). We will discuss these in further detail below, by first beginning with differentiation of monocytes to macrophages.

#### 1.3.3.1 Differentiation of Monocytes to Macrophages

PAMPs and the recognition of DAMPS is needed for the migration of monocytes to the site of inflammation (75, 82). This causes the release of various chemoattractants to encourage migration of monocytes to the site of inflammation where they can then differentiate into macrophages dependent on signals from the local microenvironment (72, 75). Chemoattracts encouraging the migration of monocytes include CCL2, CCL7, CCL8 and M-CSF (18, 72). Monocyte chemoattractant protein-1 (MCP-1) also attracts monocytes to the site, and is secreted by endothelial cells, T cells and fibroblasts (75). Cytokines such as TNF$\alpha$ secreted from macrophages causes the expression of adhesion molecules such as selectins, integrins and Immunoglobulin super family enabling monocyte adhesion and trans-endothelial migration (75).

In the bowel, blood monocytes are recruited by the CCR2/CCL2 axis (45). In response to infection, monocytes accumulate in the mucosa in response to CCL2 and are then activated by recognition of PAMPs by PRRs (45, 84). In response to the tissue microenvironment, monocytes then begin to differentiate into macrophages, and in the process, alter their expression of surface markers. CD14 and TLR2 expression on monocytes is downregulated as they differentiate into macrophages (79). Following monocyte migration into the tissue they may then be exposed to granulocyte-macrophage colony stimulating factor (GM-CSF) and become M1 macrophages with MDM the most common form of macrophage within the bowel (45, 72, 85). New macrophages arise mainly for tissue defence and to restore homeostatic balance (73,

75). Tissue resident macrophages are responsible for sensing the environment and raising an alarm if needed; they release signals which then recruit immune cells and causes M1 differentiation for fighting infection (43). Once the infection has been resolved, tissue restoration begins which requires M2 differentiation (42). During resolution of inflammation, macrophages also play an important role in the removal of apoptotic cells (82). If however, once the insult is cleared activated macrophages remain unregulated and persist, this can then lead to disease (34).

#### 1.3.3.2 Macrophage Polarisation and Subsets

Macrophages are very heterogenous and plastic in nature, reading cues from the microenvironment to become M1 or M2 macrophages from MΦ and in some cases, re-polarise (75, 78, 80, 84). Below we discuss the phenotype of M1 and M2 macrophages, their differences, and similarities (Figure 1.10).

##### 1.3.3.2.1 Proinflammatory M1 Macrophages

M1 macrophages are classically activated, proinflammatory in nature and are polarised by either LPS or Th1 associated cytokines such as IFNγ and GM-CSF (18, 42, 72, 75). M1 macrophages are anti-microbial and remove pathogens through the NAPDH cascade and ROS production (75). M1s produce proinflammatory mediators such as citrulline, NOS, ROS, and cytokines such as IL-1a/b, IL-6, IL-12, IL-23 and TNF$\alpha$ (34, 73, 75, 80). CD86 and CD80 expression is also highest in M1 cells (72).

M1s further promote production of Th1 and Th17 by producing IFNγ and chemokines such as CXCL8 and CXCL10 which in turn recruits Th1 cells (75). Th1 in turn also produce IFNγ which activates M1 to produce proinflammatory cytokines, ROS and turn arginine into nitric oxide, creating a feedback loop (77). Chemokines produced as

a result of this also include CXCL5, CXCL8, CXCL9, CXCL10 and CXCL13 (77). M1 macrophages are involved in defence however can contribute to chronic inflammation and autoimmunity through uncontrolled tissue damage (73, 75). In disease, elevated M1 levels are seen in the IBD mucosa and in patients with high Body Mass Index (BMI), Rheumatoid Arthritis (RA) and liver diseases including NASH and PSC (37, 77, 86).

#### 1.3.3.2.2 Regulatory M2 Macrophages

M2 macrophages are anti-inflammatory in nature and are involved in the phagocytosis of bacteria, wound healing, and repair, however, detrimentally are associated with cancer and fibrosis (72, 75). M2 macrophages can phagocytose pathogens without any proinflammatory cytokines release and thus are useful in removing parasites (34). M2 macrophages are alternatively activated and involved in tissue remodelling and helminth infection, causing allergy and tumour progression when inappropriately activated (80). M2 are known for their low IL-12 and high IL-10 expression and are induced by PRRs-PAMPs (34, 75). *In vivo* M2 are polarised mainly through Th2 cytokines such as IL-4 and IL-6 which signal via STA6 and IL4Ra, or IL-10 which signals via STAT3 and IL-13 (75, 80). M2 can also be polarised by granulocytes and can then go on to produce matrix metalloproteinases (MMPs) and other Growth Factors (GF) (34). Once activated, M2 macrophages secrete a combination of anti-inflammatory mediators including glucocorticoids, IL-10, TGF-$\beta$, polyamines and ornithine (73). M2 macrophages are known for their high expression of CD206, a C type lectin receptor and CD163 which is a scavenger receptor (75). These macrophages also express co-stimulatory molecules needed to activate T Cells including CD80 and CD86 (34). The mediators released by M2 such as CCL17,

CCL18, CCL22 and CCL24 can recruit Th2, Tregs and eosinophils contributing to the adaptive immune response (75).

There are four main known subtypes of M2 macrophages, M2a, M2b, M2c and M2d. M2a are polarised through IL-4 or IL-13 and express high levels of CD206 (75, 80, 81). M2b are activated through immune complexes, TLR agonists or IL-1R and go on to produce pro- and anti-inflammatory cytokines such as IL-10 or IL-6 (75, 80). M2c are derived through IL-10 and strong anti-inflammatory signals and produce high levels of IL-10 and TGF-β (75, 80, 81). M2d contrastingly are activated through TLR agonists and produce IL-10 and VEGF (75). Under homeostatic conditions, tissue resident macrophages in the colon display a M2-like phenotype (18). However, excessive amounts of M2 can be detrimental as they are unable to combat infection (34).

Phenotypically, both M1 and M2 macrophages differ in their structure as under a microscope, M1 appear circular whereas M2 macrophages appear spindlier and fibroblast-like (18). M1 have high phagocytic activity, antigen presentation and antibacterial capacity whereas M2 have low (Table 1.5) (18). M1 macrophages use anaerobic glycolysis whereas M2 require oxidative glucose and fatty acid metabolism to function (75). These differences enable both populations to efficiently manage an immune response to remove pathogens and fight infection but also prevent tissue damage, resulting in a M1/M2 balance. Crucially, a disbalance in this ratio can lead to inflammation, atherosclerosis, and cancer (72, 80). Excessive M1 macrophages are associated with proinflammatory illnesses whereas elevated M2 are seen in tumours and helminth infections (72). This balance could thus potentially be manipulated for therapy but as of yet, it has been difficult to identify mediators which could facilitate this (72).

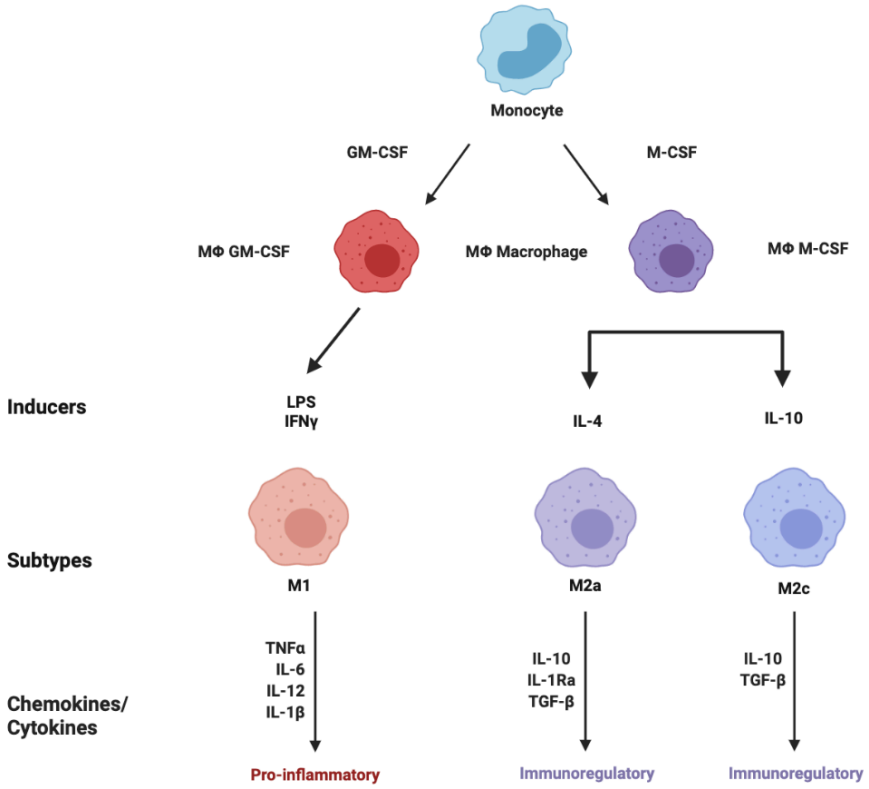



**Figure 1.10: Polarisation of Monocytes into M1, M2a and M2c Macrophage Populations**

Monocytes treated with either granulocyte - macrophage colony stimulating factor (GM-CSF) or macrophage colony stimulating factor (M-CSF) develop into MΦ GM-CSF or MΦ M-CSF respectively. Further polarisation of MΦ GM-CSF with Lipopolysaccharide (LPS) and Interferon gamma (IFNγ) results in the production of M1 which produce proinflammatory mediators such as TNFα and IL-6. Treatment of MΦ M-CSF with IL-4 induces results in the production of the M2a subpopulation of M2 macrophages which produce IL-10, IL-1Ra and TGF-β. Contrastingly, treatment of MΦ M-CSF with IL-10 results in the production of M2c which produce IL-10 and TFG-b promoting an immunoregulatory phenotype. Figure produced using Biorender.com.

**Table 1.5: Differences Between M1 and M2 Macrophage Populations**

| | M1 | M2 |
|---|---|---|
| **Activation State** | Classically | Alternative |
| **Metabolism** | Anaerobic | Oxidative and Fatty Acid |
| **Expression Markers** | CD80<br>CD86<br>HLA-DR | CD206<br>IL1R2<br>HLA-DR<br>CD163 |
| **Polarisers** | IFNY<br>LPS | IL-4<br>IL-1Ra<br>IL-10<br>TGF-Beta |
| **Produce** | IL-6<br>IL-8<br>TNF-alpha<br>CXCL1<br>CXCL2<br>CXCL3<br>ROS | IL-10<br>LTC4<br>TGF-beta<br>CCL17<br>CCL18<br>CCL22<br>CCL24 |
| **Major Role** | Cytotoxic<br>Anti-microbial<br>Proinflammatory | Wound healing<br>Repair<br>Regulatory |
| **In Disease** | Chronic inflammation<br>Autoimmunity | Fibrosis<br>Chronic infection |

#### 1.3.3.3 Macrophage Plasticity

Macrophages are highly plastic in nature wherein cells are polarised towards one phenotype and then, responding to cues in the microenvironment, are then stimulated to adopt another phenotype (72, 79, 81). For example, M-CSF polarisation develops regulatory M2 cells, however, if cells are exposed to GM-CSF first and then polarised *further* with M2 cytokines, M2 macrophages develop a proinflammatory phenotype

(72). This suggests perturbed regulatory M2 cells could potentially form within a diseased environment and exacerbate illness.

In the colon, tissue resident macrophages are more M2-like and highly tolerogenic maintaining homeostasis, whilst still possessing phagocytic and APC activity. MDMs, which arise in the colon in response to infections are more M1-like and during the resolution of inflammation are either apoptised or reprogrammed into M2 in response to the environmental milieu (37, 84). The mediators of this process remain unknown. Studies suggest that repolarisation of M1 to M2 within the colon in disease could be perturbed producing an M1/M2 disbalance and defunct macrophages which cannot fully generate resolution of inflammation (72). These macrophages could then in turn also influence the liver through the gut-liver axis.

#### 1.3.3.4 Macrophages in IBD and Disease

Colon macrophages can phagocytose and produce constitutively high levels of IL-10 but lack NO and ROS and thus are more tolerogenic (37, 45). They also express high levels of MHCII and produce TNF$\alpha$ implicated in antigen presentation and activating Tregs (45). Under homeostatic conditions ileal macrophages express CD163, CD64, MHCII, CD68 and CD14, with resident macrophages expressing lower CD14 levels (45). Newly MDMs however express high levels of CD14 alongside MHC11, CD163, CD209 and Cd11c, making them more responsive to antigens within the tissue (45).

Many studies have highlighted the role macrophages play in colitis (30, 34). In IBD, as the mucosal barrier disintegrates, macrophages infiltrate into the intestinal lumen and mucosa where they accumulate, causing a thickened mucosa (30, 37, 44). This alters tissue integrity and contributes to the inefficiency of the immune response within IBD (37). Expression of co-stimulatory molecules on macrophages including CD40, TLRs,

CD80, CD86 and TREM1, a PRR, are upregulated during disease making them more responsive and crucially less tolerogenic to antigens (34). These tissue infiltrating macrophages have high levels of TREM-1, CD14 and CD89 and NF-κb, secreting greater pro-inflammatory cytokines such as IL-6, IL-8, IFNγ and TNFα which contributes to this influx of inflammatory mediators (26, 30). An increased number of $CD14^{high}$ macrophages are found in the ileal and mucosa of CD with high CD33, CD64 and CX3CR1 expression and low levels of HLA-DR (30). Studies suggest M1 recruit Th17 and Th1 and persist in CD, without acquiring an M2 phenotype (18, 37, 44). Similarly in UC, an influx of M1s is seen, along with an abnormal M2 response which contribute to inflammation and recruitment of Th2 (18). Caradonna *et al.,* (2000) interestingly found that peripheral MDMs from UC or CD patient blood had significantly impaired phagocytic capability in comparison to control. This thus suggests that during inflammation, peripheral monocytes may be able to influence the phenotype of macrophages within the gut, exacerbating disease. Murine models have greatly aided our understanding of IBD and provide an efficient method in gaining insights into potential mediators in human disease (88). There are numerous IBD mice models, with the Dextran Sodium Sulphate (DSS) model most commonly used and highlighting macrophages as key players in pathophysiology (26, 88). More detailed analysis of mouse models in IBD can be found in **Appendix B**.

The contribution of macrophages to IBD pathogenesis makes them a key target for therapeutics in IBD. Biologics such as Infliximab can induce M2 macrophages expressing CD68 and CD206 in responders and promote wound healing (82). Colony stimulating factor is important for macrophage survival, as blocking CSFR1 reduces monocyte to macrophage development and could be targeted to prevent expansion of macrophages within the colon (45, 82). MCP-1 is secreted by epithelial cells, causing

migration of monocytes into LP, which is upregulated in disease (89). Thus, preventing the recruitment of monocytes to the LP could also be targeted which could dampen the adaptive immune response in IBD (77). Monocytes and macrophages are also integral to T cell responses in the colon, another key avenue of investigation in IBD, which we discuss next.

## 1.4 CD4+ T Lymphocytes

Alterations in the T cell adaptive immune response are reported during IBD (3). T helper cells are separated into subsets dependent on their polarising cytokines, core transcription factor expression and distinct cytokine production (Table 1.6) (47, 90). The subsets arise once they differentiate from Naïve T cells (Th0) into specialised subsets expressing Cluster of Differentiation (CD) 4 or CD8 which perform specific roles (91). CD4 T cells are broadly defined as helper T cells, helping to mediate an immune response, with CD8 T cells classified as cytotoxic, involved in removal of infected cells (91). Before considering the roles of T cell subsets in intestinal inflammation it is important to clearly define which subsets are of interest.

**Table 1.6: T Helper Cell Subsets[1]**

| T Helper Cell Subset | Polarising Cytokines | Transcription Factor | Cytokines Produced |
|---|---|---|---|
| Th1 | IL-12, IFNγ | T Bet | IFNγ, TNFα |
| Th2 | IL-4 | GATA3 | IL-4, IL-5, IL-13 |
| Th9 | IL-4, TGF-β | IRF4, PU.1 | IL-9 |
| Th17 | IL-1, IL-6, IL-23, TGF--β | RORγ | IL-17A, IL-17F, IL-21, IL-22, IL-25, IL-26 |
| Th22 | IL-6, TNFα | AhR | IL-22 |
| Tfh | IL-6, IL-21 | Bcl6 | IL-21 |
| Tregs | TGF-β, IL-2 | FoxP3 | TGF-β, IL-10 |

[1] Adapted from *Golubovskaya and Wu, 2016; Kim and Cantor, 2014 and Tripathi and Lahesmaa, 2014*

Th1 and Th2 cells are highly associated with IBD (See 1.1.7). Crohn's is historically associated with Th1 cells which are generated through STAT1 activation via IFNγ released by APCs (2, 9, 18). Th1 secrete IFNγ which activates the bactericidal activity of macrophages (4). Th1 also produce IL-1, IL-2, TNFα and IFNγ which can inhibit

Th2 cells (2). UC contrastingly is more associated with a Th2 phenotype (20). Th2 are generated by APC via IL-4 secretion which activates STAT6 at the cell surface which migrates into the nucleus and activates GATA3, the master regulator required for Th2 (2, 92). Th2 cells produce IL-4, IL-5, IL-13, which limit Th1 and help to limit Helminth infections (2, 4). In CD, a greater proportion of Th1 cytokines such as IFNγ and IL-12 are seen in the mucosa, but in UC, increased IL-5 and IL-13 are present and linked to Th2 cells (2, 4). A balance of Th1 and Th2 cells is imperative as excessive amounts of either Th1 or Th2 cells has been associated with the two forms of IBD (2).

### 1.4.1 Tregs and Th17 Cells

Although historically Th1 and Th2 cells were believed to be the key T cell mediators in IBD, both Tregs and Th17 may play a more crucial role (2, 4). Under homeostatic conditions, Tregs and Th17 work in balance to remove pathogens and maintain a controlled immune response in the bowel (2, 4, 28). In IBD, Th17 produce proinflammatory mediators such as IL-17A and IL-17F which perpetuate inflammation whereas Tregs become dysfunctional causing a disturbance within the normal Treg/Th17 regulatory balance (47, 48). Below we discuss further the role of both Tregs and Th17 cells within IBD and the bowel.

#### 1.4.1.1 Tregs

Tregs play a key role in immune tolerance and constitute approximately 10% of circulating CD4+ T Cells (93-97). Two forms of Tregs have been identified, natural Tregs (nTregs) and induced Tregs (iTregs) (2). Thymus derived Tregs are referred to as nTregs and iTregs are those which are induced peripherally from CD4+ T cells (98-100). Tregs express the transcription factor Forkhead box P3 (FoxP3) and CD25, the

alpha chain component of the IL-2 receptor, which enable immune tolerance when activated (99, 101, 102). Stabilisation of FoxP3 results in inhibition of IL-2 production and can upregulate the expression of CTLA-4 which is needed for characteristic Treg function (90, 94) By suppressing the activity of APC, Tregs can control the immune response and hence limit unnecessary damage, promoting homeostasis and maintaining immune tolerance (99, 103). Tregs are believed to limit IBD through the release of anti-inflammatory cytokines such as IL-10 (46, 93, 104). In IBD, however a reduced presence of Tregs in the intestinal mucosa and patient blood is reported (2, 46). Along with reduced Treg numbers, a change in Treg phenotype has also been reported, exacerbating inflammation (2, 46). Due to their versatility and role in many immune diseases, Tregs have become targets for therapies (2, 99).

#### 1.4.1.2 Th17

Th17 cells are a subset of CD4+ effector T cells which provide defence against pathogens but also contribute to autoimmunity due to their proinflammatory nature (90). Th17 cells develop from Th0 cells in the presence of CD161, IL-21, IL-6 and, or, TGF-β and the binding of IL-23 to the IL-23R which activates STAT3 (4). This then leads to the activation of the retinoid related organ receptor gamma (RORγ), the transcription factor needed for polarisation to a Th17 phenotype (2, 90). Th17 cells then can secrete IL-17A, IL-17F, IL-21 and IL-23, all pro-inflammatory cytokines (2, 4, 47). IL-23 is required to stabilise Th17 polarisation whilst IL-17 is important for host defence against pathogens (47, 92). IL-17 is also a chemoattractant, recruiting immune cells such as neutrophils to prolong inflammation (3, 102). Thus, Th17 are equipped to provide key defences to eliminate pathogens (48, 102). However,

excessive Th17 and their pro-inflammatory products also links Th17 to the pathogenesis of autoimmune disorders such as RA, IBD and cancer (47, 48).

IL-17 is thought to play an integral role in the pathogenesis of both UC and CD (4). Th17 cells, and their secretome (e.g., IL-17A/F, IL-21, and IL-22) is associated with IBD pathogenesis in humans and mouse models (3, 91). High numbers of Th17 cells and excessive accumulation of their by-products is observed in IBD patients with a higher proportion of Th17 in IBD mucosa and blood in comparison to healthy individuals (2, 4). Interestingly, some studies have shown that Th17 cells can be protective as IL-17-targetting drugs exacerbate colitis (4, 105). Thus greater research is needed to determine the impact of Th17 cells in IBD pathogenesis (28).

#### 1.4.1.3 Th17/Treg Balance in IBD

Th17 and Tregs maintain a healthy balance within the gut with Tregs suppressing the immune response whilst Th17 cells eradicate pathogens (28, 102, 104). Importantly, this homeostatic balance appears to be disrupted in IBD since an imbalance in the Th17/Treg ratio is observed, with a rise in Th17 cells, and a fall in Tregs reported in some studies (2, 28). Interconnected drivers of the Treg/Th17 ratio are TGF-β and IL-6, key common mediators for Treg/Th17 differentiation (28). During inflammation elevated IL-6 alongside reduced TGF-β promotes the production of Th17 whilst concurrently downregulating Treg production (2, 4, 28). Conversely, high concentrations of TGF-β inhibit the IL-23 receptor, promoting FoxP3 expression and inhibiting RORγt (28). A key finding which has widened our understanding of the Treg/Th17 balance is the evidence for cellular plasticity of Tregs and their ability to evolve Th17-like phenotypes (Figure 1.11) (2). These plastic Tregs behave like various T helper subsets, including more pro-inflammatory inclined phenotypes such

as Th17, losing their usual suppressive ability and contributing to disease pathology (93, 102). Some studies suggest that Treg plasticity is a part of normal Treg function where they change their phenotype in response to circumstances but still retain their expression of FoxP3 (97). Omenetti and Pizarro (2015) show that Tregs are able to differentiate into Th17 cells, where they secrete IL-17 but are still suppressive in nature. Koenen *et al.,* (2008) similarly showed that conventional Tregs could be differentiated into Tregs which produced IL-17 and expressed CCR6 and RORγt. Th17 cells are also plastic in nature and can adopt a Th1 phenotype where they produce IFNγ (4). Annunziato *et al.,* (2007) found that Th17 cells in CD could produce both IL-17 and IFNγ suggesting plasticity (4). Stimulating Th17 with IL-12 causes an increase in the expression of T-bet and IFNγ with concurrent downregulation of RORγ and IL-17. This demonstrates IL-17 secreting cells can become more Th1-like whilst expressing CD161, a surface marker of Th17 progenitors, suggesting both Th1 and Th17 contribute to inflammation in IBD (4). Similar to Treg plasticity, the mechanisms which control the change in Th17 phenotype still remain unknown. Thus, although it is documented that both Tregs and Th17 cells are imbalanced in IBD and can display plasticity, studies into this mechanism are still highly limited. Understanding mediators that could control the Treg and Th17 phenotype is of great interest due to the therapeutic potential of inducing plasticity. ***The Ikaros Family of Transcription Factors*** are thought to be some such mediators capable of influencing both Th17 and Treg development, alongside crucially, Treg plasticity.

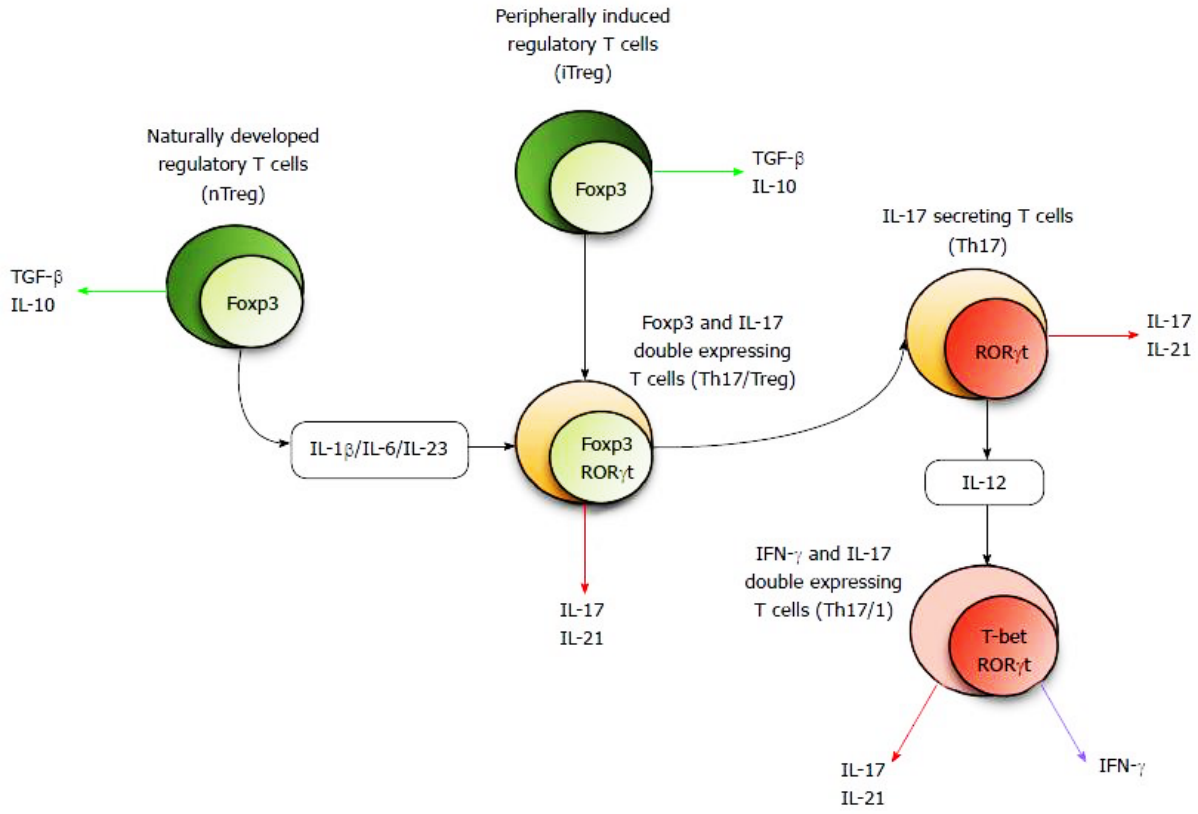



**Figure 1.11: Factors Influencing the Plasticity of Regulatory T Cells and T helper 17 (Th17) Cells**
Tregs can be influenced by cytokines such as IL-6 and IL-23 to present a Th17-like phenotype, whereas Th17 cells when exposed to IL-12 can develop a Th1-like phenotype. Figure adapted from Ueno *et al.,* (2015).

## 1.5 The Ikaros Family of Transcription Factors

The Ikaros family of proteins are a family of zinc finger transcription factors consisting of five members: ***Aiolos***, ***Eos***, ***Helios***, ***Ikaros*** and ***Pegasus*** (Table 1.7) (107, 108). The Ikaros family is highly ubiquitous and homologous, with variants found in numerous cell types such as lymphocytes and neurons, and expression of members also seen in different species such as mice and zebrafish (107). Since the discovery of Ikaros in 1992, a multitude of roles for the family in many systems throughout the body have been discovered from T and B lymphocyte development, apoptosis, cell cycle arrest, adaptive immunity, and effector functions (107, 109-113). The Ikaros family have been shown to be key to development of humans and other species with deletion of one or more Ikaros family members, resulting in loss of all lymphoid lineages (114). Complications in the Ikaros family have been linked to various leukaemia's, whilst GWAS highlight the families' involvement in autoimmune disorders such as Systemic Lupus Erythematosus (SLE), and most relevant to my thesis, IBD (113, 115).

**Table 1.7: Genes Encoding the Five Members of the Ikaros Family**

| Transcription Factor | Encoding Gene | Chromosome Location |
|---|---|---|
| Aiolos | IKZF3 | 17q12-21.1 |
| Eos | IKZF4 | 12q13.2 |
| Helios | IKZF2 | 2q34 |
| Ikaros | IKZF1 | 7p12.2 |
| Pegasus | IKZF5 | 10q26.13 |

### 1.5.1 Ikaros Family: Structure

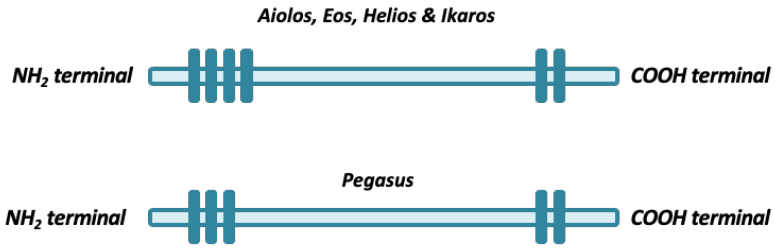
The Ikaros family of transcription factors are similar to the Krüppel family of transcription factors which contain the distinctive *C2-H2* arrangement of zinc fingers (116, 117). Ikaros proteins contain two highly conserved zinc finger motifs with the alignments found to be conserved across species, however, Pegasus does display some divergence (Figure 1.12) (108, 118, 119). The zinc fingers are comprised of a zinc atom surrounded in a specific composition by four cysteine and, or, histidine residues (118). A *C2-HC* cysteine residue is characteristic, with two '*C'* terminal Krüppel-like C2-H2 zinc fingers involved in interactions with the same or other family members to form homo- and heterodimers (108, 110, 120, 121). The C-terminal zinc fingers are also capable of interactions with other proteins (110, 122). At the amino or '*N'* terminal, the four zinc fingers here enable DNA binding of the factors to key targets (110, 117, 121, 122). Pegasus is divergent here as it contains three zinc fingers at the *'N'* terminal (107). The consensus Ikaros family DNA binding site is ***'GGGAA'*** and for the divergent member, Pegasus, it is '***GNNNGNNG'*** (120).

The proteins can undergo post-translational modification and alternative splicing to yield different isoforms of the Ikaros family (107, 110). Such splicing may explain functional diversity and roles in disease (See 1.5.5.2) (107, 109, 117, 123). Studies have shown that if members lose one or more of their zinc fingers, they can become '*dominant negative isoforms'* where they dimerise with family members, however, are unable to bind DNA thus obliterating their usual mode of action (96, 113).

(A)




(B)




(C)

| Zinc Finger | Function |
|---|---|
| ZF1 | Contain binding site specificity to target gene and thus help bind DNA |
| ZF2 | Contains DNA motif to bind DNA directly |
| ZF3 | Contains DNA motif to bind DNA directly |
| ZF4 | Contain binding site specificity to target gene and thus help bind DNA<br>* No ZF4 in Pegasus |
| ZF5 | Protein interactions including homo- and hetero- dimerisation |
| ZF6 | Protein interactions including homo- and hetero- dimerisation |

**Figure 1.12: Structure and Function of Ikaros Family Members**
**(A)** Schematic of the Amino (NH2) and Carboxy (CH2) terminal of standard Ikaros family members. **(B)** Aiolos, Eos, Helios and Ikaros contain 4 zinc fingers (represented by dark blue horizontal bars) at their N terminal, with Pegasus containing 3. **(C)** Table describing functions of each zinc finger.

### 1.5.2 Expression of the Ikaros Family

The Ikaros proteins are observed in numerous organs and cell types. Eos and Pegasus appear to be the most widely distributed throughout the body, with their expression observed in the liver, brain, heart and skeletal muscle (110). Previous studies have shown expression of Ikaros in the brain and involvement in development of the nervous system, however newer studies also highlighted its expression in other organs such as the liver (110). Cellular distribution of the transcription factors is also highly ubiquitous throughout the body, ranging from precursors to mature cell types. Thymic cells have a high expression of Helios, with many studies describing the role of the Ikaros family in CD4+ T cells (96, 123). Ikaros, Aiolos and Helios expression has been seen in lymphoid cells, and Helios and Ikaros expression also reported in erythroid cells (110).

### 1.5.3 Regulation of Gene Transcription

The Ikaros family can act as both repressors and activators of gene transcription via high affinity binding to DNA through the *N-terminal* (107, 124).

The three key steps involved in initiating gene repression include *(123)*:

*i.* *Chromatin remodelling*

*ii.* *RNA Polymerase II transcription initiation complex*

*iii.* *Altering chromosome conformation*

Chromatin remodelling is one of the key methods by which the Ikaros family can control gene expression (107). In cells, the nucleosome is found covered by chromatin surrounded by histones which can extend *N* terminals out from the core to interact with other proteins or DNA. It is these *N* terminals which can be de/acetylated to alter chromatin conformation and ultimately regulate gene transcription (Figure 1.13) (125).

Ikaros family members localise to peri-centromeric heterochromatin around the nucleolus and bind to co-repressors such as Sin3A/B and Mi-2 beta (Mi-2β), a chromatin remodelling partner enabling access to the nucleosome (83, 107, 126, 127). These co-repressor and transcription factor complexes can then bind to Histone Deacetylase (HDAC) 1 or 2 components of the NuRD (nucleosome-remodelling and histone deacetylate) complex which enable deacetylation of histones. HDACs are able to deacetylate histones which makes the locus unavailable for transcription regulators to bind which can then lead to gene silencing through a condensed phenotype of the chromatin (103, 109, 125, 126). The co-repressor/transcription factor/HDAC complex is recruited to the promoter of target genes via the recognised sequence of DNA of gene at the heterochromatin, leading to histone deacetylation and thus repression of the gene (122, 125). The family also regulate transcription via interaction with RNA Polymerase II and the RNA Pol II transcription initiation complex (110, 123).

### 1.5.4 The Ikaros Family in Disease

Alterations in Ikaros family member expression have been identified in diseases and disorders such as IBD and leukaemia (123). Mutations in Ikaros are associated with leukaemia and lymphomas, with Aiolos found in chronic lymphocytic leukaemia and Helios also identified in T Cell Acute Lymphoblastic Leukaemia (T-ALL) (107). GWAS studies have identified SNPs in IKZF3, the Aiolos encoding gene in IBD (128). Autosomal mutations in Pegasus have also been associated with thrombocytopenia, again highlighting the pleiotropic nature of the transcription factors (129). Next, we divulge further into each member of the Ikaros family, discussing their discovery and their role in disease.

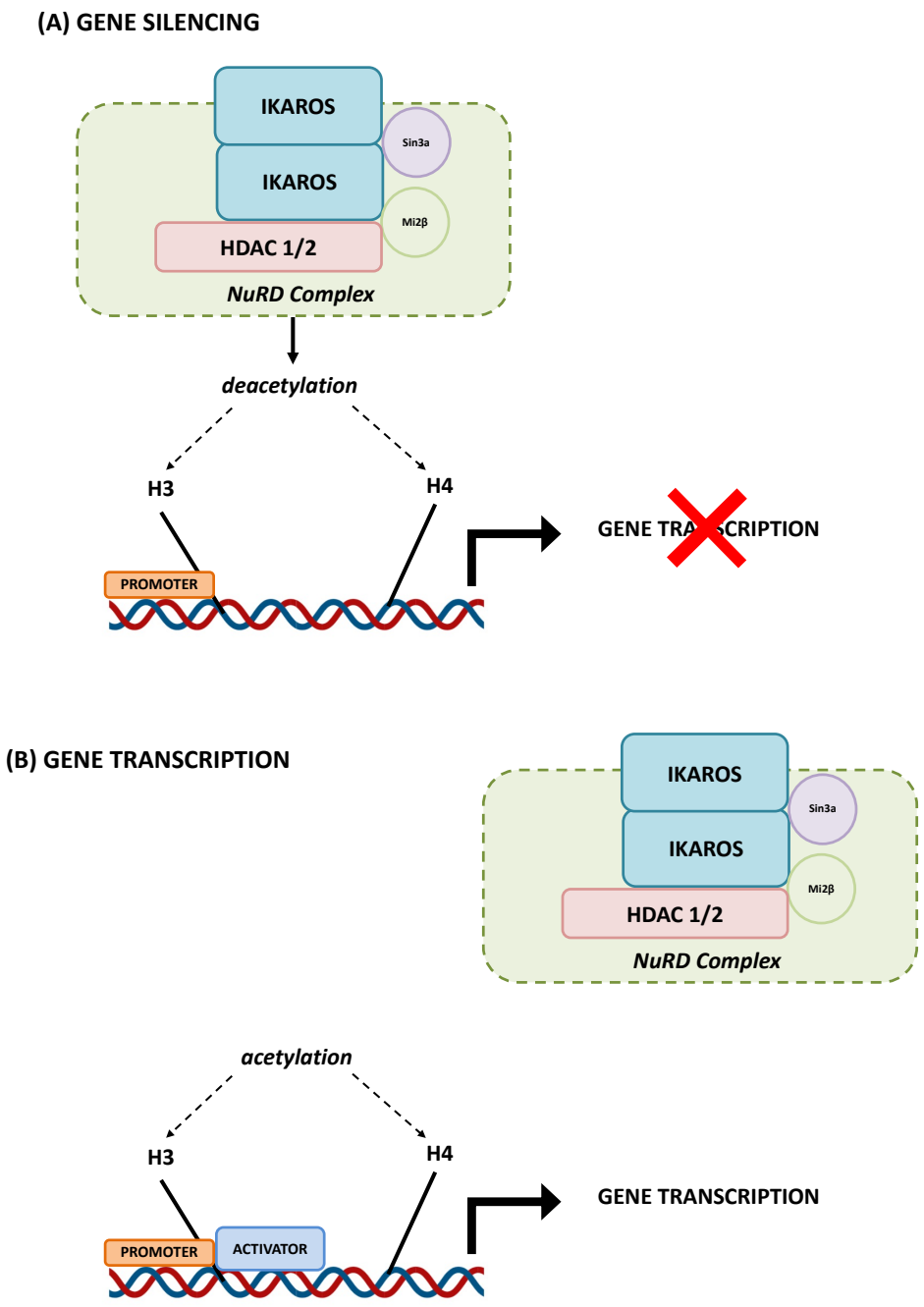



**Figure 1.13: Ikaros and the Nucleosome-Remodelling and Histone Deacetylate (NuRD) Complex Can Regulate Gene Transcription**
**(A) GENE SILENCING:** Histones H3 and H4 can be deacylated by Ikaros homodimers (in this example) binding to components of the NuRD complex, HDAC1/ HDAC2, Mi2B and Sin3a. This ensures a closed conformation of the gene and therefore no gene transcription. **(B) GENE TRANSRIPTION:** Dependent on cell type, by binding to the NuRD complex and, Mi-2b which is a chromatin remodelling partner, Ikaros can move the complex away from histones, enabling acetylation of histones H3 and H4 and access for activators at the promoter, enabling gene transcription.

### 1.5.5 Ikaros

Ikaros, encoded by IKZF1, or ZNFN1A1, is the founding member of the Ikaros family, discovered in 1992 during a T cell lineage transcription regulator screening by Georgopoulos *et al.,* (1992) (110, 115, 122, 130, 131). Ikaros is found on the short arm of chromosome 7 at 7p12.2 and its main isoform is formed of 519 amino acids (132, 133). Ikaros is formed of 8 exons, with Exon 1 involved in the regulation of gene transcription along the promoter (133). Exons 4, 5 and 6 encode the 4 *N* terminal zinc fingers implicated in DNA binding, with exon 8 encoding the 2 fingers at the *C* terminal (133). Protein binding occurs at *ZF5* and *ZF6* (122, 126). Ikaros binds to the conventional Ikaros family DNA binding consensus 5'***GGGAA***3' (115, 120, 125, 134). Homology between the mouse and human form of Ikaros is 95%, with orthologues seen in both Drosophila and Zebrafish (120, 122, 130). Ikaros is related to the Drosophila gene *Hunchback*, which is involved in the regulation of GTP-ase Activating Protein (GAP) (126, 130).

#### 1.5.5.1 The Role of Ikaros

Multiple roles for Ikaros have been identified in development of CD4+ T Cells (including Th1, Th17 and Tregs), B cells and myeloid cells (Section 3.1.4) (110, 135, 136). Ikaros can also function as a tumour suppressor, modulate myeloid lineage expression and most importantly, act as transcription repressor (122, 134, 135, 137). Ikaros can also regulate NF-κB and Notch target genes including Gata3 and Runx1 and promotes apoptosis in erythroid cells by binding to SMAD6 and SMAD7 (107). Recent studies have shown that Ikaros can act as an activator, and a repressor of specific genes (138). For example, Ikaros is an activator of STAT4, UL-7 and Rag1a whilst repressing T-bet expression (107). Ikaros also plays a key role in modulating T

Cell Receptor (TCR) signalling, in a similar way to how Aiolos modulates B Cell Receptor (BCR) signalling (109).

### 1.5.5.2 Ikaros Isoforms and Splice Variants

Since the discovery of Ikaros, numerous Ikaros isoforms have been identified (Figure 1.14) (116, 126, 133, 135, 137). Pre-mRNA splicing of transcripts results in the formation of isoforms of varying size, from 50 to 72kDa (131, 138, 139). The Ikaros isoforms can form complexes that are stable in solution which have different functional phenotypes (139). Payne *et al.,* (2003) found expression of Ikaros isoforms, both binding and non-binding forms, in progenitors and mature cells suggesting Ikaros is expressed throughout hematopoietic differentiation in different guises for its various roles. The group also discovered the Ikaros isoform, Ik-x, which is highly expressed in myeloid and modulated during myeloid cell differentiation (131, 133, 140). There are two identifiable subsets of Ikaros isoforms, *functional* and *dominant negative* isoforms (122). Ik-1 is the largest, most functional, and most common in lymphoid and erythroid lineages (131, 137, 139). Ik-1 protein is seen in B Cells, NK Cells and nucleated erythrocytes whilst Ikaros isoforms Ik-1-4 are present in many forms of leukaemia (113, 131). Contrastingly, splicing isoforms Ik-5 to Ik-9, have lower expression and comprise of the dominant negative isoforms (117, 133). Ik-6 and Ik-7 are the most dominant negative isoforms of Ikaros, preventing DNA-binding isoforms from forming and are seen in many malignancies (122, 133). Ik-6 is a short splice isoform of 37kDa and is the most potent dominant negative repressor (125, 138). This isoform is the most prevalent isoform found in patients with childhood Acute Lymphoblastic Leukaemia (ALL) (113).

The different splice variants of Ikaros are also found in different locations. For example, Ik-1 and Ik-2 are most abundant and are frequently expressed in the nucleus whereas Ik-3 and Ik-4 are found in the cytoplasm of fibroblasts (117, 137, 141).

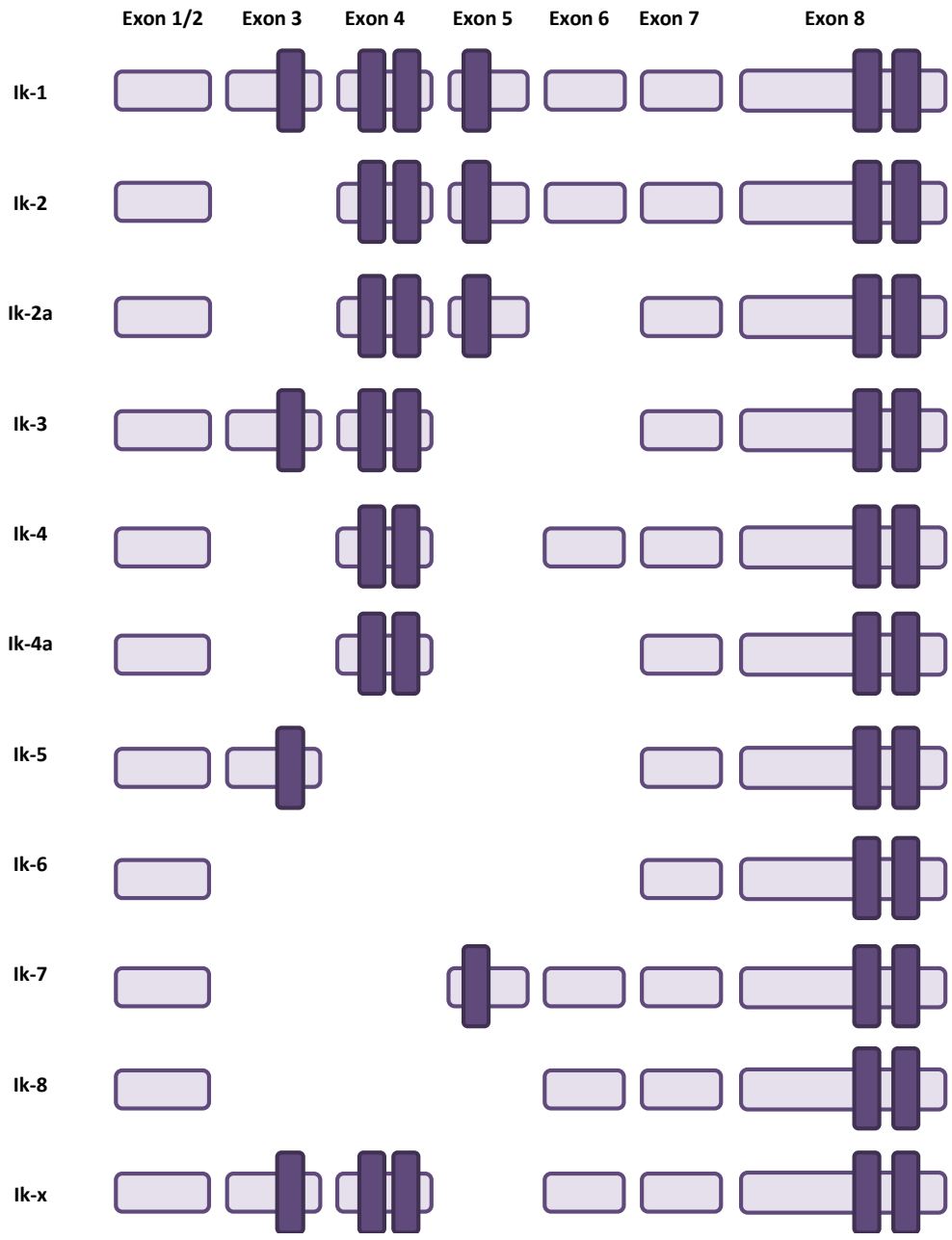



**Figure 1.14: Schematic of Ikaros Isoforms**
Diagram depicting different Ikaros splice variants of common Ikaros isoforms from Ik-1 to Ik-x. Light purple horizontal bars represent the exons, with dark purple bars representing zinc fingers.

### 1.5.5.3 Ikaros, CK2 and Cell Cycle Control

Ikaros can be regulated by Casein Kinase 2 (CK2) (110, 133). CK2 can phosphorylate Ikaros, decreasing its DNA affinity and prevents its binding to target gene promoters (Figure 1.15) (110). CK2 thus is able to mediate the role of Ikaros in different biological functions (141, 142). Protein phosphatase 1 (PP1) can in turn inhibit CK2-mediated Ikaros phosphorylation (110, 133). Through CK2, Ikaros can control cell cycle progression, survival and death through its role in repression (122). In the cell cycle, studies have shown that Ikaros has a role in daughter cell formation from mother cells (122). Ikaros can modulate genes involved in cell cycle progression having a negative effect on cyclins with an opposite effect on cell cycle inhibitors such as p21 (141). In the study by Georgopoulos (2017), the group found that Ikaros has a conserved *ser/thr* residue at the *C* terminal which can be phosphorylated by CK2 during G1-2 transition, resulting in reduced DNA binding (Figure 1.16) (109, 122). Thus, aberrations in Ikaros function can influence cell survival and death which could influence disease pathogenesis.

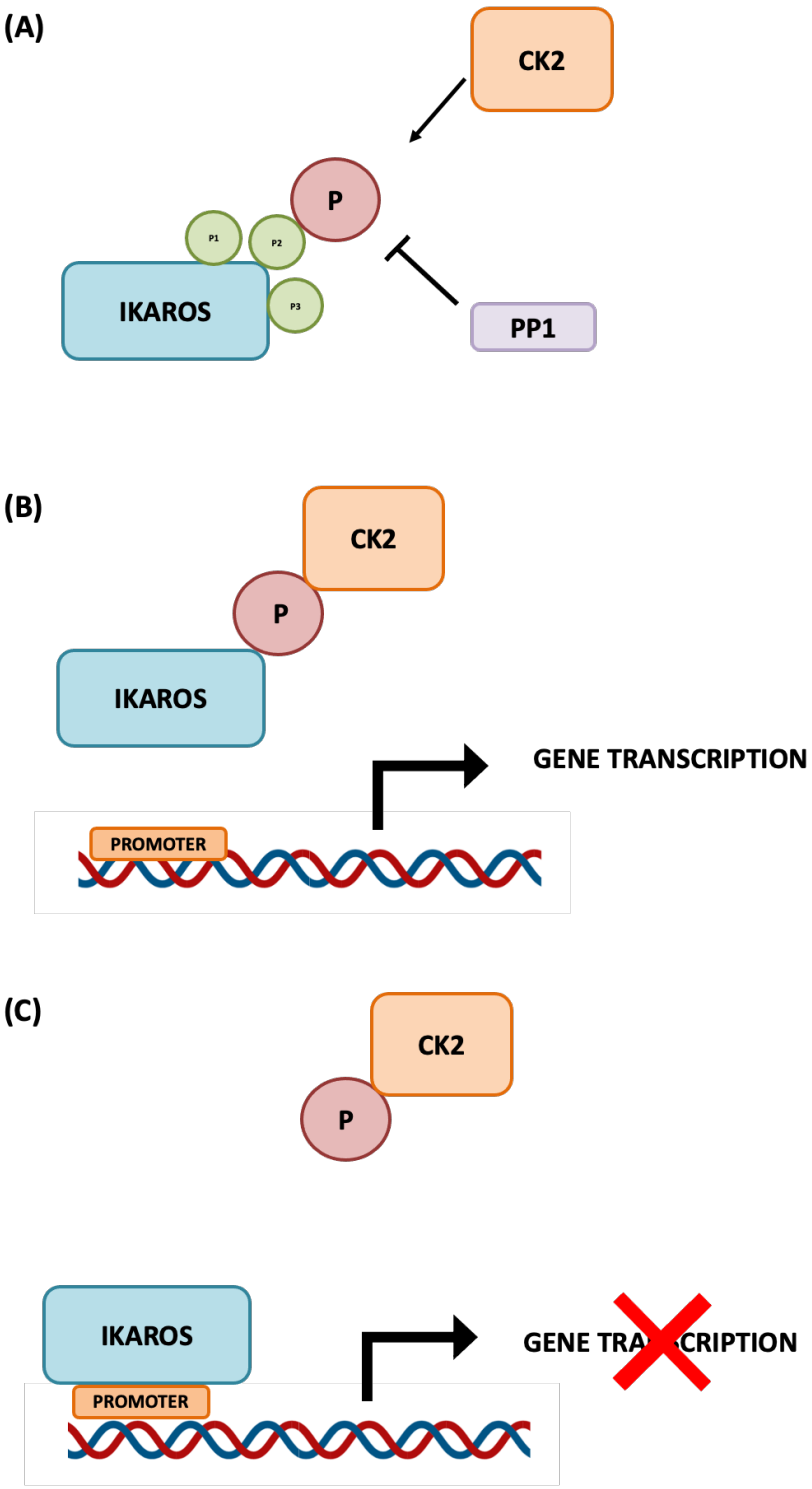



**Figure 1.15: Ikaros and CK2 Mediated Gene Transcription**
**(A)** Ikaros can be phosphorylated by Casein Kinase 2 (CK2) at phosphorylation sites P1, P2 and P3. The CK2 inhibitor Protein phosphatase 1 (PP1) can reverse CK2 mediated phosphorylation. **(B)** When phosphorylated, Ikaros is unable to bind to the promoter and thus, in this case, unable to repress gene transcription. **(C)** When CK2 does not phosphorylate Ikaros, Ikaros is able to bind the promoter and prevent gene transcription.

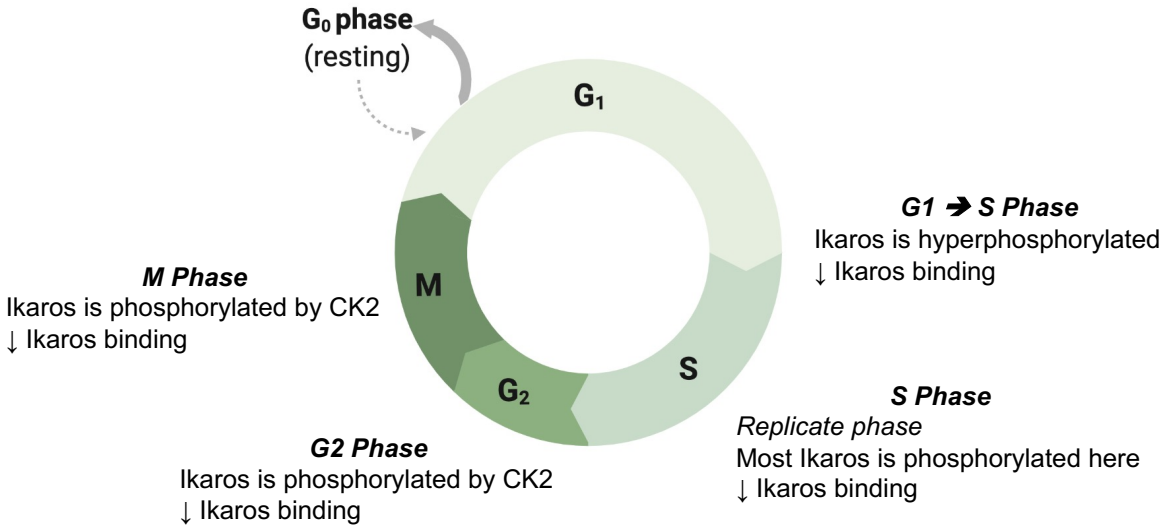



**Figure 1.16: Ikaros Phosphorylation Enables Cell Cycle Progression**
Phosphorylation of Ikaros by Casein Kinase 2 (CK2) throughout the cell cycle, reduces Ikaros binding promoting cell cycle progression. Image adapted from *Biorender.com*.

### 1.5.5.4 Ikaros Expression in Cells and Tissue

Ikaros is expressed throughout tissue such as in the brain and liver, with the highest expression of Ikaros observed in lymphopoietic tissue including the spleen, thymus, and lymph nodes (110, 122, 137). mRNA expression of Ikaros can be found in all cells but corresponding protein levels vary (131). The highest Ikaros expression is seen in immature thymocytes, with Ikaros also found in Hematopoietic Stem Cells (HSCs), myeloid and erythroid precursors, T and B cells, NK cells and lymphoid and neural progenitor cells (109, 110, 122, 137). Many studies have focused on the role of Ikaros in thymocytes where it is highly expressed (108). Here Ikaros can impact the differentiation of CD4+ T Cells into Th17 by promoting production of IL-17 and other Th17 related genes (See 3.1.4) (143). This suggests Ikaros has an important role in determination of T cell lineage (143). Low levels of Ikaros are found in monocytes but

is then upregulated in Monocyte-DC cultures (136). Matulić *et al.,* (2010) have described Ik-1 expression in Jurkat, MOLT-4, NALM-1 and RAJI cell lines but no Ik-6.

#### 1.5.5.5 Ikaros in Disease

Ikaros mutations result in multiple autoimmune disorders and diseases in humans and murine models (132). Ikaros mutations are implicated in SLE, B Cell-ALL (B-ALL), ALL, Acute Myeloid Leukaemia (AML), common variable B cell immunodeficiency (CVID), IBD, and respiratory tract infections (107, 115, 132, 133, 135, 139, 144, 145). Mutations in the IKZF1 gene are also seen in GWAS studies investigating IBD, SLE and T1D (146).

Homozygous global knock out of Ikaros (Ikaros$^{(-/-)}$) results in lack of B cell development in mice (139). An effect of Ikaros$^{(-/-)}$ was also seen in the myeloid lineages with an increase in differentiated macrophages with a corresponding decrease in neutrophils (107). Payne *et al.,* (2003) also found Ikaros null mice have myeloid and erythroid defects alongside complications in lymphoid cells. Similarly, Gómez-del Arco *et al.,* (2004) found myeloid precursors increase in Ikaros$^{(-/-)}$ whereas B and T cells decrease, therefore suggesting Ikaros can influence the myeloid and lymphoid pathways in alternate ways (141). A dominant negative Ikaros mutation also results in a lack of T cells before and after birth resulting in very quick death for mice (107).

The role of Ikaros mutations in cancer have also been of great interest (117). Ikaros knockdown in T cells and lack of dominant isoforms can lead to malignancies in T cells (117). Particular Ikaros isoforms also play a role in disease as in childhood B-ALL, a decrease in Ik-1 and Ik-2 is found with a rise in Ik-4 to Ik-8 isoforms (117). The dominant negative Ik-6 isoform is found in different forms of leukaemia and is seen in a third of T–ALL cases, being termed an *oncogenic isoform* (83, 122, 133). In

childhood AML cases, Gorzkiewicz and Walczewska (2015) found 7/10 cases possess the Ik-6 isoform. This isoform was also seen in acute & chronic myeloid leukaemia and myeloproliferative neoplasm (122). Studies have shown Ik-6 upregulates Bcl-XL which is an anti-apoptotic protein (132). Bcl-XL is also involved in the differentiation and survival of monocytes and macrophages suggesting a role for Ikaros in their regulation (122).

### 1.5.6 Aiolos

Aiolos (ZNFN1A3, IKZF3), is a 509 amino acid homologue of Ikaros located at chromosome 17q11.2~21, first identified in 1997 (117, 147-149). Sixteen different isoforms of Aiolos have now been identified with expression distributed throughout development in various cell types (107, 149). Developmentally, Aiolos appears later than Ikaros, with expression seen during the late foetal thymus stage (150). Aiolos is expressed in lymphocytes and is upregulated as precursors become double positive with expression seen in pre-B cells, CD4+ T cells (including Th17), B cells and plasma cells in the bone marrow (107, 110, 148-150). We will discuss this role of Aiolos in CD4+ T Cells, and in particular Th17 cells in greater detail later in this thesis (See 3.1.1). Expression of Aiolos is however reportedly not seen in myeloid and erythroid precursors, hematopoietic progenitors, or HSCs (110, 150).

Aiolos can form homodimers similar to the other Ikaros family members and can signal through NuRD to influence DNA transcription (148, 149). Interestingly, Aiolos homodimers have been shown to be better transcription activators than Ikaros (150). In lymphocytes, previous studies have shown that Ikaros and Aiolos associate with each other quite regularly (151). Ikaros has also been shown to promote Aiolos expression, alongside NF-$\kappa$B, STAT3, AhR, and TGF-$\beta$ (110). Aiolos has a similar

dimerisation and binding pattern as Ikaros but is still able to form heterodimers with other family members such as Helios (107, 110, 137, 147, 150, 152).

#### 1.5.6.1 Aiolos and its Role in B Cells

The greatest expression of Aiolos is observed in B lymphocytes where it is key to function, proliferation, and differentiation (100, 110, 112, 115, 148, 150). Defects in Aiolos lead to inefficient B Cell development, with studies showing Aiolos is anti-proliferative and loss of Aiolos increases pre- and immature B cells (107, 113, 117). Aiolos is also involved in modulating BCR signalling and promotes Fc$\gamma$R inhibited signalling therefore a cell needs a higher threshold for activation (113, 117). This is similar to the role that Ikaros plays in T cells (109). Aiolos global knock out in a mouse model resulted in the production of B cell lymphomas with an increase in serum levels of both IgG and IgE, B cell precursors and a reduction in B cell tolerance, supporting the importance of Aiolos in B cell behaviour (114, 148).

#### 1.5.6.2 Role of Aiolos in Disease

Mutations in Aiolos have been associated with many diseases such as B-ALL and IBD (128). Elevated Aiolos expression is found in cancers, SLE and RA as well as lymphomas and is believed to promote metastasis, hence is a valuable target for cancer therapy (110, 148). Aiolos knockdown in T Cells also results in a more intense forms of colitis through its influence on both Th1 and Th17 (128). A study by Webb *et al.,* (2015) reported that the Aiolos encoding gene IKZF3 is implicated in PBC, another autoimmune disease of the liver associated with CD4+ T cells and in particular, Th17 cells. Aiolos can also regulate cell apoptosis, suggesting this could be perturbed in

disease, specifically in cancer (110, 154). A key drug of investigation has been Thalidomide, which we will discuss in detail in this thesis (See 6.1).

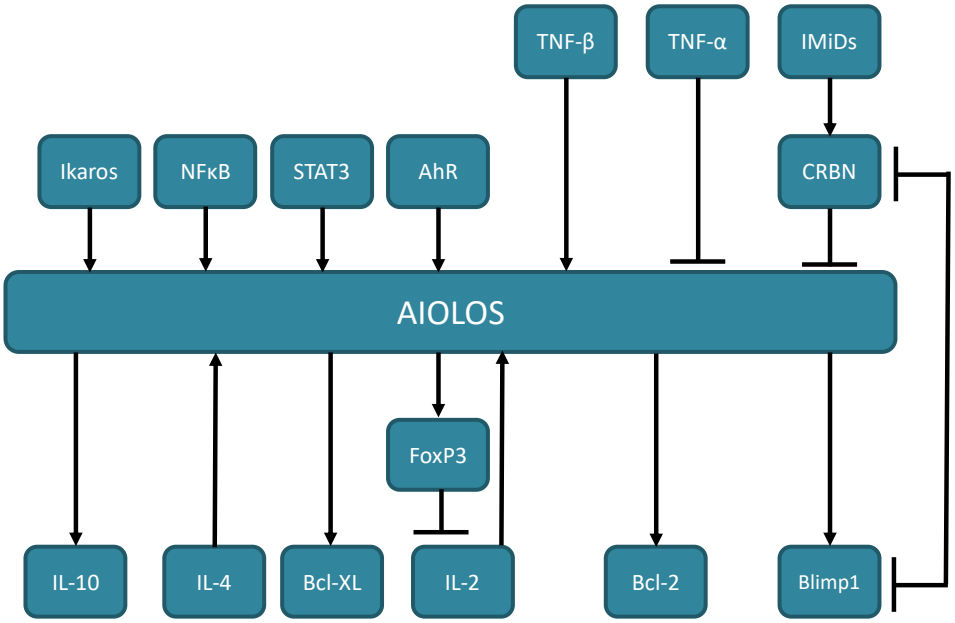



**Figure 1.17: Proposed Regulation Pathways of Aiolos**
Aiolos is inhibited by Immunomodulatory drugs (IMiDs) through the action of Cereblon (CRBN) and TNFα. In turn, Aiolos is regulated by Ikaros, NF-κB, STAT3, AhR, IL-2, IL-4, and TNF-b. In turn, Aiolos can regulate IL-10, Bcl-XL, Bcl-2 and FoxP3. Figure adapted from Fan and Lu (2016).

### 1.5.7 Eos

Eos (IKZF4), named after the Goddess of Dawn in Greek mythology, was first discovered in 1999 by Honma *et al.,* (1999) whilst screening genes involved in astrocyte culture (155). According to Greek mythology, Eos is believed to be responsible for opening the gates of heaven allowing the sun to rise and was known to ride on the back of Pegasus (137, 155). During initial investigations into the Ikaros family, some studies refer to Eos as Daedalus, however Eos is now the standard

nomenclature (109). A protein of 522-585 amino acids with a molecular weight of 58.5-70kDa (dependent on splice variant), Eos has the classic Ikaros family structure, with four zinc motifs at its *N* terminal and 2 at the *C* terminal (119, 121, 124, 137, 156). In zebrafish, one homologue for Eos has been found (118).

Eos expression throughout the human body is broad with protein identified in the brain, liver, kidney, spleen, heart, and muscle (110, 116, 121, 137). Eos has also been observed in both the Central Nervous System (CNS) and Peripheral Nervous System (PNS) (121). Different splice variants of Eos may have different functions or roles in different regions of the body. For example, Eos present in the CNS and PNS is of a different isoform than that found in the lymphoid lineage (121). Honma *et al.,* (1999) were unable to identify Eos expression in the liver, kidney, spleen, or lung, with the main source of Eos identified within the developing nervous system. Recent studies and our work have however broadened our understanding of Eos expression, with our group finding detectable expression of Eos within the liver and bowel (110, 118). Eos can form heterodimers with other Ikaros family members, binding through the *C* terminal and can behave as a gene repressor (121, 156). The *C* terminal of Pegasus and Eos share an 80% sequence homology, and like Pegasus, Eos is also believed to play an important role in development (119, 124). Previous studies suggest that Eos is however most similar to Helios, with a sequence homology between both of 83.3% (107, 121, 137). Eos binds to the consensus ***'GGGAA'*** recognition site common to members of the Ikaros family (116). Eos also contains a PEDLA motif which CtBP, a co-repressor, can bind to and through this interaction, is able to limit gene expression (116, 157).

### 1.5.7.1 Eos Expression and Function in Immune Cells

Eos is involved in a multitude of process such as osteoclast differentiation to skeletal and cardiac muscle (110). Eos is also involved in regulation of gamma-globin gene regulation during erythroid differentiation (156). In cell lines, high levels of Eos have been reported in THP-1s (137). Expression of Eos has mainly been investigated in lymphocytes, monocytes, Treg, CD8+ T cells and other Th cell subsets (107, 110, 158). A key finding by Hu *et al.,* (2007) found that MITF and PU.1, transcription factors which interact with Eos, are found in macrophages and monocytes, suggesting a role for the transcription factor in the myeloid lineage (134). Indeed, some of the highest expression levels of Eos in are reported in monocytes, however research into Eos and its expression in myeloid populations is still limited (107). Eos may also positively regulate Th1 as a reduction in IFNγ is seen in Eos knockout mice models (123). Global deletion of Eos in mouse models has shown that there is a delay in onset of symptoms of autoimmunity suggesting Eos may also be present in APCs or innate immune cells which then influence the activation of effector T Cells (158). Gokhale *et al.,* (2019) have also shown Eos is needed for activation of CD4+ and CD8+ T cells.

A key role of Eos is that it binds to and can regulate FoxP3-mediated gene expression thus suggesting Eos may play a role in Treg function, development and, or stability (97, 119, 159). Lack of Eos results in loss of Treg suppressive function (See 3.1.2) (123, 157). By directly interacting with FoxP3, Eos stabilises FoxP3 and enables Foxp3-mediated inhibition of IL-2 with studies showing Eos depletion prevents Treg suppression of IL-2 (94, 157). Pan *et al.,* (2009) similarly found that selective siRNA knockdown of Eos in Tregs, permits IL-2 production by preventing the interaction between FoxP3 and the IL-2 promoter. This thus supports the role of Eos as an

intermediary of FoxP3-mediated gene transcription indicating a key role in Treg function which will be explored in this thesis (155).

#### 1.5.7.2 Eos in Disease

Studies have identified the involvement of Eos in various diseases such as HTVL-1 infection, autoimmunity, insulin resistance, IBD and Polycystic Ovary Syndrome (PCOS) (110, 123, 160, 161). Koskinen *et al.,* (2020) found different Eos genotypes were associated with insulin resistance in PCOS, a common endocrine disorder, although the link is still unknown. Similarly, Eos was identified as one of the potential causative genes of PCOS by Censin *et al.,* (2021) implicating Eos in diseases not solely associated with immune cells. Eos can also bind to the transcriptional regulator oncoprotein Tax, a transactivating protein involved in upregulating IFNγ, cell survival and viral gene expression implicated in Human T cell leukaemia virus type 1 (HTVL-1) (162). Naito *et al.,* (2019) found significant lower levels of Eos in PBMCs of patients with HTVL-1 in comparison to normal, with Tax influencing Eos expression although the mechanism was undetermined. The group found HTVL-1 leads to plasticity of Tregs from suppressive to inflammatory phenotype suggesting that low levels of Eos may correlate with changes in Treg phenotype (See 3.1.2) (162). Similarly, Sharma *et al.,* (2013) reported that changes in Treg function through reprogramming of cells in the thymus was dependent on a reduction in Eos expression whilst maintaining FoxP3 expression (97). The group found that loss of Eos-expressing cells resulted in the inability for Tregs to aid APCs to activate naïve T cells (97). Sharma *et al.,* (2013) found that under IL-6-reduced circumstances an Eos-stable Treg population is produced, with no reprogramming of Tregs or loss of Eos. With IL-6, a Treg population is produced which can lose Eos and reprogram into T helper cells under conditions

present in the microenvironment (155). We will discuss the role of the Ikaros family and Eos in Treg plasticity further in Chapter 3.

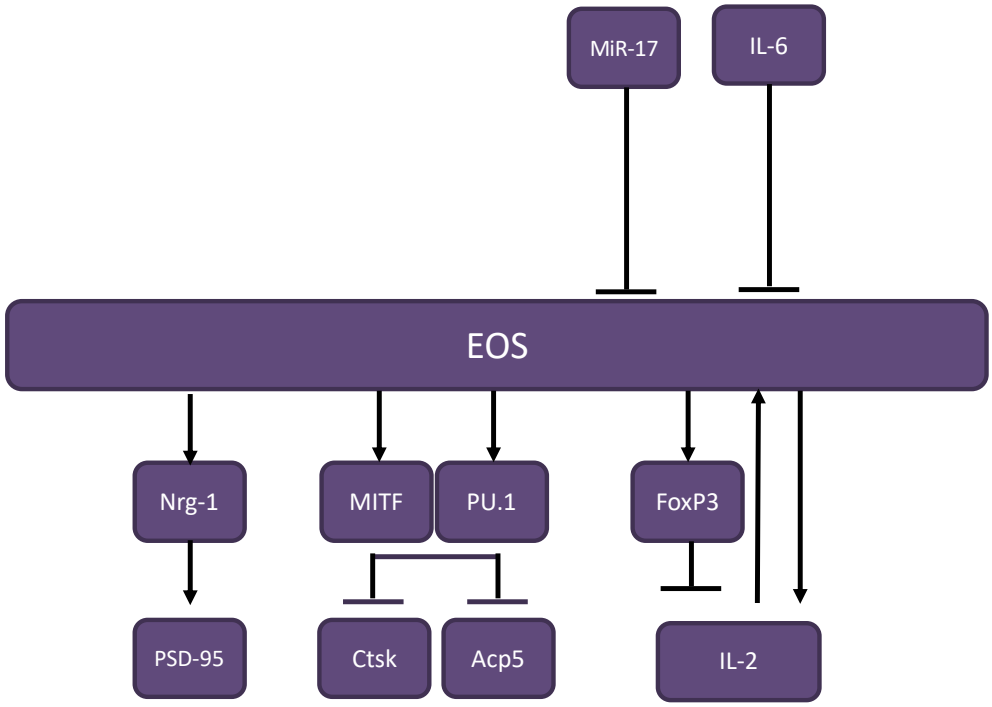



**Figure 1.18: Proposed Regulation Pathways of Eos**
Eos is inhibited by the microRNA MiR-17 and the IL-6 cytokine. Contrastingly, Eos is involved in the regulation of Nrg-1, MITF, PU.1, IL-2 and FoxP3. Figure adapted from Fan and Lu (2016).

### 1.5.8 Helios

Helios also known as ZNFN1A2 or IKZF2, was first identified in 1998 by Hahm *et al.,* (1998) when the group was investigating Ikaros-related genes (152). Through purification of Ikaros complexes they identified and named the 70kDa protein Helios which they found had high homology with Ikaros (117, 139, 152). The group identified two isoforms of Helios, naming them Helios A and B (later renamed Hel-1 and Hel-2),

with approximately 8 isoforms of Helios now identified through further studies (117, 137, 139, 152). Hel-1 and Hel-2 are the longer, more common isoforms of Helios (113, 117). Short splice variants Hel-5 to Hel-8 act as negative isoforms by forming dimers which can limit signalling (96, 113, 138). In terms of structure, Eos has been shown to have the most sequence similarity to Helios (107, 137). Helios however can still co-localise and heterodimerise with both Aiolos and Ikaros (152). In zebrafish, one homologue for Helios has been found (118).

#### 1.5.8.1 Helios Expression in Tissue

Most Helios expression is observed in the thymus and is found in the foetal liver and yolk sac which are key sites of haematopoiesis (117, 163). Helios is believed to be implicated in the hematopoietic system and lymphoid development hence its expression at key sites such as the thymus are fitting to its role (116, 139). Alongside the thymus, Helios expression has also been seen in the respiratory tract, kidney, lymph nodes and brain but in adult, expression is mainly seen in the spleen and thymus (137, 163). Some studies have reported lack of Helios expression in organs such as the liver (139).

#### 1.5.8.2 Cellular Expression of Helios

Helios is expressed in lymphoid, erythroid, epidermal keratinocytes, HSCs, thymocytes, embryonic cells and B Cells (96, 107, 109, 110, 115). Helios is also expressed in transitional single positive CD8+ thymocytes and single positive CD4+ cell lineages with expression levels changing throughout the development (96, 99). There are also differing expression levels of Helios in different cell types with expression in HSCs low, but higher in T cells and Tregs (109). Helios is highly

expressed in proliferative thymocytes, whereas naïve T Cells are Helios negative (98, 108). Helios may play an inhibitory role in some cell types. For example silencing of Helios is needed for B cells (107). Similarly, no upregulation of Helios is seen during Th17 differentiation (128). Some studies have found lack of Helios expression in monocytes, DC or macrophages, B Cells, CD8 cells and Th1 and Th2 subsets, but again this has been contested in recent work (100). Helios expression has been greatly reported in CD4+ T cell subsets, and in particular, Tregs (114, 139). Studies have found that Helios is expressed in 60-70% of all circulating Tregs in healthy patients, with the highest Helios expression seen in FoxP3+ Tregs (52, 103, 163). This is discussed further in Section 3.1.3.

#### 1.5.8.3 Role of Helios in Disease

The discovery of Helios and its presence in key lymphocytic cells makes it a key target of investigation for roles it may have in disease. Correlations between Helios expression and disease have been seen in SLE, T1DM, RA and Leukaemia (107, 115, 164). A higher percentage of Helios+ Tregs are found in SLE active patients during chronic infection (110). A greater presence of Helios+ Tregs are also seen in cancer patients (52). Hel-1 and Hel-2 are found in the blood, whereas Helios splice variants were seen in tumour cell lines and leukemic patients by Matulić *et al.,* (2010) suggesting differences in Helios isoform expression in health and disease. Helios mutations also greatly associate with T-ALL (107, 115). Similarly, Chan (2019) found that Helios may have a role in maintaining AML stem cell activity and also repression of myeloid differentiation, which appears perturbed in AML.

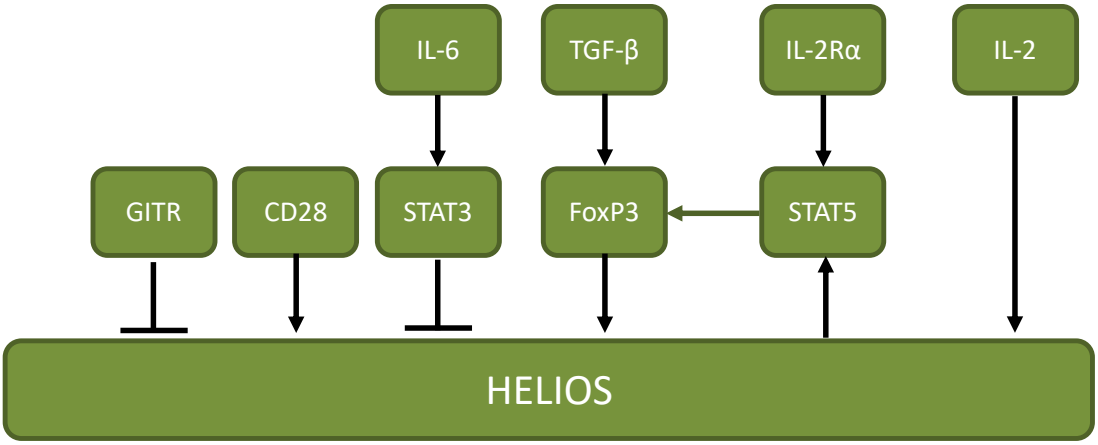



**Figure 1.19: Proposed Regulation Pathways of Helios**
Helios is inhibited by GITR and IL-6 through the cytokines influence on STAT3. Contrastingly, Helios is regulated by CD28, IL-2, TGF-beta and FoxP3. Figure adapted from Fan and Lu (2016).

### 1.5.9 Pegasus

Pegasus, the most divergent member of the Ikaros family was first identified in 2000 by Perdomo *et al.,* (2000) (110, 120, 137). Named after the infamous winged horse from Greek mythology, Pegasus and its role have remained elusive since its initial discovery (129). Pegasus has a molecular weight of 46.5kDa and the gene is found on Chromosome 10 (137, 166). Pegasus has a greater similarity to Hunchback and appears to have a more primitive non-hematopoietic role within development unlike other family members (107). Another way in which Pegasus differs is that it contains *three zinc fingers* at its *N* terminal in comparison to the classic four seen with the others (Figure 1.12) (107, 118). Although Pegasus is similar to Aiolos and Ikaros, sharing the typical *C* terminal, it is at the *N* terminal domain where it differs most where it contains a different DNA recognition domain: ***'GNNNGNNG'*** in comparison to all other family members (120, 124, 137). Interestingly, it has been reported that Pegasus is unable to form heterodimers with either Eos or Ikaros, although data on its interactions with other family members is limited (107). Another difference identified by John *et al.,*

(2013) was that unlike other family members which localise to the heterochromatin for gene regulation, Pegasus instead localised away from the nucleolus, in an *'alternative macromolecular organelle'*. John *et al.,* (2013) also identified three Pegasus variants with differences seen in their non-coding regions in zebrafish. By inferring knowledge from other family members, we can hypothesise these variants may have individual roles in regulation of gene expression or disease. Together, these highlight the multitude of ways in which Pegasus differs from the conventional Ikaros family members.

Pegasus is broadly expressed throughout the body, with expression seen in the liver, brain, kidney, heart, skeletal tissue and during embryogenesis (100, 107, 110, 116, 118, 137). Pegasus is found in different cellular populations such as naïve, effector, memory and mature CD8 T Cells, although its expression is lower than Ikaros in T Cells (138). Recent studies have also highlighted the key role that Pegasus plays in the megakaryocytic lineage (166).

#### 1.5.9.1 The Role of Pegasus in Development

Although the Ikaros family in general have a key role in immune cells, Pegasus seems to be an anomaly having a predominant role in development (120). Sharing homology to Hunchback, Pegasus plays a key role in embryonic development where it can regulate homeodomain genes (120). Zebrafish contain an orthologue of Pegasus which shares great homology to the human form, with three isoforms of Pegasus identified (120). Pegasus knockdown in zebrafish, causes a *'disordered left right asymmetry in the gut'* and incorrect gut intestine looping, suggesting a key role for Pegasus in the gut (120). Target genes of Pegasus were also identified including the *pitx2* gene which is involved in left-right asymmetry, which was negatively regulated

by Pegasus. Similarly, *cdx4*, *apc11* and *cxxxc1* were also found to be negatively regulated by Pegasus whereas *srp54*, *cbx31* and *pbx1* were positively regulated (120). These observations plus the structural and genetic divergence between Pegasus and other Ikaros family members suggests Pegasus may have distinct functions.

#### 1.5.9.2 Pegasus and Its Role in Platelet Development and Disease

Recent studies investigating mutations in the IKZF5 gene have found this can cause a delay in development, with a reduction seen in the number of both T and B cells, although the mechanisms contributing to this are still unknown (166). Most recently, IKZF5 has also been implicated in megakaryopoiesis, the process which enables development of platelets (129, 166). Heterozygous mutations have been identified in Pegasus which have been linked to inherited thrombocytopenia in recent studies (166, 167). A paper by Vannucchi (2019) also highlighted how autosomal mutations in IKZF5 could cause thrombocytopenia, a disease resulting in platelet abnormalities. Interestingly, the group found that Pegasus mutations caused a milder and rarer form of thrombocytopenia in comparison to other known thrombocytopenia-causing mutations (129). Similarly, Leinoe *et al.,* (2020) investigating the platelets of patients with IKZF5 mutations, found disturbed function, an elongated structure alongside disturbances in the arrangement of filamin, alpha and beta tubulin and myosin and overall, a lower platelet count. These platelets also had additional morphological changes with empty vacuoles and membranes, less alpha granules and disorganised cytoskeleton (166). Together, the limited data on Pegasus suggests a key role for the transcription factor in both development and platelet function, however due to the pleiotropic nature of the family, further investigation of the transcription factor could identify novel roles for the family member.

## 1.6 Summary, Hypothesis and Aims

In my introduction, I have introduced IBD, its prevalence, pathogenesis and most importantly, the scientific need for better diagnosis, treatment, and management of the disease. I then discussed the gut-liver axis and the contribution of key immune cell populations to disease pathology. I concluded my introduction by introducing the Ikaros family, a family of zinc finger transcription factors which have a role in gene regulation and who appear to play a role in IBD. In this thesis, I investigate the Ikaros family in the context of IBD hypothesising that ***'the Ikaros family play an integral role in IBD pathogenesis through their role in mediating macrophage phenotype'***.

Below I summarise the aims and objectives of each chapter in this thesis (Table 1.8), followed by the Methods utilised in my thesis. I then begin my project by discussing the expression of the Ikaros family within Tregs and Th17 cells.

**Table 1.8: Aims and Objectives of Each Thesis Chapter**

| CHAPTER | AIMS | Objectives |
|---|---|---|
| **Chapter 3** | To investigate expression of the Ikaros Family in Tregs | I. To document Ikaros family expression in CD4+ Cells<br>II. To verify Treg and Non-Treg associated family members in our samples<br>III. To document if expression of family members was influenced by IBD-induced inflammation |

| | | |
|---|---|---|
| **Chapter 4** | To investigate Ikaros Family expression in the bowel and liver | I. Verify if the Ikaros Family is expressed within bowel and liver tissue<br>II. Identify which cells express Ikaros family members<br>III. Determine what happens to Ikaros Family expression levels in diseased tissue |
| **Chapter 5** | To investigate Ikaros Family expression within macrophage populations | I. To ascertain if the Ikaros family is expressed within monocytes and macrophage subsets<br>II. If the Ikaros family is expressed, to determine if members have differential expression within different macrophage subsets<br>III. To determine if bowel disease has any impact of Ikaros family expression within the macrophage population in the bowel<br>IV. To determine if there is differential expression of macrophages and the Ikaros Family within different regions (stricture, distal and proximal) of resected tissue |
| **Chapter 6** | To investigate the effect of therapeutics on Ikaros Family expression in macrophages | I. To ascertain if Pomalidomide could affect Ikaros family expression with macrophage subsets<br>II. Determine what impact IBD has on systemic Ikaros family expression within monocytes and macrophages<br>III. Distinguish donor and patient derived monocyte and macrophage Ikaros family expression differences<br>IV. Determine whether biological intervention in the form of Infliximab can impact Ikaros family expression within monocytes and MDM |
| **Chapter 7** | To investigate Eos knockdown in THP-1 derived macrophages | I. To analyse the impact of Eos knockdown on MΦ macrophage function and phenotype |

# Chapter 2: Methods

## 2.1 Ethics and Use of Human Biomaterials

This study involved the use of human biomaterials in the form of blood and tissue samples. All were collected with written, informed patient consent and were approved by our local ethical review boards. Approvals for the liver studies were provided under the Centre for Liver Research project ethics codes 18-WA-0214 "*Liver inflammation*" and 19-WA-0139 "*Fibrosis*". These covered both use of human liver tissue and blood samples from patients and normal controls. In some cases, surplus venesected blood from hemochromatosis (HFE) patients was also utilised. HFE is a hereditary condition which impacts iron homeostasis within an afflicted individual. Regular phlebotomy which helps lower the amount of systemic iron and this blood was thus available for our studies (168).

IBD patient bowel and blood samples were provided under the *Tissue Remodelling and Fibro-Stenosis in Crohn's Disease (TRAFIC)* study, approval reference number RRK6508. The study provided a mix of Healthy Control, UC and CD bowel biopsies, Biologic Naïve and anti-TNF$\alpha$ treated blood samples alongside resection material for RNASeq analysis. Bowel sections for imaging were provided under the *'Chemokines involved in the development of PSC, idiopathic IBD and Colorectal Cancer'* ethics, approval reference number RRK2431. Additional Endocytoscopy Study ethics IRAS ID: 227882 also provided a mix of Healthy Control and UC bowel samples, alongside blood samples from patients who had low level UC inflammation (169).

## 2.2 Cell Culture

### 2.2.1. Peripheral Blood Mononuclear Cells (PBMCs)

#### 2.2.1.1 Isolation and Culture of Peripheral Blood Mononuclear Cells (PBMCs)

Isolation of Peripheral blood mononuclear cells (PBMCs) was conducted using the Ficoll gradient centrifugation method in accordance with manufacturer's protocol (GE Healthcare, Life Sciences, Buckinghamshire, UK). Blood was diluted in Phosphate Buffered Saline (PBS, Oxoid, ThermoFisher Scientific, Leicestershire, UK) at a 1:1 dilution, with 25ml of the resulting solution layered onto 15ml of Ficoll in a 50ml Falcon tube. The tube was centrifuged for 20 minutes at 800 x g, with acceleration at 5 and deceleration brake at 2. Once the centrifugation period was complete, the mononuclear cell layer was removed using a 1ml Pasteur pipette and placed into a fresh 50ml Falcon tube. PBS was added to wash the cells and the tube was then centrifuged at 800 x g for 5 minutes, with acceleration and deceleration set at 9 for all further washes. The supernatant was then discarded, and cells re-suspended in 50ml of PBS and centrifuged for 5 minutes at 1100rpm. The supernatant was discarded, and cells re-suspended in PBS for counting using Trypan Blue (Sigma Aldrich, Paisley, UK) at a ratio of 1:1 to determine live cells using a haemocytometer. Cells were then either used straight away, placed into culture or frozen into Cryovials in 1ml of Cryostor™ Cryopreservation Media (Sigma Aldrich, Paisley, UK) and stored at -80$^{o}$C. For culture, isolated PBMCs or enriched subsets isolated from PBMCs were maintained in ***complete medium*** consisting of Roswell Park Memorial Institute Medium (RMPI) 1640 Medium (Sigma Aldrich, Paisley, UK) supplemented with 10% Foetal Calf Serum (FCS, Sigma Aldrich, Paisley, UK) and 1% L-Glutamine (Life

Technologies, Paisley, UK) and 1% Penicillin-Streptomycin (Life Technologies, Paisley, UK). Cells were incubated at 37$^{o}$C with 5% $CO_2$.

#### 2.2.1.2 Selection of CD4 Positive (CD4+) PBMCs

CD4+ T Cells were enriched from PBMCs using the MojoSort™ Human CD4+ T Cell Isolation kit by BioLegend® (San Diego, US). Isolated PBMCs were counted and re-suspended in *'MACS Buffer'* consisting of 10ml PBS, 0.2% EDTA (Sigma Aldrich, Poole, UK) and 2% Heat-Inactivated FCS (Sigma Aldrich, Poole, UK) at a density of 100 million cells/ml of MACS buffer. CD4+ cells were then enriched using the MojoSort™ Human CD4 T Cell Isolation protocol. Firstly, the *Biotin-Antibody Cocktail* was added to the cells at a ratio of 1µl:10µl cells in MACS buffer and left on ice for 15 minutes. Following incubation, *Streptavidin Nanobeads* beads were added to the cells at a ratio of 1µl:10µl and left on ice for 15 minutes. Next, the tube was placed into an EasySep™ magnet (STEMCELL Technologies, Vancouver, CA) for 5 minutes, after which the cell solution was poured into a fresh tube and washed with 3mls of MACS buffer and centrifuged for 5 minutes at 2000 rpm. The cells were then counted as above and re-suspended in complete medium or PBS.

#### 2.2.1.3 Enrichment of Monocytes From PBMCs

Enrichment of $CD14^{+}CD16^{+}$ expressing monocytes from PBMCs was conducted using the MACS® Miltenyi Biotec Pan Monocyte Isolation Kit (Miltenyi Biotec, Bergisch Gladback, Germany). All steps were conducted using pre-cooled reagents and equipment. Isolated PBMCs were re-suspended at a concentration of 40µl/ $10^7$ million cells in MACS buffer (prepared as PBS, 0.4%, 0.8M EDTA and 0.5% FCS). The manual magnetic labelling instructions were followed according to the manufacturers'

guidelines. FcR Blocking reagent at 10 μl per $10^7$ million cells and *Biotin-Antibody Cocktail* also at 10μl per $10^7$ million cells were added to cells and left for 5 minutes at 4°C. Following incubation, 30μl MACS buffer per $10^7$ cells was added to the cell suspension and then *Anti-Biotin Microbeads* at 20μl per $10^7$ cells were added for 10 minutes at 4°C. The LS+ Selection MACS® Column (Miltenyi Biotec, Bergisch Gladback, Germany) was used for isolation and prepared prior to manual cell separation by running 3mls of MACS buffer through the column. After Anti-Biotin antibody incubation, 3mls of MACS buffer was added to the cell suspension, which was then placed onto the LS+ column, with $CD14^+CD16^+$ cells eluting out of the column. The eluted monocytes were washed with PBS, and either re-suspended in RLT Buffer and stored at -20°C for RNA isolation (Section 2.4) or washed with PBS and re-suspended in complete medium for further experiments. Flow analysis demonstrated an 80% enrichment of $CD14^+CD16^+$ expressing monocyte subsets (Figure 2.1).

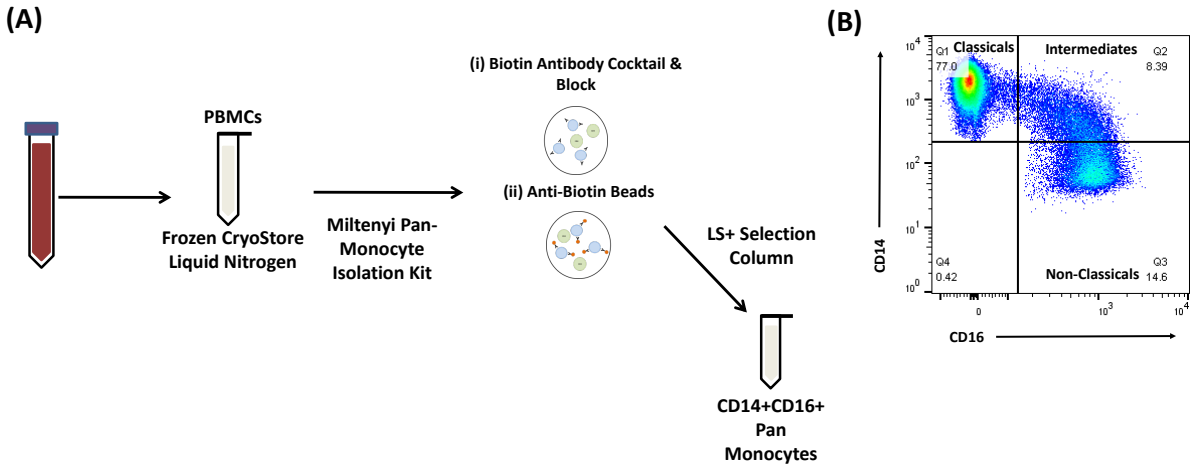



**Figure 2.1: The MACS® Miltenyi Biotec Pan Monocyte Isolation Kit**
**(A)** Using the Miltenyi Biotec Pan Monocyte Isolation Kit, CD14+CD16+ double positive monocytes were isolated from either fresh or frozen PBMC samples. cell A biotin antibody cocktail and block were added to the cell suspension and incubated followed by addition of anti-biotin beads. The monocytes were then eluted through LS+ columns using manual magnetic elution. **(B)** Expression of CD14 and CD16 surface markers was confirmed using Flow Cytometry which showed that approximately 85% of cells eluted expressed both CD14+ and CD16+, with staining intensity analysis showing that classical, intermediate, and non-classical monocytes were present in the eluted Pan-monocyte pool.

### 2.2.1.4 Polarisation of PBMC-Derived Monocytes into Macrophages

Monocyte-derived macrophages were achieved using a polarisation method adapted from the Wallace group (170) (Dr Graham Wallace, Institute of Inflammation and Ageing, University of Birmingham). Enriched pan-monocytes (See above) were re-suspended in complete medium at a concentration of 1 million cells/ml in a 12 well plate. The final volume of the wells was made up to 2ml with GM-CSF (10ng/ml, Miltenyi Biotec, Bergisch Gladback, Germany) added to wells for a M1 phenotype and M-CSF (50ng/ml, Miltenyi Biotec, Bergisch Gladback, Germany) added to wells for a M2 phenotype, and left for 72 hours. After 72 hours, the plates were centrifuged at 500 x g for 5 minutes, the medium removed, and wells washed with PBS. Fresh medium with either GM-CSF (for M1) or M-CSF (for M2 cells) was then added to the wells for 48 hours. After 48 hours, the plate was centrifuged at 500 x g for 5 minutes and the

medium removed, with wells washed with PBS. The appropriate polarisers were then added to the plate and left to incubate for 24 hours (Table 2.1). After incubation, the plates were centrifuged at 500 x g for 5 minutes and supernatants harvested. For RNA isolation, the cells were washed with PBS and 350μl prepared RLT Buffer added to each well (Section 2.4). For analysis via Flow Cytometry, wells were washed with Dulbecco's PBS (Sigma Aldrich, Paisley, UK) and then 500μl cold Non-Enzymatic Cell Dissociation Solution (1X, Sigma Aldrich, Paisley, UK) was added to each well. The plates were placed in the incubator for 30 minutes, after which the cellular contents of each well were harvested into FACs tubes, and the flow cytometry protocol conducted as below (Section 2.3). For Western Blotting, cell lysates were collected in 250μl pre-prepared CelLytic™ MT Cell Lysis Reagent (henceforth CelLytic™ Sigma Aldrich, Paisley, UK) containing Roche cOmplete™ ULTRA Tablets (50x Stock, Roche, Basel, Switzerland) and Roche PhosSTOP™ (25x Stock, Roche, Basel, Switzerland) and stored at -80$^{o}$C.

**Table 2.1: Primary Monocyte to Macrophage Polarising Conditions**

| Macrophage Phenotype | Polarisers/ Concentration | Manufacturer | Catalogue Number |
|---|---|---|---|
| MΦ - GM-CSF | GM-CSF (10ng/ml) | Miltenyi Biotech | 130-093-865 |
| MΦ - M-CSF | M-CSF (50ng/ml) | PeproTech | 300-25 |
| M1 | GM-CSF (10ng/ml) | Sigma-Aldrich | L5418 |
| | LPS (50ng/ml) | ImmunoTools | 11343534 |
| | IFNγ (20ng/ml) | | |
| M2a | M-CSF (50ng/ml) | PeproTech | 200-04 |
| | IL-4 (20ng/ml) | | |
| M2c | M-CSF (50ng/ml) | PeproTech | 200-10 |
| | IL-10 (20ng/ml) | | |

GM-CSF, Granulocyte-macrophage colony stimulating factor; IFNγ, Interferon gamma; IL, Interleukin; LPS, Lipopolysaccharide; M-CSF, macrophage colony stimulating factor.

### 2.2.2 THP-1

#### 2.2.2.1 Culture of THP-1 Cells

THP-1 cells are an immortalized monocyte-like cell line used in this body of work (43, 74, 80). For maintenance of THP-1s, cells were seeded at a density of 500,000-800,000 cells/ml with intermittent Trypan Blue staining conducted to determine cell viability. Cells were maintained in *complete medium* and incubated at 37$^{o}$C with 5% $CO_2$.

#### 2.2.2.2 THP-1 Differentiation to Macrophages in Vitro

For *in vitro* differentiation of THP-1 cells, I adapted a published method by Shiratori *et al.,* (2017). THP-1 cells were seeded in 12 well plates at a density of 500,000 cells/well in a final well volume of 2mls. The cells were left either untreated or stimulated with 50ng/ml of Phorbol 12-myristate 12-acetate (PMA) (Sigma Aldrich, Paisley, UK) for 48 hours. After 48 hours, the plates were centrifuged at 500 x g for 5 minutes, the medium removed, and cells washed with PBS and replaced with fresh medium for 72 hours. Following the rest period, the plate was centrifuged for 5 minutes at 500 x g, the medium removed, and wells washed with PBS. Cells were left untreated or exposed to macrophage polarisers added to appropriate wells for 24 hours (Table 2.2). After incubation, the plate was centrifuged for 5 minutes at 500 x g and the supernatants harvested. Cells were then harvested as mentioned above (Section 2.2.1.4).

**Table 2.2: THP-1 to Macrophage Polarising Conditions**

| Macrophage Phenotype | Polarisers/ Concentration | Manufacturer | Catalogue Number |
|---|---|---|---|
| MΦ | PMA (50ng/ml) | Sigma-Aldrich | P8139 |
| M1 | LPS (50ng/ml) | Sigma-Aldrich | L5418 |
| | IFNγ (20ng/ml) | ImmunoTools | 11343534 |
| M2a | IL-4 (20ng/ml) | PerproTech | 200-04 |
| M2c | IL-10 (20ng/ml) | PerproTech | 200-10 |

IFNγ, Interferon gamma; IL, Interleukin; LPS, Lipopolysaccharide; PMA, Phorbol 12-myristate 13-acetate.

## 2.3 Flow Cytometric Analysis of Protein Expression

Flow Cytometry is a versatile method providing rapid quantitative analysis of protein levels present on both membranous and intracellular area of cells. Due to the nature of this project, flow cytometry provided a potential means of assaying proteins such as the Ikaros family in different cell subsets.

### 2.3.1 Extracellular and Intracellular Staining of Proteins

Flow Cytometry was conducted on samples using the eBioscience™ FoxP3/Transcription Factor FoxP3 Permeabilisation kit (Invitrogen, ThermoFisher Scientific, Leicestershire, UK) in accordance with manufacturer's instructions. Cells were harvested into 5ml FACs tubes (Becton, Dickinson and Company, New Jersey, US) with Live-Dead staining conducted using the Zombie Aqua™ Fixable Viability Kit (BioLegend, San Diego, CA, US) diluted 1:500 in PBS and left for 20 minutes at room temperature. The cells were washed with 2% FBS-PBS and centrifuged for 5 minutes at 2000rpm. Extracellular staining was then conducted with the appropriate antibodies and IgG controls (Table 2.3) for 25 minutes on ice. The cells were then washed with PBS and fixed for an hour with pre-prepared eBioscience FoxP3 Fixation solution in accordance with manufactures instructions. After incubation, the cells were washed

with PBS followed by a wash with Permeabilisation Buffer. Intracellular staining with the appropriate antibodies and IgG Controls (Table 2.3) was then conducted for 45 minutes at 4ºC. Following incubation, cells were washed once with Permeabilisation Buffer and then with PBS. Cells were suspended in 300µl of PBS at 4ºC until they were ready to be analysed.

The CyAn ADP Flow Cytometer by Beckman Coulter or the BD LSR Fortessa X-20 was used for analysis of samples. The data was then analysed offline using FlowJo™ Software Version 10 (Becton, Dickinson and Company, New Jersey, US).

**Table 2.3: List of Flow Cytometry Antibodies**

| Name | Conjugate | Manufacturer Name | Catalogue Number |
|---|---|---|---|
| Aiolos | BV421 | BD Horizon | 565217 |
| Armenian Hamster IgG,κ | PerCPCy5.5 | BioLegend | 400931 |
| BV605 | CD4 | BD Horizon | 562658 |
| BV650 | CD45RA | BioLegend | 304135 |
| CD127 | PeCy7 | Invitrogen | 25-128-42 |
| CD14 | BUV395 | BD Horizon | 563561 |
| CD14 | PE | Miltenyi | 130-110-577 |
| CD14 | BV786 | BD | 563698 |
| CD16 | PeCy7 | BioLegend | 302016 |
| CD163 | SB600 | Invitrogen eBioscience™ | 63-1639-42 |
| CD206 | PeDazzle CF594 | BD Horizon | 564063 |
| CD25 | PeDazzle CF594 | BioLegend | 356126 |
| CD284 | SB645 | Invitrogen eBioscience™ | 64-9917-42 |
| CD3 | PE | Miltenyi Biotec | 130-091-374 |
| CD3 | FITC | BioLegend | 300306 |
| CD3 | BV421 | BD Horizon | 562426 |
| CD3 | BV711 | BD Horizon | 563725 |
| CD3 | APC Vio770 | Miltenyi Biotec | 130-096-610 |
| CD4 | PerCPCY5.5 | BioLegend | 300530 |
| CD4 | APC | BioLegend | 300514 |
| CD4 | BV510 | BD Horizon | 562970 |

| | | | |
|---|---|---|---|
| CD4 | APC CY7 | BioLegend | 300518 |
| CD4 | BV786 | BD Horizon | 563877 |
| CD4 | BUV395 | BD Horizon | 564724 |
| CD4 | PE | BioLegend | 300508 |
| CD45 | SB780 | Invitrogen eBioscience™ | 78-9458-42 |
| CD45RA | BV785 | BioLegend | 304140 |
| CD45RA | BV650 | BioLegend | 304135 |
| CD56 | PE | Invitrogen eBioscience™ | 12-0567-42 |
| CD56 | PECY7 | BioLegend | 304628 |
| CD66b | PE | Invitrogen eBioscience™ | 12-0666-42 |
| CD80 | SB702 | Invitrogen eBioscience™ | 67-0809-42 |
| CD83 | PE | Invitrogen eBioscience™ | 12-0839-42 |
| CD86 | PeCY5 | Invitrogen eBioscience™ | 12-0869-42 |
| FoxP3 | APC | Invitrogen | 17-4776-42 |
| Helios | PerCPCy5.5 | BioLegend | 137230 |
| HLA-DR | APC eFluor 780 | Invitrogen eBioscience™ | 47-9956-42 |
| Ikaros | 488 | BD Pharmigen | 564867 |
| IL-2 | PE | eBioscience | 12-7029-41 |
| Mouse IgG1,κ | PerCPCy5.5 | BioLegend | 400149 |
| Mouse IgG1,κ | BV711 | BioLegend | 400167 |
| Mouse IgG1,κ | BUV395 | BD | 563547 |
| Mouse IgG1κ | FITC | BioLegend | 400110 |
| Mouse IgG1κ | BV785 | BioLegend | 400169 |
| Mouse IgG1κ | PeDazzle CF594 | BioLegend | 400176 |
| Mouse IgG1κ | PE | BioLegend | 400140 |
| Mouse IgG1κ | BV510 | BioLegend | 400171 |
| Mouse IgG1κ | PECY7 | eBioscience | 25-4714-42 |
| Mouse IgG1κ | BV421 | BD Horizon | 562438 |
| Mouse IgG1κ | BV650 | BioLegend | 400163 |
| Mouse IgG1κ | BV605 | BioLegend | 400161 |
| Mouse IgG1κ | APC | BioLegend | 400121 |
| Mouse IgG2b | BV785 | BioLegend | 400356 |
| Mouse IgG2αk | BV650 | BioLegend | 400265 |
| Mouse IgG2αk | BV605 | BioLegend | 400269 |

Antibodies added to samples suspended within FACs tubes in either Permeabilisation Buffer or Brilliant Violet Staining Buffer (Becton, Dickinson and Company, New Jersey, US) to a final volume of 100μl

### 2.3.2 Flow Cytometry: Compensation Beads

Accurate flow analysis requires compensation of fluorophores to ensure that a corrected signal of positive staining is measured, and background staining is excluded. Thus, the Anti-mouse Ig,κ/Negative Control Compensation Particles from BD™ (Becton, Dickinson and Company, New Jersey, US) were used in our flow cytometry protocol. The compensation beads were briefly vortexed and then one drop each of the positive anti-Mouse IgG and Negative Control (approximately 60μl per drop) were added to each FACs tube. Antibodies for each fluorochrome were added to FACs tube to create single colour compensation beads (Table 2.4). The tubes were covered and placed at room temperature for 30 minutes after which the beads were washed with 3mls of PBS at 2000rpm for 5 minutes. After the wash, 500μl of PBS was added to each tube and stored at 4$^{o}$C until needed.

**Table 2.4: List of Antibodies Used for Flow Cytometry Compensation**

| Compensation | Antibody | Manufacturer | Catalogue Number |
|---|---|---|---|
| APC Vio770 | CD3 | Miltenyi Biotec | 130-096-610 |
| PerCPCy5.5 | CD4 | BioLegend | 300530 |
| FITC | CD3 | BioLegend | 300306 |
| PE | CD3 | Miltenyi Biotec | 130-091-374 |
| APC | CD4 | BioLegend | 300514 |
| PeCy7 | CD56 | BioLegend | 304628 |
| PeCF594 (Dazzle) | CD25 | BioLegend | 356126 |
| BV 510 | CD4 | BD Horizon | 562970 |
| BV 421 | CD4 | BD Horizon | 562426 |
| APC CY7 | CD4 | BioLegend | 300518 |
| BV711 | CD3 | BD Horizon | 563725 |
| BV786 | CD4 | BD Horizon | 563877 |
| BUV395 | CD4 | BD Horizon | 564724 |
| BV605 | CD4 | BD Horizon | 562658 |
| BV650 | CD45RA | BioLegend | 304135 |
| PECY5 | CD86 | Invitrogen eBioscience ™ | 12-0869-42 |

### 2.3.3 Eos Antibody Titration

Due to a lack of commercially validated anti-Eos flow antibodies, we utilised an unconjugated Rabbit Anti-Eos antibody from Novus Biologics (NBP2-53305, 0.2mg/ml) coupled with a secondary fluorescent antibody. All other antibodies in our panel were of a different species, thus we could ensure only the Eos antibody was captured with the anti-Rabbit secondary. The conditions outlined in Table 2.5 were used to investigate appropriate conditions. PBMCs were isolated as before, and the flow cytometry procedure conducted until the washes after fixation. The primary antibodies were then added to cells for 1 hour at 4$^{o}$C. After incubation the cells were washed twice with permeabilisation buffer. Secondary antibodies of either Alexa Fluor 488 goat anti-rabbit IgG H+L (FITC, Invitrogen, ThermoFisher Scientific, Leicestershire, UK) or Alexa Fluor 647 goat anti-rabbit IgG H+L (APC, Invitrogen, ThermoFisher Scientific, Leicestershire, UK) were added and incubated at 4$^{o}$C for 1 hour. The cells were then washed with permeabilisation buffer and then PBS for 5 minutes at 2000 rpm and then suspended in PBS for analysis via flow cytometry. Through data analysis using FlowJo we found the optimum concentrations were 1$\mu$g/ml of anti-Eos antibody and a 1:1000 APC secondary dilution. It is however important to note limitations of this method in relation to the sensitivity of the secondary and higher Mean Fluorescence Intensity values due to the nature of the antibodies.

**Table 2.5: Conditions Assayed For Optimisation of Unconjugated Anti-Eos Antibody And Appropriate Secondary Antibody For Flow Cytometry**

| | Anti-Rabbit IgG (0.5 µg/ml) | Anti-Rabbit IgG (1µg/ml) | Anti-Rabbit IgG (1.5 µg/ml) | Anti-Rabbit IgG (2 µg/ml) | Anti-Eos Antibody (0.5µg/ml) | Anti-Eos Antibody (1µg/ml) | Anti-Eos Antibody (1.5µg/ml) | Anti-Eos Antibody (2 µg/ml) |
|---|---|---|---|---|---|---|---|---|
| APC Secondary (1:500) | X | X | X | X | X | X | X | X |
| APC Secondary (1:1000) | X | X | X | X | X | **X** | X | X |
| APC Secondary (1:1500) | X | X | X | X | X | X | X | X |
| FITC Secondary (1:500) | X | X | X | X | X | X | X | X |
| FITC Secondary (1:1000) | X | X | X | X | X | X | X | X |
| FITC Secondary (1:1500) | X | X | X | X | X | X | X | X |

***X***; represents ideal Eos antibody and secondary antibody concentration

### 2.3.4 Flow Cytometry: Sorting Cells

To sort cells into specific populations of interest for downstream analysis, isolated PBMCs were washed in PBS, counted, and then re-suspended at 5 million cells per 50µl in PBS. A proportion of unstained cells were removed to enable efficient sorter set-up and compensation. Cells were labelled for 30 minutes on ice with a selection of antibodies (Table 2.6). After incubation, cells were washed with 2% FBS-PBS and then placed in sorting buffer consisting of PBS, 6.5% BSA (Gibco™, ThermoFisher Scientific, Leicestershire, UK) and 0.2% EDTA (Avantar™, VWR Life Sciences, Randor, Pennsylvania, US). Cells were sorted using a MoFlo Astrios Cell Sorter

(Beckman Coulter, California, US) by Dr Paula Pietroni in our sorting facility. Some cells were also retained for concurrent flow cytometry staining. Cells were sorted into two populations, Tregs and Non-Tregs using cell surface markers to distinguish between both populations. Tregs were identified as $CD3^{+}CD4^{+}CD127^{low}CD25^{high}$ and Non-Tregs as $CD3^{+}CD4^{+}CD25^{-}CD127^{low/-}$. After sorting, collected cells were washed with PBS and lysed in RLT Buffer, and stored at -80°C (See section 2.4).

**Table 2.6: List Of Antibodies Used For Sorting Tregs And Non-Tregs**

| Antibody | Manufacturer | Catalogue Number | Volume/$5x10^6$ cells (µl) |
|---|---|---|---|
| CD4 BV786 | BD Horizon | 564724 | 1 |
| CD3 BV711 | BD Horizon | 563725 | 1 |
| CD127 PeCY7 | Invitrogen | 25-128-42 | 2 |
| CD25 Pe Dazzle CF594 | BioLegend | 356126 | 2 |
| Zombie Aqua | BioLegend | 423101 | 1:500/sample |

## 2.4 Cell Harvesting and RNA Extraction

RNA was isolated from lysed cells collected in RLT buffer using commercially available kits developed by Qiagen (Hilden, Germany) as described in Table 2.7. Protocols were conducted in accordance to manufactures instructions. Donor, NASH, and PSC liver tissue RNA for clinical data correlations (Section 4.2.7) were kindly provided by Dr Emma Shepherd. RNA concentration was determined using the Nanodrop™ 1000 (ThermoFisher Scientific, Massachusetts, US). Concentrations were provided as ng/ml along with absorbance values for 280/260nm and 260/230nm. The absorbance values provide an indication of the purity of the nucleic acid with values closer to 2 for RNA indicating a higher level of purity (171).

**Table 2.7: Qiagen RNA Extraction Kits Used For Appropriate Starting Materials**

| QIAGEN RNA EXTRACTION KIT | STARTING MATERIAL |
|---|---|
| RNeasy Plus Micro Kit | <50,000 cells |
| RNeasy Micro Kit | <500,000 cells |
| RNeasy Mini Kit | > 500,000 cells |
| | Bowel Biopsies |
| All samples lysed in RLT buffer prepared as 1ml RLT buffer: 10μl Beta-mercaptoethanol: | |
| < 5 x $10^6$ Cells – 350μl RLT Buffer | |
| > 5 x $10^6$ / a single bowel biopsy / 1$cm^3$ liver tissue - 600μl RLT Buffer | |

## 2.5 Real-Time Quantitative Polymerase Chain Reaction (RT- qPCR)

In this project we utilised Real-Time Quantitative Polymerase Chain Reaction (henceforth referred to as qPCR) to detect gene products within samples.

### 2.5.1 cDNA Preparation

The iSCRIPT ™ cDNA Synthesis Kit from Bio-Rad (Hercules, California, US) was used to convert RNA into cDNA for transcript analysis via qPCR. The kit contained a 5X reaction mix and the enzyme *Reverse Transcriptase*, which along with RNA and water completed the final 20μl reaction mix (Table 2.8).

**Table 2.8: One Reaction Mix of iSCRIPT ™ cDNA Synthesis Kit**

| Component | Amount (μl, Total Volume 20μl) |
|---|---|
| 5X iScript Reaction Mix | 4 |
| iScript Reverse Transcriptase | 1 |
| RNA | *Variable** |
| Water | *Variable** |
| * Dependent on final concentration of RNA required for experiment | |

The SensoQuest LabCycler (Göttingen, Germany) was used for conversion of RNA into cDNA using the conditions highlighted below in Table 2.9. The prepared cDNA was then diluted using RNase-free water at a ratio of 1:4 and stored at -20ºC until needed.

**Table 2.9: Steps for cDNA Synthesis**

| PCR Reaction Step | Time (Minute/s) | Temperature (ºC) |
|---|---|---|
| Priming | 5 Minutes | 25ºC |
| Reverse Transcription | 20 Minutes | 46ºC |
| Reverse Transcriptase Inactivation | 1 Minute | 95ºC |
| Hold | Infinity | 4ºC |

### 2.5.2 qPCR: Methodology

The Applied Biosystems® TaqMan® Universal Master Mix II with UNG (ThermoFisher Scientific, Leicestershire, UK) was used for qPCR. Standard housekeeping genes used throughout this thesis included *18S*, *SRSF4* and *RPS9* as endogenous controls. Individual data figures highlight which housekeeping gene was used for each experiment. To assay transcriptional expression of genes, the diluted cDNA was prepared with a typical reaction mixture as highlighted in Table 2.10. The Assay ID for target genes are highlighted in Table 2.11.

**Table 2.10: Components of One Taq Man® Universal Master Mix Reaction Per Well in a 384-Well Plate**

| Component | Per Reaction (µl) |
|---|---|
| Gene Assay | 0.5 |
| Taq Man Buffer | 5 |
| Water | 1.5 |
| cDNA | 3 |

**Table 2.11: Assay ID For Target Genes Used in This Thesis**

| Target Gene | Manufacturer | Assay ID |
|---|---|---|
| 18s | ThermoFisher Scientific | 4318839 |
| Aiolos | ThermoFisher Scientific | Hs00232635_m1 |
| Eos | ThermoFisher Scientific | Hs00223842_m1 |
| FoxP3 | ThermoFisher Scientific | Hs01085834_m1 |
| GAPDH | ThermoFisher Scientific | Hs04420632_g1 |
| Helios | ThermoFisher Scientific | Hs00212361_m1 |
| Ikaros | ThermoFisher Scientific | Hs00958474_m1 |
| Pegasus | ThermoFisher Scientific | Hs00223846_m1 |
| RPS9 | ThermoFisher Scientific | Hs02339424_g1 |
| SRSF4 | ThermoFisher Scientific | Hs00900675_m1 |

The 7900HT Fast Real-Time PCR System (ThermoFisher Scientific, Leicestershire, UK) was used for PCR cycling. The system parameters were as below (Table 2.12) for 40 PCR cycles. Data was analysed using the SDS RQ Analyser software (ThermoFisher Scientific, Leicestershire, UK).

**Table 2.12: PCR Cycles and Steps**

| Step | Temperature | Time |
|---|---|---|
| **UNG Incubation** | 50°C | 2 minutes |
| **Polymerase Activation** | 95°C | 10 minutes |
| **Denature** | 95°C | 15 seconds |
| **Anneal/Extend** | 60°C | 1 minute |

### 2.5.3 Analysis of PCR Data

Following the PCR cycle, the results were received as Cycle Threshold (CT) values which were analysed by normalising the baseline threshold value to 0.1 x $10^3$. PCR data was then normalised to the appropriate housekeeping gene and analysed as described in Table 2.13.

**Table 2.13: Analysing PCR Data**

| Value | Definition/Equation |
|---|---|
| **CT** [1] | Cycle Threshold Value |
| **∆CT** [2] | Sample CT – Housekeeping Gene CT |
| **∆∆CT** [3] | ∆CT – Control ∆CT |
| **Fold Change** [4] | $2^{\wedge \Delta\Delta CT}$ |

1. The cycle threshold value (CT) is achieved following the PCR run cycle.
2. To normalise the CT values, delta-CT **(∆CT)** values are calculated by subtracting the housekeeping gene CT value from the sample CT value for each sample.
3. Delta-delta CT **(∆∆CT)** then involves subtracting the control sample delta CT value from the delta CT value of your sample to normalise your data to the control.
4. The fold change indicates the gene expression relative to the background.

## 2.6 Immunohistochemistry

Representative Mouse and Rabbit IgG control images for all forms of IHC in this thesis are in **Appendix A**. Selection of imaged regions was chosen at random to avoid bias and therefore, results represent the spread of staining throughout tissue with no specific region of interest chosen from each tissue section (See **Appendix A**).

### 2.6.1 Haematoxylin and Eosin Staining

To assess structural differences of diseased and healthy tissues, Haematoxylin and Eosin (H&E) staining was conducted using the below method (Table 2.14). After the

final Xylene wash, a drop of DPX Phthalate-free Mounting Media (CellPath, Powys, UK) was added to the section, covered with a 24mm x 40 mm coverslip, and left in a fume hood to dry. Sections were imaged on the Zeiss Axioscan Slide Scanner (Carl Zeiss, Oberkochen, Germany) and offline analysis completed using Zen Blue light software (Carl Zeiss, Oberkochen, Germany).

**Table 2.14: Haematoxylin and Eosin Staining of Paraffin Embedded Tissue**

| Reagent | Time (Minutes/Seconds) | No. of Washes |
|---|---|---|
| Xylene | 2 Minutes | x3 |
| Acetone (Alcohol) | 2 Minutes | x2 |
| Water | 2 Minutes | x2 |
| Haematoxylin Harris | 4 Minutes | x1 |
| Water | 2 Minutes | x1 |
| Acid Alcohol | 30 Seconds | x1 |
| Water | 2 Minutes | x1 |
| Scott's Tap Water Substitute | 30 Seconds | x1 |
| Water | 2 Minutes | x1 |
| Eosin | 1 Minute | x1 |
| Water | 2 Minutes | x2 |
| Acetone (Alcohol) | 2 Minutes | x4 |
| Xylene | 2 Minutes | x3 |
| **Mount in DPX Substitute Solution** | | |

### 2.6.2 3,3'-Diaminobenzidine (DAB) Immunohistochemistry

Staining with peroxidase conjugated antibodies and 3,3'-Diaminobenzidine (DAB) substrate is a common method used to enable identification of proteins within tissue. For this, tissue from both bowel and liver was fixed in formalin and then embedded in paraffin wax. Tissue sections were cut at 5μm thickness and mounted onto charged glass slides ready for use when needed. The DAB IHC protocol was then conduced as described in Table 2.15. Primary antibody and dilutions are described in Table 2.16. After the final Xylene wash, a drop of DPX Phthalate-free Mounting Media was added

to the section and covered with a 24mm x 40 mm coverslip and left in a fume hood to dry. Slides were imaged on the Zeiss Axioscan Slide Scanner and offline analysis completed using Zen Blue light software to randomly select an average of 5-8 regions from each section (Carl Zeiss, Oberkochen, Germany). Semi-quantitative analysis was performed using Fiji Image J Software.

**Table 2.15: 3,3'-Diaminobenzidine (DAB) Protocol of Paraffin Embedded Tissue**

| Step | Reagent | Time (Minute/Seconds) | No of Washes |
|---|---|---|---|
| 1 | **REHYDRATION:** Xylene | 3 Minutes | x3 |
| 2 | **REHYDRATION:** Industrial Denatured Alcohol | 3 Minutes | x3 |
| 3 | **REHYDRATION:** Water | 3 Minutes | x2 |
| 4 | **Antigen Retrieval Tris-based Antigen Unmasking Solution** (pH 9, Vector Laboratories, California, US) 20 Minutes HIGH Microwave Power | | |
| 5 | 0.1% TBS-Tween 20 | 3 Minutes | x2 |
| 6 | **BLOXALL®** (Vector Laboratories, California, US) 10 Minute Incubation | | |
| 7 | 0.1% TBS-Tween 20 | 3 Minutes | x2 |
| 8 | **2x Casein** (10X, Vector Laboratories, California, US) 10 Minute Incubation | | |
| 9 | **Primary Antibody** Diluted in 0.1% TBS-Tween 20 1 hour Incubation | | |
| 10 | 0.1% TBS-Tween 20 | 3 Minutes | x2 |

| | | | |
|---|---|---|---|
| 11 | **Two Drops**<br>ImmPRESS® Horse Anti-Mouse IgG Polymer Peroxidase or<br>ImmPRESS® Horse Anti-Rabbit IgG Polymer Peroxidase<br>(Vector Laboratories, California, US)<br>30 Minute Incubation | | |
| 12 | 0.1% TBS-Tween 20 | 3 Minutes | x3 |
| 13 | **DAB Substrate**<br>(Vector Laboratories, California, US)<br>5 Minute Incubation | | |
| 14 | Deionised water | 3 Minutes | x1 |
| 15 | **Haematoxylin (Mayers)**<br>45 Seconds | | |
| 16 | Hot Water | 2 Minutes | x1 |
| 17 | **DEHYDRATION:**<br>Industrial Denatured Alcohol | 3 Minutes | x3 |
| 18 | **DEHYDRATION:**<br>Xylene | 3 Minutes | x3 |
| **Mount in DPX Substitute Solution** | | | |

**Table 2.16: Antibodies and Their Dilutions Used in 3,3'-Diaminobenzidine (DAB) Immunohistochemistry**

| Antibody | Species | Manufacture | Catalogue Number | Concentration | Dilution |
|---|---|---|---|---|---|
| Aiolos | Rabbit | Novus Biologics | NBP2-24495 | 1mg/ml | 1:50 |
| Eos | Rabbit | Novus Biologics | NBP2-53305 | 0.2mg/ml | 1:50 |
| Helios | Mouse Monoclonal | R&D | MAB73091 | 100μg | 1:2000 |
| Ikaros | Mouse | BD Pharmingen | R32-1149 | 0.5mg/ml | 1:100 |
| Ikaros | Rabbit | Novus Biologics | NBP2-75536 | 1mg/ml | 1:50 |
| Pegasus | Rabbit | Novus Biologics | NBP1-80021 | 0.5mg/ml | 1:50 |
| CD68 | Mouse IgG1 κ | BioLegend | 916104 | 0.5mg/ml | 1:200 |
| CD4 | Rabbit | Abcam | Ab133616 | 0.166mg/ml | 1:100 |
| LEAF ™ Purified Mouse IgG1 κ Isotype Control | Mouse | BioLegend | MG1-45 | 1mg/ml | Variable |
| Rabbit IgG | Rabbit | Agilent, DAKO | X0903 | 20mg/ml | Variable |

### 2.6.3 Opal Dye™ for Multiplex Staining

Opal Dye™ (Opal™) is a method of multiplexing IHC which uses indirect IHC fluorescence to amplify a signal through labelled secondary antibody (172). Opal™ fluorophores are covalently bound to tyramide molecules, which are amplified during staining, with up to 8 markers co-stained theoretically without cross-reactivity (173). Primary antibodies are optimised by DAB and through *singleplexes* before Opal™ co-staining (172). Opal™ is advantageous as antibodies of the same species can be co-

stained without cross-reactivity as fluorophores are covalently bound to epitopes and antibodies removed by stripping (172). As all our Ikaros antibodies were of Rabbit IgG isotype, this method was suitable for us to assess co-expression of family members with CD68. Opal™ was conducted as described in Table 2.17, with the antibodies and dilutions described in Table 2.18. Slides were mounted using Immunomount™ (Shandon, ThermoFisher Scientific, Leicestershire, UK), covered with 24mm x 40 mm glass cover slips and left at 4°C until ready to be imaged using the Vectra® Polaris™ system (Akoya Biosciences, Massachusetts, US) by Miss Emma Hurlestone at the Human Biomaterials Resource Centre, University of Birmingham, and images analysed offline using Phenochart Software (Akoya Biosciences, Massachusetts, US) and Fiji Image J Software for semi-quantitative analysis. Quantified regions were selected at random as above to avoid bias.

**Table 2.17: Opal Dye™ Multiplex Protocol of Paraffin Embedded Tissue**

| Step | Reagent | Time (Minute/Seconds) | No of Washes |
|---|---|---|---|
| 1 | **REHYDRATION:** Xylene | 3 Minutes | x3 |
| 2 | **REHYDRATION:** Industrial Denatured Alcohol | 3 Minutes | x3 |
| 3 | **REHYDRATION:** Water | 3 Minutes | x2 |
| 4 | **Antigen Retrieval Tris-based Antigen Unmasking Solution** (pH 9, Vector Laboratories, California, US) 20 Minutes HIGH Microwave Power | | |
| 5 | 0.1% TBS-Tween 20 | 3 Minutes | x2 |
| 6 | **BLOXALL®** (Vector Laboratories, California, US) | | |

| | | | |
|---|---|---|---|
| | 10 Minute Incubation | | |
| 7 | 0.1% TBS-Tween 20 | 3 Minutes | x2 |
| 8 | **2x Casein**<br>(10X, Vector Laboratories, California, US)<br>10 Minute Incubation | | |
| 9 | **Primary Antibody**<br>Diluted in 0.1% TBS-Tween 20<br>1 hour Incubation | | |
| 10 | 0.1% TBS-Tween 20 | 3 Minutes | x2 |
| 11 | **Two Drops**<br>**ImmPRESS® Horse Anti-Mouse IgG Polymer Peroxidase** or<br>**ImmPRESS® Horse Anti-Rabbit IgG Polymer Peroxidase**<br>(Vector Laboratories, California, US)<br>30 Minute Incubation | | |
| 12 | 0.1% TBS-Tween 20 | 3 Minutes | x3 |
| 13 | **100µl Opal Dye™**<br>(PerkinElmer, Boston, MA, US)<br>Diluted 1:150 in 0.1% TBS-Tween 20<br>10 Minute Incubation | | |
| 14 | 0.1% TBS-Tween 20 | 3 Minutes | x3 |
| 15 | **Repeat Steps 4-14 For Each Additional Primary Antibody/Opal Dye™**<br>**Move to Step 15 after additional of final Opal Dye™** | | |
| 15 | **100µl of Hoechst Ready Flow™ Reagent 33342**<br>(Invitrogen, ThermoFisher Scientific, Leicestershire, UK)<br>Diluted 2 Drops: 100µl in 0.1% TBS-Tween 20<br>10 Minute Incubation | | |
| 16 | 0.1% TBS-Tween 20 | 3 Minutes | x1 |
| 17 | Deionised Water | 3 Minutes | x1 |
| **Mount in Immunomount™** | | | |

**Table 2.18: Antibodies and Their Dilutions Used in Opal Dye™ Staining of Tissue**

| Antibody | Species | Manufacturer | Catalogue Number | Dilution | Opal Dye™ |
|---|---|---|---|---|---|
| Aiolos | Rabbit | Novus Biologics | NBP2-24495 | 1:50 | 570 |
| Eos | Rabbit | Novus Biologics | NBP2-53305 | 1:50 | 570 |
| Helios | Mouse Monoclonal | R&D | MAB73091 | 1:2000 | 570 |
| Ikaros | Rabbit | Novus Biologics | NBP2-75536 | 1:50 | 570 |
| Pegasus | Rabbit | Novus Biologics | NBP1-80021 | 1:50 | 570 |
| CD68 | Mouse IgG1 κ | BioLegend | 916104 | 1:100 | 690 |
| LEAF ™ Purified Mouse IgG1 κ Isotype Control | Mouse | BioLegend | MG1-45 | Dependent on Antibodies | 570/690 |
| Rabbit IgG | Rabbit | Agilent, DAKO | X0903 | Dependent on Antibodies | 570 |

## 2.7 RNASeq Methodology

### 2.7.1 Resection Sample Processing for Bulk RNASeq Analysis

Resection samples were collected under the TRAFIC ethics (See Section 3.2) from 9 patients requiring surgery for CD related strictures attending the Queen Elizabeth Hospital in Birmingham (Table 5.1). Pathologists defined the resection as areas of stricturing and fibrosis (stricture) as well as areas proximal and removed (distal) to inflamed and damaged mucosa. Tissue from each of the three sites was placed into RNAlater® (Qiagen, UK) for storage at -80$^{o}$C until processing.

RNA was batch processed by Dr Louisa Jeffery and Miss Sarah Akiror from samples using the RNeasy on column extraction kit according to manufacturer's instructions (Qiagen UK). RNA was quantified using Qubit (Life Technologies, Carlsbad, California, US) and 0.5ng was used to prepare indexed cDNA QIAseq UPX 3' Transcriptome libraries. These were quantified and quality controlled using the QIAseq Library Quant Assay Kit and Tapestation analysis and sequenced on the Miseq and Nextseq Illumina platforms to a depth of 1 to 3 million reads/sample. Fastq files were obtained through BaseSpace and reads demultiplexed aligned, quantified, and normalized using the CLC Genomics Workbench (Qiagen, Venio, Netherlands). In total, 27 samples were used for analysis.

Downstream bioinformatic analysis was performed By Dr Animesh Acharjee to identify key macrophage specific gene clusters (Table 2.19) and co-expression with members of the Ikaros gene family in each sample. The analytical approach has been previously described and allowed analysis of specific macrophage clusters within the data set (169). We used a correlation based hierarchical clustering analysis to confirm the genes behave in a similar way (174). Differential expression analysis between conditions was conducted with the limma package (175). Library size was estimated using a reduced maximum likelihood estimator with 500 iterations. Initial fitting was performed using a robust M-estimation, and moderated test statistics were computed by empirical Bayes. An FDR-corrected P value $<0.05$ was considered and filtered for further downstream data analysis. We used the supervised classification method called partial least-squares discriminant analysis (PLS-DA) (176). Cross-validation was performed to predict and estimate the model performance (whether models were over fitted). We used variable importance in the projection scores (VIP) to prioritise the genes and this was used more than one to select the macrophage genes impacting

the Distal, Proximal and Stricture categories. Pathway enrichment was analysed using gene ontology and Kyoto encyclopaedia of genes and genomes (KEGG).

**Table 2.19: Genes For Identifying Macrophage Populations From RNASeq Data**

| МΦ | M1 | M2a | M2c |
|---|---|---|---|
| BAX | C1QB | ABCG2 | C1QB |
| BCL2 | CCL1/8 | ALDH1A2 | CD14 |
| CD163 | CCR7 | CABLES1 | CD163 |
| ITGB2 | CD14 | CACNA1G, | FAM20A |
| MMP9 | CD80 | CACNB4 | IL2RA |
| NRP1 | CD86 | CCL22 | JAK3 |
| | CFB | CD1C | MMP7 |
| | CLEC4E | CD23 | PDPN |
| | CSF1R | CD68 | SIGLEC10 |
| | CXCL9/10/11 | ITAGM | SOCS3 |
| | FCGR1A | LRRC4 | SPI1 |
| | FCGR1B (CD64) | MEST | VCAN |
| | CD86 | MORC4 | |
| | GBP1 | RAMP1, | |
| | HIF1A | TNFRSF11A | |
| | IL1b | OLFML3 | |
| | IL23A | TAL1 | |
| | IL6 | TSPAN7 | |
| | IRF1 | | |
| | LPS | | |
| | TNF | | |
| | TNFα | | |
| | VEGFA | | |

## 2.8 Western Blotting for Protein Quantification

To assess the protein levels of the Ikaros family in cell samples, Western Blotting was used. First, to assess amount of protein in samples, a BCA Assay was used.

### 2.8.1 BCA Assay

The Pierce BSA Standard protein assay kit (ThermoFisher Scientific, Leicestershire, UK) was used to determine the protein concentration in harvested samples. Samples

were thawed, briefly vortexed and then lysed with a 18G needle (Terumo™ Agani™, ThermoFisher Scientific, Leicestershire, UK) and a Leur-Lock™ 1ml syringe (Becton, Dickinson and Company, New Jersey, US). The samples were then centrifuged at 10,000g for 20 minutes at 4°C, and the supernatant retained. Samples were diluted 1:1 with pre-prepared CelLytic™ and plated in duplicate in a 96 well plate. Bovine Serum Albumin (BSA, 2mg/ml, ThermoFisher Scientific, Leicestershire, UK), standards were prepared (0-2000 μg/ml) according to manufacturer's instructions and added in duplicate to the plate. The coloured reagents from the BCA kit were mixed at a ratio of 50:1 for A: B and then 200μl of the mix added to each well and incubated at 37°C for 30 minutes. After incubation, absorbance of the plate was read at 560nm using the Bio-Tek, Synergy HT plate reader (Vermont, US) and Gen5 Software (Bio-Tek, Vermont, US). The data was normalised to blanks and unknown protein concentrations interpolated by rearranging $y=m\chi+c$ to find '$\chi$'.

### 2.8.2 Western Blot Protocol

Laemmli buffer (4X, Bio-Rad, Hercules, California, US) was added to cell lysates with sample volumes/concentrations normalised using pre-prepared CelLytic™. The samples were heated at 95°C for 5 minutes, briefly centrifuged and then loaded into wells. The Mini-gel Tank (Invitrogen, ThermoFisher Scientific, Leicestershire, UK) and pre-made 12-well, Invitrogen™ Novex™ WedgeWell™ 12% Tris-Glycine 1mm Mini Protein Gels (ThermoFisher Scientific, Leicestershire, UK) were used for experiments. For running buffer, the Ultrapure 10X Tris (0.25M)/ Glycine (1.92M)/ SDS (1%) (National Diagnostics, Atlanta, Georgia, US) was prepared to a working volume of 1L. In one well, 5μl of the Thermo Scientific™ PageRuler™ Plus Pre-stained Protein Ladder 10-250kDa (ThermoFisher Scientific, Leicestershire, UK) was added to enable

identification of molecular weights. The gel was then run at 50V for 5 minutes to ensure all the samples were aligned, after which the voltage was increased to 200V for 35 minutes. The Trans-Blot® Turbo™ RTA Transfer Kit, Nitrocellulose (Bio-Rad, Hercules, California, US) alongside the Trans-Blot® Turbo™ (Bio-Rad, Hercules, California, US) were used to transfer proteins onto nitrocellulose membranes. A transfer '*sandwich'* was prepared by placing filter stacks on the transfer cassette, followed by a nitrocellulose membrane, the gel and then covered with a final stack of filter paper. Air bubbles were removed and then placed into the Trans-Blot®, with the gel transferred at 2.5A, 16V for 10mins.

Following the transfer, 5ml of Ponceau S Staining (Sigma Aldrich, Paisley, UK) was added to each membrane to check the transfer. The membrane was imaged on the Bio-Rad ChemiDoc™ Imager (Bio-Rad, Hercules, California, US), using the *colorimetric* exposure setting. The membrane was then washed with water to remove the stain and then washed thrice for five minutes with TBS-Tween 20 (0.05%). The blot was then blocked for an hour with gentle agitation with 5% Milk (Marvel, Premier Foods, Hertfordshire, UK)–TBS-Tween 20 (0.05%) at room temperature. After blocking, the primary antibody (Table 2.20) made up in the blocking buffer was then added and left on a shaker overnight at 4$^{o}$C.

The next day, the primary antibody was removed, and the blot washed thrice for five minutes with TBS-Tween-20. The secondary antibody (Rabbit Anti-Mouse IgG Peroxidase or Goat Anti-Rabbit IgG Peroxidase (Sigma Aldrich, Paisley, UK) was diluted in 5% Milk-TBST at 1.5μl:3000μl and then added to the blot and left at room temperature with gentle agitation for an hour. The blot was then washed with TBS-Tween 20 for one 15 minute wash and two 5 minute washes. Following this, the blot was transferred to TBS and lightly dried. The Thermo Scientific™ Pierce™ ECL Plus

Western Blotting Substrate (ThermoFisher Scientific, Leicestershire, UK) was then prepared to a final volume of 1.6mls. The solution was added onto the blot for 5 minutes, in limited light conditions. The blot was then imaged with the ChemiDoc™ Imager using the *chemiluminescence* setting to visualise bands and the *colorimetric* exposure for protein ladder visualisation. For staining with housekeeping antibodies (beta-actin or GAPDH, Table 2.19), the blot was washed for 5 minutes using TBS-Tween 20 and then 5ml of Restore™ Plus Western Blot Stripping Buffer (ThermoFisher Scientific, Leicestershire, UK) was added to the blot and placed on an incubator for 10 minutes on a rocker. The blot was then washed for 5 minutes using TBS-Tween 20 and then blocked for an hour with 5% Milk. The housekeeping antibody made up in the blocking buffer was added and left overnight at 4$^{o}$C and imaged the next day using the same method as described above.

**Table 2.20: Antibody Dilutions Used in Western Blotting**

| Antibody | Species | Manufacture | Catalogue Number | Concentration | Dilution |
|---|---|---|---|---|---|
| Aiolos | Rabbit | Novus Biologics | NBP2-24495 | 1mg/ml | 1:500 |
| Eos | Rabbit | Novus Biologics | NBP2-53305 | 0.2mg/ml | 1:250 |
| Helios | Mouse | R&D | MAB73091 | 100μg | 1:500 |
| Ikaros | Mouse | BD Pharmingen | R32-1149 | 0.5mg/ml | 1:500 |
| Ikaros | Rabbit | Novus Biologics | NBP2-75536 | 1mg/ml | 1:500 |
| Pegasus | Rabbit | Novus Biologics | NBP1-80021 | 0.5mg/ml | 1:500 |
| Beta-Actin | Rabbit | Sigma | SAB5600204 | 100μg | 1:5000 |
| GAPDH | Mouse | Invitrogen | AM4300 | 100μg | 1:10,000 |

## 2.9 Enzyme-Linked ImmunoSorbent Assay (ELISA)

The R&D Systems® ELISA kits were used for the detection of cytokines in supernatants from our macrophage cell cultures, with protocols conducted in accordance with manufacturer's instructions.

### 2.9.1 IL-10 ELISA

The R&D Systems, Human IL-10 Quantikine ELISA Kit (Bio-techne, Minnesota, US) was used to assay the concentration of IL-10 released from different polarised macrophage populations. Samples were diluted 1:4 using Calibrator Diluent RD5C if it was believed they may contain a high concentration of IL-10. The reagents required for the protocol were prepared in accordance with the manufactures protocol (See **Appendix A.2**) and brought to room temperature before beginning the experiment. The protocol was conducted according to manufacturer's instructions. The optical density of the wells was read within 30 minutes using a plate reader (Bio-Tek, Synergy HT, Vermont, US) and Gen5 Software (Bio-Tek, Vermont, US) at 450nm and wavelength correction set to 540/570nm. The standard curve was then plotted, and unknowns interpolated from the line by rearranging $y=m\chi+c$ to find $\chi$.

### 2.9.2 IL-12 ELISA

The R&D Systems, Human IL-12 Quantikine ELISA Kit (Bio-techne, Minnesota, US) was used to assay the concentration of IL-12 released from different polarised macrophage populations. Samples were diluted in complete medium in a 1:4 dilution if necessary. All reagents were brought to room temperature before use and the protocol conducted in accordance with manufactures instructions (See **Appendix A.2**). The optical density of each well was measured using the Bio-Tek, Synergy HT

microplate reader and Gen5 Software at 490nm (wavelength correction set to 650 nm to 690 nm) within 30 minutes of addition of the stop solution.

## 2.10 Testing Effects of Pomalidomide on Macrophage Ikaros Family Expression

Pomalidomide is an immunomodulatory drug which has been shown to selectively target Aiolos and Ikaros for degradation thus we decided to investigate the impact the drug can have on macrophage polarisation and phenotype (See Chapter 6). The method was adapted from Yu *et al.,* (2019) who reported that treatment of THP-1 with Pomalidomide at 10μM was sufficient to induce IKFZ-1 knockdown at 24 hours (145). Thus THP-1 cells were plated at 1 million cells/ml and pre-treated with 10μM Pomalidomide for 24 hours in a 24 well plate (short term stimulation) or Pomalidomide was maintained throughout differentiation protocols (long-term stimulation). For short-term stimulation, after incubation, 500,000 cells were plated per well in a 12 well plate with the well volume topped up to 2mls. The cells were then either left untreated or treated with PMA (50ng/ml) for 48 hours. After incubation, the plates were centrifuged at 500 x g for 5 minutes and then the medium removed, wells washed with PBS and fresh complete medium added to the wells for 72 hours. After rest, polarisers to a MΦ or M1 phenotype were added to each well for 24 hours (Table 2.2). After polarisation, the plates were centrifuged at 500 x g for 5 minutes and the medium removed, and wells washed with PBS. Contrastingly, to assess the long-term impact of Pomalidomide, the protocol as described above (Section 2.2.2.2) was followed with cells either treated with 10μM Pomalidomide or left untreated (Control) throughout the protocol. After treatment, the plates were centrifuged at 500 x g for 5 minutes, the

medium removed, and wells washed with PBS. For both experiments, the cells were then harvested for RNA isolation and qPCR analysis as described above.

## 2.11 Short interference RNA (siRNA)

We used siRNA knockdown to investigate the impact of Ikaros family knockdown on macrophage phenotype and function. The family member we investigated in this study was Eos, based on data surrounding its role in Treg suppressive function and our findings of high expression within THP-1 cells and CD68+ macrophages (93, 119, 137, 159).

### 2.11.1 Silencer Select & Lipofectamine RNAiMAX Reagent

The Silencer Select Lipofectamine RNAiMAX (ThermoFisher Scientific, Leicestershire, UK) protocol was used in our experiments. Alongside the Eos-targeting siRNA (*siEos*), we used a GAPDH positive control (*siGAPDH*) and a negative pool siRNA (*Negative Pool*) and Opti-MEM media only (*Control*) as our experimental controls. To reconstitute the siRNA (5nmol), the vial was centrifuged briefly, and the siRNA re-suspended using nuclease-free water to a final concentration of 100μM. A 10μM working stock concentration using nuclease-free water was then prepared.

### 2.11.2 siRNA Experimental Design

A brief walkthrough of the experimental design is described in Figure 2.2. THP-1 cells were seeded at the desired concentration in appropriate wells (Table 2.21) and then treated with 50ng/ml of PMA for 48 hours.

**Table 2.21: Lipofectamine RNAiMAX Cell Seeding Conditions**

| Plate Size | Cell Number | Final Volume (μl) |
|---|---|---|
| 6 Well | 1,000,000 | 2000 |
| 24 Well | 250,000 | 1000 |
| 96 Well | 40,000 | 200 |

The PMA was then removed, and cells left to rest for 48 hours in complete medium. For the final 24 hours, RPMI was added to the wells to serum-starve the cells. The wells were then washed with PBS in preparation for the siRNA. The Lipofectamine RNAiMAX was first diluted in Opti-MEM medium (Gibco™, ThermoFisher Scientific, Leicestershire, UK) in accordance with the table below:

**Table 2.22: Lipofectamine RNAiMAX Opti-Mem Media to Lipofectamine RNAi Max Ratio**

| | 96 Well (μl) | 6 Well (μl) |
|---|---|---|
| Opti-Mem Media | 25 | 150 |
| Lipofectamine RNAiMAX | 1.5 | 9 |

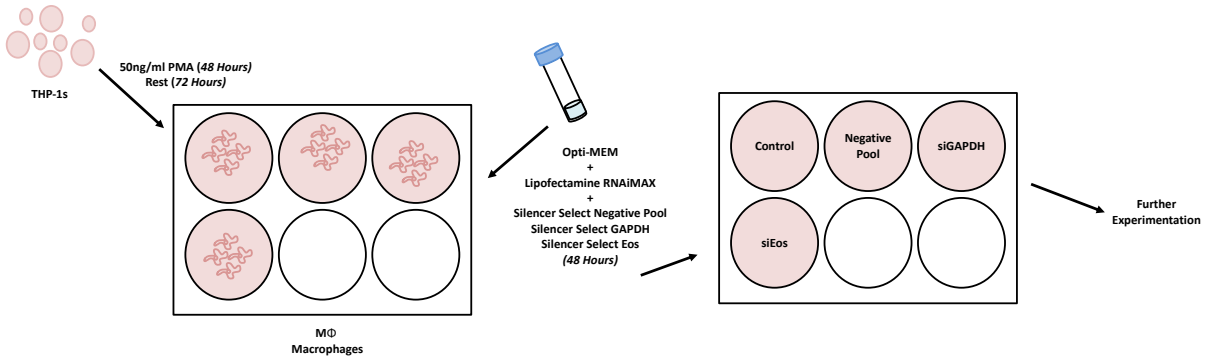



**Figure 2.2: Lipofectamine RNAiMAX and Silencer Select Protocol Walkthrough** THP-1s were seeded at a density of 500,000 cells/well in a 6 well plate, stimulated with 50ng/ml PMA and left for 48 hours. After a 72-hour period of rest, MΦ developed which were then treated with Opti-Mem alone (Control) or Opti-Mem and Lipofectamine RNAiMAX and either silencer select (SS) Negative Pool, SS GAPDH knockdown (siGAPDH) or SS Eos knockout (siEos) for 48 hours. The cells were then ready for further experimentation to determine the impact of Eos knockdown on MΦ in comparison to control.

Each of the targeting siRNAs (Anti-Eos, Negative Pool and anti-GAPDH) were then diluted in Opti-MEM medium as per Table 2.23. The siRNA was then added to the diluted Lipofectamine in a 1:1 ratio (Table 2.24), left to incubate for 5 minutes at room temperature and then added to the wells as described in Table 2.25.

**Table 2.23: Lipofectamine RNAiMAX Opti-Mem Media to siRNA Ratio**

| | 96 Well (μl) | 6 Well (μl) |
|---|---|---|
| Opti-Mem Media | 25 | 150 |
| siRNA (10μM) | 0.5 (5pmol) | 3 (30pmol) |

**Table 2.24: Diluted Lipofectamine RNAiMAX Reagent to Diluted siRNA Ratio**

| | 96 Well (μl) | 6 Well (μl) |
|---|---|---|
| **Diluted siRNA** | 25 | 150 |
| **Diluted Lipofectamine Reagent** | 25 | 150 |

**Table 2.25: Lipofectamine RNAiMAX siRNA-Lipid Complex and Final siRNA Concentration Per Well**

| Component | 96 Well | 6 Well |
|---|---|---|
| siRNA-lipid complex/well | 10μl | 250μl |
| Final siRNA used/well | 1 pmol | 25 pmol |

The cells were then incubated with siRNA for 48 hours at 37$^{o}$C after which the wells were washed twice with PBS. For RNA extraction, cells were harvested as previously described (Section 2.4). To assess changes in the secretion of mediators by the cells, after 48 hours of incubation with the siRNA, wells were washed twice with PBS and 1ml of complete medium was added to each well and the plate incubated at 37$^{o}$C overnight. The next day, the plate was centrifuged at 500 x g for 5 minutes after which the supernatant was retained, and the wells lysed for RNA extraction. To determine

the cell viability of cells, using the 96 well plate experimental design, the cultured plate was spun at 500 x g for 5 minutes, wells washed twice with PBS and 100µl fresh Opti-MEM was added to each well. To assess the cell viability, 20µl of reconstituted CellTiter 96® AQueous Solution Reagent was added into each well and the plate incubated at 37°C. The absorbance of the plate was read at 490nm using the Bio-Tek, Synergy HT plate reader and Gen5 Software, with regular readings taken at every hour over a four-hour period.

### 2.11.3 Vybrant™ Phagocytosis Assay

To determine if Eos knockdown could impact the phagocytic capacity of THP-1-derived macrophages, the Vybrant™ Phagocytosis Assay (ThermoFisher Scientific, Leicestershire, UK) was used. Using siRNA protocol conditions for a 96-well plate, surrounding wells were also supplied with complete medium to reduce the impact of evaporation during culturing. Conditions are described in Table 2.26, with each condition replicated in quadruple.

**Table 2.26: Vybrant Phagocytosis Assay Conditions**

| Condition | Well Contents |
|---|---|
| Negative Control | No Cells |
| Positive Control | Opti-Mem Media only |
| Negative Pool | Opti-Mem Media + SS Negative Pool siRNA |
| siGAPDH | Opti-Mem Media + SS GAPDH siRNA |
| siEos | Opti-Mem Media + SS Eos siRNA |

SS, silencer select; siGAPDH, silencer select GAPDH siRNA; siEos, silencer select Eos siRNA

After a 48-hour incubation with the siRNA, the plate was washed twice with PBS and 200µl of fresh complete medium added to each well and placed in the incubator at

37°C for an hour. During this incubation, the fluorescein-tagged E. *coli* BioParticle suspension (5mg/ml) was prepared by resuspending the E. *coli* in HBSS and 4.5mL of deionised water. The mix was sonicated using the Qsonica sonicator (Newton, US) with 2 X 10 second pulses and kept on ice until ready to use. After an hour, the medium was removed from the wells. Immediately, 100µl of the prepared BioParticle suspension was added to all wells. The plate was then wrapped in foil and placed in an incubator for 2 hours. During this incubation, trypan blue was prepared by re-suspending its contents in 4 mL of deionized water. The mixture was then briefly sonicated again as above. After a 2 hour incubation, the BioParticle suspension was removed from each well and 100µl of the trypan blue suspension was added to each well. This was left to incubate for 1 minute at room temperature. After this, the trypan blue was removed from each well and the plate read immediately with ~480 nm excitation and ~520 nm emission using the Bio-Tek, Synergy HT plate reader and Gen5 Software. The blank reading was then subtracted from all wells and then data from each group of replicates grouped to provide an average reading for each experimental condition. The data was then normalised to the Negative Pool.

### 2.11.4 Proteome Profiler - Human Cytokine Array

The R&D Proteome Profiler - Human Cytokine Array (Bio-techne, Minnesota, US) was used to assess the cytokine profile changes in siRNA treated THP-1 macrophage cultures. Eos knockdown was conducted as described in 2.10.2. Supernatants were defrosted on ice, and pooled (200µl from each *experimental replicate* to make a final volume of 600µl). All reagents were brought to room temperature before use. Serving as a blocking buffer, 2ml of Array Buffer 4, was added onto each membrane in a 4-well multi dish and incubated for an hour on a rocker. Samples were prepared by

adding 600µl of the pooled supernatants to 0.5ml of Array Buffer 4 and the final volume made up to 1.5ml using Array Buffer 5. The Detection Antibody Cocktail was reconstituted with 100µl of deionised water and 15µl of the cocktail then added to each sample and incubated for an hour at room temperature. Once the block was completed, the sample/antibody mixture added to each well and incubated overnight at 2-8$^{o}$C on a rocker.

The next day, the membranes were washed for 10mins using the 1X wash buffer prepared according to manufactures instructions, with the wash repeated three times. The Streptavidin-HRP was prepared according to manufactures instructions and 2ml of the diluted Streptavidin-HRP was added onto each membrane and incubated for 30 minutes at room temperature. After incubation, the washes were repeated, and membranes dried lightly and placed onto plastic wrap. The Chemi Reagent Mix was prepared to yield 1ml of mix per membrane and added to each membrane for 1 minute. The membranes were then wrapped in cling film and imaged on the Bio-Rad ChemiDoc™ Imager. The *chemiluminescence* setting was used to image the blots, with exposure times varying from 5-20 minutes. Images were analysed using Fiji Image J Software to determine the relative density of each blot. The data was then normalised to the Negative Pool.

## 2.12 Graphing and Statistical Analysis

All data was analysed and presented using GraphPad Prism Version 9 Software (San Diego, US (GraphPad, Software Inc., Sand Diego, CA, USA). Dependent on the requirements of the experiments, the statistical analysis methods utilised in this thesis include *unpaired T tests* for comparison between two groups and *Pearson Correlation* for correlating clinical data. For data sets comparing more than two conditions *one*

*way Analysis of Variance (ANOVA)* and *two-way ANOVA* was used in conjunction with the post-hoc *Tukeys* or *Sidak's multiple comparison tests*. All results presented in this report were expressed as mean ± SEM. *NS* represents non-significant data. A *p value* of less than 0.05 was considered statistically significant.

# Chapter 3: The Role of The Ikaros Family in Treg and Th17 Polarisation and Plasticity

## 3.1 Introduction

Both Tregs and Th17 cells have been shown to express members of the Ikaros family, making them clear targets for investigating the Treg/Th17 balance, and most importantly, Treg and Th17 plasticity in disease (96-98, 123, 128, 143, 163, 177). Below, I summarize the existing literature on roles of family members in Treg and Th17 polarisation and the role they could play in influencing plasticity (Figure 3.1).

### 3.1.1 Aiolos Influences Th17 and Treg Polarisation

Aiolos is integral to CD4+ T Cells, with work by Ridley *et al.,* (2020) concluding Aiolos is a regulator of CD3/CD28 mediated IL-10 production by CD4+ T Cells. Many studies have also highlighted the importance of Aiolos expression in Th17 differentiation and function (128, 177). Aiolos inhibits IL-2, with IL-2 an inhibitor of Th17 differentiation (119, 123, 128). TNF-alpha inhibitor (TNFi) also promotes Aiolos expression within Th17 which suggests TNF$\alpha$ may negatively regulate Aiolos (110, 179). Aiolos is also expressed by Tregs and promotes Th17 differentiation but also production of IL-10 (96, 110, 128). Quintana *et al.,* (2012) using Aiolos-deficient murine models found that CD4+ T cells from these mice were unable to differentiate into Th17 cells. The group found that under Th17 polarising conditions Aiolos upregulates both STAT3 and AhR during Th17 differentiation (128). Aiolos can bind to the IL-10 promoter and promote production of IL-10 in Th17 and in CD4+ T Cells, creating a positive feedback loop (110, 178, 179). Similarly, Evans *et al.,* (2014) found that Th17 can switch between producing either IFNγ or IL-10 dependent on stimuli. Th17 cells which are exposed to anti-TNF$\alpha$ have increased IL-10 production and higher Aiolos expression and are functionally distinct to conventional Th17 cells (179). Together these offer a potential mechanism in which Aiolos could help mediate Treg/Th17 plasticity.

### 3.1.2 Eos Promotes Treg Polarisation and Prevents Th17 Development

High expression of Eos is observed in Tregs although some uncertainty surrounding its role remains (46, 157, 158). IKZF4 is highly expressed in Tregs and believed to be needed for their stability and in particular, their suppressor mechanisms (93, 119, 159). Previous studies have shown that Eos can bind to FoxP3, behaving as a co-repressor, and is needed to maintain Treg function (158, 180). Eos along with co-repressors can help stabilize Foxp3 after it binds its target site, resulting in either repression of IL-2 or enhancement of CTLA-4 expression, thus fully committing the cell to the Treg phenotype (94). Conversely, Eos knockdown results in the loss of suppressive capability of Tregs and promotes a proinflammatory phenotype *in vitro* and *in vivo* (46, 119, 155). A selective knockout of Eos in Tregs also causes production of proinflammatory mediators such as IL-17 from these cells, suggesting Treg plasticity (119, 123). Rieder *et al.,* (2015) in a global knockdown of Eos in mice found development of severe EAE, with concurrent high levels of IL-17 and T cells in the peripheral and central nervous systems (119). The group concluded that lack of Eos resulted in upregulation of IL-17 and IFNγ and thus promoted differentiation of T cells into a Th17 phenotype (119).

Further investigations have identified both Eos-labile and Eos-stable populations of Tregs (96, 97). Eos-labile populations, which amount to 30-50% of Tregs, are identified as those who rapidly lose their Eos expression in comparison to a population of Tregs which stably express Eos (Eos-stable) (97, 155). Eos can inhibit the expression of IL-2 however studies have shown that decreased FoxP3 binding to IL-2 occurs with Helios knockdown not with Eos (96, 103). There are also differences in the expression of Eos depending on the stimulation state with basal Eos expression in resting Treg upregulated when cells are activated (119).

There is also growing evidence that Eos can influence plasticity of Tregs (155). Pan *et al.,* (2009) demonstrated that Eos is needed for FoxP3 dependent Treg suppressive function and Eos knockdown causes a loss in Treg activity and instead promotes other effector Th phenotypes (46, 97, 162). Sharma *et al.,* (2013) found that there is a population of Tregs expressing FoxP3+ that can alter expression of Eos during inflammation (97). This suggests that during inflammation, Tregs lose Eos expression which enables Tregs to become plastic as they express FoxP3 and also have effector T cell-like properties (123). IL-6, which is needed for the downregulation of Eos expression, has been shown to convert Tregs into Th cells whilst retaining their FoxP3 expression (97, 110). By reprogramming thymic Tregs using IL-6, Rieder and Shevach (2013) identified both positive and negative Eos Treg populations. Eos-labile and Eos-stabile cells were equally suppressive in nature in *in vitro* studies and in their ability to supress *in vivo* colitis but Eos-labile cells 'reprogrammed' in the draining lymph node (155). These Tregs were not suppressive in nature, were unable to limit IBD and could induce colitis (155).

Eos also appears to have a downregulatory role in Th17 differentiation. Inhibition of Eos by the MicroRNA *miR-17* promotes Th17 development with Th17 cells themselves possessing low Eos expression (119, 123, 128). IKZF4 can also limit the production of IL-17A in Th17-like plastic Tregs (93). In turn, *miR-17* targets Eos which in turn leads to promotion of Th17 differentiation (110). Mice without the Eos-targeting miRNA, *miR17-92*, have reduced severity of EAE, an increase in Eos expression in T cells and concurrent decrease in IL-17 (119). Together, this suggests that Eos could influence both Tregs and Th17 to influence plasticity.

### 3.1.3 Helios is a Marker of Tregs

Studies suggest around 60-70% of Tregs may express Helios to some degree in both mice and humans. Helios is implicated in Treg differentiation, and may differentiate between natural Tregs and induced Tregs, making Helios a key target of investigation (98, 163). Helios has been used in studies to differentiate subsets of both CD4+ and FoxP3+ Treg cells, and along with TIGIT co-expression, used to identify memory Tregs (110, 181). There are both Helios positive (Helios+) and Helios negative (Helios-) Tregs which differ in function. Helios+ cells are immunosuppressive whereas Helios- Tregs are less suppressive in nature (99, 110, 181). Elkord *et al.,* (2015) found Helios+ Tregs proliferate more readily than Helios-Tregs *in vitro* and secrete IL-10 but not IL-2 or IFNγ. This suggests Helios is a marker of activated Tregs which are more suppressive and stable than those who lack Helios expression (96, 99, 164). Fan and Lu (2016) also found Helios+ Tregs suppress TCR stimulation and antigen specific responses, whilst inhibiting IFNγ and IL-17 production. IL-12, a proinflammatory cytokine, targets Helios+ Tregs whereas anti-TNF$\alpha$ increases Helios- Tregs and inhibits Helios+ Treg expansion (52). TNF$\alpha$ alongside anti-IL-12 can lead to the expansion of Helios+ Tregs suggesting cues in the microenvironment could influence the Helios positive or negative phenotype of Tregs (52).

Interestingly, similar expression of Helios in Tregs which are FoxP3+ and RORγt+, i.e., '*plastic'* Tregs has also been seen (123). This thus offers the potential for Helios to play a role in Treg plasticity. Other studies have found that Helios+ Tregs lack Aiolos expression but express Eos, whereas Helios- contrastingly express Aiolos (96, 110). This supports the previous notion that whereas Aiolos is associated with pro-inflammatory cell phenotypes, Helios and Eos are associated with regulatory cells (110, 128, 177).

### 3.1.4 Ikaros is Key to Treg and Th17 Polarisation

Ikaros is extremely important for Th17 cell polarisation. Inhibition of Ikaros activity, inhibits production of IL-17 and Th17 associated cytokines and genes such as RORγt and IL-17 (123, 143). To promote a Th17 phenotype, Ikaros can repress FoxP3 and Tbx21 (143). Under Th17-polarising conditions, Ikaros results in histone modifications for Th17-associated genes promoting gene expression (143). Ikaros and Aiolos both silence the IL-1 locus which affects the IL-2/STAT5 pathway, a negative regulator of Th17, therefore they can regulate and promote Th17 formation (123). There are however some studies showing that Ikaros deletion in CD4+ T cells has no impact on IL-17 or RORγ under Th17 polarising conditions. These cells however had higher T-bet and IFNγ levels suggesting Ikaros may play an important role in other T cell subsets (123). Ikaros is certainly required for IL-10 production in CD4+ T cells (122). Global Ikaros knockout was found to result in reduction in both natural and peripheral Tregs (123). This therefore suggests Ikaros is needed for both Th17 and Tregs due to the normal inhibition pattern of TGF-β and FoxP3 (143). This supports a key role for Ikaros in promoting Th17 and a proinflammatory phenotype, whilst also suggesting Ikaros may play a role in regulating Treg and Th17 plasticity through its influence on both arms of the Treg/Th17 balance.

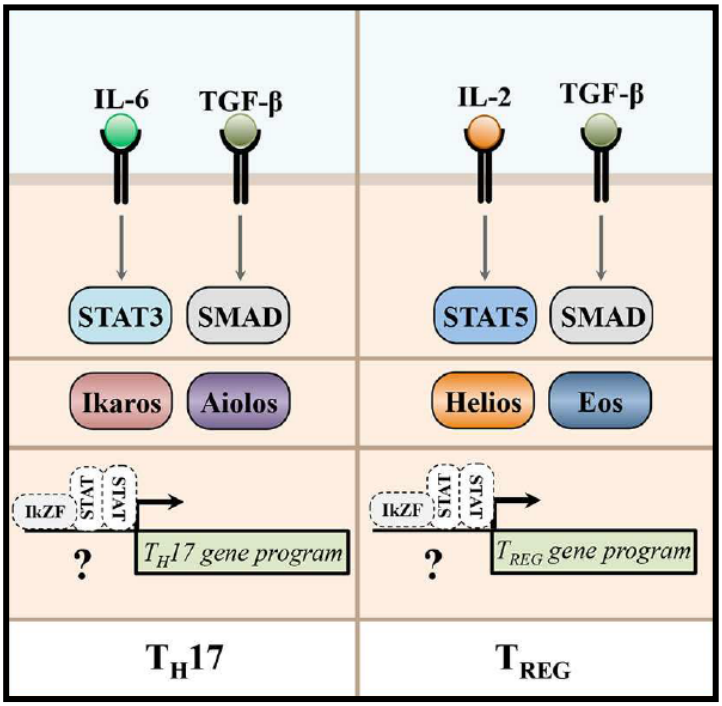



**Figure 3.1: Influence of Ikaros Family Members on Regulatory T Cell (Treg) and T helper 17 (Th17) Gene Expression**
Ikaros and Aiolos are implicated in the Th17 gene program through interactions between IL-6 and TGFB with STAT3 and SMAD respectively. Contrastingly, Helios and Ikaros are involved in Treg gene expression through IL-2 and TGF-B interactions with STAT5 and SMAD interactions. Questions remain around the activity and association of the transcription factors in regulating gene programs. Figure adapted from Powell *et al.,* 2019.

Together, previous studies of the Ikaros family show that the family is expressed and could potentially play a role in orchestrating the plasticity of Tregs and Non-Tregs (96-98, 123, 128, 143, 163, 177). Therefore, to begin this project, we confirmed the expression of the Ikaros family in these cell populations to corroborate our findings with known literature and confirm our detection methods and reagents were suitable for further experimentation on monocytes and macrophages which are the main focus of the thesis. As there are no viable commercial flow cytometry antibodies available

for either Eos or Pegasus, we used an unconjugated mouse anti-Eos antibody (Section 2.3.3) to identify its expression levels in sorted populations.

Our objectives for this chapter were thus:

I. To document Ikaros family expression in CD4+ Cells

II. To verify Treg and Non-Treg associated family members in our samples

III. To document if expression of family members was influenced by IBD-induced inflammation

## 3.2 Results

### 3.2.1 Sorting of Tregs Vs Non-Tregs from PBMCs

To identify Ikaros family expression within Treg and Non-Treg populations, we cell sorted these populations from total PBMCs (section 2.3.4). Tregs were identified as $CD3^{+}CD4^{+}CD127^{low}CD25^{high}$ and Non-Tregs as $CD3^{+}CD4^{+}CD25^{-}CD127^{low/-}$ using the gating strategy described below in Figure 3.2. Sorting for Tregs vs Non-Tregs from PBMCs was confirmed at both a protein level using Flow Cytometry and RNA level using FoxP3 as a marker of Tregs in qPCR. Using qPCR in Figure 3.3, RNA expression levels of FoxP3 were significantly higher ($p<0.01$) in Tregs in comparison to Non-Tregs where there was little to no expression of the Treg-identifying transcription factor, confirming sorting of cell populations.

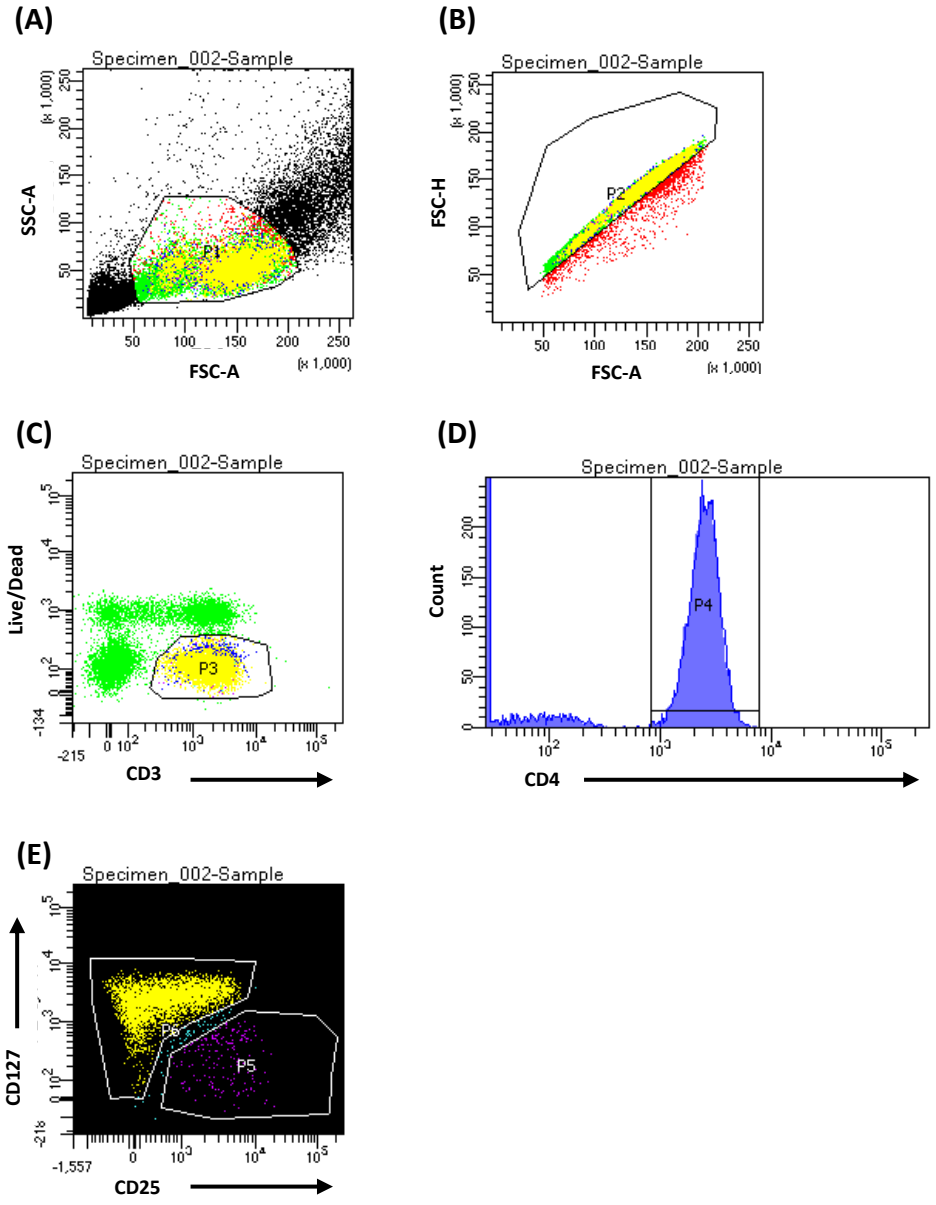



**Figure 3.2: Gating Strategy For Sorting of Tregs and Non-Tregs From Peripheral Blood Mononuclear Cells (PBMCs)**

**(A)** Cells were gated out from debris and then **(B)** Singlets were gated with doublets excluded. **(C)** CD3+ cells and cells which were Live/Dead stain negative were gated out from the cell population with **(D)** CD4+ positive cells selected from this group. **(E)** Tregs were identified as those which expressed $CD3^{+}CD4^{+}CD127^{low}CD25^{high}$ and Non-Tregs as those which expressed $CD3^{+}CD4^{+}CD25^{low}CD127^{low/med}$. Representative blots derived from MoFlo Astrios Cell Sorter are shown. *N=4. P; Gated populations, P1; Lymphocytes, P2; Singlets, P3; CD3+Live/Dead- Cells, P4; CD4+ Cells, P5; Tregs, P6; Non-Tregs.*

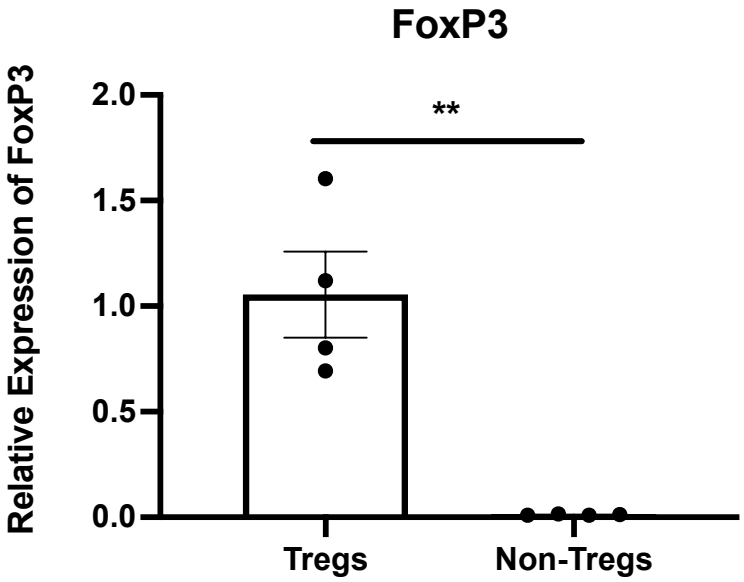



**Figure 3.3: Confirming Treg Vs Non-Treg Sorting Through Expression of FoxP3** Tregs and Non-Tregs were sorted from blood derived peripheral blood mononuclear cells from Hemochromatosis blood. Total RNA was isolated from each population and levels of FoxP3 were analysed via qPCR to confirm that the cells had been sorted into Tregs ($CD3+CD4+CD25^{high}CD127^{low}$) and Non-Tregs ($CD3+CD4+CD25^{low}$ $CD127^{med/high}$). Data was normalised to Tregs. Results are presented as mean ± SEM. *N=4,* FoxP3 ** $p<0.01$, *unpaired T Test. Housekeeping Gene: RPS9.*

### 3.2.2. Expression of Ikaros Family Members in Treg Populations

From these sorted populations, total RNA was isolated, and qPCR used to assess Ikaros family expression (Figure 3.4). Levels of Ikaros, Aiolos and Pegasus were comparable in both Tregs and Non-Tregs populations. Contrastingly, expression of Eos was significantly higher ($P<0.05$) in Tregs in comparison to Non-Tregs. Similarly, expression of Helios was four-fold higher in Tregs ($p<0.01$) in comparison to Non-Tregs.

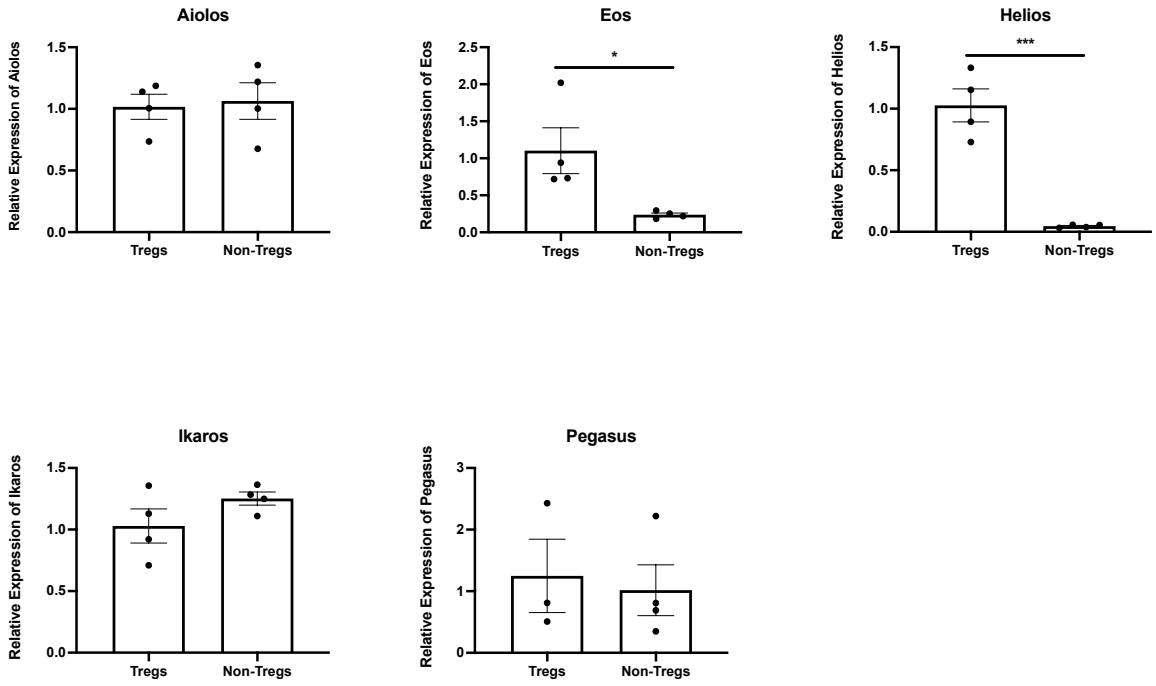



**Figure 3.4: Expression of the Ikaros Family in Sorted Tregs and Non-Tregs**
Tregs (CD3+CD4+CD25$^{high}$CD127$^{low}$) and Non-Tregs (CD3+CD4+CD25$^{low}$ CD127$^{med/high}$) were sorted from blood derived peripheral blood mononuclear cells from Hemochromatosis blood. Total RNA was isolated from each population and levels of the Ikaros Family of Transcription Factors were then analysed via qPCR. Data was normalised to Tregs. Results are presented as mean ± SEM. *N=4, Eos * p<0.05; Helios ***, unpaired T Test. Housekeeping Gene: RPS9.*

### 3.2.3 Protein Expression of The Ikaros Family in Tregs and Non-Tregs

Next, we analysed Ikaros family protein expression by flow within Treg and Non-Treg populations, using the gating strategy described in Figure 3.5. Mean Fluorescence Intensity (MFI) values of the Ikaros family in Tregs and Non-Tregs (Figure 3.6) suggest that Ikaros was abundantly expressed at protein level in both cell populations, in agreement with the PCR data. There was moderate expression of Eos which was possibly higher in Tregs and similar moderate expression of Aiolos in both cell types. In contrast to the PCR data, Helios was only expressed to a low level in the Treg populations.

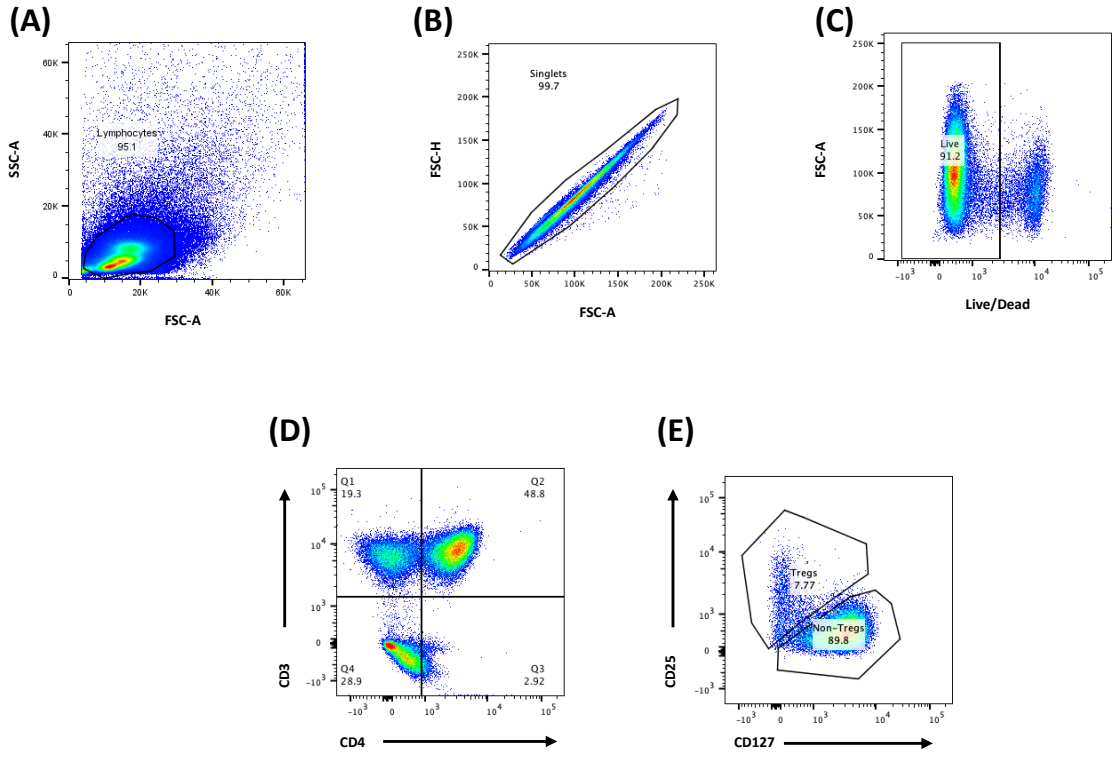



**Figure 3.5: Gating Strategy For Identifying Treg and Non-Treg Populations**
**(A)** Cell populations were identified and gated out from debris and then from the lymphocyte population **(B)** Singlets were gated with doublets excluded. **(C)** Live/Dead stain negative cells gated out from the cell population with **(D)** CD4+ and CD3+ double positive cells selected from this group. **(E)** Tregs were identified as $CD3^{+}CD4^{+}CD127^{low}CD25^{high}$ and Non-Tregs as $CD3^{+}CD4^{+}CD25^{low}CD127^{low/med}$. Representative images shown. *N=4.*

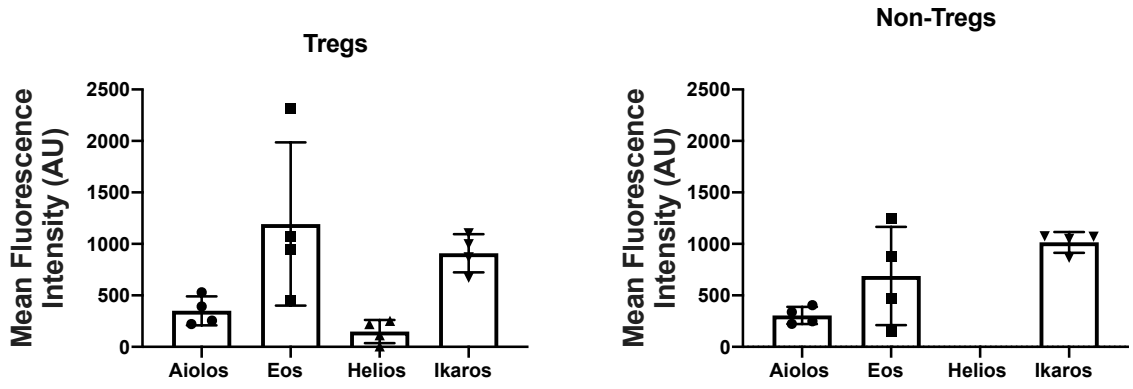



**Figure 3.6: Expression of the Ikaros Family in Tregs and Non-Tregs**
Tregs (CD3+CD4+CD25$^{high}$CD127$^{low}$) and Non-Tregs (CD3+CD4+CD25$^{low}$ CD127 $^{med/high)}$ were gated from total blood derived peripheral blood mononuclear cells from Hemochromatosis blood and analysed by Flow Cytometry using FlowJo V10 software. Levels of the Ikaros Family of Transcription Factors were then assessed in both populations. Results are presented as mean ± SEM. *N=4. NS. One Way ANOVA.*

### 3.2.4 Mild UC Inflammation is Associated with Lower Expression of the Ikaros Family

With our findings supporting previous literature (96-98, 123, 128, 143, 163, 177), we next decided to investigate the impact of inflammation in the context of IBD on Ikaros family expression in PBMCs. We used PCR to assess RNA levels of the Ikaros family present in circulating CD4+ T cells from HFE and mildly inflamed UC patients (Figure 3.7). Comparison of HFE CD4+ T cells and those from UC showed that relative expression levels of Aiolos, Eos and Helios were similar in both. Expression of Ikaros ($p<0.05$) and Pegasus ($p<0.001$) were found to be significantly lower in CD4+ peripheral cells from patients with UC, with almost a 50% decrease in Pegasus expression.

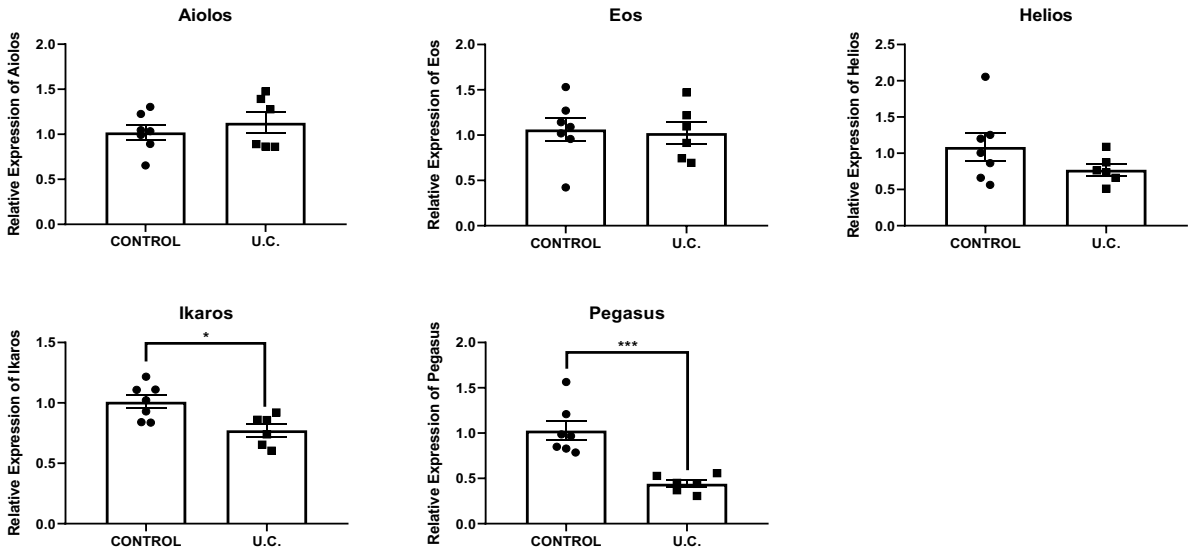



**Figure 3.7: Relative Expression Levels of Helios, Ikaros and Pegasus are Lower in Ulcerative Colitis in Comparison to Hemochromatosis**

CD4 expressing peripheral blood mononuclear cells were isolated from hemochromatosis (HFE) blood (Control) and ulcerative colitis (U.C) patient blood. RNA was extracted and expression of Ikaros Family Transcription Factors measured by qPCR. Expression is shown for each group relative to the level in Control. Results are presented as mean ± SEM*. HFE N=7; U.C. N=6, Ikaros p<0.05; Pegasus p<0.001, Unpaired T Test. Housekeeping Gene: RPS9.*

## 3.3 Discussion

Our results here are consistent with previous findings reporting Eos and Helios expression is significantly associated with Tregs and the regulatory phenotype, with slightly higher expression of Aiolos and Ikaros in Non-Treg populations (Figures 3.4 & 3.6) (97, 109, 110, 119, 128, 135, 136, 159). We have also identified novel Pegasus expression in both cell populations. At a global CD4+ T cell level, our study shows that the Ikaros family is impacted by inflammation, with lower levels of Ikaros, Pegasus and Helios in peripheral blood from UC patients in comparison to Control (Figure 3.7). It is necessary to acknowledge that we used blood from HFE donors rather than healthy controls as a comparator, and there are reports of altered lymphocyte phenotype and function in this context (182, 183). Thus, we should repeat our analysis using age matched healthy donors. Nevertheless, it is possible that either Helios, Ikaros and possibly Pegasus positive cells may be recruited into tissue as a consequence of IBD or the systemic inflammatory effects of the disease alter expression. As levels of both the Treg and Th17-associated transcription factors were lower, this supports previous data from our lab which has shown inflammation influences both branches of the Treg and Th17 balance (Section 3.1). Similarly, since there is increased presence of Treg and Th17-associated transcription factors due to greater Th17 cells and Th17-cell mediators within IBD, we can hypothesise that these cells may be present in the bowel rather than periphery (3). For Pegasus, there is no publicly available data on its expression within CD4+ T cells in disease, or in IBD, thus our results here provide novel insight into its expression in disease.

A significant reduction within Ikaros expression in UC samples also signifies that mild inflammation within the bowel has systemic effects on Ikaros expression. However, one might expect an increase in Ikaros expression as previous studies on blood cells

have suggested elevated Ikaros levels correlate with disease (184). Although reagents used to identify the protein and sources of cells vary between labs, our data suggests a reduced expression in active disease. Lower levels of Ikaros in T cells has been associated with lymphoid malignancy and there is certainly an increased cancer risk in patients with IBD (117, 185, 186). This lack of Ikaros could in turn lead to the activation of genes normally regulated or repressed by Ikaros leading to disease (109). We also know that elevated Ikaros levels have been reported in lymphocytes and macrophages within the bowel and liver tissue so we may again be seeing a reduction of positive cells in the periphery (187, 188). Notably as patients within our study had mild UC inflammation, and we were not able to fully compare protein and mRNA levels for all family members in all cell subpopulations we need further work to confirm our findings. Isolating PBMCs from patients with moderate or severe IBD, and healthy controls could help us investigate this hypothesis. Thus, as we delve into the next chapter, we look at Ikaros levels within tissue to gain an insight to Ikaros family expression at the site of inflammation.

### 3.3.1 Summary

To begin my thesis, I have tested the reagents available to me by confirming that the Ikaros family of proteins are expressed in Tregs and Non-Tregs, with the data supporting previous reports. Novel data in regard to expression of Pegasus in particular was also generated but needs confirmation. Most interestingly, analysis of peripheral CD4+ T Cells from patients with mild UC demonstrated lower levels of Helios, Ikaros and Pegasus in comparison to Control, implicating the Ikaros family in IBD. In the next chapter, we move on to discuss expression of the Ikaros family within bowel tissue and the implications of their expression in disease pathology.

# Chapter 4: Ikaros Family Expression Within The Bowel And Liver

## 4.1 Introduction

In the previous Chapter, I was able to demonstrate how IBD was able to influence systemic Ikaros family expression levels in CD4+ T Cells. In this next Chapter, I document the histological effects of bowel inflammation in the form of CD and UC on bowel structure and then introduce the concept of Ikaros family expression in the bowel. As I was based within the Centre for Liver and Gastrointestinal Research (CLGR) at UoB, I was also able to access liver tissue from a mixture of Donor and autoimmune liver diseases. Not only was this useful in optimisation of experiments, Ikaros family expression is seldom studied within the liver, particularly in PSC-IBD and therefore would provide us with novel insights. Having previously introduced the bidirectional relationship between the gut and the liver in the introduction, we hypothesise that the Ikaros family could play a potential role in mediating immune response within the gut-liver axis.

The objectives of this Chapter were therefore to:

I. Verify if the Ikaros Family is expressed within bowel and liver tissue
II. Identify which cells express Ikaros family members
III. Determine what happens to Ikaros Family expression levels in diseased tissue

## 4.2 Results

In this investigation I had access to blood samples from healthy individuals and patients with either IBD or chronic liver disease as comparators. I was also able to source formalin fixed tissue samples from inflamed and uninflamed bowel resections and fresh tissue from liver explant material or donors not used for transplantation. These formed the basis for my analysis of Ikaros family expression. Table 4.1 shows demographic data from the NASH and PSC liver tissue used in this project.

**Table 4.1: Demographic Results For Liver Transplant Patients With Non-alcoholic Steatosis (NASH) and Primary Sclerosing Cholangitis (PSC) Used in this Investigation**

| DISEASE | GENDER | AGE (Years) | HEIGHT (M) | WEIGHT (KG) | BMI | DIAGNOSIS (PATHOLOGY) | AST (IU/L) | ALT (IU/L) | ALP (IU/L) | BILIRUBIN (µmol/L) | MELD SCORE | GGT (IU/L) | ALBUMIN (g/L) | CRP (mg/L) |
|---|---|---|---|---|---|---|---|---|---|---|---|---|---|---|
| NASH | F | 68 | 1.64 | 75.4 | 28.03 | NASH | | 541 | 35 | 60 | N | | 20 | 12 |
| NASH | F | 55 | 1.68 | 62.1 | 22 | NAFLD / HFE | | N | N | 124 | 23 | | 35 | 5 |
| NASH | M | 48 | 1.74 | 126.6 | 41.82 | NASH | | 26 | 111 | 18 | 9 | | 39 | 3 |
| NASH | F | 67 | 1.67 | 69 | 24.74 | NASH | | 1491 | 58 | 78 | N | | 33 | 21 |
| NASH | M | 50 | 1.74 | 106.3 | 35.11 | NASH | N | 29 | 136 | 136 | 20 | n | 35 | 3 |
| NASH | M | 58 | 1.82 | 115.5 | 34.87 | NASH | N | N | 101 | 31 | 15 | 47 | 40 | N |
| NASH | F | 62 | 1.55 | 86.6 | 36.05 | NASH | 40 | 22 | 196 | 22 | N | 134 | 36 | N |
| PSC | F | 50 | 1.7 | 76.7 | 26.85 | PSC | 71 | 42 | 314 | 29 | N | 105 | 26 | N |
| PSC | F | 26 | 1.58 | 49.8 | 19.95 | PSC | | 696 | 304 | 31 | 8 | | 27 | 26 |
| PSC | F | 51 | 1.74 | 70.8 | 23.38 | PSC | | 493 | 213 | 74 | 13 | | 34 | 57 |
| PSC | M | 50 | 1.8 | 96.6 | 29.81 | PSC | | 857 | 295 | 54 | 52 | | 20 | 24 |
| PSC | M | 30 | 1.86 | 83.3 | 25.32 | PSC | 171 | 75 | 504 | 169 | 18 | 138 | 31 | N |
| PSC | F | 60 | 1.55 | 51.8 | 21.56 | PSC | N | 571 | 44 | 73 | N | N | 32 | 29 |
| PSC | F | 64 | 1.86 | 59.4 | 24.72 | PSC | N | 48 | 999 | 77 | N | N | 36 | N |
| PSC | M | 36 | 1.7 | 62.8 | 21.73 | PSC | N | 122 | 1111 | 266 | 17 | N | 35 | 17 |
| PSC | M | 22 | 1.92 | 76.4 | 20.72 | PSC | N | 1595 | 657 | 129 | N | N | 24 | 24 |

Liver function clinical data collected prior to or at time of transplant including Albumin (g/L), Bilirubin(µmol/L), C-Reactive Protein (mg/L), Alkaline Phosphatase (ALP, IU/L), Alanine Aminotransferase (ALT, IU/L) Aspartate Transaminase (AST, IU/L), Gamma-glutamyl transferase (GGT, IU/L) MELD Score (Model for End-Stage Liver Disease) were collected pre- Non-alcoholic Steatosis (NASH) and Primary Sclerosing Cholangitis (PSC) patient surgery. The age, height, weight, Body Mass Index (BMI) and official clinical diagnosis (from Pathology team QEHB) were also recorded. *NASH = N=7, PSC = N=9.*

### 4.2.1 Inflammatory Bowel Disease Upsets the Normal Structure of the Bowel

Comparing the structure of 'healthy', CD and UC bowel as means to assess level of inflammation is a technique used in the clinical setting to diagnose patients with the various stages of IBD. Therefore, I also began by using H&E staining of tissue sections to document the structural differences between 'normal' or healthy, CD and UC bowel tissue available to me. Figure 4.1 shows a representative image of the normal histological appearance of the colon in which the *mucosa*, the *muscularis mucosa* and the *submucosa* can be identified. Each compartment is highly defined and segregated from the other regions enabling easy identification of the structural components of the bowel. Highly organised crypt structures are visible throughout the mucosa embedded within the stroma, containing epithelial cells on the outer crypt and goblet cells towards the lumen. In Figure 4.1A, the submucosa containing connective tissue can be seen, followed by a layer of smooth muscle known as the muscularis mucosa. At the bottom, the mucosa containing numerous crypts surrounded by the multicellular (including macrophages and lymphocytes) containing stroma can be identified. The crypts (Figure 4.1B) are highly organised structures surrounded by myofibroblasts, containing a ring of epithelial cells on the outside, followed by mucus-secreting goblet cells outside of the lumen of the crypt structure. This highly organised structure enables efficient function of bowel tissue.

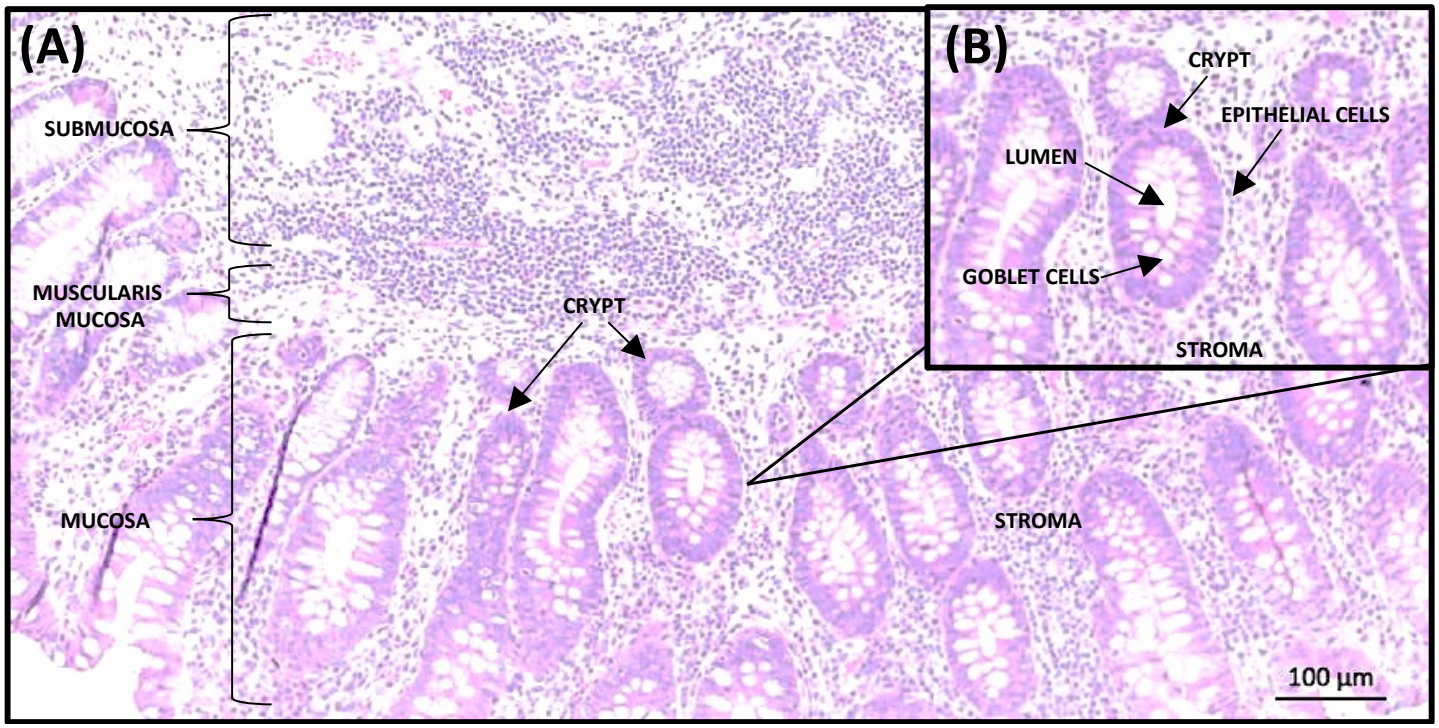



**Figure 4.1: Structure of the Normal Colon**
Haematoxylin and Eosin staining of Formalin-Fixed Paraffin-Embedded (FFPE) was used to stain the nucleus and organelles within a section of normal colon tissue. **(A)** Annotated section of normal colon highlighting the distinct layers and key components of the tissue. **(B)** Magnified cross section of a crypt and stroma. Scale bar represents 100 µm. Representative images are shown. Magnification x20. *N=1.*

### 4.2.2 Crohn's Disease and Ulcerative Colitis Disrupts Bowel Structure

In contrast to healthy, the architecture of the colon becomes profoundly altered in disease. Figure 4.2 shows a representative image of a colon biopsy from a patient with CD undergoing a routine scoping to assess severity of IBD. Analysis of a cross section from this CD biopsy shows the extent to which inflammation damages the architecture of the bowel tissue. Alongside disruptions in the organisation of the bowel tissue, structures within the bowel become enlarged due to inflammation and influx of immune cells. There is also disruption in the organisation of the mucosa/submucosa with areas merging due to inflammation. The uniformed structure of the crypt is disrupted with a mixture of crypt elongation and crypt abscesses readily observed.

Similar to CD, in UC, inflammation can be observed throughout the bowel tissue, with problems in identifying the distinct anatomical regions of the bowel due to disfiguration resulting from inflammation. Figure 4.3 shows a representative section of UC colon in which structures within the bowel appear enlarged and there are no distinct compartments visible. Large granulomas are observed throughout the tissue owing to the infiltration of immune cells within the mucosa. Alongside this, there is a distinct loss of the usual crypt structure due to crypt abscesses, with the stroma infiltrated with lymphocytes.

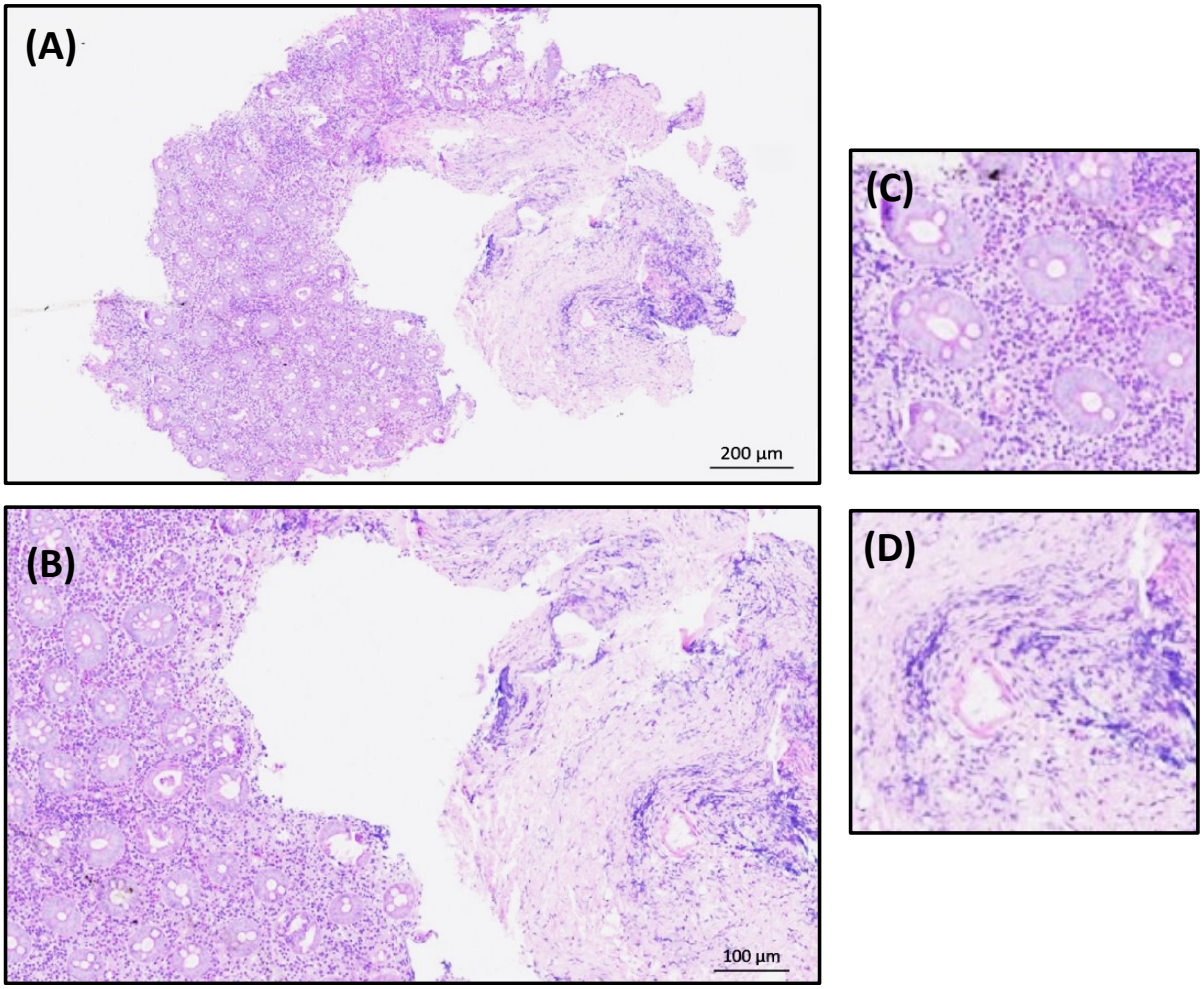



**Figure 4.2: Haematoxylin and Eosin Staining of Crohn's Diseased Tissue**
Haematoxylin and Eosin staining of Formalin-Fixed Paraffin-Embedded (FFPE) tissue was used to stain the nucleus and the organelles within a section of Crohn's Disease bowel biopsy. **(A**) Image depicting the total area of the biopsy. Scale bar represents 200 µm. **(B)** Closer image of biopsy identifying structures within the tissue. Scale bar represents 100 µm. From B, magnification of the mucosa **(C)** highlighting altered crypt structure and **(D)** submucosa displaying an inflamed vessel along with inflammatory cell accumulation. Representative images are shown. Magnification x20. *N=1*

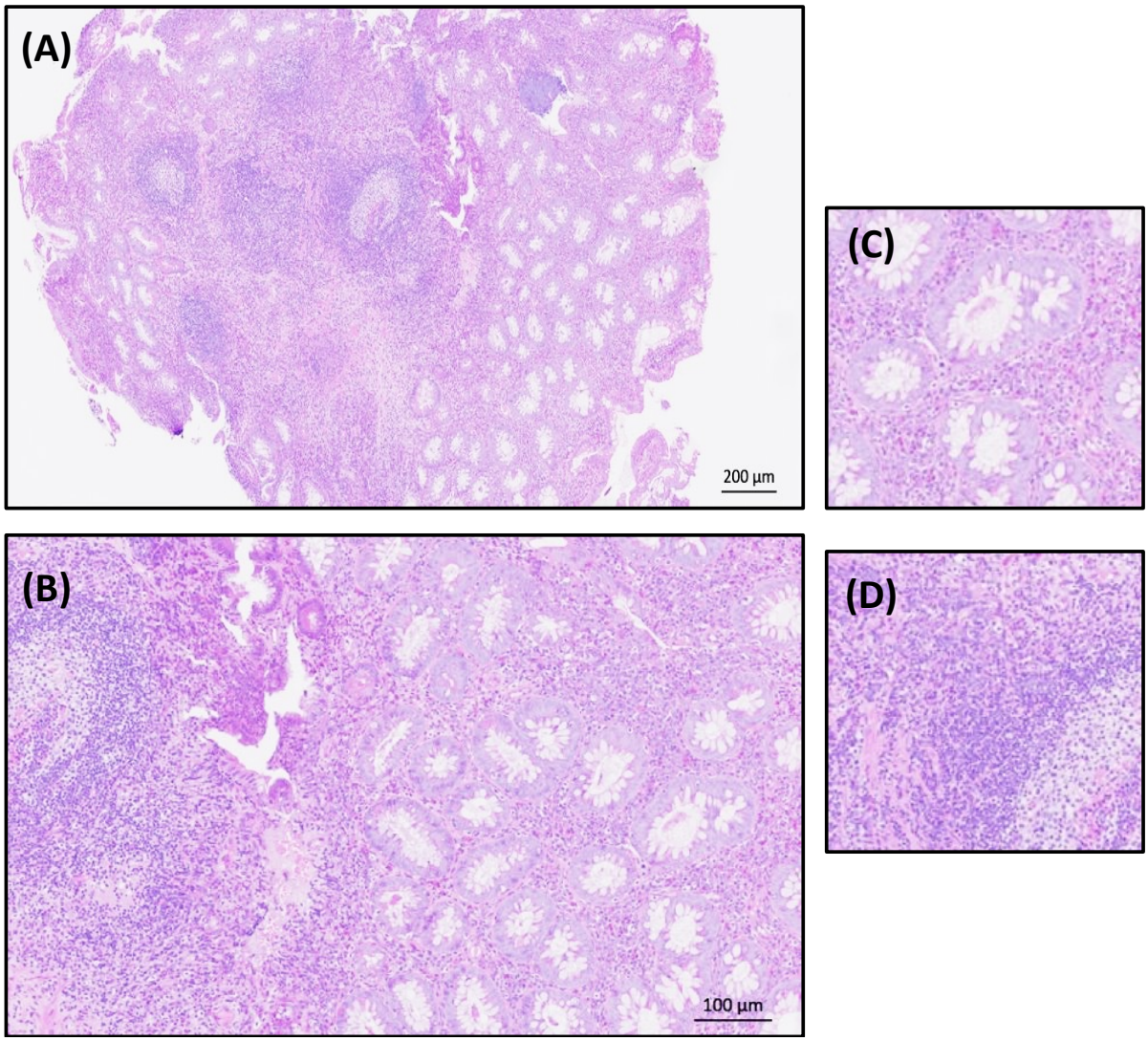



**Figure 4.3: Haematoxylin and Eosin Staining of Ulcerative Colitis Bowel Tissue**
Haematoxylin and Eosin staining of Formalin-Fixed Paraffin-Embedded (FFPE) tissue was used to stain the nucleus and the organelles within a section of Ulcerative Colitis bowel biopsy. **(A)** Image depicting the total area of the biopsy. Scale bar represents 200 µm. **(B)** Closer image of biopsy identifying structures within the tissue. Scale bar represents 100 µm. From B, magnification of the mucosa **(C)** showing enlarged crypts and **(D)** submucosa displaying inflammatory loci. Representative images are shown. Magnification x20. *N=1.*

### 4.2.3 The Ikaros Family is Expressed Within the Bowel Tissue

Previous studies have described expression of the Ikaros family in various cellular populations, and organs such as the liver, however data on the expression of the family in bowel is limited (110, 118). Therefore, we began this study by assessing the expression of the family in inflamed and uninflamed FFPE colon sections. Using DAB-IHC, the protein expression of all Ikaros family members was assessed in inflamed vs non-inflamed matched tissue. Our results show that all members of the Ikaros family were expressed within the bowel structure, with expression of family members upregulated during inflammation (Figures 4.4-4.8). Expression of the transcription factors was seen dispersed throughout the mucosa during inflammation, with concentrated expression observed in granulomas. To quantify the *'amount'* of protein present, the percentage area DAB positive was determined by randomly selecting regions (*n*) from each '*N*', and Image J software used to determine arbitrary values for positive staining. Results were normalised to matched tissue stained with either a Rabbit or Mouse IgG and then averaged for each *N*.

Expression of Aiolos was found throughout the bowel section, with higher levels of Aiolos positive areas in inflamed tissue in comparison to non-inflamed. Staining for Aiolos was observed within the crypt and stroma in the mucosa, within lymphocytes. Similarly, levels of Eos were found to be higher in inflamed tissue in comparison to non-inflamed tissue. Within the inflamed tissue, expression was seen within the mucosa in lymphocytes throughout the tissue around the crypts within the stroma. Both Helios and Ikaros were also elevated in inflamed tissue in comparison to non-inflamed, with Ikaros expression possessing the highest protein expression in inflamed tissue in comparison to all other transcription factors. Expression of both transcription factors was seen within lymphocytes in inflamed tissue. Ikaros expression in the

representative image was greatly upregulated in the submucosa, with heavy clusters of lymphocytes within granulomas observed. Pegasus contrastingly had the lowest protein expression out of all the transcription factors, with similar expression levels of the protein observed in both inflamed and non-inflamed tissue. Expression of Pegasus was seen within the stroma in lymphocytes in both inflamed and uninflamed tissue.

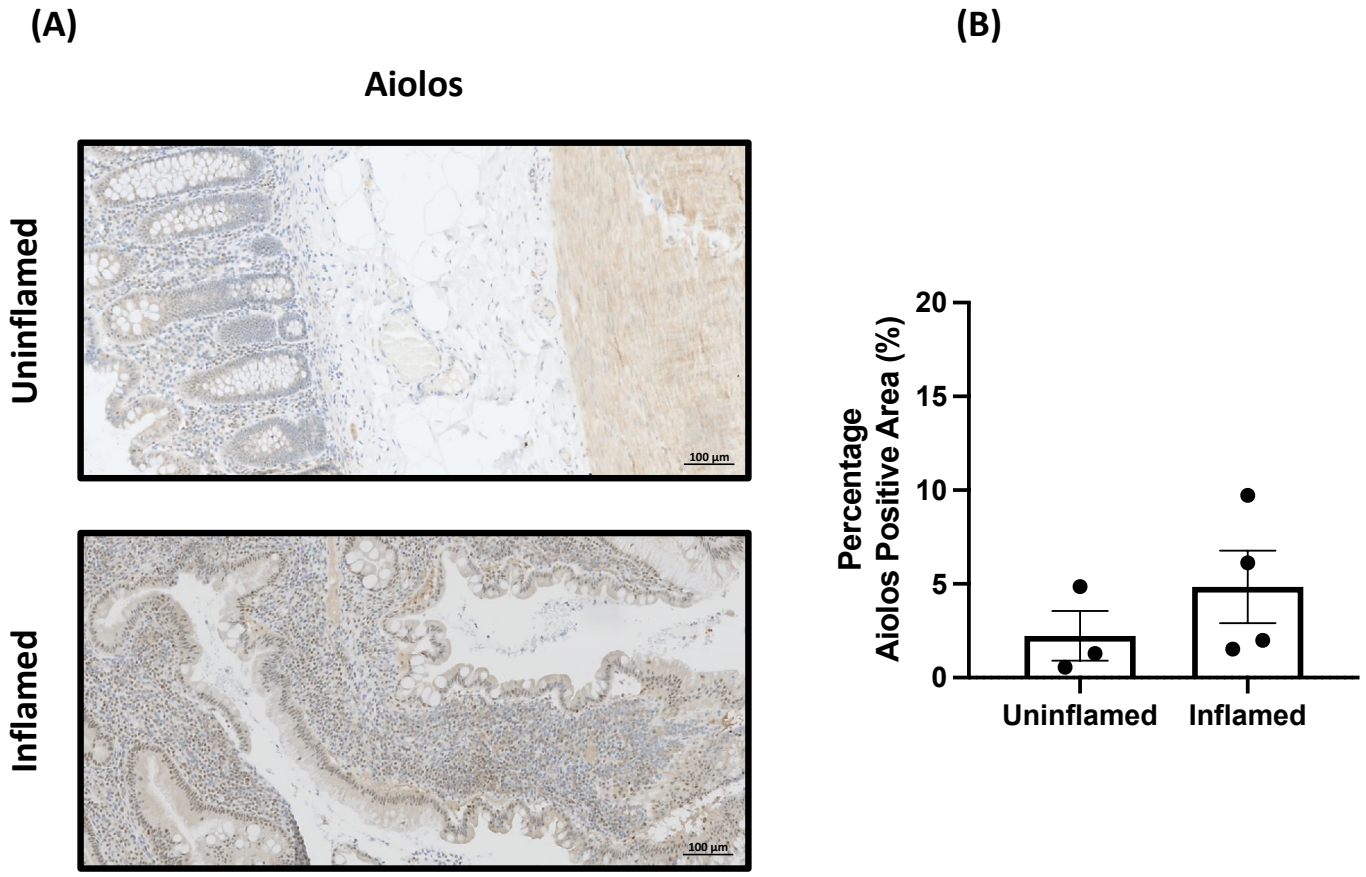



**Figure 4.4: Expression of Aiolos in Uninflamed and Inflamed Bowel**
**(A)** 3,3'-diaminobenzidine (DAB) staining was used to assess the presence of Aiolos in both inflamed and uninflamed bowel tissue. Haematoxylin was used for nuclear staining. **(B)** The percentage Aiolos Positive Area (%) was determined by randomly selecting 5-8 regions (*n*) from each sample (N) and Image J software used to determine values for positive DAB staining. Dots represent average staining of regions (*n*) in each *N*. Results are normalised to appropriate IgG controls and presented as Mean ± SEM. Representative images are shown. Magnification x20. Scale Bar represents 100µm. *Non-Inflamed, N=3, n=20; Inflamed, N=4, n=26. NS. Unpaired T Test.*

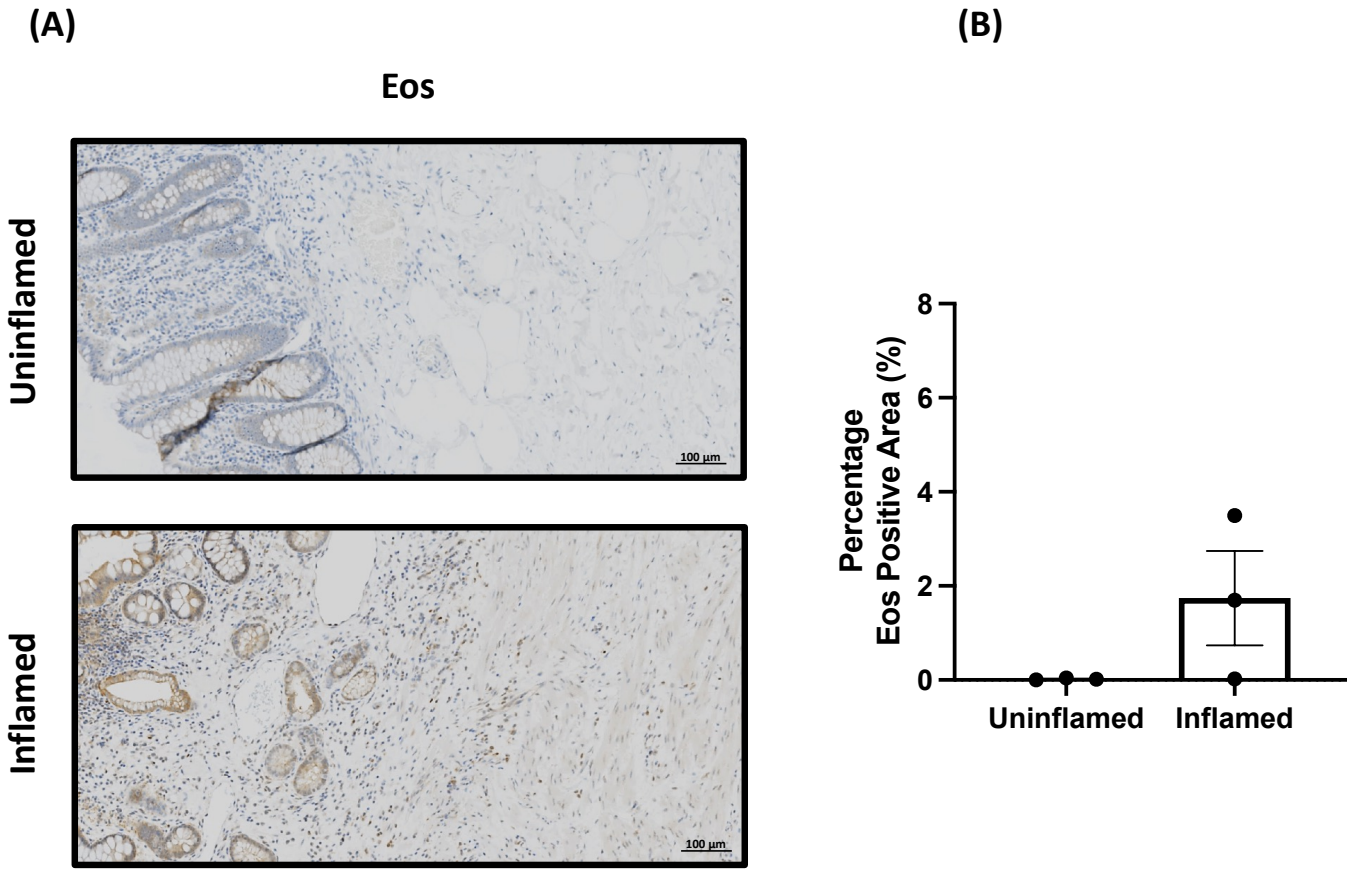



**Figure 4.5: Eos Expression in Inflamed Bowel in Comparison to Uninflamed**
**(A)** 3,3'-diaminobenzidine (DAB) staining was used to assess the presence of Eos in both inflamed and uninflamed bowel tissue. Haematoxylin was used for nuclear staining. **(B)** The percentage Eos Positive Area (%) was determined by randomly selecting 5-8 regions (*n*) from each sample (N) and Image J software used to determine values for positive DAB staining. Dots represent average staining of regions (*n*) in each *N*. Results are normalised to appropriate IgG controls and presented as Mean ± SEM. Representative images are shown. Magnification x20. Scale Bar represents 100µm. *Non-Inflamed, N=3, n=20; Inflamed, N=4, n=25. NS. Unpaired T Test.*

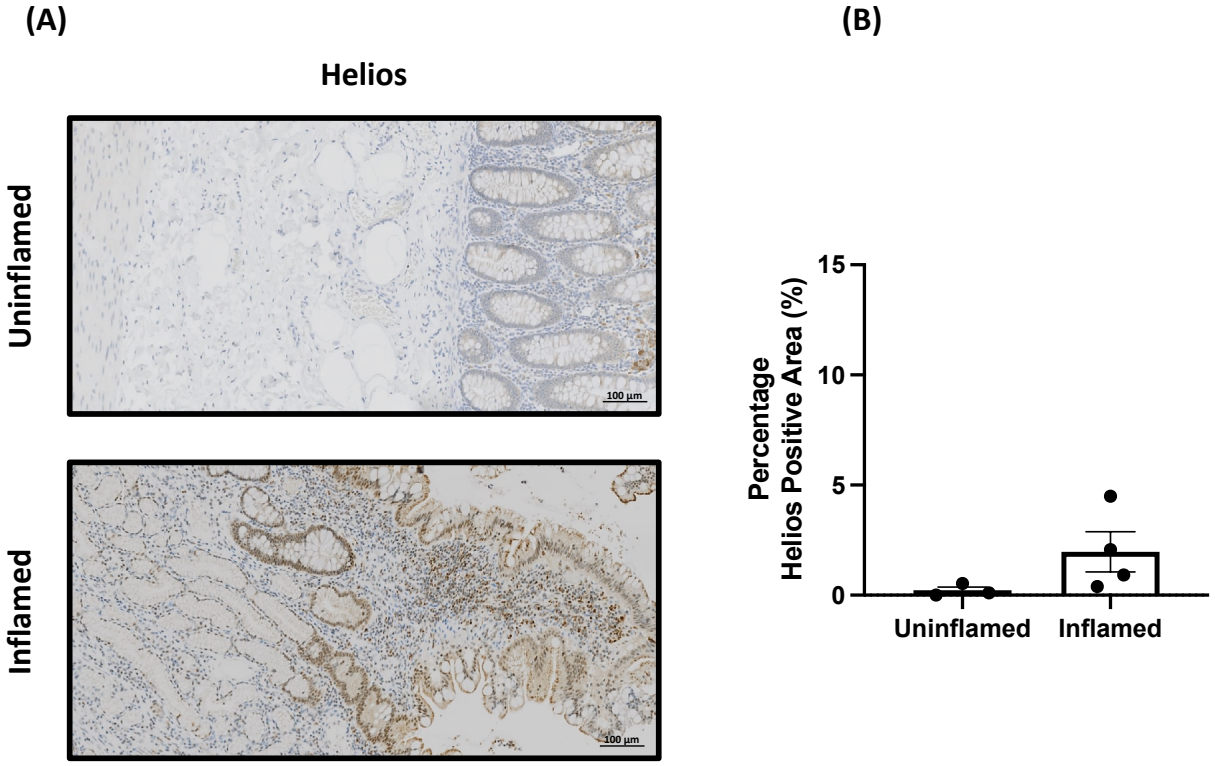



**Figure 4.6: Expression of Helios in Uninflamed and Inflamed Bowel**
**(A)** 3,3'-diaminobenzidine (DAB) staining was used to assess the presence of Helios in both inflamed and uninflamed bowel tissue. Haematoxylin was used for nuclear staining. **(B)** The percentage Helios Positive Area (%) was determined by randomly selecting 5-8 regions (n) from each sample (N) and Image J software used to determine values for positive DAB staining. Dots represent average staining of regions (n) in each N. Results are normalised to appropriate IgG controls and presented as Mean ± SEM. Representative images are shown. Magnification x20. Scale Bar represents 100µm. Non-Inflamed, N=3, n=19; Inflamed, N=4, n=30. *NS*. Unpaired T Test.

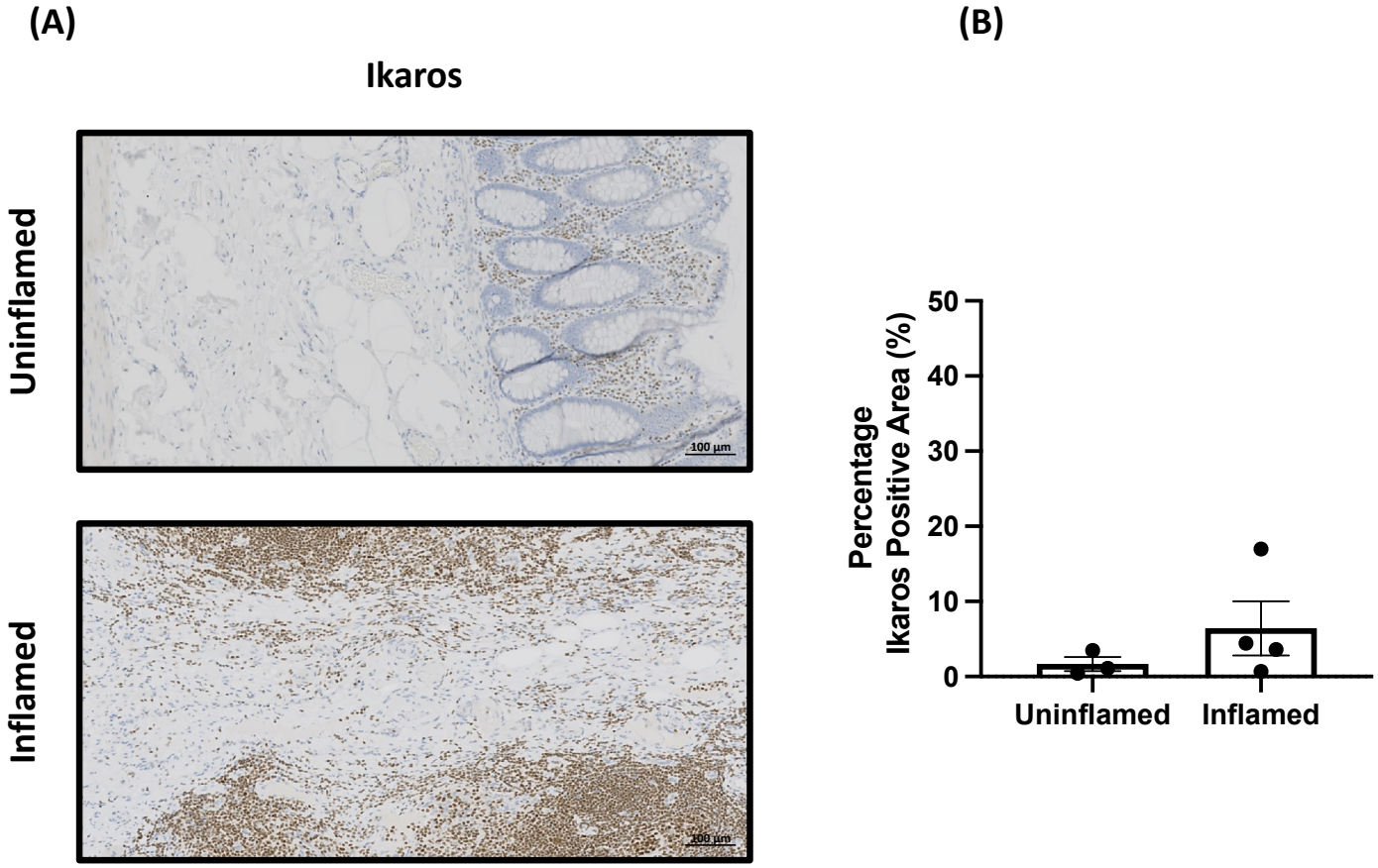



**Figure 4.7: Ikaros Expression in Inflamed Bowel in Comparison to Uninflamed**
**(A)** 3,3'-diaminobenzidine (DAB) staining was used to assess the presence of Ikaros in both inflamed and uninflamed bowel tissue. Haematoxylin was used for nuclear staining. **(B)** The percentage Ikaros Positive Area (%) was determined by randomly selecting 5-8 regions (*n*) from each sample (N) and Image J software used to determine values for positive DAB staining. Dots represent average staining of regions (*n*) in each *N*. Results are normalised to appropriate IgG controls and presented as Mean ± SEM. Representative images are shown. Magnification x20. Scale Bar represents 100µm. *Non-Inflamed, N=3, n=20; Inflamed, N=4, n=27. NS. Unpaired T Test.*

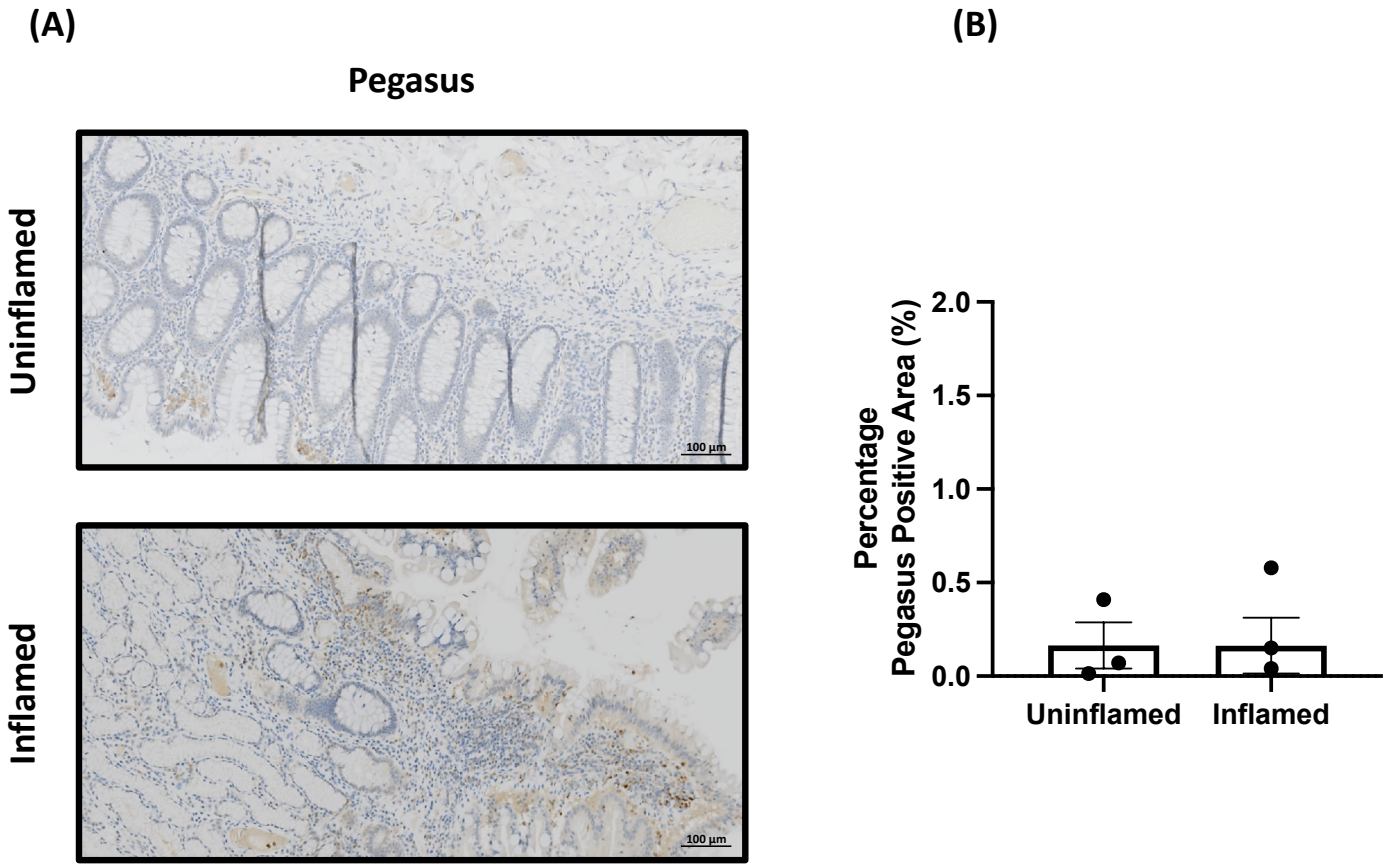



**Figure 4.8: Expression of Pegasus in Uninflamed and Inflamed Bowel**
**(A)** 3,3'-diaminobenzidine (DAB) staining was used to assess the presence of Pegasus in both inflamed and uninflamed bowel tissue. Haematoxylin was used for nuclear staining. **(B)** The percentage Pegasus Positive Area (%) was determined by randomly selecting 5-8 regions (*n*) from each sample (N) and Image J software used to determine values for positive DAB staining. Dots represent average staining of regions (*n*) in each *N*. Results are normalised to appropriate IgG controls and presented as Mean ± SEM. Representative images are shown. Magnification x20. Scale Bar represents 100µm. *Non-Inflamed, N=3, n=20; Inflamed, N=4, n=27. NS. Unpaired T Test.*

### 4.2.4 Higher Expression of Aiolos and Ikaros mRNA is Found in Diseased Tissue Samples

To further quantify the effect of disease on Ikaros family expression within the bowel, I performed qPCR on samples from non-diseased (referred to as '*Healthy'* below) and UC bowel tissue. RNA was extracted from biopsies from UC patients and Healthy donors and qPCR conducted (Figure 4.9). Comparison of Healthy and UC biopsies found that UC samples exhibited higher relative expression levels of both Ikaros and Aiolos. Contrastingly, levels of Eos, Helios and Pegasus were found to be similar in both patient groups.

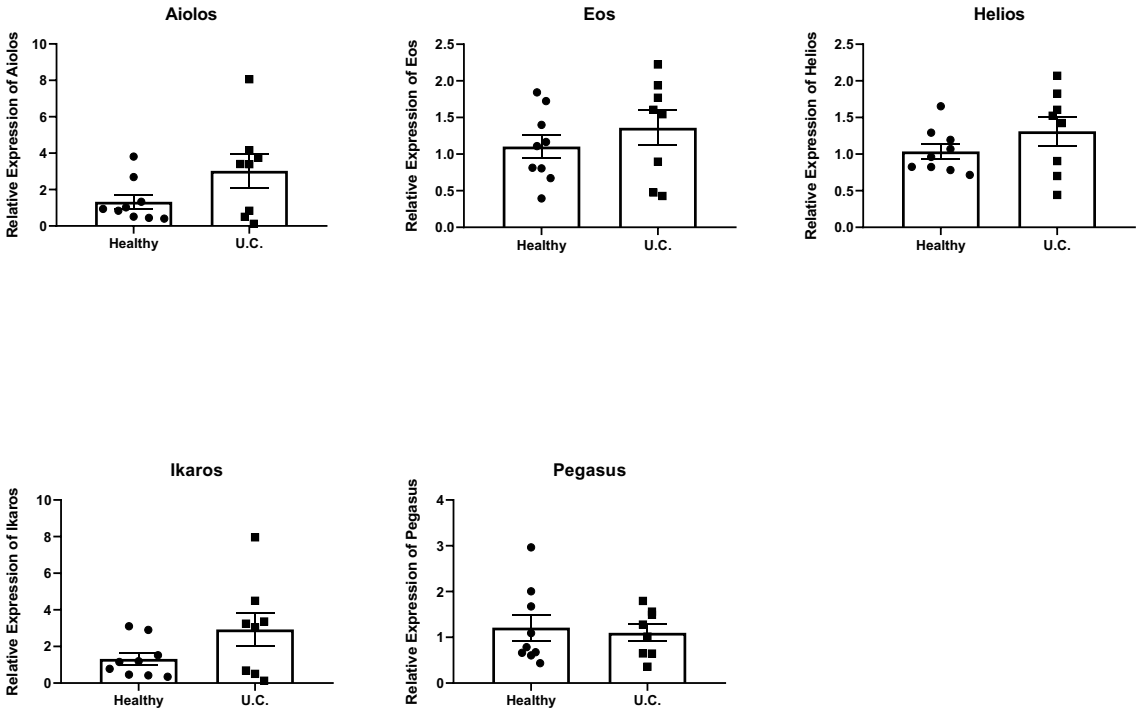



**Figure 4.9: Relative Expression Levels of Aiolos and Ikaros is Higher in Biopsies From Patients With UC in Comparison to Healthy Donors**

Total RNA was extracted from healthy donor (Healthy) and Ulcerative Colitis (U.C.) bowel biopsies and expression of the Ikaros Family of Transcription Factors measured by qPCR. Expression is shown for each group relative to the level in healthy donors. Symbols represent individual biopsies. Results are presented as mean ± SEM. *Healthy N=9; UC N= 8, NS. Unpaired T-test. Housekeeping Gene: RPS9.*

### 4.2.5 Liver Inflammation Perturbs Liver Structure

As PSC is a disease of interest in relation to IBD, we also decided to investigate expression of the Ikaros family in this condition. For comparison I used samples of donor liver and another chronic liver disease, NASH, as diseased control. As with the bowel tissue above, H&E staining was used to assess the impact of the autoimmune disease on normal tissue structure.

#### 4.2.5.1 Donor Liver has a Regular Liver Structure, Interspersed With Fatty Droplets

Normal donor material was used as a comparator throughout and rather than biopsies, I had access to explanted liver tissue collected for transplantation surgery for these analyses. H&E staining of donor material showed that the tissue retained its organised structure, with clear visibility of the hepatocytes, cholangiocytes and vascular structures. The tissue retained its usual zonal architecture and apart from normal resident immune cells there was little evidence of any inflammation. Of note, the majority of donor tissue available for research has been rejected for use in transplantation due to suspected fatty degeneration. In agreement I observed numerous fatty droplets dispersed throughout the tissue, mostly presenting as macrovesicular lipid within hepatocytes in pericentral areas (Figure 4.10).

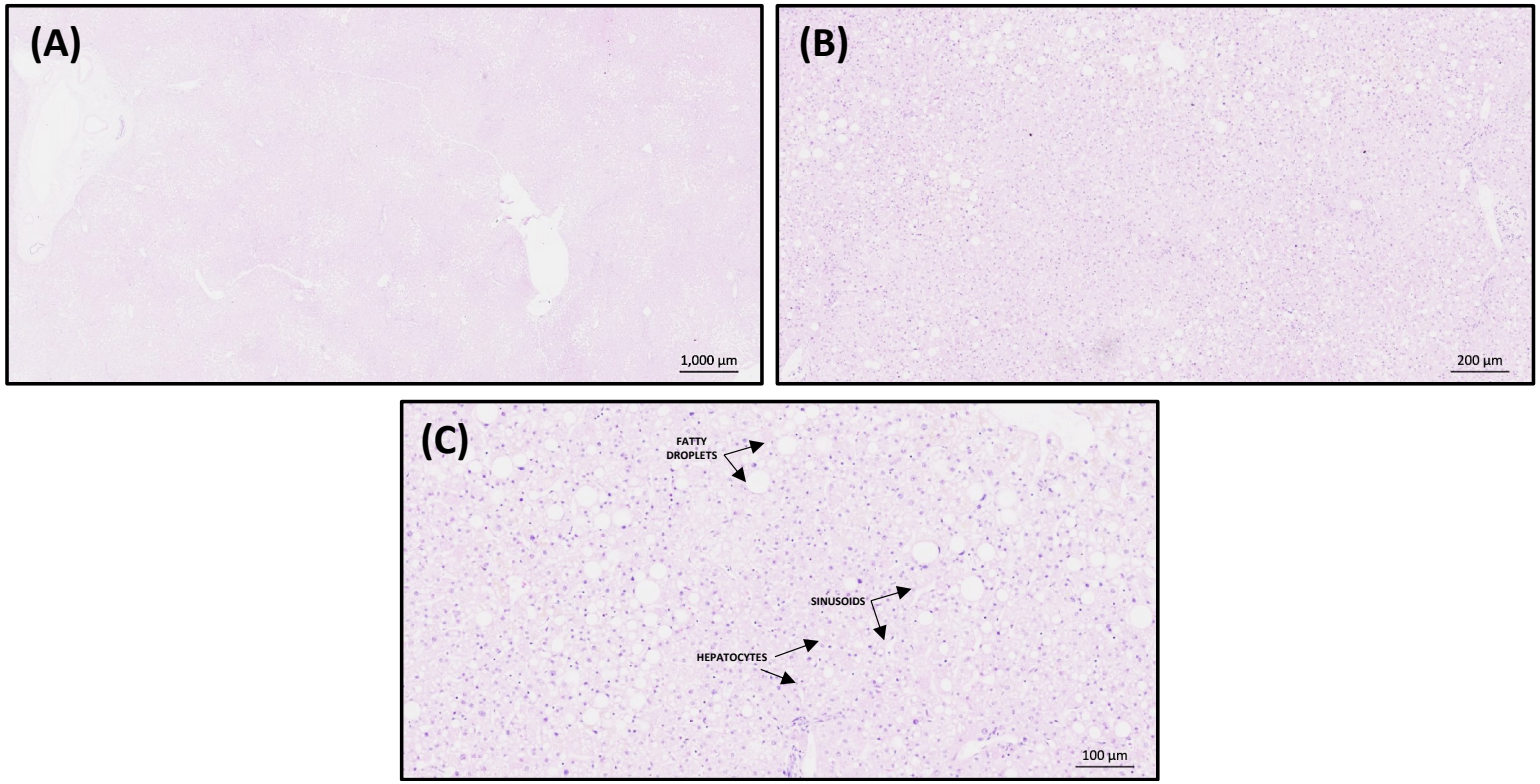



**Figure 4.10: Haematoxylin and Eosin Staining of Donor Liver Tissue**
Haematoxylin and Eosin staining of Formalin-Fixed Paraffin-Embedded (FFPE) tissue was used to stain the nucleus and the organelles within a section of donor liver tissue. **(A)** Overview of liver tissue structure. Scale bar represents 1000 µm. **(B)** Closer image of liver tissue identifying regions within the tissue. Scale bar represents 200 µm. **(C)** Labelled section of donor tissue identifying representative hepatocytes, fatty droplets and sinusoids which are labelled with black arrows. Scale bar represents 100 µm. Representative images are shown. Magnification x20. *N=1.*

#### 4.2.5.2 Immune Infiltration and Fibrosis is Common in PSC

In comparison to donor liver tissue, observations of the PSC liver tissue confirmed significant architectural disruption and immune cell infiltrate (Figure 4.11). These samples were collected upon explant for transplantation and thus exhibited features of cirrhosis such as bridging fibrosis and the presence of regenerative nodules. Inflammatory cell infiltrate was observed throughout the tissue and particularly dense in the scarred areas around the portal tracts. Presence of a ductular proliferative response was also seen in this area.

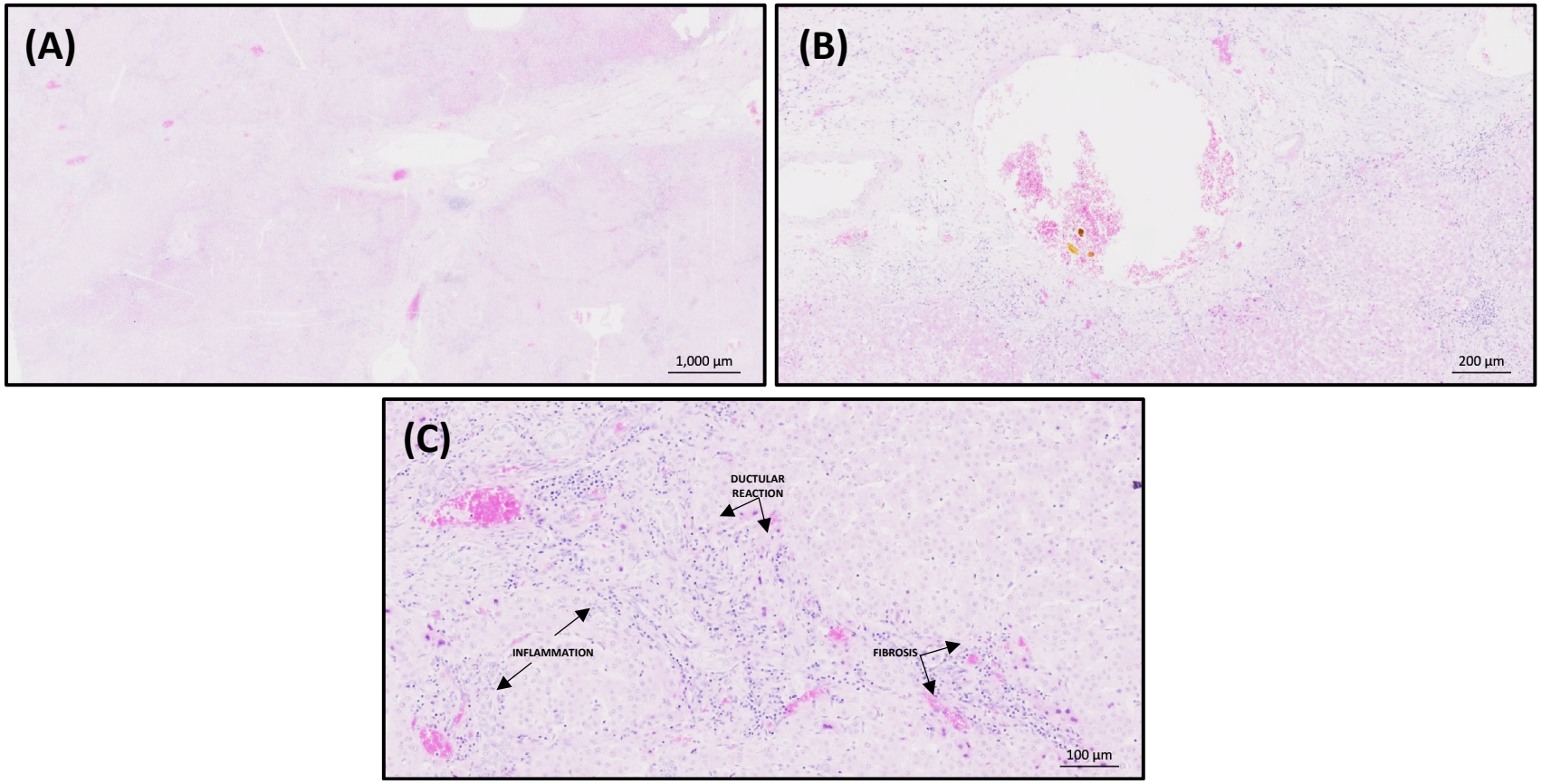



**Figure 4.11: Haematoxylin and Eosin Staining of Primary Sclerosing Cholangitis Liver Tissue**
Haematoxylin and Eosin staining of Formalin-Fixed Paraffin-Embedded (FFPE) tissue was used to stain the nucleus and the organelles within a section of Primary Sclerosing Cholangitis (PSC) Liver Tissue. **(A)** Overview of PSC liver tissue structure. Scale bar represents 1000 µm. **(B)** Closer image of liver tissue identifying regions within PSC tissue. Scale bar represents 200 µm. **(C)** Labelled section of PSC tissue identifying representative fibrosis, ductular reaction and inflammation within the tissue labelled with black arrows. Scale bar represents 100 µm. Representative images are shown. Magnification x20. *N=1*

### 4.2.6 Ikaros Family Expression in Liver

Similar to the bowel, data regarding the expression of the Ikaros family in the liver is limited, with some studies even arguing that the family is absent within the liver (110). Thus, we simultaneously aimed to document if firstly the Ikaros family was expressed in the liver and then secondly what impact inflammation, resulting from NASH, PSC, PSC-IBD, had on expression of the family. Using DAB-IHC we analysed expression levels of the Ikaros family in liver tissue. Semi-quantitative analysis was conducted as before.

#### 4.2.6.1 Aiolos Expression is Elevated in Diseased Tissue

Comparison of the percentage positive Aiolos staining in Donor, NASH, PSC and PSC-DAB liver sections revealed that expression of Aiolos is elevated in NASH, PSC and PSC-IBD tissue in comparison to Donor, although not significantly (Figure 4.12). In Donor liver, limited expression of Aiolos was seen in lymphocytes. In NASH contrastingly, greater Aiolos expression was seen within fibrotic regions, again in lymphocytes. In PSC, concentrated Aiolos expression was seen in lymphocytes around the portal areas, with expression of Aiolos also seen in Kupffer-like structures within the liver.

#### 4.2.6.2 PSC Tissue Has Significantly Higher Expression Levels of Eos in Comparison to Donor

Figure 4.13 shows that Eos expression was found to be higher in PSC tissue in comparison to Donor, NASH ($p<0.05$) and PSC-IBD liver sections. Across all tissue, expression of Eos could be seen in macrophage-like structures within the liver. Greater expression of Eos was seen within PSC tissue, especially in lymphocytes around the portal areas.

#### 4.2.6.3 Helios Expression is Significantly Higher in PSC Liver in Comparison to NASH and PSC-IBD

PSC liver sections had higher expression of Helios in comparison to NASH and PSC-IBD liver tissue (Figure 4.14). Low Helios expression was seen throughout the liver tissue, spread throughout Donor and NASH in lymphocytes. In PSC, greater Helios expression was in lymphocytes and Kupffer-like cells with less expression of Helios seen in PSC-IBD tissue within lymphocytes and around sinusoids.

#### 4.2.6.4 Ikaros is Expressed in Diseased and Donor Liver Tissue

Ikaros expression was observed throughout the tissue of all liver types assessed, with positivity in lymphocytes (Figure 4.15). Ikaros expression was seen within Donor tissue around arteries, veins, and the portal area, with concentrated expression of Ikaros seen in lymphocytes. Heavy expression of Ikaros was seen in both PSC and PSC-IBD portal areas, again concentrated within lymphocytes. Although expression was slightly higher in NASH and PSC tissue, this was not significantly higher than levels observed in Donor or PSC-IBD tissue.

#### 4.2.6.5 PSC and PSC-IBD Liver Express Greater Protein Levels of Pegasus

In comparison to Donor, levels of Pegasus were higher in PSC and PSC-IBD liver (Figure 4.16). Little to no expression of Pegasus was seen within Donor tissue sections. Greater staining was seen in NASH tissue within macrophage-like structures in the tissue. In PSC, greater Pegasus staining was seen in lymphocytes and in macrophage-like structures. In the representative image, greater Pegasus expression can be seen in the portal region in a mix of lymphocytes and macrophages.

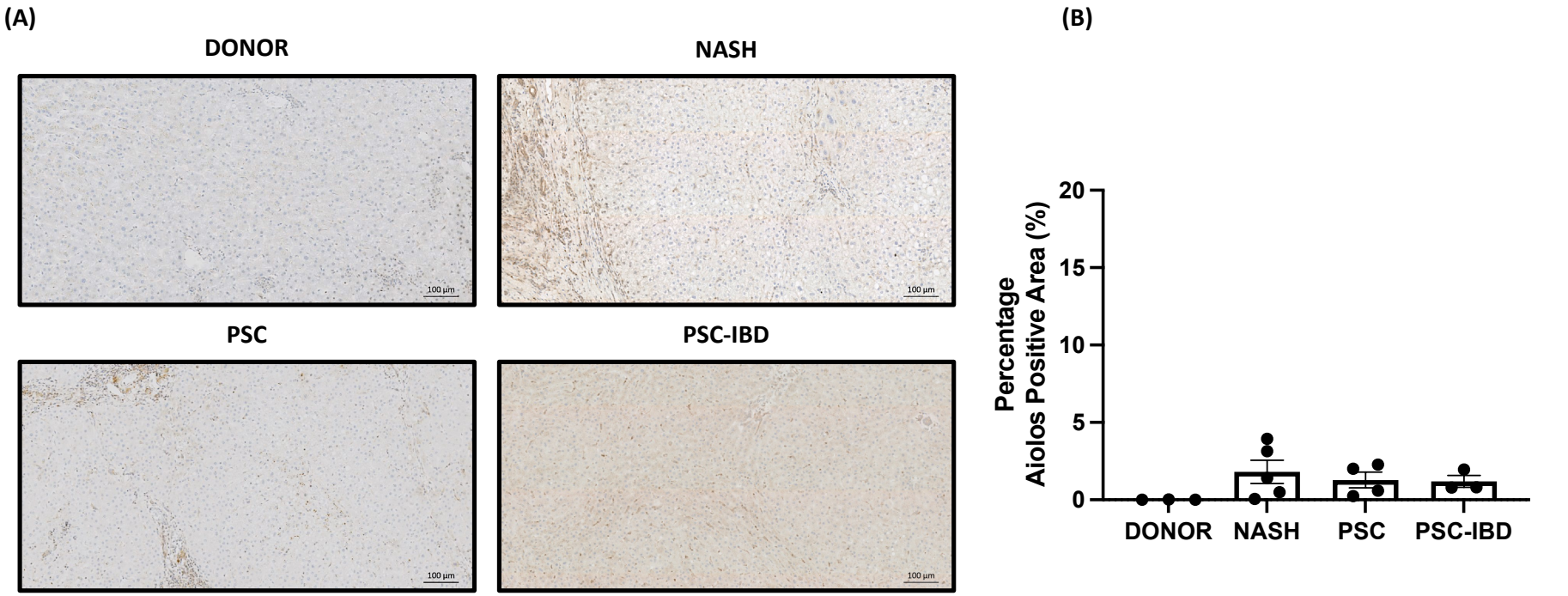



**Figure 4.12: Expression of Aiolos in Donor, Non-alcoholic Steatohepatitis (NASH), Primary Sclerosing Cholangitis (PSC) and PSC-Inflammatory Bowel Disease (PSC-IBD) Liver Tissue**

**(A)** 3,3'-diaminobenzidine (DAB) staining was used to view the presence of Aiolos in Donor, NASH, PSC and PSC-IBD Liver Sections. Haematoxylin was used for nuclear staining. **(B)** For quantitative analysis, the percentage Aiolos Positive Area (%) was determined by randomly selecting 5-8 regions (*n*) from each sample (*N*) and Image J software used to determine values for positive DAB staining. Dots represent average staining of regions (*n*) in each *N*. Results are normalised to appropriate IgG controls and presented as Mean ± SEM. Representative images are shown. Magnification x20. Scale Bar represents 100µm. *Donor, N=3, n=15; NASH, N=5, n=25; PSC, N=5, n=25; PSC-IBD, N=3, n=15. NS. One way ANOVA and Tukey's Multiple Comparison Test.*

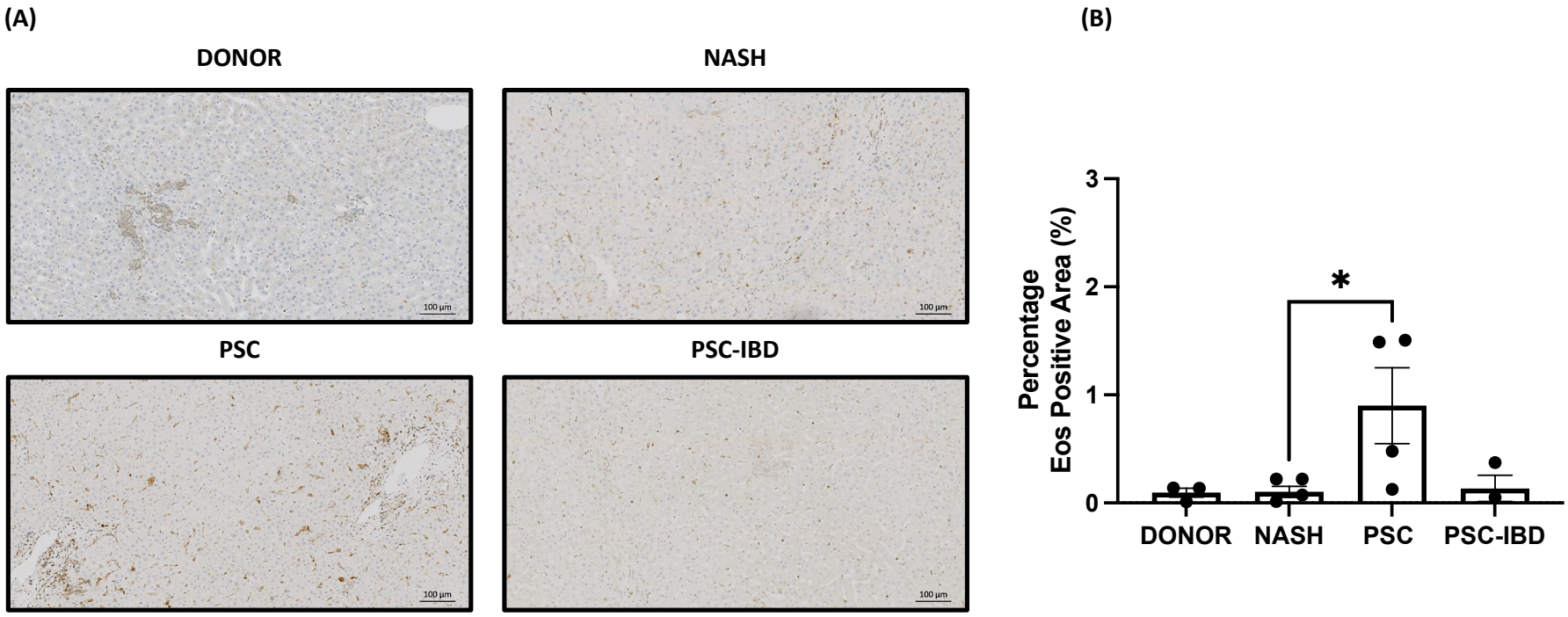



**Figure 4.13: Expression of Eos in Donor, Non-alcoholic Steatohepatitis (NASH), Primary Sclerosing Cholangitis (PSC) and PSC-Inflammatory Bowel Disease (PSC-IBD) Liver Tissue**

**(A)** 3,3'-diaminobenzidine (DAB) staining was used to view the presence of Eos in Donor, NASH, PSC and PSC-IBD Liver Sections. Haematoxylin was used for nuclear staining. **(B)** For quantitative analysis, the percentage Eos Positive Area (%) was determined by randomly selecting 5-8 regions (*n*) from each sample (*N*) and Image J software used to determine values for positive DAB staining. Dots represent regions and bars represent the mean. Results are normalised to appropriate IgG controls and presented as Mean ± SEM. Representative images are shown. Magnification x20. Scale Bar represents 100µm. *Donor, N=3, n=15; NASH, N=5, n=25; PSC, N=5, n=25; PSC-IBD, N=3, n=15. NASH Vs PSC * P<0.05. One way ANOVA and Tukey's Multiple Comparison Test.*

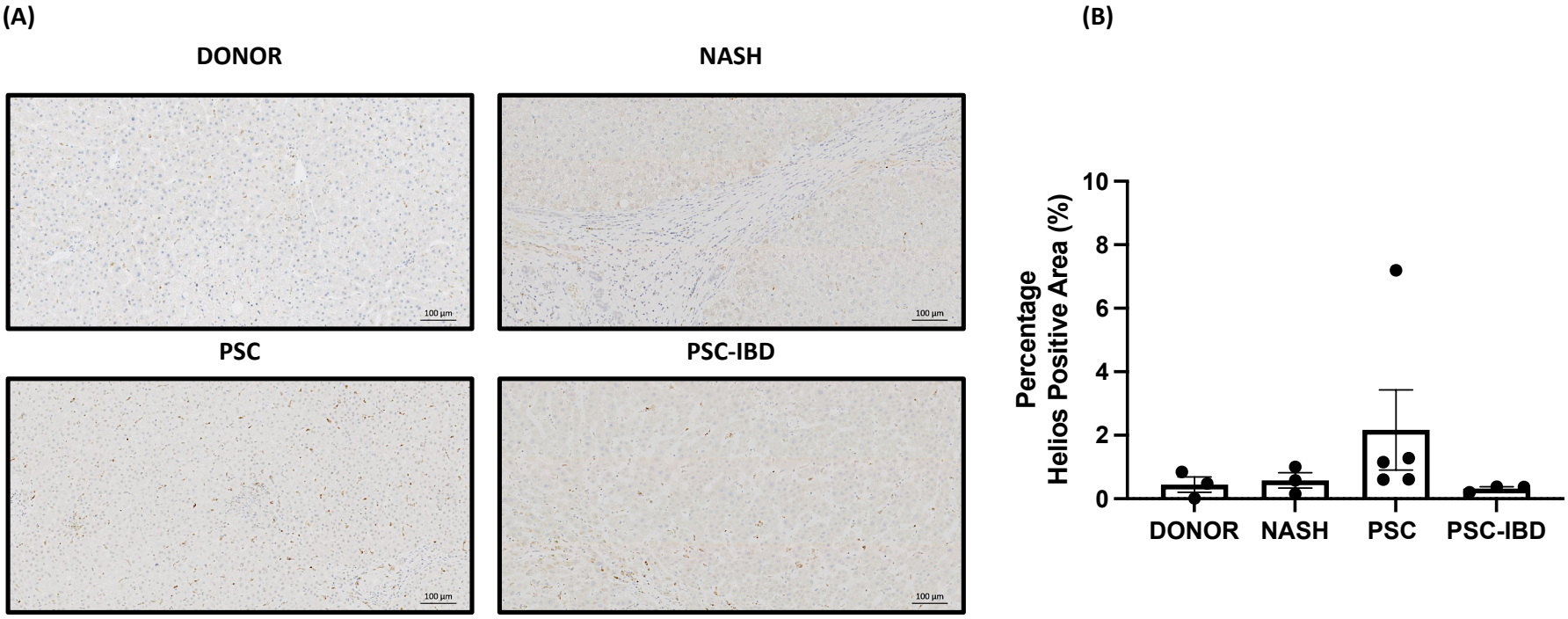



**Figure 4.14: Expression of Helios in Donor, Non-alcoholic Steatohepatitis (NASH), Primary Sclerosing Cholangitis (PSC) and PSC-Inflammatory Bowel Disease (PSC-IBD) Liver Tissue**

**(A)** 3,3'-diaminobenzidine (DAB) staining was used to view the presence of Helios in Donor, NASH, PSC and PSC-IBD Liver Sections. Haematoxylin was used for nuclear staining. **(B)** For quantitative analysis, the percentage Helios Positive Area (%) was determined by randomly selecting 5-8 regions (*n*) from each sample (*N*) and Image J software used to determine values for positive DAB staining. Dots represent regions and bars represent the mean. Results are normalised to appropriate IgG controls and presented as Mean ± SEM. Representative images are shown. Magnification x20. Scale Bar represents 100µm. *Donor, N=3, n=15; NASH, N=5, n=25; PSC, N=5, n=25; PSC-IBD, N=3, n=15. NS. One way ANOVA and Tukey's Multiple Comparison Test.*

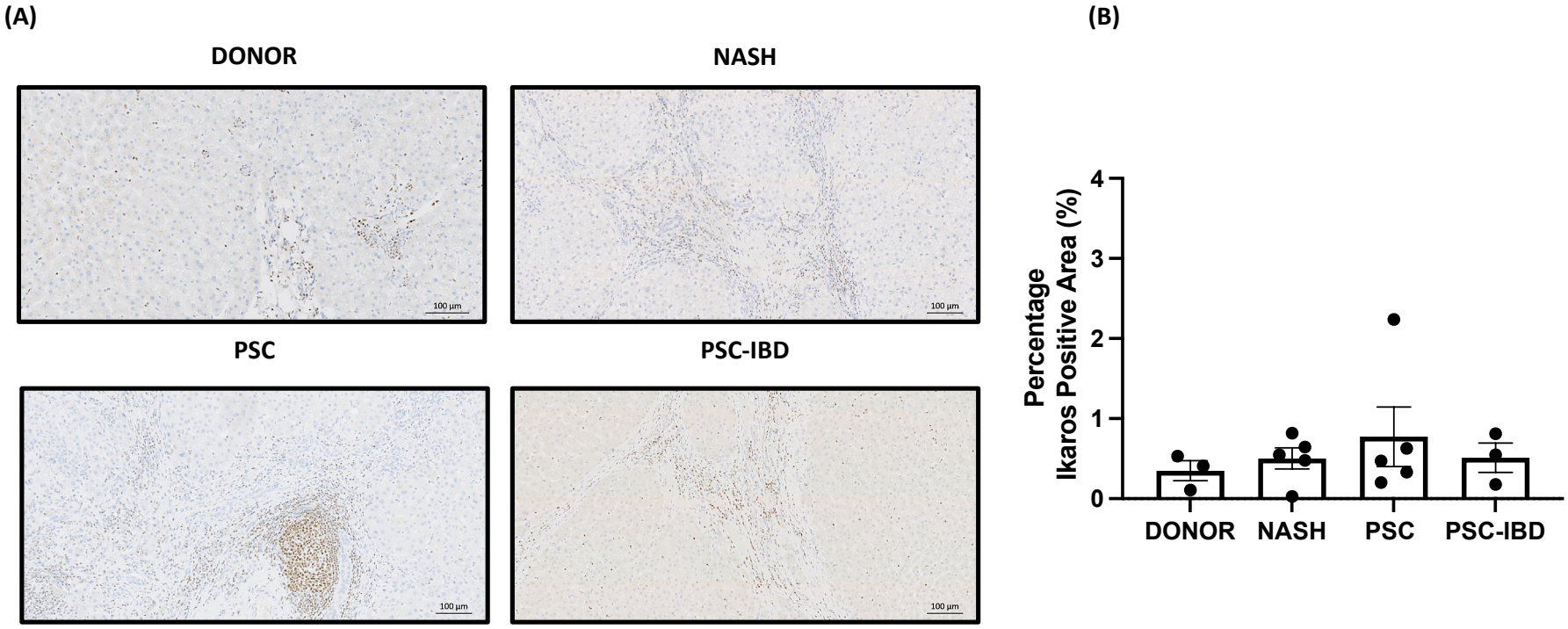



**Figure 4.15: Expression of Ikaros in Donor, Non-alcoholic Steatohepatitis (NASH), Primary Sclerosing Cholangitis (PSC) and PSC-Inflammatory Bowel Disease (PSC-IBD) Liver Tissue**

**(A)** 3,3'-diaminobenzidine (DAB) staining was used to view the presence of Ikaros in Donor, NASH, PSC and PSC-IBD Liver Sections. Haematoxylin was used for nuclear staining. **(B)** For quantitative analysis, the percentage Ikaros Positive Area (%) was determined by randomly selecting 5-8 regions (*n*) from each sample (*N*) and Image J software used to determine values for positive DAB staining. Dots represent regions and bars represent the mean. Results are normalised to appropriate IgG controls and presented as Mean ± SEM. Representative images are shown. Magnification x20. Scale Bar represents 100µm. *Donor, N=3, n=15; NASH, N=5, n=25; PSC, N=5, n=25; PSC-IBD, N=3, n=15. NS. One way ANOVA and Tukey's Multiple Comparison Test.*

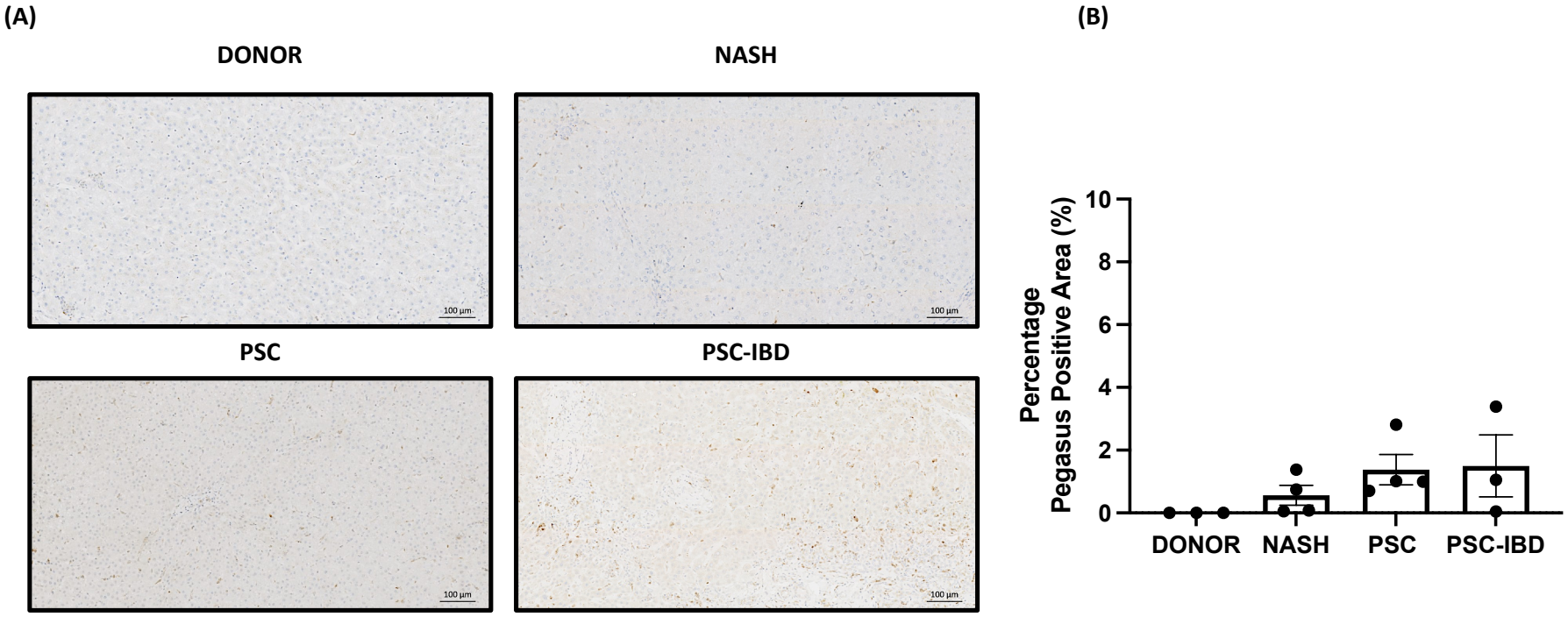



**Figure 4.16: Expression of Pegasus in Donor, Non-alcoholic Steatohepatitis (NASH), Primary Sclerosing Cholangitis (PSC) and PSC-Inflammatory Bowel Disease (PSC-IBD) Liver Tissue**

**(A)** 3,3'-diaminobenzidine (DAB) staining was used to view the presence of Pegasus in Donor, NASH, PSC and PSC-IBD Liver Sections. Haematoxylin was used for nuclear staining. **(B)** For quantitative analysis, the percentage Pegasus Positive Area (%) was determined by randomly selecting 5-8 regions (*n*) from each sample (*N*) and Image J software used to determine values for positive DAB staining. Dots represent regions and bars represent the mean. Results are normalised to appropriate IgG controls and presented as Mean ± SEM. Representative images are shown. Magnification x20. Scale Bar represents 100µm. *Donor, N=3, n=15; NASH, N=5, n=25; PSC, N=5, n=25; PSC-IBD, N=3, n=15. NS. One way ANOVA and Tukey's Multiple Comparison Test.*

### 4.2.7 Primary Sclerosing Cholangitis Liver has Higher Expression of the Ikaros Family at a RNA level in Comparison to Donor Liver

We next analysed the RNA expression levels of the family in Donor, PSC and NASH liver tissue by qPCR (Figure 4.17). Our results showed that RNA levels of all members of the family were higher in PSC in comparison to Donor. NASH, used as a disease control, also displayed higher expression of the Ikaros family in comparison to Donor. However, levels of Eos, Ikaros and Helios were highest in PSC tissue. Significant increases in Aiolos expression ($p<0.01$) in both NASH and PSC tissue were observed in comparison to Donor. Helios and Ikaros were both significantly upregulated in NASH ($p<0.05$) with a trend for increased expression in PSC. Levels of Pegasus was again higher in diseased tissue in general but only significantly higher ($p<0.01$) in PSC tissue.

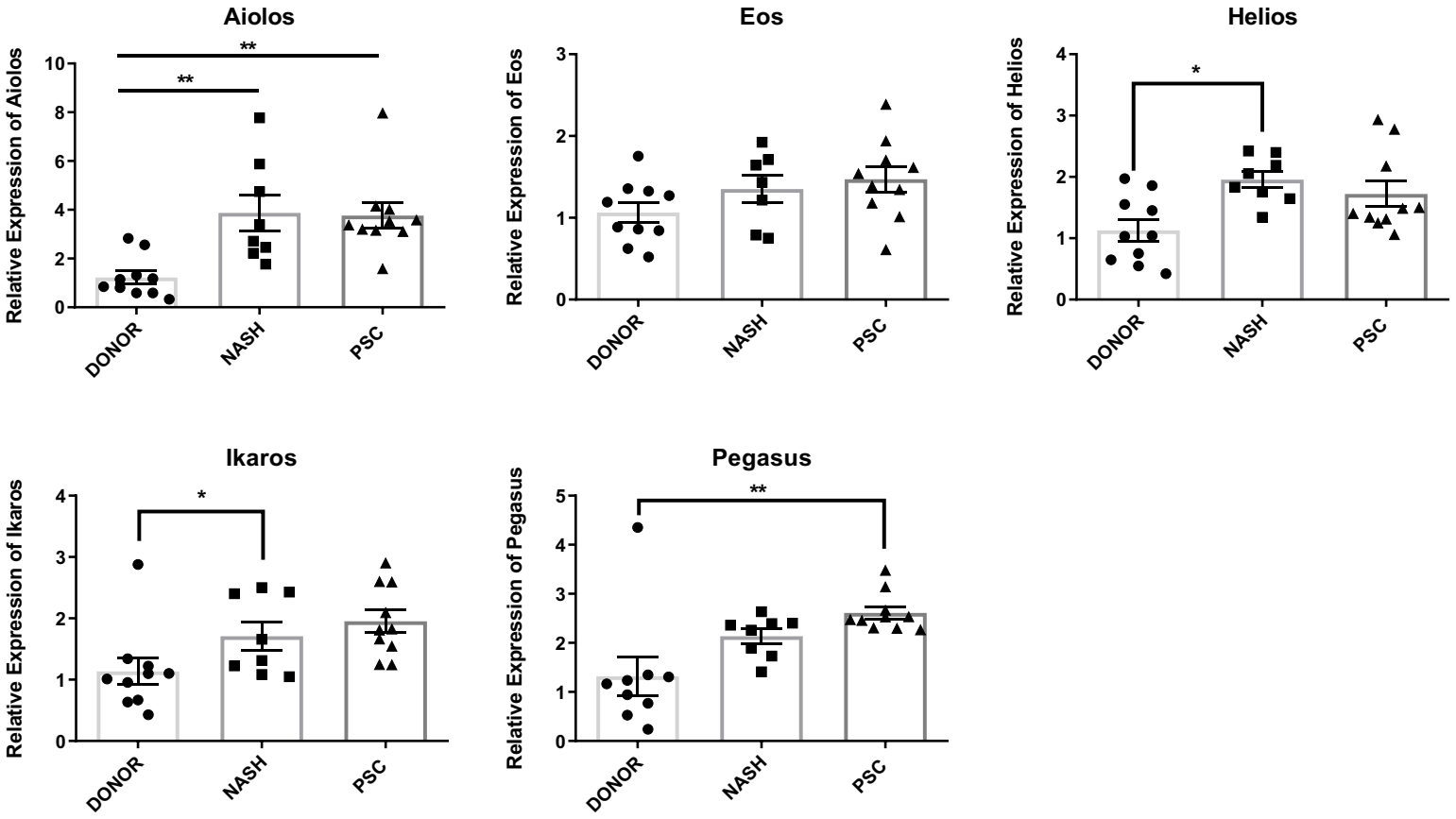



**Figure 4.17: Diseased Liver has Higher Relative Expression Levels of the Ikaros Family in Comparison with Donor Liver**
Total RNA was extracted from donor (Donor), Primary Sclerosing Cholangitis (PSC) and Non-alcoholic steatohepatitis (NASH) liver 1cm3 cubes and expression of the Ikaros Family of Transcription Factors measured by qPCR. Expression is shown for each group relative to the level in Donor. Results are presented as mean ± SEM. Symbols represent individual liver samples. Donor *n*= 10; NASH *n*=7; PSC *n*=10. *Aiolos ** p<0.01; Helios * P<0.05; Ikaros * P<0.05; Pegasus ** p<0.01. One way ANOVA and Tukey's Multiple Comparison Test. Housekeeping Gene: SRSF4.*

### 4.2.8 Expression of Ikaros Family RNA Correlates with Markers of Disease Severity

Where possible, we collated anonymised patient clinical data for the clinical samples I used in my expression analyses. This demographic data is summarised in Table 4.1 at the beginning of this chapter. With this data, we correlated expression of the Ikaros family in diseased liver with patient liver function clinical markers including Albumin, Bilirubin, BMI, C-Reactive Protein (CRP), Alkaline Phosphatase (ALP) and Alanine Aminotransferase (ALT) from pre-surgery.

Within NASH liver a slight positive correlation between expression of Aiolos and Albumin, Bilirubin and ALP was seen with a slight negative linear regression observed between Aiolos expression and CRP and ALT (Figure 4.18). A positive association between expression of Eos with ALP, Bilirubin and BMI was also seen with a corresponding negative association observed between Eos expression and ALT and CRP (Figure 4.19). A significantly positive correlation between expression of Helios and Bilirubin ($p<0.05$) was found with a contrasting negative association observed between Helios expression and Albumin, ALT, BMI, and CRP (Figure 4.20). A positive correlation between expression of Ikaros and Albumin, ALP and Bilirubin was seen with a negative correlation observed between Ikaros expression and ALT and CRP (Figure 4.21). A positive correlation was also seen between expression of Pegasus and ALP, ALT, Bilirubin and CRP with a significant negative linear regression observed between Pegasus expression and BMI ($P<0.05$) (Figure 4.22).

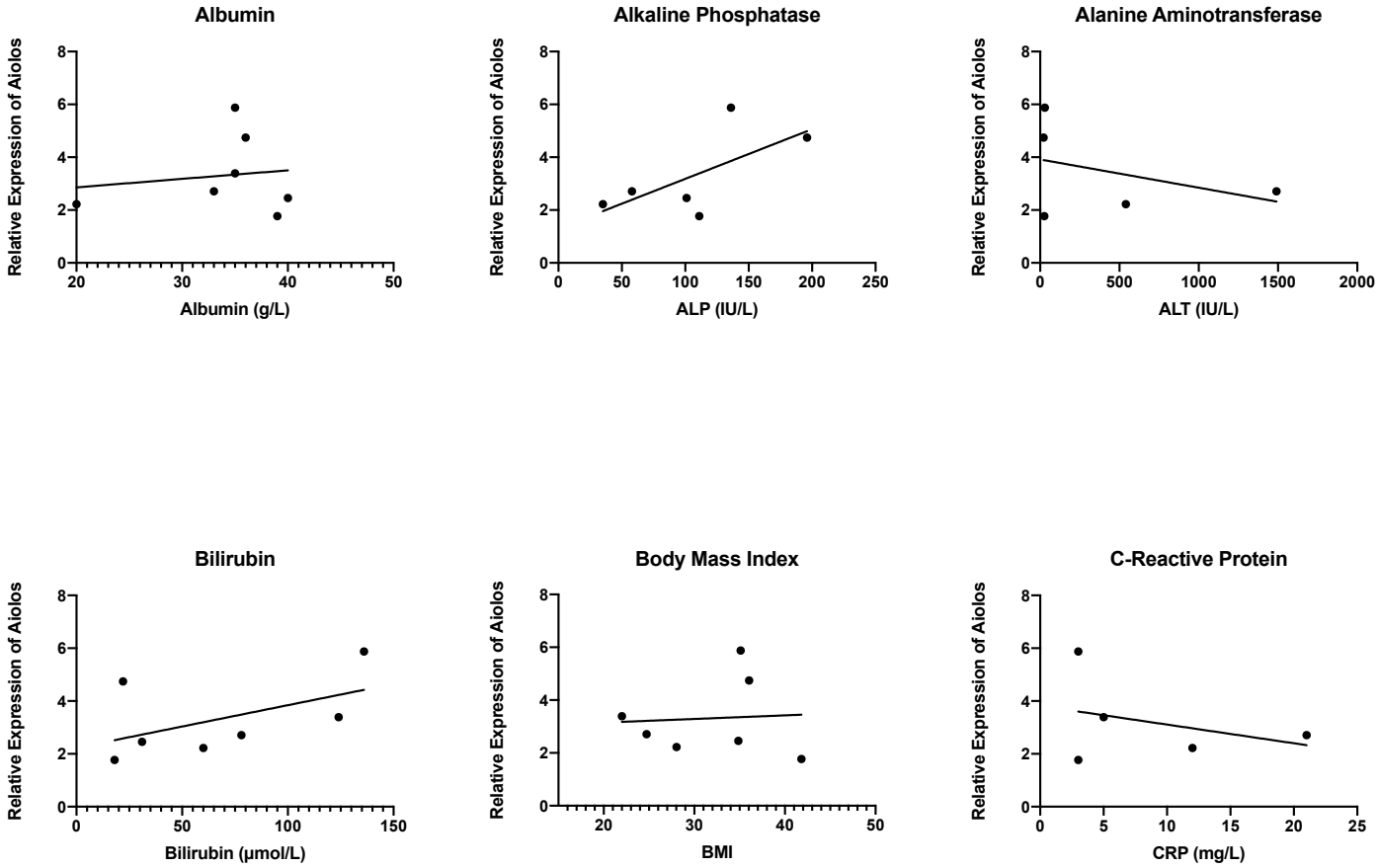



**Figure 4.18: Correlations Between Aiolos and Patient Liver Function Markers in Non-alcoholic Steatohepatitis Liver**
Total RNA was isolated from whole Non-alcoholic Steatohepatitis (NASH) liver segments and quantitative PCR performed to analyse relative expression levels of the Ikaros Family member Aiolos. Data was normalised to donor livers (data not shown) and then correlated against patient liver function clinical data *(Albumin, Bilirubin, Body Mass Index (BMI), C-Reactive Protein (CRP), Alkaline Phosphatase (ALP), Alanine Aminotransferase (ALT))* from pre-NASH surgery. Dots represent individual liver samples. *N=4-7. NS. Pearson Correlation. Housekeeping Gene: SRSF4.*

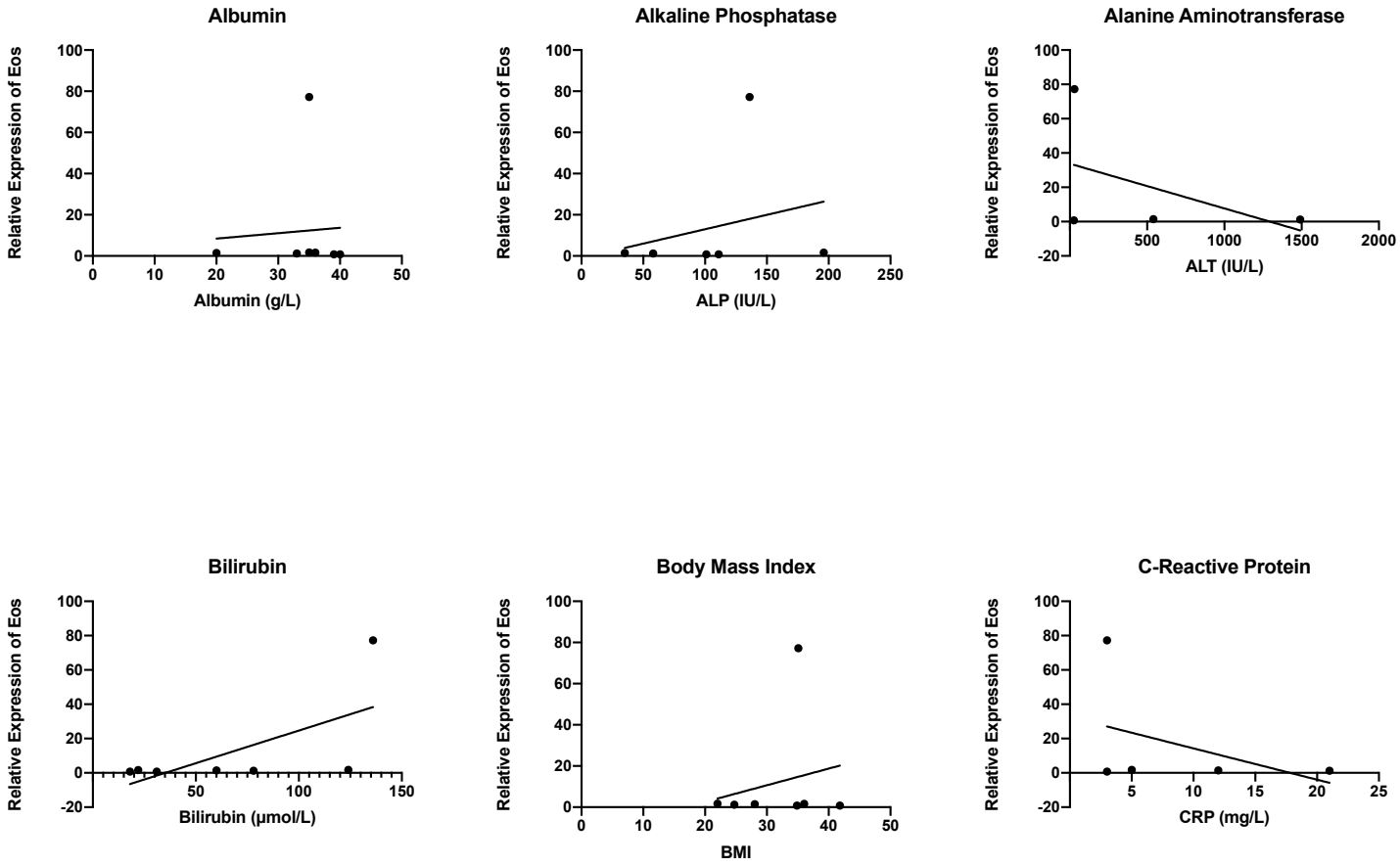



**Figure 4.19: No Clear Correlation Exists Between Eos and Patient Liver Function Markers in Non-alcoholic Steatohepatitis Liver**

Total RNA was isolated from whole Non-alcoholic Steatohepatitis (NASH) liver segments and quantitative PCR performed to analyse relative expression levels of the Ikaros Family member Eos. Data was normalised to donor livers (data not shown) and then correlated against patient liver function clinical data *(Albumin, Bilirubin, Body Mass Index (BMI), C-Reactive Protein (CRP), Alkaline Phosphatase (ALP), Alanine Aminotransferase (ALT))* from pre-NASH surgery. Dots represent individual liver samples. *N=4-7. NS. Pearson Correlation. Housekeeping Gene: SRSF4*

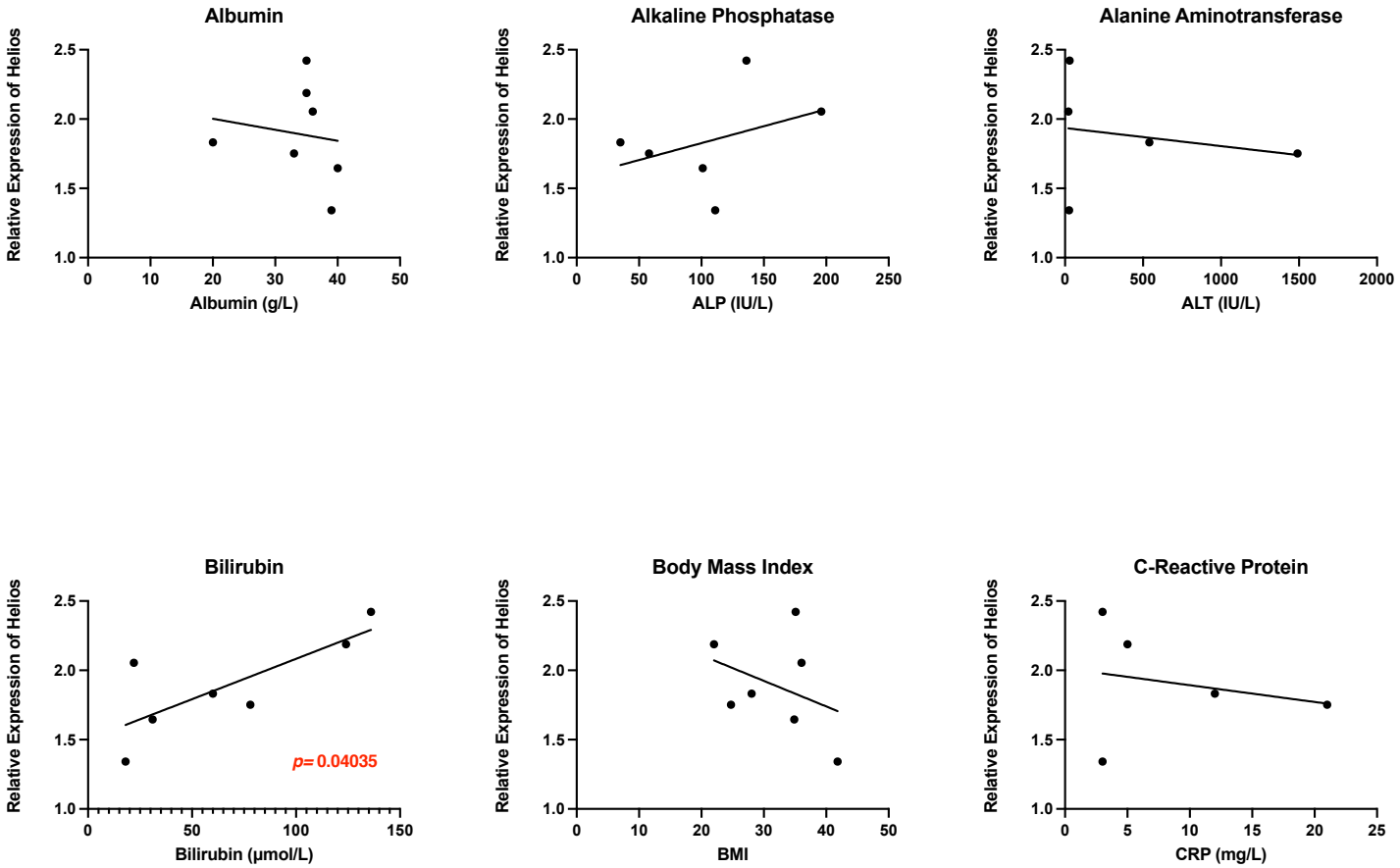



**Figure 4.20: A Trend For Correlation Exists Between Helios and Body Mass Index in Non-alcoholic Steatohepatitis Liver**
Total RNA was isolated from whole Non-alcoholic Steatohepatitis (NASH) liver segments and quantitative PCR performed to analyse relative expression levels of the Ikaros Family member Helios. Data was normalised to donor livers (data not shown) and then correlated against patient liver function clinical data *(Albumin, Bilirubin, Body Mass Index (BMI), C-Reactive Protein (CRP), Alkaline Phosphatase (ALP), Alanine Aminotransferase (ALT))* from pre-NASH surgery. Dots represent individual liver samples. *N=4-7. Bilirubin Vs Helios * P < 0.05, Pearson Correlation. Housekeeping Gene: SRSF4.*

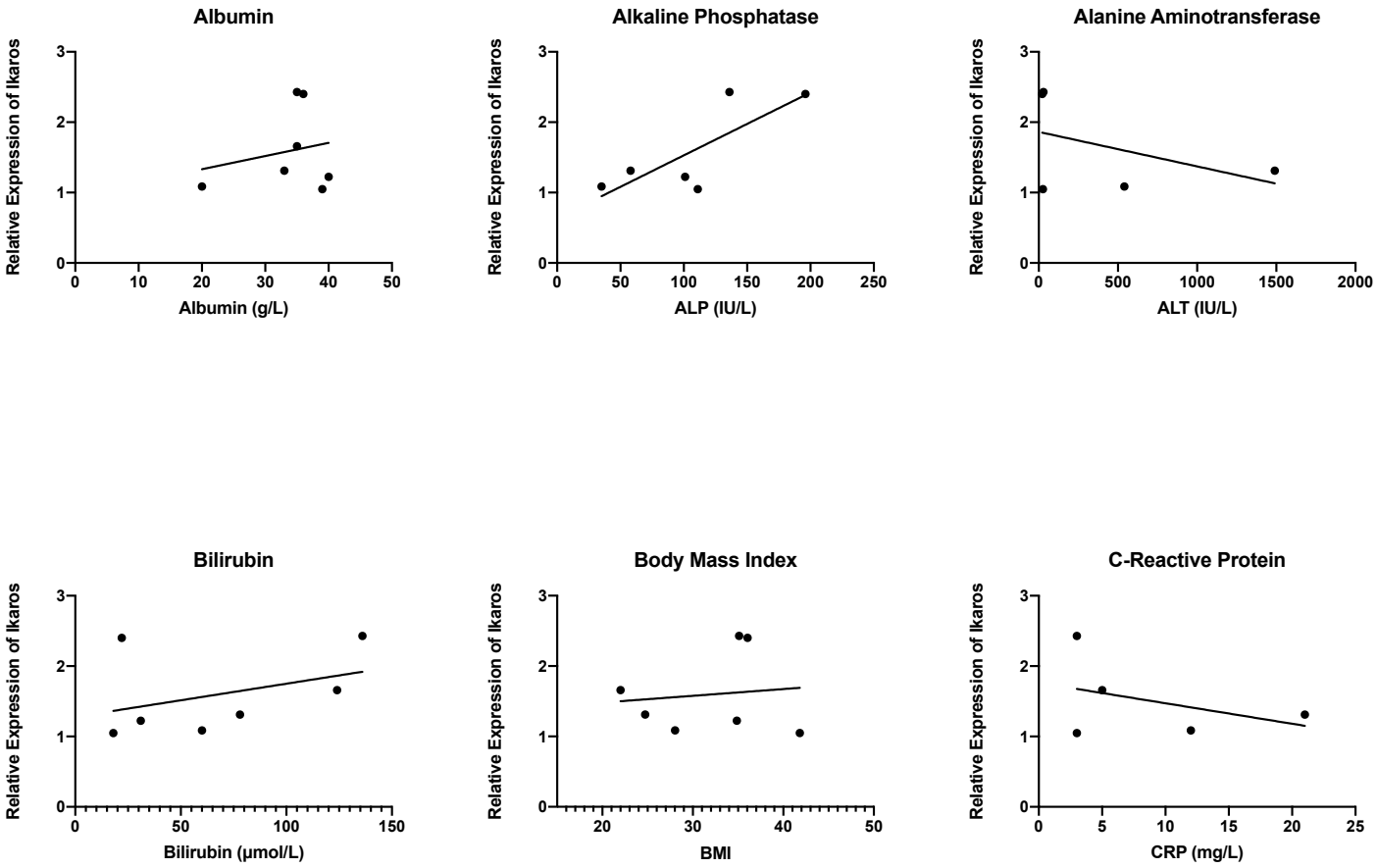



**Figure 4.21: Correlations Between Ikaros and Patient Liver Function Markers in Non-alcoholic Steatohepatitis Liver**
Total RNA was isolated from whole Non-alcoholic Steatohepatitis (NASH) liver segments and quantitative PCR performed to analyse relative expression levels of the Ikaros Family member Ikaros. Data was normalised to donor livers (data not shown) and then correlated against patient liver function clinical data *(Albumin, Bilirubin, Body Mass Index (BMI), C-Reactive Protein (CRP), Alkaline Phosphatase (ALP), Alanine Aminotransferase (ALT))* from pre-NASH surgery. Dots represent individual liver samples. *N=4-7. NS, Pearson Correlation. Housekeeping Gene: SRSF4*

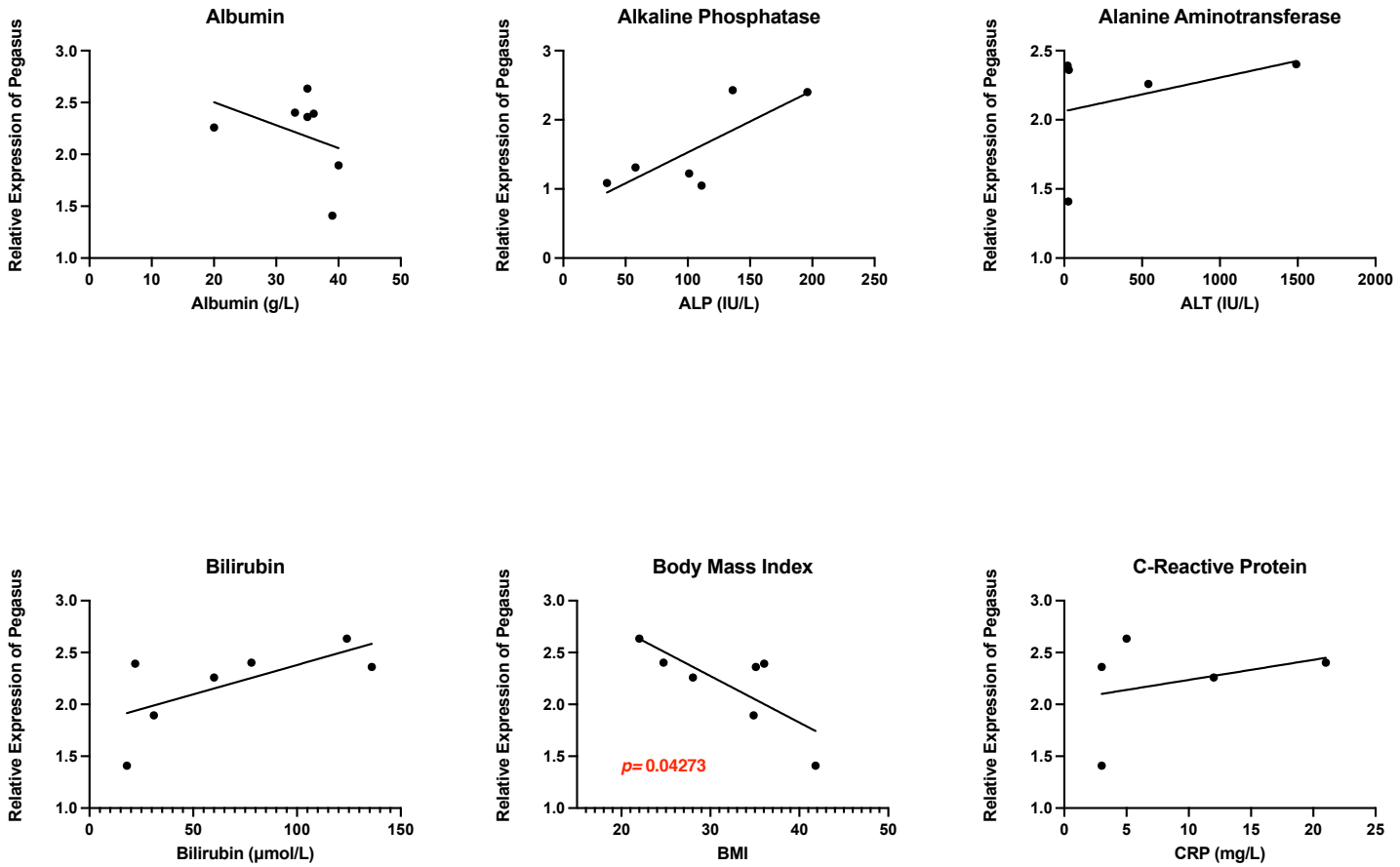



**Figure 4.22: A Negative Correlation Exists Between Pegasus and Body Mass Index in Non-alcoholic Steatohepatitis Liver**
Total RNA was isolated from whole Non-alcoholic Steatohepatitis (NASH) liver segments and quantitative PCR performed to analyse relative expression levels of the Ikaros Family member Pegasus. Data was normalised to donor livers (data not shown) and then correlated against patient liver function clinical data *(Albumin, Bilirubin, Body Mass Index (BMI), C-Reactive Protein (CRP), Alkaline Phosphatase (ALP), Alanine Aminotransferase (ALT))* from pre-NASH surgery. Dots represent individual liver samples. *N=4-7. BMI Vs Pegasus *P < 0.05, Pearson Correlation. Housekeeping Gene: SRSF4*

Similar to NASH, we also correlated expression of the Ikaros family against PSC patient clinical data including Albumin, Bilirubin, BMI, CRP, ALP, ALT collected pre-PSC surgery. Our correlation studies suggest a slight positive correlation between expression of Aiolos and Albumin, ALP and BMI with a slight negative linear regression observed between Aiolos expression and ALT (Figure 4.23). No correlation was observed between Aiolos and Bilirubin or CRP. A significant positive correlation between expression of Eos and BMI ($p<0.05$) was seen with a slight negative association observed between Eos expression and Albumin, ALP, ALT and Bilirubin (Figure 4.24). Similarly, a significant positive correlation between expression of Helios and BMI ($p<0.01$) was seen with a negative linear regression observed between Helios expression and Albumin, ALP, ALT and Bilirubin and CRP (Figure 4.25). A positive correlation between expression of Ikaros and BMI and CRP was found with a negative linear regression observed between Ikaros expression and ALT and Bilirubin (Figure 4.26). A slight positive correlation between expression of Pegasus and ALT was observed with a negative linear regression found between Pegasus expression and BMI (Figure 4.27). No correlation was observed between Pegasus and Albumin, ALP, Bilirubin or CRP.

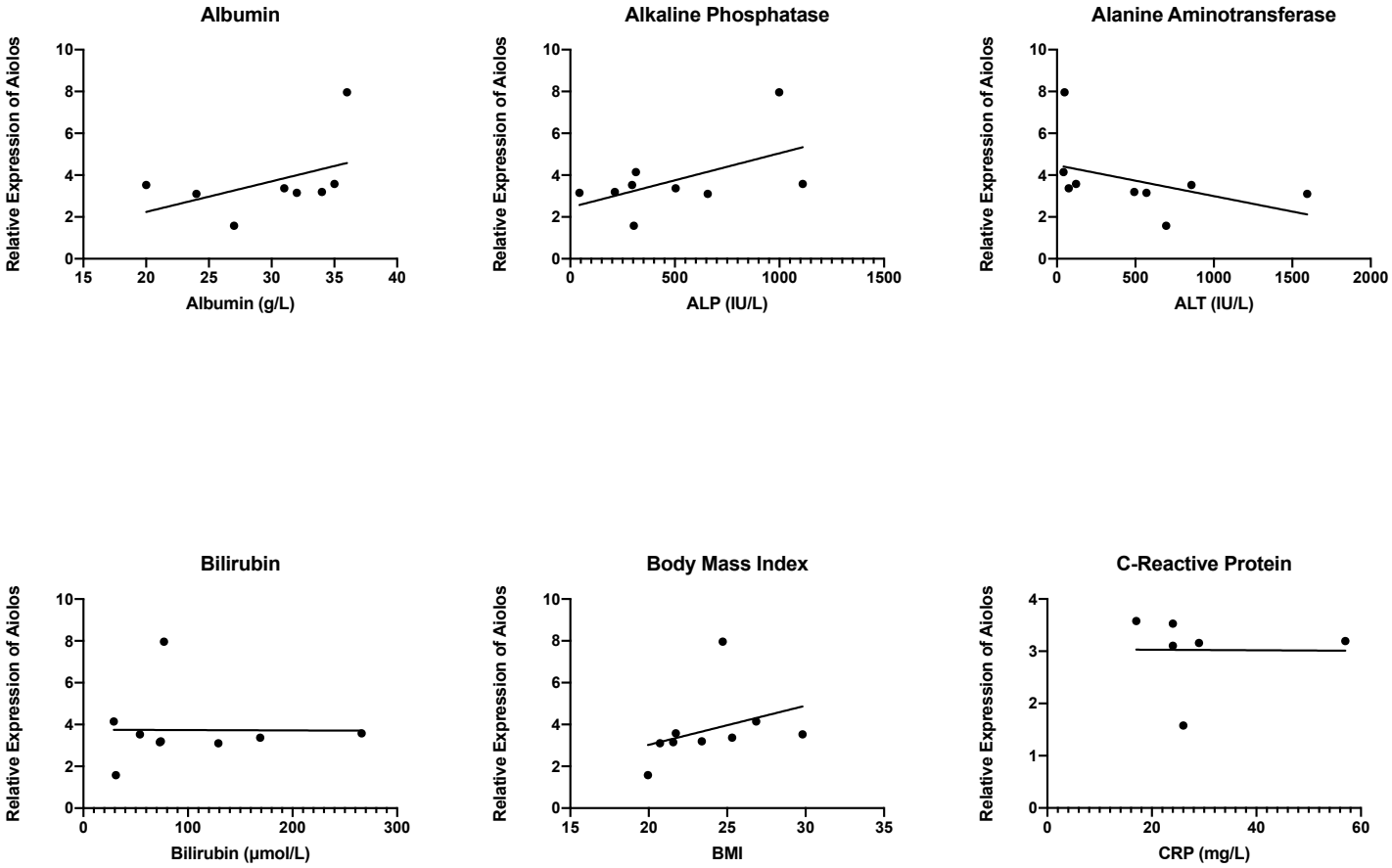



**Figure 4.23: Correlations Between Aiolos and Patient Liver Function Markers in Primary Sclerosing Cholangitis Liver**
Total RNA was isolated from whole Primary Sclerosing Cholangitis (PSC) liver segments and quantitative PCR performed to analyse relative expression levels of the Ikaros Family member Aiolos. Data was normalised to donor livers (data not shown) and then correlated against patient liver function clinical data *(Albumin, Bilirubin, Body Mass Index (BMI), C-Reactive Protein (CRP), Alkaline Phosphatase (ALP), Alanine Aminotransferase (ALT))* from pre-PSC surgery. Dots represent individual liver samples. *N=4-7. NS, Pearson Correlation. Housekeeping Gene: SRSF4*

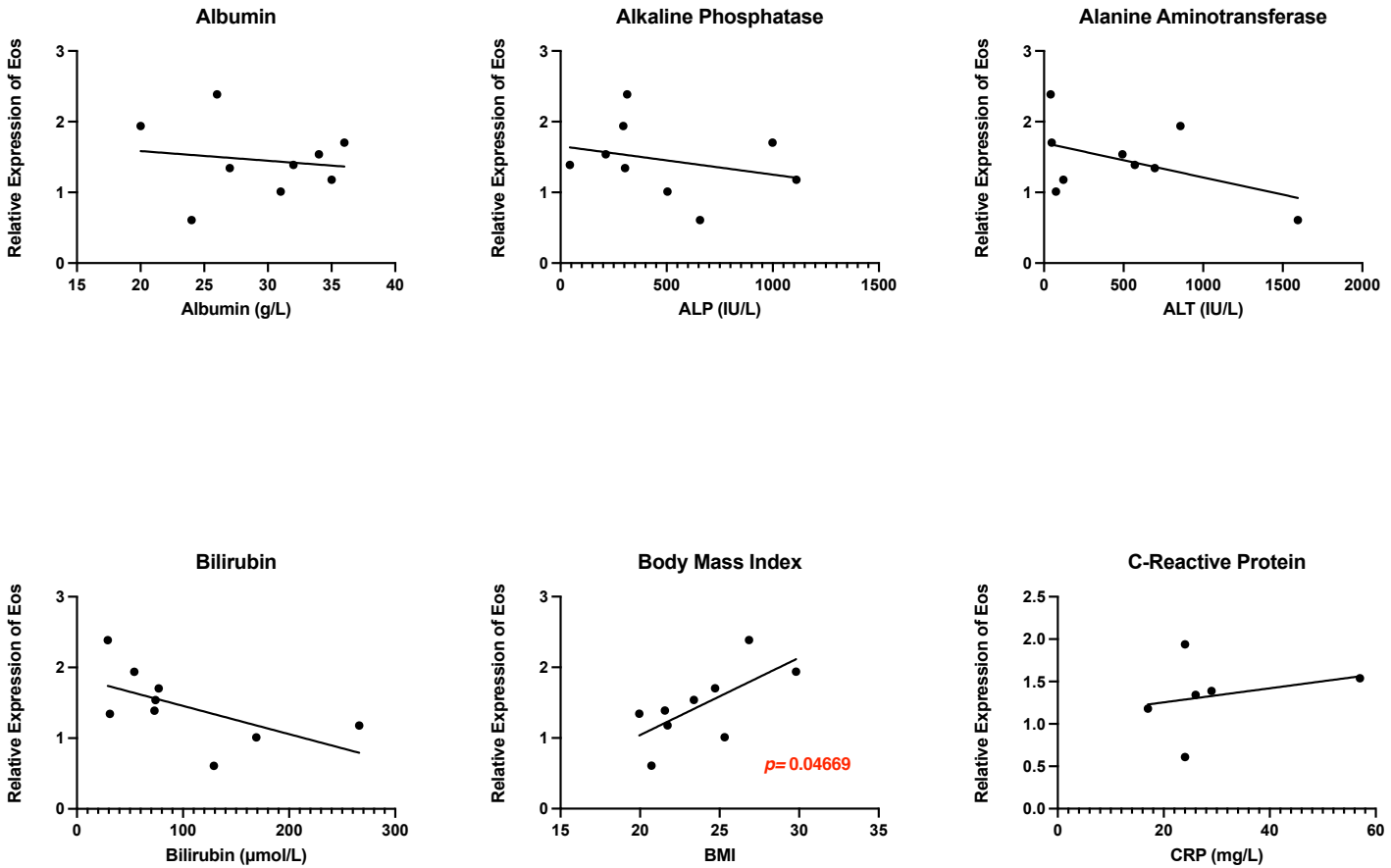



**Figure 4.24: A Positive Trend Exists Between Eos and Body Mass Index in Primary Sclerosing Cholangitis Liver**
Total RNA was isolated from whole Primary Sclerosing Cholangitis (PSC) liver segments and quantitative PCR performed to analyse relative expression levels of the Ikaros Family member Eos. Data was normalised to donor livers (data not shown) and then correlated against patient liver function clinical data *(Albumin, Bilirubin, Body Mass Index (BMI), C-Reactive Protein (CRP), Alkaline Phosphatase (ALP), Alanine Aminotransferase (ALT))* from pre-PSC surgery. Dots represent individual liver samples. *N=4-7. BMI Vs Eos * P < 0.05, Pearson Correlation. Housekeeping Gene: SRSF4.*

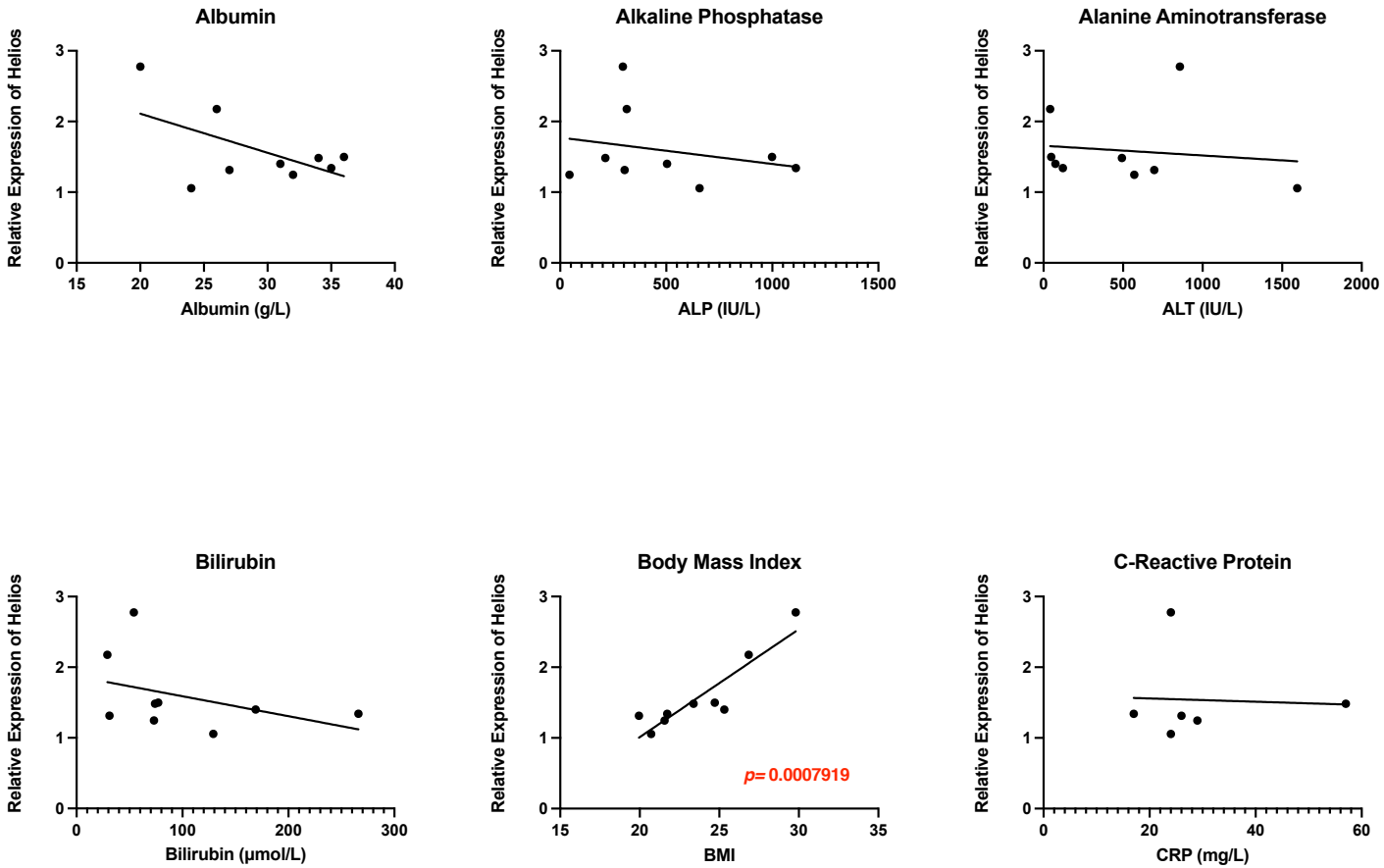



**Figure 4.25: A Positive Correlation Exists Between Helios and Body Mass Index in Primary Sclerosing Cholangitis Liver**
Total RNA was isolated from whole Primary Sclerosing Cholangitis (PSC) liver segments and quantitative PCR performed to analyse relative expression levels of the Ikaros Family member Helios. Data was normalised to donor livers (data not shown) and then correlated against patient liver function clinical data *(Albumin, Bilirubin, Body Mass Index (BMI), C-Reactive Protein (CRP), Alkaline Phosphatase (ALP), Alanine Aminotransferase (ALT))* from pre-PSC surgery. Dots represent individual liver samples. *N=4-7. BMI Vs Helios *** P < 0.05, Pearson Correlation. Housekeeping Gene: SRSF4.*

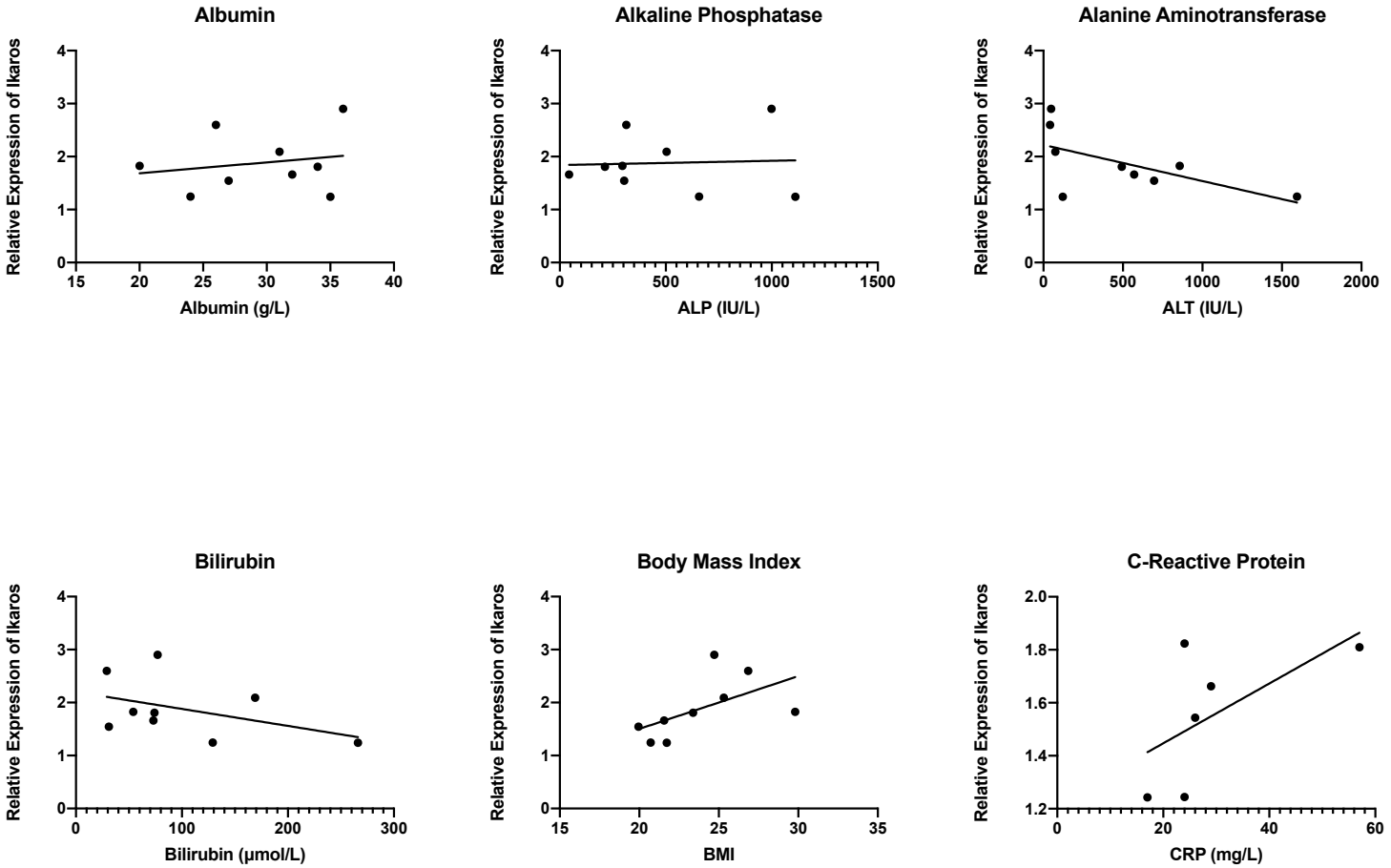



**Figure 4.26: Correlations Between Ikaros and Patient Liver Function Markers in Primary Sclerosing Cholangitis Liver**
Total RNA was isolated from whole Primary Sclerosing Cholangitis (PSC) liver segments and quantitative PCR performed to analyse relative expression levels of the Ikaros Family member Ikaros. Data was normalised to donor livers (data not shown) and then correlated against patient liver function clinical data *(Albumin, Bilirubin, Body Mass Index (BMI), C-Reactive Protein (CRP), Alkaline Phosphatase (ALP), Alanine Aminotransferase (ALT))* from pre-PSC surgery. Dots represent individual liver samples. *N=4-7. NS, Pearson Correlation. Housekeeping Gene: SRSF4.*

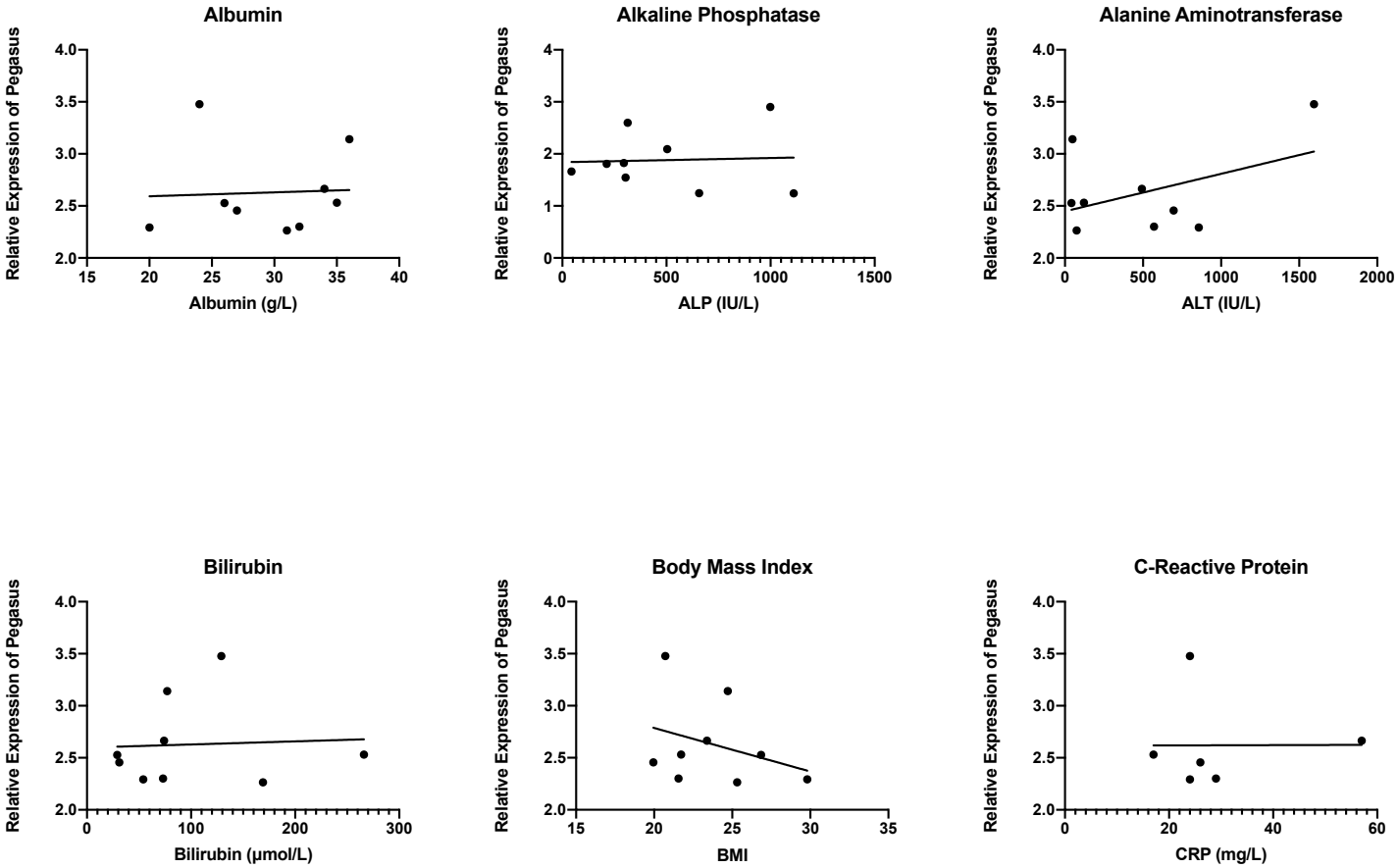



**Figure 4.27: Correlations Between Pegasus and Patient Liver Function Markers in Primary Sclerosing Cholangitis Liver**
Total RNA was isolated from whole Primary Sclerosing Cholangitis (PSC) liver segments and quantitative PCR performed to analyse relative expression levels of the Ikaros Family member Pegasus. Data was normalised to donor livers (data not shown) and then correlated against patient liver function clinical data *(Albumin, Bilirubin, Body Mass Index (BMI), C-Reactive Protein (CRP), Alkaline Phosphatase (ALP), Alanine Aminotransferase (ALT))* from pre-PSC surgery. Dots represent individual liver samples. *N=4-7. NS, Pearson Correlation. Housekeeping Gene: SRSF4.*

## 4.3 Discussion

### 4.3.1 What Happens to Tissue Structure in IBD?

Along with a patient history and biochemical parameters such as faecal calprotectin level, endoscopic classification methods are used by clinicians to diagnose and grade IBD. During endoscopy, it is routine to take biopsies which are fixed in formalin and analysed by pathologists who are then able to reaffirm results from the endoscopy. Biopsies from patients are viewed under a microscope to consider characteristic markers of IBD to identify if the disease is quiescent, inactive, or active, and to what degree (189, 190). It is important to note however that IBD is a dynamic disease and because of flares and remission, biopsies only provide a snapshot of disease at a specific point (190).

When comparing 'normal' or 'healthy' colon (Figure 4.1) with diseased CD (Figure 4.2) and UC samples (Figure 4.3) we found extensive tissue damage resulting from inflammation in IBD. Excessive infiltration by immune cells such as neutrophils, epithelial damage and changes in bowel architecture are hallmarks of IBD (189-191). Architecturally, differences in the crypt structure are also seen, with crypt shortening, deformation and a reduction in crypt density common in IBD (190). Abnormalities in the mucosa and metaplasia of Paneth cells can also be identified in biopsies (190). Importantly since, UC and CD share histological features which can make it hard to distinguish between the two, it is recommended to take multiple biopsies from areas of the ileum or the colon as some regions within the bowel may be unaffected (190). Assessing biopsies in this way provides *'a correct diagnosis in 64% of CD and 74% of UC cases'* (190).

In Figure 4.2, H&E staining of CD tissue showed some characteristic cryptitis with crypt elongation or abscesses, indicating damage to normal bowel tissue integrity.

This lack of crypt integrity has major consequences as crypts are a major site for renewal of key cell types in the bowel such as goblet cells, Paneth cells and enterocytes (35, 39). Compared to healthy bowel tissue, accumulation of immune cells was also evident alongside distortions in the regular tissue structure supporting the presence of inflammation within the bowel. However, we were unable to identify all key markers of CD as biopsies are superficial, and CD is a deep tissue penetrating disease. For UC, changes in the architecture include extreme distortion of the tissue structure and mucosal surface, alongside a reduction in crypt density, superficial ulcers and pseduopolyps (Table 4.2)(189). A diffuse lymphocyte infiltrate in the LP and mucosa was also seen. This is in agreement with my samples where several lymphoid aggregates were identified throughout the mucosa (Figure 4.3) (189, 190). Distortion of crypt structure, alongside cryptitis, where neutrophils infiltrate into the crypt epithelium and crypt abscess were also identified in our samples (189). These evident differences in the H&E of CD and UC disease course can then help aid diagnosis in the clinic.

**Table 4.2: Changes in Tissue Architecture in CD and UC Distinguishable by Biopsies and Resections**

| | CD | UC |
|---|---|---|
| Crypt architecture abnormalities | Discontinuous | Continuous |
| Chronic Inflammation | Discontinuous | Continuous |
| Patchiness | Common | Uncommon |
| Localisation | Transmural | Superficial, Transmural and/or submucosa |
| Lymphoid aggregates | Common, Transmural | Frequent in mucosa and submucosa |
| Granulomas | Present | Absent |
| Acute Inflammation | Discontinuous | Continuous |
| Crypt Abscesses | Uncommon | Common |
| Mucin Depletion | Uncommon or mild | Present |
| Muscular Hypertrophy | Present | Absent |
| Paneth Cell Metaplasia | Uncommon | Present |

Adapted from Magro *et al.,* (2013)

### 4.3.2 Phenotypic Changes in PSC Tissue

Comparison of the H&E stains of Donor and PSC tissue (Figures 4.10 & 4.11) confirmed the changes in tissue structure resulting from autoimmunity. Hepatic steatosis is part of the *'extended criteria'* of donor grafts, which includes NAFLD livers, as although not favourable, these livers are more readily available (192). Although the donor liver accessible to us had failed to meet transplantation criteria and was thus often steatotic, the tissue architecture was relatively normal with no immune cell infiltration present in the tissue. In the donor samples we used, steatosis was either absent or would be classed as mild. In contrast, the PSC samples had significant disruption of normal lobular architecture with clear signs of inflammation and fibrosis, in keeping with the fact the tissue was explanted upon transplantation. PSC can be classified in stages ranging from Stage 1: portal inflammation, Stage 2: periportal inflammation, Stage 3: septal inflammation and Stage 4: cirrhosis (193). The majority of our examples were in the cirrhosis stage as would be expected in explant samples. Thus, I observed characteristic 'onion-skin' fibrosis in PSC, alongside non-specific inflammation and bridging fibrosis with the presence of regenerative nodules in some cases (Figure 4.11). I also observed that the colour of sections also differed greatly, with some samples displaying a yellow/green tinge characteristic of cholestasis in PSC.

### 4.3.3 Ikaros Family Expression in the Liver and Bowel

Once I was reassured that my tissue samples were representative of the diseases in question, I next performed analyses to specifically test whether members of the Ikaros family were present. Within the bowel samples, an infiltration of immune cells within the mucosa and submucosa was clearly seen with corresponding upregulation of

protein levels of Ikaros family members. Various studies have shown that there is an increase in CD4+ T cells and innate immune cells such as macrophages present in IBD tissue (26). We also know that the Ikaros family are expressed by these cells and therefore their upregulation in our tissue is not unexpected (2-4). Similarly, in NASH, PSC and PSC-IBD, immune cell infiltration is believed to contribute to the pathogenesis of these diseases, with Ikaros family expression seen in these cell populations (56, 194). However, to our knowledge, no other study has investigated the expression of the Ikaros family in liver tissue, or compared their expression in Donor, NASH, PSC and PSC-IBD tissue. Similarly, investigations of the levels of the Ikaros family in inflamed and uninflamed human bowel due to IBD are not reported. Thus, our work is some of the first discussing the expression of Ikaros family members in both bowel and liver disease.

#### 4.3.3.1 Ikaros Family Expression Within the Bowel

We found that all members of the Ikaros family were expressed within the bowel, with all bar Pegasus upregulated within inflamed bowel. The Human Protein Atlas (THPA) reports greater expression of Aiolos in the colon than the liver, with detectable expression seen in both (195, 196). Previous studies also describe Aiolos expression within the colon, localised to CD4+ lymphocytes and B Cells (128, 187). We similarly saw this in our DAB-IHC analysis and PCR experiments with higher Aiolos expression seen in inflamed bowel tissue (Figure 4.4 & 4.9). In disease, elevated Aiolos expression has been found in cancers, SLE and RA (110) (See 1.5.6). Li *et al.,* (2014) for example found high expression of Aiolos correlates with poor survival in human lung cancer. This supports our findings of elevated Aiolos expression in IBD and disease in comparison to ‘normal’. This elevated Aiolos expression could then

contribute to pathogenesis through its role on the proinflammatory Th17 phenotype seen in disease, or through dysregulated B cell or T cell function.

We also observed an increase in Eos protein expression in diseased tissue from CD patients (Figure 4.5) which was present throughout the layers of the bowel, with expression seen in lymphocytes. This supports previous literature as Eos is expressed in cells including Tregs, CD8+ T Cells and monocytes, which we know infiltrate the bowel in disease (107, 110, 158). Our genetic analysis of material from patients with UC also suggest RNA levels of Eos were slightly higher in U.C bowel in comparison to Healthy (Figure 4.9), again supporting the concept that it is the infiltrating immune cells which express Eos in IBD.

To our knowledge, there is no data in the public domain on expression or presence of Helios in normal or diseased bowel tissue in humans. The HPA, suggests high Helios expression throughout normal colon which was similar to our findings (195, 196). We found higher Helios expression in inflamed bowel tissue in comparison to uninflamed, with expression throughout the mucosa and submucosa (Figure 4.6). As mentioned previously, Helios expression is crucial for Tregs. An interesting Helios knockout study by Sebastian *et al.,* (2016) in Tregs found that although the deficient Tregs had normal *in vitro* suppressor function and functioned in an *in vivo* IBD model, they had impaired control of T cell expansions and mediation of Tfh and Th1 cells. The group hypothesised that lack of Helios may make Tregs constitutively active encouraging an inappropriate immune response (114). Interestingly, the group also found that these mice developed an enlargement of the liver and hepatic lipidosis. Mice deficient in Helios also developed NAFLD with an elevation of serum alkaline phosphatase levels (114). Correlating our liver patient data with clinical markers (Figure 4.20), we too saw a slight positive correlation between relative Helios expression and Alkaline

Phosphatase levels suggesting a link between Helios positive cells and tissue damage (33). Due to the gut-liver axis (Section 1.2.1), it is not surprising that disease in one organ can be translated to the other, with common mediators between both.

In the bowel, Ikaros expression was higher in inflammation (Figure 4.7), in common with the other family members. This also agreed with previous reports as Ikaros was expressed throughout the bowel in lymphocyte aggregates in diseased tissue, as has been seen in normal colon tissue (195, 196). Ikaros has been linked to IBD, with Ikaros variants reported in IBD (132, 146)(See 1.5.5). Javierre *et al.,* (2011) found that Ikaros was expressed in lymphocytes within the colon and colorectal cancer samples and is hypermethylated in colorectal cell lines. In normal colon samples Ikaros was unmethylated (187). The authors suggested that Ikaros function is cell type specific, with Ikaros hypermethylation causing more aggressive tumours (187). Certainly, Ikaros expression is found in colorectal cancer cell lines including RKO, LOVO and CACO-2 supporting a role for Ikaros in bowel cancer (187). I found that Ikaros expression was elevated in UC samples in comparison to Healthy (Figure 4.9). This suggests that in the bowel, in both UC and CD, Ikaros is upregulated in disease and therefore may exacerbate inflammation which could be dependent on its methylation state.

For Pegasus, no annotated protein expression has been reported in either the bowel or the liver, and to date its role remains unknown (110, 118, 195, 196). In contrast to the other family members and to the hepatic compartment, I found that Pegasus protein and RNA expression within the bowel was similar in both inflamed and uninflamed bowel (Figure 4.8 & 4.9), suggesting Pegasus may not be directly involved in bowel inflammation. Given the structural differences between Pegasus and its

family members, and documented roles in development, this may reflect unique functions of this under investigated protein.

It is however important to note that a limitation of IHC-DAB in the bowel was that some positive staining appeared to be epithelial and non-specific which may have influenced the true amount of staining present. For future analysis therefore determining a more accurate quantitative method such as that discussed in Section 5.2.12 could provide greater accuracy.

#### 4.3.3.2 Ikaros Family Expression Within the Liver

Our RNA and IHC analysis found that all members of the Ikaros family were indeed expressed within liver tissue, with many members upregulated in tissue during disease.

Our results show that Aiolos expression was upregulated in diseased liver tissue, compared to little observed in Donor liver tissue (Figure 4.12). Comparing RNA levels of Aiolos in Donor and diseased liver tissue, we found significantly higher expression of Aiolos in NASH and PSC suggesting Aiolos plays a role in liver disease (Figure 4.17). Previous studies report expression of Aiolos in the liver and malignant hepatocyte cell lines such as Hep3B, although not in the tissue of the diseases we investigated (197, 198). Interestingly, a GWAS study by Webb *et al.,* (2015) did identify SNPs in the Aiolos encoding gene IKZF3 in PBC but did not further consider the role of Aiolos. As Aiolos is expressed in a plethora of cell types including B cells, CD4+ T Cells and as we report, macrophages, the increase in total expression can be explained by the influx of immune cells seen in disease (107, 110, 148-150). This would be in keeping with our immune cell localization of staining.

Like Aiolos, Eos expression was higher in diseased tissue than in Donor, with significantly higher expression of Eos in PSC tissue (Figure 4.13). Eos was also found in lymphocytes, and macrophage-like structures within the tissue, suggesting a role for Eos in Kupffer cells which has not been reported. Although hepatic protein expression has been reported, we were unable to find any publicly available immunochemical data to support cell-specific expression (110, 118, 121, 137, 195, 196). At a gene level I found relative expression of Eos was similar in Donor and diseased tissue suggesting gene and protein regulation may be distinct (Figure 4.17). Interestingly, a positive correlation was found between Eos and BMI in PSC (Figure 4.24) (See below) which may suggest a link to obesity.

Helios expression was similarly higher in PSC tissue than donor material (Figure 4.14), but in contrast, levels in both NASH and PSC-IBD were *lower* than controls. This suggests that in some diseases, Helios may be downregulated. Investigating Helios expression through THPA, we found abundant Helios expression in 'normal' liver, with great positive staining of hepatocytes and lymphocytes (195-197). The expression of Helios in lymphocytes and its known association with Tregs heavily suggests that this Helios expression is Treg-associated (52, 103, 163). Helios is expressed in the foetal liver, therefore our findings support continued Helios expression through into adulthood (163). Interestingly, RNA levels of Helios were significantly elevated in whole NASH tissue in comparison to Donor (Figure 4.17). This again supports the notion of differential regulation of family members at a protein and RNA level. We could hypothesise that this suggests Helios is upregulated at an RNA level due to the loss of protein under inflammatory conditions (199). Similarly, higher Pegasus expression was observed in PSC and PSC-IBD tissue in comparison to staining in Donor samples. We also found highest RNA expression in PSC tissue (Figure 4.16)

suggesting that Pegasus may play a role in PSC-related disease. We were able to correlate Pegasus expression to BMI in NASH, with higher BMI values correlating with lower Pegasus expression (Figure 4.22). Our results however suggest that elevated Pegasus expression may play a role in mediating liver disease.

In contrast to the members above, we observed slightly elevated levels of Ikaros protein and RNA expression in PSC and NASH ($p<0.05$) (Figure 4.15). This supports previous studies which have suggested elevated Ikaros levels correlate with disease (3). Although the THPA does not describe expression in normal tissue, my data and others report expression of Ikaros in both foetal and adult liver (110, 122, 137, 195, 196). Most recently, Ikaros has been implicated in HCC where it negatively regulates MDIG (mineral dust-induced gene) and MYC, two genes that are overexpressed in HCC (200). Most interestingly, RNA analysis from snap-frozen HCC and control liver blocks found HCC livers had a *lower* level of Ikaros expression (200). This therefore suggests that Ikaros plays a vital role in regulating gene expression, which is perturbed in illness due to the loss of Ikaros. As an example, Zhang *et al.,* (2014) report that Ikaros represses CD133, which is a marker *'for enrichment of cancer stem cells'* (201). Here Ikaros binds to CtBP to form a complex which then binds the CD133 promoter and inhibits CD133 expression (201). This group also found low Ikaros expression in HCC which correlated with greater mortality (201). In NASH and PSC however, the opposite appears to be true since elevated Ikaros levels appear to contribute to disease. This has been seen in individuals with CVD and T2DM (188). Concrete confirmation of Ikaros-dependent gene regulation in acute liver injury come from a study investigating Ikaros expression and function during liver transplantation (188). Here, high levels of Ikaros correlated with *'worse human liver transplant function'* (188). Using a rodent transplantation model, the group found elevated levels of Ikaros

in liver macrophages upon reperfusion, with lower SIRT1 levels, and increased inflammasome activation, all of which contributed to greater hepatocyte damage in liver transplants (188). This again supports the upregulation of Ikaros in inflammation-related liver disease, suggesting Ikaros could be an efficient therapeutic target. However, to date it is not clear whether Ikaros may be upregulated at a genetic or protein level but again may not migrate from the cytoplasm into the nucleus to impact gene expression. In our results (Figure 4.15 and Figure 5.23) it does appear that the vast majority of Ikaros staining is nuclear.

### 4.3.4 Ikaros Family Correlations with Liver Clinical Data

As I had access to anonymised clinical data for the patients from whom I had tissue samples, I was able to do correlation analysis. The significant findings are summarised in Table 4.3.

**Table 4.3: Summary of Clinical Data Correlations**

| DISEASE | CORRELATION | P VALUE | ASSOCIATION |
|---|---|---|---|
| NASH | Bilirubin (µmol/L) Vs Helios | *0.0403* | Positive |
| NASH | BMI[1] Vs Pegasus | *0.0427* | Negative |
| PSC | BMI[1] Vs Eos | *0.0467* | Positive |
| PSC | BMI[1] Vs Helios | *0.0008* | Positive |

[1] **BMI: Body Mass Index**

Our results suggest correlations between certain Ikaros family members and clinical markers. There was a clear link between BMI and Eos, Helios and Pegasus suggesting that the Ikaros family may play a role in obesity and metabolism. A strong positive correlation was seen with Helios and BMI value in PSC suggesting that Helios

may play a role in obesity-mediated disease. Patients with a high BMI have an increase in inflammatory cells, thus expression of Ikaros family members in Th17 cells, M1s and even Tregs could understandably increase in these conditions (86). Similar associations with BMI are reported in T1DM and Tregs, with a study by Wu *et al.,* (2019) suggesting high BMI had a negative correlation with Tregs (86, 202). Treg cell expression of Helios has been linked to obesity and insulin resistance in diabetes, but here expression decreased within the adipose tissue with increasing BMI (86, 199). Thus, it is possible that cell specific expression of members of the Ikaros family may be influenced by tissue metabolic status. Another hypothesis is as Tregs are less present within chronic inflammation such as obesity itself but elevated in autoimmunity such as NASH, the upregulated Helios expression and its association could be through the inflammation.

Interestingly, Chrousos and Kino (2005) found that Ikaros is involved in psychological stress responses through the Hypothalamic-Pituitary-Adrenal (HPA) axis and could in turn influence metabolism and obesity. Mutations in Ikaros could make an individual more vulnerable to stress and hence stress associated with IBD pathophysiology (Section 1.1.6) provides another mechanism by which the Ikaros family could influence IBD (203). The group hypothesised that individuals with lower expression of Ikaros would theoretically have reduced alpha-MSH (melanocyte stimulating hormone) and beta-endorphin production through lack of Ikaros regulation. This would then cause increased appetite and corresponding decreased metabolism leading to obesity. In support of this Ezzat *et al.,* (2005) show that Ikaros knockdown in mice models resulted in weight loss which could be circumvented through exogenous addition of glucocorticoid treatment (204). Interestingly, Ikaros null mice exhibited compensatory upregulation of other family members such as Eos which could also contribute to

disease (204). Therefore, my observed negative correlation of Pegasus and BMI in NASH are similar to what has been proposed by Chrousos and Kino (2005) and regulation of weight by Ikaros. This offers the potential that Pegasus may regulate appetite in NASH and could be a target for NASH management. Contrastingly, positive correlations of both Eos and Helios with BMI in PSC suggests elevated levels of both transcription factors may promote weight gain and contribute to increased BMI.

In NASH, a positive correlation between elevated Bilirubin levels and Helios was also found (Figure 4.20). Although there is limited data on Helios expression in NASH, a correlation between Helios and Bilirubin suggests a link between the transcription factor and inflammation within the liver. A study by Vaeth *et al.,* (2019) saw that deletion of Stim1 and Stim 2, two genes required for formation of the calcium release activated calcium channels (CRAC) in Tregs, prevented Treg formation and downregulated Helios (205). Specifically in the liver, these mice exhibited lymphocyte infiltration around their bile ducts and displayed a phenotype which resembled PBC (205). Overall, the results suggest a link between Helios and Treg differentiation and that compromised regulation leads to biliary inflammation as seen in PSC.

Although we were able to assess Ikaros family protein and RNA levels in '*normal'* and diseased bowel and liver tissue, there were some limitations to our work enforced by sample availability which could be addressed in future studies. RNA levels were measured in UC biopsies whereas protein was detected by IHC in CD resected samples, thus the results cannot be compared. Our RNA levels were assessed in whole tissue therefore our results do not identify specific cellular expression. We also lacked IBD clinical data from samples. Overall, analysis of the Ikaros family in matched tissue and blood from Donor and diseased would provide greater clarity on the relationship between protein and RNA expression of the family. Selecting regions of

interests for analysis alongside cell-specific Ikaros family expression would also provide insight into the mechanisms of action of the transcription factors. We addressed this partially, by tissue staining technique Opal™ which will be discussed in further detail in the next chapter.

### 4.3.5 Summary

Our findings in both the liver and the bowel in disease support our hypothesis that the Ikaros Family could play a role in disease due to their deviations in expression from normal (Figure 4.28). We have also identified expression of family members within macrophages in the liver, suggesting a key role for the family in this cell population. Correlations between family members and clinical markers reinforce this relationship, suggesting further investigation could implicate family members as targets in liver and bowel disease.

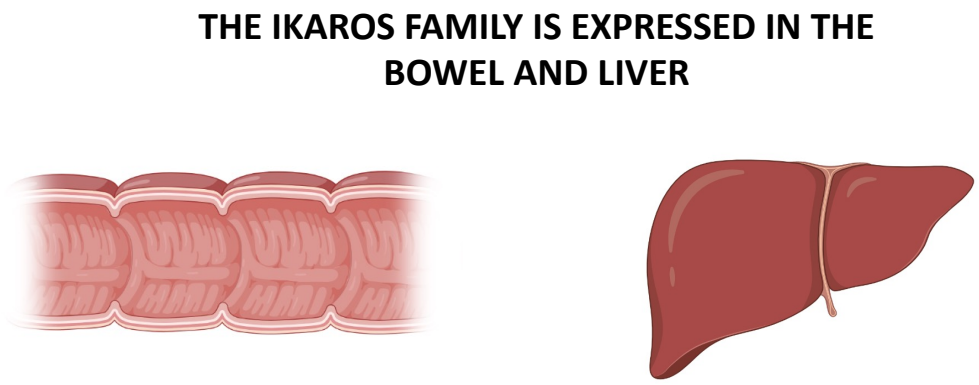



**Figure 4.28: Summary Diagram For Chapter 4**
Summary diagram of the key findings from the *Ikaros Family Expression Within The Bowel And Liver* thesis chapter. In the inflamed colon, higher levels of Aiolos, Eos, Helios and Ikaros protein was found in comparison to uninflamed. In the liver, Primary Sclerosing Cholangitis (PSC) tissue had higher levels of Aiolos RNA and Eos, Helios, and Pegasus protein. Correlating clinical markers with Ikaros family expression within liver tissue, a positive correlation was observed between BMI and Helios and Eos in PSC tissue, with a negative correlation between Pegasus and BMI. In NASH, a positive correlation between Bilirubin and Helios was seen. *NASH, Non-alcoholic Steatohepatitis; PSC, Primary Sclerosing Cholangitis*

# Chapter 5: Ikaros Family Expression Within Monocytes and Macrophages

## 5.1 Introduction

In our previous chapter, we reported that all members of the Ikaros family were expressed within the bowel and liver appearing within macrophage-like structures within the tissue. To our knowledge, Ikaros family expression within macrophages in the bowel and liver is virtually unexplored. Previous studies have indicated that certain members of the Ikaros family are expressed within myeloid populations, with no data available for Pegasus (113). Investigation into the function of the Ikaros family is even more limited, but there are some studies which have focused on the role of Ikaros in macrophage function (142). Ikaros expression has been reported in macrophage populations, with studies suggesting Ikaros isoforms Ik-1 and Ik-2 are expressed in these cells (83, 139, 142, 206). In childhood AML, Ik-6 is common suggesting a lack of normal Ikaros function may contribute to the abnormal myeloid phenotype seen in patients (122, 142). Oh *et al.,* (2018) found that Ikaros could play a role in macrophages by regulation of chromatin state and that Ikaros was needed for a sufficient response to LPS-induced bacterial induction of inflammatory gene expression. Bruns *et al.,* (2016) also saw Ikaros expression in macrophages and using an Ikaros knockdown in macrophages found an increase in the Th17 response suggesting a rise in proinflammatory mediators. Interestingly, the group found that expression of Ikaros was higher in M2-like macrophages and that crucially, Ikaros could be used to influence macrophage polarisation (206).

Data on other Ikaros family members however is limited. A study by John and Ward (2011) suggested the highest expression levels of Eos are seen in monocytes in comparison to other immune cell subtypes. The study by Hu *et al.,* (2007) also discussed the influence of Eos on MITF and PU.1 in osteoclasts which are also found in macrophages and monocytes suggesting a potential link to investigate Eos function

in both populations. Interestingly, Thornton *et al.,* (2010) did not find Helios expression in monocytes or macrophages. Similarly, there is no data to the best of our knowledge reporting macrophage expression of Aiolos and Pegasus. Thus, new insights generated as a result of my work will advance our understanding of whether cell plasticity and polarisation linked to Ikaros family expression is important for IBD pathophysiology.

Therefore, the objectives of this chapter were:

I. To ascertain if the Ikaros family is expressed within monocytes and macrophage subsets
II. If the Ikaros family is expressed, to determine if members have differential expression within different macrophage subsets
III. To determine if bowel disease has any impact of Ikaros family expression within the macrophage population in the bowel
IV. To determine if there is differential expression of macrophages and the Ikaros Family within different regions (stricture, distal and proximal) of resected tissue

## 5.2 Results

### 5.2.1 Quantitation of Macrophages in the Healthy, Crohn's Disease and Ulcerative Colitis Bowel Biopsies

We began by first observing the localization and number of CD68-expressing (CD68+) macrophages present in bowel sections from normal, CD and UC colon biopsies. Using DAB-IHC, we observed staining for CD68+ macrophages in all three types of bowel sections, with high CD68+ expression observed particularly in CD tissue sections, surrounding crypts. UC bowel also had comparably greater CD68+ staining in comparison to normal tissue (Figure 5.1) both in inter-crypt areas and aggregates of inflammatory cells. To quantitatively assess macrophage abundance in uninflamed vs inflamed bowel sections, we additionally stained CD68 using the same primary antibody and Opal™ 690 (Figure 5.2) and calculated the percentage area CD68+ in randomly selected regions (*n*) from each *N* using Image J. Our results found macrophages throughout the tissue in both normal and diseased sections. Quantitation confirmed that the number of CD68+ macrophages was significantly higher ($p<0.01$) in inflamed bowel in comparison to uninflamed bowel (Figure 5.2B). Representative IgG images are present in Appendix A.

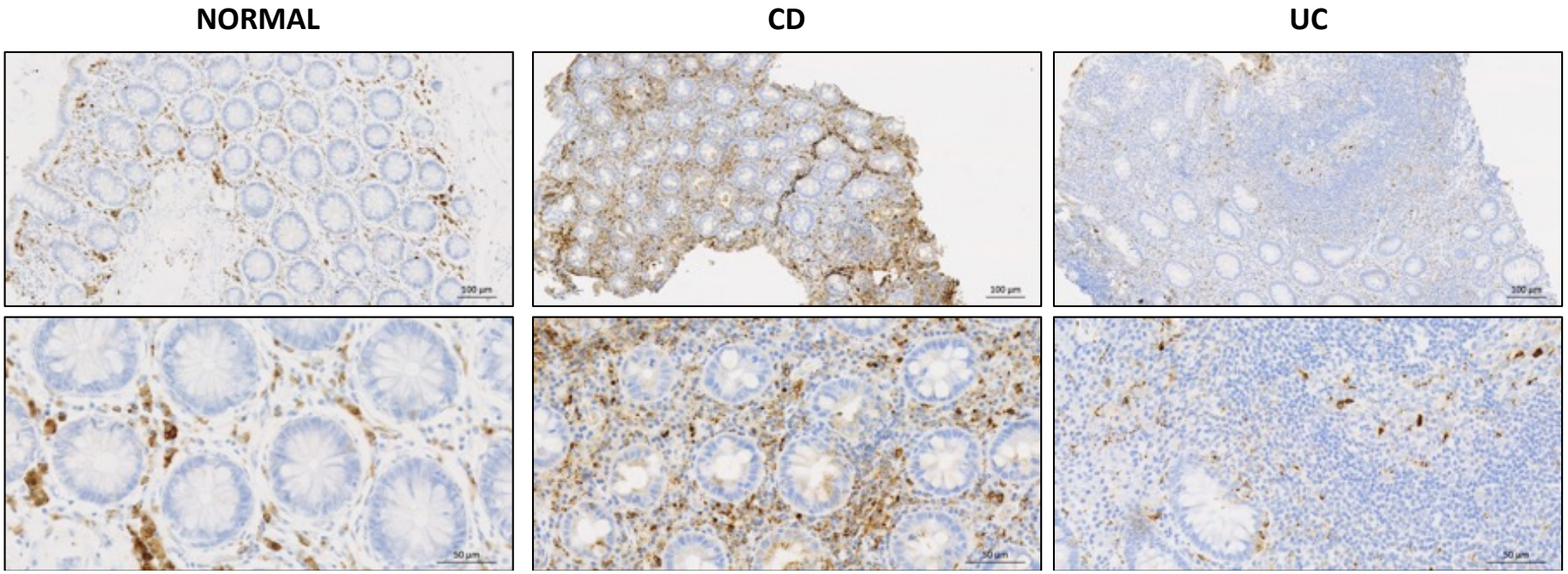



**Figure 5.1: Expression of CD68 in the Bowel**
3,3'-diaminobenzidine (DAB) staining was used to view the presence of CD68+ Macrophages in the bowel. Normal (uninflamed tissue), Chron's Disease (CD) and Ulcerative Colitis (UC) bowel sections were all found to express CD68. Representative images for each tissue category are shown. *Magnification x20.Top row:* Scale Bar represents 100µm. *Bottom row:* Scale Bar represents 50µm. *N=1.*

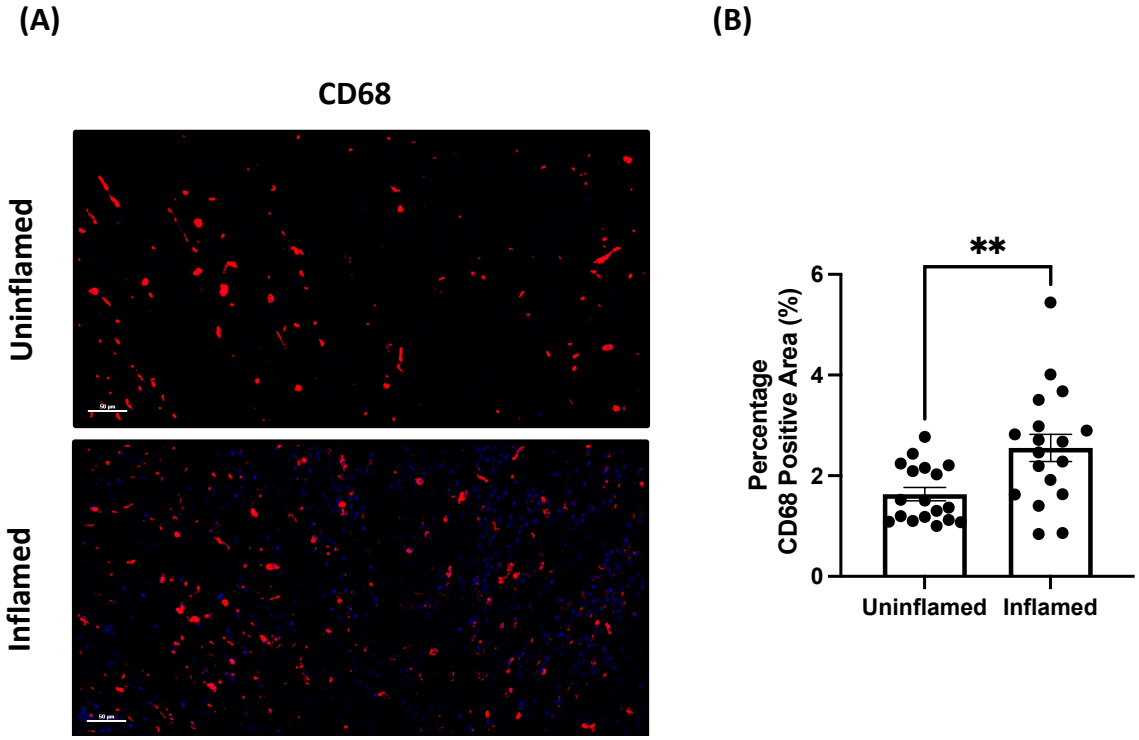



**Figure 5.2: CD68-Expressing Macrophage Expression in Uninflamed and Inflamed Bowel**

**(A)** Opal Dye™ 690 was used to view the presence of CD68 positive (CD68+) macrophages in uninflamed and inflamed bowel tissue (stained in red). DAPI was used as the nuclear stain (stained in blue). **(B)** Semi-quantitative analysis of CD68+ cells present in tissue was conducted on 10 fields of view from an N of 3 matched uninflamed and inflamed tissue regions using Image J Software. Slides were imaged using the Vectra Polaris system and Phenochart software. Dots represent regions and bars represent the mean. Results are presented as Mean ± SEM. Magnification *x20.* Scale Bar represents 50µm. *Non-Inflamed, N=3, n=10; Inflamed, N=3, n=10.* **p<0.01, *Unpaired T Test.*

### 5.2.2 Quantitation of Macrophages in the Liver

Liver tissue contains resident macrophages known as Kupffer Cells which are integral to liver innate immunity (55, 56, 207). To assess the impact of inflammation on CD68+ macrophages in the liver, DAB-IHC staining was conducted on donor and inflamed PSC, PSC-IBD and NASH tissue, with quantitative analysis conducted on randomly selected regions (*n*) from each N. Our results (Figure 5.3) show that CD68+ expression in PSC and PSC-IBD liver tissue was significantly ($p<0.0001$) increased compared to Donor tissue. Similarly, CD68+ expression in PSC and PSC-IBD was significantly higher ($p<0.01$) than in NASH.

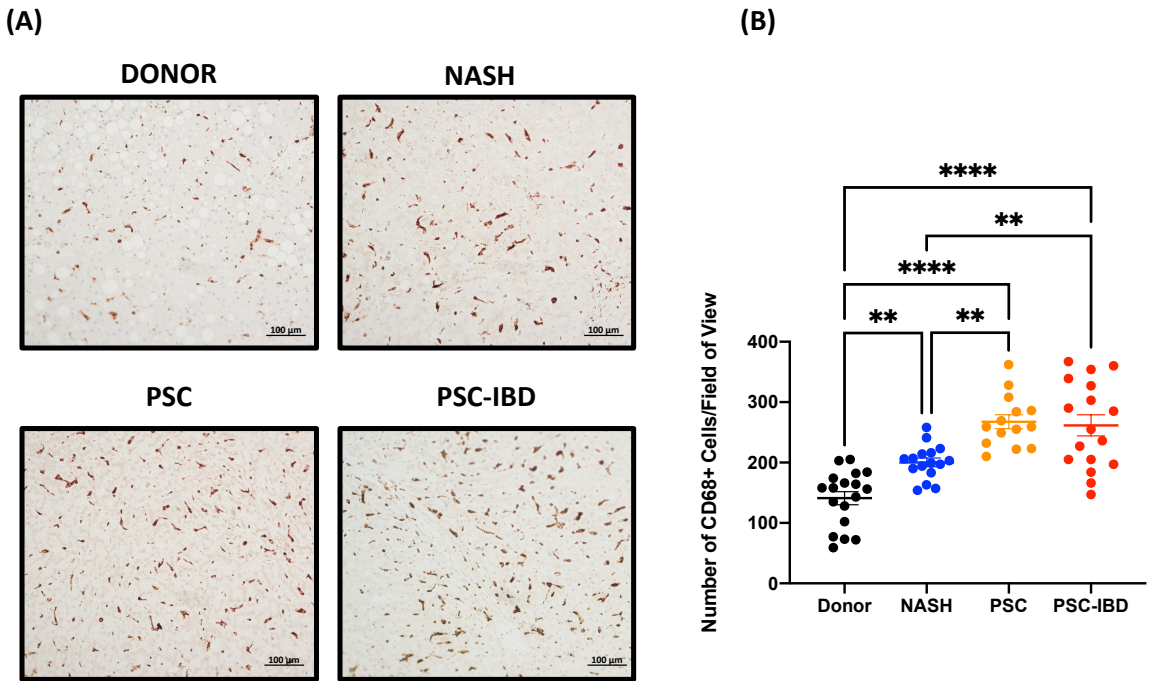



**Figure 5.3: CD68+ Macrophage Staining in Liver**
3,3'-diaminobenzidine (DAB) staining was used to view the presence of CD68 positive (CD68+) cells in liver tissue. **(A)** Donor, NASH, PSC and PSC-IBD liver tissue were found to express CD68+ markers of Kupffer Cells. **(B)** Semi-quantitative analysis of CD68+ cells present in tissue was conducted on an average of 3-5 fields of view from an *N* of 3 diseased tissue using Image J Software. Results are presented as mean ± SEM. Representative images are shown. Magnification x20. Scale Bar represents 100µm.*N=3, n=3-5. Donor Vs NASH **P<0.01; Donor Vs PSC **** p<0.0001; Donor Vs PSC-IBD **** p<0.0001; NASH Vs PSC ** p<0.01; NASH Vs PSC-IBD ** p<0.01 one-way ANOVA and Tukey's Multiple Comparison Test.*

### 5.2.3 Basal Expression of the Ikaros Family in Monocytes and the THP-1 Cell Line

To further investigate the role of the Ikaros family in the myeloid cell lineage, it was imperative for us to establish baseline expression of the family in peripheral blood-derived monocytes and the established monocyte-like cell line, THP-1. Using RNA extraction and qPCR, we found both type of cells expressed mRNA for all members of the Ikaros family at similar expression levels and thus could be used for further experimentation (Figure 5.4)

We also confirmed expression of Ikaros family proteins within THP-1 cells using flow cytometry with the gating strategy described in Figure 5.5. Flow analysis of THP-1 cells found that the highest MFI value was of Eos, with Aiolos expression the lowest with an MFI of 1587AU (Figure 5.6). Helios and Ikaros expression had comparable means in THP-1 cells by Flow Cytometry. Due to a lack of suitable Pegasus flow antibody, MFI values for the transcription factor were not assessed.

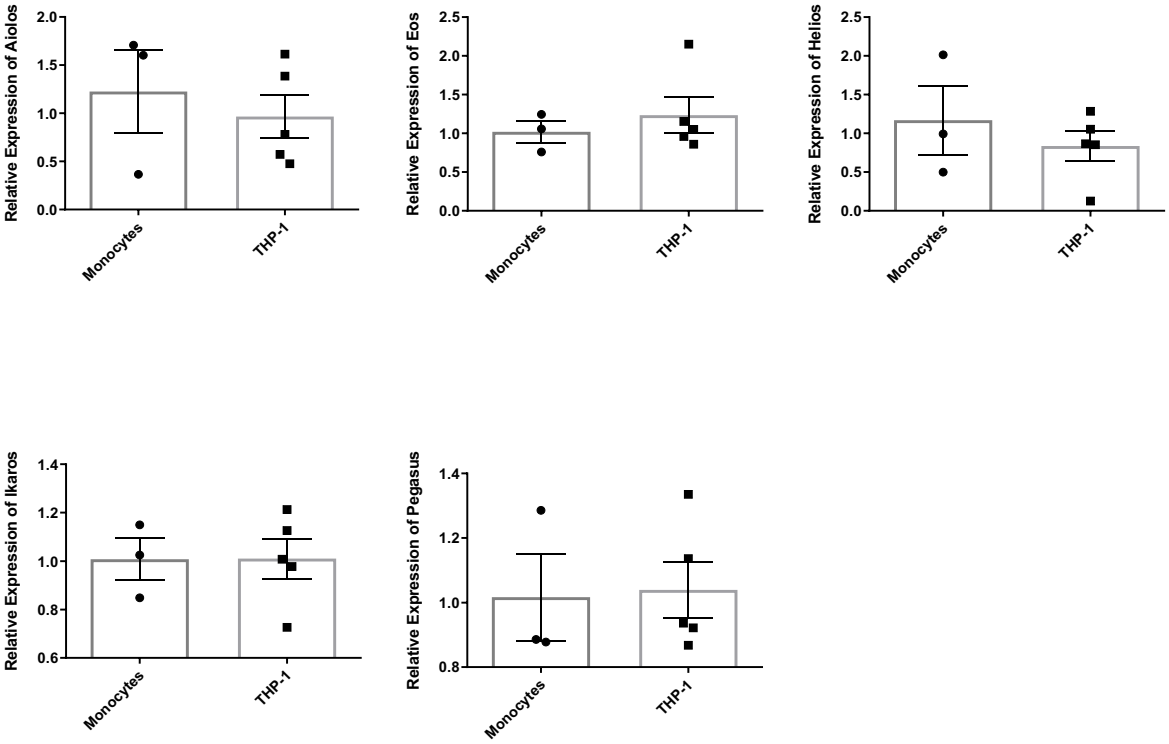



**Figure 5.4: Monocytes From Peripheral Blood Mononuclear Cells Have Similar Expression Levels of the Ikaros Family of Transcription Factors as the THP-1 Cell Line**

Blood-derived pan monocytes were isolated from hemochromatosis blood (monocytes) and alongside THP-1 cells were lysed for RNA extraction. qPCR was then conducted to assess expression levels of the Ikaros family of Transcription Factors in both cell types. Data was normalised to monocyte expression. Results are presented as mean ± SEM. Monocytes, *N=3,* THP-1, *N=5. NS. Unpaired T-test. Housekeeping Gene: RPS9.*

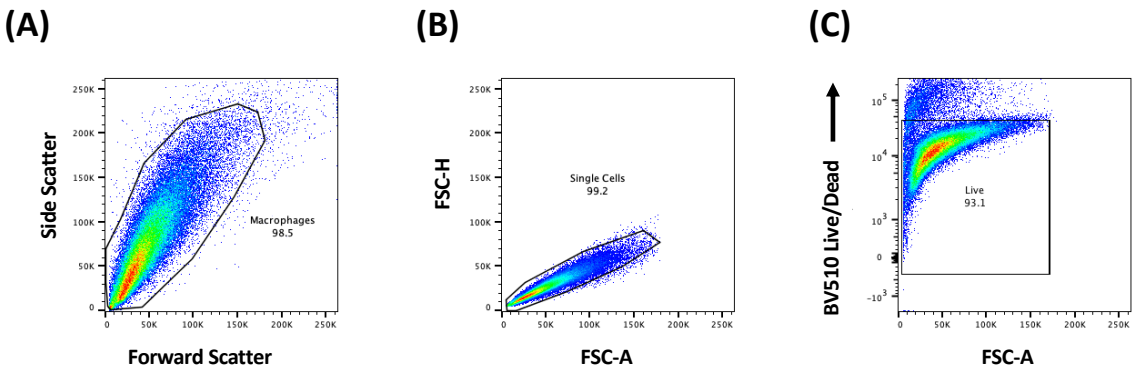



**Figure 5.5: THP-1 Derived Macrophage Flow Cytometry Gating Strategy**
**(A)** Gate cells to exclude debris with macrophage population identified, **(B)** Doublets excluded to identify singlet populations only and **(C)** Dead cells identified as those which are live/dead cell stain positive. Representative plots are shown.

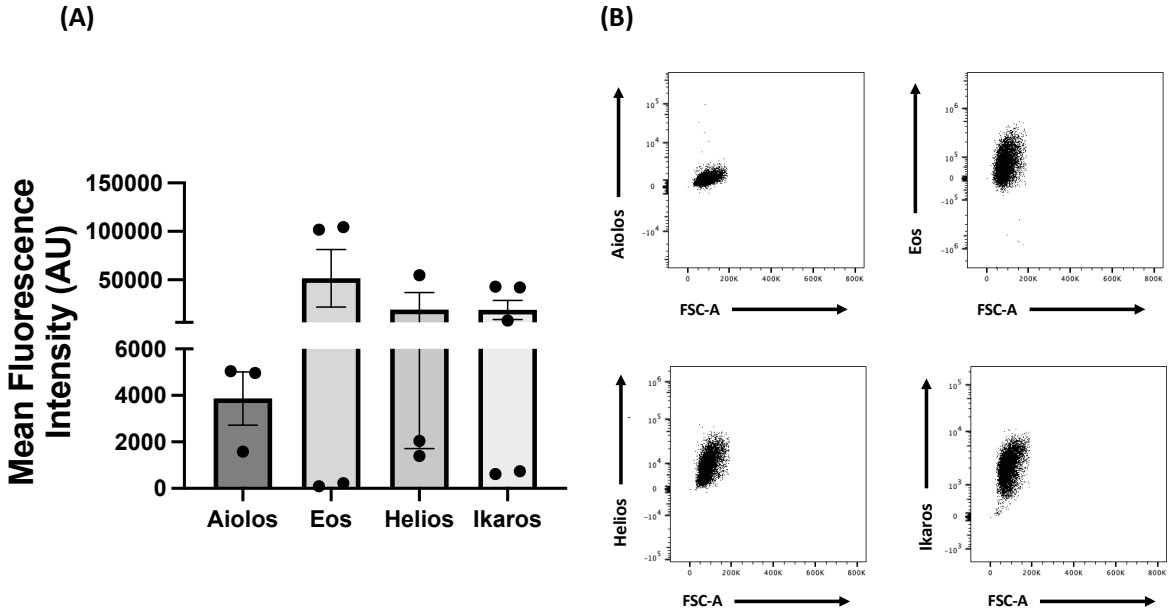



**Figure 5.6: THP-1 Cells Express Protein Levels of Aiolos, Eos, Helios and Ikaros**
Total THP-1 populations were analysed for protein expression of Ikaros family members, Aiolos. Eos, Helios, and Ikaros by Flow Cytometry and analysed using FlowJo V10 software to determine Mean Fluorescence Intensity (MFI, Arbitrary Units, AU). **(A)** MFI values were normalised to unstained samples. **(B)** Representative flow cytometry plots for each transcription factor are shown. *N=3, n=3-5. NS. One-Way ANOVA.*

### 5.2.4 Polarising the THP-1 Cell Line into Macrophages

To investigate the role of the various transcription factors in macrophages, we needed to optimise a method for macrophage polarization. We began by establishing if the THP-1 cell line could be polarised into different macrophage subsets (MΦ, M1, M2a and M2c) using the method described in Section 2.2.2.2, with the aim to replicate this in primary cells. To confirm their polarised phenotype, the supernatants from the THP-1/Macrophage cultures were analysed for IL-12 and IL-10 secretion using ELISA kits. Figure 5.7 shows that the M2c population i.e., the subset polarised using IL-10, secreted the highest concentration of IL-10 at approximately 3500pg/ml. In contrast IL-12 production was more widespread amongst in different macrophage populations (Figure 5.8) but tended to be produced at very low concentrations. M1 macrophages had the highest secretion of IL-12 at 0.3pg/ml with lower levels of IL-12 secretion seen in both THP-1 and M2a culture supernatants.

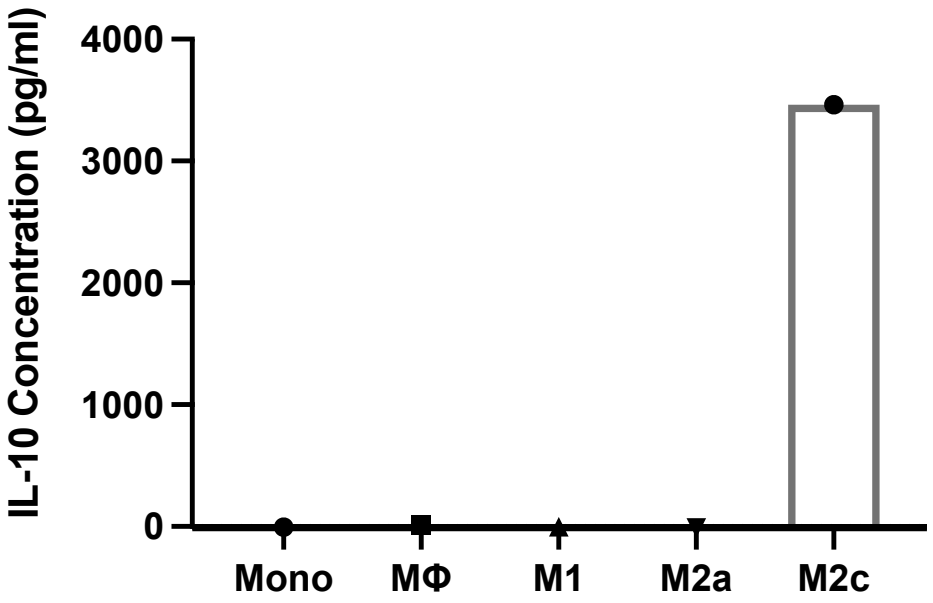



**Figure 5.7: Differentiated THP-1 M2c Macrophages Secrete the Most IL-10**
THP-1 cells were left untreated (THP-1) or polarised to Macrophages (MΦ) using PMA (50ng/ml). They were then further polarised to M1 = PMA (50ng/ml) + IFNγ (20ng/ml) + LPS (20ng/ml), M2a = PMA (50ng/ml) + IL-4 (20ng/ml), M2c = PMA (50ng/ml) + IL-10 (20ng/ml) for 24 hours. After incubation, the supernatants were harvested and used for quantification of IL-10 using the R&D Quantikine ELISA kit. *N=1.*

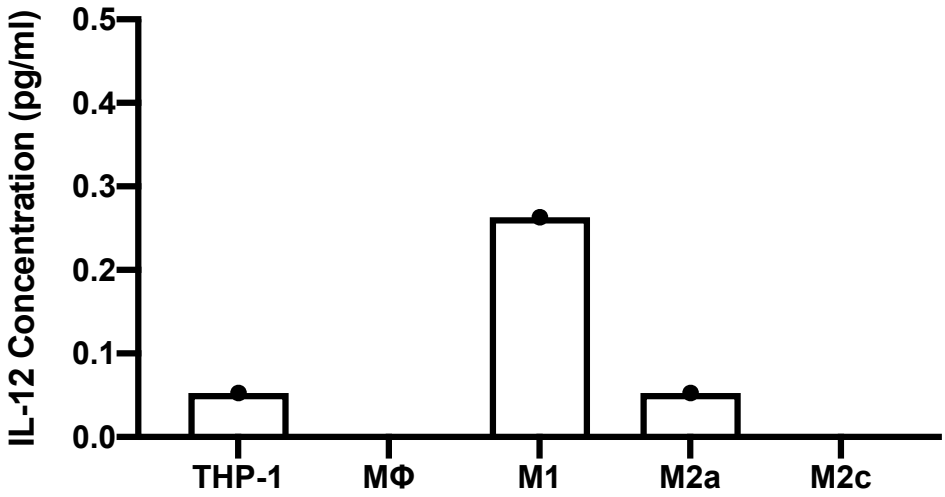



**Figure 5.8: Differentiated THP-1 M1 Macrophages Secrete the Most IL-12**
THP-1 cells were left untreated (THP-1) or polarised to Macrophages (MΦ) using PMA (50ng/ml). They were then further polarised to M1 = PMA (50ng/ml) + IFNγ (20ng/ml) + LPS (20ng/ml), M2a = PMA (50ng/ml) + IL-4 (20ng/ml), M2c = PMA (50ng/ml) + IL-10 (20ng/ml)) for 24 hours. After incubation, the supernatants were harvested and used for quantification of IL-12 using the R&D Quantikine ELISA kit. *N=1.*

### 5.2.5 Polarised THP-1 Derived Macrophages Express Macrophage Subtype-Specific Surface Markers

To assess the success of our THP-1-derived macrophage culture, we cultured cells as above and harvested cells after polarisation to either MΦ, M1, M2a or M2c for flow analysis. The aim of this was to ensure that each macrophage subtype expressed cell surface markers which from known literature were found to be associated with particular subtypes. The cell surface markers analysed included CD86, HLA-DR, CD80, CD163, CD206, CD14 and CD16 using the gating strategy described in Figure 5.9. Analysis of surface markers of macrophage differentiation found that our polarisation method was successful, with all populations expressing CD45 (Figure 5.10) (208). Expression of HLA-DR, CD80 and CD86 was highest in M1 populations supporting previous literature (Table 1.5, Chapter 1). In contrast, expression of CD206 and CD163 was highest in the M2a populations, again supporting previous literature which highlights both of these expression markers as M2-related (75, 80, 81)

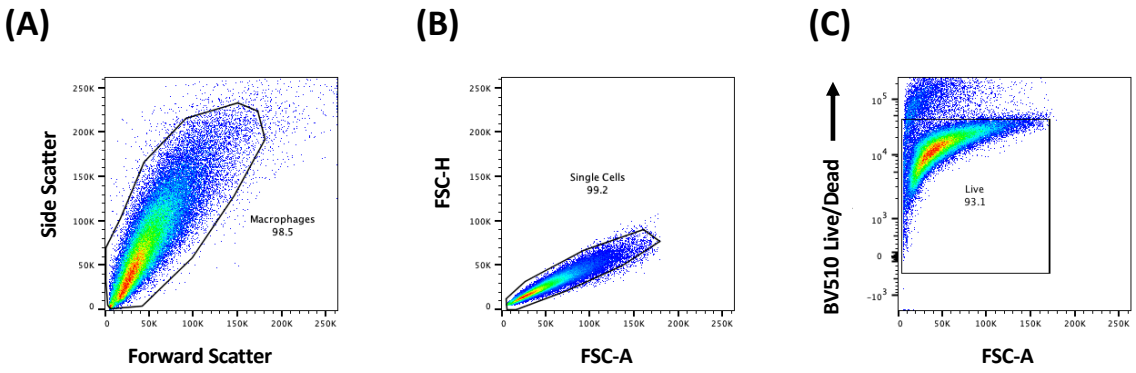



**Figure 5.9: THP-1 Derived Macrophage Flow Cytometry Gating Strategy**
**(A)** Cells were gated to exclude debris with macrophage population identified, **(B)** Doublets were then excluded to identify singlet populations and **(C)** Dead cells were identified as those which are live/dead cell stain positive. Representative plots shown. *FlowJo V10.*

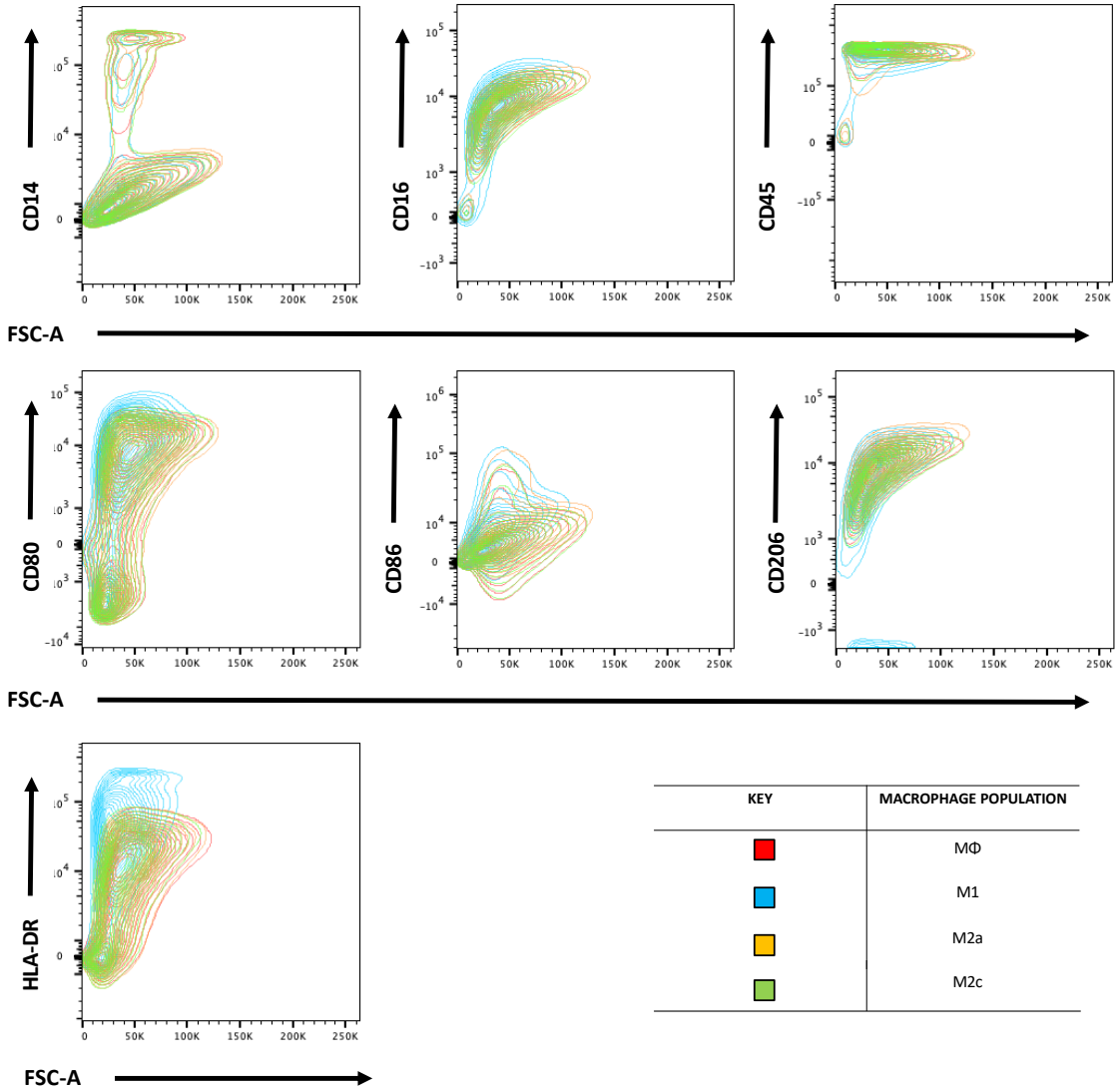



**Figure 5.10: Markers of Macrophage Differentiation**
THP-1 cells were left untreated (THP-1) or polarised to Macrophages (MΦ) using PMA (50ng/ml). They were then further polarised to M1 = PMA (50ng/ml) + IFNγ (20ng/ml) + LPS (20ng/ml), M2a = PMA (50ng/ml) + IL-4 (20ng/ml), M2c = PMA (50ng/ml) + IL-10 (20ng/ml) for 24 hours. The cells were harvested and then stained with markers of macrophage differentiation; CD14, CD16, CD45, CD80, CD86, CD206 and HLA-DR for flow cytometry analysis. *N=2.* Representative plots are shown. *FlowJo V10.*

### 5.2.6 RNA Expression of the Ikaros family in THP-1 derived Macrophage Populations

To investigate the RNA expression levels of the Ikaros family in THP-1 cells and macrophages, THP-1 cells were left unpolarised or stimulated with PMA (50ng/ml) and various effectors to polarise them into macrophage subsets (MΦ, M1 and M2a and M2c) *in vitro*. Expression of the Ikaros family was then analysed by qPCR (Figure 5.11). We observed significantly higher levels of Aiolos ($p<0.01$) in M1-like macrophages and in contrast significantly higher levels of Helios ($p<0.01$) in M2a-like macrophages. THP-1 cells and macrophage populations all expressed similar levels of both Ikaros and Eos whereas polarised macrophage populations had significantly higher levels of Pegasus (M2a, $p<0.05$; M2c, $p<0.01$) in comparison to THP-1 cells.

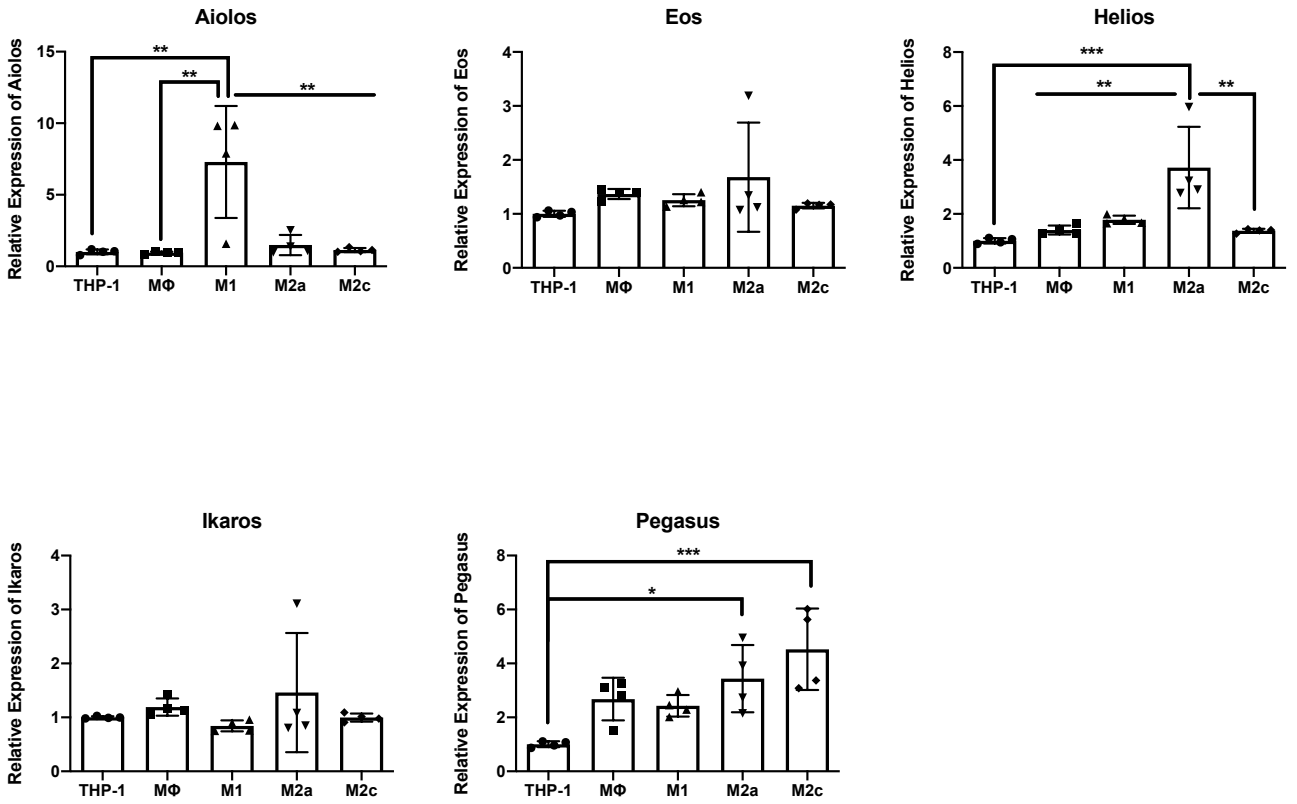
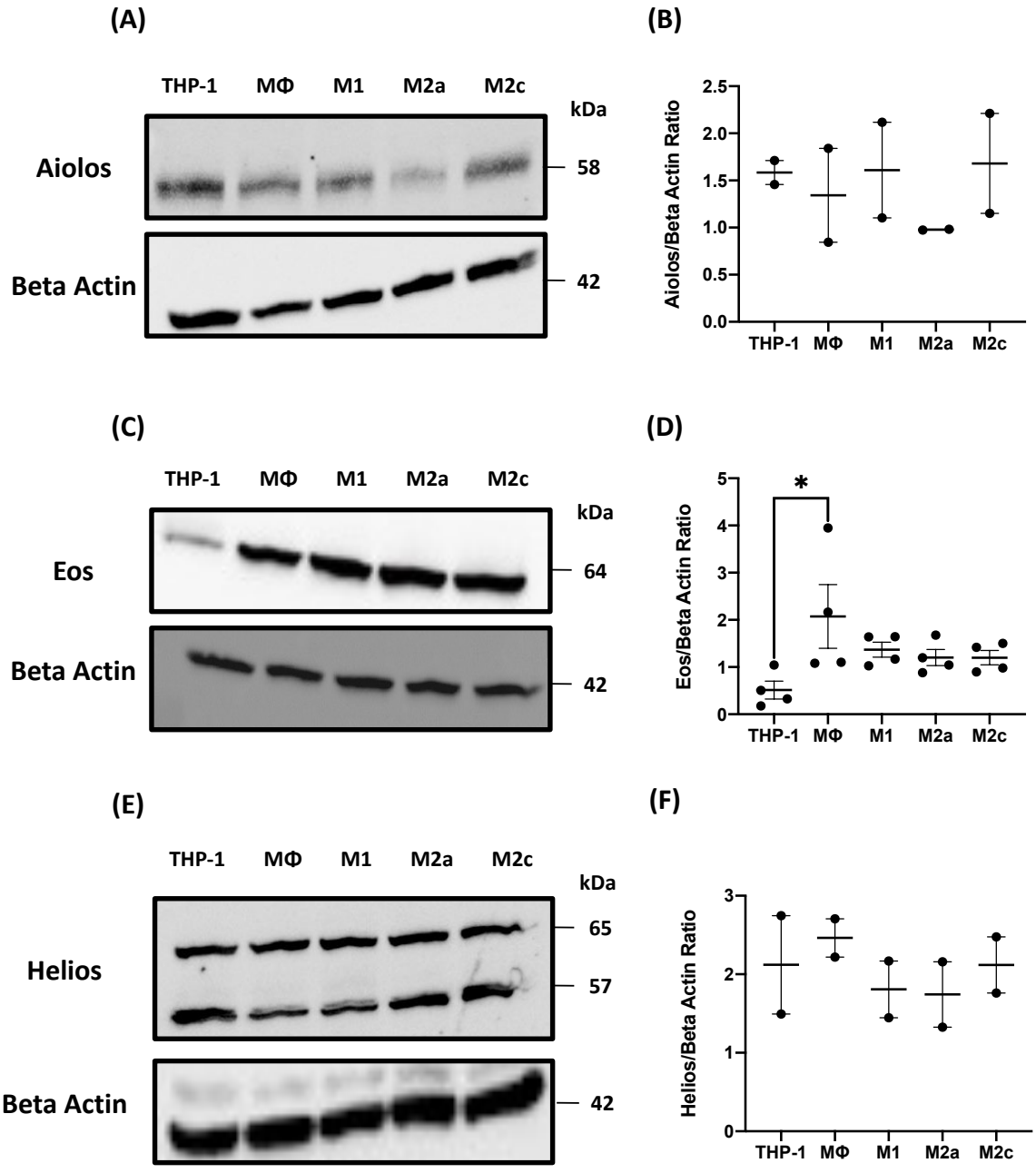



**Figure 5.11: Polarisation of THP-1s Into Different Macrophage Populations Alters the RNA Expression of the Ikaros Family**
THP-1 cells were left untreated or treated with PMA to polarise them to Macrophages (MΦ). They were then left untreated or incubated with mediators to polarise them to further macrophage subsets (MΦ = PMA (50ng/ml), M1 = PMA (50ng/ml) + IFNγ (20ng/ml) + LPS (20ng/ml), M2a = PMA (50ng/ml) + IL-4 (20ng/ml), M2c = PMA (50ng/ml) + IL-10 (20ng/ml). Total RNA was extracted from samples and measured by qPCR. Expression is shown for each group relative to the level in THP-1. Results are presented as mean ± SEM. *N=4. Aiolos *** p< 0.001; Helios *** p< 0.001; Pegasus ** p<0.01. One way ANOVA and Tukey's Multiple Comparison Test. Housekeeping Gene: RPS9.*

### 5.2.7 Protein Expression of Ikaros Family Members in THP-1-Derived Macrophages

Protein lysates were also harvested from the cell populations and used to determine protein expression of the Ikaros family through Western Blotting (Figure 5.12). All members of the Ikaros family were found to be expressed at protein level in THP-1 cells and THP-1-derived macrophages. Relative levels of expression normalised to a housekeeping gene (GAPDH or Beta-actin, both of which remained expressed across the differentiation spectrum) were determined using Image J software to provide relative quantification of amounts of transcription factor in each cell population. The highest protein levels of Aiolos were found in THP-1, M1 and M2c populations, with M2a populations expressing the least amount of Aiolos (Figure 5.12A & 5.12B). Eos contrastingly had higher expression levels throughout all populations, with significantly higher levels ($p<0.05$) seen in MΦ in comparison to THP-1 cells (Figure 5.12C & 5.12D). Helios expression was observed throughout all populations, with similar expression seen in all populations (Figure 5.12E & 5.12F). Ikaros similarly was expressed in all populations with similar expression levels seen in all, asides from M2c which had slightly lower expression (Figure 5.12G & 5.12H). In contrast, significantly higher levels ($p<0.05$) of Pegasus were seen in M1 populations in comparison to MΦ and M2c macrophage populations (Figure 5.12I & 5.12J).


(A)
THP-1
MΦ
M1
M2a
M2c
kDa
Aiolos
58
Beta Actin
42
(B)
Aiolos/Beta Actin Ratio
2.5
2.0
1.5
1.0
0.5
0.0
THP-1
MΦ
M1
M2a
M2c
(C)
THP-1
MΦ
M1
M2a
M2c
kDa
Eos
64
Beta Actin
42
(D)
Eos/Beta Actin Ratio
*
5
4
3
2
1
0
THP-1
MΦ
M1
M2a
M2c
(E)
THP-1
MΦ
M1
M2a
M2c
kDa
Helios
65
57
Beta Actin
42
(F)
Helios/Beta Actin Ratio
3
2
1
0
THP-1
MΦ
M1
M2a
M2c

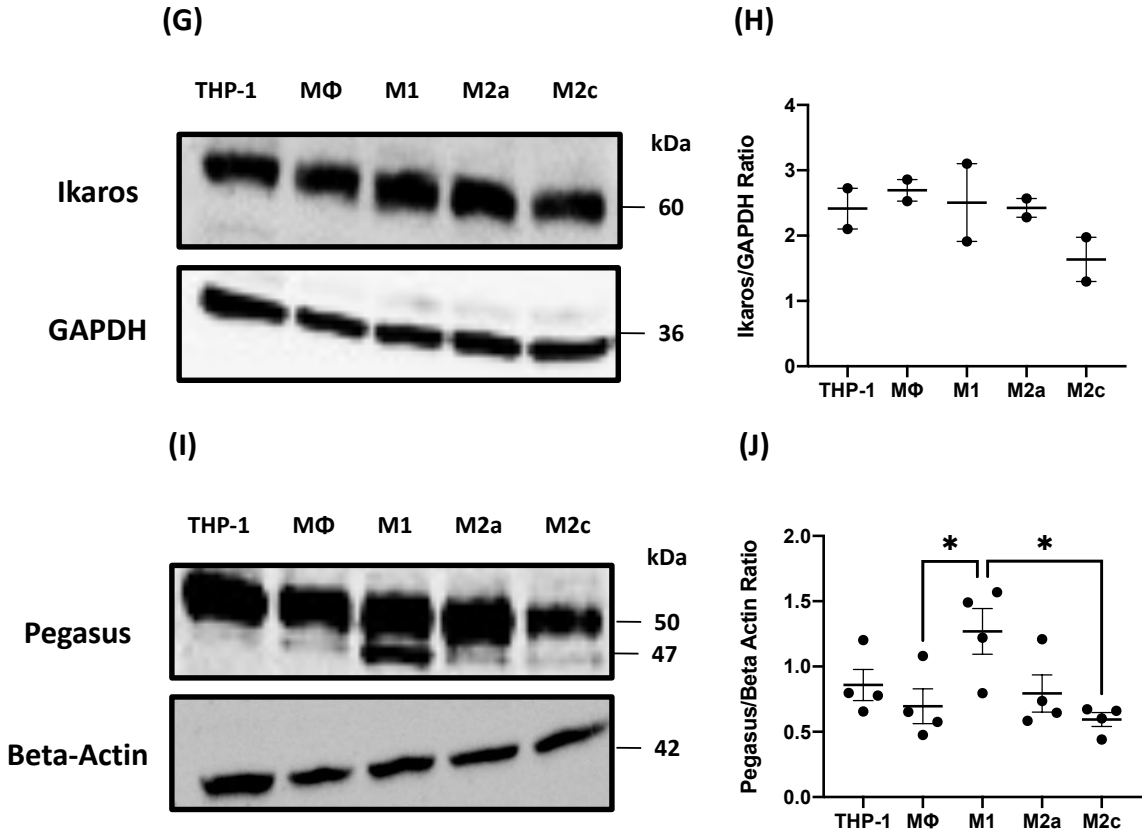



**Figure 5.12: Polarisation of THP-1s Into Different Macrophage Populations Alters the Protein Expression of the Ikaros Family**

THP-1 cells were left untreated or treated with PMA to polarise them to Macrophages (MΦ). They were then left untreated or incubated with mediators to polarise them to further macrophage subsets (MΦ = PMA (50ng/ml), M1 = PMA (50ng/ml) + IFNγ (20ng/ml) + LPS (20ng/ml), M2a = PMA (50ng/ml) + IL-4 (20ng/ml), M2c = PMA (50ng/ml) + IL-10 (20ng/ml). Protein lysates were then extracted from samples, concentration determined by Bicinchoninic acid (BCA) assay and protein presence visualised by Western Blotting. Representative blots for proteins are shown. (A) & (B) Aiolos; (C) & (D) Eos; (E) & (F) Helios; (G) & (H) Ikaros; (I) & (J) Pegasus. GAPDH and Beta-Actin were used as housekeeping genes. Relative protein quantification was determined by normalising protein to housekeeping gene using Image J software. Results are presented as mean ± SEM. Average molecular weights of proteins in Kilodalton (kDa) are shown. *N=2-4*. Eos * $p<0.05$; Pegasus * $p<0.05$. *One way ANOVA and Tukey's Multiple Comparison Test.*

Using the same gating strategy and method described above we analysed expression of Ikaros family members in macrophage populations by flow cytometry. Our results (Figure 5.13A & 5.13B) showed that all members of the Ikaros family were found to be expressed at protein levels in THP-1 cells and THP-1-derived macrophages. Both Aiolos and Helios had their highest MFI values in THP-1, although overall, Aiolos had the lowest MFI values of all family members. Helios expression was dramatically lower in all macrophage populations in comparison to its expression within THP-1 cells. Ikaros expression was highest in THP-1 cells, but again was expressed within macrophages, with the highest expression within M2a populations. Expression of Eos was similar throughout all populations, with slightly higher expression within M2c.

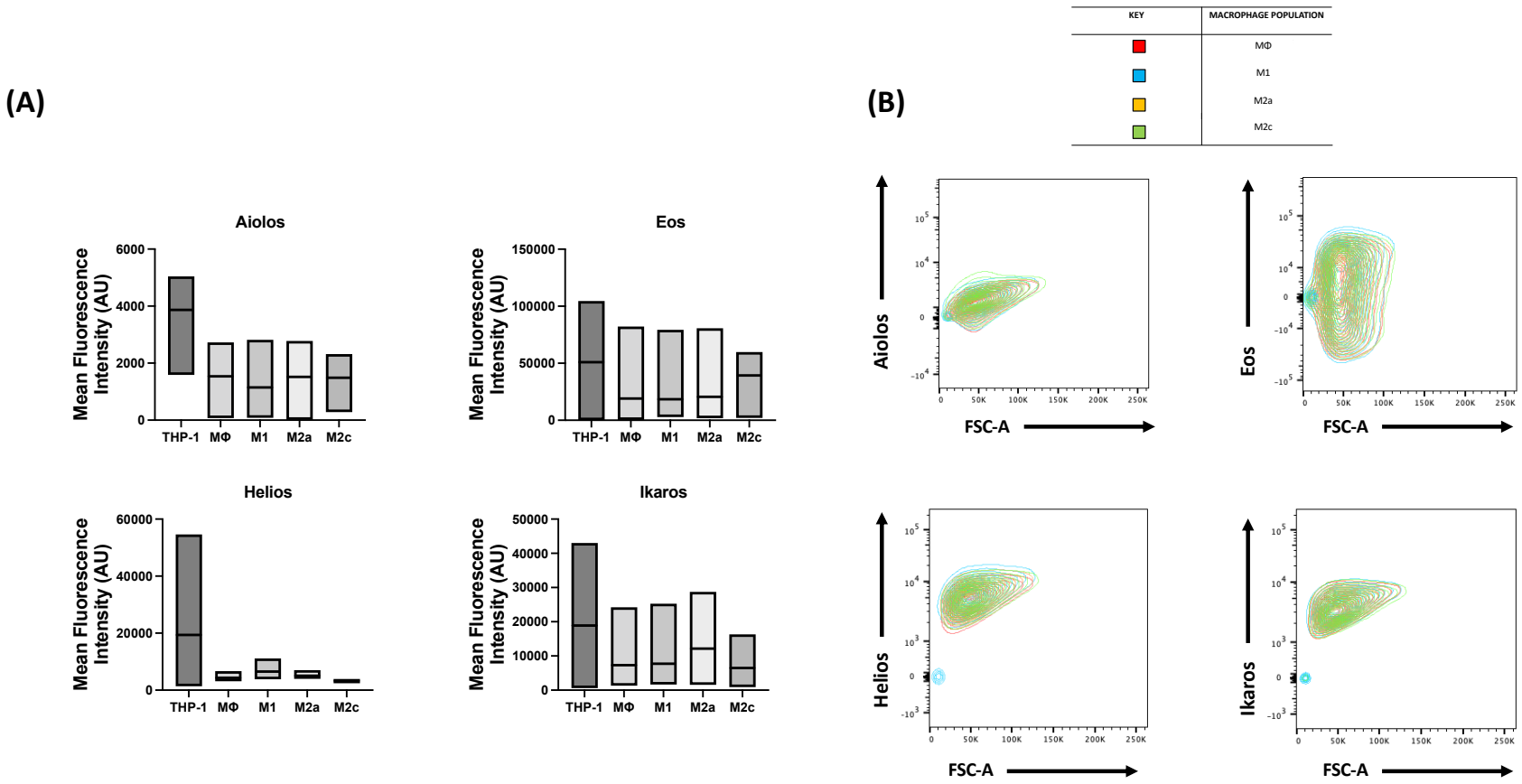



**Figure 5.13: THP-1 –Derived Macrophages Express Protein Levels of Aiolos, Eos, Helios And Ikaros**
THP-1 cells were left untreated (THP-1) or polarised to Macrophages (MΦ) using PMA (50ng/ml). They were then further polarised to M1 = PMA (50ng/ml) + IFNγ (20ng/ml) + LPS (20ng/ml), M2a = PMA (50ng/ml) + IL-4 (20ng/ml), M2c = PMA (50ng/ml) + IL-10 (20ng/ml) for 24 hours. After incubation, the cells were harvested for flow cytometry analysis of protein expression levels of Ikaros family members, Aiolos, Eos, Helios and Ikaros. **(A)** Data was analysed using FlowJo V10 software to determine Mean Fluorescence Intensity (Arbitrary Units, AU). **(B)** Representative flow cytometry plots for each transcription factor in each macrophage population are shown. *N=3, n=3-5. NS. One Way ANOVA. FlowJo V10.*

### 5.2.8 Blood Derived M2 Macrophage Subtypes Secrete the Highest Levels of IL-10, Whilst M1 Macrophages Produce Most IL-12

Once I had optimised my THP-1 to macrophage culture, I performed similar differentiation experiments using primary cells from blood samples (Section 2.2.1.4). Supernatants collected from cultured monocytes and macrophage populations were analysed by ELISA to quantify cytokine production. Figure 5.14 shows that both M2a and M2c subclasses of macrophage were found to express significantly higher ($p<0.001$) levels of IL-10 in comparison to all other subtypes analysed. Interestingly we also observed a modest production by M1 macrophages differentiated from blood cells, in contrast to what I observed in THP-1 cultures (Figure 5.7).

I next measured IL-12 production and M1 macrophages were found to have significantly higher ($p<0.01$) secretion of IL-12 in comparison to all other macrophage populations analysed. This is in keeping with what I observed with THP-1 cells, however the quantity produced was much higher for primary cells (100pg/ml as opposed to less than 1pg/ml) (Figures 5.15 & 5.8)

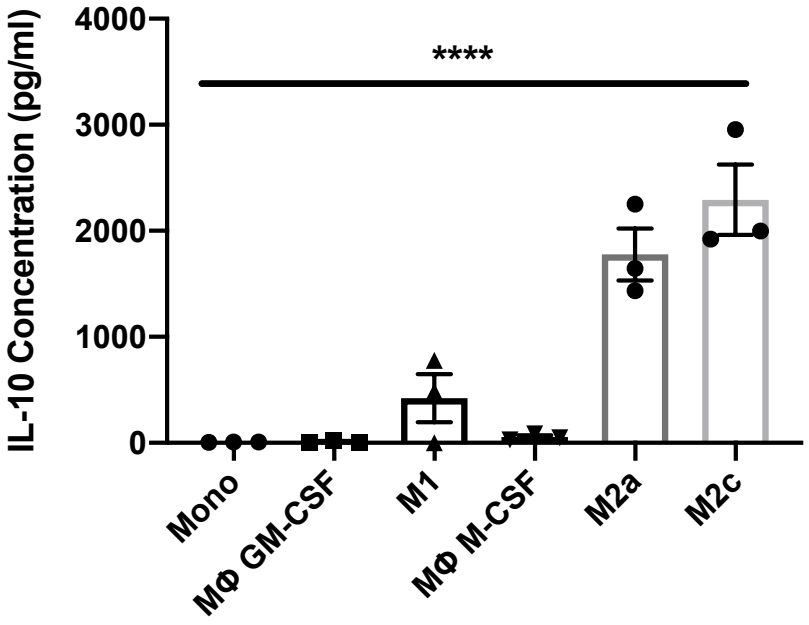



**Figure 5.14: Blood-derived M2 Macrophages Secrete IL-10**
Blood-derived monocytes were isolated from hemochromatosis blood and left untreated (Monocytes, Mono) or polarised to Macrophages (MΦ) using GM-CSF (10ng/ml) and M-CSF (50ng/ml). They were then further polarised to M1 (GM-CSF + IFNγ (20ng/ml) + LPS (50ng/ml)), M2a (M-CSF+ IL-4 (20ng/ml)) or M2c (M-CSF + IL-10 (20ng/ml)) for 24 hours. After incubation, the supernatants were harvested and used for quantification of IL-10 using the R&D Quantikine ELISA kit. Results are presented as mean ± SEM. *N=3. **** p<0.001 one-way ANOVA and Tukey's Multiple Comparison Test.*

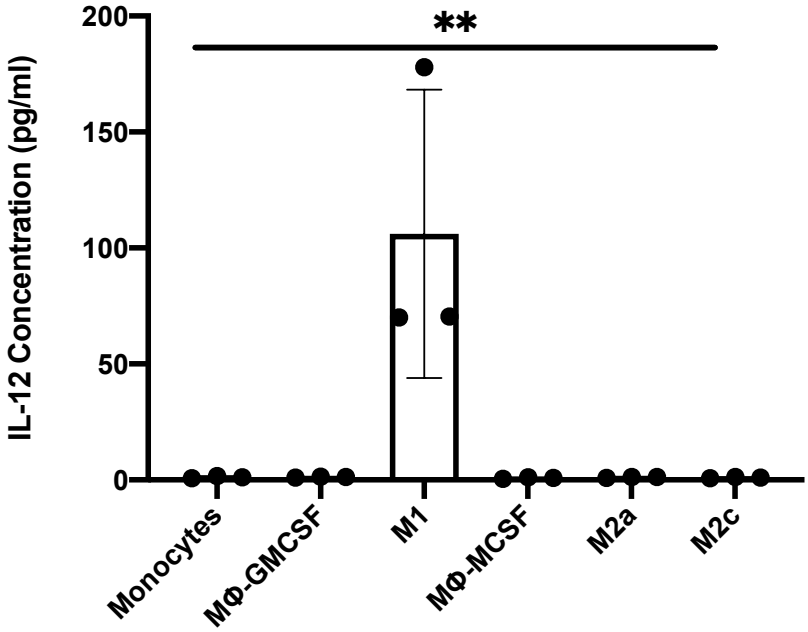



**Figure 5.15: Blood-derived M1 Macrophages Secrete IL-12**
Blood-derived monocytes were isolated from hemochromatosis blood and left untreated (Monocytes, Mono) or polarised to Macrophages (MΦ) using GM-CSF (10ng/ml) and M-CSF (50ng/ml). They were then further polarised to M1 (GM-CSF + IFNγ (20ng/ml) + LPS (50ng/ml)), M2a (M-CSF+ IL-4 (20ng/ml)) or M2c (M-CSF + IL-10 (20ng/ml)) for 24 hours. After incubation, the supernatants were harvested and used for quantification of IL-12 using the R&D Quantikine ELISA kit. Results are presented as mean ± SEM*. N=3. ** p<0.01 one-way ANOVA and Tukey's Multiple Comparison Test.*

### 5.2.9 Primary Monocyte-Derived Macrophages Express Defined Surface Markers Specific to Macrophage Subtypes

To assess the success of primary monocyte to macrophage polarisation, we cultured cells as mentioned in Section 2.2.1.4 and harvested cells after polarisation to either MΦ-GM-CSF, M1, MΦ-M-CSF, M2a or M2c for flow analysis. The cell surface markers analysed included CD86, CD45, HLA-DR, CD80, CD163, CD206, CD14 and CD16 following the gating strategy described in Figure 5.16. All populations expressed CD45, a leukocyte marker (209). Expression of HLA-DR, CD80 and CD86 was highest in M1 populations which had correspondingly lower CD163 expression supporting previous literature (Figure 5.17) (75). In contrast, expression of CD206 and CD163 was highest in the M2a populations, supporting known literature.

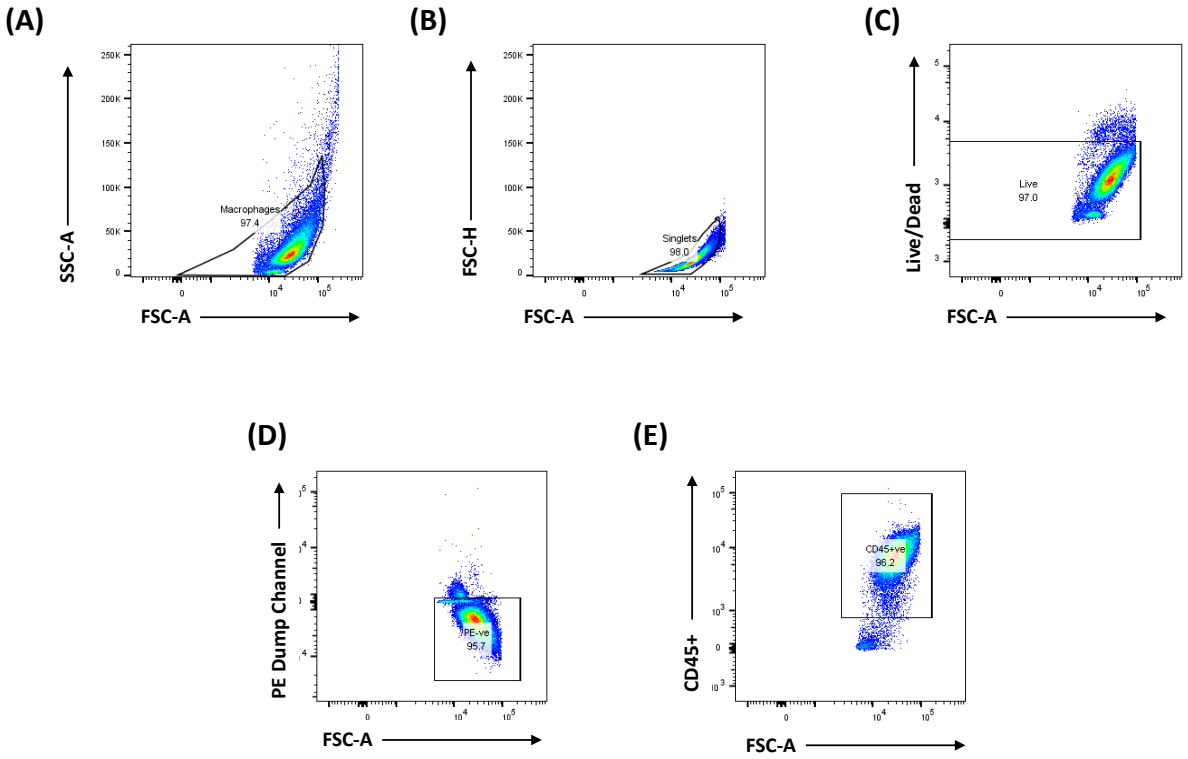



**Figure 5.16: Gating Strategy For Flow Cytometry Analysis of Surface Markers Present on Primary Monocyte-Derived Macrophages**

Blood-derived monocytes were isolated from hemochromatosis blood and left untreated (Monocytes, Mono) or polarised to Macrophages (MΦ) using GM-CSF (10ng/ml) and M-CSF (50ng/ml). They were then further polarised to M1 (GM-CSF + IFNγ (20ng/ml) + LPS (50ng/ml)), M2a (M-CSF+ IL-4 (20ng/ml)) or M2c (M-CSF + IL-10 (20ng/ml)) for 24 hours. After polarisation, the cells were harvested for flow cytometry analysis to determine phenotypic markers for specific cell populations. (A) Cells were first gated to exclude debris, (B) the singlet population identified followed by (C) exclusion of positive stained dead cells to gate live cells. (D) Cells which stained positive for PE-labelled antibodies in our 'dump channel' were gated out, and then (E) CD45 positive cells were identified and analysed for expression of macrophage associated cell surface markers. Representative plots shown. *FlowJo V10.*

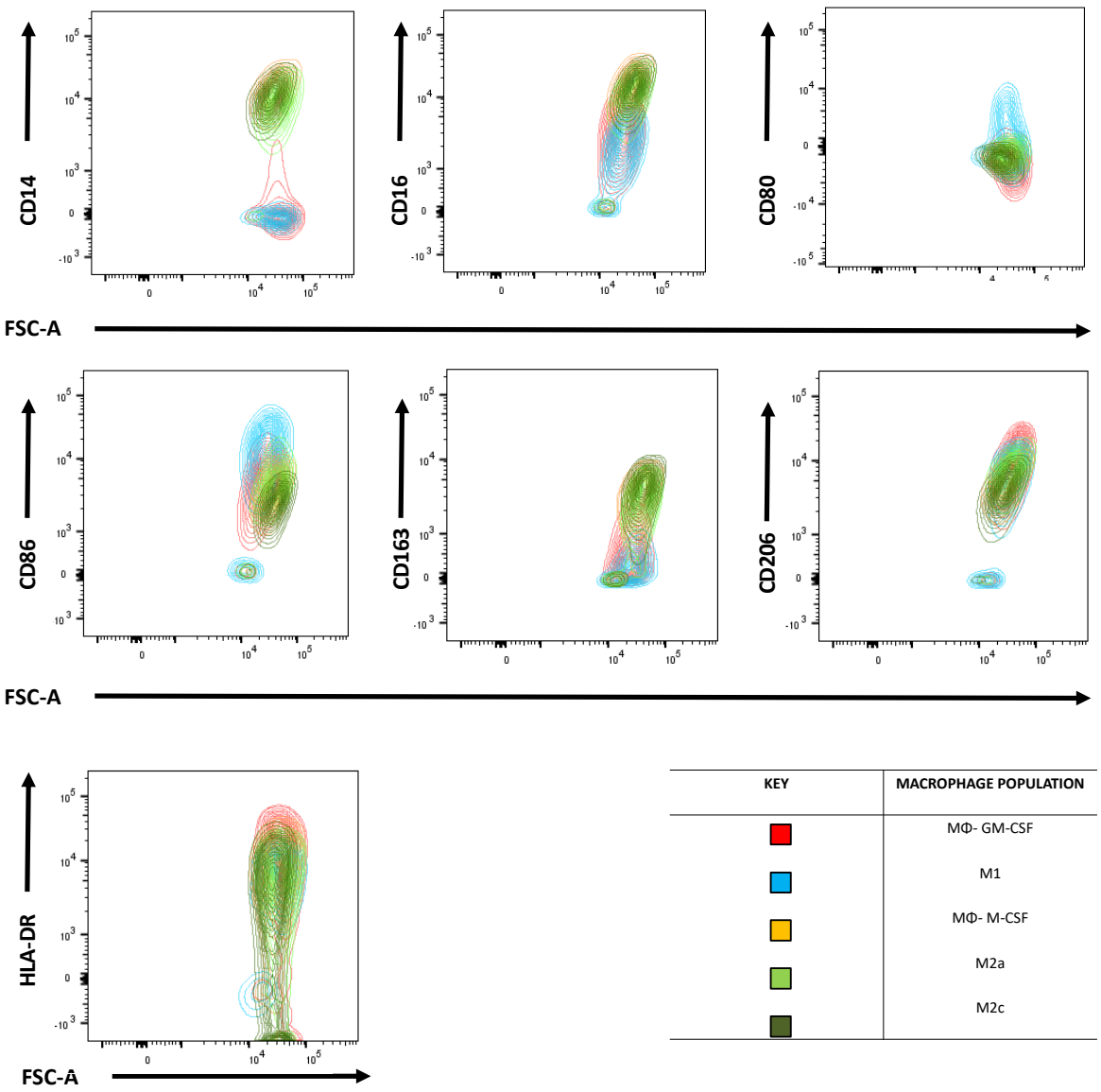



**Figure 5.17: Flow Cytometry Analysis of Surface Markers Present on Primary Monocyte-Derived Macrophages**

Blood-derived monocytes were isolated from hemochromatosis blood and left untreated (Monocytes, Mono) or polarised to Macrophages (MΦ) using GM-CSF (10ng/ml) and M-CSF (50ng/ml). They were then further polarised to M1 (GM-CSF + IFNγ (20ng/ml) + LPS (50ng/ml)), M2a (M-CSF+ IL-4 (20ng/ml)) or M2c (M-CSF + IL-10 (20ng/ml)) for 24 hours. After polarisation, the cells were harvested for flow cytometry analysis to determine phenotypic markers for specific cell populations. Cells were first gated, singlets identified followed by determination of live cells. Cells which stained positive for PE-labelled antibodies in our 'dump channel' were gated out, and then CD45 positive cells analysed for expression of macrophage associated cell surface markers including CD86, HLA-DR, CD80, CD163, CD206, CD14 and CD16. *N=2.* Representative plots are shown. *FlowJo V10.*

### 5.2.10 Polarisation of PBMC-Derived Monocytes into Various Macrophage Populations Alters the Expression of the Ikaros Family

We next moved to assessing levels of Ikaros family expression in macrophages derived from PBMCs (Figure 5.18). Here we generally noted lower relative expression of mRNA for Ikaros family members compared to the differentiated THP-1 cells (Figure 5.11). There were also different expression patterns across the differentiation spectrum. Levels of Aiolos expression were significantly lower ($p<0.01$) in macrophage populations in comparison to monocytes. Expression levels of Eos in macrophage subsets was higher than in untreated monocytes, whereas Ikaros expression was similar throughout monocyte and macrophage populations (as we saw for THP-1 cells). Helios was expressed in macrophage subsets, with its highest expression observed in the M2c populations, again agreeing with our findings using THP-1 cells. Highest expression of Pegasus was observed in monocytes, with significantly lower levels ($p<0.01$) in both GM-CSF treated MΦ and M1 macrophages and M2a ($P<0.05$). This agrees with relatively high expression in most of our differentiated THP-1 subsets.

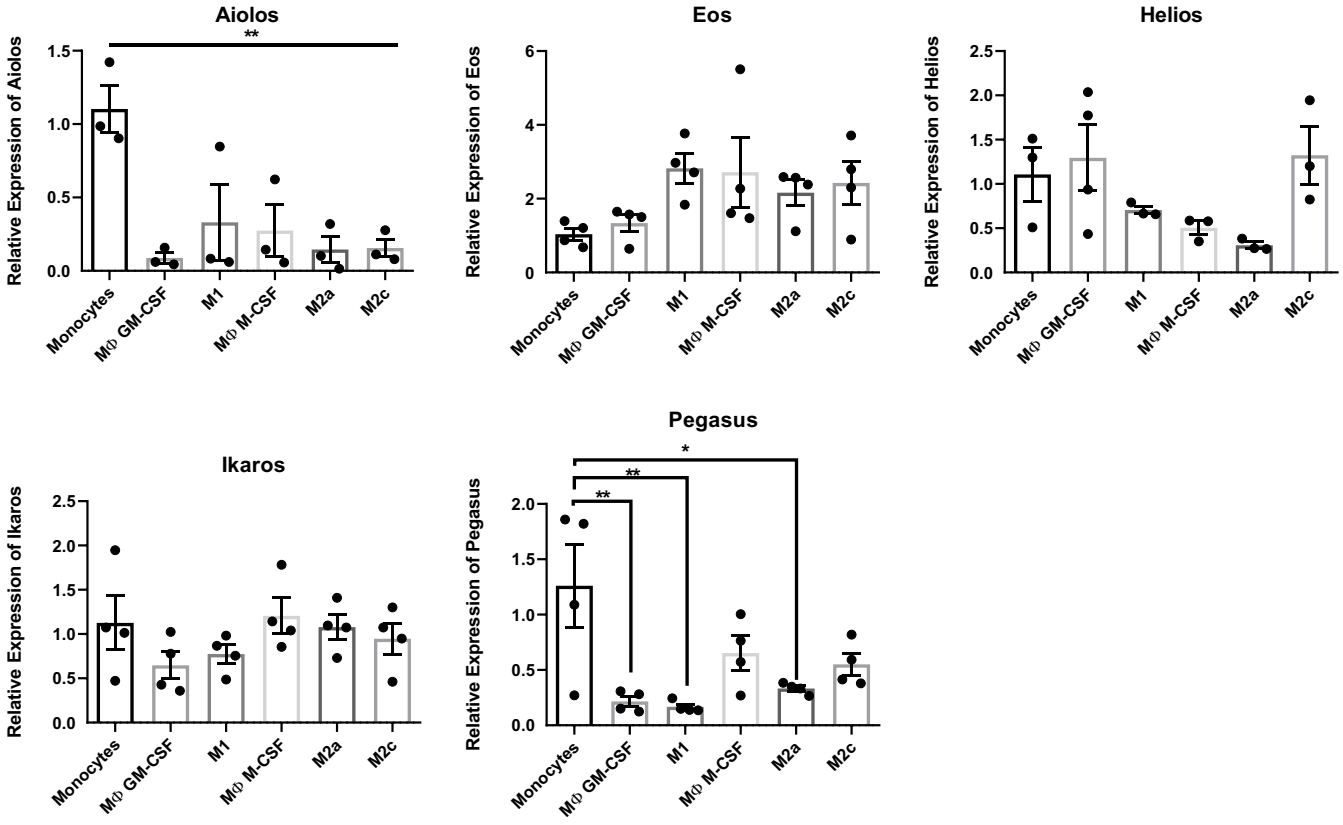



**Figure 5.18: Polarisation of PBMC-Derived Monocytes Into Different Macrophage Populations Alters The Expression of the Ikaros Family**

Blood-derived monocytes were isolated from hemochromatosis blood (control) and left untreated (Monocytes, Mono) or polarised to Macrophages (MΦ) using GM-CSF (10ng/ml) and M-CSF (50ng/ml). They were then further polarised to M1 (GM-CSF + IFNγ (20ng/ml) + LPS (50ng/ml)), M2a (M-CSF+ IL-4 (20ng/ml)) or M2c (M-CSF + IL-10 (20ng/ml)) for 24 hours. Total RNA was extracted from samples and measured by qPCR. Expression is shown for each group relative to the level housekeeping gene. Results are presented as mean ± SEM. *N=3-4*. *One way ANOVA and Tukey's Multiple Comparison Test. Housekeeping Gene: RPS9.*

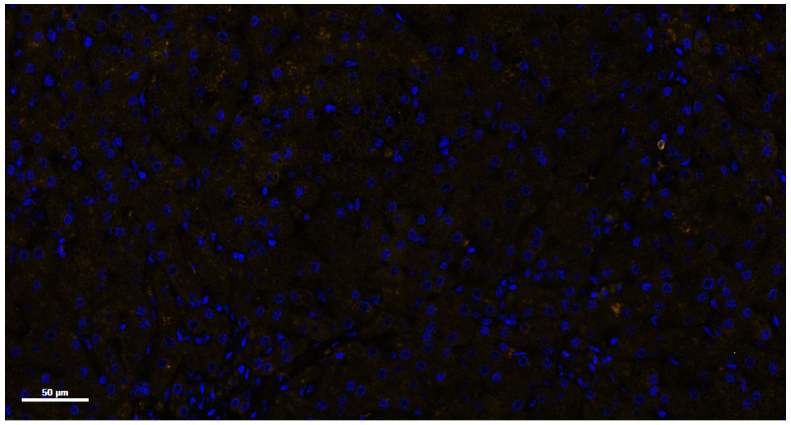
### 5.2.11 Ikaros Family Transcription Factors are Co-expressed with CD68 in Kupffer Cells

We next decided to confirm whether the Ikaros family members are expressed by macrophages, within tissue. To do this we first began by optimising the Opal™ method using PSC-IBD tissue (Section 2.6.3). PSC liver tissue is highly inflamed and known to contain significant numbers of CD68+ macrophages, and for our study, more readily available than bowel tissue. Thus, CD68 was used as a macrophage marker and was stained alongside the transcription factors. Figure 5.19 shows representative fields of view from the analysis. Here it is clear that as expected there are significant numbers of macrophages within the parenchyma of PSC liver tissue, and that some are dual positive for Ikaros family members. The proportion of dual positive cells and the intensity of staining for transcription factors varied from protein to protein. Helios and Pegasus were the most highly expressed and interestingly there appeared to be significant numbers of cells that expressed Eos but were not CD68+. For reference, examples of CD68 and Ikaros-family expressing macrophages are highlighted with white arrows and in inset squares.

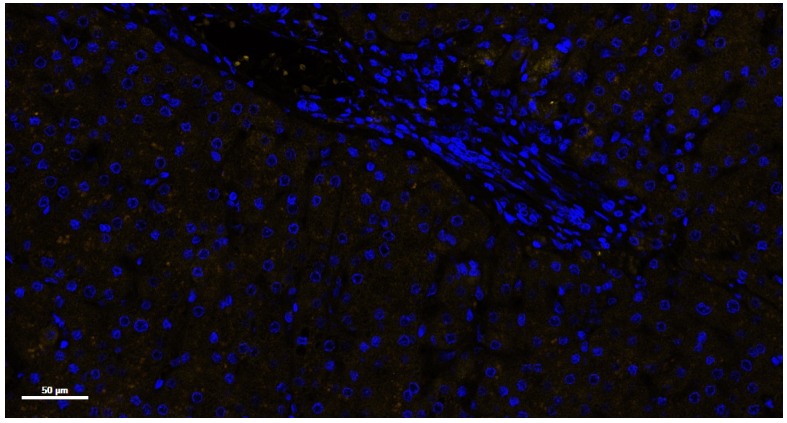
**Overleaf > Figure 5.19: Ikaros Family Members Co-localise with CD68-Expressing Macrophage Expression in Primary Sclerosing Cholangitis (PSC) Tissue**

Opal Dye™ 690 was used to view the presence of CD68 positive (CD68+, in red) macrophages, with Opal Dye™ 570 (in yellow) used to stain for members of the Ikaros Family of Transcription Factors (Aiolos, Eos, Helios, Ikaros and Pegasus) in PSC liver tissue. Slides were imaged using the Vectra Polaris system and Phenochart software. Single representative images are shown. White arrows highlight CD68 and Ikaros family co-expressing macrophages. *Inset:* Magnified images of co-expressing macrophages. DAPI was used as the nuclear stain (in blue). Magnification *x20.* Scale Bar represents 50μm. *N=3*

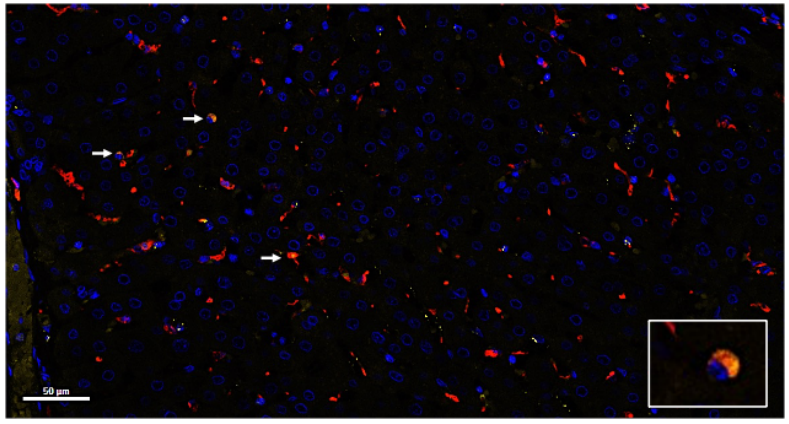
Mouse IgG



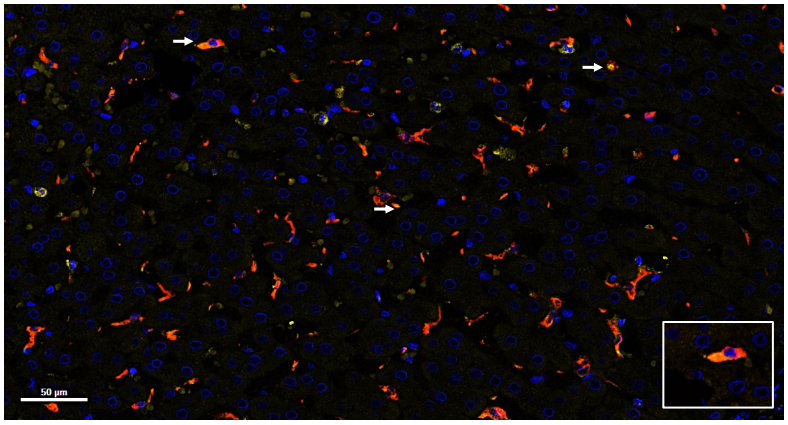

Rabbit IgG



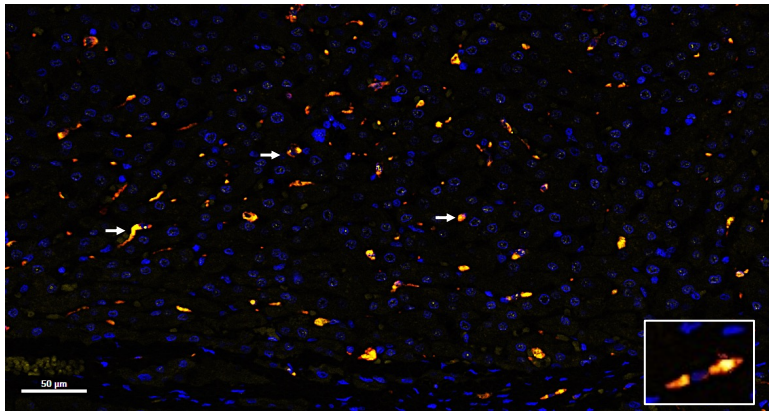

Aiolos



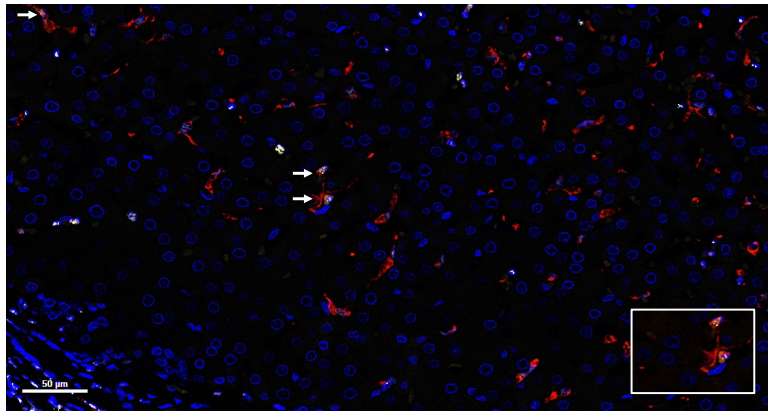

Eos



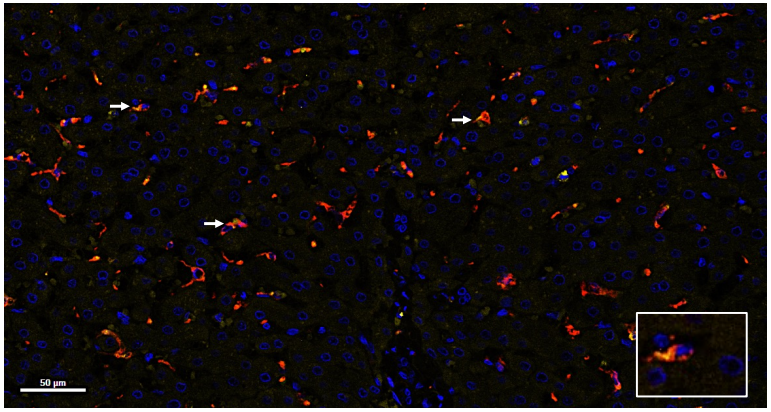
**Helios**




**Ikaros**




**Pegasus**



### 5.2.12 CD68-Expressing Macrophages in the Bowel Co-express the Ikaros Family of Transcription Factors

Once we had completed optimisation of the Opal™ method on liver tissue, we then moved on to assessing the expression of the Ikaros family in both uninflamed and inflamed colon tissue. CD68 was used as a positive marker of macrophages and stained alongside the transcription factors as before. Figure 5.20-5.24 show that there was positive staining for all Ikaros family members within CD68-expressing macrophages in the colon. Qualitative analysis of Ikaros family expression found upregulation of the transcription factors within inflamed bowel tissue. CD68 expression was also similarly upregulated in inflamed tissue in comparison to uninflamed. Quantitative analysis found that levels of Aiolos+CD68+ cells was higher in inflamed bowel in comparison to uninflamed, with significantly higher levels of Eos+CD68+ cells ($p<0.01$) and Helios+CD68+ cells ($p<0.05$). Similar levels of Ikaros+CD68+ and Pegasus+CD68+ double positive cells were seen in inflamed and uninflamed tissue. For reference, examples of CD68 and Ikaros-family expressing macrophages are highlighted with white arrows and in inset squares.

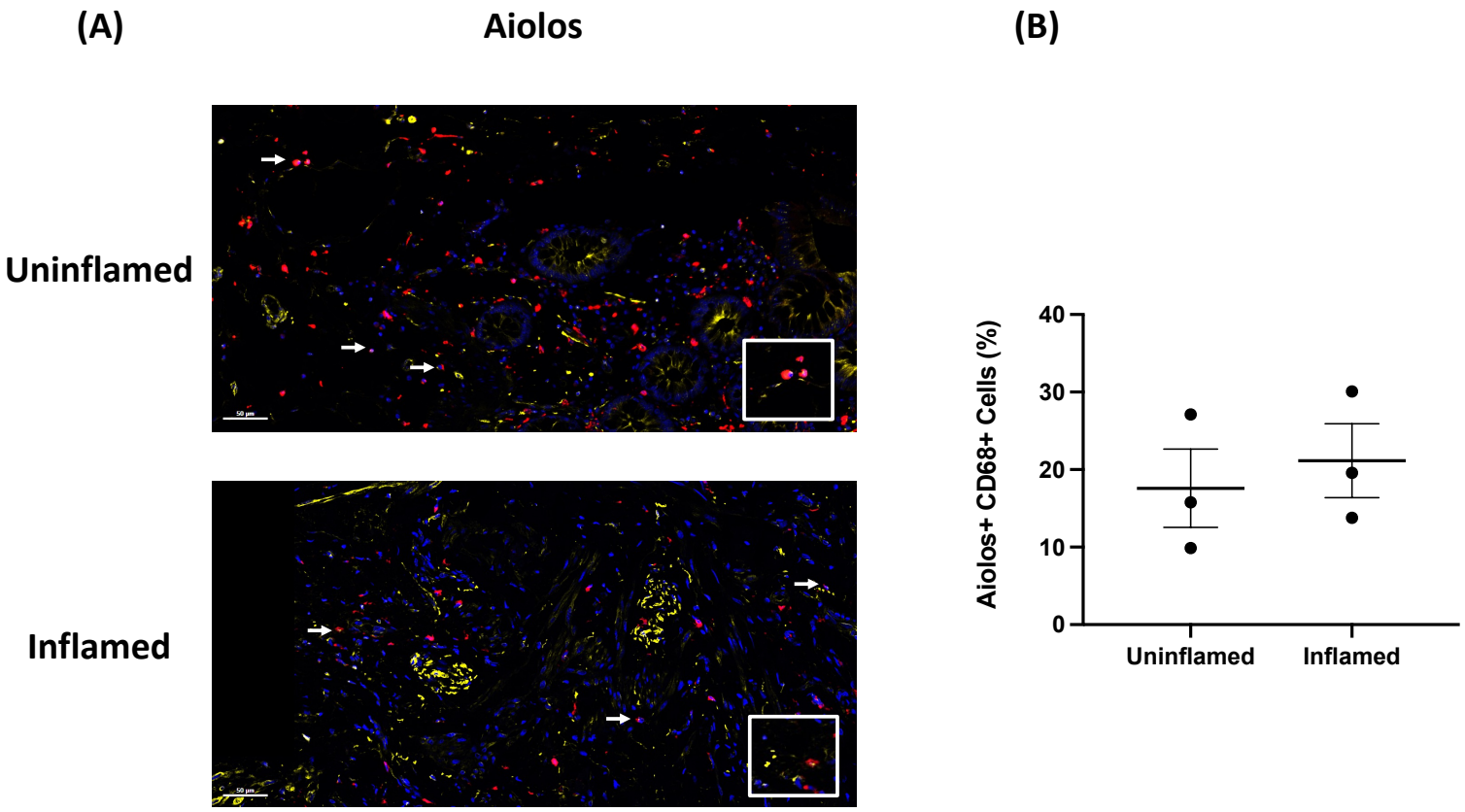



**Figure 5.20: Aiolos Co-localises with CD68-Expressing Macrophages in Uninflamed and Inflamed Bowel Tissue**
Opal Dye ™ 690 was used to view the presence of CD68 positive (CD68+, in red) macrophages, with Opal Dye ™ 570 used to stain for Aiolos (in yellow) in matched uninflamed and inflamed bowel tissue. Slides were imaged using the Vectra Polaris system and Phenochart software. **(A)** Single representative images are shown. White arrows highlight CD68 and Aiolos co-expressing macrophages. *Inset*: Magnified images of co-expressing macrophages. DAPI was used as the nuclear stain (in blue). **(B)** For quantitative analysis, 7-11 regions (*n*) were randomly selected from each sample (*N*) and Image J software used to count Aiolos and CD68 double positive cells in tissue. Dots represent average staining of regions (*n*) in each *N*. Results are presented as Mean ± SEM. Magnification *x20.* Scale Bar represents 50µm. *Non-Inflamed, N=3, n=30; Inflamed, N=3, n=30. NS, Unpaired T Test.*

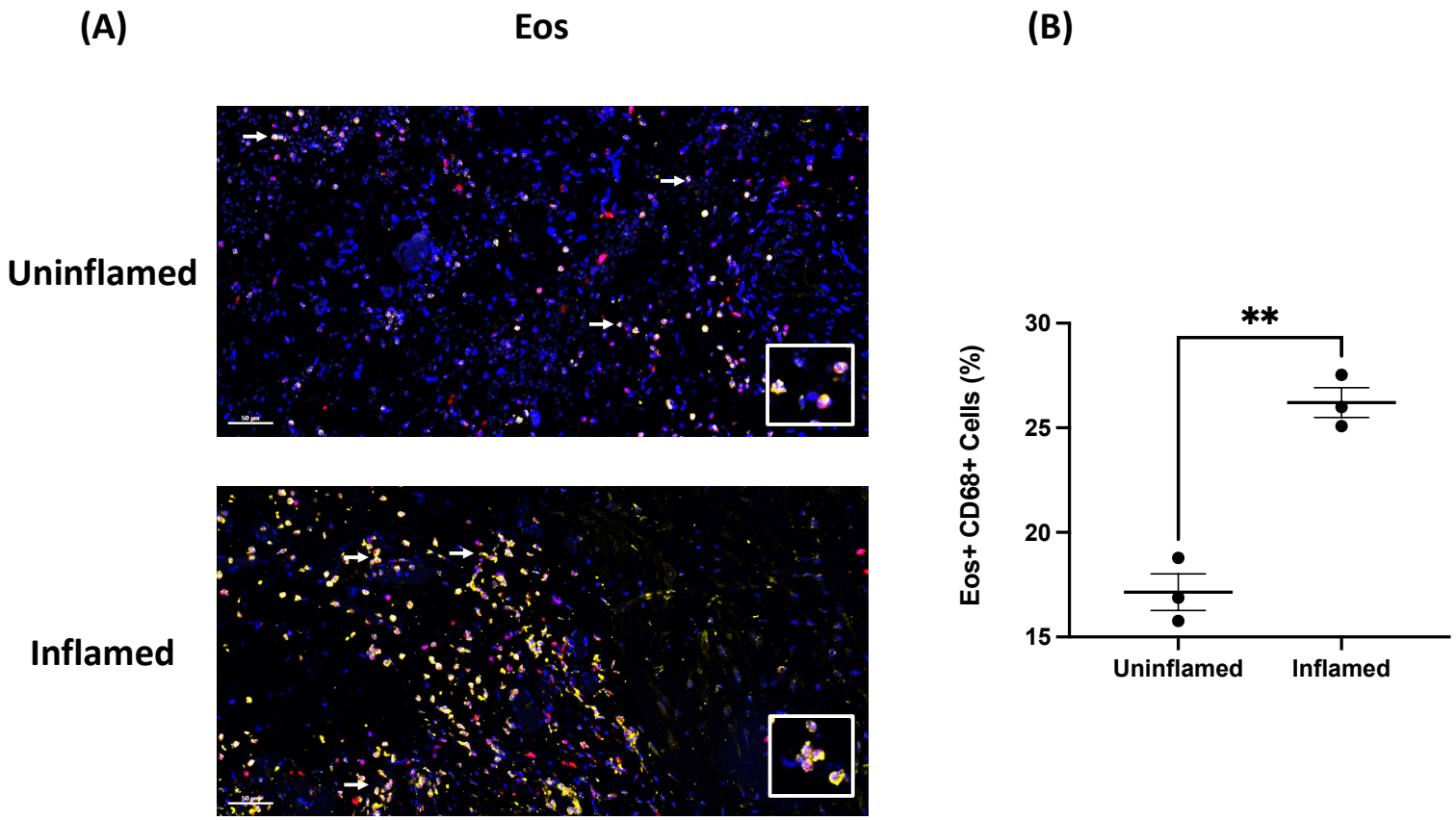



**Figure 5.21: Eos Co-localises with CD68-Expressing Macrophages in Uninflamed and Inflamed Bowel Tissue**
Opal Dye ™ 690 was used to view the presence of CD68 positive (CD68+, in red) macrophages, with Opal Dye ™ 570 used to stain for Eos (in yellow) in matched uninflamed and inflamed bowel tissue. Slides were imaged using the Vectra Polaris system and Phenochart software. **(A)** Single representative images are shown. White arrows highlight CD68 and Eos co-expressing macrophages. *Inset*: Magnified images of co-expressing macrophages. DAPI was used as the nuclear stain (in blue). **(B)** For quantitative analysis, 7-11 regions (*n*) were randomly selected from each sample (*N*) and Image J software used to count Eos and CD68 double positive cells in tissue. Dots represent average staining of regions (*n*) in each *N*. Results are presented as Mean ± SEM. Magnification *x20.* Scale Bar represents 50µm. *Non-Inflamed, N=3, n=32; Inflamed, N=3, n=39. ** p<0.01, Unpaired T Test.*

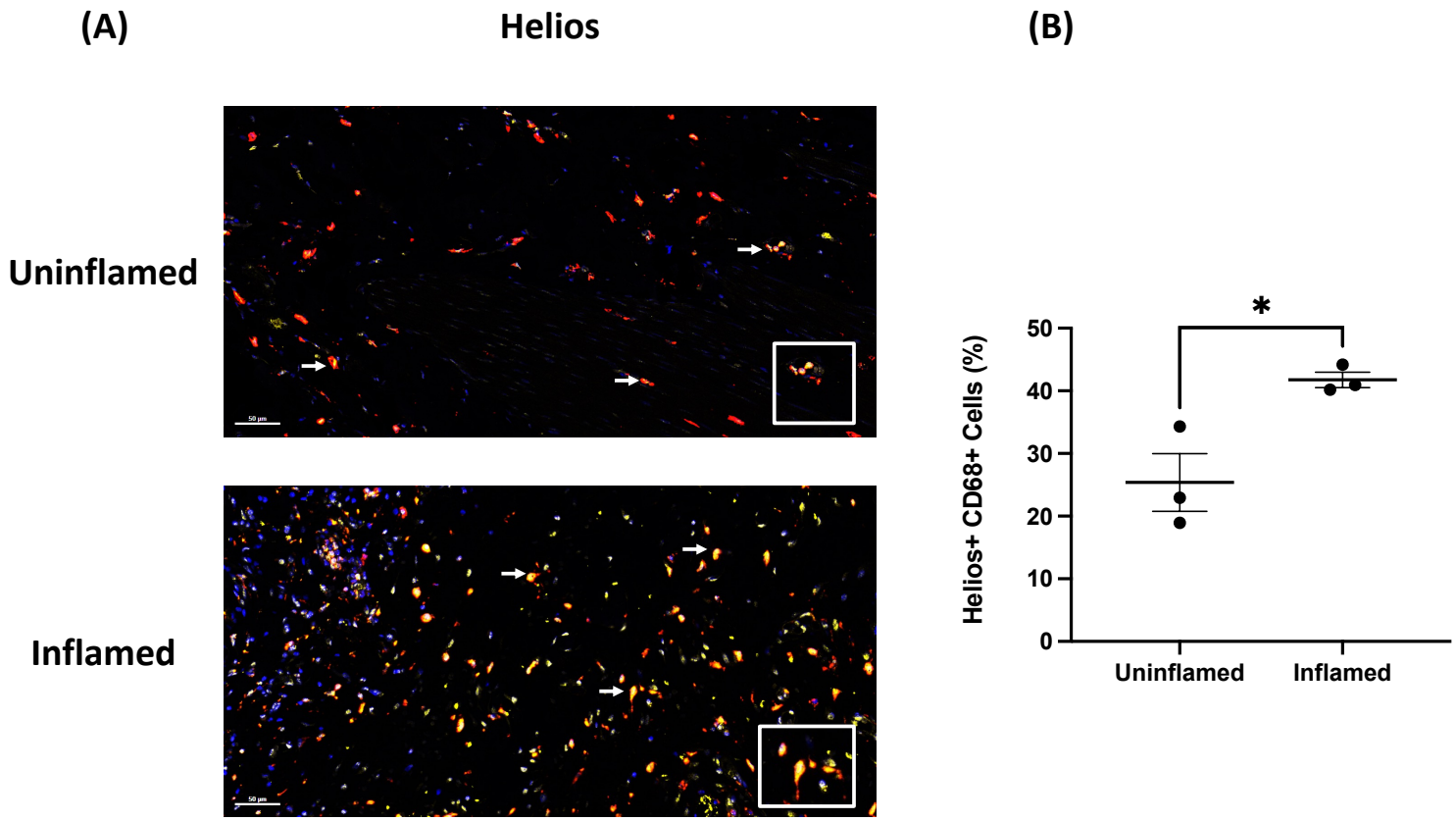



**Figure 5.22: Helios Co-localises with CD68-Expressing Macrophages in Uninflamed and Inflamed Bowel Tissue**
Opal Dye ™ 690 was used to view the presence of CD68 positive (CD68+, in red) macrophages, with Opal Dye ™ 570 used to stain for Helios (in yellow) in matched uninflamed and inflamed bowel tissue. Slides were imaged using the Vectra Polaris system and Phenochart software. **(A)** Single representative images are shown. White arrows highlight CD68 and Helios co-expressing macrophages. *Inset*: Magnified images of co-expressing macrophages. DAPI was used as the nuclear stain (in blue). **(B)** For quantitative analysis, 7-11 regions (*n*) were randomly selected from each sample (*N*) and Image J software used to count Helios and CD68 double positive cells in tissue. Dots represent average staining of regions (*n*) in each *N*. Results are presented as Mean ± SEM. Magnification *x20.* Scale Bar represents 50µm. *Non-Inflamed, N=3, n=29; Inflamed, N=3, n=27. * p<0.05, Unpaired T Test.*

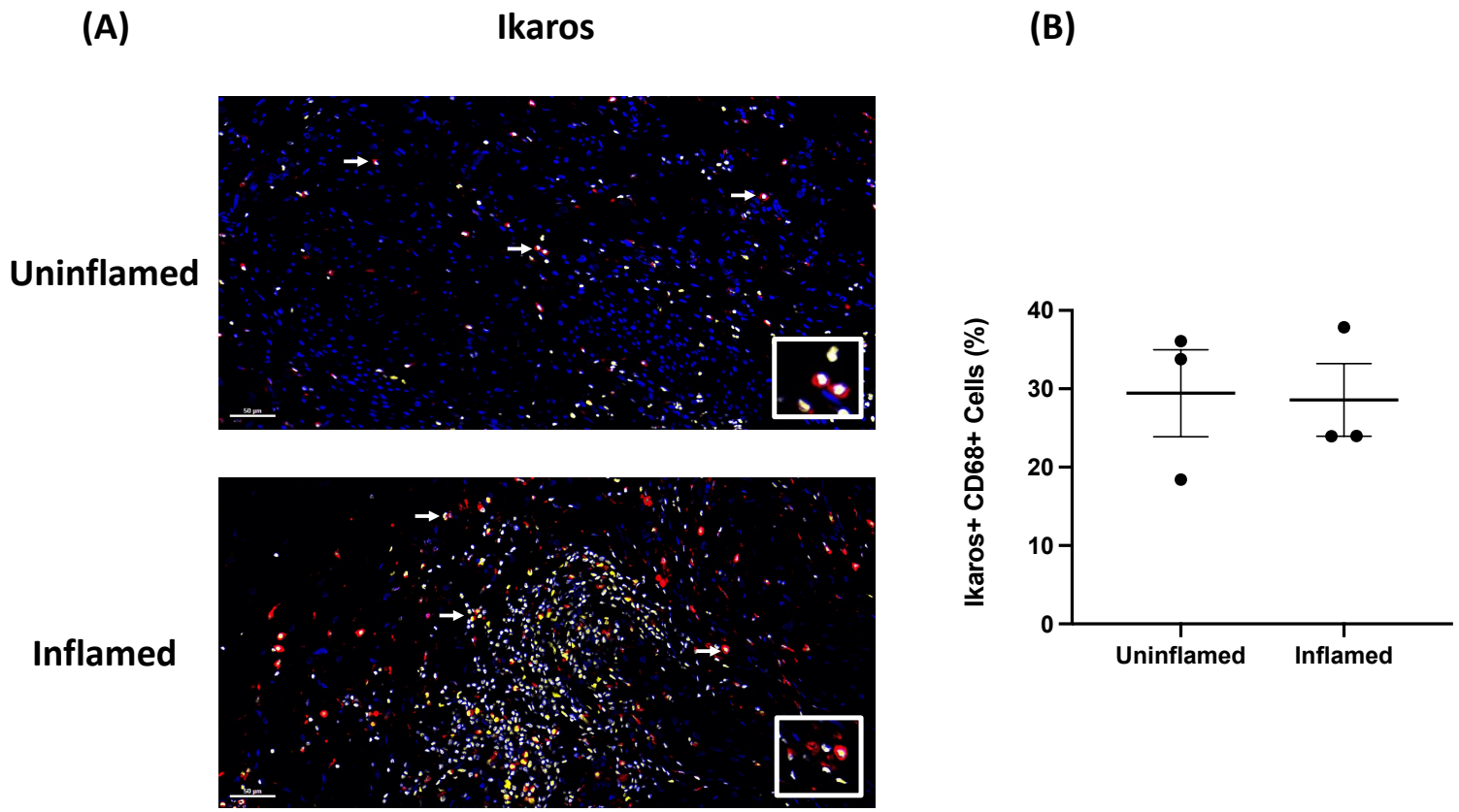



**Figure 5.23: Ikaros Co-localises with CD68-Expressing Macrophages in Uninflamed and Inflamed Bowel Tissue**
Opal Dye ™ 690 was used to view the presence of CD68 positive (CD68+, in red) macrophages, with Opal Dye ™ 570 used to stain for Ikaros (in yellow) in matched uninflamed and inflamed bowel tissue. Slides were imaged using the Vectra Polaris system and Phenochart software. **(A)** Single representative images are shown. White arrows highlight CD68 and Ikaros co-expressing macrophages. *Inset*: Magnified images of co-expressing macrophages. DAPI was used as the nuclear stain (in blue). **(B)** For quantitative analysis, 7-11 regions (*n*) were randomly selected from each sample (*N*) and Image J software used to count Ikaros and CD68 double positive cells in tissue. Dots represent average staining of regions (*n*) in each *N*. Results are presented as Mean ± SEM. Magnification *x20.* Scale Bar represents 50µm. *Non-Inflamed, N=3, n=30; Inflamed, N=4, n=27. NS, Unpaired T Test.*

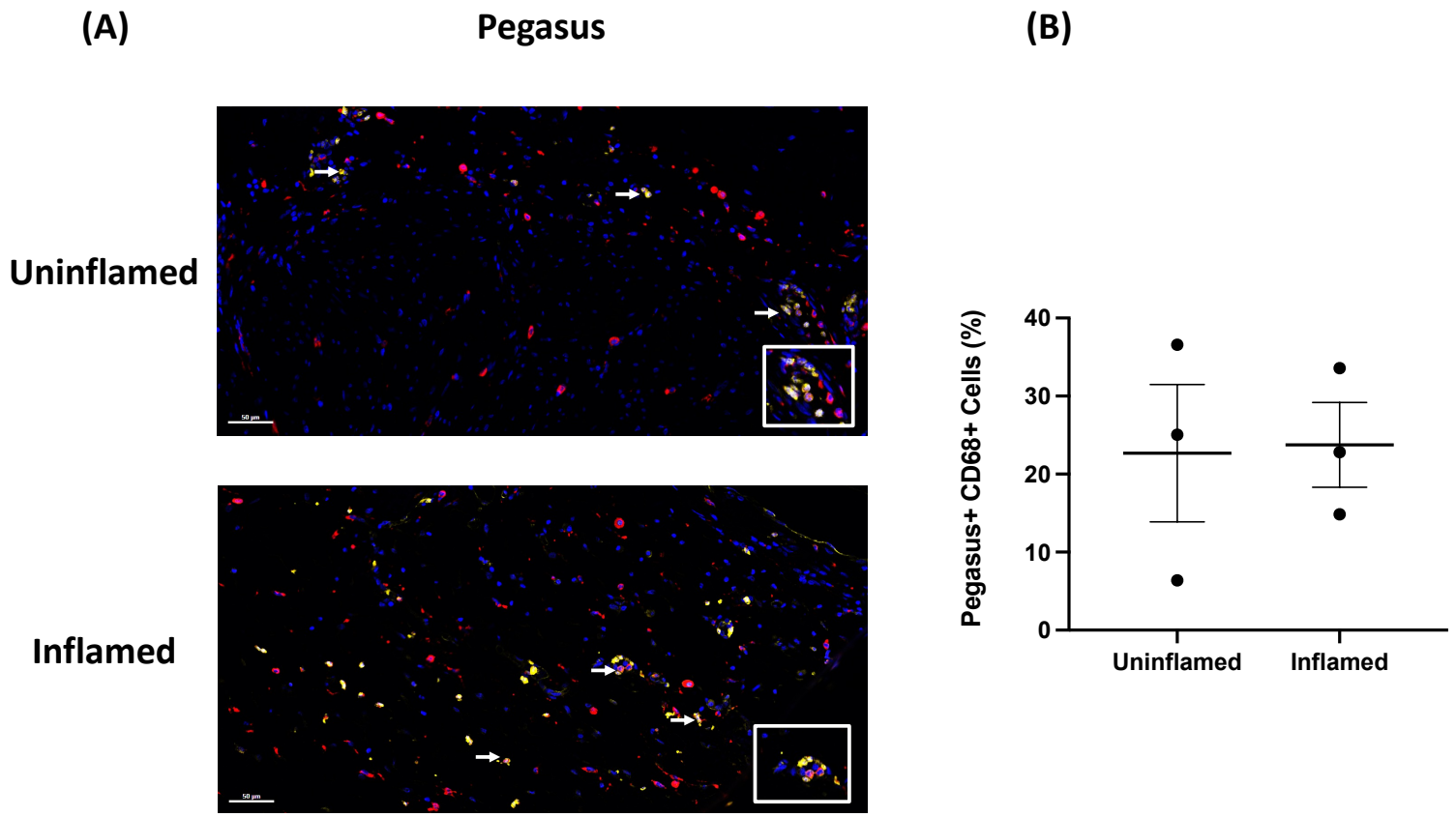



**Figure 5.24: Pegasus Co-localises with CD68-Expressing Macrophages in Uninflamed and Inflamed Bowel Tissue**
Opal Dye ™ 690 was used to view the presence of CD68 positive (CD68+, in red) macrophages, with Opal Dye ™ 570 used to stain for Pegasus (in yellow) in matched uninflamed and inflamed bowel tissue. Slides were imaged using the Vectra Polaris system and Phenochart software. **(A)** Single representative images are shown. White arrows highlight CD68 and Pegasus co-expressing macrophages. *Inset*: Magnified images of co-expressing macrophages. DAPI was used as the nuclear stain (in blue). **(B)** For quantitative analysis, 7-11 regions (*n*) were randomly selected from each sample (*N*) and Image J software used to count Pegasus and CD68 double positive cells in tissue. Dots represent average staining of regions (*n*) in each N. Results are presented as Mean ± SEM. Magnification *x20.* Scale Bar represents 50µm. *Non-Inflamed, N=3, n=29; Inflamed, N=3, n=27. NS, Unpaired T Test.*

### 5.2.13 RNASeq Data Analysis From CD Resections

Tissue was collected from patients with CD undergoing surgical resection as described in Section 2.7. Whole tissue RNASeq analysis was then conducted on 9 samples from resected material (Table 5.1), with a focus on Ikaros family and macrophage gene expression.

#### 5.2.13.1 Hierarchical Clustering for Macrophage Genes in Resection Samples

We began by using unsupervised hierarchical clustering to assess which specific macrophage gene signatures clustered or grouped together in our biopsy samples. The genes of interest were chosen based on their identification as cardinal features of key macrophage subsets (Table 2.19). Figure 5.25 shows the dendrogram generated when gene expression was assessed in all samples. There are two main populations which broadly include the more inflammatory M1 genes vs the more regulatory M2 genes, although there was a wide distribution of macrophage genes across clusters.

## Table 5.1: RNASeq Resection Patient Samples and Clinical Data

| CELL ID | SAMPLE ID | AGE (YEARS) | GENDER | DIAGNOSIS DURATION | MONTREAL CLASSIFICATION FOR LOCATION-CD | MONTREAL CLASSIFICATION (FOR BEHAVIOUR) | HAEMOGLOBIN (g/L) | CRP (mg/ml) | ALBUMIN (g/L) | ACTIVITY ON IMAGING | STRICTURE ON IMAGING | EPISODE OF SURGERY |
|---|---|---|---|---|---|---|---|---|---|---|---|---|
| C1 | BRC FCD 009-PROXIMAL | | | | | | | | | | | |
| C2 | BRC FCD 009-STRICTURE | 19 | Male | < 6 months | L1 ileal | B3 penetrating | 137 | 26 | 45 | Moderate inflammation | Inflammatory | Primary resection |
| C3 | BRC FCD 009-DISTAL | | | | | | | | | | | |
| C4 | BRC FCD 010-PROXIMAL | | | | | | | | | | | |
| C5 | BRC FCD 010-STRICTURE | 35 | Female | 5 to 9 years | L3 ileocolonic | B3 penetrating | 127 | 23 | 39 | Moderate inflammation | Mixed | Primary resection |
| C6 | BRC FCD 010-DISTAL | | | | | | | | | | | |
| C7 | BRC FCD 012-PROXIMAL | | | | | | | | | | | |
| C8 | BRC FCD 012-STRICTURE | 55 | Female | >20 years | L1 ileal | B2 stricturing | 134 | 3 | 43 | Moderate inflammation | Mixed | Secondary resection |
| C9 | BRC FCD 012-DISTAL | | | | | | | | | | | |
| C10 | BRC FCD 016-PROXIMAL | | | | | | | | | | | |
| C11 | BRC FCD 016-STRICTURE | 37 | Male | 6 to 12 months | L3 ileocolonic | B3 penetrating | 139 | 49 | 43 | Mild inflammation | Mixed | Primary resection |
| C12 | BRC FCD 016-DISTAL | | | | | | | | | | | |
| C13 | BRC FCD 017-PROXIMAL | | | | | | | | | | | |
| C14 | BRC FCD 017-STRICTURE | 39 | Male | 10 to 20 years | L1 ileal | B2 stricturing | 145 | 5 | 36 | Moderate inflammation | Mixed | Primary resection |
| C15 | BRC FCD 017-DISTAL | | | | | | | | | | | |
| C16 | BRC FCD 019-PROXIMAL | | | | | | | | | | | |
| C17 | BRC FCD 019-STRICTURE | 26 | Male | 10 to 20 years | L3 ileocolonic | B3 penetrating | 94 | 1 | 40 | Severe active inflammation | Mixed | Primary resection |
| C18 | BRC FCD 019-DISTAL | | | | | | | | | | | |
| C19 | BRC FCD 003-PROXIMAL | | | | | | | | | | | |
| C20 | BRC FCD 003-STRICTURE | 54 | Male | >20 years | L1 ileal | B2 stricturing | 129 | 16 | 43 | Severe active inflammation | Inflammatory | Primary resection |
| C21 | BRC FCD 003-DISTAL | | | | | | | | | | | |
| C22 | BRC FCD 004-PROXIMAL | | | | | | | | | | | |
| C23 | BRC FCD 004-STRICTURE | 63 | Female | >20 years | L3 ileocolonic | B2 stricturing | 128 | 2 | 38 | Mild inflammation | Mixed | Tertiary resection |
| C24 | BRC FCD 004-DISTAL | | | | | | | | | | | |
| C25 | BRC FCD 005-PROXIMAL | | | | | | | | | | | |
| C26 | BRC FCD 005-STRICTURE | 24 | Male | 10 to 20 years | L1 ileal | B2 stricturing | 139 | 34 | 46 | Moderate inflammation | Mixed | Primary resection |
| C27 | BRC FCD 005-DISTAL | | | | | | | | | | | |

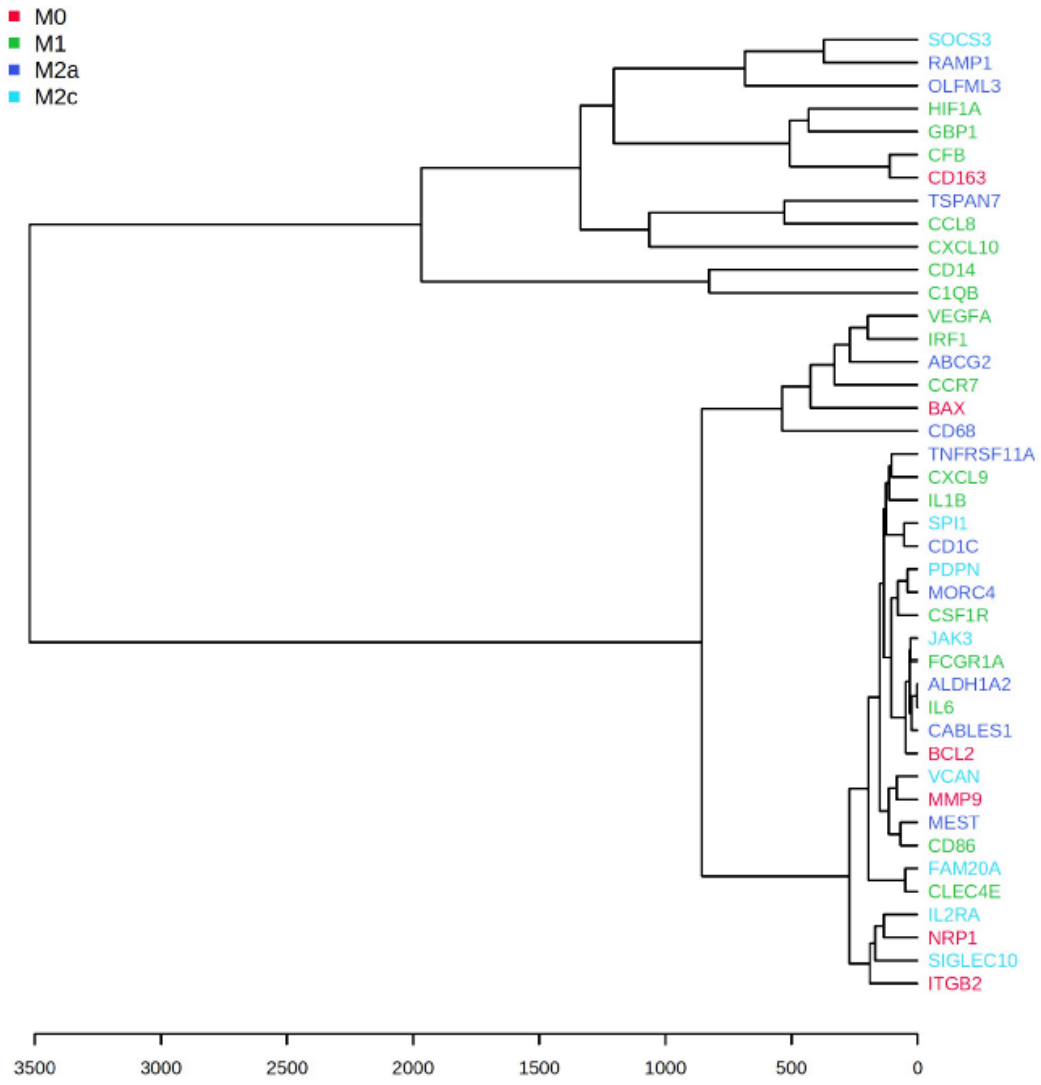



**Figure 5.25: Dendrogram Showing Outcome of Hierarchical Clustering For Macrophage Genes in Resection Samples**

Transcriptome libraries extracted from CD resection samples were sequenced on the NextSeq Illumina platform. Macrophage genes were clustered using Hierarchical clustering (distance measure using Euclidean, and clustering algorithm on ward. D) to highlight shared gene signatures in the indicated macrophage populations (MΦ, M1, M2a and M2c). Genes are indicated in different colours. The scale below shows the heights of the dendrogram from the distance matrix. Data were generated from *N= 9 samples, n=27.*

Next, we compared the genetic signatures that best discriminated biopsy tissue from the proximal, distal and strictured areas of the colon in CD using variable importance in the projection scores (VIP) to prioritize the genes. Figure 5.26 shows the 15 genes that best separated anatomical areas (VIP score greater than 1) and the location in which expression was most abundant (indicated by heatmaps to right of image). Most of the top 15 genes (13/15) were enriched in the strictured area with Guanylate binding protein 1 (GBP1), Olfactomedin-like protein 3 (OLFML3), Complement factor B and Interferon Regulatory Factor 1 (IRF1) being the most significant. Interestingly the distal region was associated with low expression of many genes with key macrophage markers such as CD163 and CD14 being reduced in this area. We also note that Ikaros appears as one of the genes with the highest VIP scores but here expression was highest in the proximal area and reduced in the stricture region. This pattern was also noted for TNFSFR11a/RANK.

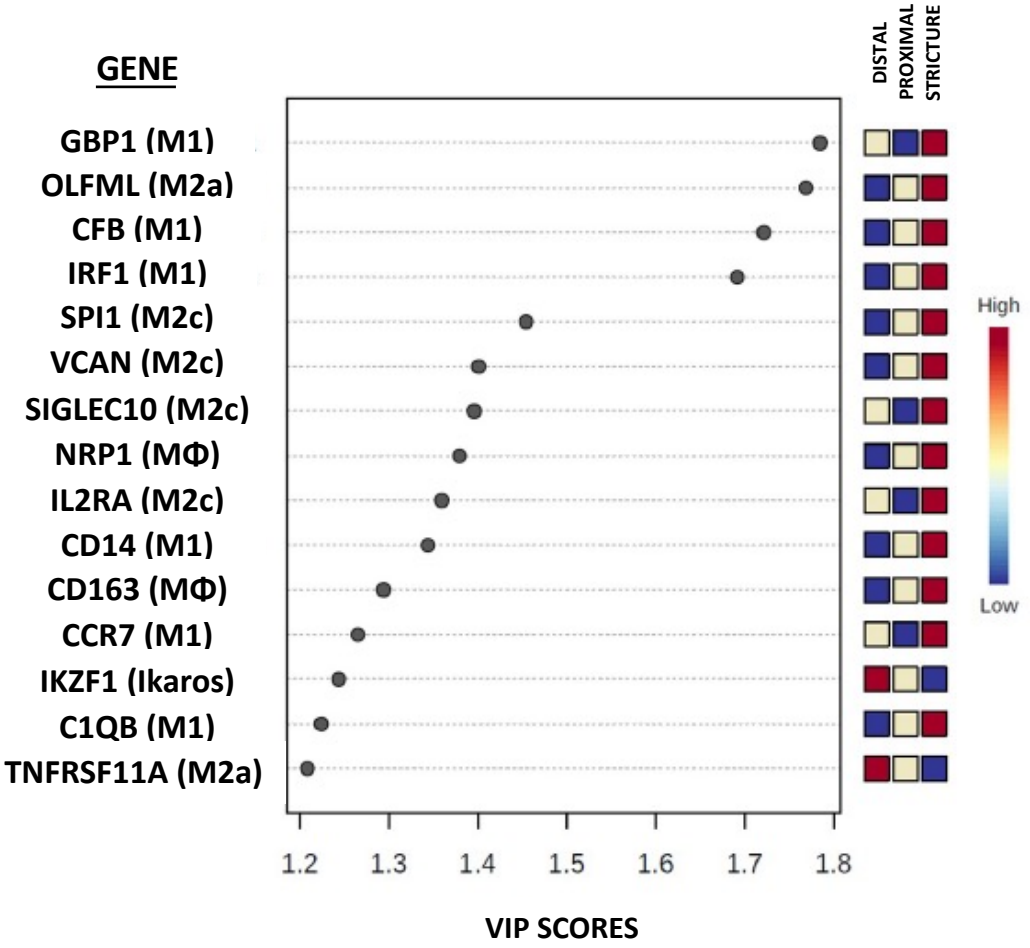



**Figure 5.26: VIP Scores Separate Key Macrophage Genes in Key Anatomical Compartments in the Injured Colon**

Transcriptome libraries extracted from 9 resection samples over 3 anatomical sites were sequenced on the NextSeq Illumina platform. 15 key macrophage genes were selected from PLS-DA modelling based on those with a 'variable importance in the projection' (VIP) score more than 1. The plot shows the 15 selected genes with a VIP score > 1 that discriminated between Distal, Proximal and Stricture categories within our biopsy dataset. Gene names and associated macrophage cluster (e.g., M1, M2c) are supplied (left). Normalized expression values (High vs. Low) of the selected genes are presented in the right-hand side heatmaps. *N= 9 samples, n=27.*

### 5.2.13.2 Pegasus Expression is Highest in Stricture Regions, With Ikaros Expression Higher in Distal Regions

We next looked at Ikaros family member gene expression to determine whether these were concentrated in the stricture, proximal or distal areas of inflamed colon. Figure 5.27A shows individual data for patients separated according to anatomical site of biopsy (stricture, proximal and distal area). There is clear and significant interindividual variation in expression across the inflamed colon. However, if gene expression is averaged across patients (Figure 5.27B) the data suggest that Ikaros and Helios are predominantly found in distal areas, Pegasus is located within the stricture region and Aiolos and Eos are found proximal to the fibrotic and strictured area. This was confirmed by our assessment of VIP scores to prioritize the genes.

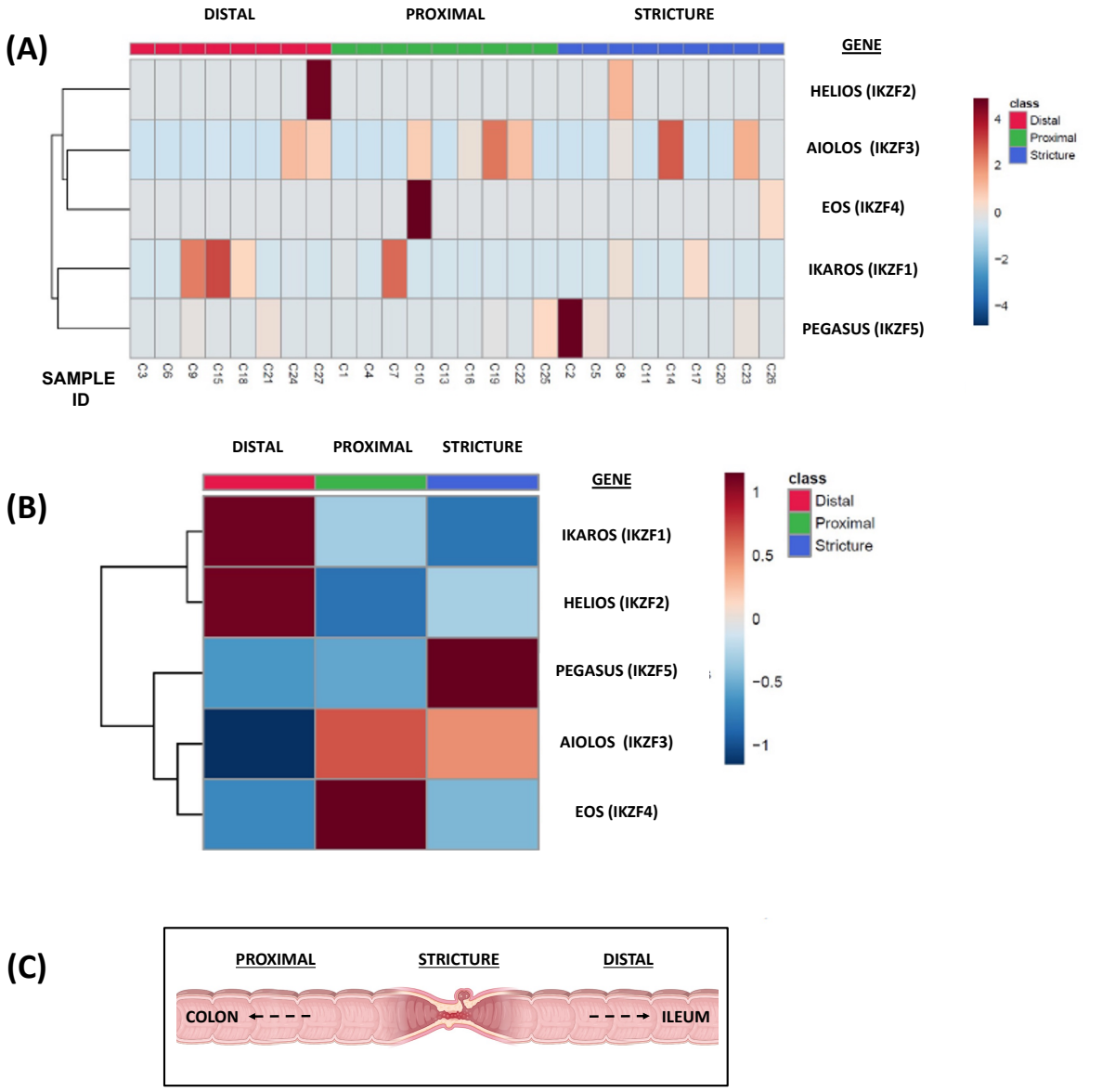



**Figure 5.27: Distribution of Ikaros Family Gene Expression in Key Anatomical Compartments in the Injured Colon**

Transcriptome libraries extracted from 9 resection samples across three anatomical sites were sequenced on the NextSeq Illumina platform. **(A)** Heatmap of the selected gene expression patterns across multiple patients (1 sample per column) in the Distal, Proximal and Stricture categories (Red to Blue indicators, top of heatmap). Genes are annotated based on hierarchical clustering with dendrogram (rows) and intensity of expression for each sample is indicated by heatmap key (right scale). **(B)** Heatmap of the average expression of the selected genes across all the patients in the Distal, Proximal and Stricture categories **(C)** Schematic of the regions attained during sample collection. *N= 9 samples, n=27.*

#### 5.2.13.3 Ikaros Has the Highest VIP Score of All Ikaros Family Members, With Greatest Expression in Distal Regions

Figure 5.28 shows ranking of relative expression of the Ikaros family across the anatomical sites. Whilst the VIP scores were lower than those observed for the macrophage-specific genes (Figure 5.26) there is clear differential expression across the colon. In contrast to the previous analysis (Figure 5.27, above), Ikaros is again the most abundant transcription factor but enriched in distal and proximal areas. Helios was again noted to be concentrated in distal areas and Pegasus was most abundant in strictures. We also again noted that Aiolos and Eos were highest in proximal areas, although these were ranked lower in the VIP scores.

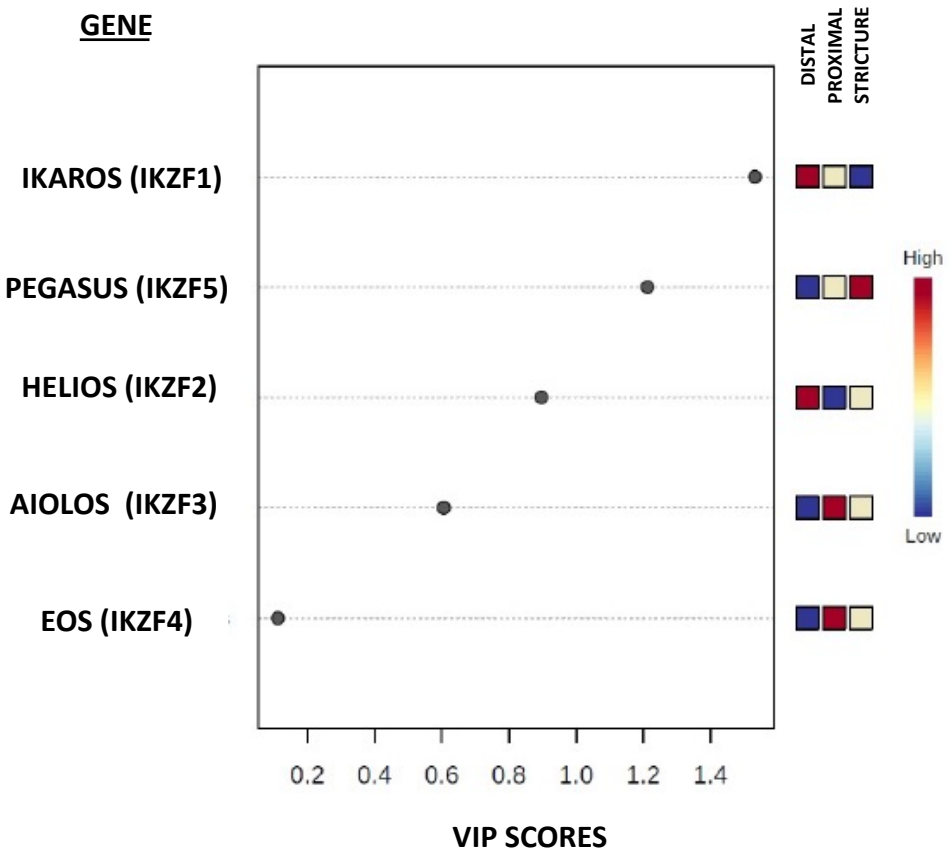



**Figure 5.28: VIP Scores Separate Ikaros Family Genes in Key Anatomical Compartments in the Injured Colon**
Transcriptome libraries extracted from 9 resection samples were sequenced on the NextSeq Illumina platform. 15 key macrophage genes were selected from PLS-DA modelling based on those with a 'variable importance in the projection' (VIP) score more than 1. The plot shows the VIP scores for Ikaros transcription factors and their relative abundance across Distal, Proximal and Stricture categories within our dataset. Gene names are supplied (left). Normalized expression values (High vs. Low) of the selected genes are presented in the right-hand side heatmaps. *N= 9 samples, n=27.*

## 5.3 Discussion

### 5.3.1 Elevated Expression of Macrophages in Diseased Bowel

In agreement with the literature, I report increased CD68+macrophages within inflamed bowel (Figure 5.1 and Figure 5.2). Macrophage numbers are increased in fibrosis in CD as seen in Figure 5.1, where greater positive staining for CD68+ macrophages visible in comparison to normal colon and UC (30, 34). In CD, macrophages migrate into the muscular layer and mesenteric fat with greater levels of CD206+ macrophages reported in CD, UC and colorectal cancer supporting our findings in inflamed tissue (18, 30). Similarly, in strictured regions of the colon we saw greater macrophage-associated genes supporting the increase in macrophages in IBD-related disease (Figure 5.26). This increase in macrophages within the bowel, with inefficient response to infection can have a detrimental response in IBD making macrophages a key therapeutic target (Section 1.3.3.5).

### 5.3.2 Macrophages Play a Key Role in Liver Disease

Similar to bowel disease, in the liver, macrophages contribute to fibrosis and disease pathogenesis of PSC as three times more macrophages are seen in PSC in comparison to Donor and PBC livers (210). In our results, expression of macrophage markers in both PSC and PSC-IBD tissue was twice that seen in Donor liver (Figure 5.3). Similar to the monocyte/macrophage recruitment seen in IBD, numerous studies support greater CD16+ monocyte recruitment and CD68+CD206+ macrophages expression in PSC liver and have linked macrophage activation to disease severity (66, 210). Increased numbers of CD68+ Kupffer cells are also found in NASH and NAFLD liver supporting our results (61). Chen *et al.,* (2019) compared PSC, PBC,

ALD, NASH and Donor liver and saw greater intermediate and non-classical monocyte infiltration in diseased livers, with the most seen in PSC. This again suggests targeting macrophages for intervention would have great therapeutic benefit in the gut-liver axis. The drivers of this monocyte infiltration are complex. In PSC, cholangiocyte senescence causes release of *'senescence-associated secretory phenotype'* (SASP), leading to greater macrophage recruitment (64). Karlsen *et al.,* (2017) similarly reported macrophage upregulation within the bile duct regions in PSC, supporting the role of macrophages in mediating fibrosis in liver disease. LSECs normally prevent Kupffer cells activation and monocyte adhesion and migration (65). In NASH however, LSEC secrete more CCL2 and upregulate VCAM-1 and ICAM-1 expression which recruits greater monocytes which then differentiate into MDM (65). Targeting monocyte recruitment in NAFLD has been investigated through the use of *Cenicriviroc*, a duel CCR2 and CRR5 antagonist which has shown promise in mice models and clinical trials (61, 62). Li *et al.,* (2020) similarly found that Cenicriviroc could help dampen fibrosis and inflammation in NASH and limit MDM production (65). Blocking CCR2/MCP-1 to prevent migration of monocytes in mouse models shows benefits in PSC, suggesting like in NASH and IBD, targeting the monocyte/macrophage axis could provide therapeutic benefits (64). Together these studies support the role for targeting macrophage production in liver disease as therapeutic intervention.

NASH was used as a disease control in studies, however, there is mounting interest in the incidence of NAFLD, NASH and IBD due to the rising global incidence of both (212, 213). Patients with IBD are thought to have a higher risk of NAFLD, with NAFLD considered a comorbidity of IBD but there still is limited data on their relationship (214). Theories suggest diet and environmental factors could influence pathogenesis of both.

Bessissow *et al.,* (2016) estimated NAFLD is present in approximately 33.6% of IBD patients, with Sartini *et al.,* (2018) finding patients with IBD develop a specific NAFLD phenotype, with a strong correlation between severe IBD and greater steatosis. Similarly, in patients who had both IBD and NAFLD, higher levels of both AST and ALT liver clinical markers were found (213). Studies however in this relationship are limited due to the chronic nature of the diseases where longitudinal studies are needed (214). However, identifying macrophages and Ikaros family expression between both offers potential targets for intervention.

### 5.3.3 Monocytes and THP-1 cells Express the Ikaros Family

We are one of the first groups to describe expression of the Ikaros family in both primary monocytes and the THP-1 cell line (Figures 5.4 & 5.6). Although studies in the past have described expression of certain family members such as Ikaros and Eos, to our knowledge, no studies have discussed the expression of other members such as Pegasus (83, 100, 107, 139, 142, 206). Our results here confirm that the Ikaros family is expressed by monocytes and THP-1s offering a potential cell line model for further study. During the COVID pandemic, this was extremely beneficial when I lacked patient samples. The novelty of the family has also caused some challenges in sourcing reagents. Differences in expression levels analysed by FACS and Western Blotting, suggests differential antibody sensitivity in methodological approaches (Figure 5.12 & 5.13). For example, we saw similar levels of Helios by Western, but lower levels in macrophage populations by flow. Although expression profiles of Ikaros and Eos were similar through both methods, the spread of samples analysed by flow suggests lysate analysis may have been more robust. The lack of conjugated Eos and

Pegasus flow antibodies supports confirming observations using FACS when better reagents are available.

### 5.3.4 Establishing our Monocyte to Macrophage Culture Method

Our method of polarising THP-1 cells was based on established methodology (81). To confirm polarisation, we used R&D Quantikine IL-10 and IL-12 ELISAs finding that M2c macrophages secreted the highest amount of IL-10 whereas M1s secrete the highest amount of IL-12, supporting known literature (Figure 5.7 & 5.8) (34, 81). A similar picture was observed in MDMs which found that significantly higher levels of IL-10 were secreted by the M2 macrophage populations (Figure 5.14)(34, 75). In contrast, M1 populations secrete significantly higher amounts of IL-12 (34). Our results thus support what is known in the literature confirming our polarization protocols worked as expected and cells were in the correct states when we assessed transcription factor expression. Further evidence comes from pre-pandemic, flow experiments on macrophage populations. Using flow to determine expression of macrophage subset markers, our results found that M1 and M2-associated cell surface markers corresponded with known literature, supporting our methodology (Figure 5.17). Cells were gated using CD14, CD16 and HLA-DR and CD206 and CD163 were highly expressed in M2 populations as expected (72, 75, 76). In M1, CD163 expression was lower, with higher CD80 and CD86 expression, again supporting known literature (72, 75). As we followed well established protocols, we were able to conclude our macrophage populations had been successfully polarised with our findings.

Although ultimately, we resorted to preliminary data using THP-1s, differences do exist in comparison to primary cells (76, 78, 79). Daigneault *et al.,* (2010) report that THP-

1 MΦ have no CD206 expression suggesting they are *classically* activated unlike MDM (79). Tedesco *et al.,* (2018) also found minimal expression of CD163 on THP-1 MΦ, a key marker found on macrophages. THP-1-derived MΦ were also found to secrete greater IL-1b and TNF$\alpha$ after stimulation than MDM (78). In a comparative analysis of proinflammatory cytokine release, Shiratori *et al.,* (2017) suggested that the polarisation of THP-1 to M1 was a more efficient than differentiation to M2, as cells also had minimal upregulation of M2-related genes (80). This supports the notion that cells are classically activated and suggests more robust stimulation or secondary signals such as cell-cell interactions are needed to drive a regenerative phenotype (79, 80). Together these studies suggest that THP-1-derived macrophages were a suitable model for our study but needs validation in primary cell models.

### 5.3.5 Ikaros Family in Macrophage Populations

In my results, I show that all members of the Ikaros family are expressed in THP-1 derived macrophages (Figure 5.11 & 5.12 & 5.13). To our knowledge, this is the first report of Ikaros family expression within THP-1 derived macrophages and highlighted key differences with primary macrophages. Although comparable differences between protein and RNA may represent differences in gene/protein regulation, we have been able to show distinct relationships of Ikaros family members with certain macrophage subsets. Primary MDMs demonstrated lower Aiolos and Pegasus RNA expression (Figure 5.18) whilst Eos expression was higher in macrophage populations in comparison to monocytes. The highest expression of Helios was seen in M2c cell populations, whilst Ikaros expression, was consistently expressed in all macrophage populations.

The lack of expression of Aiolos mRNA in primary macrophages was interesting to note and may suggest a lack of importance in macrophage behaviour. In agreement, low monocyte expression of Aiolos was reported by Billot *et al.,* (2010). However, at the protein level, detectable Aiolos were found, with lowest levels in the M2a populations (Figure 5.12). Together, our findings suggest Aiolos expression may be redundant within macrophages for their effector function but may be required for their development or survival such as its role in B cells (107, 113, 117).

In contrast, elevated Pegasus protein in THP-1-derived M1 populations suggests Pegasus may play a significant role in M1 function. We identified two protein bands of slightly differing molecular weights (Figure 5.12) in M1 populations suggesting isoform variation. We know that different Ikaros isoforms have different roles in cell types, health and disease suggesting an alternative Pegasus isoform within M1 may have a distinct functional role in comparison to other subsets (Section 1.5.9) (113, 138). This altered Pegasus expression in M1 is also of great interest therapeutically and could potentially be used to target M1 macrophages. However, it is important to note the variations between expression levels in primary cells and THP-1.

Eos protein expression levels were significantly higher in macrophages in comparison to THP-1 cells alone. At an RNA level, Eos expression was slightly higher in M2 populations suggesting a role for Eos in regulatory macrophages. Although there are studies highlighting Eos expression in monocytes and macrophages, little has been done to investigate comparative functions in these cells (107, 110, 134, 158). Together, our study is of one the first to find that Eos is expressed in all macrophage populations suggesting it is vital for their survival and function. In the next chapter, we use this knowledge to investigate the role of Eos in macrophage phenotype.

Ikaros was similarly expressed throughout all THP-1 and MDM populations at a RNA level (Figure 5.11 & 5.18). At a protein level however, Ikaros had lower expression in THP-1 derived M2c populations in comparison to other populations, albeit in a modest number of experiments. Previous studies have described expression of Ik-1, Ik-2, and Ik-x isoforms in macrophage populations, with greater Ikaros expression observed in inflammatory monocytes (83, 131, 140, 142). Such studies suggest that Ikaros is expressed within macrophages and required for functions such as regulator of chromatin state, response to LPS and influencing macrophage polarisation (83, 107, 206).

Helios expression was elevated in the M2 populations suggesting that Helios may have a role in a regulatory phenotype, similar to its expression and association with Tregs (98, 108). Helios had similar protein expression levels in all macrophage populations I studied thus suggesting Helios expression could be integral to macrophages, comparable to Ikaros expression (Figure 5.12). However, our findings dispute those by Thornton *et al.,* (2010) who did not find Helios RNA expression in monocytes or in macrophages in mice and focussed on expression in Treg. This may suggest interspecies differences but highlights the need for further work in this area.

### 5.3.6 All Ikaros Family Members Co-Express With CD68

To supplement our cellular protein and RNA expression data the Opal™ method was used to stain for expression of Ikaros family members in CD68+ macrophages in both the liver and the bowel. Our results confirmed all members of the family were expressed by CD68+ macrophages, one of the first studies to report this.

Opal™ staining is very sensitive and specific and is therefore useful for detecting low expression markers, and thus was deemed appropriate for detecting the Ikaros family

(173). In comparison to Chapter 4, dual staining could also ensure we could quantitate CD68 and Ikaros family double positive staining and ignore background epithelial or muscularis staining. We used Opal™ 570 for the Ikaros family which has the highest brightness on the Vectra Polaris with an excitation of 494nm and emission of 525nm to ensure we could capture all positive staining (173). For CD68, we used Opal™ 690 which has an excitation of 676nm and emission of 694nm, with low brightness on the Vectra Polaris and had been previously optimised within our group.

In our results, significantly greater expression of Helios+CD68+ and Eos+CD68+ was seen in inflamed tissue in comparison to uninflamed (Figure 5.21 & 5.22). Greater expression of Ikaros+CD68+ and Aiolos+CD68+ macrophages were also seen in inflamed tissue although not significant (Figure 5.20 & 5.23). Pegasus+CD68+ macrophages were of equal amounts in inflamed and uninflamed tissue (Figure 5.24). This supports upregulation of Ikaros family members during inflammation and the findings observed in our phenotypic studies (Chapter 4). Through this method we were also able to identify nuclear staining patterns of the family, such as Ikaros, compared to some cytosolic staining observed with Aiolos. Not all Ikaros family expression co-localised with CD68: some was seen within lymphocytes supporting known expression data on the family (Chapter 1 & 3). Ideally, for future work it would be beneficial to choose regions of interest (ROI) in our IHC analysis rather than the unbiased method we utilised in this work, as the spread of staining was vast which impacted individual *n* analysis. For example, selecting like-for-like ROI such as the mucosa in uninflamed and inflamed tissue to compare would give greater accuracy into staining patterns of family members within bowel regions. It is also important to note that the tissue samples used within DAB and Opal analysis were not matched and could explain discrepancies within our results.

Taking together our phenotypic findings in this chapter however, we hypothesise that the Ikaros family expression may help determine the M1 or M2-like phenotype of macrophages in disease similar to their proposed role in the Treg/Th17 balance. Both Aiolos and Ikaros are affiliated with Th17 cells, with Eos and Helios expression greatly associated with a Treg phenotype (46, 177, 181, 216). Observations of Aiolos expression in M1 populations and Helios expression in M2c macrophages, the regulatory macrophage phenotype support the potential role of the Ikaros family in mediating the inflammatory vs regulatory phenotype of macrophages. Elevated Helios and Eos expression within CD68+ macrophages also suggests the upregulation of regulatory factors in disease. Although not much is known about Eos, a review by Yu *et al.,* (2021) found Helios+ Tregs are upregulated in diseases such as SLE (blood), RA (synovial fluid) and colorectal cancer tissue, but have altered functionality. The group found these Tregs lacked certain cytokine production such as IL-10 or IFNγ, whereas Helios-Tregs produced such cytokines. The group hypothesised this difference could relate to the role of Helios in Treg stability or its influence is microenvironment-specific, with the heterogeneity of results leaving conclusions open. This therefore proposes the factors could be upregulated to promote a regulatory phenotype or aid macrophage plasticity which may detrimentally impact macrophage phenotype. In our next chapter, we discuss functional studies carried out in this project to investigate this theory.

### 5.3.7 Limitations of Our IHC Study

Biopsies although beneficial for diagnosis, are difficult to image in a research context due to issues arising with their storage, orientation, superficial nature, and size. Samples available for research are often remnants from clinical diagnostics and thus

can be small. Another limitation for my project was limited biopsies per patients. Between 4-6 biopsies were taken from patients, with two used for basic diagnostics, leaving in some cases only 2 biopsies for imaging. This was challenging as we were unable to optimise antibodies and provide sufficient controls with such limited tissue. For this reason, we began by optimising staining using liver tissue as it was readily available in the CLGR.

Because of the sample processing time and challenges associated with Opal™, much of my analysis relied on simpler DAB-IHC. These are straightforward however only one marker can be assessed per slide; staining can be affected by thickness of tissue and issues with background reactivity are common as discussed before (173). When using DAB-IHC we were unable to identify marker interactions or colocalization and thus we decided to use multiplexing to assess co-expression of CD68 and the Ikaros family (218). For our co-expression studies, we were able to attain larger sections from archived material from resected colon. This material contained uninflamed and inflamed regions and enabled us to view a greater tissue architecture of the bowel. Although this tissue was efficient for DAB, we did encounter issues with Opal™. Mainly, this was loss of tissue integrity due to the repeated cycles of antigen stripping (172). The archived bowel was relatively old and therefore there may have been issues with its preservation which could have affected the efficiency of the staining. Multiplexing must also be highly optimised but itself is extremely labour intensive and has a risk of human error which can lead to batch variance (172, 173, 218). This thus makes Opal™ labour intensive as it can take prolong periods to establish antibody pairings and to determine appropriate dilutions following the optimisation of singleplexes (173). For optimisation we also used liver tissue sections, which have higher autofluorescence staining than bowel tissue which may have affected the

antibody efficiency dilutions. All samples were also FFPE, contributing to background autofluorescence, which we tried to overcome using established methods of double blocking with Bloxall™ and Casein (172, 173). Finally, although theoretically, antibodies which are well established for DAB should work for Opal™, we did have issues with efficient staining of certain members of the family, namely Aiolos and Pegasus. For future studies, ideally testing multiple isoforms may be beneficial. However, multiplexing for us was invaluable as we were limited by the lack of validated flow cytometry antibodies for both Pegasus and Eos and species cross reactivity of available primary antibodies for dual staining. We had initially planned to multiplex two Ikaros family members (a regulatory and an inflammatory-associated member), CD4, CD64 and DAPI per slide but due to time limitations this was not possible.

### 5.3.8 RNASeq Data Analysis

In this pilot study, we have found differential expression of Ikaros family members within resected colon material providing a novel insight into the Ikaros family in IBD. Up to 70% of CD patients can develop strictures 10 years after their initial diagnosis, with many requiring surgery to remove the obstructive tissue (219). Our RNASeq samples are from resections in patients with CD and for the majority of patients, this was their primary resection (Table 5.1).

Strictured regions of tissue are known to contain a mixture of cell types such as myofibroblasts producing extracellular matrix (ECM) components, fibroblasts, epithelial and endothelial cells, CD4+ T cells, and macrophages which work in concerted action to cause tissue damage (220). Aggregates of lymphocytes in strictures are common, with greater ECM deposition of components such as fibronectin and collagen within the tissue (219, 221). Thus, as the Ikaros family is

expressed in many of these cell types, their elevated expression within these samples is predictable (96, 110, 123).

Our data generated from this RNASeq database is novel as we attained three distinct regions from surgical resections: the distal, proximal and stricture regions. This has enabled us to identify specific gene signatures in each individual region of the diseased colon. Most importantly, we are one of the first groups to discuss the expression of Ikaros family members within these three regions. As macrophages are highly implicated within IBD, it is not surprising to see that we were able to readily identify both a M1 proinflammatory cluster and a M2 regulatory cluster within our data set (Figure 5.25) (30, 45, 82). Macrophages are key to stricture pathogenesis, with elevated CD68+ macrophages identified in IBD tissue by us and other groups (Figure 5.2) (30, 45). Greater IL-36+ macrophage presence alongside myofibroblasts have been reported in strictures (221). An increase in CD68+ macrophages is also reported in fibrotic regions, supporting the elevated macrophage gene expression observed in the strictured region of our samples (221). By identifying genetic signatures using VIP, it was interesting to note that the majority of macrophage genes were again present within the stricture region (Figure 5.26). Again, based on previous studies this is fitting as immune cell infiltrate is greatly increased within strictures alongside an increase in macrophages and their mediators (30, 45, 220).

Fang *et al.,* (2015) compared paediatric IBD and colitis murine models to correlate genomic signatures of IBD in mice and humans using colon total RNASeq, similar to our approach. They similarly found upregulation of genes including IRF1 (M1), GBP1 (M1) OLFML3 (M2a) and TNFRSF11A (M2a) which were all identified within our study (222). Another study by Holgersen *et al.,* (2015) analysed colon biopsies from UC, CD and non-IBD control samples, conducting total RNASeq and presenting fold change

values in their results. The group found 115 '*literature defined genes'* which were *'significantly differentially expressed'* within IBD samples. Of these genes, two were also seen in our results: IL2Ra and CCR7 which we identified via their high VIP scores. Other macrophage related genes such as CXCL9, MMP9 and CD86 were also identified in their upregulated IBD gene set, supporting the role of macrophages in IBD pathogenesis.

Notably, we have used a whole tissue sequencing approach rather than single cell analysis. Thus, although some of our identified genes will be restricted to macrophages, others will not. For example, OLFML3, which was identified in both our study and Fang *et al.,* (2015), although associated with M2a, is also expressed by fibroblasts. Thus our reported increased stricture expression could relate to fibroblast presence within the stricture region and ECM remodelling (224).

One limitation of our work is that we lacked healthy control samples within our study to help interpret data. Thus, data from other groups for spatial differences in immune cell populations along the healthy colon provide insight into homeostatic functions of the colon from which we can infer Ikaros family expression (225). James *et al.,* (2020) analysed single cell (sc) RNASeq data from '*healthy steady-state'* donor colon isolating cells from the LP. The group identified similar populations of Tregs in both the proximal and distal colon (225). Interestingly, the group found there was a greater presence of B cells in distal colon in comparison to proximal (225). Tyler *et al.,* (2020) contrastingly used tissue digestion of biopsies to stain cells with flow cytometry markers and found greater presence of B cells within proximal regions in normal colon, along with greater monocytes, macrophages and CD8+ T cells. In contrast, the group found more CD4+ T cells and plasma cells in distal areas (226). As biopsies were used in this study, this does limit the penetration into the tissue architecture, and can explain

the differences in cell phenotypes observed in each region. For example, with greater numbers of B cells in the proximal region, we might expect greater Aiolos expression here due to its association with B cells (226).

A key finding from our study was that the Ikaros family is indeed expressed differentially within the colon during IBD, with elevated Ikaros and Helios expression in distal regions and elevated Pegasus and Aiolos expression within the stricture (Figures 5.27 & 5.28). Interestingly, Aiolos expression was higher within the proximal region, along with Eos expression, suggesting a role for these transcription factors away from the stricture site. To our knowledge, this has not been reported in the public domain.

Elevated expression of Pegasus and Aiolos within the stricture suggests a role in stricture pathogenesis. For Pegasus we can hypothesise that the increase in Pegasus could be due to elevated macrophage presence based on our finding of Pegasus expression within macrophages (Figure 5.24). Furthermore, we can also speculate the local increase in Pegasus may reflect increase in platelet accumulation at the strictured region (129, 166). A release of inflammatory mediators at the site of stricturing can lead to blood clot formation through the release thrombin, which encourages platelet recruitment and degranulation of platelets, forming further blood clots (220).Thrombocytosis is thought to correlate with small bowel obstructions post-colon surgery and thus Pegasus could potentially be associated with this risk (227, 228). This thus suggests that perhaps Pegasus could function as a marker of risk**.** Interestingly, the patient with the highest expression of Pegasus in the stricture was the youngest and most recently diagnosed (< 6 months, see Table 5.1). Although more insight is needed, it is promising to see a potential correlation between duration of diagnosis and, or age, with Pegasus expression.

Although Eos had the lowest VIP score of all members, the higher expression of Eos in the proximal samples could support its elevated expression in cells such as monocytes, macrophages and Tregs which are present in this region under homeostatic conditions (97, 119, 159, 226)(See above). It was also interesting to note that the individual with most elevated expression of Eos within the proximal region was also the only member of the data set to display mild inflammation based on clinical scores (Table 5.1). This again supports the notion of elevated expression of Eos, a regulatory transcription factor within the proximal region with elevated regulatory cell presence.

Elevated expression of Ikaros and Helios within distal regions could be due to their expression within CD4+ T cells within this region where they are more prevalent under homeostatic conditions as reported by Tyler *et al.,* (2020). I have discussed within this thesis the role of both Ikaros and Helios within CD4+ T cells populations, mainly Tregs and Th17 cells and thus elevated expression of these transcription factors within the colon in IBD could be explained by the influx of CD4+ T Cells in disease (52, 103, 110, 135, 136, 163). Aiolos expression within the stricture could similarly be due to its expression in macrophages or CD4+ T cells, with its elevated expression in proximal sites due to its association with B cells, which are more prevalent within this area (107, 110, 149, 226). We can also speculate the differences in Ikaros family expression could be due to the migration of cells to the site of inflammation and as the tissue shows a snapshot of time post-surgery, this could in some sense provide some insight into differences. These observed differences in Ikaros family expression could then be used to correlate disease course or outcome of surgery, identifying novel clinical IBD markers.

Although our study has provided a novel insight into the expression of the Ikaros family within the different regions of a CD resection, there are however caveats to the study. Firstly, the population size in our pilot study is small. The age range of patients varies from 19 to 63 and the ratio of female: male is 3:9, which could in turn influence the results. In Figure 5.27, we can see the variability of the Ikaros family expression within samples, and how for example, high expression of a member in one donor can skew the average expression of the members across each region. A major caveat in RNASeq analysis within IBD is a lack of standardized methodology for analysing cell populations in human samples and lack of robust public sequencing databases to compare. The starting material for studies also varies, for example James *et al.,* (2020) used cadaveric donor material with Fang *et al.,* (2015) analysing data from a mix of studies using biopsies and regions of colon from paediatric IBD donors.

Although RNASeq data provides us with great insights into the potential role of the Ikaros family in IBD, we could greatly benefit from scRNASeq which could help correlate expression with cell type. This would support the limited tissue staining studies I was able to perform. We also have no region of 'healthy' colon from individuals to provide a robust control. The proximal and distal regions were used as 'internal controls' but may be influenced by spread of the disease due to their physical proximity to the stricture.

### 5.3.9 Summary

Our study is one of the first to identify co-expression of Ikaros family members with CD68+ myeloid cells, confirming that Ikaros family proteins are expressed within macrophages in both the liver and the bowel. Associations of Ikaros family members within distinct regions of resections also provides insights into their potential role in

disease pathology. These finding are novel and important foundations for future studies with patient material. The Ikaros family have been under investigated in the past with expression and function studies focussing on lymphocytes. Together, our results and studies have shown that macrophages are present and functionally implicated in both bowel and liver disease, making them an excellent therapeutic target. Co-expression of Ikaros family members also suggests that macrophages could be targeted through the Ikaros family using therapeutics such as Pomalidomide which we attempt in the next chapter. Although macrophages can be targeted through the CCR2-CCL2/CCL7 axis, it is important to note the widespread expression of these chemokine receptors across the differentiation spectrum. Thus broad targeting of all cells may make individuals more susceptible to disease via additional impact on macrophages key to tissue repair (44). Thus, by selective targeting of Ikaros family members to promote changes in macrophage plasticity, one could in turn influence the regulatory and inflammatory phenotype of macrophages to promote the resolution of inflammation.

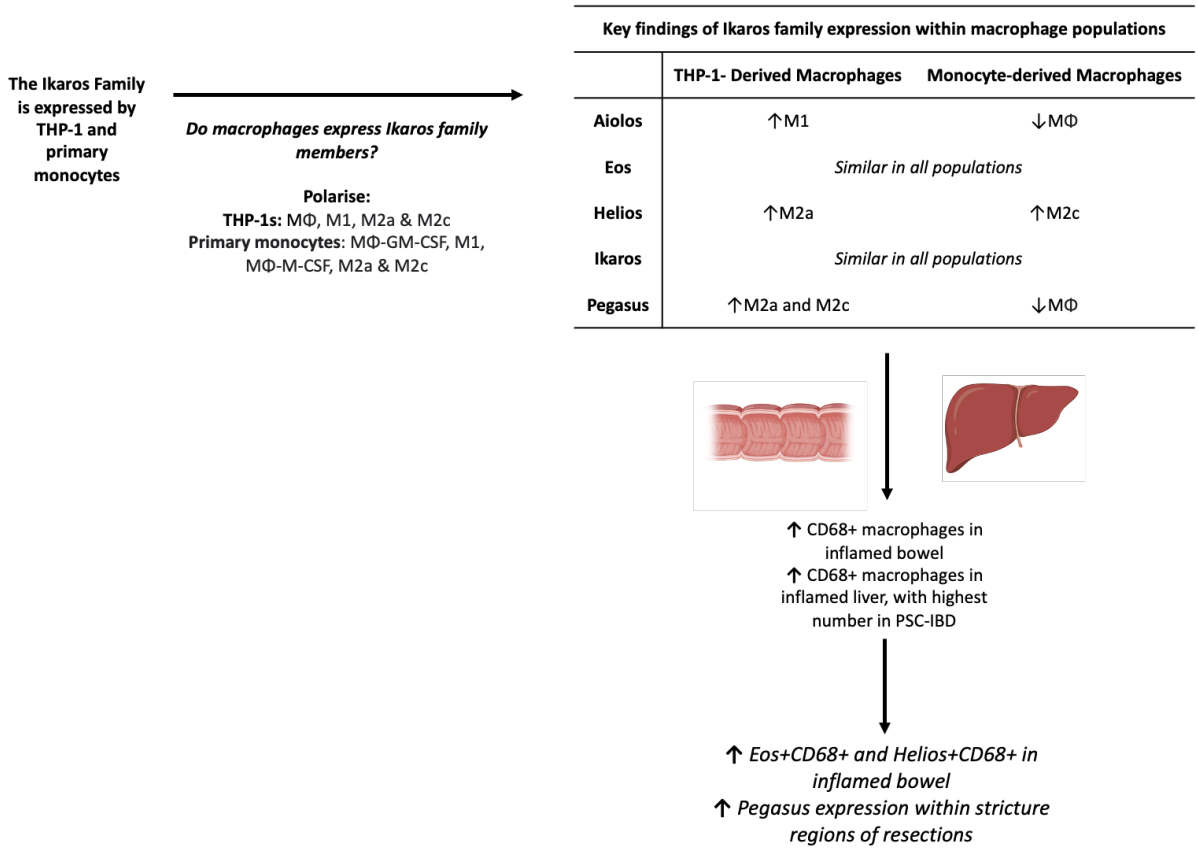



**Figure 5.29: Summary of Findings From Chapter 5**
Summary diagram of the key findings from the *Ikaros Family Expression In Monocytes And Macrophages* chapter. The Ikaros family was summarised to be expressed within THP-1s and primary monocytes. Polarisation to various macrophage subtypes found Ikaros family expression in THP-1 derived and monocyte derived macrophages which are summarised within the table in the figure. Next, in both colon and liver tissue, elevated levels of CD68 expressing (CD68+) macrophages were seen during inflammation. Importantly, we saw a significant increase in Eos positive (Eos+) CD68+ macrophages and Helios positive (Helios+) and CD68+ macrophages in inflamed bowel.

# Chapter 6: Impact of IBD and Therapeutic Intervention on Ikaros Family Expression

## 6.1 Introduction

In this Chapter, I discuss the impact of IBD and the therapeutics Pomalidomide and Infliximab on Ikaros Family expression within macrophage populations. As mentioned in Section 1.1.8, anti-TNF$\alpha$ therapies such as Infliximab have shown the greatest promise in promoting remission in UC and CD, with Thalidomide, a readily available drug, showing promise in promoting remission (8, 9, 229). TNF$\alpha$ is an attractive target within IBD as studies have shown it contributes massively to inflammation seen within IBD with high levels found in the mucosa, serum and stool of CD patients (9). Anti-TNF antibody can also induce apoptosis in T cells and monocytes, helping to manage inflammatory cells (9). Infliximab can also induce M2 macrophages expressing CD68 and CD206 promoting a regulatory macrophage phenotype in patients (82). Thus, we can hypothesise that Infliximab may influence Ikaros family expression within macrophages. Pomalidomide contrastingly is a derivative of Thalidomide which is not yet routinely used within the clinic for IBD management. Below, I introduce Thalidomide, its derivates and the impact they have on certain Ikaros family members, in particular, Aiolos and Ikaros, within IBD models.

### 6.1.1 Thalidomide, Lenalidomide and Pomalidomide: Immunomodulatory Drugs and The Ikaros Family

Due to the growing interest in the role of Aiolos and Ikaros in cancer, many therapeutics have been investigated which could target and dampen the effect of both transcription factors. One such drug able to target Aiolos and Ikaros is Thalidomide. Thalidomide is an immunomodulatory drug (IMiD) which has also been shown in some studies to promote remission in IBD (7, 230). Thalidomide is a synthetic piperidinyl isoindole glutamic acid derivative which is known to inhibit release of TNF$\alpha$ and other

cytokines from monocytes. Although now more commonly used to treat multiple myeloma, Thalidomide was originally developed as a sedative and for management of headaches, colds, and nausea (12, 230). Marketed in 1957 as a treatment of myeloma, Thalidomide was withdrawn in 1961 because of its severe side effects on unborn foetuses (10, 12). It has since been discovered that Thalidomide interacts with a target protein called Cereblon which regulates expression of downstream targets like p63, explaining its detrimental effects on foetal limb development (231). Thalidomide was then reintroduced in 1988 by the FDA with updated guidance regarding dosage and side effects (12). Thalidomide has shown promise in management of IBD (12). Limited systemic reviews have shown promise of Thalidomide in CD management, promoting greater remission and a reduction in steroid use, although more research is needed in UC management (229). Thalidomide's legacy however has led to development of drug analogues, of which Pomalidomide and Lenalidomide are examples (7, 12, 232, 233). Both Lenalidomide and Pomalidomide slightly differ in their chemical structure and maintain a similar level of activity to Thalidomide, with reduced side effects (Figure 6.1) (233). Although there are concerns regarding efficient delivery of IMiDs to the gastrointestinal tract and their broad side effects, the ability to influence the function of T cells, NK cells, B cells and monocytes is attractive (234).

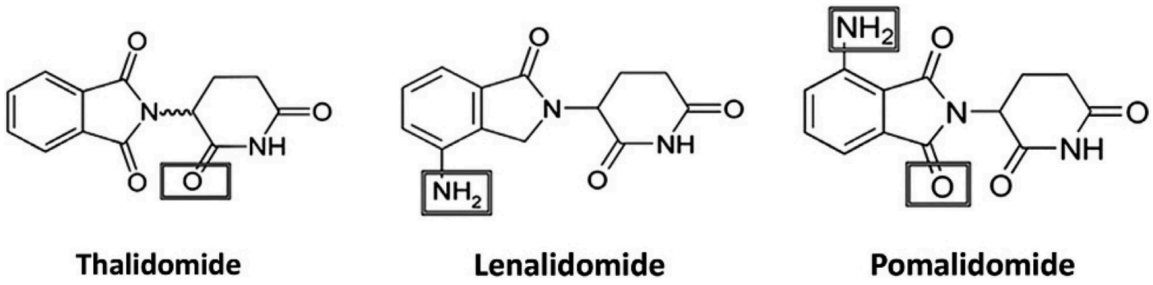



**Figure 6.1: Chemical Structure of Thalidomide and its Derivatives**
The chemical structure of the Immunomodulatory drugs (IMiDs) Thalidomide, Lenalidomide and Pomalidomide highlight the structural differences within this group of drugs. All three IMiDs behave as Cereblon modulators. Key differences in each drug are highlighted by a black outlined square. Image adapted from Chanan-Khan *et al.,* (2013)

Lopez-Millan *et al.,* (2017) demonstrated that both IMiDs were capable of attenuating experimental acute colitis in murine models. In murine IBD models, Lenalidomide treated mice had a higher survival rate and a depletion in inflammation (233). Contrastingly, Pomalidomide resulted in a survival rate of approximately 40%, with some improvement in inflammation observed (233). Bolomsky *et al.,* (2017) also found treatment with Lenalidomide down regulated Aiolos and Ikaros, causing apoptosis in multiple myeloma. The group found that treatment of T cells with Lenalidomide decreased both Aiolos and Ikaros with a concurrent increase in IL-2 production (232). This was also seen by Gandhi *et al.,* (2014) who suggested that by degrading Ikaros and Aiolos, T cell co-stimulation via upregulation of IL-2 occurs.

Thus, IMiDs function by supressing and downregulating inflammation, inhibiting proliferation of lymphocytic cells and proinflammatory cytokines whilst upregulating the secretion of anti-inflammatory cytokines (233). Like Thalidomide, IMiDs mediate these effects through *Cereblon*-targeted ubiquitination and degradation of proteins via the proteasome (144, 232). Both Ikaros and Aiolos have been shown to bind to

Cereblon, which is the substrate receptor of the cullin ring 4 ligase (CRL4) E3 ubiquitin ligase complex making them suitable targets for IMiDs (Figure 6.2) (109, 110, 144, 232, 233).

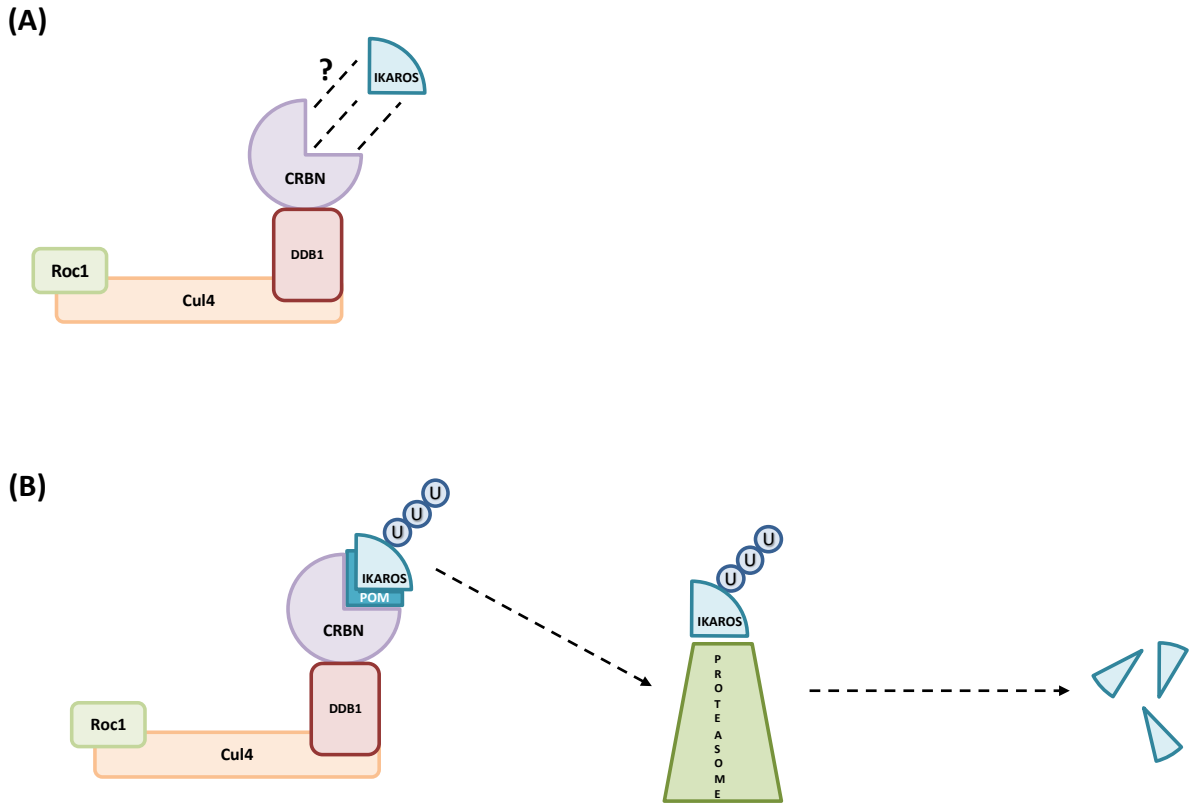



**Figure 6.2: Pomalidomide-Mediated Degradation of Ikaros**
The Cullin ring 4 ligase (CRL4) E3 ubiquitin ligase complex contains the components Cul4, DDB1, Roc1 and Cereblon (CRBN). **(A)** In the absence of Pomalidomide (POM.), it is unknown if Aiolos or Ikaros can bind to CRBN as substrates (marked with a question mark). **(B)** Under conditions of Pomalidomide or Lenalidomide, CRBN is able to bind to Ikaros or Aiolos and tag them for Ubiquitination (U) which then leads to their degradation via the proteasome. For ease of viewing, only Pomalidomide and Ikaros are shown but can be substituted with either Lenalidomide or Aiolos. *Cul 4, cullin 4; DDB1, DNA damage binding protein-1; Roc1, regulator of cullins 1.* Figure adapted from Gandhi *et al.,* (2014).

### 6.1.2 The Ikaros Family and Thalidomide

By its association with Cereblon, Pomalidomide is able to degrade Aiolos and Ikaros, with studies demonstrating Pomalidomide exhibits greater Ikaros and Aiolos degradation than other members of the IMiD family (144, 235). In human studies, Bolomsky *et al.,* (2017) noted correlations between the expression levels of Ikaros in T Cells, B Cells and monocytes and clinical response in patients following treatment with IMiDs for Multiple Myeloma and thus suggested using Ikaros as a marker of IMiD activity (232). Interestingly, patients who had higher Ikaros levels in B Cells, T Cells and monocytes before treatment had better clinical outcome, although the link was not investigated further by the group (232).

Lenalidomide treatment of patients with haematological cancers has also been shown to decrease numbers of CD16+ non-classical monocytes in the periphery, highlighting the impact of Ikaros knockdown on monocytes and macrophages (144). There are also limited instances describing the ability of Thalidomide and other IMiDs to influence macrophages during cancer therapy, suggesting Ikaros (and Aiolos) knockdown could influence macrophages in disease (206). Together, studies suggest a potential role for IMiDs in IBD management. These drugs are readily available and have shown promise in limited human studies and murine models (10). Due to their influence on Ikaros family members, and the evidence linking them to macrophage biology, they may influence IBD pathology through key immune cells such as macrophages. Thus, this will be explored further in my experimental approach.

Taking together this knowledge of Pomalidomide and its impact on Ikaros family members, I used THP-1-derived macrophages to assess the drugs' impact on macrophage expression of Ikaros family members. Alongside this, I also investigate the expression of the Ikaros family within MDMs derived from Control (HFE), Biologic

Naïve and anti-TNFα treated patient samples to ascertain the impact of IBD and anti-TNFα treatment.

Together, the objectives of this section were:

I. To ascertain if Pomalidomide could affect Ikaros family expression with macrophage subsets
II. Determine what impact IBD has on systemic Ikaros family expression within monocytes and macrophages
III. Distinguish donor and patient derived monocyte and macrophage Ikaros family expression differences
IV. Determine whether biological intervention in the form of Infliximab can impact Ikaros family expression within monocytes and MDM

## 6.2 Results

Whilst Pomalidomide can target Aiolos and Ikaros for degradation little is known about its effect on other family members or on macrophages. Thus, we cultured THP-1 and THP-1-derived macrophages with 10μM Pomalidomide (Section 2.9). Treatment was performed either pre-Macrophage polarisation for the short culture (Figure 6.3) or during the full culture protocol (Figure 6.4) to assess the impact of short and long culture with Pomalidomide on Ikaros family expression.

### 6.2.1 Short-term Pomalidomide Culture Alters Ikaros Family Expression

THP-1 cells were first incubated with 10μM Pomalidomide for 24 hours before polarising cells to macrophages. Figure 6.3 shows that undifferentiated THP-1 cells expressed Aiolos, Eos, Helios, Ikaros and Pegasus RNA as previously demonstrated (Figure 5.11) with the lowest expressed being Helios (Figure 6.3). Treatment with Pomalidomide for 24 hours did not significantly alter expression of family members in undifferentiated cells. As before, MΦ differentiation induced an increase in Helios expression and Aiolos and Helios both increased in cells differentiated to M1 macrophages. Short term exposure to Pomalidomide reduced Aiolos ($p<0.05$), Ikaros and Pegasus expression in M1 macrophages. Interestingly for MΦ macrophages, Eos was increased by treatment whereas Helios expression decreased. Table 6.1 describes the significant differences between populations.

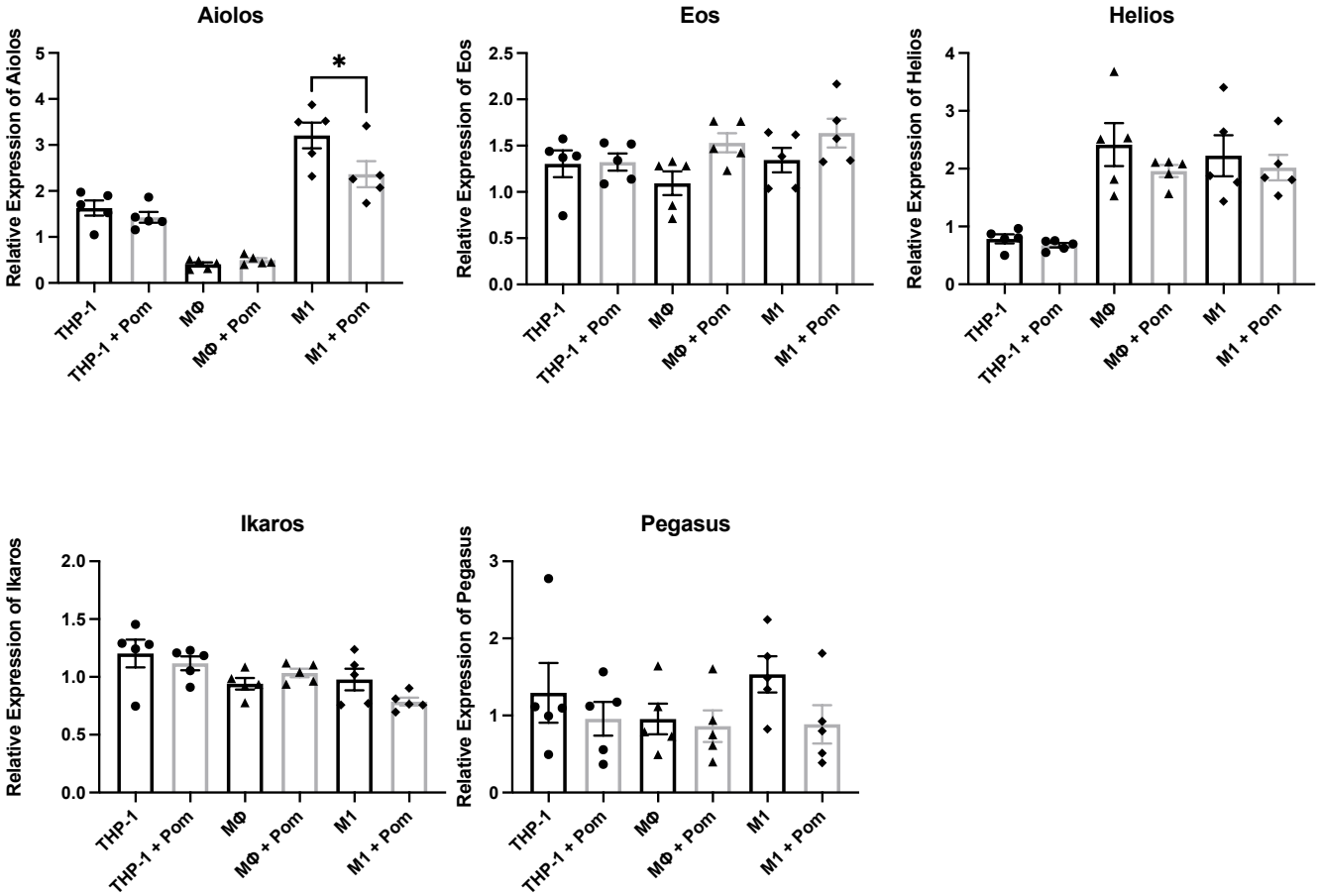



**Figure 6.3: Pomalidomide Addition Alters Expression of the Ikaros Family in Macrophages**
THP-1 cells were polarised to MΦ macrophages with addition of PMA. The cells were then left untreated or incubated with mediators to polarise them further to different macrophage subsets (MΦ = PMA (50ng/ml), M1 = PMA (50ng/ml) + IFNγ (20ng/ml) + LPS (20ng/ml), M2a = PMA (50ng/ml) + IL-4 (20ng/ml), M2c = PMA (50ng/ml) + IL-10 (20ng/ml)). The macrophages were then cultured with or without Pomalidomide (Pom.) 10μM for 24 hours, after which, cells were harvested, RNA isolated and qPCR conducted. Results are presented as mean ± SEM. *N=2, n=5. one-way ANOVA and Tukey's Multiple Comparison Test. Aiolos, M1 VS M1 + Pomalidomide * p < 0.05. Housekeeping Gene: RPS9.*

**Table 6.1: Statistical Analysis of 24-hour Pomalidomide Addition to MΦ and M1 Macrophages**

| | Aiolos | Eos | Helios | Ikaros | Pegasus |
|---|---|---|---|---|---|
| **THP-1 vs. THP-1 + Pom** | ns | ns | ns | ns | ns |
| THP-1 vs. MΦ | ** | ns | *** | ns | ns |
| THP-1 vs. MΦ + Pom | ** | ns | * | ns | ns |
| THP-1 vs. M1 | **** | ns | ** | ns | ns |
| THP-1 vs. M1 + Pom | ns | ns | * | ** | ns |
| THP-1 + Pom vs. MΦ | ** | ns | *** | ns | ns |
| THP-1 + Pom vs. MΦ + Pom | * | ns | ** | ns | ns |
| THP-1 + Pom vs. M1 | **** | ns | ** | ns | ns |
| THP-1 + Pom vs. M1 + Pom | * | ns | ** | * | ns |
| **MΦ vs. MΦ + Pom** | ns | ns | ns | ns | ns |
| MΦ vs. M1 | **** | ns | ns | ns | ns |
| MΦ vs. M1 + Pom | **** | ns | ns | ns | ns |
| MΦ + Pom vs. M1 | **** | ns | ns | ns | ns |
| MΦ + Pom vs. M1 + Pom | **** | ns | ns | ns | ns |
| **M1 vs. M1 + Pom** | * | ns | ns | ns | ns |

### 6.2.2 Pomalidomide Addition Alters Expression of the Ikaros Family in Macrophages

Next, the influence of long-term incubation with Pomalidomide was assessed by exposing THP-1 cells to 10μM Pomalidomide (+Pomalidomide) before and after polarising cells to various macrophage subsets using PMA (50ng/ml) (Figure 6.4). Data was normalised to control (subsets without Pomalidomide treatment) with basal expression of each transcription factor similar to what we have previously described (Figure 5.11). In contrast to the short-term treatment (Figure 6.3) it appeared that there was a reduction in Eos expression in undifferentiated cells whereas levels of Pegasus and Ikaros increased. Aiolos, Eos and Helios expression remained suppressed in MΦ and M1 macrophages. Within M2 macrophages exposed to Pomalidomide, higher Helios and Ikaros expression was seen in comparison to Control.

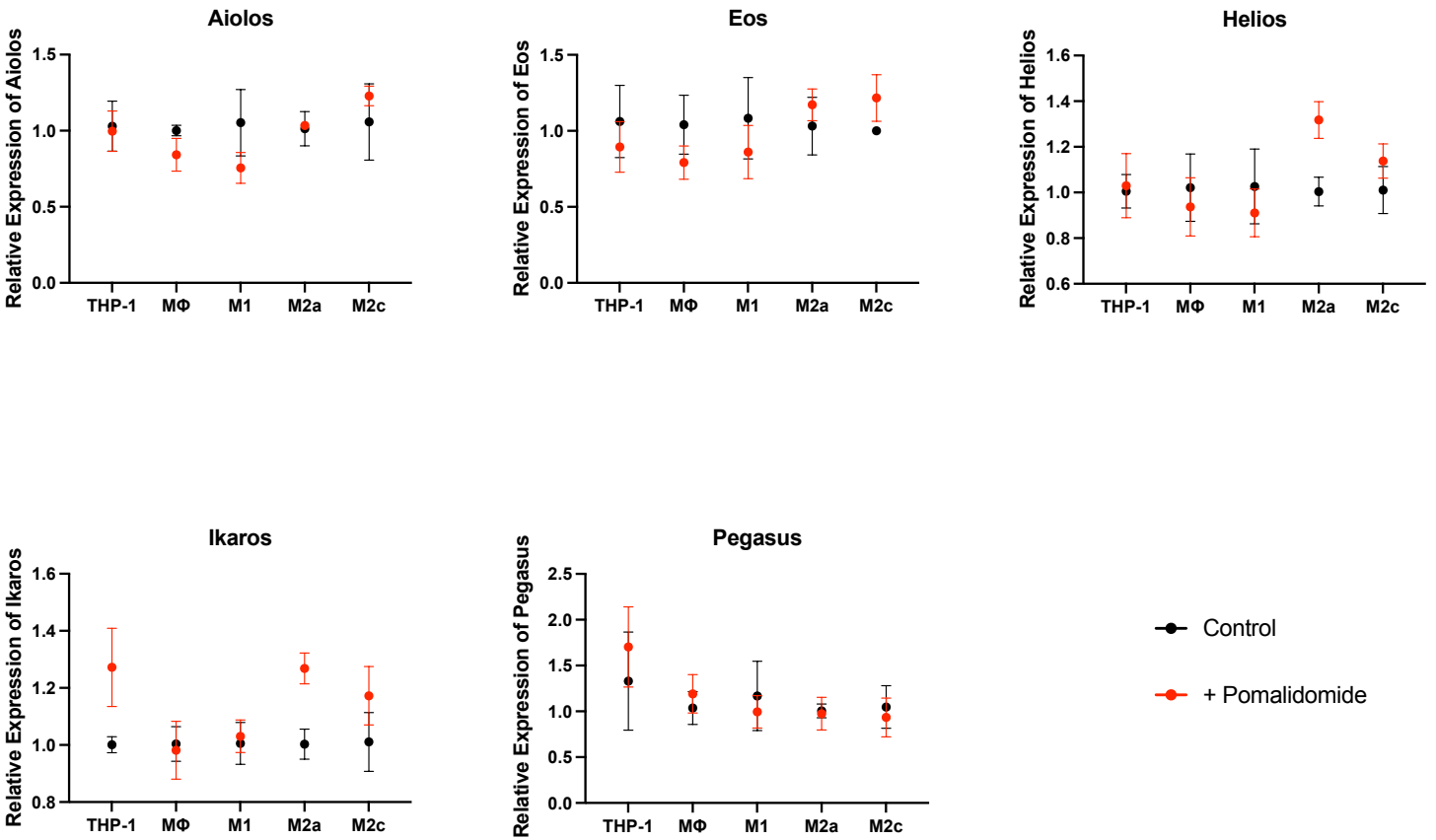



**Figure 6.4: Prolonged Pomalidomide Culture Alters Expression of the Ikaros Family in Macrophages**
THP-1 cells were polarised to MΦ macrophages with addition of PMA. The cells were then left untreated or incubated with mediators to polarise them further to different macrophage subsets (MΦ = PMA (50ng/ml), M1 = PMA (50ng/ml) + IFNγ (20ng/ml) + LPS (20ng/ml), M2a = PMA (50ng/ml) + IL-4 (20ng/ml), M2c = PMA (50ng/ml) + IL-10 (20ng/ml)). Cells were also left untreated or treated with addition of Pomalidomide (10μM) throughout the culture. RNA was extracted from samples and measured by qPCR. Results are presented as mean ± SEM. *Control, N=3; +Pomalidomide, N=5. Two-way ANOVA. NS. Housekeeping Gene: RPS9.*

### 6.2.3 Freezing and Thawing Cells Alters Expression of Ikaros Family Members Compared to Freshly Isolated Cells

As part of the TRAFIC study (Section 2.1), patient PBMCs were collected and stored at -80°C for later analysis and crucially for us, these samples proved beneficial during the COVID pandemic. Prior to the COVID pandemic, we were keen to assess the impact that freezing had on the expression of the Ikaros family, as to our knowledge, there was no known evidence for this in the literature. Thus, analysis of frozen samples served a dual purpose: both allowing me to continue my studies whilst clinics were suspended and generating useful data on the impact of cryopreservation.

Therefore, fresh and frozen matched HFE PBMC samples were compared to assess differences in expression levels of the transcription factors (Figure 6.5). Cells were polarized to different macrophage populations by addition of indicated cytokines for 24 hours. The various macrophage populations were lysed, the RNA extracted and analysed for expression levels of the transcription factors, with data normalised to '*fresh'* samples. Our results show a general trend for higher expression levels in frozen samples in comparison to fresh. Frozen samples had slightly higher expression of Aiolos, Helios and Ikaros in monocytes. Thawed cells differentiated to MΦ had a tendency for elevated Eos and Ikaros expression, whilst Pegasus was elevated in M2 populations.

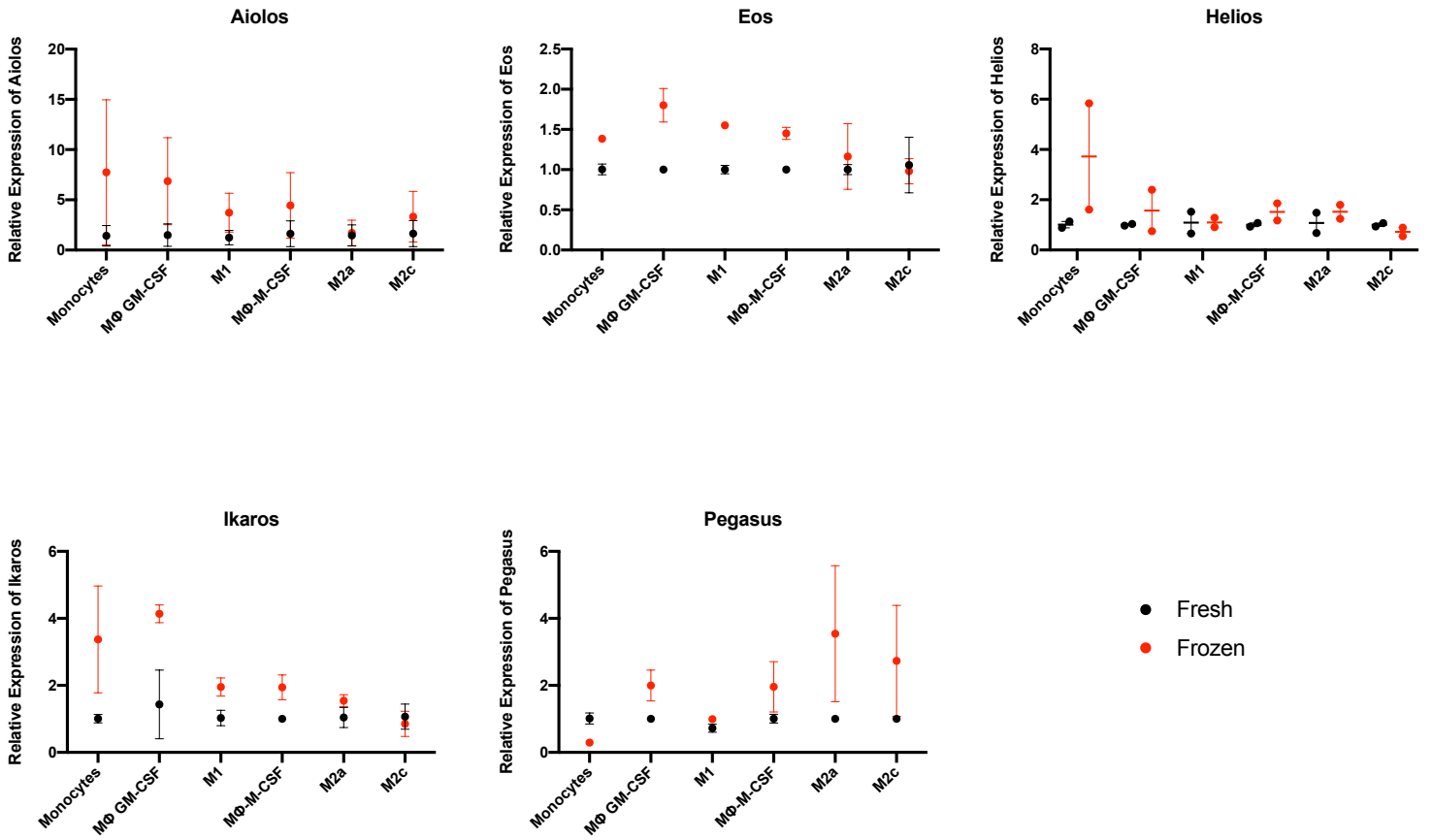



**Figure 6.5: Comparison of Fresh and Frozen Peripheral Blood Mononuclear Cells-Derived Monocyte to Macrophage Culture** Monocytes were isolated from the same peripheral blood mononuclear cells (PBMCs) donor following isolation or frozen and then isolated. The monocytes were then left untreated (Monocytes, Mono) or polarised to Macrophages (MΦ) using GM-CSF (10ng/ml) and M-CSF (50ng/ml). They were then further polarised to M1 (GM-CSF + IFNγ (20ng/ml) + LPS (50ng/ml)), M2a (M-CSF+ IL-4 (20ng/ml)) or M2c (M-CSF + IL-10 (20ng/ml)) for 24 hours. The cells were the lysed and RNA extracted for qPCR analysis. Results were normalised to the housekeeping gene RPS9, and then further normalised to the mean of fresh samples to determine relative expression of each sample. Results are presented as mean ± SEM. *Fresh, N=2; Frozen, N=2. Housekeeping Gene: RPS9.*

### 6.2.4 Diseased Patient Macrophages have Differential Expression of Ikaros Family Transcription Factors in Comparison to Control

Monocytes were isolated from both Controls (HFE) and Biologic Naïve *frozen* IBD patient samples to assess differences in Ikaros family expression in disease. Our results showed that expression levels of the Ikaros family differed in Biologic Naïve patients with IBD in comparison to Control (Figure 6.6). There was much variability between different patient samples, but it appeared that Eos expression was increased in M2 macrophages and was significantly increased in monocytes compared to controls ($p<0.05$). Both Helios and Ikaros appeared to be more abundant in samples across the spectrum, with significant increase in Helios expression in MΦ macrophages ($p<0.05$). Aiolos and Pegasus expression tended to be reduced in all patient samples across the macrophage differentiation spectrum.

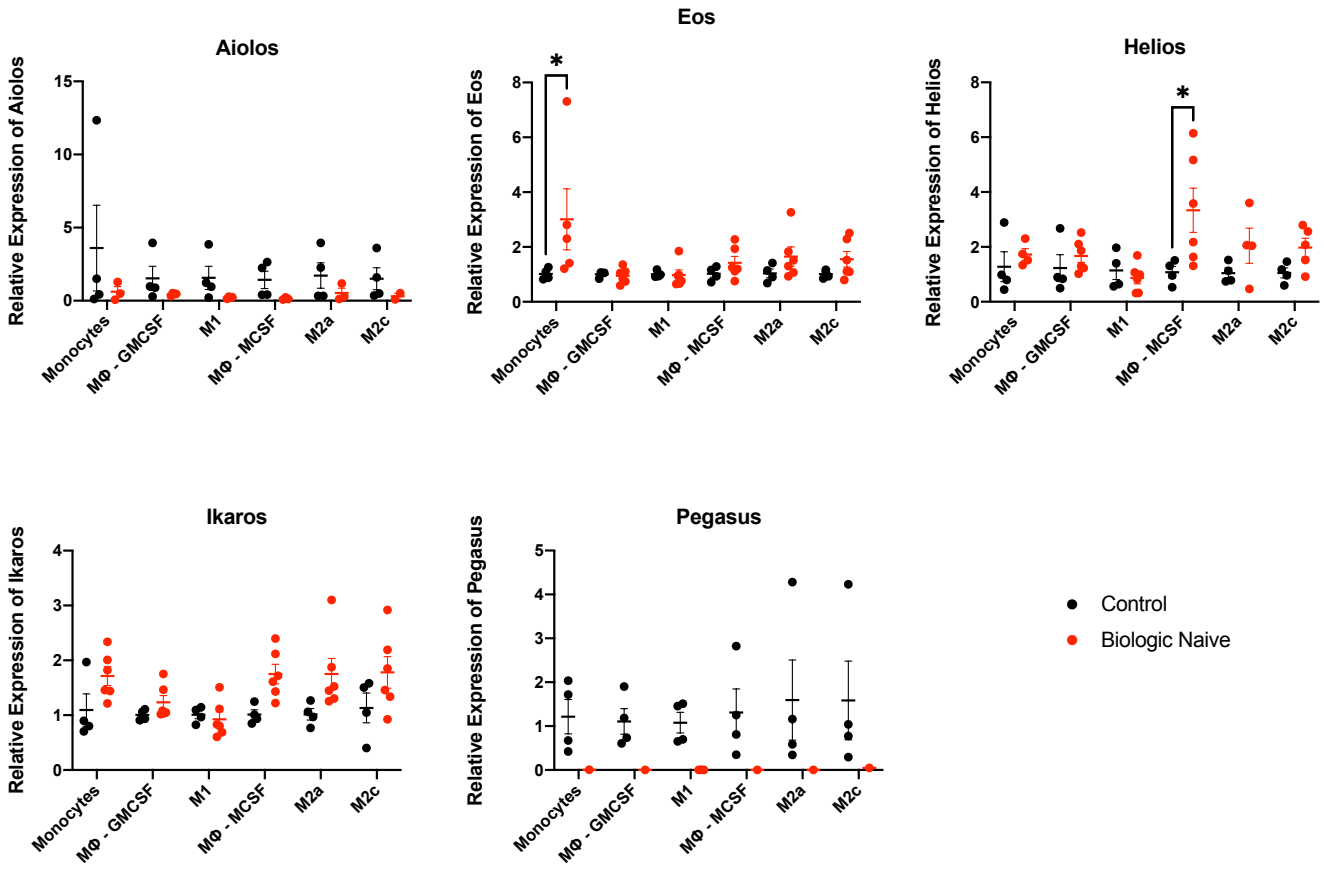



**Figure 6.6: Comparison of Ikaros Family Levels in Control and Biologic Naïve Diseased Patient Samples**
Monocytes were isolated from either hemochromatosis (Control) peripheral blood mononuclear cells (PBMCs) donors or from Biologic Naïve newly diagnosed IBD patient samples. The monocytes were then left untreated (Monocytes, Mono) or polarised to Macrophages (MΦ) using GM-CSF (10ng/ml) and M-CSF (50ng/ml). They were then further polarised to M1 (GM-CSF + IFNγ (20ng/ml) + LPS (50ng/ml)), M2a (M-CSF+ IL-4 (20ng/ml)) or M2c (M-CSF + IL-10 (20ng/ml)) for 24 hours. The cells were the lysed and RNA extracted for qPCR analysis. Results were normalised to the housekeeping gene RPS9, and then further normalised to Control Values. Results are presented as mean ± SEM. *Control; N=4, Biologic Naïve; N=6. Eos * p<0.05; Helios * p<0.05. Two-way ANOVA and Tukey's Multiple Comparison Test. Housekeeping Gene: RPS9.*

### 6.2.5 Elevated Levels of IL-12 Secretion Are Found in M1 Populations Isolated From Untreated IBD Blood

Supernatants were harvested from cultured macrophage populations of either Control or Biologic Naïve peripheral blood samples, similar to the method discussed in Section 2.8. Comparison of IL-12 secretion from supernatants found elevated IL-12 secretion in Biologic Naive M1 populations in comparison to Control M1 (Figure 6.7). All other populations had comparable levels of IL-12 in both control and Biologic Naive samples. This supports previous literature which has shown elevated IL-12 levels in IBD patients in comparison to control (236).

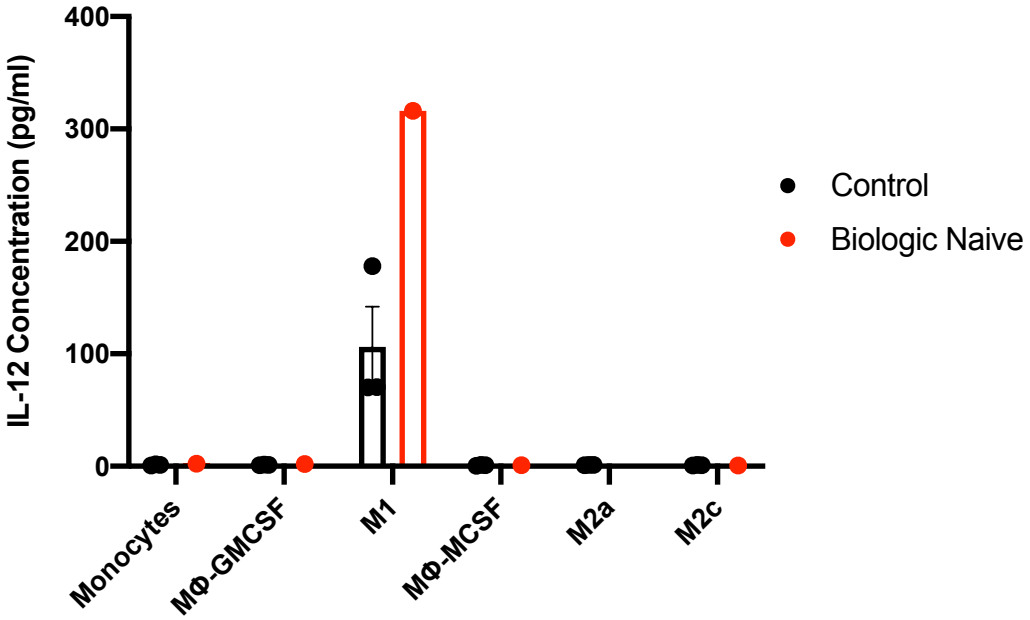



**Figure 6.7: Biologic Naïve Inflammatory Bowel Disease (IBD) M1 Macrophages Secrete Greater IL-12 in Comparison to Control**

Blood-derived monocytes were isolated from hemochromatosis blood (control) or untreated IBD biologic naïve blood (BNV) and left untreated (Monocytes, Mono) or polarised to MΦ) using GM-CSF (10ng/ml) and M-CSF (50ng/ml). They were then further polarised to M1 (GM-CSF + IFNγ (20ng/ml) + LPS (50ng/ml)), M2a (M-CSF+ IL-4 (20ng/ml)) or M2c (M-CSF + IL-10 (20ng/ml) ) for 24 hours. After incubation, the supernatants were harvested and used for quantification of IL-12 using R&D Quantikine ELISA kit. Results are presented as mean ± SEM. *Control, N=3; Biological Naive, N=1.*

### 6.2.6 Impact of Anti-TNFα treatment on Ikaros Family Expression in Macrophages

Anti-TNFα targeting monoclonal antibody, known in the clinic as Infliximab, is a common treatment used for the management of IBD (6, 11, 12, 30, 52). In the TRAFIC study, alongside Biologic Naïve patients we were able to attain peripheral blood sample from patients treated with anti-TNFα therapy. Monocytes were isolated from these samples and polarized to various macrophage populations as before. Ikaros family expression levels in anti-TNFα treated, Control and Biologic Naive macrophage populations (as mentioned above) were then compared. However, not all transcription factors were expressed at mRNA level in the anti-TNFα treated samples and thus have been omitted from the results shown below. As I was only able to attain readouts from 2 anti-TNFα treated patient samples, I was unable to statistically compare findings.

#### 6.2.6.1 Anti-TNFα Treatment Increases Expression of Eos in Monocytes

In comparison to Control monocyte populations (Figure 6.8A & Figure 6.6), Eos expression was almost 40 times higher in samples from patients treated with anti-TNFα. However, expression of Eos was comparable in Control and anti-TNFα-treated macrophage populations. Similarly in comparison to the Biologic Naïve monocyte populations (Figure 6.8B and Figure 6.6), expression of Eos was greatly elevated in anti-TNFα treated monocyte populations. Similar expression was observed in all differentiated macrophage populations in both populations.

#### 6.2.6.2 Anti-TNFα Treatment Lowers Ikaros Expression in Macrophage Populations

Ikaros expression was also slightly elevated in anti-TNFα treated samples compared to Control, with higher Ikaros expression also observed in MΦ-M-CSF populations (Figure 6.9A and Figure 6.6). Contrastingly, lower expression of Ikaros was seen in both M1 and M2c populations in blood from patients exposed to anti-TNF$\alpha$. Comparing Biologic Naïve and anti-TNFα treated samples, higher expression of Ikaros was seen in Biologic Naïve populations, with a general trend for lower Ikaros expression levels in the anti-TNFα treated populations (Figure 6.9B and Figure 6.6).

#### 6.2.6.3 Helios Expression is Elevated in M2c Macrophage Populations Following Anti-TNFα Treatment

After treatment with anti-TNFα we could not detect Helios expression in macrophage populations from all patients. However, in MΦ-M-CSF and M2c populations where Helios expression was detected, elevated expression of Helios was seen post anti-TNFα treated patients in comparison to Control (Figure 6.10A and Figure 6.6) and Biologic Naïve (Figure 6.10B and Figure 6.6). Contrastingly, lower expression of Helios was observed in MΦ-GM-CSF and M1 populations in anti-TNFα treated samples, in comparison to Control and Biologic Naïve.

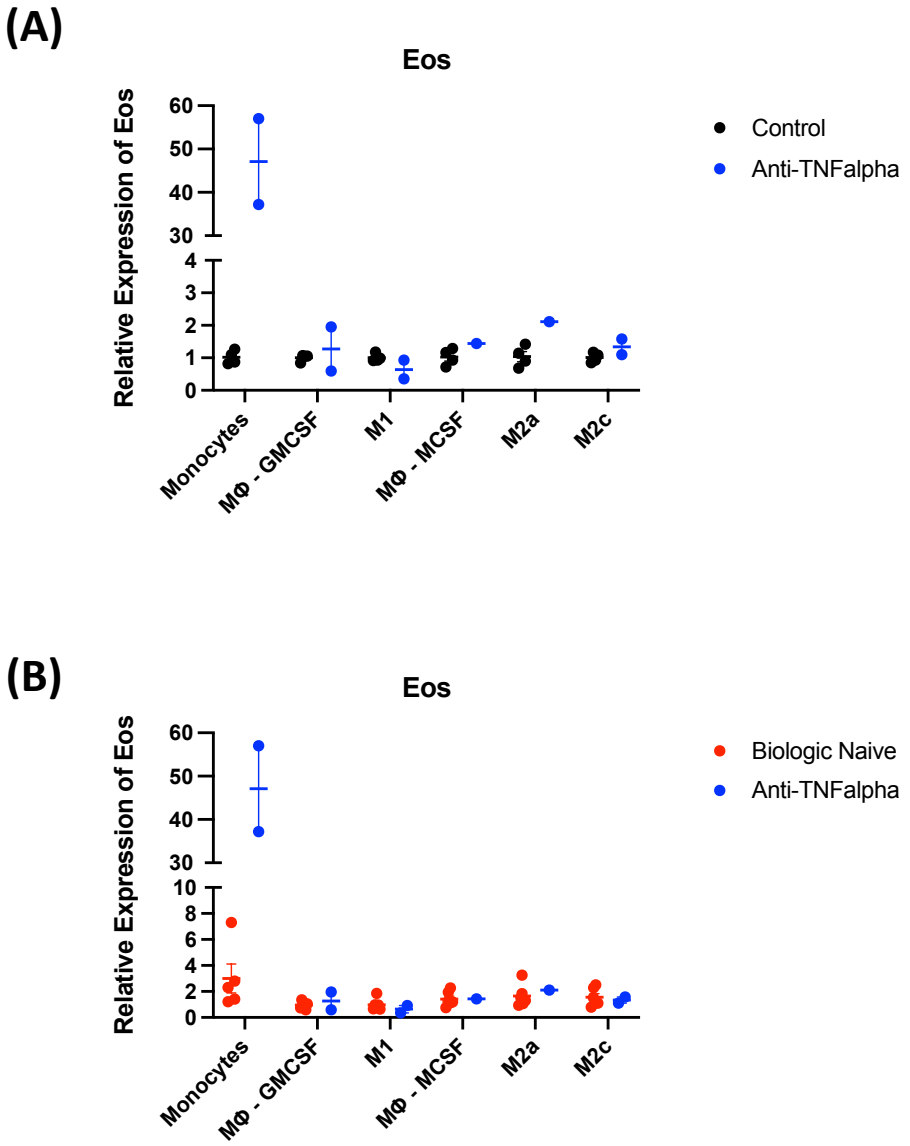



**Figure 6.8: Expression Of Eos in Control and Anti-TNFα Treated IBD Patient Samples**

Monocytes were isolated from either hemochromatosis (Control) peripheral blood mononuclear cells (PBMCs) donors, from Anti-TNFα treated IBD patient samples or from Biologic Naïve newly diagnosed IBD patient samples. The monocytes were then left untreated (Monocytes, Mono) or polarised to Macrophages (MΦ) using GM-CSF (10ng/ml) and M-CSF (50ng/ml). They were then further polarised to M1 (GM-CSF + IFNγ (20ng/ml) + LPS (50ng/ml)), M2a (M-CSF+ IL-4 (20ng/ml)) or M2c (M-CSF + IL-10 (20ng/ml)) for 24 hours. The cells were the lysed and RNA extracted for qPCR analysis. Results were normalised to the housekeeping gene RPS9, and then further normalised to Control Values. Results are presented as mean ± SEM. **(A)** Control Vs Anti-TNFα; **(B)** Biologic Naïve Vs Anti-TNFα. *Anti-TNFalpha; N=2, Biologic Naïve; N=6, Control; N=4. Housekeeping Gene: RPS9.*

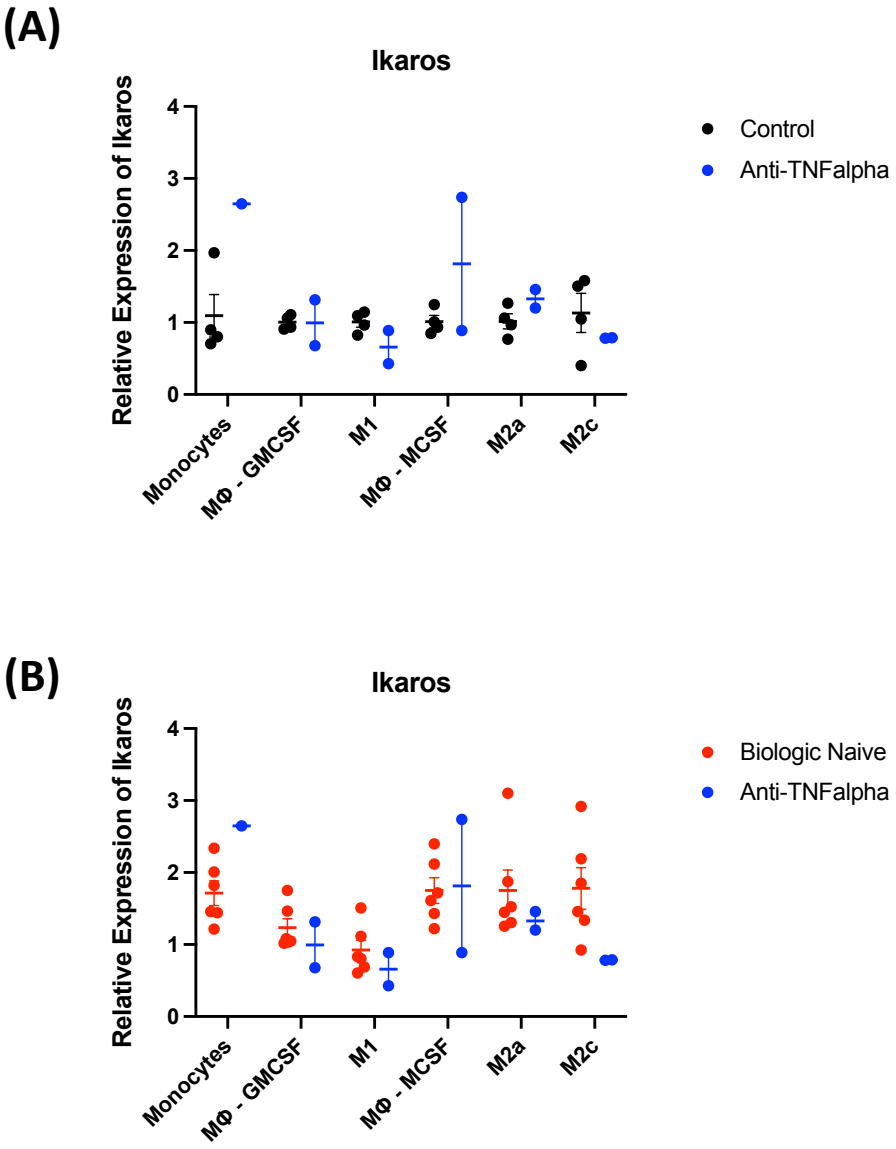



**Figure 6.9: Expression of Ikaros in Control and Anti-TNFalpha Treated IBD Patient Samples**

Monocytes were isolated from either hemochromatosis (Control) peripheral blood mononuclear cells (PBMCs) donors, from Anti-TNFalpha treated IBD patient samples or from Biologic Naïve newly diagnosed IBD patient samples. The monocytes were then left untreated (Monocytes, Mono) or polarised to Macrophages (MΦ) using GM-CSF (10ng/ml) and M-CSF (50ng/ml). They were then further polarised to M1 (GM-CSF + IFNγ (20ng/ml) + LPS (50ng/ml)), M2a (M-CSF+ IL-4 (20ng/ml)) or M2c (M-CSF + IL-10 (20ng/ml)) for 24 hours. The cells were the lysed and RNA extracted for qPCR analysis. Results were normalised to the housekeeping gene RPS9, and then further normalised to Control Values. Results are presented as mean ± SEM. **(A)** Control Vs Anti-TNFalpha; **(B)** Biologic Naïve Vs Anti-TNFalpha. *Anti-TNFalpha; N=2, Biologic Naïve; N=6, Control; N=4. Housekeeping Gene: RPS9.*

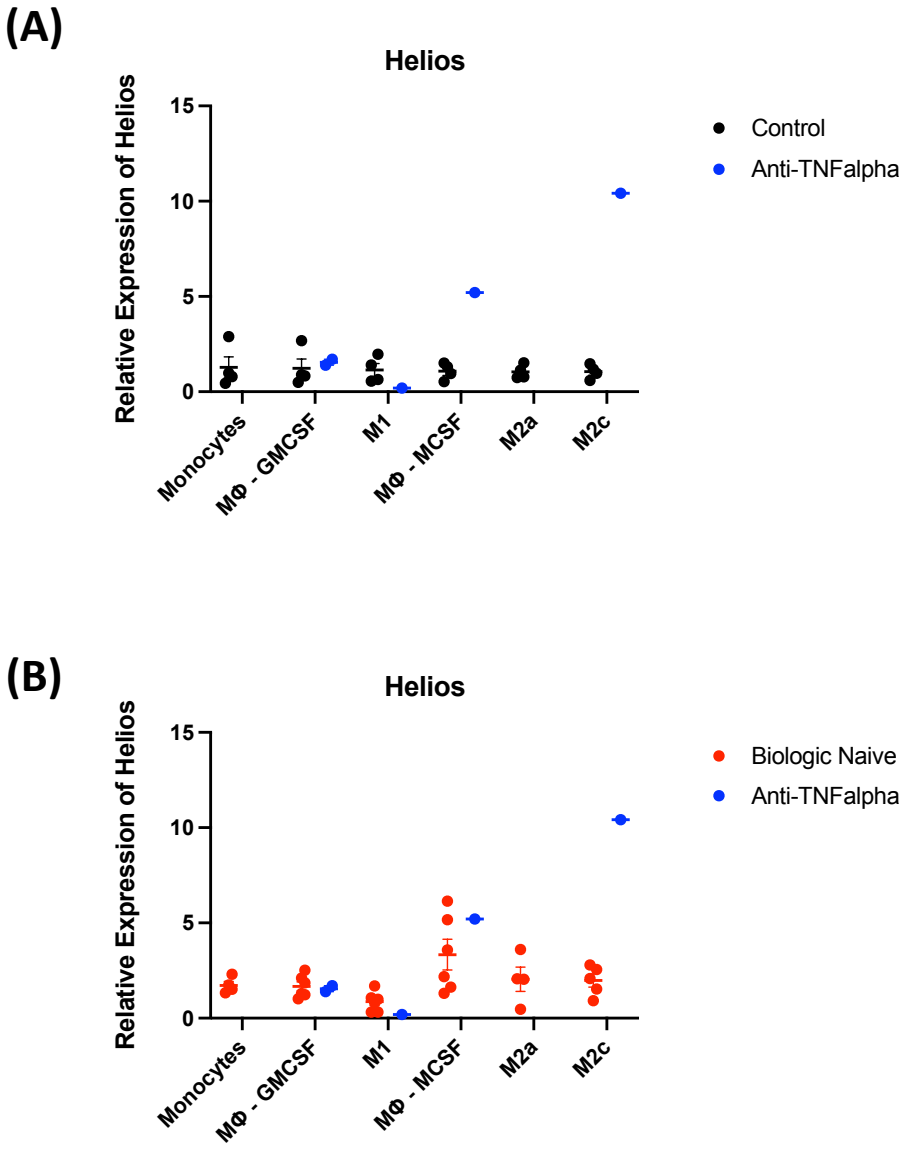



**Figure 6.10: Expression of Helios in Control and Anti-TNFalpha Treated IBD Patient Samples**

Monocytes were isolated from either hemochromatosis (Control) peripheral blood mononuclear cells (PBMCs) donors, from Anti-TNFalpha treated IBD patient samples or from Biologic Naïve newly diagnosed IBD patient samples. The monocytes were then left untreated (Monocytes, Mono) or polarised to Macrophages (MΦ) using GM-CSF (10ng/ml) and M-CSF (50ng/ml). They were then further polarised to M1 (GM-CSF + IFNγ (20ng/ml) + LPS (50ng/ml)), M2a (M-CSF+ IL-4 (20ng/ml)) or M2c (M-CSF + IL-10 (20ng/ml)) for 24 hours. The cells were the lysed and RNA extracted for qPCR analysis. Results were normalised to the housekeeping gene RPS9, and then further normalised to Control Values. Results are presented as mean ± SEM. (A) Control Vs Anti-TNFalpha; (B) Biologic Naïve Vs Anti-TNFalpha. *Anti-TNFalpha; N=2, Biologic Naïve; N=6, Control; N=4.NS. Housekeeping Gene: RPS9.*

## 6.3 Discussion

### 6.3.1 Pomalidomide Targets Expression of all Ikaros Family Members

As mentioned above Pomalidomide is a drug readily used in the clinical setting for treatment of multiple myeloma. It is suggested to act by selectively targeting Aiolos and Ikaros for proteasomal degradation in common with other similar IMiDs which mediate Cereblon-dependent degradation (145, 231, 235). As a validated drug, with limited clinical data on its use within IBD management, Thalidomide and in particular, Pomalidomide, was an attractive tool for us to assess the impact of Aiolos or Ikaros reduction in macrophages (233).

Our protocol for culturing and treating THP-1-derived macrophages with Pomalidomide was based on the method described by Yu *et al.,* (2019) who found that 10μM Pomalidomide was sufficient to induce a decrease in Aiolos and Ikaros expression. In contrast, studies with rodent models report use of 50mg/kg$^{-1}$/day which is significantly higher than the dose sufficient to induce a response in THP-1 cells (233). In humans, the dose for treatment of myeloma is 4mg/day for 21 days of a 28-day cycle, again much higher than that used in our studies (237). With a much lower dose of Pomalidomide however, our results show a significant decrease in Aiolos in the M1 macrophage population following addition of Pomalidomide (Figure 6.3). This supports previous literature suggesting that Pomalidomide selectively targets Aiolos, alongside Ikaros, for degradation (145, 233, 235, 238). The lack of a more pronounced effect on Ikaros was surprising but levels of Ikaros were lower in M1 cells after Pomalidomide treatment. Levels of Pegasus were also lower in M1 treated with Pomalidomide suggesting Pegasus could also be a target of IMiD-dependent degradation. To our knowledge, there is not yet evidence of impact of IMiDs on Eos, Helios, or Pegasus. Thus, our results are some of the first to show that Pomalidomide

may have off-target effects on other members of the Ikaros family, which may be time dependent. However, since Pegasus has been reported to self-associate with other family members it is possible that indirect downregulation may relate to impact of Pomalidomide on Ikaros or Aiolos (137). Importantly downregulation of members of the Ikaros family other than Ikaros and Aiolos may explain why some people have a less than favourable response to IMiDs (229).

We next incubated cells with Pomalidomide for the full duration of the protocol to assess the impact of long-term culture with Pomalidomide. This is more relevant therapeutically as Pomalidomide is delivered continuously, over a prolonged period in clinical settings (1mg-4mg daily) (237). Again, levels of Aiolos were lower in M1 macrophages following treatment with Pomalidomide (Figure 6.4). This is significant since our data suggests that the M1 macrophages express the highest amount of Aiolos (Figure 5.11). Thus, under inflammatory conditions, where an increase in M1 macrophages is observed, targeting of Aiolos (and Ikaros) using Pomalidomide may have an impact on the local proinflammatory response. However, since no studies have assessed the impact of Aiolos knockdown on macrophage phenotype, further work would be required.

The effects of Pomalidomide on expression of Eos were more complex and time dependent. Eos expression was reduced after long term exposure in THP-1, MΦ and M1 which differed from what was seen with short term pre-treatment with Pomalidomide, although not significant. Interestingly, here we saw that in the M2 populations, there was an increase in Eos expression. Both these support the hypothesis that increased Eos expression and its association with M2, or a more regulatory phenotype of macrophages may be linked to reduced inflammation or better outcome. Certainly, studies with knockout animals suggest that lack of Eos impacts T

cell differentiation and is implicated in Treg function (46, 119). Lower levels of Eos were seen in M1 macrophages, again supporting the hypothesis that Eos exhibits reduced expression within inflammatory cell populations such as Th17 cells (119, 128). Therefore, therapeutically targeting Eos may promote a more regulatory environment and aid resolution. Increasing the number of M2 macrophages in the colon could benefit the bowel by repairing tissue damage caused by the uncontrolled immune response seen during IBD (43, 75). However, it is important to note that dysregulation of the M1/M2 ratio is often associated with chronic diseases such as atherosclerosis (80). Therefore, although M2 macrophages could help promote tissue repair, excessive amounts could contribute to fibrosis and inefficient immune response to pathogens (34, 37).

Similarly, Helios expression was also higher in the M2a macrophage populations following addition of Pomalidomide. This is in agreement with previous studies of Helios function showing that Helios is upregulated in Th2 cells in response to OVA *and* IL-4 suggesting a link between Helios and IL-4 (123). Interestingly, I observed that Ikaros levels were higher in both the THP-1 and M2 populations following treatment with Pomalidomide. There is data from two studies confirming that Ikaros expression is present in macrophages with higher levels in M2-like macrophages (139, 206). Ikaros is believed to influence macrophage polarisation, thus investigating the phenotype of M2 macrophages post-Pomalidomide treatment may offer an insight into the impact of upregulated Ikaros expression on function (206). One study by Bruns *et al.,* (2016) for example suggests that Ikaros knockdown in macrophages resulted in an increase in the Th17 response. Ikaros may therefore be needed to maintain a regulatory phenotype of macrophages. This suggests that although targeting Ikaros may seem attractive to limit chronic inflammation, this could unintentionally exacerbate

inflammation depending on context and cells impacted. In contrast to Ikaros expression, Pegasus expression was slightly reduced in M1 and M2 populations following addition of Pomalidomide. As we saw with Helios, this again suggests that IMiDs may also target the other members of the Ikaros family. Little is known about the functional impact of Pegasus knockdown in macrophages, or immune cells in general. Our novel results here suggest that Pegasus is expressed within macrophage populations and can also be influenced using IMiDs. Thus, future studies of the contribution of this transcription factor to macrophage function would be of interest.

### 6.3.2 Expression of the Ikaros Family in Frozen PBMC Samples

Comparing fresh and frozen macrophage samples, I noted a greater expression of Ikaros family RNA in some frozen macrophage populations in comparison to fresh (Figure 6.5). For Aiolos, Eos and Ikaros, fresh and frozen populations showed a similar expression across selected macrophage populations, suggesting that expression of the factors in these populations is stable. This is in agreement with one study by Bolomsky *et al.,* (2017) who in a small patient cohort saw a comparable percentage of Ikaros-positivity in fresh and frozen bone marrow mononuclear cells. This suggests levels of Ikaros may be relatively stable. Pegasus however is a notable outlier, with higher gene expression observed in frozen macrophages. Although there is no publicly available data available on this, we can speculate that this may be due to instability of the Pegasus which may mean it degrades rapidly in fresh cells. This difference could also be due to its distinctive structure in comparison to other family members (Section 1.5.9) (120, 124, 137).

We did note some other phenotypic changes between fresh and frozen cells. As a group we found that a greater number of monocytes could be isolated from fresh HFE

samples compared to stored IBD samples. This may reflect the fact that the HFE samples were '*fresher'* than the stored IBD samples and therefore there was less loss of cells in samples (239). It could also reflect the less inflamed nature of these patients having venesection and impact of peripheral whole blood cell counts. If cells are migrating into the inflamed colon of our IBD patients then the isolated cell return may be less, suggesting an altered white blood cell count (240).

For our study of the comparison of fresh vs frozen samples, we utilised HFE blood as it was more readily accessible in comparison to IBD patient blood. HFE blood was used as a '*control'* in the CLGR with many published studies from the group utilising this pool of patients (241, 242). HFE blood is believed to be a relatively suitable control once patients have undergone phlebotomy to remove excess iron (243). Ideally, we would have liked to have been able to compare differences in fresh and frozen PBMC populations from patient samples. We were also only able to replicate this experiment with two matched samples, thus we should be cautious in drawing firm conclusions.

### 6.3.3 Expression of the Ikaros Family in Biologic Naïve IBD Samples

To our knowledge my work is some of the first to assess Ikaros family expression in IBD. This data provides a means to ascertain if the Ikaros family are biomarkers which could help diagnose or stratify disease, and to assess treatment response. Non-responsiveness to therapeutics, is a key issue in the management of IBD patients thus being able to identify at risk patients would improve their clinical care (9, 53).

RNA expression of Aiolos in Control macrophage populations was very low in comparison to the monocyte populations and similar to the expression of Aiolos observed in fresh samples (See Figure 6.6). Interestingly, expression in all Biologic Naïve populations was much lower, with minimal expression observed throughout

populations. Billot *et al.,* (2010) described 'almost undetectable levels' of Aiolos RNA in monocytes isolated from healthy PBMCs but did not analyse expression levels in macrophage populations. The very low level of Aiolos expression in monocytes contrasts somewhat with our study, but both suggest that biological function of Aiolos may be less significant in healthy individuals. Another study analysing Aiolos expression in monocytes compared differences in expression of Aiolos protein in cells from SLE and RA patients and controls (244). Both these diseases are associated with IBD and the authors report that RA and SLE CD14+ monocytes have elevated expression of Aiolos (110, 146, 244). Although this confirms our report that Aiolos is expressed by monocytes, it differs from our findings since diseased patient cohorts expressed *higher* amounts of Aiolos in this study. Our diseased Biologic Naïve patient samples expressed *lower* levels of Aiolos in monocyte and macrophage populations. This difference may relate to the nature of the patient cohorts and the extent of their inflammation. Significant numbers of macrophages infiltrate the diseased colon and thus we may have lost activated populations from the periphery (30, 37, 44). Another key difference is that we assessed RNA levels rather than protein. Cai *et al.,* (2016) for example used flow cytometry to assess protein levels of Aiolos within samples and thus the differences we may see with our RNA data may be due to differences in protein stability and RNA levels. Thus, ideally, it would be useful to ascertain protein levels in future studies to confirm our findings. Aiolos is known to be key to B cell and T cell biology but no difference in Aiolos expression in CD4+ T cells and CD19+ B Cells was reported in control and SLE (244). Thus, it was reassuring to see the difference in monocyte Aiolos expression since this has been largely under investigated (113, 117). Elevated Aiolos expression in CD14+ monocytes also correlated with clinical markers such as ESR, creatinine, CRP, and albumin (244).

Together this suggests that in autoimmune disease such as SLE and RA, elevated Aiolos could be used as another clinical marker for diagnosis (244). Upon further investigation into the family members, this offers the potential for the family to aid IBD diagnosis. Although clinical data for patients was collected in our study, due to time constraints, we were unable to access this data. This lack of clinical data also means we are unable to ascertain the impact of any treatment programs on Ikaros family expression.

Studies investigating Eos in disease have mainly focussed on its downregulation or role in Tregs, with to our knowledge, no studies on Eos upregulation in disease (160, 161). Under homeostatic conditions, monocytes generally have high expression of Eos in comparison to other cell types (107, 110, 158). Perhaps elevated expression of Eos could signal greater activation of monocytes? Thus, we hypothesised that Eos expression may correlate with the regulatory phenotype of macrophages as seen with Tregs (46, 157, 158). Comparing monocyte populations, we found Eos expression was significantly higher ($P<0.05$) in Biologic Naïve patients in comparison to Control which could be a sign of active inflammation or infection. Or contrastingly, Eos expression may be linked to the upregulation of regulatory genes to promote a balanced approach to inflammation as is similar to what is seen in Tregs. Interestingly, the findings mimic those seen in Figure 5.21 with upregulated Eos+CD68+ macrophage in inflamed bowel supporting changes in Eos levels systemically and at the site of inflammation. Although studies on Eos expression in monocytes is limited, other similar family members such as Ikaros for example are upregulated in disease (83, 139, 142, 206, 232). Oh *et al.,* (2018) found monocytes which produce IL-6 and TNF$\alpha$ have higher Ikaros protein expression, suggesting that inflammatory monocytes upregulate expression of at least one Ikaros family member. In the next chapter, we investigate

Eos knockdown to investigate this theory. In mouse models, Eos knockdown promotes a proinflammatory phenotype, and global Eos knockdown results in a decrease in Tregs and subsequent colitis in mice (46). Eos knockdown in Tregs results in the loss of suppressive capability and promotes a proinflammatory phenotype (119, 155). In keeping with our elevated expression in diseased patient monocytes, these data suggest that upregulation of Eos may be a mechanism to promote a regulatory phenotype and to combat the inflammatory environment.

In Biologic Naïve samples, expression of Helios was elevated in all assayed populations asides from M1 macrophages in comparison to control. This was particularly marked for MΦ-MCSF Biologic Naïve populations. It had been previously reported that monocytes derived from 'healthy donors' lack Helios expression, but we report that during inflammation expression of Helios is upregulated (100). If we hypothesise that like Ikaros, Helios expression is upregulated in monocytes and macrophages we can infer that perhaps the elevated expression in M-CSF treated macrophage populations is due to the role of Helios in favouring regulation, similar to the mechanism of Eos described above.

Similar to Helios, we observed a general trend of higher expression levels of Ikaros expression in Biologic Naïve populations, asides from M1 cells. We know from previous studies Ikaros is upregulated during disease, supporting our observed results (83, 139, 142, 206, 232). Ikaros is able to influence macrophage polarisation, with higher Ikaros expression seen in M2-like macrophage populations in studies, supported by the higher expression of Ikaros seen in M-CSF-treated macrophage populations in our study (139, 206). Although the role of Ikaros in M2 macrophages is unknown we do know that Ikaros is needed to regulate the chromatin state of macrophages and enable an efficient macrophage response (142). This suggests

elevated Ikaros may be implicated in the macrophage immune response in IBD. Reduced expression of Ikaros within inflammatory M1 macrophages in Biologic Naïve samples is extremely interesting. Ikaros is upregulated by LPS and required for LPS-induced inflammatory gene expression in macrophages (142). However contrastingly, Ikaros is known to repress the iNOS promoter in response to LPS (and IFNγ) preventing the release of iNOS and NO (83). Both mediators are produced by M1 macrophages and are key to their optimal functional. Our results suggest that lower levels of Ikaros may enable enhanced activation of M1 and release of proinflammatory mediators to exacerbate inflammation. Elevated Ikaros levels also have a potential to influence macrophage survival (Section 1.5.5.3)(122, 132). Thus, elevated Ikaros levels could potentially promote inflammation by driving activation and persistence of inflammatory macrophages.

Although Pegasus expression was observed in control monocyte populations and elevated in macrophages there was almost a complete lack of Pegasus expression in Biologic Naïve patient populations. This suggests that in IBD patients, an unknown mechanism causes the loss of Pegasus expression in the periphery. This may suggest that Pegasus plays an important role in the pathogenesis of the disease or is somehow impacted by the inflammation seen in IBD. Pegasus could potentially be used as a marker in the clinic: could lack of Pegasus diagnose disease or indicate responsiveness or non-responsiveness to a drug?

### 6.3.4 Impact of Infliximab Therapy on Ikaros Family Expression

TNF$\alpha$ regulates intestinal permeability, epithelial cell growth, apoptosis and MMP production, playing a vital role in gut biology (26). Elevated TNFα levels therefore are extremely detrimental and can contribute to colitis. Thus, targeting TNF therapeutically

has been extensively explored in IBD (245, 246). In the clinic, anti-TNFα treatment is a broad spectrum biologic and is used to treat IBD, psoriasis and RA, amongst other diseases (178). Infliximab, a TNF-targeting drug, was first approved over 20 years ago as for use in treating moderate to severe cases of IBD (246). A *'chimeric monoclonal anti-TNF IgG1 antibody'*, Infliximab is efficient in managing IBD in some individuals however there are issues with primary nonresponse and secondary loss of response (246)(Chapter 1). Thus, strategies to identify patients at risk of relapse or non-response are vital.

Through the TRAFIC study we received a small number of samples from patients post treatment with Infliximab. We report that there was no detectable expression of Aiolos, or Pegasus observed in treated patient cells. Since Aiolos was observed in Biologic Naïve populations our results suggest targeting TNFα may have reduced Aiolos expression in the periphery. However, a previous study by Evans *et al.,* (2014) found that TNF$\alpha$ inhibitor (TNFi) *promotes* Aiolos expression in IL-17+CD4+ T cells *in vitro* (110, 178). Similarly, using a CD14+ monocyte and CD4+ T Cell co-culture, Ridley *et al.,* (2020) showed Aiolos expression increased in Th17 cells when cells were treated with anti-TNF$\alpha$ (178). Their work suggests that monocytes can influence Aiolos expression in CD4+ T Cells, especially Th17, and that TNF could repress Aiolos (110, 178, 179). Anti-TNFα treatment is also believed to cause induction of IL-10 by Th17 cells coinciding with upregulation of Aiolos, promoting a regulatory, not pro-inflammatory, phenotype (179). This therefore suggests that Aiolos function may be manipulated in future to induce plasticity as a therapeutic strategy, however further work is needed to clarify its relationship with TNFα.

Contrastingly, Eos expression in anti-TNFα treated samples was higher than Control populations and comparable to the Biologic Naïve diseased macrophage populations

(Figure 6.8). However, monocytes from patients treated with anti-TNFα had a significantly higher expression of Eos compared to Control and Biologic Naïve donors. This equated to a fold gene expression change of 45 in the treated patients compared to 3 in naïve patients, suggesting anti-TNFα upregulates Eos expression. There is some previous evidence suggesting that Eos and TNFα may have an inverse relationship, and thus blocking TNFα signalling, may in turn increase Eos expression (158). Similarly mice with Eos knockdown Tregs have higher levels of TNFα in CD8+ T Cells isolated from tumours (158). This suggests that Eos may regulate and repress TNFα in monocytes, supporting literature which suggests Eos functions as a repressor. Elevated Eos expression may also suggest the shift towards a more regulatory phenotype since Eos is upregulated in activated Tregs (119). Although we need greater patient numbers, the evidence points to a role of Eos promoting a more regulatory and anti-inflammatory role in monocytes. Furthermore, there is potential for Eos as a marker of anti-TNFα treatment dependent on the outcome of patients. By correlating clinical data and responsiveness of individuals, the expression level of Eos could help determine the effectiveness of Infliximab as a treatment option for patients. There was also a general trend for lower expression of Ikaros in anti-TNFα treated patients (Figure 6.9). This would support the notion that reduced Ikaros expression signals a reduction in proinflammatory mediators and inflammation. Ikaros is a positive regulator of TNF$\alpha$ and Ikaros knockout monocytes secrete less TNFα with a correlation between siRNA knockdown efficiency and cytokine reduction in MDMs (142, 144). Lenalidomide treatment of patient cells *in vitro*, causes a decrease in secretion of TNFα suggesting a reduction in pro-inflammatory mediators (144). In addition Ik-7 expressing mice have elevated levels of TNFα supporting the notion that Ikaros is a positive regulator of TNFα (247). This in combination with upregulated Eos

levels suggests lower Ikaros expression levels in monocytes could be used as markers of successful TNFα treatment in patients.

Helios expression was not observed in monocytes and M2a macrophages in anti-TNFα treated patients (Figure 6.10). Where it was present, levels of Helios were lower in MΦ-GM-CSF and M1 populations in comparison to Biological Naïve, but higher Helios levels were observed in the M2c populations. Previous studies suggest that anti-TNFα treatment of Helios *positive* Tregs results in their inhibition, whilst contrastingly increasing expansion of Helios *negative* Tregs (52, 77, 110). Again CD14+CD16+ monocytes were important for the changes in Treg *via* secretion of TNFα (52, 77). Similar to the relationship between Ikaros and TNFα, this suggests that Helios may potentially behave as a positive regulator of TNFα, with its role changing dependent on cell type (144). Ultimately, the question remains as to whether this is beneficial or not. We know from the studies on Helios expression in Tregs, that Helios is key to maintenance of Treg suppressive function (98, 108). A global IKZF2 knockdown increases production of TNFα from Tregs, suggesting a shift of Tregs to a proinflammatory phenotype (123). If we apply this to macrophages, a reduction in Helios expression in M1 subsets may in turn cause release of excess proinflammatory cytokines. Together, this would further support our theory that the Ikaros family are key to polarisation of macrophage phenotype, and when lost, result in plasticity. Another interesting find from comparing Biologic Naïve and anti-TNFα patients was the elevated Helios expression in M2c, not M2a populations in the anti-TNFα population. IL-10 drives polarisation of M2c macrophages and it has been shown that Helios+ Tregs secrete and possess high levels of IL-10 (99, 164). Studies on Aiolos expression in Th17 cells following anti-TNFα treatment report promotion of IL-10

production and Aiolos expression (179). Given that the structure of the Ikaros family members is so similar, TNFα could impact Helios expression in a similar manner.

Together, this study represents pilot data from a limited sample size (6 Biologic Naïve, 2 Anti-TNFα and 4 HFE Control samples). We collected more samples however not all samples yielded sufficient monocyte numbers or RNA for cDNA preparation (Table A.3). We were also limited by sample access constraints during the COVID pandemic. Storage of frozen samples was also not consistent which may have impacted the outcome of cell differentiation experiments. To negate this, we treated all samples in a similar manner when thawed, kept cell concentrations consistent and normalised RNA and cDNA to limit variation during qPCR. For future work, if unable to use fresh samples, batch stored samples would omit storage length variability.

### 6.3.5 Summary

Together, our pilot study has shown that Pomalidomide can influence expression levels of all Ikaros family members within macrophage populations. For the first time, we have also shown that Biologic Naïve IBD patients have altered Ikaros family expression levels in monocytes and macrophage populations in comparison to Control, suggesting the Ikaros family could play a role in macrophage phenotype and/or disease pathophysiology in IBD. Treatment with anti-TNFα altered Ikaros family expression, with complete lack of Aiolos and Pegasus, and elevated levels of Eos in monocytes, suggesting potential as markers of disease. We hypothesise that expression of Ikaros family members in macrophage populations following treatment with anti-TNFα could signify plasticity of macrophages.

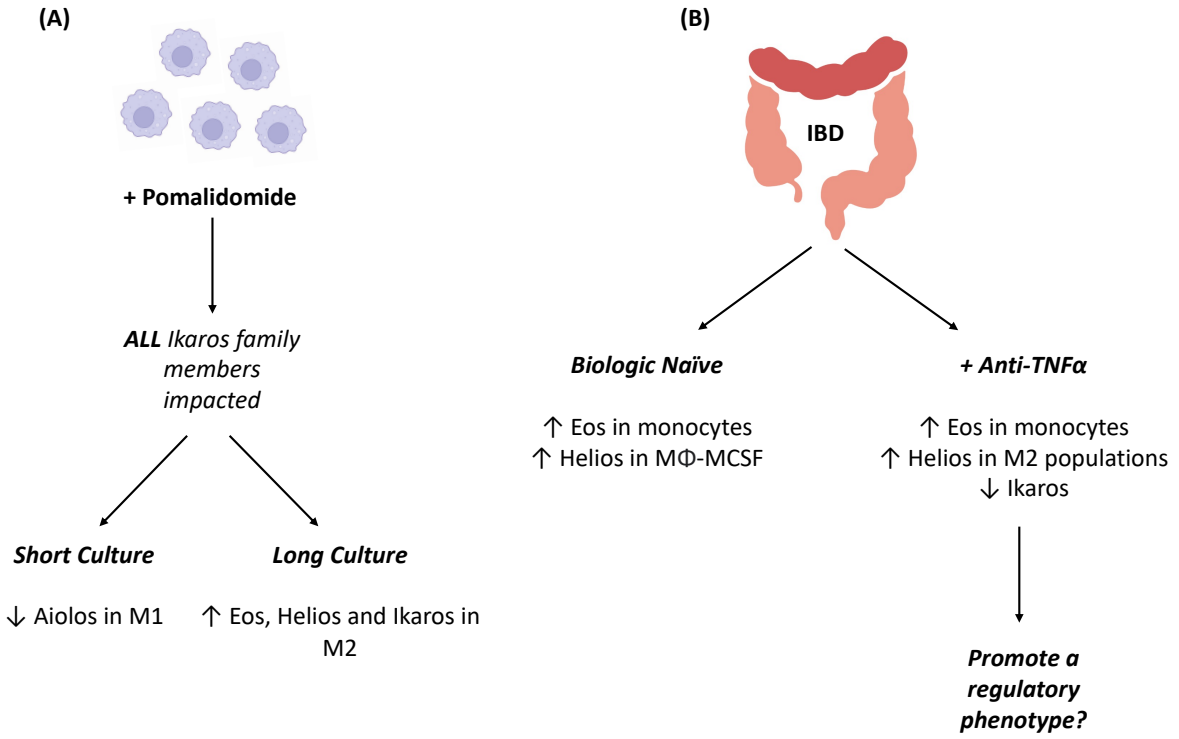



**Figure 6.11: Summary Diagram of Chapter 6**
Graphical summary of key findings from Chapter 6, *Impact of IBD and therapeutic intervention on Ikaros Family Expression*. **(A)** Using Pomalidomide (10μM) in a short (pre-treatment with Pomalidomide for 24 hours) and long culture (with Pomalidomide for duration of culture) with polarised macrophage subsets (THP-1, MΦ, M1, M2a and M2c), we found that all Ikaros family members were impacted by the drug. Significantly in the short culture, lower levels of Aiolos were observed in M1 following Pomalidomide treatment. In the long culture, higher levels of Eos, Helios and Ikaros were seen in M2 populations. **(B)** Peripheral blood monocytes were isolated from blood samples from patients with IBD, both Biologically Naïve or treated with anti-TNFα. Some monocytes were the differentiated into different macrophage subsets including MΦ-GM-CSF, M1, MΦ-M-CSF, M2a and M2c. Significant increases in Eos were found in monocytes in comparison to Control, with an increase in Helios in MΦ-MCSF populations in Biological Naïve also observed in comparison to Control. In Anti-TNFα treated samples, an increase in Eos was observed in monocytes, an increase in Helios expression in M2 populations and a decrease in Ikaros expression in all macrophage populations in comparison to Control. We hypothesise this promotes a regulatory phenotype of macrophages.

# Chapter 7: Selective Eos Knockdown In Macrophages

## 7.1 Introduction

Having established within our previous Chapter that Eos is upregulated in CD68+ macrophages within inflamed bowel and liver tissue and within Biologically Naïve patient monocytes, we summarised that bowel inflammation has an impact on Eos expression within the monocyte and macrophage population. Thus, we decided to investigate the role of Eos within macrophages to determine if Eos is needed for macrophage survival, and, or function.

Thus, the objective of this chapter was:

I. To analyse the impact of Eos knockdown on MΦ macrophage function and phenotype

To address this objective, I used Lipofectamine RNAiMAX and Silencer Select siRNA to selectively target and knockdown Eos within THP-1-derived MΦ macrophages (Methods, Chapter 2). After confirming a successful knockdown, I used these cells within the Vybrant Phagocytosis Assay to assess changes in phagocytic capacity compared to untreated cells. To assess phenotypic changes, I used a cytokine array to compare the cytokine and chemokine secretion of Eos knockdown MΦ with Control.

## 7.2 Results

### 7.2.1 Lipofectamine RNAiMAX and Silencer Select Significantly Reduce Eos Expression in THP-1-derived MΦ Macrophages

As described in Chapter 2 the Lipofectamine RNAiMAX protocol was used to knockdown Eos in THP-1-derived MΦ macrophages to assess the impact of Eos on macrophage function and phenotype. In a 6 well plate, 500,000 THP-1s were seeded and exposed to the siRNA mix. Cells were harvested after incubation and qPCR conducted to analyse expression levels of Eos and other Ikaros family members (Figure 7.1). Using the Lipofectamine RNAiMAX reagent, we found levels of Eos were significantly reduced ($p<0.05$) in comparison to Control (siRNA culture conditions with no siRNA) in the Eos knockdown (siEos). Similarly, expression levels of the positive control, GAPDH, were also significantly reduced ($p<0.05$) in the GAPDH knockdown (siGAPDH) in comparison to the Control. Although Ikaros expression levels were lower in the siEos knockdown in comparison to Control, this was not significant. Thus, we were satisfied that our assay was working correctly, even though we saw baseline fluctuations with our Negative Pool reagents.

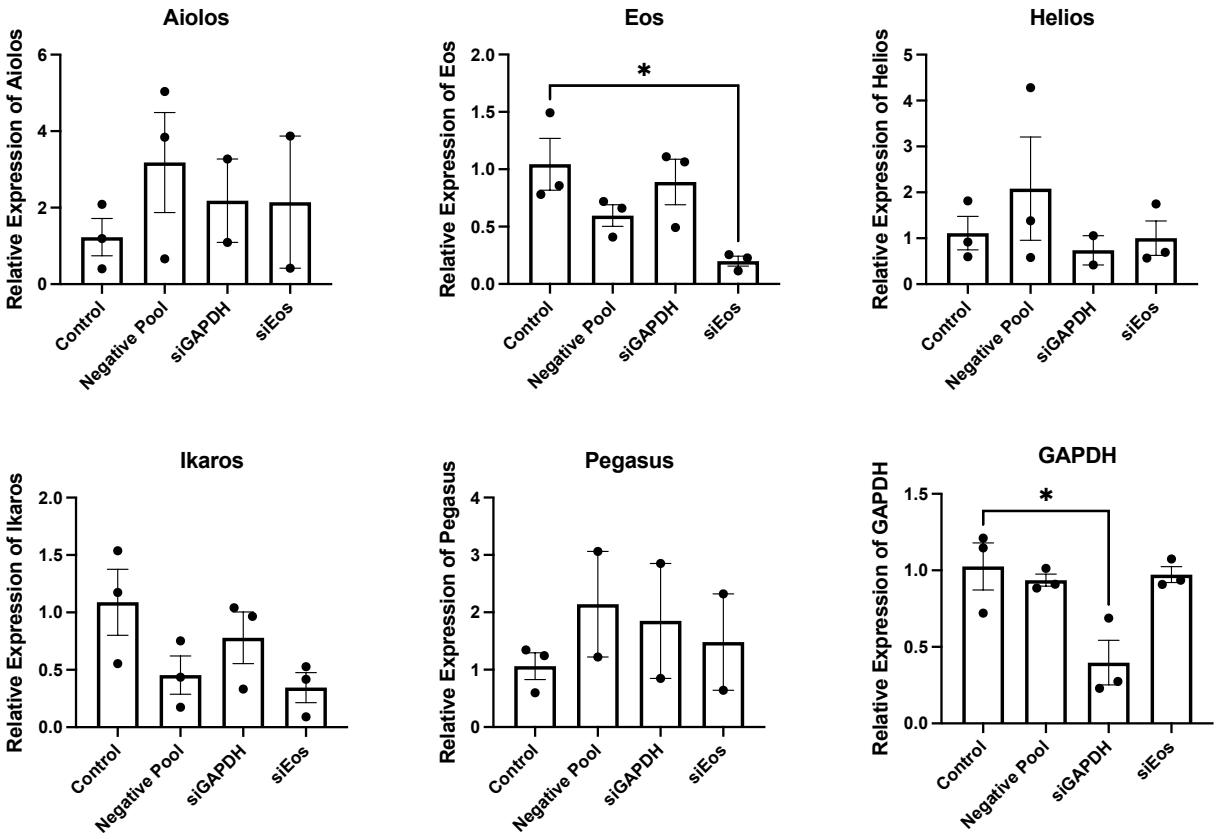



**Figure 7.1: Lipofectamine RNAiMAX and Silencer Select Reduces Eos Expression**
THP-1 cells were seeded at 500,000 cells/ml and polarised to MΦ macrophages with addition of 50ng/ml PMA. The cells were then left untreated in Opti-Mem Medium (Control) or treated with Lipofectamine RNAiMAX and either Silencer Select (SS) Negative Targeting Pool (Negative Pool), SS GAPDH Positive (siGAPDH) and SS Eos Targeting siRNA (siEos) for 48 hours. The cells were then lysed, RNA extracted, and qPCR conducted to analyse gene expression levels. Results are normalised to Control. Results presented as mean ± SEM.*N=3*. *Eos *p<0.05; GAPDH * p<0.05. one-way ANOVA and Tukey's Multiple Comparison Test. Housekeeping Gene: RPS9.*

### 7.2.2 Eos Knockdown Macrophages Retain Cell Viability During Culture

We next assessed the impact of our siRNA protocol on cell viability using CellTiter 96® (Section 2.11.2) to ensure this protocol did not alter cell viability or induce apoptosis. Data was normalised to Control. Figure 7.2 showed that the percentage cell viability displayed little change over the four-hour period of treatment with individual siRNAs or control reagents. However, we did observe that cells exposed to the Control and Negative Pool had higher cell viability in comparison to siEos and siGAPDH. This did not change across the incubation period.

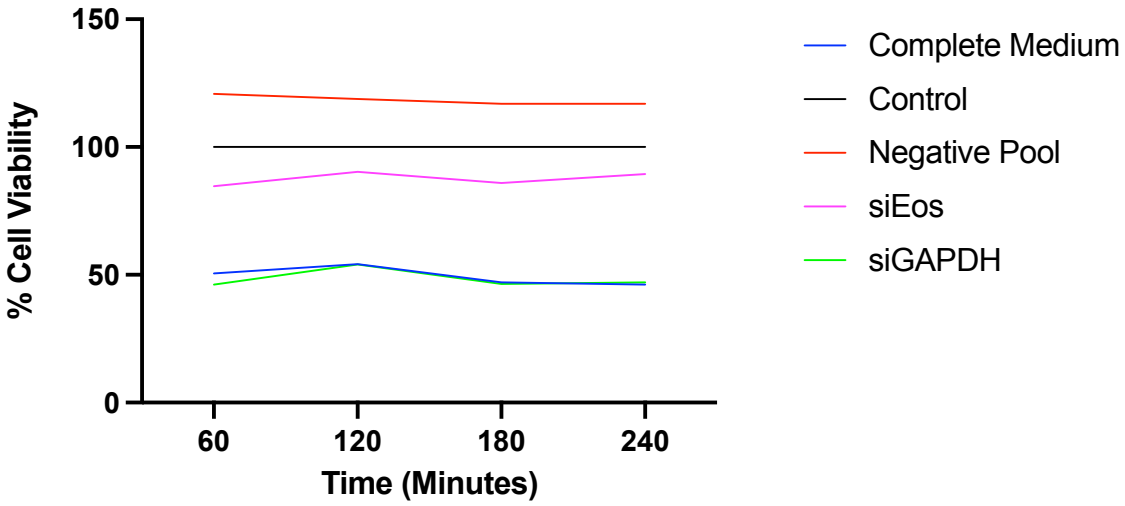



**Figure 7.2: Lipofectamine® RNAiMAX and Silencer Select Have Minimal Impact on Cell Viability**
The CellTiter 96® Aqueous Solution was used to determine the cell viability of THP-1 cells incubated with Opti-Mem alone (Control), Complete Medium (Complete Medium), or Opti-Mem and Lipofectamine RNAiMAX and either Silencer Select (SS) Negative Targeting Pool) Negative Pool, SS GAPDH Positive (siGAPDH) and SS Eos Targeting siRNA (siEos). *N=1, n=5. NS.*

### 7.2.3 The Lipofectamine RNAiMAX Method is Sufficient to Knockdown Eos in a 96 Well Plate Culture

To ensure our method of knockdown was successful in a 96-well plate set-up for experiments, we adapted the siRNA protocol for 40,000 cells/well in a 96-well plate and then harvested RNA from cultured cells (Figure 7.3). Our results showed that Eos was comparably reduced in the siEos population in the 96-well format. The expression of GAPDH in the siGAPDH also decreased in relative expression in comparison to Control.

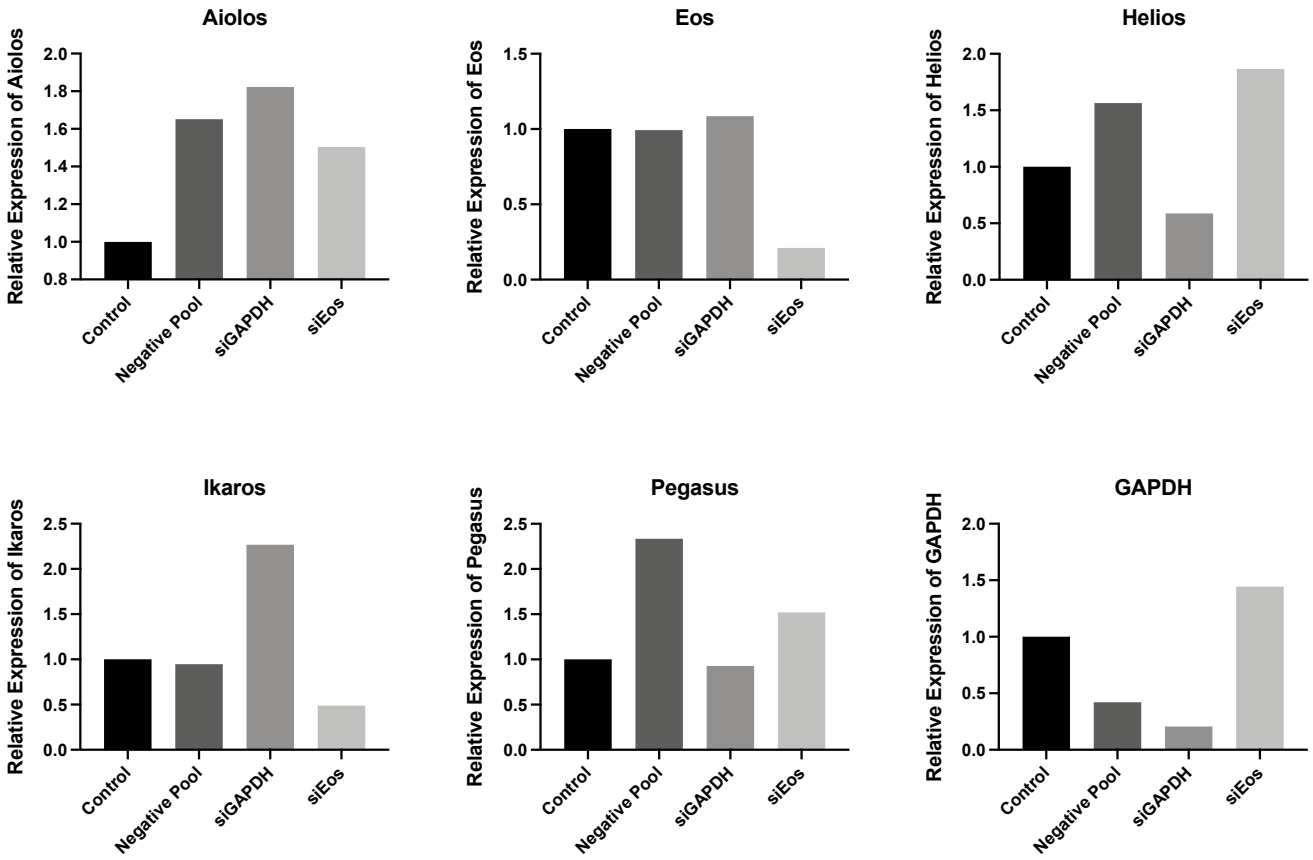



**Figure 7.3: Lipofectamine RNAiMAX and Silencer Select Reduces Eos Expression**
THP-1 cells were seeded at 40,000 cells/well in a 96 well plate and polarised to MΦ macrophages with addition of 50ng/ml PMA. The cells were then left untreated in Opti-Mem Medium (Control) or treated with Lipofectamine RNAiMAX and either Silencer Select (SS) Negative Targeting Pool (Negative Pool), SS GAPDH Positive (siGAPDH) and SS Eos Targeting siRNA (siEos) for 48 hours. The cells were then lysed and pooled from 4 wells for each condition, RNA extracted, and qPCR conducted to analyse gene expression levels. Results are normalised to Control. Results presented as mean. *N=1. Housekeeping Gene: RPS9.*

### 7.2.4 Eos Knockdown Within Macrophages Impacts Their Phagocytic Capacity

Next, using the Vybrant™ Phagocytosis Assay (Section 2.10.3), the ability of siEos MΦ to phagocytose fluorescein labelled *E. coli* was compared to Control. Figure 7.4 shows that the capacity of differentiated siEos MΦ to phagocytose *E. coli* particles decreased by approximately 50% in comparison to both the Negative Pool and the siGAPDH population. Phagocytosis capacity was also decreased in comparison to Control cells (30% lower).

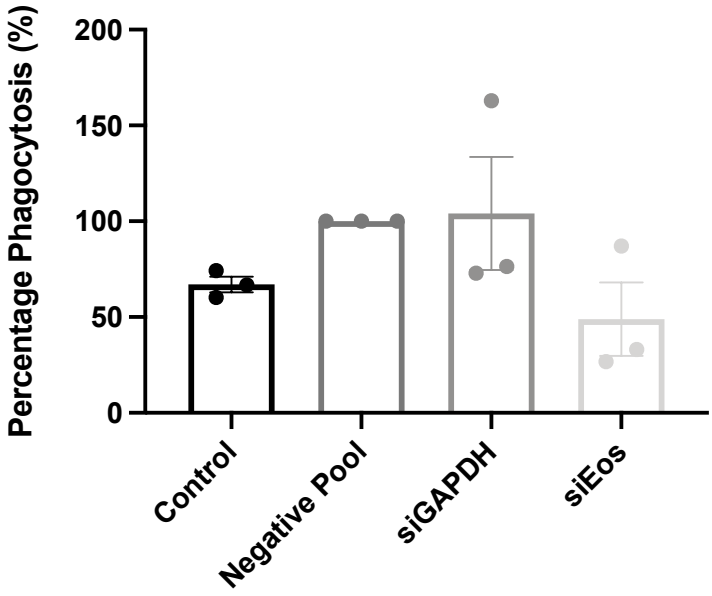



**Figure 7.4: Eos Knockdown Suggests A Reduction in Phagocytic Capacity of PMA-Polarised THP-1 Macrophages**

THP-1 cells were transformed into MΦ following addition of PMA (50ng/ml) and then treated with Opti-Mem (Control), Lipofectamine RNAiMAX Silencer Select (SS) Negative Targeting Pool) Negative Pool, SS GAPDH Positive (siGAPDH) and SS Eos Targeting siRNA (siEos). Using the Vybrant ™ Assay to determine phagocytic capacity of cells, a fluorescein-tagged E. *coli* BioParticle suspension was added to cells for an hour, followed by a fluorescent BioParticle suspension for two hours and quenched with a Trypan Blue suspension. The plate was read at a 480 excitation with our results finding Eos knockdown reduced the capacity of cells to phagocytose. Results are normalised to the Negative Pool. Results presented as mean ± SEM.*N=3. One-Way ANOVA. NS*

### 7.2.5 Eos Knockdown is Sustained Post siRNA Treatment Following Addition of Complete Medium

To assess the secretome of treated cells, post-siRNA treatment, we incubated cells with 1ml of complete medium to then collect the supernatant 24 hours later to maximize analyte concentration. Thus, we analysed Ikaros family gene expression at the same timepoint to determine if Eos knockdown was sustained post-siRNA treatment. Figure 7.5 shows that levels of Eos significantly ($p<0.01$) decreased in siEos in comparison to Control. Similarly, in comparison to the Negative Pool and siGAPDH populations, Eos expression was again significantly (Negative Pool; $p<0.01$, siGAPDH $p<0.05$) lower. A significant decrease ($p<0.01$) in GAPDH was also observed in siGAPDH in comparison to Control. Again, in comparison to the Negative Pool and siEos, the level of GAPDH expression was significantly ($p<0.01$) lower. Thus, results were similar to our earlier data (Figure 7.1) and knockdown was maintained in the intervening 24-hour period. In comparison to the usual cultural method, a greater significant reduction in both Eos and GAPDH was found.

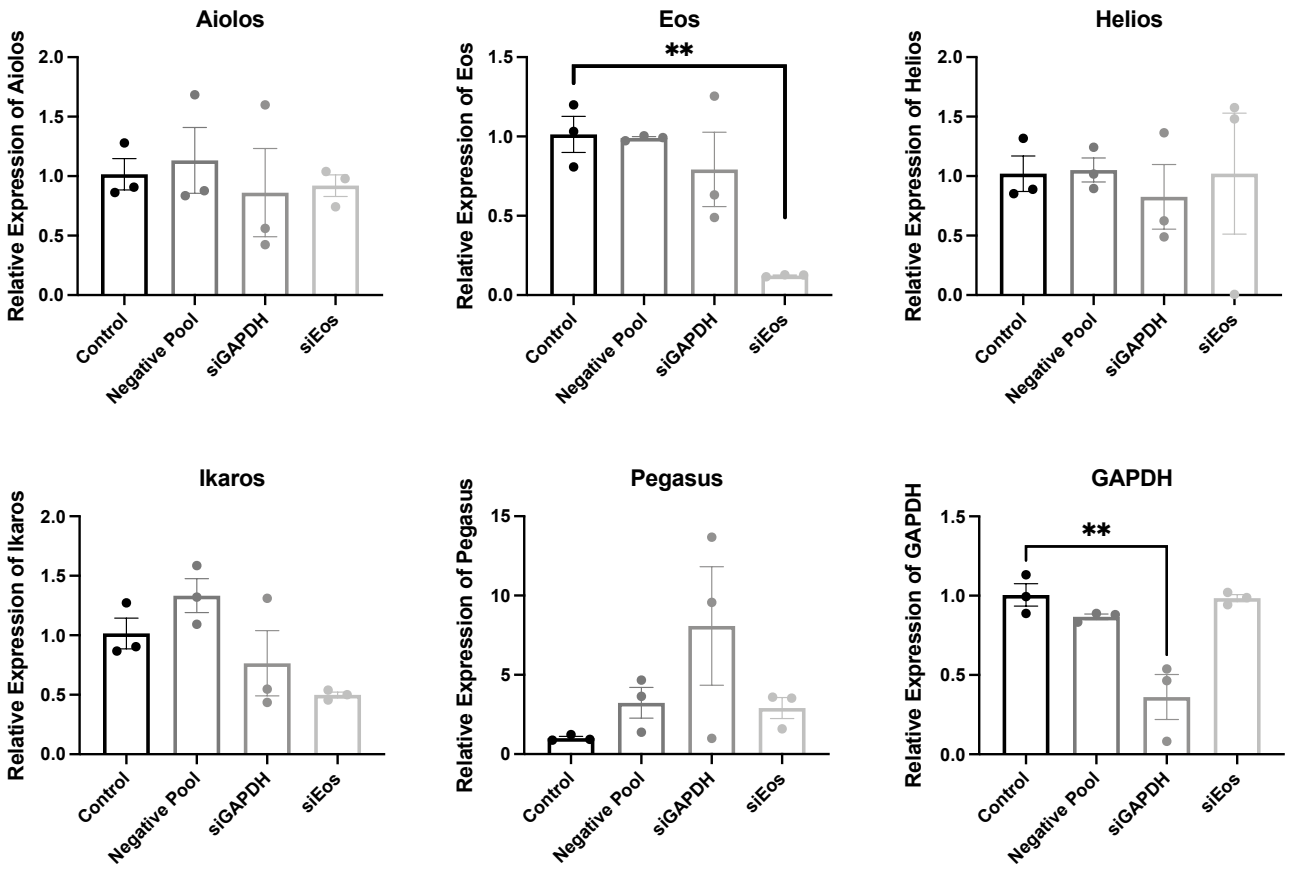



**Figure 7.5: Eos Knockdown is Sustained Post siRNA Treatment and Following Addition of Complete Medium**
THP-1 cells were polarised to MΦ macrophages with addition of PMA (50ng/ml) for 48 hours and then left to rest for 72 hours. The cells then were left untreated (control) or treated with Lipofectamine RNAiMAX and either a Negative Pool siRNA (Negative Pool), a GAPDH siRNA knockdown (GAPDH $^{(-/-)}$) or Eos siRNA knockdown (Eos $^{(-/-)}$) for 48 hours. After incubation with the siRNA, complete medium was added to the wells for 24 hours after which the cells were lysed for RNA harvest and supernatants kept for further analysis. Results are presented as mean ± SEM and normalised to Control. *N=3, Eos **p<0.01; Ikaros * p<0.05; GAPDH ** p<0.01. one-way ANOVA and Tukey's Multiple Comparison Test. Housekeeping Gene: RPS9.*

### 7.2.6 Eos knockdown in Macrophages Reduces IL-2 Secretion but Increases IL-17E and IL-8 secretion

To assess the change in secretome by siEos macrophages in comparison to Control macrophages, we utilised the R&D Proteome Profiler (Section 2.10.4). Following siRNA incubation, cells were retained in 1ml of fresh complete medium for a further 24 hours. The supernatants were then harvested, pooled from 3 independent experiments, and used for the profiler assay. Results were normalised to the Negative Pool.

Figure 7.6 shows that lower levels of IL-1a were seen in the siEos MΦ in comparison to all other populations, whereas a complete lack of IL-2 was seen in both the GAPDH and Eos knockdown. Similar levels of IL-13 were seen in Control and siEos while contrastingly, the highest level of IL-8 production was seen in the siEos population compared to the other populations. IL-16 and IL-17E also increased after knockdown. Contrastingly, slightly lower levels of IL-18 were observed in siEos in comparison Control.

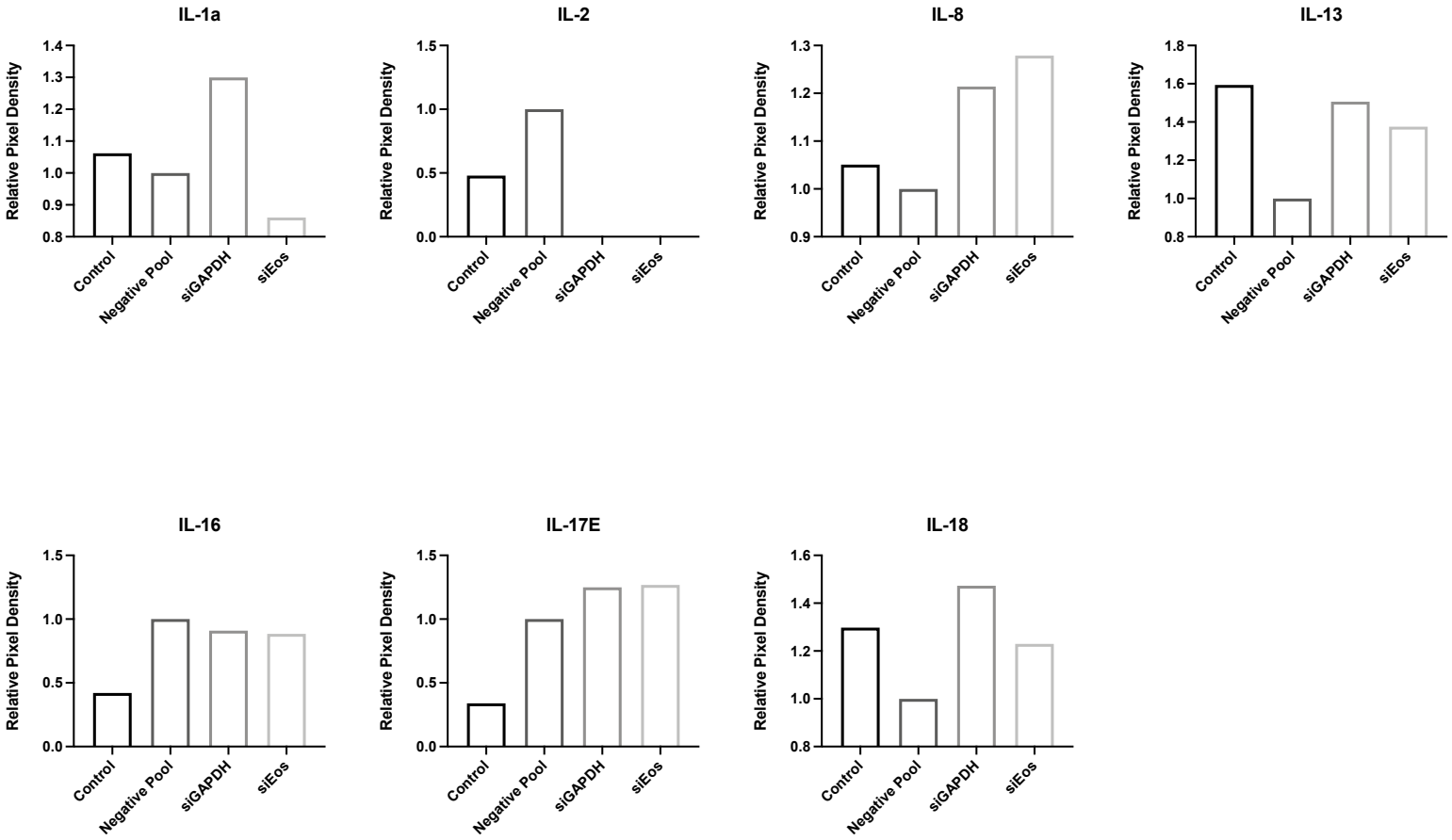



**Figure 7.6: Eos Knockdown in THP-1 Macrophages Alters Cytokine Secretion**
THP-1 cells were seeded at 500,000 cells/ml and polarised to MΦ macrophages with addition of 50ng/ml PMA. The cells were then left untreated in Opti-Mem Medium (Control) or treated with Lipofectamine RNAiMAX and either Silencer Select (SS) Negative Targeting Pool (Negative Pool), SS GAPDH Positive (siGAPDH) and SS Eos Targeting siRNA (siEos) for 48 hours. After incubation, 1ml of complete medium was added to cells and the supernatants collected from samples after 24 hours for analysis via the R&D Proteome Profiler. Samples from three independent experiments were pooled for each condition and Pixel Density calculated using Image J software. Results are relative to the Negative Pool. *N=3, N=1*.

When analysing levels of CCL5, no CLL5 was seen in either the siGAPDH or siEos, whereas siEos had higher levels of CD40L in comparison to Control (Figure 7.7). In comparison to Control, siEos had almost double expression levels of CXCL1. siEos also had the highest presence of CXCL10 in comparison to all other populations, with the biggest increase of all factors seen in CXCL10. Similar levels of ICAM-1 were seen in all populations, with MIF, MIP1a/b, and SERPIN E1 levels appearing slightly higher in siEos.

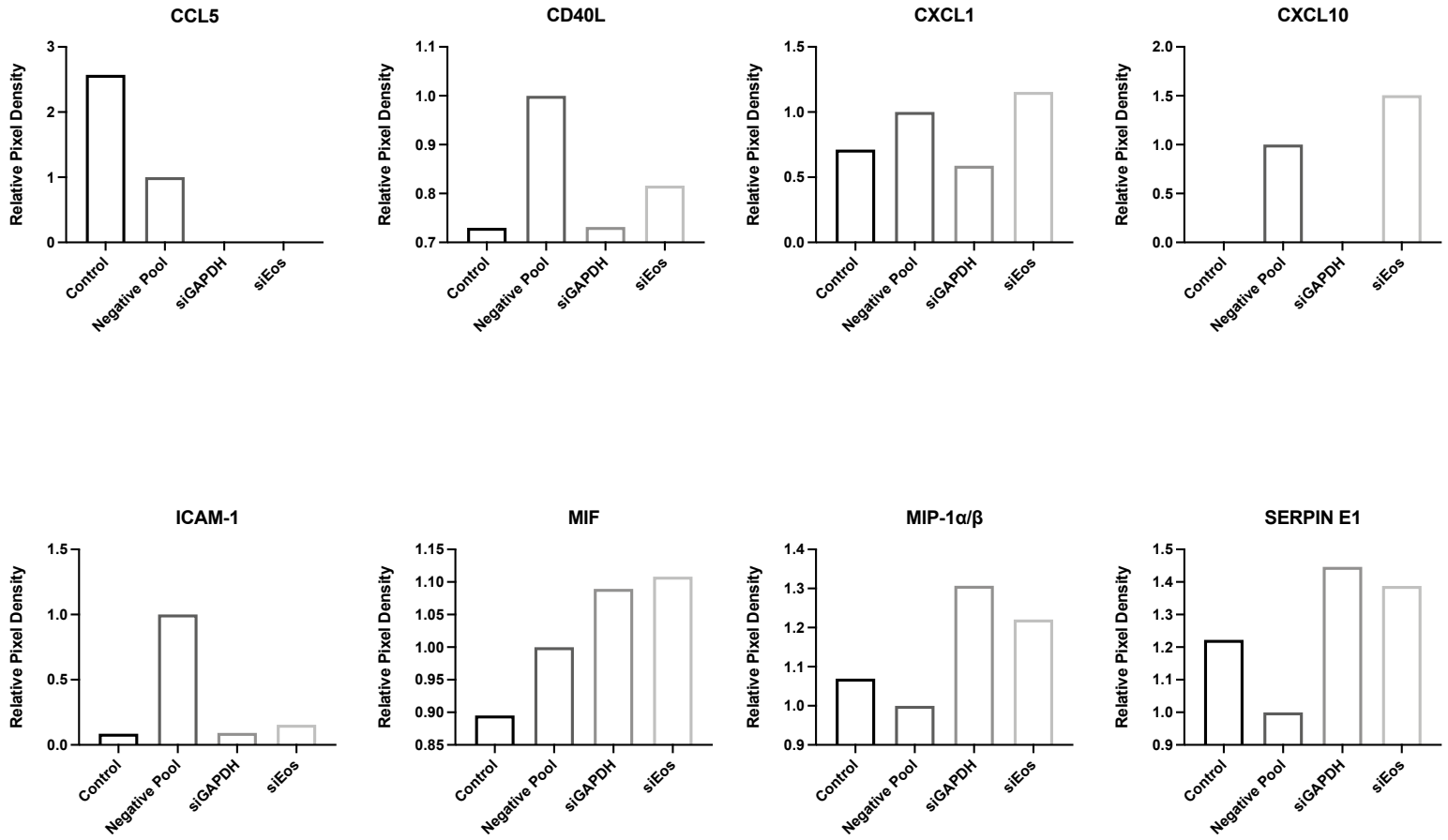



**Figure 7.7: Eos Knockdown in THP-1 Macrophages Alters Chemokine Secretion**
THP-1 cells were seeded at 500,000 cells/ml and polarised to MΦ macrophages with addition of 50ng/ml PMA. The cells were then left untreated in Opti-Mem Medium (Control) or treated with Lipofectamine RNAiMAX and either Silencer Select (SS) Negative Targeting Pool (Negative Pool), SS GAPDH Positive (siGAPDH) and SS Eos Targeting siRNA (siEos) for 48 hours. After incubation, 1ml of complete medium was added to cells and the supernatants collected from samples after 24 hours for analysis via the R&D Proteome Profiler. Samples from three independent experiments were pooled for each condition and Pixel Density calculated using Image J software. Results are relative to the Negative Pool. *N=3, N=1*

## 7.3 Discussion

### 7.3.1 Eos Knockdown Effects the Phagocytic Capacity of Macrophages

To fully investigate the role of the Ikaros family in macrophages, we decided to use siRNA to knockdown members and then assess any changes which arose. We initially began by investigating Eos as mentioned in the introduction, conducting the protocol in THP-1 cells with the goal of optimising the method for use in primary MDM cultures. This was complicated by the effects of COVID on laboratory and sample access. Thus, we worked with THP-1-macrophage cultures, with the aim to investigate knockdown in primary cells in future.

Using the Lipofectamine RNAiMAX method, we observed a significant and specific reduction in Eos expression, suggesting this method was appropriate for further experimentation (Figure 7.1). We did note however, that levels of Ikaros were also lower in the Eos knockdown samples, albeit not significantly. Further experimentation is required to clarify whether this particular siRNA had off target effects on Ikaros expression, which may relate to structural similarity. Of note our siGAPDH also worked appropriately. Assessing cell viability was key to confirm that the knockdown had no off-target effects, since a certain reduction in cell viability is expected for most siRNA knockdown methods. We confirmed that the siEos population and Control population retained good viability after treatment. Importantly a reduction in viability was observed after GAPDH knockdown. This protein has been shown to play roles in energy metabolism and stress responses in a variety of cells, with cytostatic effects reported after depletion in cancer cell lines (248). Thus, inability of cells to attach and adhere to wells for survival or impact of knockdown on cell metabolism may explain our viability reduction. Therefore, for future experiments, it would be key to assay another housekeeping gene as a control.

Next, we investigated the functional impact of siEos in macrophages. Phagocytosis is a key mechanism used by macrophages to help limit infection and inflammation (2, 43, 73, 81). Thus, any limitation on this ability could be extremely detrimental to the homeostatic balance within the gut. My experiments (Figure 7.4) highlighted a reduction in the phagocytic capacity of siEos macrophages, suggesting Eos plays a key role in the ability of macrophages to clear pathogens. This may contribute to the exacerbation and or accumulation of pathogenic material in the LP. In this regard, Caradonna *et al.,* (2000) have previously shown that peripheral MDMs from UC or CD patients had significantly impaired phagocytic capability in comparison to control. This contributed to the exacerbation of disease. Thus, drugs used therapeutically in IBD which have off target effects on Eos, could potentially reduce the capability of cells to phagocytose and exacerbate disease. I also performed a cytokine array to assess the impact of siEos secretome production (Figure 7.6 & 7.7). This provided interesting initial results suggesting chemokines and cytokines within the NF-κb pathway could be impacted by siEos, although further work and replicates are needed to confirm this finding. This is similar to previous studies showing that the Ikaros family is able to influence this pathway (83, 249). Interestingly, impact on this pathway is complex and cell dependent. When investigating the regulation of iNOS production in macrophages, Cho *et al.,* (2008) found that Ikaros repressed the gene through NF-κb loci, thereby activating iNOS production. However, a contrasting study by Oh *et al.,* (2018) suggests that LPS addition stimulated macrophages and increased Ikaros expression which then had a positive impact on the NF-κb pathway. Clearly Ikaros may have a multitude of roles dependent on context and therefore to consider the family as solely *'gene repressors'* may not be accurate. Thus, the roles of the Ikaros family need to be investigated further in different immune cells under different conditions (such as

normal vs diseased, resting vs polarized) to fully assess likely roles of targeted inhibition.

One of the mediators upregulated in our knockdown experiments was CD40L. This binds to CD40 found on macrophages and is the second stimulation signal required by macrophages after IFNγ (250). In chronic diseases such as atherosclerosis, CD40L ligation by ligands such as Mac-1 drives inflammation and in IBD, the proportion of gut macrophages expressing CD40 increases (250-252). However, the link between Eos function and CD40L is novel. CD40L is a marker of Treg stability and overexpression of Eos has negative consequences on T cells by impairing CD40L upregulation resulting in inefficient helper T cells (97). In Eos-labile Treg populations there an increase in CD40L expression (119). This supports our observation in the siEos macrophages, where a greater expression of CD40L was seen in comparison to Control. This could potentially hint towards reprogramming of cells to a more effector phenotype, with a greater capacity for cells to become activated due to their upregulated CD40L expression.

CXCL1, a chemokine which binds to CXCR2 was also greater in siEos (142). Interestingly this chemokine is produced by gut macrophages during intestinal wall stress and reduces the contractile ability of the intestine (253). Serum levels of CXCL1 increase in patients with IBD where it has been suggested to contribute to the proinflammatory environment (254). Elevated levels of CXCL1 have also been identified in CD and UC data RNASeq data sets (222). However it is also important for recruitment of restorative macrophages to the gut during DSS colitis, and here mice deficient in CXCL1 exhibit more severe injury (255). The chemokine is also important for cytokine production by Th17 cells (142). I demonstrated that in siEos MΦ, expression levels of CXCL1 were almost double that of Control cells which could

suggest adoption of a more inflammatory phenotype. CXCL10 was also found to be elevated in the siEos MΦ population. The chemokine, typically induced by IFNγ binds to CXCR3 and promotes recruitment of lymphocytes to the inflamed gut and liver (75, 242, 256). The local production is suggested to derive from M1 macrophages which promote generation of Th1 and Th17 by expressing chemokines such as CXCL10 which in turn recruit Th1 cells and is associated with cytokines such as IFNγ, TNFα and LPS (75). Elevated levels of CXCL10 have also been seen in RNASeq analysis of CD and UC data sets (222). This again suggests a proinflammatory shift in siEos MΦ in comparison to Control.

Effects of Ikaros family members on Treg/Th17 polarisation have been widely described (123, 143)(Section 3.1). IL-17E is a Th17- associated cytokine which was upregulated in my knockdown experiments (110). This is similar to studies with Eos knockdown in Tregs which find an upregulation of IL-17 and other Th17 related products (93, 119, 123, 128). Similarly, I also demonstrated elevated levels of IL-8 in siEos MΦ. IL-8 binds CXCR1/2 and is implicated in the chemotaxis of monocytes and found expressed on M1 macrophages (30, 80). Expression of IL-8 has been linked to disease severity and risk of relapse in IBD and is involved in neutrophil recruitment into the inflamed bowel (257, 258). Elevated levels of IL-8 suggest greater recruitment of monocytes to enable a more pronounced immune response, promoting the notion of a proinflammatory shift in the MΦ phenotype (30). Interestingly, Lenalidomide treatment (targeting Aiolos and Ikaros), significantly increases expression of IL-8 *and CCL2* in monocyte-derived DC cultures (238). Thus, knockdown of Eos may have a similar impact on IL-8 expression levels, and consequent anti-inflammatory effects.

In contrast to the above, my study found reductions in the expression of both IL-1a and IL-2 within siEos MΦ. IL-1a is another proinflammatory cytokine produced by macrophages which contributes to inflammation (259). Its analogue, IL-1b is associated with macrophage function and Boutboul *et al.,* (2018) found that patients with germline homozygous mutations in Ikaros have a defective response to TLR stimulation leading to reduced IL-1b production (89, 259). Similarly, in our study, we saw a reduction in IL-1a expression in siEos MΦ suggesting Eos may play a role in activating IL-1a expression. IL-1a is needed to activate the proinflammatory response of macrophages and acts as a DAMP for the immune system (259). Thus, our reported reduction after Eos knockdown could be beneficial. However, IL-1a is also required for efficient removal of phagocytosed pathogens (259). This is in agreement with the results from my phagocytosis experiments (Figure 7.4) which saw a reduction in phagocytic capacity of siEos macrophages, suggesting potential inefficient macrophage function. Similarly, the lack of IL-2 in siEos MΦ supports the notion of inefficient immune cell response. Previous studies on Eos have highlighted a key role for Eos in IL-2 expression, whereas other family members such as Helios and Aiolos, are known to supress its expression (103, 119). Eos has been found to be needed for IL-2 production of CD4 cells *in vitro* (119). Eos knockout cells have reduced proliferation when stimulated and Rieder *et al.,* (2015) hypothesised that this is due to reduction in IL-2 production (123). IL-2 is key for Treg function thus a lack of IL-2 again suggests an inflammatory phenotype of the macrophages which could promote autoimmunity (99, 101, 102).

### 7.3.2 Summary and Limitations of this Chapter

siEos MΦ displayed characteristics of proinflammatory macrophages suggesting a change from the conventional homeostatic uncommitted MΦ phenotype, supporting our hypothesis that Eos expression could influence macrophage phenotype (46, 157, 158). Interestingly, in our previous chapters, we have seen upregulated Eos expression in both blood (Figure 6.6) and tissue-derived (Figure 5.21) macrophages which suggests Eos overexpression may contribute to an inefficient or proinflammatory macrophage response in disease. Together, our novel findings suggest a role for Eos in controlling macrophage phenotype through plasticity. The changes observed in CD40L, IL-2 and IL-17 production in the Eos knockdown are useful for further experimentation focussed on macrophage plasticity, since they are established markers for investigating Treg plasticity (97). Thus, further analysis of surface markers may establish if the macrophages have indeed undergone plasticity towards a pro-inflammatory phenotype due to the lack of Eos. For further experimentation, it would also be key to replicate the array without pooling of experimental repeats for each condition. Due to project constraints, we were unable to individually assay the experimental repeats nor conduct the siRNA knockdown in primary cells thus for future work this would be our priority. Another key limitation of our study is the lack of functional studies investigating the role of Eos in macrophage function. To our knowledge, at the time of writing this thesis, there are no published papers available in the public domain investigating the role of Eos in macrophages or macrophage plasticity. Interestingly, we have also seen elevated Eos+CD68+ macrophages in inflamed bowel (Figure 5.21) supporting a role for Eos in IBD although the reason remains unknown.

Thus, further work is needed to determine the full impact of Eos knockdown *and* overexpression on the phenotype of macrophages: this includes assaying changes in phenotypic markers in siEos MΦ, comparing differences in donor and patient MΦ plasticity studies and scRNASeq on cells *in situ*.

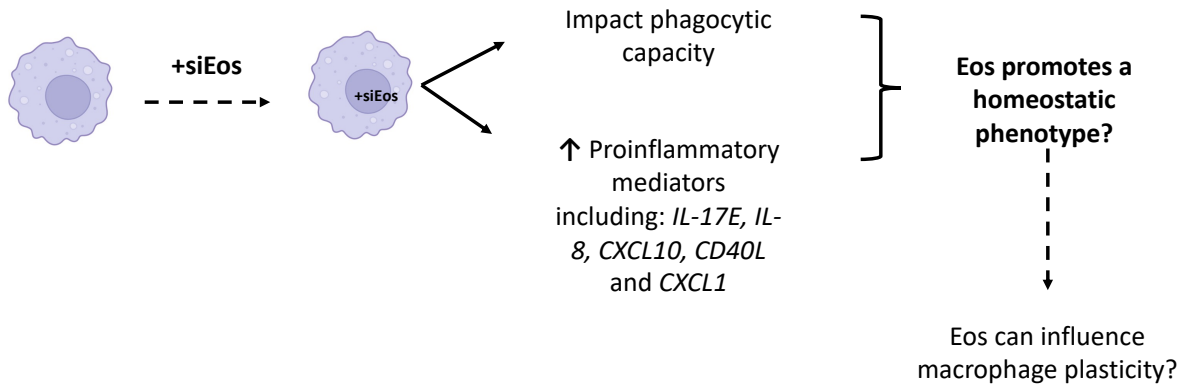



**Figure 7.8: Summary Diagram for Chapter 7**
Summary of the key findings from Chapter 7, *Investigating Selective Eos Knockdown In MΦ Macrophages*. THP-1 derived resting macrophages (MΦ) were treated with anti-Eos targeting siRNA (siEos) and assayed for changes in phenotype and function. These macrophages were found to have reduced phagocytic capacity and an increase in proinflammatory mediator production in comparison to untreated macrophages. siEos, Silencer Select Eos Targeting siRNA.

# Chapter 8: Concluding Discussion

## 8.1 Key Conclusions of my Thesis

The findings in my thesis have greatly increased our knowledge on the under investigated Ikaros family of transcription factors. The work in this project has proven that the family is not only expressed within macrophages, but members of the family have differential expression within subsets and are influenced by inflammation status and biologic intervention (Figure 8.1). Beginning this project in Chapter 3, I was able to reassert known expression data of Ikaros family members within Treg and Non-Treg populations, reporting Helios as a marker of Tregs (100, 114). Using patient samples, we were able to identify that mild UC inflammation altered systemic levels of Ikaros family members within CD4+ T Cells, and identified novel data on Pegasus expression in IBD.

In Chapter 4, we took this knowledge of alterations within systemic levels of Ikaros family members in response to IBD, to assess their expression within bowel tissue during inflammation. Due to the gut-liver axis, I used this knowledge to investigate the Ikaros family within PSC-IBD, to explore whether the Ikaros family could link both the liver and gut (55). Our results showed that the Ikaros family is indeed expressed within the bowel and liver, and certain members are impacted in both during inflammation. Using correlation analysis of clinical markers and the Ikaros family in liver disease, I showed that correlations exist between Eos, Helios and Pegasus and BMI in PSC and NASH which is previously unreported. This offers the potential for the family members as clinical markers and highlights a novel role for Pegasus. We were also able to access resected material from patients undergoing CD-mediated resections, providing us with novel data regarding differential Ikaros family expression within regions of resections.

Through IHC analysis, we found that the Ikaros family is expressed within lymphocytes in both tissues, but also appeared to stain macrophages within liver tissue. We took this knowledge into Chapter 5, where we aimed to discover if the Ikaros family could play a role within macrophages. We know from limited literature that Ikaros and Eos are present within macrophages with roles in regulation, however to our knowledge this has not been investigated in the capacity of the bowel, liver or in various macrophage subsets (107, 142).

In my thesis, I have shown that CD68+ expressing macrophages are upregulated significantly in the bowel and in PSC-IBD (29, 55, 56). Most importantly, I have shown that all members of the Ikaros family are expressed by THP-1 cells, primary monocytes and MDMs, with differential expression levels. Through the use of multiplex staining, I have also shown that there is a significant increase in both Eos+CD68+ and Helios+CD68+ cells within inflamed bowel in comparison to uninflamed implicating the transcription factors within disease pathology. This was also seen in pilot mouse data (**Appendix B**).

I next investigated differences within Ikaros Family expression in MDMs derived from Control, Biologic Naïve or anti-TNF$\alpha$-treated PBMCs to ascertain if donor variances in family members existed. In Chapter 6, I found an increase in Eos expression in monocytes from Biologic Naïve patients, with elevated Eos expression in those treated with anti-TNF$\alpha$. Helios was also upregulated within the MΦ-MCSF populations with a greater elevation following anti-TNF$\alpha$ treatment. What was most interesting is that both Eos and Helios are known to promote a regulatory phenotype in comparison to the other family members and therefore we can hypothesise their upregulation in response to inflammation and anti-TNF$\alpha$ treatment may be to mitigate inflammation. The use of Infliximab within the clinic aims to dampen the global inflammatory

response, therefore a corresponding reduction in the more proinflammatory inclined Ikaros in macrophage populations supports this theory (30). Together this suggests that Eos may be upregulated in response to inflammation, to manage inflammation. To further support this hypothesis, we saw that both Helios+CD68+ and Eos+CD68+ macrophages were significantly upregulated in inflamed bowel tissue. We know that macrophages are upregulated within the bowel in IBD as a means to combat inflammation and repair tissue and thus both Eos and Helios could contribute to this (30, 37, 44). From our RNA data we know that Eos is found in all macrophage subtypes suggesting it is vital for macrophage function, with Helios associating more greatly with MΦ-GM-CSF and M2c macrophage populations, again the regulatory cell phenotype. We next investigated how we could manipulate the transcription factors through the use of therapeutics and knockdown models. In Chapter 6, I have shown that expression of the Ikaros Family in macrophages can be manipulated using readily available drugs like Pomalidomide or using siRNA. We found Pomalidomide depleted levels of Aiolos in M1 in the short culture, supporting previous literature on IMiD-dependent Aiolos downregulation and potentially encouraging a regulatory phenotype (144, 235). Contrastingly in the long culture, we found an increase in Ikaros and Helios in M2 populations with Pomalidomide. From available literature and from our results in this thesis, we know that both proteins appear to have a greater association with M2 cells (Chapter 5) (206). Therefore, our results appear to suggest within M2 macrophages, Pomalidomide favours their upregulation, however further investigation is needed to determine if this could promote a regulatory macrophage phenotype.

In Chapter 7, I have also shown that Eos knockdown within MΦ macrophages promotes a proinflammatory phenotype suggesting Eos is needed for the homeostatic phenotype of macrophages. An impact in phagocytic capacity was also seen which

mimics the loss in capacity seen within macrophages in the bowel in IBD (87). These macrophages are less effective and therefore suggests Eos is vital for efficient macrophage function within the bowel. To support the change in phenotype, we also saw a decrease in IL-2, but corresponding increase in levels of IL-17E, IL-8. CXCL5, CXCL10, CD40L and CXCL1, all alluding to a proinflammatory phenotype. Together our work suggests lack of Eos may promote a proinflammatory phenotype in macrophages. Our finding of elevated Eos expression within monocytes in Biologic Naïve, anti-TNF$\alpha$-treated samples, along with inflamed bowel tissue suggests Eos upregulation may encourage a more homeostatic phenotype of macrophages to combat inflammation and promote tissue rebuilding, or contrastingly, this upregulation results in an inefficient macrophage response. Although more work is needed, this greatly supports a role for Eos in mediating the phenotype and thus plasticity of macrophages.

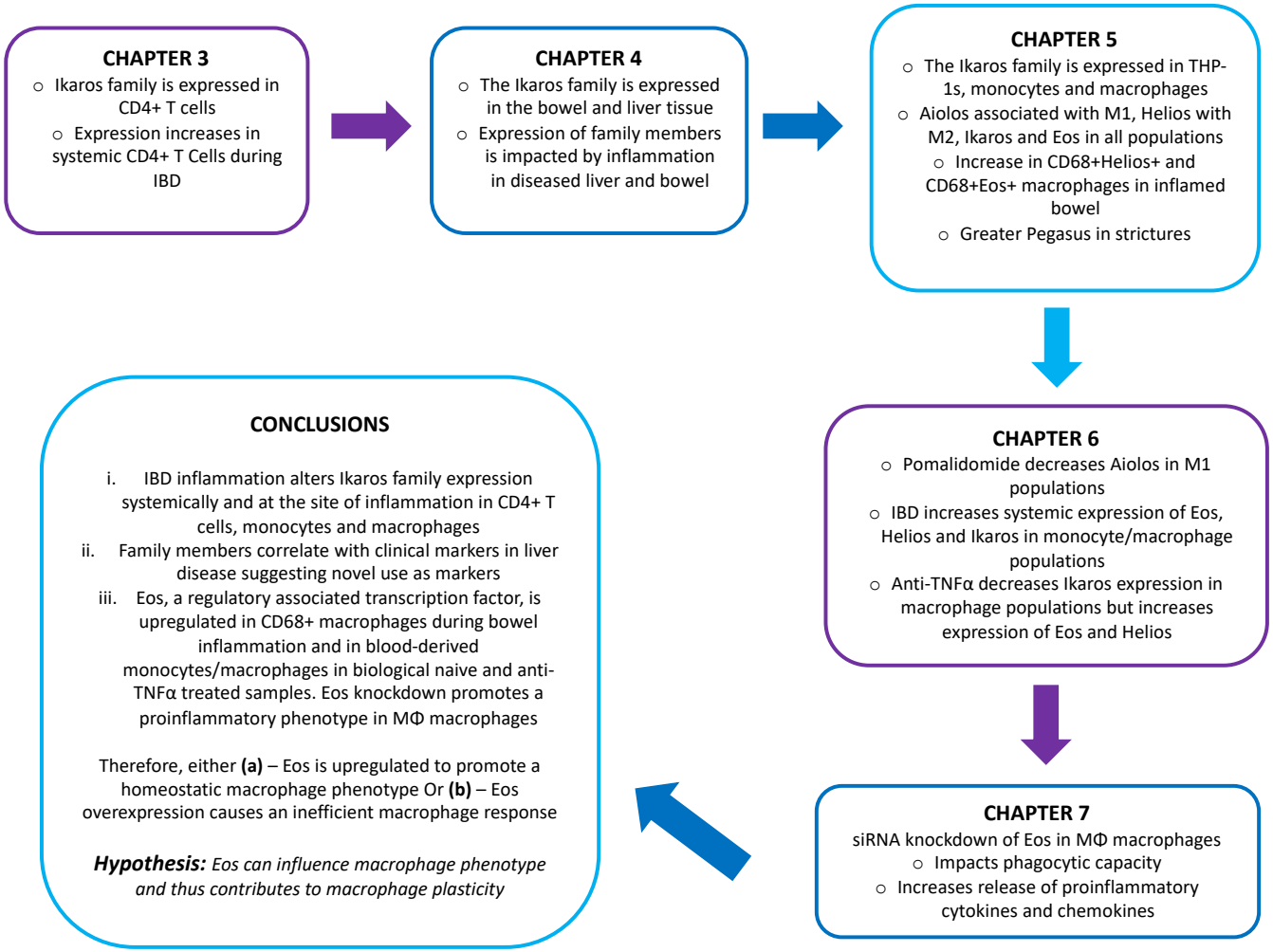



**Figure 8.1: Key Conclusions of This Thesis**
A summary of key findings from each results chapter in this thesis. *CD68+, CD68 positive; MΦ, macrophages; M1, Proinflammatory macrophages; M2, Regulatory macrophages; TNFα, TNF alpha.*

## 8.2 Significance of Key Findings

My project overall has used multiple complementary strategies to generate novel insights about an under-explored transcription factor family. For example in 2021, 5 articles were published investigating Eos, with only 1 available through the PubMed database for Pegasus (260). My work has shown that the family is expressed within macrophages and thus could influence macrophage plasticity – a key investigative target for restoring the homeostatic M1/M2 balance within IBD. We have also found the relatively under investigated member, Pegasus, correlates with disease markers such as BMI in NASH and has elevated presence in bowel strictures, offering potential novel roles for the transcription factor. I have also shown that during sample storage and subsequent thawing, Pegasus expression at an RNA level is lost. Interestingly, we did not see this with our Control samples therefore leading us to hypothesise that potentially, instability of patient monocytes in comparison to Control may cause this. For future studies therefore this would be a key topic to investigate. We have also seen clinical correlations between Ikaros family members and clinical markers again supporting a role for the family as diagnostic tools. For example, Ikaros was found to associate with M2 macrophages, however, was also downregulated by anti-TNF$\alpha$ offering potential avenues of functional investigations which could be correlated with treatment outcome. Other clinical implications from my work come from assessing the impact of Pomalidomide. I have shown that Pomalidomide can impact all members of the Ikaros family which therefore opens the possibility of off-target effects within individuals. This finding could be further investigated and help to determine if these off target effects could impact a person's propensity to side effects or responsiveness to Pomalidomide.

## 8.3 Future Directions of Work

Like any research project, there are always more questions to be asked and limitations to be addressed. However, due to the COVID pandemic, we experienced unique access limitations which could be readily addressed with easing of restrictions: both in the lab and clinic. A key limitation of our study was the lack of fresh clinical samples, in part due to the COVID pandemic but also due to delays in securing ethical approvals at the beginning of the project. For future studies, matched IBD blood and tissue samples would help correlate data for expression of Ikaros Family members with disease stage. This would permit assessment of whether the family members have potential as prognostic or diagnostic markers and if levels in the blood could correlate with bowel or liver disease severity. Next, alongside observing expression within inflamed and inflamed bowel regions, tissue samples from healthy control, UC and CD would permit more extensive characterisation of expression using tools like scRNASeq, spatial transcriptomics, or Flow Cytometry. I was able to generate some interesting data from my Opal™ experiments, but this was preliminary in nature and not without limitations. Future studies would greatly benefit from fresher tissue, and I could also optimise the method further and add more markers to take full advantage of the methodology. Alongside this, we could find resources to use INFORM technology (Akoya Biosciences) to successfully analyse the tissue.

Following from our pilot siRNA data we could next investigate siEos in different macrophage populations and then use this methodology to investigate other family members, ideally within MDMs. Alternately, detailed analysis of cell specific murine knockout models in the context of disease would provide insights to link our expression data to disease outcome. A more extensive functional characterisation could then be carried out on these cells such as measuring migratory or adhesive functions as well

as cytokine release. Luminex technology to assess cytokine and chemokine changes across multiple healthy and diseased cell donors could circumvent the caveats of pooled samples. Whilst I have robust data for gene expression, the connection between gene and protein expression has not been fully explored. In part this related to a lack of validated antibodies for all members of the family. This has been a prevalent issue for others who have also assessed Eos levels through mRNA and not protein detection (158, 162). For future work, we could try an indirect staining approach for an unconjugated Pegasus IHC antibody similar to what we did for Eos. As we have found links between the Ikaros family in liver and bowel disease, it would be interesting to explore this further and see which other co-morbidities such as RA may be linked to Ikaros family function (13). We also know that diet plays a key role in both IBD and NASH thus it would be interesting to see the impact that dietary components could have on the Ikaros family and in turn on macrophage phenotype (9, 11, 12, 55).

## 8.4 Conclusion

To conclude, my thesis has demonstrated novel expression and functional data on Ikaros family members within myeloid cells in bowel and liver disease. The findings of my work suggest that the Ikaros Family could function as markers of disease severity due to their responsiveness in disease and biologic treatment, whilst identifying a novel functional role for members in macrophages. As mentioned in the introduction of this thesis, IBD remains a great medical burden, with its management restricted due to the lack of efficient clinical markers to determine prognosis, severity, and responsiveness to current therapies. My work offers a potential for the Ikaros family to function as clinical targets and markers through non-invasive imaging and systemic culture methods which could help better manage patient treatment.

# References


1. Gasparetto M, Guariso G. Highlights in IBD Epidemiology and Its Natural History in the Paediatric Age. Gastroenterol Res Pract. 2013;2013:829040.
2. Huang Y, Chen Z. Inflammatory bowel disease related innate immunity and adaptive immunity. Am J Transl Res. 2016;8(6):2490-7.
3. Zhang Y-Z, Li Y-Y. Inflammatory bowel disease: pathogenesis. World journal of gastroenterology. 2014;20(1):91-9.
4. Galvez J. Role of Th17 Cells in the Pathogenesis of Human IBD. ISRN Inflamm. 2014;2014:928461.
5. Ye Y, Pang Z, Chen W, Ju S, Zhou C. The epidemiology and risk factors of inflammatory bowel disease. Int J Clin Exp Med 2015;8(12):22529-42.
6. Windsor JW, Kaplan GG. Evolving Epidemiology of IBD. Current Gastroenterology Reports. 2019;21(8):40.
7. Yang C, Singh P, Singh H, Le ML, El-Matary W. Systematic review: thalidomide and thalidomide analogues for treatment of inflammatory bowel disease. Aliment Pharmacol Ther. 2015;41(11):1079-93.
8. Kim DH, Cheon JH. Pathogenesis of Inflammatory Bowel Disease and Recent Advances in Biologic Therapies. Immune Netw. 2017;17(1):25-40.
9. Kucharzik T, Maaser C, Lugering A, Kagnoff M, Mayer L, Targan S*et al.,*. Recent Understanding of IBD Pathogenesis: Implications for Future Therapies. Inflamm Bowel Dis. 2006;12:1068–83.
10. Guariso G, Gasparetto M. Treating children with inflammatory bowel disease: Current and new perspectives. World J Gastroenterol. 2017;23(30):5469-85.
11. Kaplan GG. The global burden of IBD: from 2015 to 2025. Nature Reviews Gastroenterology & Hepatology. 2015;12(12):720-7.
12. Fakhoury M, Negrulj R, Mooranian A, Al-Salami H. Inflammatory bowel disease: clinical aspects and treatments. J Inflamm Res. 2014;7:113-20.
13. Ye BD, McGovern DP. Genetic variation in IBD: progress, clues to pathogenesis and possible clinical utility. Expert Rev Clin Immunol. 2016;12(10):1091-107.
14. Alatab S, Sepanlou SG, Ikuta K, Vahedi H, Bisignano C, Safiri S*et al.,*. The global, regional, and national burden of inflammatory bowel disease in 195 countries and territories, 1990–2017: a systematic analysis for the Global Burden of Disease Study 2017. The Lancet Gastroenterology & Hepatology. 2020;5(1):17-30.
15. Wilks S, Moxon W. Lectures on pathological anatomy: Longmans, Green; 1889.
16. Crohn BB, Ginzburg L, Oppenheimer GD. Regional ileitis: A pathologic and clinical entity. The American Journal of Medicine. 1952;13(5):583-90.
17. Kirsner JB. Historical origins of current IBD concepts. World journal of gastroenterology. 2001;7(2):175-84.
18. Isidro RA, Appleyard CB. Colonic macrophage polarization in homeostasis, inflammation, and cancer. Am J Physiol Gastrointest Liver Physiol. 2016;311(1):G59-73.
19. Chang CW, Wong JM, Tung CC, Shih IL, Wang HY, Wei SC. Intestinal stricture in Crohn's disease. Intest Res. 2015;13(1):19-26.
20. Weismuller TJ, Trivedi PJ, Bergquist A, Imam M, Lenzen H, Ponsioen CY*et al.,*. Patient Age, Sex, and Inflammatory Bowel Disease Phenotype Associate With Course of Primary Sclerosing Cholangitis. Gastroenterology. 2017;152(8):1975-84 e8.

21. Ouyang Q, Tandon R, Goh KL, Pan GZ, Fock KM, Fiocchi C*et al.,*. Management consensus of inflammatory bowel disease for the Asia-Pacific region. J Gastroenterol Hepatol. 2006;21(12):1772-82.
22. Ricciuto A, Kamath BM, Griffiths AM. The IBD and PSC Phenotypes of PSC-IBD. Curr Gastroenterol Rep. 2018;20(4):16.
23. Park KT, Ehrlich OG, Allen JI, Meadows P, Szigethy EM, Henrichsen K*et al.,*. The Cost of Inflammatory Bowel Disease: An Initiative From the Crohn's & Colitis Foundation. Inflamm Bowel Dis. 2020;26(1):1-10.
24. Ng SC, Shi HY, Hamidi N, Underwood FE, Tang W, Benchimol EI*et al.,*. Worldwide incidence and prevalence of inflammatory bowel disease in the 21st century: a systematic review of population-based studies. The Lancet. 2017;390(10114):2769-78.
25. Burisch J, Jess T, Martinato M, Lakatos PL, EpiCom E. The burden of inflammatory bowel disease in Europe. J Crohns Colitis. 2013;7(4):322-37.
26. Heinsbroek SE, Gordon S. The role of macrophages in inflammatory bowel diseases. Expert Rev Mol Med. 2009;11:e14.
27. Morais LH, Schreiber HLt, Mazmanian SK. The gut microbiota-brain axis in behaviour and brain disorders. Nat Rev Microbiol. 2021;19(4):241-55.
28. Omenetti S, Pizarro TT. The Treg/Th17 Axis: A Dynamic Balance Regulated by the Gut Microbiome. Front Immunol. 2015;6:639.
29. Konturek PC, Harsch IA, Konturek K, Schink M, Konturek T, Neurath MF*et al.,*. Gut(-)Liver Axis: How Do Gut Bacteria Influence the Liver? Med Sci (Basel). 2018;6(3).
30. Kuhl AA, Erben U, Kredel LI, Siegmund B. Diversity of Intestinal Macrophages in Inflammatory Bowel Diseases. Front Immunol. 2015;6:613.
31. Karaiskos C, Hudspith BN, Elliott T, Rayment NB, Avgousti V, Sanderson JD. Defective macrophage function in crohn's disease: role of alternatively activated macrophages in inflammation. Gut. 2011;60(Suppl 1):A143-A4.
32. Berkowitz L, Schultz BM, Salazar GA, Pardo-Roa C, Sebastian VP, Alvarez-Lobos MM*et al.,*. Impact of Cigarette Smoking on the Gastrointestinal Tract Inflammation: Opposing Effects in Crohn's Disease and Ulcerative Colitis. Front Immunol. 2018;9:74.
33. Charpentier C, Chan R, Salameh E, Mbodji K, Ueno A, Coeffier M*et al.,*. Dietary n-3 PUFA May Attenuate Experimental Colitis. Mediators Inflamm. 2018;2018:8430614.
34. Steinbach EC, Plevy SE. The role of macrophages and dendritic cells in the initiation of inflammation in IBD. Inflamm Bowel Dis. 2014;20(1):166-75.
35. Rao J, Wang J. Regulation of Gastrointestinal Mucosal Growth. . San Rafael (CA): Morgan & Claypool Life Sciences;; 2010.
36. Azzouz L, Sharma S. Physiology, Large Intestine. reasure Island (FL): StatPearls Publishing; 2021 [updated 2021 Aug 9. Available from: https://www.ncbi.nlm.nih.gov/books/NBK507857/.
37. Han X, Ding S, Jiang H, Liu G. Roles of Macrophages in the Development and Treatment of Gut Inflammation. Front Cell Dev Biol. 2021;9:625423.
38. Ogobuiro I, Gonzales J, Tuma F. Physiology, Gastrointestinal Treasure Island (FL): StatPearls Publishing; 2021 [updated 2021 Apr 25. Available from: https://www.ncbi.nlm.nih.gov/books/NBK537103/.
39. Collins JT, Nguyen A, Badireddy M. Anatomy, Abdomen and Pelvis, Small Intestine NCBI: StatPearls Publishing; 2020 [Available from: https://www.ncbi.nlm.nih.gov/books/NBK459366/?report=classic.

40. Costa J, Ahluwalia A. Advances and Current Challenges in Intestinal in vitro Model Engineering: A Digest. Front Bioeng Biotechnol. 2019;7:144.
41. Sun Y, Li L, Xie R, Wang B, Jiang K, Cao H. Stress Triggers Flare of Inflammatory Bowel Disease in Children and Adults. Front Pediatr. 2019;7:432.
42. Lukic A, Larssen P, Fauland A, Samuelsson B, Wheelock CE, Gabrielsson S*et al.,*. GM-CSF- and M-CSF-primed macrophages present similar resolving but distinct inflammatory lipid mediator signatures. FASEB J. 2017;31(10):4370-81.
43. Forrester MA, Wassall HJ, Hall LS, Cao H, Wilson HM, Barker RN*et al.,*. Similarities and differences in surface receptor expression by THP-1 monocytes and differentiated macrophages polarized using seven different conditioning regimens. Cell Immunol. 2018;332:58-76.
44. Caer C, Wick MJ. Human Intestinal Mononuclear Phagocytes in Health and Inflammatory Bowel Disease. Front Immunol. 2020;11:410.
45. Bain CC, Mowat AM. The monocyte-macrophage axis in the intestine. Cell Immunol. 2014;291(1-2):41-8.
46. Pan F, Yu H, Dang EV, Barbi J, Pan X, Grosso JF*et al.,*. Eos mediates Foxp3-dependent gene silencing in CD4+ regulatory T cells. Science. 2009;325(5944):1142-6.
47. Kim HJ, Cantor H. CD4 T-cell subsets and tumor immunity: the helpful and the not-so-helpful. Cancer Immunol Res. 2014;2(2):91-8.
48. Koenen HJ, Smeets RL, Vink PM, van Rijssen E, Boots AM, Joosten I. Human CD25highFoxp3pos regulatory T cells differentiate into IL-17-producing cells. Blood. 2008;112(6):2340-52.
49. Kastl AJ, Jr., Terry NA, Wu GD, Albenberg LG. The Structure and Function of the Human Small Intestinal Microbiota: Current Understanding and Future Directions. Cell Mol Gastroenterol Hepatol. 2020;9(1):33-45.
50. Kobayashi T, Siegmund B, Le Berre C, Wei SC, Ferrante M, Shen B*et al.,*. Ulcerative colitis. Nat Rev Dis Primers. 2020;6(1):74.
51. Nakase H, Uchino M, Shinzaki S, Matsuura M, Matsuoka K, Kobayashi T*et al.,*. Evidence-based clinical practice guidelines for inflammatory bowel disease 2020. J Gastroenterol. 2021;56(6):489-526.
52. Zhong H, Yazdanbakhsh K. Differential control of Helios+/− Treg development by monocyte subsets through disparate inflammatory cytokines. Blood. 2013;121(13):2494-502.
53. Roda G, Jharap B, Neeraj N, Colombel JF. Loss of Response to Anti-TNFs: Definition, Epidemiology, and Management. Clin Transl Gastroenterol. 2016;7:e135.
54. Lamb CA, Kennedy NA, Raine T, Hendy PA, Smith PJ, Limdi JK*et al.,*. British Society of Gastroenterology consensus guidelines on the management of inflammatory bowel disease in adults. Gut. 2019;68(Suppl 3):s1.
55. Kalra A, Yetiskul E, Wehrle C, Tuma F. Physiology, Liver Treasure Island (FL): StatPearls Publishing; 2021 [updated 2021 May 9 Available from: https://www.ncbi.nlm.nih.gov/books/NBK535438/.
56. Kubes P, Jenne C. Immune Responses in the Liver. Annu Rev Immunol. 2018;36:247-77.
57. Abdel-Misih SR, Bloomston M. Liver anatomy. Surg Clin North Am. 2010;90(4):643-53.
58. Kalo E, Read S, Ahlenstiel G. Targeting Gut–Liver Axis for Treatment of Liver Fibrosis and Portal Hypertension. Livers. 2021;1(3):147-79.
59. Trefts E, Gannon M, Wasserman DH. The liver. Curr Biol. 2017;27(21):R1147-r51.

60. Krishna M. Microscopic anatomy of the liver. Clin Liver Dis (Hoboken). 2013;2(Suppl 1):S4-S7.
61. Kazankov K, Jorgensen SMD, Thomsen KL, Moller HJ, Vilstrup H, George J*et al.,*. The role of macrophages in nonalcoholic fatty liver disease and nonalcoholic steatohepatitis. Nat Rev Gastroenterol Hepatol. 2019;16(3):145-59.
62. Wang T, Ma C. The hepatic macrophage pool in NASH. Cell Mol Immunol. 2021;18(8):2059-60.
63. Guicciardi ME, Trussoni CE, Krishnan A, Bronk SF, Lorenzo Pisarello MJ, O'Hara SP*et al.,*. Macrophages contribute to the pathogenesis of sclerosing cholangitis in mice. J Hepatol. 2018;69(3):676-86.
64. Cadamuro M, Girardi N, Gores GJ, Strazzabosco M, Fabris L. The Emerging Role of Macrophages in Chronic Cholangiopathies Featuring Biliary Fibrosis: An Attractive Therapeutic Target for Orphan Diseases. Front Med (Lausanne). 2020;7:115.
65. Li H, Zhou Y, Wang H, Zhang M, Qiu P, Zhang M*et al.,*. Crosstalk Between Liver Macrophages and Surrounding Cells in Nonalcoholic Steatohepatitis. Front Immunol. 2020;11:1169.
66. Bossen L, Vesterhus M, Hov JR, Farkkila M, Rosenberg WM, Moller HJ*et al.,*. Circulating Macrophage Activation Markers Predict Transplant-Free Survival in Patients With Primary Sclerosing Cholangitis. Clin Transl Gastroenterol. 2021;12(3):e00315.
67. Chung BK, Henriksen EKK, Jorgensen KK, Karlsen TH, Hirschfield GM, Liaskou E. Gut and Liver B Cells of Common Clonal Origin in Primary Sclerosing Cholangitis-Inflammatory Bowel Disease. Hepatol Commun. 2018;2(8):956-67.
68. Benedict M, Zhang X. Non-alcoholic fatty liver disease: An expanded review. World J Hepatol. 2017;9(16):715-32.
69. Mertz A, Nguyen NA, Katsanos KH, Kwok RM. Primary sclerosing cholangitis and inflammatory bowel disease comorbidity: an update of the evidence. Ann Gastroenterol. 2019;32(2):124-33.
70. Loftus EV, Jr., Harewood GC, Loftus CG, Tremaine WJ, Harmsen WS, Zinsmeister AR*et al.,*. PSC-IBD: a unique form of inflammatory bowel disease associated with primary sclerosing cholangitis. Gut. 2005;54(1):91-6.
71. Eksteen B, Grant AJ, Miles A, Curbishley SM, Lalor PF, Hübscher SG*et al.,*. Hepatic endothelial CCL25 mediates the recruitment of CCR9+ gut-homing lymphocytes to the liver in primary sclerosing cholangitis. J Exp Med. 2004;200(11):1511-7.
72. Mia S, Warnecke A, Zhang XM, Malmstrom V, Harris RA. An optimized protocol for human M2 macrophages using M-CSF and IL-4/IL-10/TGF-beta yields a dominant immunosuppressive phenotype. Scand J Immunol. 2014;79(5):305-14.
73. Italiani P, Boraschi D. From Monocytes to M1/M2 Macrophages: Phenotypical vs. Functional Differentiation. Front Immunol. 2014;5:514.
74. Bosshart H, Heinzelmann M. THP-1 cells as a model for human monocytes. Ann Transl Med. 2016;4(21):438.
75. Shapouri-Moghaddam A, Mohammadian S, Vazini H, Taghadosi M, Esmaeili SA, Mardani F*et al.,*. Macrophage plasticity, polarization, and function in health and disease. J Cell Physiol. 2018;233(9):6425-40.
76. Marimuthu R, Francis H, Dervish S, Li SCH, Medbury H, Williams H. Characterization of Human Monocyte Subsets by Whole Blood Flow Cytometry Analysis. J Vis Exp. 2018(140).
77. Roberts CA, Dickinson AK, Taams LS. The Interplay Between Monocytes/Macrophages and CD4(+) T Cell Subsets in Rheumatoid Arthritis. Front Immunol. 2015;6:571.

78. Tedesco S, De Majo F, Kim J, Trenti A, Trevisi L, Fadini GP*et al.,*. Convenience versus Biological Significance: Are PMA-Differentiated THP-1 Cells a Reliable Substitute for Blood-Derived Macrophages When Studying in Vitro Polarization? Front Pharmacol. 2018;9:71.
79. Daigneault M, Preston JA, Marriott HM, Whyte MK, Dockrell DH. The identification of markers of macrophage differentiation in PMA-stimulated THP-1 cells and monocyte-derived macrophages. PLoS One. 2010;5(1):e8668.
80. Chanput W, Mes JJ, Savelkoul HF, Wichers HJ. Characterization of polarized THP-1 macrophages and polarizing ability of LPS and food compounds. Food Funct. 2013;4(2):266-76.
81. Shiratori H, Feinweber C, Luckhardt S, Linke B, Resch E, Geisslinger G*et al.,*. THP-1 and human peripheral blood mononuclear cell-derived macrophages differ in their capacity to polarize in vitro. Mol Immunol. 2017;88:58-68.
82. Na YR, Stakenborg M, Seok SH, Matteoli G. Macrophages in intestinal inflammation and resolution: a potential therapeutic target in IBD. Nat Rev Gastroenterol Hepatol. 2019;16(9):531-43.
83. Cho SJ, Huh JE, Song J, Rhee DK, Pyo S. Ikaros negatively regulates inducible nitric oxide synthase expression in macrophages: involvement of Ikaros phosphorylation by casein kinase 2. Cell Mol Life Sci. 2008;65(20):3290-303.
84. Ireland LV, Mielgo A. Macrophages and Fibroblasts, Key Players in Cancer Chemoresistance. Front Cell Dev Biol. 2018;6:131.
85. Hine AM, Loke P. Intestinal Macrophages in Resolving Inflammation. J Immunol. 2019;203(3):593-9.
86. Wu D, Han JM, Yu X, Lam AJ, Hoeppli RE, Pesenacker AM*et al.,*. Characterization of regulatory T cells in obese omental adipose tissue in humans. Eur J Immunol. 2019;49(2):336-47.
87. Caradonna L, Amati L, Lella P, Jirillo E, Caccavo D. Phagocytosis, Killing, Lymphocyte-Mediated Antibacterial Activity, Serum Autoantibodies, and Plasma Endotoxins in Inflammatory Bowel Disease. The American Journal Of Gastroenterology. 2000;95:1495-502.
88. Eichele DD, Kharbanda KK. Dextran sodium sulfate colitis murine model: An indispensable tool for advancing our understanding of inflammatory bowel diseases pathogenesis. World J Gastroenterol. 2017;23(33):6016-29.
89. McAlindon MEH, C.J.; Mahida, Y.R. Expression of interleukin 1? and interleukin 1? converting enzyme by intestinal macrophages in health and inflammatory bowel disease. Gut. 1998;42:214-9.
90. Lee YK, Mukasa R, Hatton RD, Weaver CT. Developmental plasticity of Th17 and Treg cells. Curr Opin Immunol. 2009;21(3):274-80.
91. Hevia A, Bernardo D, Montalvillo E, Al-Hassi HO, Fernandez-Salazar L, Garrote JA*et al.,*. Human colon-derived soluble factors modulate gut microbiota composition. Front Oncol. 2015;5:86.
92. Golubovskaya V, Wu L. Different Subsets of T Cells, Memory, Effector Functions, and CAR-T Immunotherapy. Cancers (Basel). 2016;8(3).
93. Butcher MJ, Filipowicz AR, Waseem TC, McGary CM, Crow KJ, Magilnick N*et al.,*. Atherosclerosis-Driven Treg Plasticity Results in Formation of a Dysfunctional Subset of Plastic IFNgamma+ Th1/Tregs. Circ Res. 2016;119(11):1190-203.
94. Heinrichs JB, D.; Veerapathran, A.; Anasetti, C.; Betts, B.; Yu, X-Z. Regulatory T-Cell Therapy for Graft-versus-host Disease
. Journal of Immunology Reasearch. 2016;1(1):1-14.

95. Lord JD. Promises and paradoxes of regulatory T cells in inflammatory bowel disease. World J Gastroenterol. 2015;21(40):11236-45.
96. Seng A, Yankee TM. The Role of the Ikaros Family of Transcription Factors in Regulatory T cell Development and Function. J Clin Cell Immunol. 2017;8(2).
97. Sharma MD, Huang L, Choi JH, Lee EJ, Wilson JM, Lemos H*et al.,*. An inherently bifunctional subset of Foxp3+ T helper cells is controlled by the transcription factor eos. Immunity. 2013;38(5):998-1012.
98. Akimova T, Beier UH, Wang L, Levine MH, Hancock WW. Helios expression is a marker of T cell activation and proliferation. PLoS One. 2011;6(8):e24226.
99. Elkord E, Abd Al Samid M, Chaudhary B. Helios, and not FoxP3, is the marker of activated Tregs expressing GARP/LAP. Oncotarget. 2015;6(24):20026-36.
100. Thornton AM, Korty PE, Tran DQ, Wohlfert EA, Murray PE, Belkaid Y*et al.,*. Expression of Helios, an Ikaros transcription factor family member, differentiates thymic-derived from peripherally induced Foxp3+ T regulatory cells. Journal of immunology (Baltimore, Md : 1950). 2010;184(7):3433-41.
101. Lord JD, Shows DM, Chen J, Thirlby RC. Human Blood and Mucosal Regulatory T Cells Express Activation Markers and Inhibitory Receptors in Inflammatory Bowel Disease. PLoS One. 2015;10(8):e0136485.
102. Sehrawat S, Rouse BT. Interplay of Regulatory T Cell and Th17 Cells during Infectious Diseases in Humans and Animals. Front Immunol. 2017;8:341.
103. Baine I, Basu S, Ames R, Sellers RS, Macian F. Helios induces epigenetic silencing of IL2 gene expression in regulatory T cells. J Immunol. 2013;190(3):1008-16.
104. Beriou G, Costantino C, Ashley C, Yang L, Kuchroo V, Baecher-Allan CaH, D. . IL-17–producing human peripheral regulatory T cells retain suppressive function. Blood. 2009;113(18):4240-9.
105. Ogawa A, Andoh A, Araki Y, Bamba T, Fujiyama Y. Neutralization of interleukin-17 aggravates dextran sulfate sodium-induced colitis in mice. Clin Immunol. 2004;110(1):55-62.
106. Annunziato F, Cosmi L, Santarlasci V, Maggi L, Liotta F, Mazzinghi B*et al.,*. Phenotypic and functional features of human Th17 cells. J Exp Med. 2007;204(8):1849-61.
107. John LB, Ward AC. The Ikaros gene family: transcriptional regulators of hematopoiesis and immunity. Mol Immunol. 2011;48(9-10):1272-8.
108. Mitchell JL, Seng A, Yankee TM. Ikaros, Helios, and Aiolos protein levels increase in human thymocytes after beta selection. Immunol Res. 2016;64(2):565-75.
109. Georgopoulos K. The making of a lymphocyte: the choice among disparate cell fates and the IKAROS enigma. Genes & Development. 2017;31:439-50.
110. Fan Y, Lu D. The Ikaros family of zinc-finger proteins. Acta Pharm Sin B. 2016;6(6):513-21.
111. Mitchell JL, Seng A, Yankee TM. Expression patterns of Ikaros family members during positive selection and lineage commitment of human thymocytes. Immunology. 2016;149(4):400-12.
112. Kioussis D. Aiolos: an ungrateful member of the Ikaros family. Immunity. 2007;26(3):275-7.
113. Matulić M, Paradzik M, Puskarić BJ, Stipić J, Antica M. Analysis of Ikaros family splicing variants in human hematopoietic lineages. Coll Antropol. 2010;34(1):59-62.
114. Sebastian M, Lopez-Ocasio M, Metidji A, Rieder SA, Shevach EM, Thornton AM. Helios Controls a Limited Subset of Regulatory T Cell Functions. J Immunol. 2016;196(1):144-55.

115. Heizmann B, Kastner P, Chan S. The Ikaros family in lymphocyte development. Curr Opin Immunol. 2018;51:14-23.
116. Perdomo J, Crossley M. The Ikaros family protein Eos associates with C-terminal-binding protein corepressors. Eur J Biochem. 2002;269(23):5885-92.
117. Rebolla A, Schmitt C. Ikaros, Aiolos and Helios: Transcription regulators and lymphoid malignancies. Immunology and Cell Biology. 2003;81:171-5.
118. John LB, Yoong S, Ward AC. Evolution of the Ikaros gene family: implications for the origins of adaptive immunity. J Immunol. 2009;182(8):4792-9.
119. Rieder SA, Metidji A, Glass DD, Thornton AM, Ikeda T, Morgan BA*et al.,*. Eos Is Redundant for Regulatory T Cell Function but Plays an Important Role in IL-2 and Th17 Production by CD4+ Conventional T Cells. J Immunol. 2015;195(2):553-63.
120. John LB, Trengove MC, Fraser FW, Yoong SH, Ward AC. Pegasus, the 'atypical' Ikaros family member, influences left-right asymmetry and regulates pitx2 expression. Dev Biol. 2013;377(1):46-54.
121. Honma Y, Kiyosawa H, Mori T, Oguri A, Nikaido T, Kanazawa K*et al.,*. Eos: a novel member of the Ikaros gene family expressed predominantly in the developing nervous system. FEBS Lett. 1999;447(1):76-80.
122. Gorzkiewicz A, Walczewska A. Functions of the Ikaros transcription factor and the role of IKZF1 gene defects in hematological malignancies. Acta Haematologica Polonica. 2015;46(1):10-9.
123. Powell MD, Read KA, Sreekumar BK, Oestreich KJ. Ikaros Zinc Finger Transcription Factors: Regulators of Cytokine Signaling Pathways and CD4(+) T Helper Cell Differentiation. Front Immunol. 2019;10:1299.
124. Westman BJP, J.; Matthews, J.M.; Crossley, M.; Mackay, J.P. Structural Studies on a Protein-Binding Zinc-Finger Domain of Eos Reveal Both
Similarities and Differences to Classical Zinc Fingers. Biochem. 2004;43(42):13318-27.
125. Koipally J, Renold A, Kim J, Georgopoulos K. Repression by Ikaros and Aiolos is mediated through histone deacetylase complexes. Embo j. 1999;18(11):3090-100.
126. Koipally J, Georgopoulos K. A molecular dissection of the repression circuitry of Ikaros. J Biol Chem. 2002;277(31):27697-705.
127. Koipally J, Heller EJ, Seavitt JR, Georgopoulos K. Unconventional potentiation of gene expression by Ikaros. J Biol Chem. 2002;277(15):13007-15.
128. Quintana FJ, Jin H, Burns EJ, Nadeau M, Yeste A, Kumar D*et al.,*. Aiolos promotes TH17 differentiation by directly silencing Il2 expression. Nat Immunol. 2012;13(8):770-7.
129. Vannucchi AM. Pegasus causes inherited thrombocytopenia. Blood. 2019;134(23):1999-2000.
130. Georgopoulos K, Moore D, Derfler B. Ikaros, an early lymphoid-specific transcription factor and a putative mediator for T cell commitment. Science. 1992;258(5083):808-12.
131. Payne KJ, Huang G, Sahakian E, Zhu JY, Barteneva NS, Barsky LW*et al.,*. Ikaros isoform x is selectively expressed in myeloid differentiation. J Immunol. 2003;170(6):3091-8.
132. Eskandarian Z, Fliegauf M, Bulashevska A, Proietti M, Hague R, Smulski CR*et al.,*. Assessing the Functional Relevance of Variants in the IKAROS Family Zinc Finger Protein 1 (IKZF1) in a Cohort of Patients With Primary Immunodeficiency. Front Immunol. 2019;10:568.
133. Olsson L, Johansson B. Ikaros and leukaemia. Br J Haematol. 2015;169(4):479-91.
134. Hu R, Sharma SM, Bronisz A, Srinivasan R, Sankar U, Ostrowski MC. Eos, MITF, and PU.1 recruit corepressors to osteoclast-specific genes in committed myeloid progenitors. Mol Cell Biol. 2007;27(11):4018-27.

135. Boutboul D, Kuehn HS, Van de Wyngaert Z, Niemela JE, Callebaut I, Stoddard J*et al.,*. Dominant-negative IKZF1 mutations cause a T, B, and myeloid cell combined immunodeficiency. J Clin Invest. 2018;128(7):3071-87.
136. Movassagh M, Laderach D, Galy A. Proteins of the Ikaros family control dendritic cell maturation required to induce optimal Th1 T cell differentiation. Int Immunol. 2004;16(6):867-75.
137. Perdomo J, Holmes M, Chong B, Crossley M. Eos and pegasus, two members of the Ikaros family of proteins with distinct DNA binding activities. J Biol Chem. 2000;275(49):38347-54.
138. Clambey ET, Collins B, Young MH, Eberlein J, David A, Kappler JW*et al.,*. The Ikaros transcription factor regulates responsiveness to IL-12 and expression of IL-2 receptor alpha in mature, activated CD8 T cells. PLoS One. 2013;8(2):e57435.
139. Hahm K, Cobb BS, McCarty ASB, K.E. Klug, C.A., Lee R, Akashi K, Weissman IL*et al.,*. Helios, a T cell-restricted Ikaros family member that quantitatively associates with Ikaros at centromeric heterochromatIn. Genes & Development. 1998;12:782–96
140. Francis OL, Payne JL, Su R-J, Payne KJ. Regulator of myeloid differentiation and function: The secret life of Ikaros. World J Biol Chem. 2011;2(6):119-25.
141. Gómez-del Arco P, Maki K, Georgopoulos K. Phosphorylation controls Ikaros's ability to negatively regulate the G(1)-S transition. Mol Cell Biol. 2004;24(7):2797-807.
142. Oh KS, Gottschalk RA, Lounsbury NW, Sun J, Dorrington MG, Baek S*et al.,*. Dual Roles for Ikaros in Regulation of Macrophage Chromatin State and Inflammatory Gene Expression. J Immunol. 2018;201(2):757-71.
143. Wong LY, Hatfield JK, Brown MA. Ikaros sets the potential for Th17 lineage gene expression through effects on chromatin state in early T cell development. J Biol Chem. 2013;288(49):35170-9.
144. Cytlak U, Resteu A, Bogaert D, Kuehn HS, Altmann T, Gennery A*et al.,*. Ikaros family zinc finger 1 regulates dendritic cell development and function in humans. Nat Commun. 2018;9(1):1239.
145. Yu HH, Reitsma JM, Sweredoski MJ, Moradian A, Hess S, Deshaies RJ. Single subunit degradation of WIZ, a lenalidomide- and pomalidomide-dependent substrate of E3 ubiquitin ligase CRL4CRBN. 2019.
146. O'Brien S, Thomas RM, Wertheim GB, Zhang F, Shen H, Wells AD. Ikaros imposes a barrier to CD8+ T cell differentiation by restricting autocrine IL-2 production. J Immunol. 2014;192(11):5118-29.
147. Morgan BS, L.; Avitahl, N.; Andrikopoulos, K.; Ikead, T.; Gonzales, E.; Wu, P.; Neben, S.; Georgopoulos, K. Aiolos, a lymphoid restricted transcription factor that interacts with Ikaros to regulate lymphocyte differentiation. The EMBO Journal. 1997;16(8):2004-13.
148. Romero F, Martínez AC, Camonis J, Rebollo A. Aiolos transcription factor controls cell death in T cells by regulating Bcl-2 expression and its cellular localization. Embo j. 1999;18(12):3419-30.
149. Wang H, Xu Z, Du W, Lin Z, Liu Z. N160 of Aiolos Determines its DNA-Binding Activity. Anat Rec (Hoboken). 2019;302(11):2014-9.
150. Georgopoulos K, Winandy S, Avitahl N. The Role of The Ikaros Gene in Lymphocyte Development and Homeostasis. Annu Rev Immunol. 1997;15:155-76.
151. Koipally J, Georgopoulos K. Ikaros interactions with CtBP reveal a repression mechanism that is independent of histone deacetylase activity. J Biol Chem. 2000;275(26):19594-602.

152. Kelley CMI, T.; Koipally, J.; Avitahl, N.; Wu, L.; Georgopoulos K.; B. A. Morgan. Helios, a novel dimerization partner of Ikaros expressed in the earliest hematopoietic progenitors. Current Biology. 1998;8:508–15.
153. Webb GJ, Siminovitch KA, Hirschfield GM. The immunogenetics of primary biliary cirrhosis: A comprehensive review. J Autoimmun. 2015;64:42-52.
154. Rebollo A, Ayllon V, Fleischer A, Martinez CA, Zaballos A. The association of Aiolos transcription factor and Bcl-xL is involved in the control of apoptosis. J Immunol. 2001;167(11):6366-73.
155. Rieder SA, Shevach EM. Eos, goddess of treg cell reprogramming. Immunity. 2013;38(5):849-50.
156. Yu HC, Zhao HL, Wu ZK, Zhang JW. Eos negatively regulates human gamma-globin gene transcription during erythroid differentiation. PLoS One. 2011;6(7):e22907.
157. Leavy O. Eos: the sound of silence. Nature Reviews Immunology. 2009;9(10):674-5.
158. Gokhale AS, Gangaplara A, Lopez-Occasio M, Thornton AM, Shevach EM. Selective deletion of Eos (Ikzf4) in T-regulatory cells leads to loss of suppressive function and development of systemic autoimmunity. J Autoimmun. 2019;105:102300.
159. Bettini ML, Pan F, Bettini M, Finkelstein D, Rehg JE, Floess S*et al.,*. Loss of epigenetic modification driven by the Foxp3 transcription factor leads to regulatory T cell insufficiency. Immunity. 2012;36(5):717-30.
160. Koskinen MK, Mikk ML, Laine AP, Lempainen J, Loyttyniemi E, Vahasalo P*et al.,*. Longitudinal Pattern of First-Phase Insulin Response Is Associated With Genetic Variants Outside the Class II HLA Region in Children With Multiple Autoantibodies. Diabetes. 2020;69(1):12-9.
161. Censin JC, Bovijn J, Holmes MV, Lindgren CM. Colocalization analysis of polycystic ovary syndrome to identify potential disease-mediating genes and proteins. Eur J Hum Genet. 2021;29(9):1446-54.
162. Naito T, Ushirogawa H, Fukushima T, Tanaka Y, Saito M. EOS, an Ikaros family zinc finger transcription factor, interacts with the HTLV-1 oncoprotein Tax and is downregulated in peripheral blood mononuclear cells of HTLV-1-infected individuals, irrespective of clinical statuses. Virol J. 2019;16(1):160.
163. Thornton AM, Shevach EM. Helios: still behind the clouds. Immunology. 2019;158(3):161-70.
164. Takatori H, Kawashima H, Matsuki A, Meguro K, Tanaka S, Iwamoto T*et al.,*. Helios Enhances Treg Cell Function in Cooperation With FoxP3. Arthritis Rheumatol. 2015;67(6):1491-502.
165. Chan SM. The Making of a Leukemic Stem Cell: A Novel Role for IKZF2 in AML Stemness and Differentiation. Cell Stem Cell. 2019;24(1):5-6.
166. Leinoe E, Kjaersgaard M, Zetterberg E, Ostrowski S, Greinacher A, Rossing M. Highly impaired platelet ultrastructure in two families with novel IKZF5 variants. Platelets. 2020:1-6.
167. Lentaigne C, Greene D, Sivapalaratnam S, Favier R, Seyres D, Thys C*et al.,*. Germline mutations in the transcription factor IKZF5 cause thrombocytopenia. Blood. 2019;134(23):2070-81.
168. Winters AC, Tremblay D, Arinsburg S, Mascarenhas J, Schiano TD. Reassessing the safety concerns of utilizing blood donations from patients with hemochromatosis. Hepatology. 2018;67(3):1150-7.
169. Iacucci M, Jeffery L, Acharjee A, Nardone OM, Zardo D, Smith SCL*et al.,*. Ultra-high Magnification Endocytoscopy and Molecular Markers for Defining Endoscopic and Histologic

Remission in Ulcerative Colitis-An Exploratory Study to Define Deep Remission. Inflamm Bowel Dis. 2021;27(11):1719-30.
170. Clayton SA, Daley KK, MacDonald L, Fernandez-Vizarra E, Bottegoni G, O'Neil JD*et al.,*. Inflammation causes remodeling of mitochondrial cytochrome c oxidase mediated by the bifunctional gene C15orf48. Sci Adv. 2021;7(50):eabl5182.
171. Teare JM, Islam R, Flanagan R, Gallagher S, Davies MG, Grabau C. Measurement of nucleic acid concentrations using the DyNA Quant and the GeneQuant. Biotechniques. 1997;22(6):1170-4.
172. Stack EC, Wang C, Roman KA, Hoyt CC. Multiplexed immunohistochemistry, imaging, and quantitation: a review, with an assessment of Tyramide signal amplification, multispectral imaging and multiplex analysis. Methods. 2014;70(1):46-58.
173. Viratham Pulsawatdi A, Craig SG, Bingham V, McCombe K, Humphries MP, Senevirathne S*et al.,*. A robust multiplex immunofluorescence and digital pathology workflow for the characterisation of the tumour immune microenvironment. Mol Oncol. 2020;14(10):2384-402.
174. Oded Maimon LR. Data Mining and Knowledge Discovery Handbook. Boston, MA: Springer; 2005. 1383 p.
175. Ristamaki R, Joensuu H, Salmi M, Jalkanen S. Serum CD44 in malignant lymphoma: an association with treatment response. Blood. 1994;84(1):238-43.
176. Helland IS. Partial Least Squares Regression and Statistical Models. Scandinavian Journal of Statistics. 1990;17(2):97-114.
177. Liston A, Gray DH. Homeostatic control of regulatory T cell diversity. Nat Rev Immunol. 2014;14(3):154-65.
178. Ridley ML, Fleskens V, Roberts CA, Lalnunhlimi S, Alnesf A, O'Byrne AM*et al.,*. IKZF3/Aiolos Is Associated with but Not Sufficient for the Expression of IL-10 by CD4+ T Cells. The Journal of Immunology. 2020;204(11):2940-8.
179. Evans HG, Roostalu U, Walter GJ, Gullick NJ, Frederiksen KS, Roberts CA*et al.,*. TNF-alpha blockade induces IL-10 expression in human CD4+ T cells. Nat Commun. 2014;5:3199.
180. McCoy K, Le Gros G. The role of CTLA-4 in the regulation of T cell immune responses. Immunol Cell Biol. 1999;77:1-10.
181. Bin Dhuban K, d'Hennezel E, Nashi E, Bar-Or A, Rieder S, Shevach EM*et al.,*. Coexpression of TIGIT and FCRL3 identifies Helios+ human memory regulatory T cells. J Immunol. 2015;194(8):3687-96.
182. Fabio G, Zarantonello M, Mocellin C, Bonara P, Corengia C, Fargion S*et al.,*. Peripheral lymphocytes and intracellular cytokines in C282Y homozygous hemochromatosis patients. J Hepatol. 2002;37(6):753-61.
183. Costa M, Cruz E, Oliveira S, Benes V, Ivacevic T, Silva MJ*et al.,*. Lymphocyte Gene Expression Signatures from Patients and Mouse Models of Hereditary Hemochromatosis Reveal a Function of HFE as a Negative Regulator of CD8+ T-Lymphocyte Activation and Differentiation In Vivo. PLOS ONE. 2015;10(4):e0124246.
184. Zhang YZ, Li YY. Inflammatory bowel disease: pathogenesis. World J Gastroenterol. 2014;20(1):91-9.
185. Mitchell JL, Yankee TM. Variations in mRNA and protein levels of Ikaros family members in pediatric T cell acute lymphoblastic leukemia. Ann Transl Med. 2016;4(19):363.
186. Axelrad JE, Lichtiger S, Yajnik V. Inflammatory bowel disease and cancer: The role of inflammation, immunosuppression, and cancer treatment. World J Gastroenterol. 2016;22(20):4794-801.

187. Javierre BM, Rodriguez-Ubreva J, Al-Shahrour F, Corominas M, Grana O, Ciudad L*et al.,*. Long-range epigenetic silencing associates with deregulation of Ikaros targets in colorectal cancer cells. Mol Cancer Res. 2011;9(8):1139-51.
188. Kadono K, Kageyama S, Nakamura K, Hirao H, Ito T, Kojima H*et al.,*. Myeloid Ikaros-SIRT1 signaling axis regulates hepatic inflammation and pyroptosis in ischemia-stressed mouse and human liver. J Hepatol. 2021.
189. Magro F, Langner C, Driessen A, Ensari A, Geboes K, Mantzaris GJ*et al.,*. European consensus on the histopathology of inflammatory bowel disease. J Crohns Colitis. 2013;7(10):827-51.
190. Geboes K. What histologic features best differentiate Crohn's disease from ulcerative colitis? Inflamm Bowel Dis. 2008;14 Suppl 2:S168-9.
191. Lee SH, Kwon JE, Cho ML. Immunological pathogenesis of inflammatory bowel disease. Intest Res. 2018;16(1):26-42.
192. McCormack L, Dutkowski P, El-Badry AM, Clavien PA. Liver transplantation using fatty livers: always feasible? J Hepatol. 2011;54(5):1055-62.
193. Nakanuma Y, Harada K, Katayanagi K, Tsuneyama K, Sasaki M. Definition and pathology of primary sclerosing cholangitis. J Hepatobiliary Pancreat Surg. 1999;6(4):333-42.
194. Yamashita M, Morio T. Inborn errors of IKAROS and AIOLOS. Curr Opin Immunol. 2021;72:239-48.
195. Uhlén M, Fagerberg L, Hallström BM, Lindskog C, Oksvold P, Mardinoglu A*et al.,*. Tissue-based map of the human proteome. Science. 2015;347(6220):1260419.
196. The Human Protein Atlas. The Human Protein Atlas [Webpage]. The Human Protein Atlas: The Human Protein Atlas; 2022 [Available from: https://v15.proteinatlas.org/.
197. Li X, Xu Z, Du W, Zhang Z, Wei Y, Wang H*et al.,*. Aiolos promotes anchorage independence by silencing p66Shc transcription in cancer cells. Cancer Cell. 2014;25(5):575-89.
198. Wang J-H, Avitahl N, Cariappa A, Friedrich C, Ikeda T, Renold A*et al.,*. Aiolos Regulates B Cell Activation and Maturation to Effector State. Immunity. 1998;9(4):543-53.
199. Eller K, Kirsch A, Wolf AM, Sopper S, Tagwerker A, Stanzl U*et al.,*. Potential role of regulatory T cells in reversing obesity-linked insulin resistance and diabetic nephropathy. Diabetes. 2011;60(11):2954-62.
200. Huo Q, Ge C, Tian H, Sun J, Cui M, Li H*et al.,*. Dysfunction of IKZF1/MYC/MDIG axis contributes to liver cancer progression through regulating H3K9me3/p21 activity. Cell Death Dis. 2017;8(5):e2766.
201. Zhang L, Li H, Ge C, Li M, Zhao F-y, Hou H-l*et al.,*. Inhibitory effects of transcription factor Ikaros on the expression of liver cancer stem cell marker CD133 in hepatocellular carcinoma. Oncotarget. 2014;5(21):10621-35.
202. Ferraro A, D'Alise AM, Raj T, Asinovski N, Phillips R, Ergun A*et al.,*. Interindividual variation in human T regulatory cells. Proc Natl Acad Sci U S A. 2014;111(12):E1111-20.
203. Chrousos GP, Kino T. Ikaros transcription factors: flying between stress and inflammation. J Clin Invest. 2005;115(4):844-8.
204. Ezzat S, Mader R, Yu S, Ning T, Poussier P, Asa SL. Ikaros integrates endocrine and immune system development. Journal of Clinical Investigation. 2005;115(4):1021-9.
205. Vaeth M, Wang YH, Eckstein M, Yang J, Silverman GJ, Lacruz RS*et al.,*. Tissue resident and follicular Treg cell differentiation is regulated by CRAC channels. Nat Commun. 2019;10(1):1183.

206. Bruns H, Mougiakakos D, Bach C, Böttcher M, Bittenbring JT, Büttner M*et al.,*. the IKZF1-IRF4 Axis Regulates Macrophage Polarization and Macrophage-Mediated Anti-Tumor Immunity. Blood. 2016;128(22):2514-.
207. Dixon LJ, Barnes M, Tang H, Pritchard MT, Nagy LE. Kupffer cells in the liver. Compr Physiol. 2013;3(2):785-97.
208. Pfau JC, Walker E, Card GL. Monoclonal antibodies to CD45 modify LPS-induced arachidonic acid metabolism in macrophages. Biochimica et Biophysica Acta (BBA) - Molecular Cell Research. 2000;1495(3):212-22.
209. Schlereth SL, Kremers S, Schrodl F, Cursiefen C, Heindl LM. Characterization of Antigen-Presenting Macrophages and Dendritic Cells in the Healthy Human Sclera. Invest Ophthalmol Vis Sci. 2016;57(11):4878-85.
210. Chen YY, Arndtz K, Webb G, Corrigan M, Akiror S, Liaskou E*et al.,*. Intrahepatic macrophage populations in the pathophysiology of primary sclerosing cholangitis. JHEP Rep. 2019;1(5):369-76.
211. Karlsen TH, Folseraas T, Thorburn D, Vesterhus M. Primary sclerosing cholangitis - a comprehensive review. J Hepatol. 2017;67(6):1298-323.
212. Chao CY, Battat R, Al Khoury A, Restellini S, Sebastiani G, Bessissow T. Co-existence of non-alcoholic fatty liver disease and inflammatory bowel disease: A review article. World J Gastroenterol. 2016;22(34):7727-34.
213. Sartini A, Gitto S, Bianchini M, Verga MC, Di Girolamo M, Bertani A*et al.,*. Non-alcoholic fatty liver disease phenotypes in patients with inflammatory bowel disease. Cell Death Dis. 2018;9(2):87.
214. Bessissow T, Le NH, Rollet K, Afif W, Bitton A, Sebastiani G. Incidence and Predictors of Nonalcoholic Fatty Liver Disease by Serum Biomarkers in Patients with Inflammatory Bowel Disease. Inflamm Bowel Dis. 2016;22(8):1937-44.
215. Billot K, Parizot C, Arrouss I, Mazier D, Debre P, Rogner UC*et al.,*. Differential aiolos expression in human hematopoietic subpopulations. Leuk Res. 2010;34(3):289-93.
216. O'Brien S. The Role of Ikaros in CD8+ T cell Biology. 2013.
217. Yu WQ, Ji NF, Gu CJ, Wang YL, Huang M, Zhang MS. Coexpression of Helios in Foxp3(+) Regulatory T Cells and Its Role in Human Disease. Dis Markers. 2021;2021:5574472.
218. Tan WCC, Nerurkar SN, Cai HY, Ng HHM, Wu D, Wee YTF*et al.,*. Overview of multiplex immunohistochemistry/immunofluorescence techniques in the era of cancer immunotherapy. Cancer Commun (Lond). 2020;40(4):135-53.
219. Honzawa Y, Yamamoto S, Okabe M, Seno H, Nakase H. Current Topics of the Mechanism of Intestinal Fibrosis in Crohn's Disease. Immuno. 2021;1(4):574-82.
220. Speca S, Giusti I, Rieder F, Latella G. Cellular and molecular mechanisms of intestinal fibrosis. World J Gastroenterol. 2012;18(28):3635-61.
221. Alfredsson J, Wick MJ. Mechanism of fibrosis and stricture formation in Crohn's disease. Scand J Immunol. 2020;92(6):e12990.
222. Fang K, Grisham MB, Kevil CG. Application of Comparative Transcriptional Genomics to Identify Molecular Targets for Pediatric IBD. Front Immunol. 2015;6:165.
223. Holgersen K, Kutlu B, Fox B, Serikawa K, Lord J, Hansen AK*et al.,*. High-resolution gene expression profiling using RNA sequencing in patients with inflammatory bowel disease and in mouse models of colitis. J Crohns Colitis. 2015;9(6):492-506.
224. Jin Y, Li JL. Olfactomedin-like 3: possible functions in embryonic development and tumorigenesis. Chin Med J (Engl). 2019;132(14):1733-8.

225. James KR, Gomes T, Elmentaite R, Kumar N, Gulliver EL, King HW*et al.,*. Distinct microbial and immune niches of the human colon. Nat Immunol. 2020;21(3):343-53.
226. Tyler CJ, Guzman M, Lundborg LR, Yeasmin S, Perez-Jeldres T, Yarur A*et al.,*. Inherent Immune Cell Variation Within Colonic Segments Presents Challenges for Clinical Trial Design. J Crohns Colitis. 2020;14(10):1364-77.
227. Ulger BV, Erbis H, Turkoglu A, Gumus M, Gul M, Arikanoglu Z*et al.,*. Mean Platelet Volume/Platelet Count Ratio: A New Diagnostic Parameter for Necrosis in Adhesive Small Bowel Obstruction—A Retrospective Cohort Study. International Surgery. 2015;100(9-10):1256-61.
228. Mohamud M, Osborne L, Jones HG, Ahmed A, Beynon J, Harris DA*et al.,*. Thrombocytosis as a Marker for Postoperative Complications in Colorectal Surgery. Gastroenterol Res Pract. 2018;2018:1978639.
229. Bramuzzo M, Ventura A, Martelossi S, Lazzerini M. Thalidomide for inflammatory bowel disease: Systematic review. Medicine (Baltimore). 2016;95(30):e4239.
230. Quach H, Ritchie D, Stewart AK, Neeson P, Harrison S, Smyth MJ*et al.,*. Mechanism of action of immunomodulatory drugs (IMiDS) in multiple myeloma. Leukemia. 2010;24(1):22-32.
231. Ito T, Handa H. Molecular mechanisms of thalidomide and its derivatives. Proc Jpn Acad Ser B Phys Biol Sci. 2020;96(6):189-203.
232. Bolomsky A, Hubl W, Spada S, Muldur E, Schlangen K, Heintel D*et al.,*. Ikaros expression in distinct bone marrow cell populations as a candidate biomarker for outcome with lenalidomide-dexamethasone therapy in multiple myeloma. Am J Hematol. 2017;92(3):269-78.
233. Lopez-Millan B, Diaz de la Guardia R, Roca-Ho H, Garcia-Herrero CM, Lavoie JR, Rosu-Myles M*et al.,*. Therapeutic effect of the immunomodulatory drug lenalidomide, but not pomalidomide, in experimental models of rheumatoid arthritis and inflammatory bowel disease. Exp Mol Med. 2017;49(2):e290.
234. Chanan-Khan AA, Swaika A, Paulus A, Kumar SK, Mikhael JR, Rajkumar SV*et al.,*. Pomalidomide: the new immunomodulatory agent for the treatment of multiple myeloma. Blood Cancer Journal. 2013;3(9):e143-e.
235. Gandhi AK, Kang J, Havens CG, Conklin T, Ning Y, Wu L*et al.,*. Immunomodulatory agents lenalidomide and pomalidomide co-stimulate T cells by inducing degradation of T cell repressors Ikaros and Aiolos via modulation of the E3 ubiquitin ligase complex CRL4(CRBN.). Br J Haematol. 2014;164(6):811-21.
236. Kashani A, Schwartz DA. The Expanding Role of Anti-IL-12 and/or Anti-IL-23 Antibodies in the Treatment of Inflammatory Bowel Disease. Gastroenterol Hepatol (N Y). 2019;15(5):255-65.
237. Dimopoulos MA, Leleu X, Palumbo A, Moreau P, Delforge M, Cavo M*et al.,*. Expert panel consensus statement on the optimal use of pomalidomide in relapsed and refractory multiple myeloma. Leukemia. 2014;28(8):1573-85.
238. Costa F, Bolzoni M, Vescovini R, Marchica V, Accardi F, Notarfranchi L*et al.,*. Lenalidomide Increases Human Dendritic Cell Maturation in Multiple Myeloma Modulating Both Monocyte Differentiation and Mesenchymal Stromal Cell Inhibitory Properties through Ikaros and Casein Kinase 1 Degradation, Respectively. Blood. 2016;128(22):4464-.
239. Barcelo H, Faul J, Crimmins E, Thyagarajan B. A Practical Cryopreservation and Staining Protocol for Immunophenotyping in Population Studies. Curr Protoc Cytom. 2018;84(1):e35.

240. Barton JC, Wiener HW, Acton RT, Go RC. Total blood lymphocyte counts in hemochromatosis probands with HFE C282Y homozygosity: relationship to severity of iron overload and HLA-A and -B alleles and haplotypes. BMC Blood Disord. 2005;5:5-.
241. Liaskou E, Zimmermann HW, Li KK, Oo YH, Suresh S, Stamataki Z*et al.,*. Monocyte subsets in human liver disease show distinct phenotypic and functional characteristics. Hepatology. 2013;57(1):385-98.
242. Oo YH, Banz V, Kavanagh D, Liaskou E, Withers DR, Humphreys E*et al.,*. CXCR3-dependent recruitment and CCR6-mediated positioning of Th-17 cells in the inflamed liver. Journal of hepatology. 2012;57(5):1044-51.
243. De Buck E, Pauwels NS, Dieltjens T, Compernolle V, Vandekerckhove P. Is blood of uncomplicated hemochromatosis patients safe and effective for blood transfusion? A systematic review. J Hepatol. 2012;57(5):1126-34.
244. Cai X, Liu X, Du S, Xu X, Liu A, Ge X*et al.,*. Overexpression of Aiolos in Peripheral Blood Mononuclear Cell Subsets from Patients with Systemic Lupus Erythematosus and Rheumatoid Arthritis. Biochem Genet. 2016;54(1):73-82.
245. Zou H, Li R, Hu H, Hu Y, Chen X. Modulation of Regulatory T Cell Activity by TNF Receptor Type II-Targeting Pharmacological Agents. Front Immunol. 2018;9:594.
246. Papamichael K, Lin S, Moore M, Papaioannou G, Sattler L, Cheifetz AS. Infliximab in inflammatory bowel disease. Ther Adv Chronic Dis. 2019;10:2040622319838443.
247. Umetsu SE, Winandy S. Ikaros is a regulator of Il10 expression in CD4+ T cells. Journal of immunology (Baltimore, Md : 1950). 2009;183(9):5518-25.
248. Phadke MS, Krynetskaia NF, Mishra AK, Krynetskiy E. Glyceraldehyde 3-phosphate dehydrogenase depletion induces cell cycle arrest and resistance to antimetabolites in human carcinoma cell lines. J Pharmacol Exp Ther. 2009;331(1):77-86.
249. Katerndahl CDS, Heltemes-Harris LM, Willette MJL, Henzler CM, Frietze S, Yang R*et al.,*. Antagonism of B cell enhancer networks by STAT5 drives leukemia and poor patient survival. Nat Immunol. 2017;18(6):694-704.
250. Jones GR, Bain CC, Fenton TM, Kelly A, Brown SL, Ivens AC*et al.,*. Dynamics of Colon Monocyte and Macrophage Activation During Colitis. Front Immunol. 2018;9:2764.
251. Carlsen HS, Yamanaka T, Scott H, Rugtveit J, Brandtzaeg P. The proportion of CD40+ mucosal macrophages is increased in inflammatory bowel disease whereas CD40 ligand (CD154)+ T cells are relatively decreased, suggesting differential modulation of these costimulatory molecules in human gut lamina propria. Inflammatory Bowel Diseases. 2006;12(11):1013-24.
252. Zirlik A, Maier C, Gerdes N, MacFarlane L, Soosairajah J, Bavendiek U*et al.,*. CD40 ligand mediates inflammation independently of CD40 by interaction with Mac-1. Circulation. 2007;115(12):1571-80.
253. Docsa T, Bhattarai D, Sipos A, Wade CE, Cox CS, Jr., Uray K. CXCL1 is upregulated during the development of ileus resulting in decreased intestinal contractile activity. Neurogastroenterol Motil. 2020;32(3):e13757.
254. Alzoghaibi MA, Al-Mofleh IA, Al-Jebreen AM. Neutrophil chemokines GCP-2 and GRO-alpha in patients with inflammatory bowel disease. J Dig Dis. 2008;9(3):144-8.
255. Shea-Donohue T, Thomas K, Cody MJ, Zhao A, DeTolla LJ, Kopydlowski KM*et al.,*. Mice deficient in the CXCR2 ligand, CXCL1 (KC/GRO-α), exhibit increased susceptibility to dextran sodium sulfate (DSS)-induced colitis. Innate Immunity. 2008;14(2):117-24.

256. Curbishley SM, Eksteen B, Gladue RP, Lalor P, Adams DH. CXCR 3 activation promotes lymphocyte transendothelial migration across human hepatic endothelium under fluid flow. Am J Pathol. 2005;167(3):887-99.
257. Murphy CT, Moloney G, Hall LJ, Quinlan A, Faivre E, Casey P*et al.,*. Use of bioluminescence imaging to track neutrophil migration and its inhibition in experimental colitis. Clin Exp Immunol. 2010;162(1):188-96.
258. Kessel C, Lavric M, Weinhage T, Brueckner M, de Roock S, Däbritz J*et al.,*. Serum biomarkers confirming stable remission in inflammatory bowel disease. Scientific Reports. 2021;11(1):6690.
259. Di Paolo NC, Shayakhmetov DM. Interleukin 1alpha and the inflammatory process. Nat Immunol. 2016;17(8):906-13.
260. PubMed. PubMed National Center for Biotechnology Information (NCBI): National Center for Biotechnology Information (NCBI); 2022 [Available from: https://www.ncbi.nlm.nih.gov/.
261. Bouladoux N, Harrison OJ, Belkaid Y. The Mouse Model of Infection with Citrobacter rodentium. Curr Protoc Immunol. 2017;119:19 5 1- 5 25.
262. Ostanin DV, Bao J, Koboziev I, Gray L, Robinson-Jackson SA, Kosloski-Davidson M*et al.,*. T cell transfer model of chronic colitis: concepts, considerations, and tricks of the trade. American journal of physiology Gastrointestinal and liver physiology. 2009;296(2):G135-G46.
263. Okayasu I, Hatakeyama S, Yamada M, Ohkusa T, Inagaki Y, Nakaya R. A novel method in the induction of reliable experimental acute and chronic ulcerative colitis in mice. Gastroenterology. 1990;98(3):694-702.
264. Dumortier A, Kirstetter P, Kastner P, Chan S. Ikaros regulates neutrophil differentiation. Blood. 2003;101(6):2219-26.
265. Castellanos JG, Woo V, Viladomiu M, Putzel G, Lima S, Diehl GE*et al.,*. Microbiota-Induced TNF-like Ligand 1A Drives Group 3 Innate Lymphoid Cell-Mediated Barrier Protection and Intestinal T Cell Activation during Colitis. Immunity. 2018;49(6):1077-89 e5.
266. Dos Anjos Cassado A. F4/80 as a Major Macrophage Marker: The Case of the Peritoneum and Spleen. Results Probl Cell Differ. 2017;62:161-79.
267. Liu Z, Gu Y, Shin A, Zhang S, Ginhoux F. Analysis of Myeloid Cells in Mouse Tissues with Flow Cytometry. STAR Protoc. 2020;1(1):100029.

# Appendix A: Chapter 2 Methods Supplementary Material

## A.1 Immunohistochemistry Supplementary Material

### A.1.1 3,3'-diaminobenzidine (DAB) Staining Controls

#### A.1.1.1 Live Tissue DAB Controls: Mouse IgG

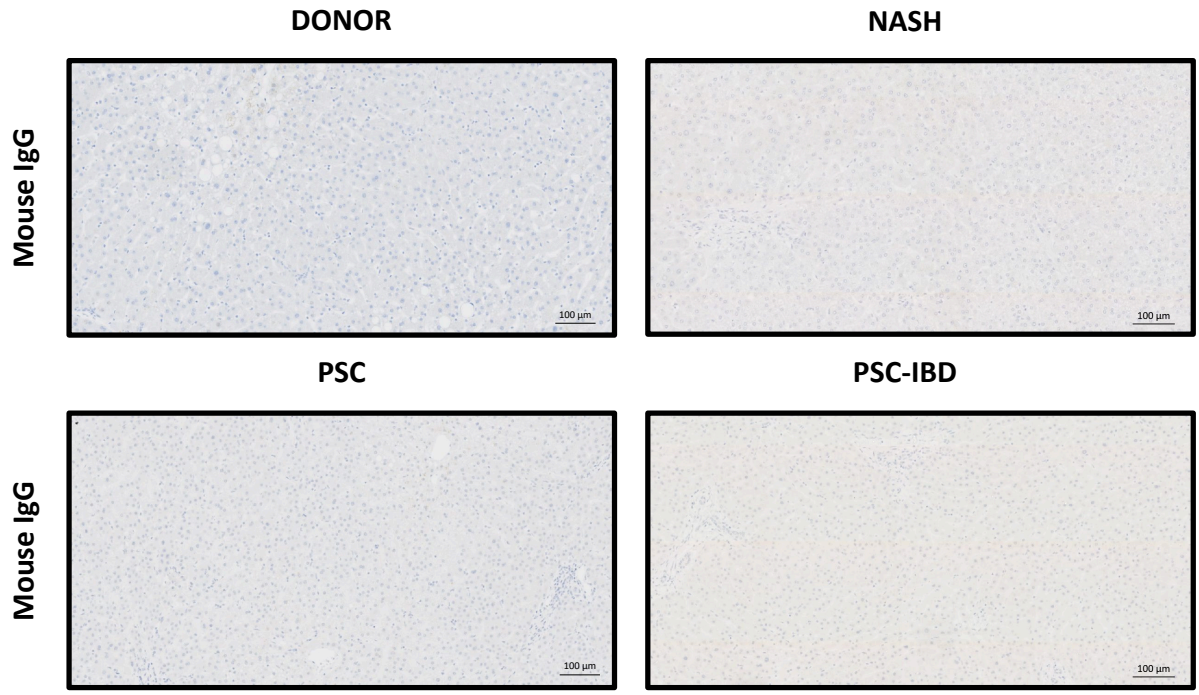



**Figure A.1: Representative Images of Isotype Matched Control Mouse IgG Liver Sections**
3,3'-diaminobenzidine (DAB) staining was conducted on Donor, Non-alcoholic steatohepatitis (NASH), Primary Sclerosing Cholangitis (PSC) and PSC-Inflammatory Bowel Disease (PSC-IBD) liver tissue looking at positive staining for Mouse IgG. Representative images are shown. Magnification x20. Scale Bar represents 100µm. *Donor, N=3; NASH, N=5; PSC, N=5; PSC-IBD, N=3.*

### A.1.1.2 Live Tissue DAB Controls: Rabbit IgG

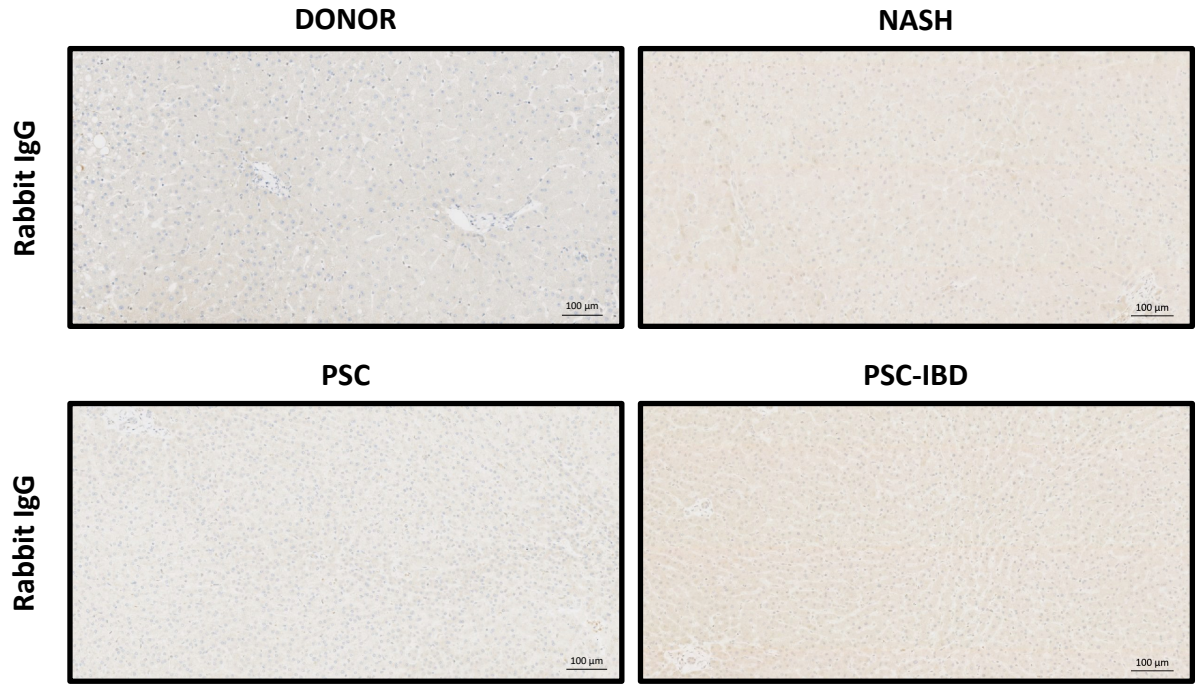



**Figure A.2: Representative Images of Isotype Matched Control Rabbit IgG Liver Sections**

3,3'-diaminobenzidine (DAB) staining was conducted on Donor, Non-alcoholic steatohepatitis (NASH), Primary Sclerosing Cholangitis (PSC) and PSC-Inflammatory Bowel Disease (PSC-IBD) liver tissue looking at expression of Rabbit IgG. Representative images are shown. Magnification x20. Scale Bar represents 100µm. *Donor, N=3; NASH, N=5; PSC, N=5; PSC-IBD, N=3.*

### A.1.1.3 Bowel Tissue Controls: Mouse and Rabbit IgG

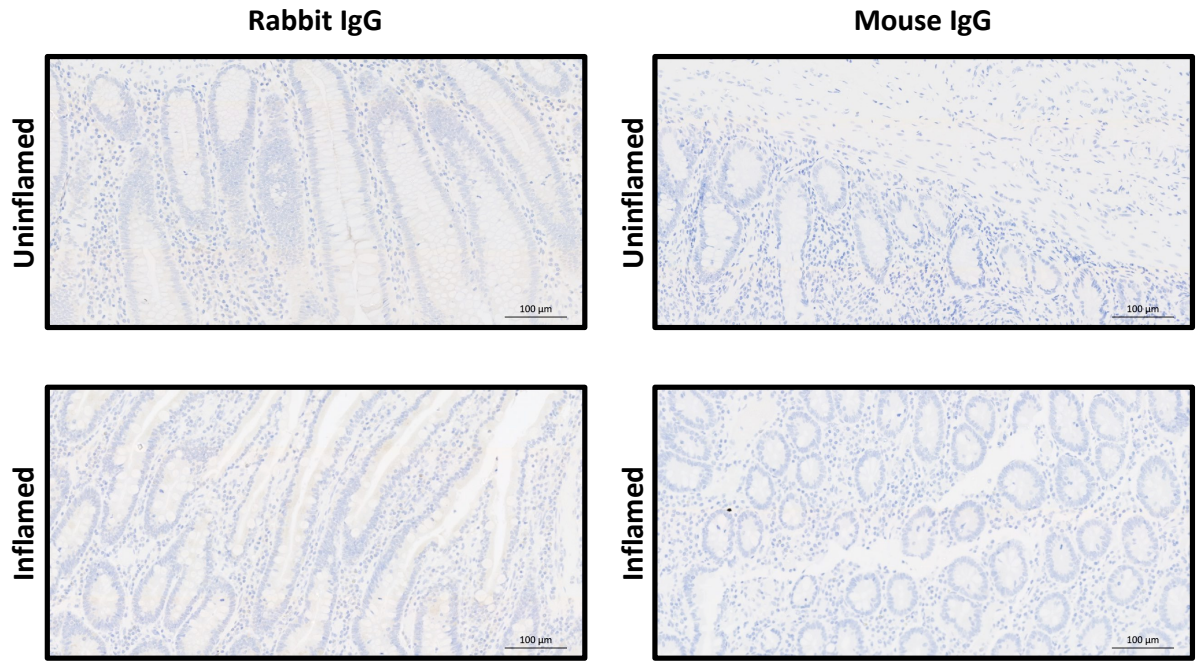



**Figure A.3: Representative Images of Isotype Matched Control Rabbit and Mouse IgG Bowel Sections**

3,3'-diaminobenzidine (DAB) staining was conducted on Inflamed and Uninflamed bowel sections stained with either Mouse IgG or Rabbit IgG. Representative images are shown. Magnification x20. Scale Bar represents 100µm. *Non-Inflamed, N=3; Inflamed, N=4.*

### A.1.2 Opal Dye™ Staining Controls

#### A.1.2.1 Bowel Mouse and Rabbit IgG

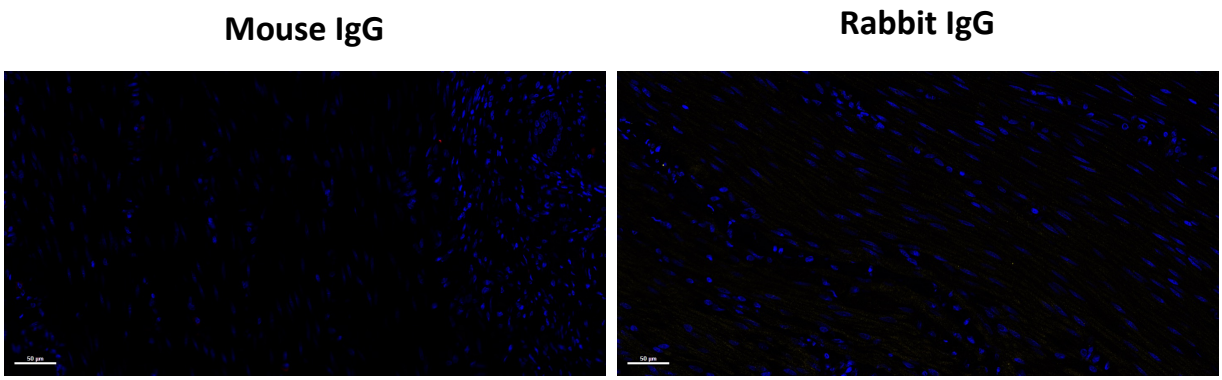



**Figure A.4: Representative Images of Isotype Matched Control Rabbit and Mouse IgG For Opal Dye™ Staining on Bowel Tissue**
For controls, Mouse IgG was stained with the Opal Dye™ 690 (in red) and Rabbit IgG stained with Opal Dye™ 570 (in yellow) on bowel tissue sections. Slides were imaged using the Vectra Polaris system and Phenochart software. Single representative images are shown. DAPI was used as the nuclear stain (in blue). Magnification *x20.* Scale Bar represents 50µm. *Mouse IgG, N=5; Rabbit IgG, N=4.*

### A.1.2.2 Liver Mouse and Rabbit IgG

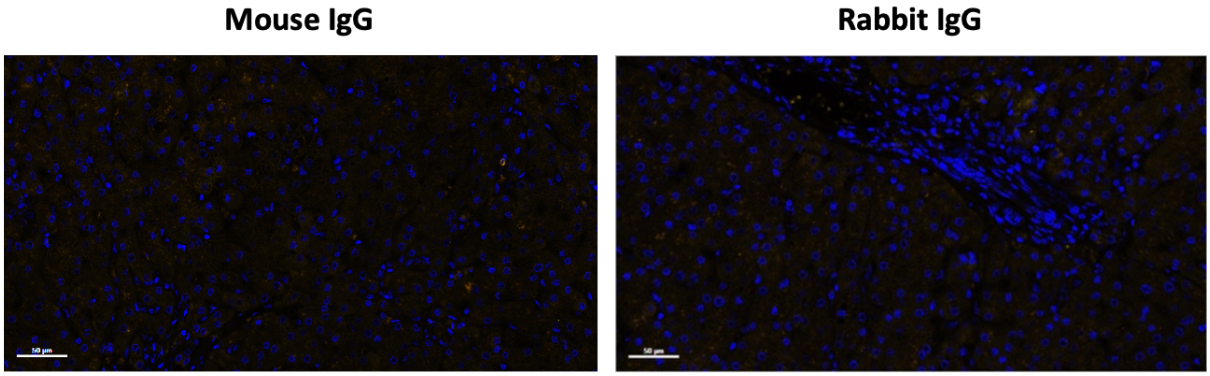



**Figure A.5: Representative Images of Isotype Matched Control Rabbit and Mouse IgG For Opal Dye™ Staining on Primary Sclerosing Cholangitis Liver Tissue**

For controls, Mouse IgG was stained with the Opal Dye™ 690 (in red) and Rabbit IgG stained with Opal Dye™ 570 (in yellow) on Primary Sclerosing Cholangitis (PSC) liver tissue sections. Slides were imaged using the Vectra Polaris system and Phenochart software. Single representative images are shown. DAPI was used as the nuclear stain (in blue). Magnification *x20.* Scale Bar represents 50µm. *Mouse IgG, N=3; Rabbit IgG, N=3.*

### A.1.3 Immunohistochemistry (IHC) Semi-Quantitative Analysis

Regions for IHC analysis in this work were randomly selected from each tissue stained to avoid bias. No region of interest was chosen therefore results in this thesis represent the staining patterns of the Ikaros family across whole bowel and liver tissue. Results were normalised to matched tissue stained with either a Rabbit or Mouse IgG and then averaged for each *N*.

#### A.1.3.1 DAB: Percentage Area DAB+

For semi-quantitation of DAB staining, ImageJ software was used. Briefly, images were opened in ImageJ, and the channels split into red, green, and blue channels. The green and red channels were closed, and analysis performed on the blue channel. To begin with, the threshold was set on isotype matched control (IMC) tissue samples for each antibody and tissue type and applied to all images. With the threshold level set, the percentage area (% area) was measured using the inbuilt analyse> measure function on Image J. The % area from the IMC was then subtracted from the corresponding stained tissue to give normalised values of DAB+ staining.

#### A.1.3.2 IHC DAB Semi-Quantitative Analysis: CD68 Counting

For counting of CD68+ Cells in DAB tissue (Section 2.6.3) as above, we set the threshold for tissues but instead of analysing percentage area DAB positive, we used the MULTI POINT tool to count the individual CD68 positive cells in liver tissue.

#### A.1.3.3 IHC Opal™ Semi-Quantitative Analysis

Using Phenochart software, 10 sections on average were randomly selected from each tissue section. The sections were then analysed using Image J Software. Briefly, images were opened in ImageJ, and the channels split into red, green, and blue channels. For CD68 analysis in the liver, the red channel was analysed with the MULTI POINT tool used to count individual CD68+ cells. In the bowel, due to the structural integrity of the tissue, we instead used the method to determine percentage area positive as above to determine the percentage area positive for CD68+ staining. To analyse CD68 and Ikaros family co-staining, the red (CD68) and green (Ikaros family) channel were merged. The percentage area staining was then measured as previously mentioned. For quantitative analysis of CD68 and Ikaros family double positive cells, 7-11 regions (*n*) were randomly selected from each sample (*N*) and Image J software used to count double positive cells in tissue. Average staining of regions (*n*) in each *N* were then reported.

## A.2 ELISA Reagent Preparation

### A.2.1 IL-10 ELISA Reagent and Standard Curve Preparation

- **Calibrator Diluent RD5C:** Prepared by diluting 1:5 RD5C: Water, therefore for 100mls of RD5C, 20ml Calibrator Diluent Concentrate was added to 80ml of water.
- **Wash Buffer:** Wash buffer was prepared by adding 20 mL of wash buffer concentrate to 480 mL of deionized water to yield 500 mL of wash buffer and mixed gently.
- **Substrate Solution:** The substrate solution was prepared no longer than 15 minutes before it was needed. Colour reagents A and B were mixed in equal volumes and protected from light.
- **Sample Preparation:** Samples were thawed and diluted 1:4 with RD5C if required.
- **Standard Preparation and Standard Curve Preparation:** The standard was prepared first by reconstituting the cytokine to produce a stock concentration of 5000pg/ml, mixed and left to sit for 15 minutes to ensure it had thoroughly reconstituted. The standard curve ranged from 500 pg/ml to 0pg/ml. To create the initial 500pg/ml, 900µl of RD5C was added to the tube with 100µl of the standard stock. In the remaining tubes, 500µl of RD5C was added and then serial dilutions made from 500pg/ml to the lowest concentration of 7.81pg/ml, by adding and then removing 500µl from each tube.

### A.2.2 IL-12 ELISA Reagent and Standard Curve Preparation

- ***Wash Buffer:*** To prepare the wash buffer, 100 mL of wash buffer concentrate was added to 900 mL of deionized to prepare 1000 mL of wash buffer
- **Substrate Solution*:*** The lyophilized Substrate was reconstituted in 6.0 mL of Substrate Diluent
- **Amplifier Solution*:*** The lyophilized Amplifier was reconstituted in 6.0 mL of Amplifier Diluent.
- ***Standard Preparation:*** The IL-12 Standard was reconstituted depending on the vial specifications and a stock solution of 40pg/ml was prepared by reconstituting with Calibrator Diluent RD5R. The range of the standard curve was from 500pg/ml as the highest standard and the Calibrator Diluent serving as the zero standard (0pg/ml).

## A.3 Patient Blood Samples

**Table A.1: Patient Blood Samples Used in Chapter 6**

| Unique TRAFIC Patient Sample Number | Date Collected and Stored | Monocytes Isolated | Sample Included in Final Analysis |
|---|---|---|---|
| ATF0015 | 28/02/2019 | 470,000 | No |
| ATF0017 | 28/06/2019 | 1.9 Million | Yes |
| ATF0019 | 04/07/2019 | 1.65 Million | Yes |
| ATF0020 | 04/09/2019 | 2.05 Million | No |
| ATF0021 | 09/08/2019 | 2.1 Million | No |
| BNV0029 | 14/02/2019 | 3.2 Million | Yes |
| BNV0030 | 28/02/2019 | 2.8 Million | Yes |
| BNV0033 | 28/06/2019 | 2.41 Million | Yes |
| BNV0035 | 01/08/2019 | 2 Million | Yes |
| BNV0036 | 02/08/2019 | 1.73 Million | Yes |
| BNV0037 | 02/08/2019 | 460,000 | No |
| BNV0041 | 01/10/2019 | 8.6 Million | Yes |

# Appendix B: The Ikaros Family and Mouse Models

## B.1 Introduction

### B.1.1 IBD Mouse Models

As our understanding of the underlying mechanisms and causes of IBD is limited, using mouse models is an efficient method to gain a better insight into its pathogenesis (88). Different methods to mimic colitis in mice include chemically induced colitis, spontaneous colitis, bacteria-induced colitis and adoptive T cell transfer methods within Rag-/- mice (88, 261, 262). The DSS mouse model is the most commonly used model for IBD (26, 88). DSS, developed by Okayasu *et al.,* (1990) is a chemical method which can be used to mimic acute, relapsing, or chronic colitis (88, 263). DSS is toxic and has anticoagulation properties, causing epithelial damage which disrupts the epithelial barrier, leading to infiltration of pathogens into the LP causing colitis (26, 88). Different dosages of DSS can be used to mimic acute or chronic forms of colitis, enabling scientists to assess varying levels of inflammation in IBD. Other IBD mouse models inducing colitis include the Trinitrobenzene Sulphonic Acid (TNBS) model, which is less popular and the well characterised *Citrobacter rodentium* (*C. rodentium*) model (26, 261).

Many murine studies have highlighted the role macrophages play in IBD (34). In mice, intestinal macrophages are replaced mainly by blood-derived monocytes (85, 250). Ly6c$^{high}$CX3CR1$^{low}$ PBMC-derived monocytes are recruited using CCR2 into the LP in mice and they gain MHCII expression as they do. The monocytes then loose Ly6c expression and begin to mature into intestinal macrophages by expressing CX3CR1$^{high}$, CD64 and F4/80 (45, 82). Similarly, in humans, CCL2 is upregulated, causing migration of classical monocytes into intestinal mucosa in CD, where they then differentiate into macrophages (30).

In DSS mice models, proinflammatory macrophage and monocyte populations accumulate in the colon with knock out of this subset reducing inflammation (26, 34). A lack of total macrophages in DSS mice models however can cause severe inflammation in the gut exacerbating colitis (26). Investigating key mediators, Steinbach and Plevy (2014) found IL10R knockout in macrophages leads to colitis development in mice models. A similar phenotype is also seen in IL-10 global knock out models where mice develop reduced tolerance and colitis (26, 34, 85).

One of the key findings through using mouse models has been the role of Th17 cells in IBD. Normally IL-17 is associated with epithelial barriers, and its loss appears to be associated with an increase in dysfunction of the barrier (4). Contrastingly, with IL-17F knockdown, a key cytokine produced by Th17, mice develop milder DSS colitis therefore suggesting IL-17F is a mediator which has a proinflammatory effects in IBD

pathogenesis (4). In mice, blocking IL-21R also prevents DSS-induced inflammation, with anti-IL21 reducing IL-17 production from cells in the LP (4). Thus, together these mouse models have supported the blocking of Th17-associated cytokines as efficient therapy for IBD management.

Mouse models can also be used to investigate the findings of GWAS studies. The NOD2 SNP identified through one of the earliest GWAS studies (See Chapter 1), was studied in mice models to provide an insight into human disease. The NOD2 knockout caused an increase in NFκB activation and severe colitis in DSS models, with greater apoptosis of macrophages coinciding with an increase in IL-1b production (13). Another GWAS identified the transmembrane protein MDR-1, which found that global knockout of MDR-1 in mice, caused the development of colitis in murine models (9). Although these are a few examples, they demonstrate the usefulness of mouse models in investigating disease-causing phenotypes in humans, which are not yet possible in human models.

### B.1.2 Ikaros Family Mouse Models

Much of our insight into the Ikaros family has come through investigating the family through murine models. For the Ikaros family, mouse models have provided an insight into their roles in development, autoimmunity and importantly, their role in key cell types such as CD4+ T Cells and macrophages.

For example, Aiolos mouse models have discussed the role of the transcription factor in IBD in the context of its impact on Th17 cells (119, 123, 128). Through these studies, it has become clearer that Aiolos is able to influence Th17 polarisation, implicating the transcription factor in the Treg/Th17 disbalance in IBD. Studies have also shown Aiolos can influence Tfh polarisation through its regulation of IL-2 (119, 128, 148). Inhibiting IL-2 increases Aiolos which in turn activates STAT3 and together Aiolos and STAT3 can induce *Bcl-6,* the Tfh master regulator, which enables differentiation of CD4+ T Cells into Tfh (123).

For Eos, murine models have helped to investigate the function of Eos, especially through loss of, or knockout Eos models. Global knockdown of Eos (Eos $^{(-/-)}$) is believed to result in autoimmunity in murine models (162). Eos $^{(-/-)}$ mice also have increased IL-17 production, supporting a switch to a more proinflammatory phenotype in absence of Eos (119). Similarly, the Eos $^{(-/-)}$ model by Powell *et al.,* (2019) resulted in global detrimental effects, causing severe Experimental Autoimmune Encephalomyelitis (EAE) with an increase in pro-inflammatory IL-17 in the Central Nervous System (CNS).Investigating its role in Tregs, Gokhale *et al.,* (2019) made conditional Eos knockout Tregs in their mouse model (158). These mice had normal suppressive function of Tregs *in vitro,* however, were more susceptible to development of EAE and were unable to inhibit the development of IBD (158). The group found that

this model resulted in upregulation of Tregs in the mice, which were less suppressive in nature, developed autoimmunity and developed infiltration of lymphocytes into non-lymphoid organs such as the lungs, liver, and kidneys. However, the group also found Eos $^{(-/-)}$ resulted in autoimmunity in mice at a later stage implicating CD8+ T cells and non-T lymphocytes into the disease pathology alongside Tregs (158).

Similar to Eos, Helios mouse models are also of great interest mainly due to its key role in Tregs and leukaemia (98). Global Helios knockdown (Helios $^{(-/-)}$) in mice can result in death at birth signifying the importance of Helios for survival (114). In another model by (110), Helios$^{(-/-)}$ mice have been shown to develop a RA phenotype. Similarly, Powell *et al.,* (2019) found Helios$^{(-/-)}$ resulted in an increase in pro-inflammatory cytokines including IL-17 and TNF$\alpha$ by Tregs, autoantibody production, increase activated T cells, whilst concurrently decreasing STAT5 activation and FoxP3. Helios$^{(-/-)}$ also resulted in a decrease in proliferation and colony formation, whilst also impacting myeloid differentiation genes therefore suggesting Helios has a role in differentiation lineages (165).

Ikaros is integral to many immune cell type and mutated Ikaros isoforms have been shown to result in defective mice from birth (117). One of the earliest papers discussing the impact of Ikaros knockdown models in mice was by Georgopoulos *et al.,* (1997). The group found that *C-terminal* deletion of Ikaros develops a Ikaros-null mutation which in mice, causes a lack of B Cells early in development (150). A lack of T Cell progenitors during foetal development coincides with this, which develop more slowly over the coming weeks with a lack of gamma delta T cells in the periphery of adult mice (150). Mice which possess a double negative isoform of Ikaros lack all lymphoid lineages with a reduction in T, B, myeloid, and erythroid cells (150). Dumortier *et al.,* (2003) using Ikaros null mice (Ikaros$^{(-/-)}$) also found total lack of B and NK cells alongside T Cell defects, with mice displaying an anaemic phenotype. Similarly, using an Ikaros dominant negative isoform, the group saw a total lack of B, T, NK, and DC Cells. This similar observation is also seen in 70% of AML patients suggesting an imperative role for Ikaros in myeloid cell function and development (122, 264). In some cases, Ikaros mutations lead to pre-B cell leukaemia in mouse models (109).

*In vitro* heterozygous mutations of Ikaros also reduces conventional monocytes within the periphery (144). In contrast, Ikaros$^{(-/-)}$ have myeloid precursor upregulation with reduction in the ability of these cells to migrate (135). Cytlak *et al.,* (2018) using Ikaros$^{(-/-)}$ in mice found a decrease in plasmacytoid DC (pDC). Boutboul *et al.,* (2018) similarly found Ikaros$^{(-/-)}$ resulted in a total lack of DC in mice. Similarly, Cytlak *et al.,* (2018) using a heterozygous mutation of Ikaros, saw this caused a reduction in pDC but increased conventional DC in humans, suggesting fully functioning Ikaros is needed for efficient DC function.

Using an Ikaros selective knockout in CD4+ T cells from mice, Umetsu and Winandy (2009) placed these cells within Th2 polarising conditions and found that they produced high levels of the Th1 cytokine IFNγ but low levels of IL-10 and IL-4, which would be expected (247). Exogenous addition of Ikaros resulted in production of Th2 cytokines IL-10 and IL-4, whilst limiting IFNγ production (a Th1 cytokine) (247). Thus Ikaros was able to regulate IFNγ in Th1 and Th2, with the group suggesting this occurs through interaction of Ikaros with GATA-3 (247). This therefore suggests Ikaros is also able to influence the polarisation and plasticity capacity of cells in response to environmental cues.

### B.1.3 Results

Mice colons were kindly provided by Veronika Matei, a member of the Dr Dave Withers group, according to their established protocol. The Withers group investigate innate lymphoid cells (ILCs) and the role of OX40L expression on ILCs in murine colitis models. Infectious '*gram negative bacteria-induced'* colitis was induced in mice by addition of *C. rodentium* and 'WT' mice expressing $OX40L^{f/f}$ were also kindly provided by the group (261). A brief description of their protocol is provided in the paper by Castellanos *et al.,* (2018). Following culling, mice colons were digested and resuspended in FACs buffer and then provided as a suspension for flow cytometry analysis in our experiments. In the colon samples, we stained for CD11b+ and F4/80, both macrophage markers and the Ikaros family. F4/80 is a marker of murine macrophages (266). CD11b is a marker expressed on myeloid cells, and was used to reinforce we had gated out a legitimate macrophage population (267). Cell populations were gated as outlined in Figure B.1, with the panel design described in Table B1.

**Table B.1: Antibody Panel For Mice Colon Staining**

| **Target** | **Fluorochrome** | **Dilution** (final volume 100μl) |
|---|---|---|
| CD11b | PE | 2:100 |
| F4/80 | PE Texas Red | 2:100 |
| Aiolos | BV421 | 3:100 |
| Eos | APC | 1:100 |
| Helios | PerCPCy5.5 | 3:100 |
| Ikaros | FITC | 1:100 |
| Live/Dead | BV510 | 1:500 |

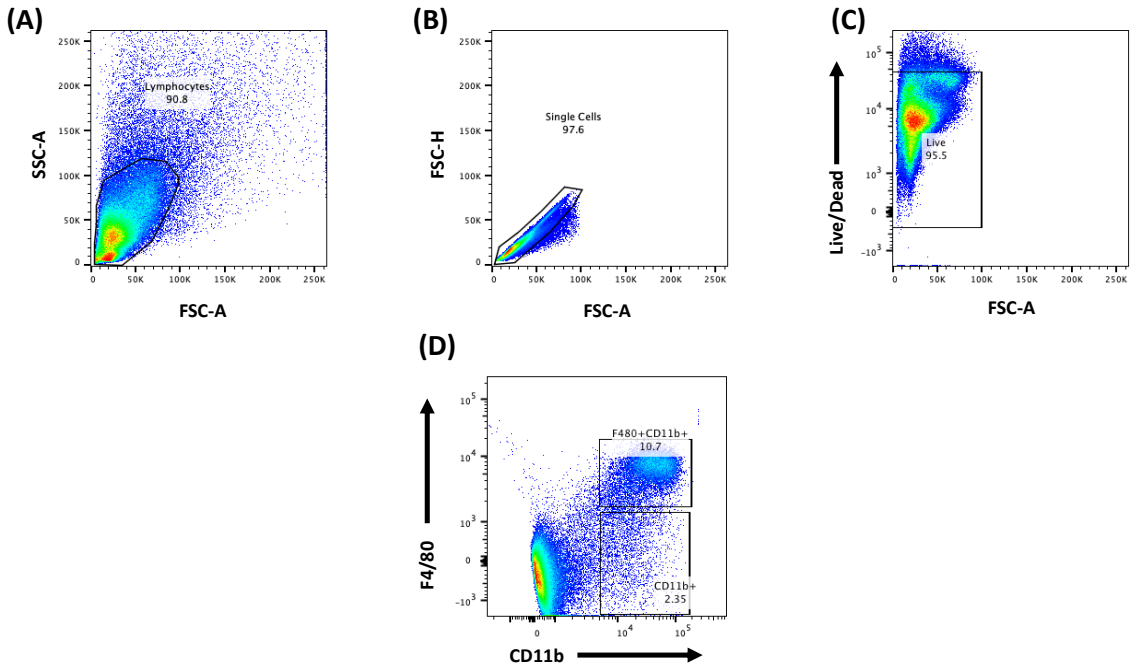



**Figure B.1: Gating Strategy for Flow Cytometry Analysis of Mice Colons**
**(A)** Cells were gated to exclude debris with total lymphocyte population identified, **(B)** Doublets were then excluded to identify singlet populations and **(C)** Dead cells were identified as those which were live/dead cell stain positive. **(D)** Using CD11b and F4/80, a CD11b+ only population and a F4/80+Cd11b+ double positive population were gated out, from which analysis for Ikaros family members was conducted. Representative plots from a 'Control' phenotype are shown. Plots derived from *FlowJo V10.*

### B.1.3.1 Eos and Helios Are Greatly Upregulated in CD11b+F4/80+ Mice Colon Macrophages

Flow cytometric analysis of CD11b+ and F4/80+ colon macrophages found that expression of Aiolos, Eos and Helios was upregulated in C. *rodentium* mice in comparison to WT (Figure B.2). Helios had the lowest MFI values in both WT and C. *rodentium* treated samples, whereas Aiolos had a slight increase in MFI values in C. *rodentium* mice in comparison to WT. Both Helios and Eos expression was almost 50% higher in MFI values in C. *rodentium* samples in comparison to WT. Eos for example, in C. *rodentium* mice had MFI values of approximately 9900AU in comparison to 5000AU in WT (Figure B.2).

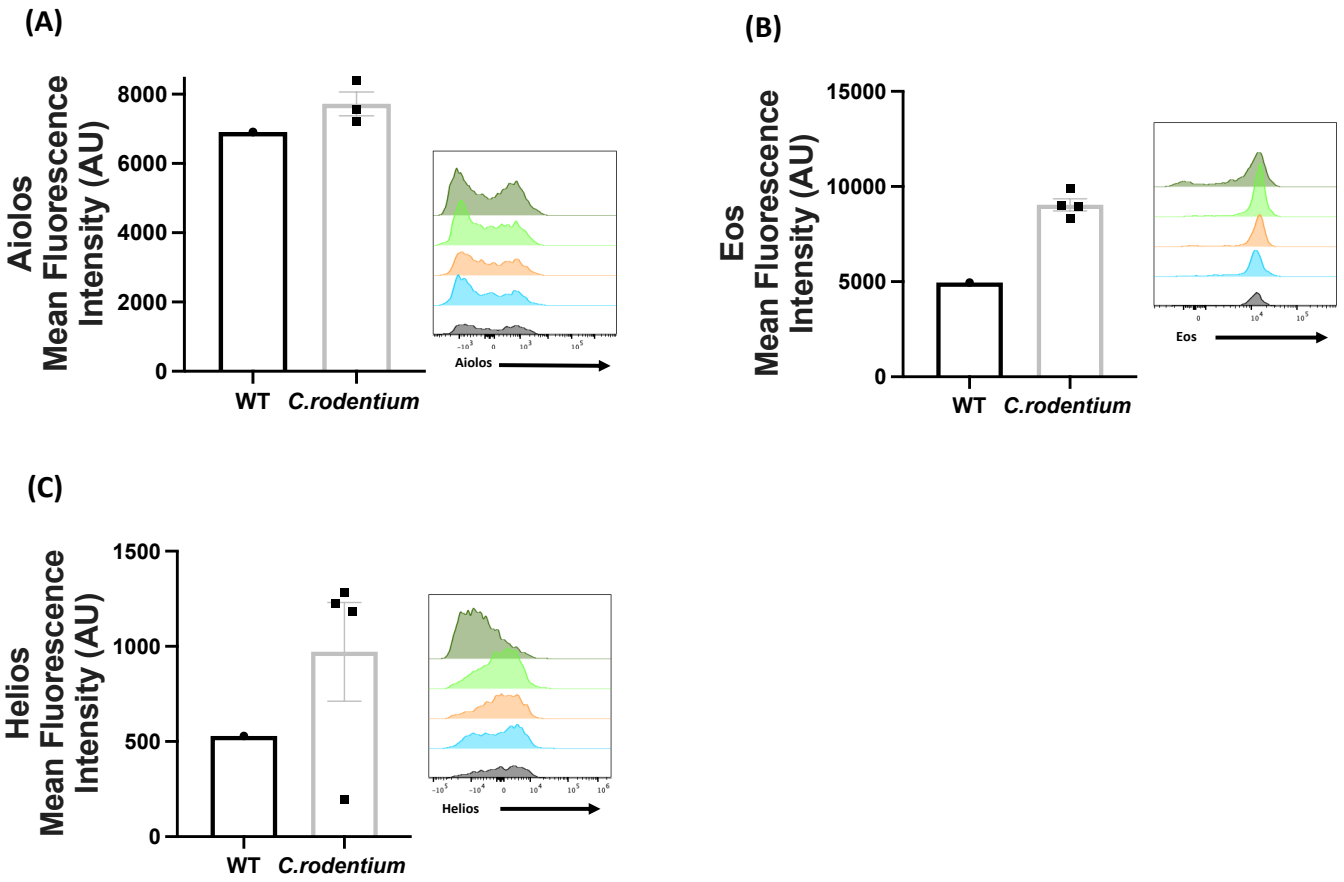



**Figure B.2: Helios and Eos are Upregulated Within *Citrobacter rodentium* Mice Colon Macrophages**

Whole mouse colon cells were isolated from *Citrobacter rodentium (C. rodentium) and* 'Wild Type' mice (WT, expressing OX40L$^{f/f}$ ) for flow cytometry analysis of protein expression levels of Ikaros family members, **(A)** Aiolos, **(B)** Eos, and **(C)** Helios. Data was analysed using FlowJo V10 software to determine Mean Fluorescence Intensity (Arbitrary Units, AU) of Ikaros family members within CD11b+F4/80+ Cells. Representative histogram plots from for each transcription factor are shown. Plots derived from *FlowJo V10.* WT, *N=1; C. rodentium, N=3-4. NS. Unpaired T Test.*

### B.1.4 Discussion

Our results have found that an increase in both Helios and Eos is observed within mice colon macrophage populations which are CD11b+ and F4/80+ (Figure B.2). The results are in part similar to what we observed within our human study data. We saw an increase in CD68+Eos+ macrophages in inflamed tissue (Figure 5.21) and an increase in Eos expression within Biologic Naive monocytes in comparison to Control (Figure 6.6). Similarly, we also saw a significant increase in CD68+Helios+ macrophages in inflamed tissue (Figure 5.22) and an increase in Helios within MΦ-M-CSF macrophages in Biologic Naïve patients in comparison to Control (Figure 6.6). Our results thus suggest that both Helios and Eos play an integral role in macrophage biology in both mice and humans, aiding the immune response. Similar to human data, data on Helios and Eos expression within mice models and in particular macrophages is limited.

For Helios, many studies have focussed on the link between Helios, CD4+ cells and Tregs in IBD, mainly due to its association with Tregs (See Chapter 3). Sebastian *et al.,* (2016) conducted a Helios selective knockout in Tregs ($Tregs^{Helios\ (-/-)}$) and found that although the Tregs had normal *in vitro* suppressor function and functioned in an *in vivo* Rag IBD model, they had impaired control of T cell expansion and mediation of Tfh and Th1 cells. Ultimately, this led to autoimmunity without the need of an antigen (114). The $Tregs^{Helios\ (-/-)}$ had low expression levels of Ki67 and Bcl-2 supporting impaired Treg expansion and survival (114). The group hypothesised that lack of Helios may make Tregs constitutively active encouraging an inappropriate immune response (114). Baine *et al.,* (2013) contrastingly injected CD4+CD25 naïve T cells into $Rag1^{(-/-)}$ mice as an IBD model and using shHelios within exogenous Tregs, found the Tregs had reduced suppressive capacity and were less protective resulting in marked colitis in mice (103). The group concluded that Tregs can develop without Helios, however lack of Helios prevents cell death (103). Similarly, in a model by Gokhale *et al.,* (2019), $Tregs^{Helios(-/-)}$ resulted in systemic autoimmunity and promoted a Th1 phenotype where the Tregs were unable to infiltrate into non-lymphoid tissue. This led to the development of a metabolic syndrome therefore mice were euthanised early. Together, these models highlight the key need for Helios in Treg function and how lack of Helios can contribute to colitis in murine IBD models. Thus, we can hypothesise that the upregulation of Helios within the C. *rodentium* mice may be to offset the inflammation resulting from the pathogen, as lack of Helios promotes autoimmunity. Similarly, Pan *et al.,* (2009) in a Rag2-/- IBD model conducted a selective knockout of Eos within Tregs, finding that these Tregs had inefficient function and failed to suppress immune responses and gene silencing. The group found that Eos impacts genes which FoxP3 represses such as effector cytokines and therefore a knockout of Eos within Tregs prevents this function (46). The group summarised that Eos is needed to limit colitis within IBD murine models thus supporting our hypothesis of upregulating Eos to manage bowel inflammation in the murine models (46).

Together, our results support the upregulation of Helios and Eos as a consequence of colonic inflammation in both mice and humans. Although more investigation is needed for the cause and purpose of this upregulation, what we can hypothesise is that upregulation is perhaps to aid the regulatory function of macrophages. This is based on our findings of upregulation of both Eos and Helios in anti-TNF$\alpha$ treated populations in comparison to Biologic Naïve patient samples. Although this was conducted on systemic PBMC populations, what we can hypothesise is the targeting of a proinflammatory mediator, TNF$\alpha$, causes the upregulation of the two transcription factors which are heavily associated with Tregs and macrophages.

Although we struggled to find studies on expression of Ikaros family members within the CD11b+/F4/80+ macrophage population in mice colon we did find a study investigating expression of Ikaros within macrophages in the liver. The model by Kadono *et al.,* (2021) assessing hepatic liver injury found that Ikaros was expressed within CD11b+ F4/80+ liver infiltrating macrophages (188). Although the group didn't delve further into other Ikaros family members, we can hypothesise that the other family members would most likely be present too. The group found that Ikaros was implicated in regulating the Sirtulin1 (SIRT1)-Ikaros mediated macrophage inflammasome pyroptosis pathway in response to ischemic-reperfusion injury (188). SIRT1 is a protein deacetylase involved in inflammation and cell senescence. An interesting finding from the group was that within biopsies from liver transplants, patients with higher BMIs had higher levels of Ikaros expression. This is similar to the findings we observed in our clinical correlations in Chapter 4, with correlations of Helios, PSC and Eos with BMI (Table 4.3). Contrastingly, the group found that lower Ikaros expression corelated with better early liver transplant function thus suggesting that Ikaros and its role within macrophage mediated pyroptosis could in part cause liver damage. Together this opens up the implication of other Ikaros family members and their role within macrophages contributing to disease pathogenesis.

There were however limitations with our pilot mice study data. For one, we were limited with how many samples we could acquire for functional analysis and thus technical replicates of our study are needed. The control samples that we acquired were also *floxed* for OX40L and therefore were not true control 'WTs'. We had also stained for Ikaros, however as our antibody was on FITC we could not accurately detect the antibody as the mice contained eYFP. Thus, for future experiments we would envisage attaining more reliable controls, along with appropriate diseased mice to assay all Ikaros family members. Optimising mice-specific antibodies could also help with attaining more reliable data. The model used within this data is also based on infection with a bacterial species, ideally therefore, other mice models such as a DSS model may provide another insight into IBD pathogenesis.